An Atlas of Opossum Organogenesis: Opossum Development

William J. Krause

Universal Publishers
Boca Raton, Florida

An Atlas of Opossum Organogenesis: Opossum Development

Copyright © 2007 William J. Krause
All rights reserved. No part of this book may be reproduced or transmitted in any form or by any means, electronic or mechanical, including photocopying, recording, or by any information storage and retrieval system, without written permission from the publisher.

Universal Publishers
Boca Raton, Florida • USA
2008

ISBN-10: 1-58112-969-6
ISBN-13: 978-1-58112-969-4

www.universal-publishers.com

An Atlas of Opossum Organogenesis

TABLE OF CONTENTS

Chapter 1 Male Reproductive System/Gamete Production....1
Chapter 2 Female Reproductive System/Gamete Production....14
Chapter 3 Shell Membrane....26
Chapter 4 Placentation....30
Chapter 5 Allantois....53
Chapter 6 Embryo Formation....61
Chapter 7 Limb Formation....89
Chapter 8 Musculoskeletal Development....105
Chapter 9 Pouch....118
Chapter 10 General Postnatal Features....123
Chapter 11 Integument....136
Chapter 12 Mesonephros....156
Chapter 13 Metanephros....176
Chapter 14 Nasal Cavity....195
Chapter 15 Trachea and Lungs....210
Chapter 16 Tongue....228
Chapter 17 Submandibular Gland....236
Chapter 18 Tooth Eruption....246
Chapter 19 Esophagus....248
Chapter 20 Stomach....258
Chapter 21 Small Intestine....279
Chapter 22 Brunner's Glands....290
Chapter 23 Colon....297
Chapter 24 Pancreas....302
Chapter 25 Liver....323
Chapter 26 Spleen....336
Chapter 27 Thymus....343
Chapter 28 Blood Cells....352
Chapter 29 Heart....360
Chapter 30 Pituitary....368
Chapter 31 Thyroid....386
Chapter 32 Parathyroid....393
Chapter 33 Adrenal....397
Chapter 34 Brain....405
Chapter 35 Ear....429
Chapter 36 Eye....437
Chapter 37 Harderian Gland....458
Chapter 38 Testis....463
Chapter 39 Ovary....468
Index....472

Introduction

The primary objective of this atlas is to gather under one cover a series of photographic illustrations and line drawings that summarize major events during organogenesis in the opossum (*Didelphis virginiana*). Many of the illustrations presented have been published previously but are scattered throughout a very diverse literature over time. The opossum is of interest because of its short gestation period (about 12.5 days) and the fact that it is born in a near embryonic state. Because of the abbreviated period of intrauterine development, the opossum is an accessible biomedical model with which to study the major events during organ development without the complications of doing intrauterine manipulations necessary if other mammalian species are used. The developing opossum can simply be examined within the marsupium (pouch) during which time the majority of organogenesis takes place. The first nine days of gestation are concerned primarily with the establishment of the three germ layers. During this period of development, opossum blastocysts float freely within uterine secretions, each prevented from physically interacting with uterine tissues by a surrounding shell membrane. Initial organogenesis commences during the last three days of the 12.5 day gestation period and continues well into the postnatal period. It is during the last three days of gestation, when the yolk sac placenta is intimately associated with the uterine mucosa that development proceeds at an astonishing rate to form functional structures that will allow for the survival of the newborn of this species. Those structures essential for survival at and immediately after birth develop precociously but follow a typical mammalian pattern of development. Such structures are generally modified in some way to allow for the survival of the young following the abbreviated gestation period. Structures not essential for immediate survival at birth (digestive and reproductive systems; lymphoid organs, ear, eyes, and hind limbs) are poorly developed at the time of birth and develop during the extended postnatal period within the pouch. Structures that appear most essential for survival at birth include the external nares, which are open and flaring, olfactory epithelium, utricle of the inner ear, lungs, cardiovascular system, mouth (which is large, open and houses a well-developed tongue), and the forelimbs which are well developed with opposable digits and epitrichial claws.

The female opossum exhibits a number of behaviors which suggest that olfaction may be important not only in guiding the newborn young to the pouch but also in locating a teat within the pouch once they arrive. Prior to birth, the female opossum sits on her haunches, licks and cleanses the vulva area, grooms the abdominal fur between the birth canal and the pouch, and thoroughly cleanses the teat area within the pouch. It should be pointed out that the newborn opossums migrate to the pouch on their own without direct physical assistance from the mother. The instinctive licking behavior of the mother may not only cleanse the migratory pathway to the teat region of the pouch, but also serve to provide olfactory cues via the saliva that guide the newborn to the pouch for teat location. At birth, opossum neonates always orient and crawl away from gravity (a negatively geotropic behavior) and travel upward toward the pouch. A band of about twenty sensory hair cells are present within the macula of the forming utricle the day prior to birth. Thus, at least one sensory region in the vestibular apparatus of the inner ear (the utricle) is capable of functioning in the newborn opossum. Mature appearing olfactory bipolar neurons, the axons of which can be traced to the developing brain, also appear in the developing nasal cavity just interior to the external nares of the opossum immediately prior to birth. During their

migration from the birth canal to the pouch, the newborn opossum uses the well-developed forelimbs and clawed digits effectively. The minute forepaws are capable of grasping and with the clawed digits the newborn young grasp the mother's fur and wriggle their way to the pouch. The female usually sits on her haunches and approximates the urogenital sinus nearer to the pouch thereby shorting the distance the young must traverse. The forelimbs of the young exhibit an overhand swimming stroke motion where the head and neck are flexed laterally followed immediately by the foreword motion of the ipsilateral foreleg. The head and neck are then flexed in the opposite direction while the deciduous claws of the forepaw grasp the fur of the mother. As the foreleg is moved backward the newborn opossum is pushed foreword. After entering the pouch, following about a ten minute journey, the head is moved in wide arcs and when the snout touches a teat it is immediately sucked into the mouth with the aid of the large, well developed tongue. The snout of the newborn is highly innervated and tactile cues also appear to be important as a final step in location and attachment to a teat. During the following two to four postnatal days, the lateral angles of the mouth seal around the teat due to a proliferation of cells within the epitrichium. As a result the mouth is sealed shut with the exception of a narrow orifice at the tip of snout that permits the entrance of the nipple. That portion of the nipple within the oral cavity swells thereby permanently anchoring the pouch young opossum to the same teat for about the next nine weeks of postnatal life.

The early prenatal development of the opossum has been detailed and illustrated by McCrady (1938). Quantitative data (organ weights, cell counts and measurements, mitotic indices) during the period of organogenesis also have been reviewed previously (Krause 1998a, 1998b). A major review of the early literature for *Didelphis virginiana* has been done Krause (2000) and its natural history reviewed and presented Krause and Krause (2004). The genome for the North American opossum (*Didelphis virginiana* Kerr) (Margulies et al. 2005) as well as the sequence of its mitochondrial DNA (Janke et al. 1994) has been determined. In this volume illustrations summarizing the major developmental events that occur during organogenesis in the opossum are gathered together and presented.

References:

Janke, A., Feldmaier-Fuchs, G., Thomas, W.K., von Haeseler, A. and Pääbo, S. (1994) The marsupial mitochondrial genome and the evolution of placental mammals. Genetics 137: 243-256.

The complete mitochondrial genome for *Didelphis virginiana* Kerr can be viewed on line at: http://www.ncbi.nlm.nih.gov/entrez/query.fcgi?db=genome&cmd=Retrieve&dopt=Overview&list_uids=10470

Krause, W.J. (1998a) A review of histogenesis/organogenesis in the developing North American opossum (*Didelphis virginiana*). Adv. Anat. Embryol. Cell Biol. 143 (I): Springer Verlag, Berlin, pp 143.

Krause, W.J. (1998b) A review of histogenesis/organogenesis in the developing North American opossum (*Didelphis virginiana*). Adv. Anat. Embryol. Cell Biol. 143 (II): Springer Verlag, Berlin, pp 120.

Krause, W.J. (2000) Information Resources on the North American Opossum (*Didelphis virginiana*): A Bibliography on its Natural History and Use in Biomedical Research. AWIC Resources Series No. 9. Animal Welfare Information Center, USDA, Agricultural Research Service, National Agricultural Library, pp 146, Baltimore Avenue, Beltsville, MD. The electronic version of this publication can be viewed on line at: http.//www.nal.usda.gov/awic/pubs/opossum/opossum.htm.

Krause, W.J. and W. A. Krause (2004) The Opossum: Its Amazing Story. Walsworth Publishing Company, Marceline, Missouri, pp 71

Margulies, E.H., Maduro, V.V.B., Thomas, P.J., Thomkins, J.P., Amemiya, C.T., Lou, M., and Green, E.D. (2005) Comparative sequencing provides insights about the structure and conservation of marsupial and monotreme genomes. Pro. Nat. Acad. Sci. USA 102: 3354-3359.

The complete genome for *Didelphis virginiana* Kerr can be viewed on line at:
GenBank AC144756. Margulies, E.H., Maduro, V.V., Thomas, P.J., Tomkins, J.P., Amemiya, C.T., Luo, M. and Green, E.D. Didelphis virginiana clone LB3-74D22, complete sequence. [Internet.] Bethesda (MD): National Library of Medicine (US). National Center for Biotechnology Information; 2003 Oct 7. Available from:
http://www.ncbi.nlm.nih.gov/entrez/query.fcgi?cmd=search&db=nucleotide&term=AC144756[accn]&doptcmdl=GenPept

McCrady, E. Jr. (1938) The embryology of the opossum. Am. Anat. Mem. 16: 1-223.

Chapter 1. Male Reproductive System/Gamete Production

Synopsis:

The structure of the adult male reproductive system is in general similar to that of most other mammals and consists of paired testes each of which is enveloped by a heavily pigmented tunica vaginalis and housed within a scrotum. The excurrent duct system of each testis consists of tubuli recti, ductuli efferentes, a ductus epididymidis, and a vas deferens. The vas deferens takes an unusual pathway by passing medial to the ureters without first having to course around the ureters before uniting the epididymides to the urethra. The urethra consists of glandular and membranous regions. The longer glandular region assumes the overall shape of a carrot and follows a U-shaped curve. The glandular portion of the urethra or prostate consists of three distinct regions that differ in position, diameter, and color. In addition to the prostate, a duct to another accessory sex gland, Cowper's glands, is linked to the male reproductive system. Each glandular unit of the latter consists of three lobes, the ducts of which unite prior to joining the urethra. The glans penis of *Didelphis* is bifid.

A unique feature of the male opossum is that its gametes (spermatozoa) exhibit distinct morphological changes as they mature and pass through the ductus epididymis. Numerous branched microvilli (stereocilia), an endocytic complex, dense granules, and multivesicular bodies located in the apical cytoplasm characterize the pseudostratified columnar epithelium lining the duct of the proximal epididymis. Such morphological features are indicative of an epithelial lining actively involved in the absorption of testicular fluid. In contrast, epithelial cells lining the ductus of the middle and distal epididymal regions exhibit morphological features (large euchromatic nuclei, large dense nucleoli, increased amounts of granular endoplasmic reticulum) indicative of protein synthesis and secretion rather than absorption. Epididymal 5-α-reductase activity has been shown to be highest in the central and distal segments of the opossum epididymis. It is within the ductus of the middle and distal regions of the epididymis where a 90° rotation of the sperm head occurs followed by pairing of spermatozoa acrosome to acrosome. The morphological transformation of epididymal spermatozoa and the phenomenon of sperm pairing are unique to *Didelphis* and other didelphid marsupials.

Acknowledgments:

Fig. 1, courtesy of and from: Martan, J. (1965). The genital system of the male opossum, *Didelphis marsupialis virginiana*, and other marsupials. Trans. Ill. State Acad. Sci. 76: 3-28.

Figs. 3, 4, 6 (bottom), 7 and 9, courtesy of and from: Kelce, W.R., W.J. Krause, and V.K. Ganjam (1987). Unique regional distribution of 4-3-Ketosteroid-5-oxidreductase and associated epididymal morphology in the marsupial *Didelphis virginiana*. Biol. Reprod. 37:403-420.

Fig. 5 (top), courtesy of and from: Holstein, A. F. (1965) Elektronenmikroskopische Untersuchungen am Spermatozoon des Opossum (*Didelphis virginiana* Kerr). Z. Zellforsch. 65: 904-914.

Figs. 5 (bottom), 8 (top), 10 and 11 (top), courtesy of and from: Krause, W.J. and J.H. Cutts (1979) Pairing of spermatozoa in the epididymis of the opossum (*Didelphis virginiana*): A scanning electron microscopic study. Arch. histol. Jap. 42:181-190.

Fig. 11 (bottom left), courtesy of and from: Bedford, J.M., J.C. Rodger, and W.G. Breed (1984). Why so many mammalian spermatozoa – a clue from marsupials? Proc. R. Soc. Lond. (B) 221: 221-233.

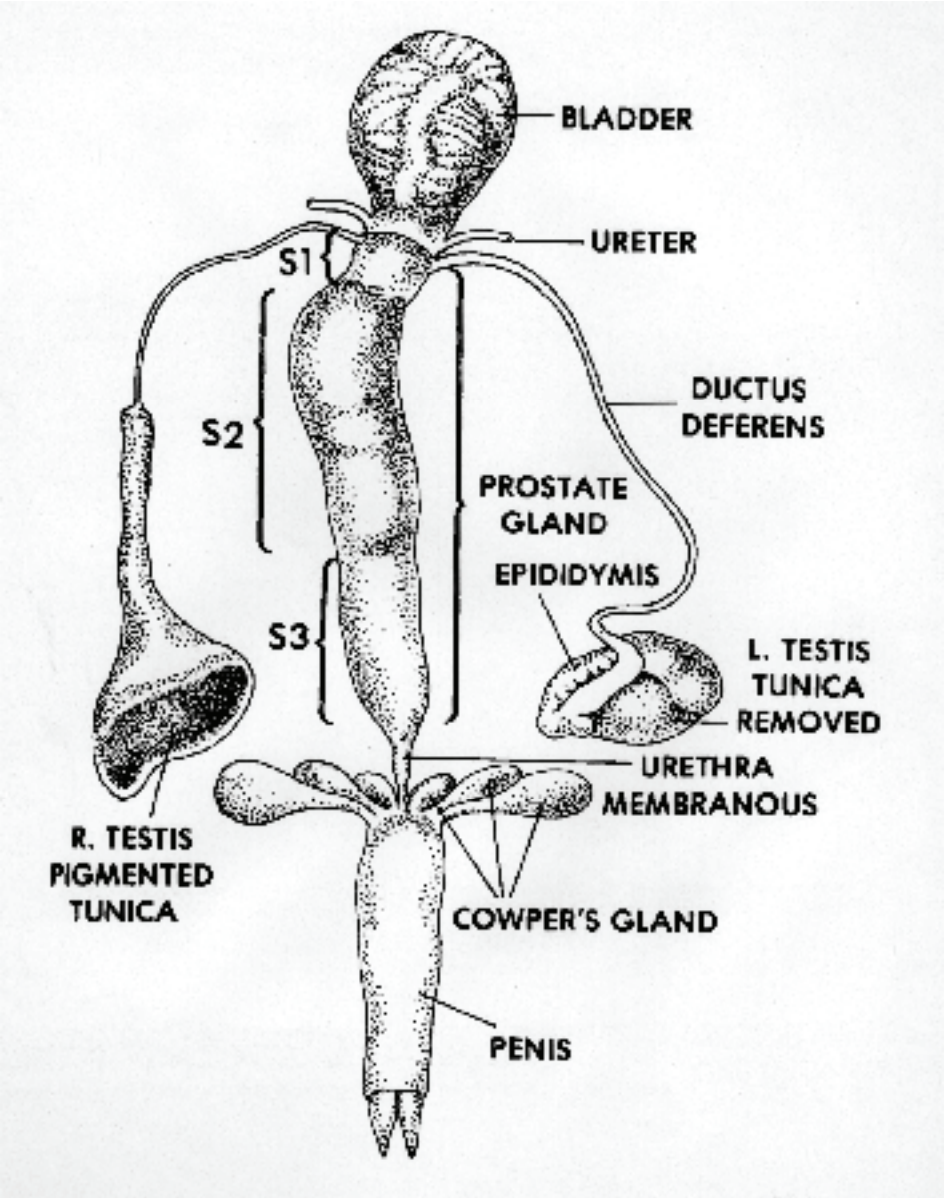

Fig. 1. A line drawing illustrates the subcomponents of the male reproductive system from a juvenile opossum. The glandular portion of the urethra (prostate) has a carrot shape and in the mature male exhibits a distinct U-shaped curve. During life the first region (prostate 1) is brown-gray in color; the second region (prostate 2) is thickest and light pink in color; and the third region (prostate 3) is gray-green in color. Each testis is housed within a highly pigmented tunica vaginalis that is blue-black in color. The contained testis is cream-white in appearance and a small conical body light green in color (containing the ductuli efferentes), separated from the head of the epididymis by a shallow groove, is observed in the mature male. The penis is bifid. These features characterize the macroscopic appearance of the adult male reproductive system.

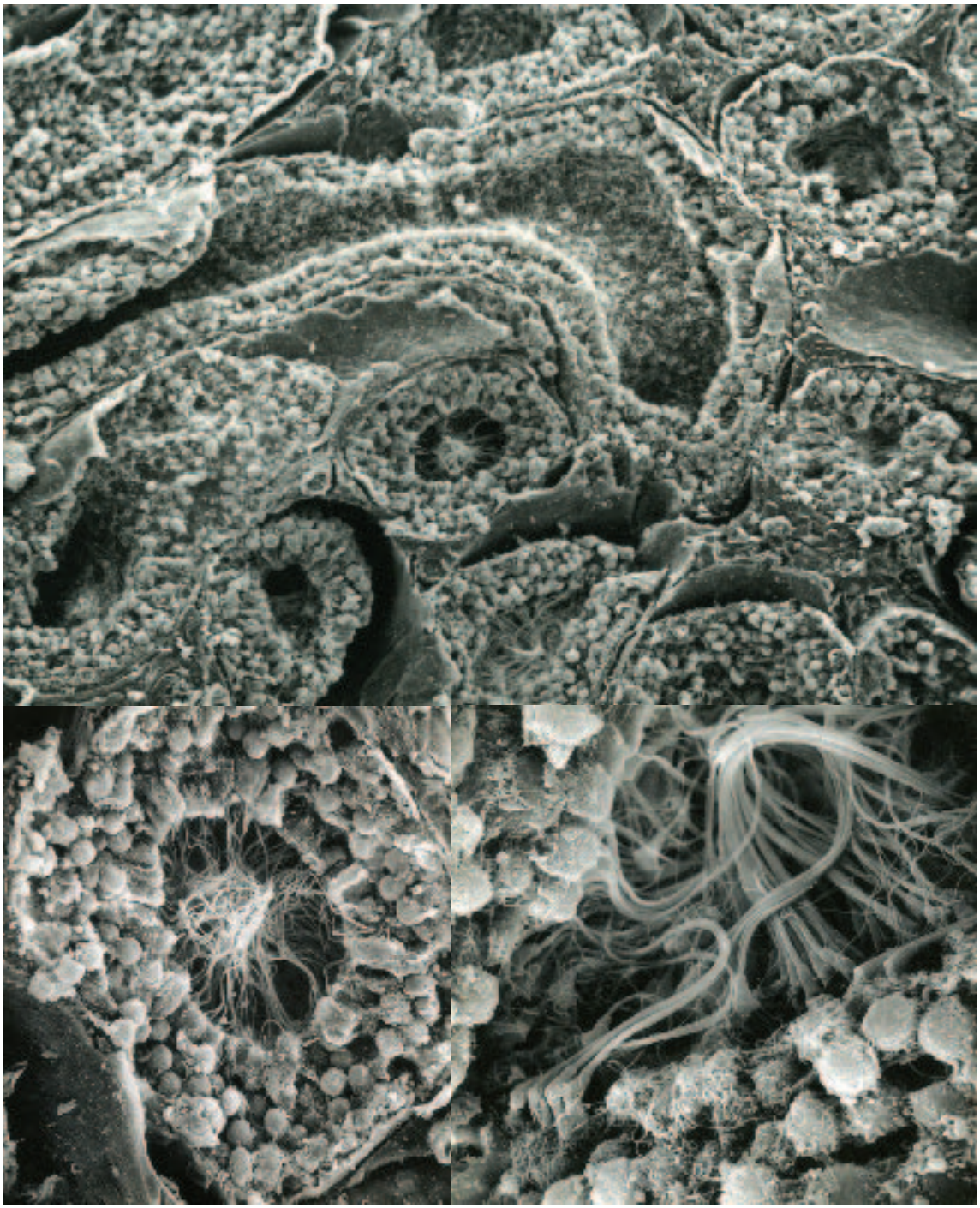

Fig. 2. (*Above*). A freeze fracture preparation of the adult testis interior illustrates numerous seminiferous tubules as viewed with the scanning electron microscope. SEM. X 200. (*Below left*). The germinal epithelium contained within a single seminiferous tubule. SEM X 500. (*Below right*). A figure that illustrates the flagella associated with spermatids just prior to their release into the lumen of the seminiferous tubule. SEM. X 2,000.

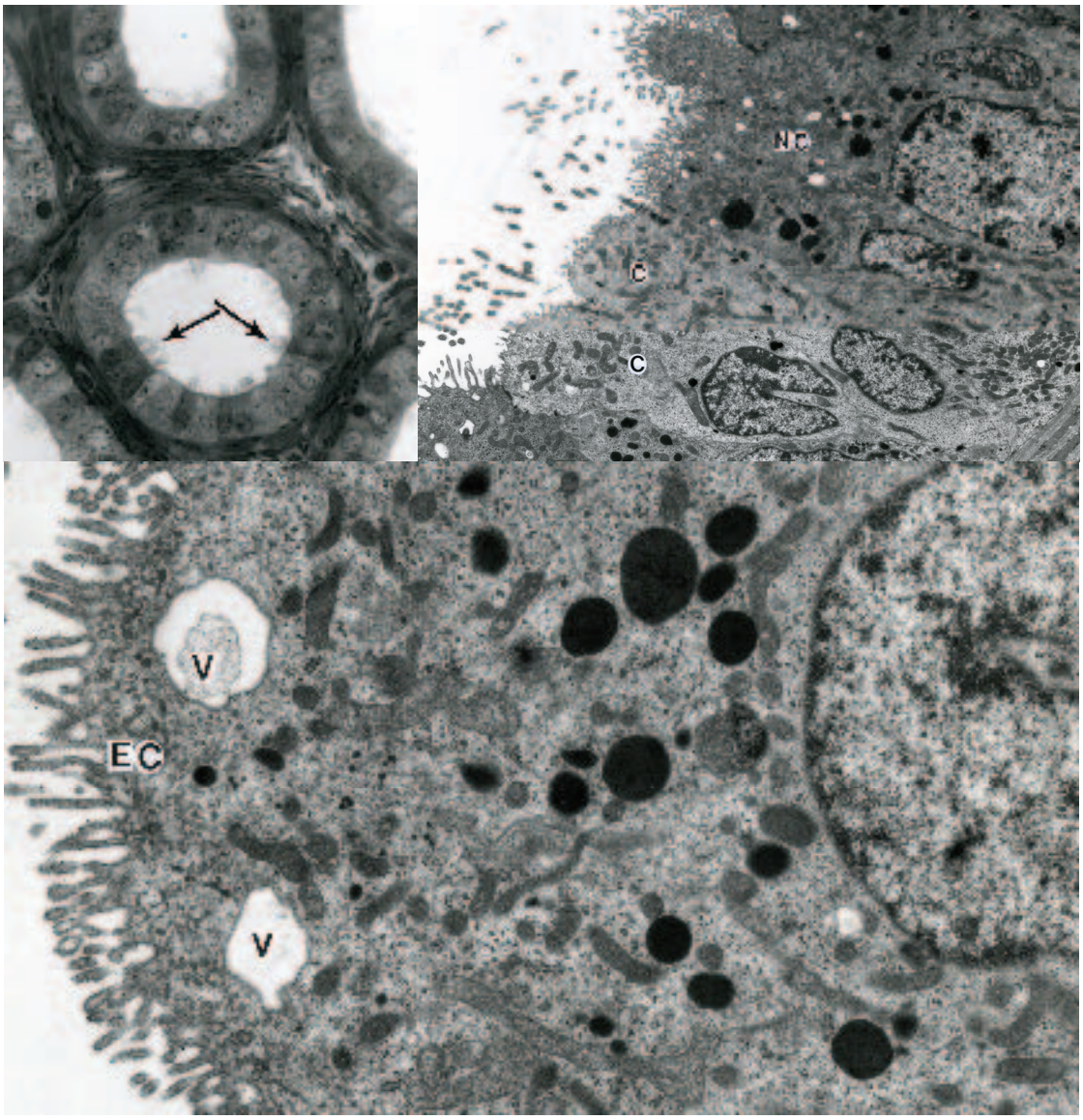

Fig. 3. (*Above left*). The ductuli efferentes are characterized by a large luminal diameter. The lining epithelial cells are of relatively low height some of which exhibit the presence of cilia (arrows). LM 780X. (*Above right*). The lining epithelium of an efferent ductule lies on a prominent basal lamina and is composed of both non-ciliated (NC) and ciliated (C) cells. TEM 4,600X . (*Below*). The apical region of the non-ciliated cell type is characterized by an endocytic complex (EC) subjacent to numerous microvilli, apical vacuoles (V) and numerous dense granules. These morphological features suggest a cell type actively engaged in absorption. TEM X 17,000.

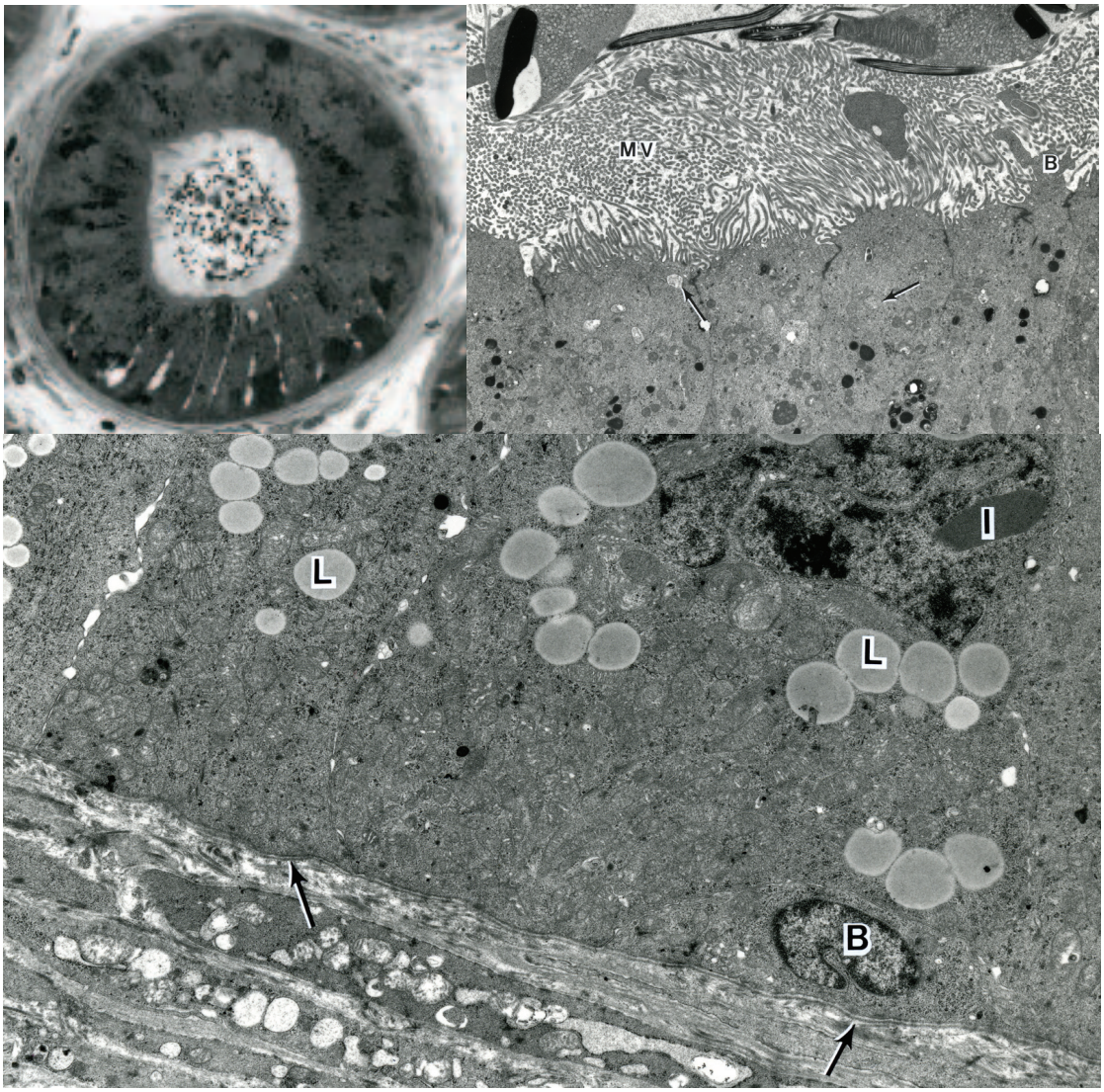

Fig. 4. (*Above left*). A light micrograph illustrates a segment of caput (head region) of the epididymis. This region of the epididymis is characterized by a tall lining epithelium and a relatively narrow lumen. Numerous dense granules fill the apical and supranuclear cytoplasm of component cells. LM X 780. (*Above right*). The apices of several epithelial cells from the proximal epididymis exhibit abundant, elaborate microvilli (MV), cytoplasmic blebs (B), an endocytic complex, dense granules, and multivesicular bodies (arrows) suggesting an absorptive function. Immature spermatozoa are seen at the top immediately adjacent to the microvilli. TEM X 7,500. (*Below*). The basal region of the epididymal lining epithelium lies on a distinct basal lamina (arrows) and the cytoplasm contains numerous lipid droplets (L) and mitochondria. A nuclear crystalloid inclusion (I) and a basal cell (B) also are shown. TEM X 9,500.

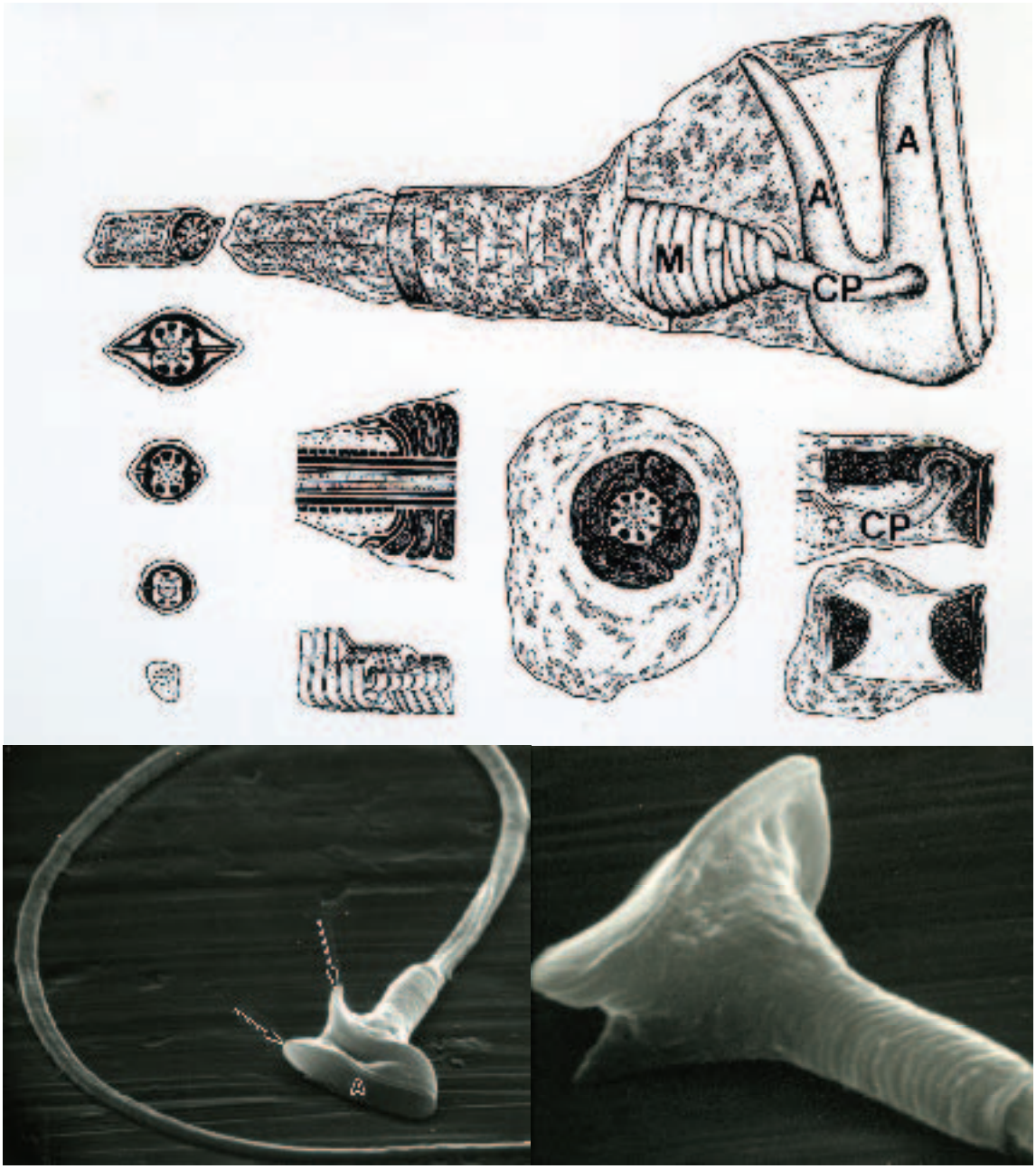

Fig. 5. (*Above*). A line drawing of an immature spermatozoon illustrates the shape and orientation of the nuclear arms (A), the elongated connecting piece (CP), the middle piece (M), and subcomponents of several regions of the tail. A large cytoplasmic droplet (residual body) envelops the nuclear region and a large portion of the middle piece. (*Below left*). The cranial view of an immature spermatozoon illustrates the two nuclear arms of the nucleus (arrows) as well as the acrosome (A) associated with the flat surface of the larger arm. Note that the length of the nucleus lies on a plane perpendicular to the long axis of the tail. SEM X 5,000. (*Below right*). The large cytoplasmic droplet obscures the details of the junction between the middle piece and nucleus of an immature spermatozoon when viewed from a caudal direction. SEM X 8,000.

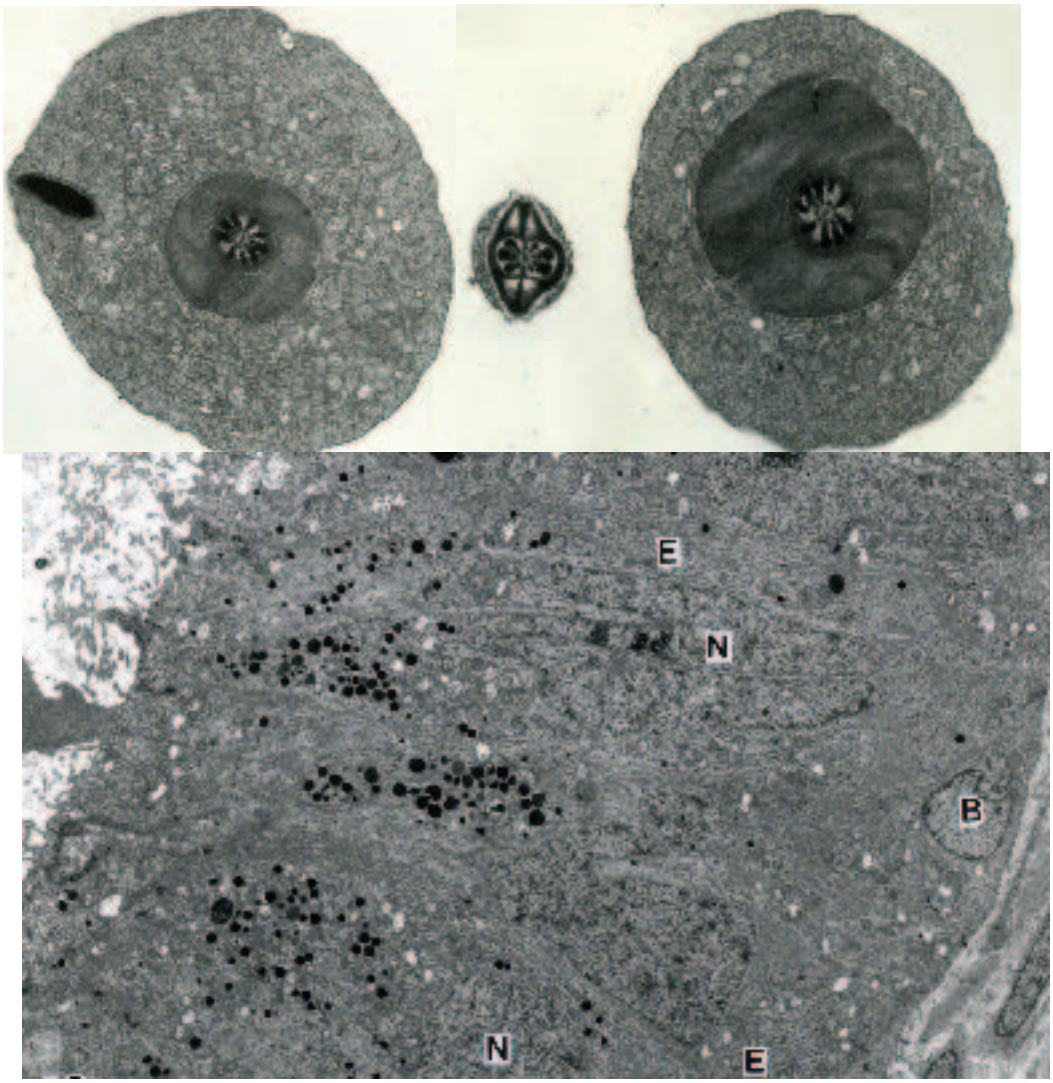

Fig. 6. (*Above left*). A portion of the cytoplasmic droplet near the nucleus of an immature spermatozoon illustrates the details of the centrally positioned middle piece, the droplet itself, and a small portion of the nucleus. TEM X 25,000. (*Above right*). A region of the middle piece but further distal along the tail as compared to the adjacent illustration as well as a portion of the tail from an additional immature spermatozoon isolated from the proximal epididymis. TEM X 25,000. (*Below*). A transmission electron micrograph through corpus epididymal epithelial cells illustrates that these cells contain abundant granular endoplasmic reticulum (E) and numerous, small electron dense granules in the supranuclear cytoplasm. Nuclei (N) are characterized by complex infoldings of the nuclear membrane. A small basal cell (B) also is shown adjacent to the basal lamina. TEM X 7,000.

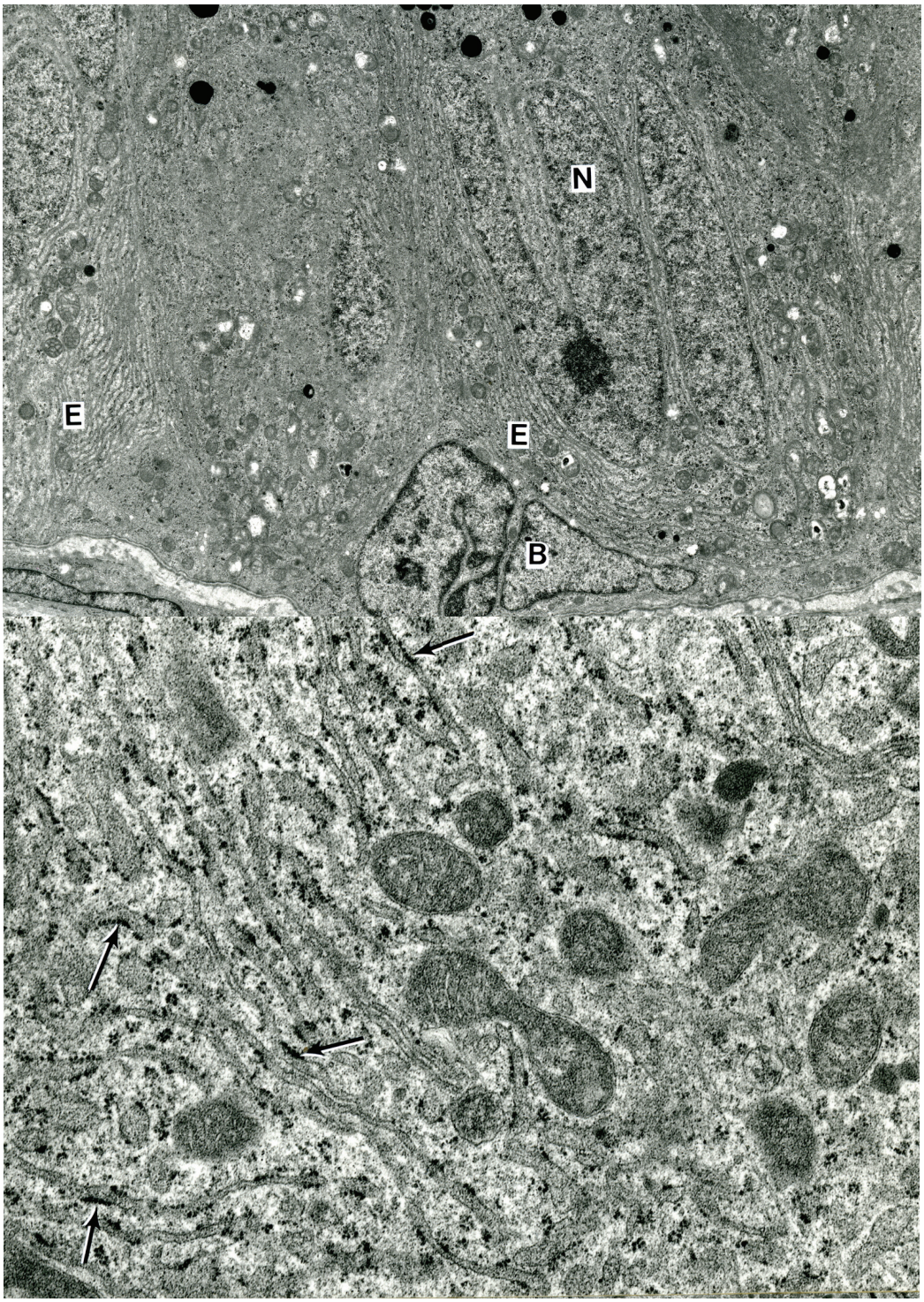

Fig. 7. (*Above*). The basal region of epithelial cells lining the corpus of the epididymis exhibits numerous profiles of granular endoplasmic reticulum (E). Note the complex nature of the nuclear profile (N) in the principal cell as well as that associated with basal cell (B). Both rest on a distinct basal lamina. TEM X 9,450. (*Below*). The granular endoplasmic from the basal region as seen at higher magnification illustrates the sparse, scattered nature of the associated ribosomes (arrows). TEM X 40,000.

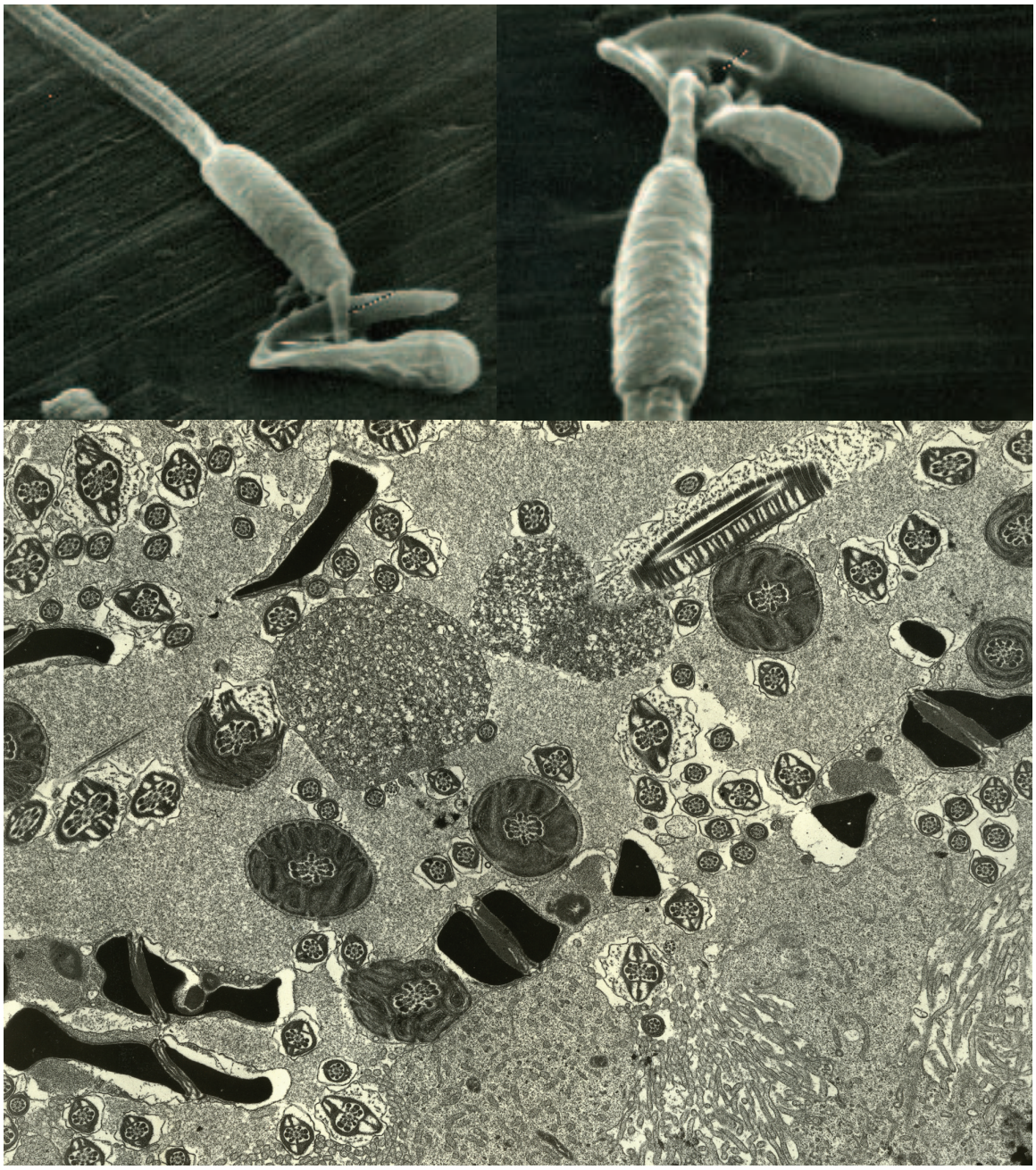

Fig. 8. (*Above left*). The heads of the majority of spermatozoa from the central epididymal region have rotated 90° and the nuclear arms lie on a plane parallel to that of the tail. The long connecting piece (large arrow) terminates in an enlargement (capitulum) that fits into the articular fossa (small arrow) of the nucleus. The acrosome and the principal and the middle piece of the tail also are shown. SEM X 5,000. (*Above right*). An additional disrupted spermatozoon (top right) viewed from a different angle demonstrates the articular fossa (arrow) as well as the medial features of the head. SEM X 5,000. (*Below*). A region of the corpus lumen illustrates both paired and unpaired spermatozoa as well as numerous sections through various regions of the tails. Note that the pairing of spermatozoa occurs acrosome-to-acrosome. TEM X 15,000.

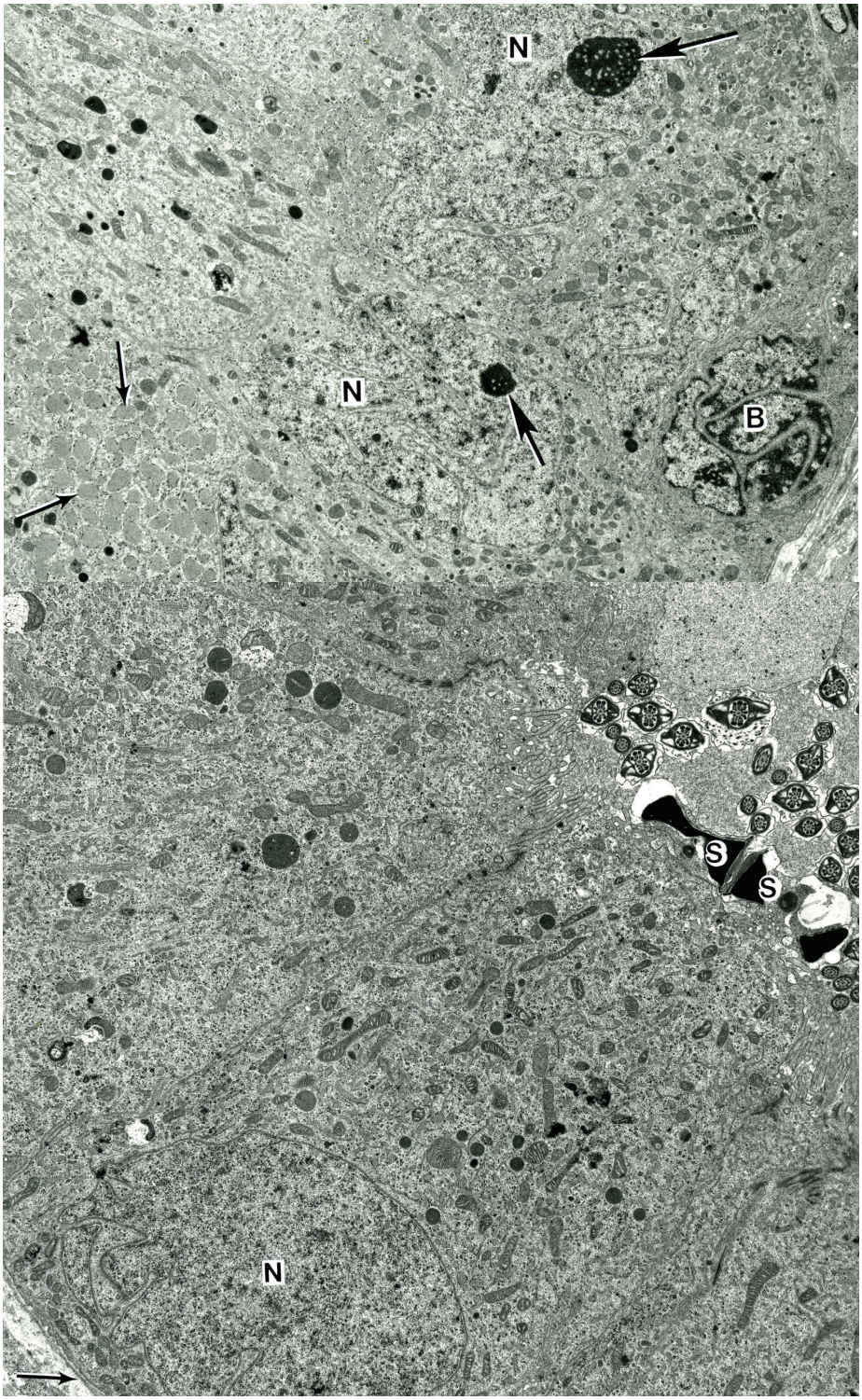

Fig. 9. (*Above*). Principal caudal epididymal cells exhibit expanded profiles of granular endoplasmic reticulum filled with amorphous material (small arrows). Note the complex nature of nuclei (N) in principal as well as basal (B) cells. Nuclei of principal cells exhibit large electron dense nucleoli (large arrows). TEM X 6,500. (*Below*). Principal cells from the distal most extent of the epididymis lie on a distinct basal lamina (arrow) and show basolateral infoldings. Paired spermatozoa (S) are shown associated with the apical surface. TEM X 7,875.

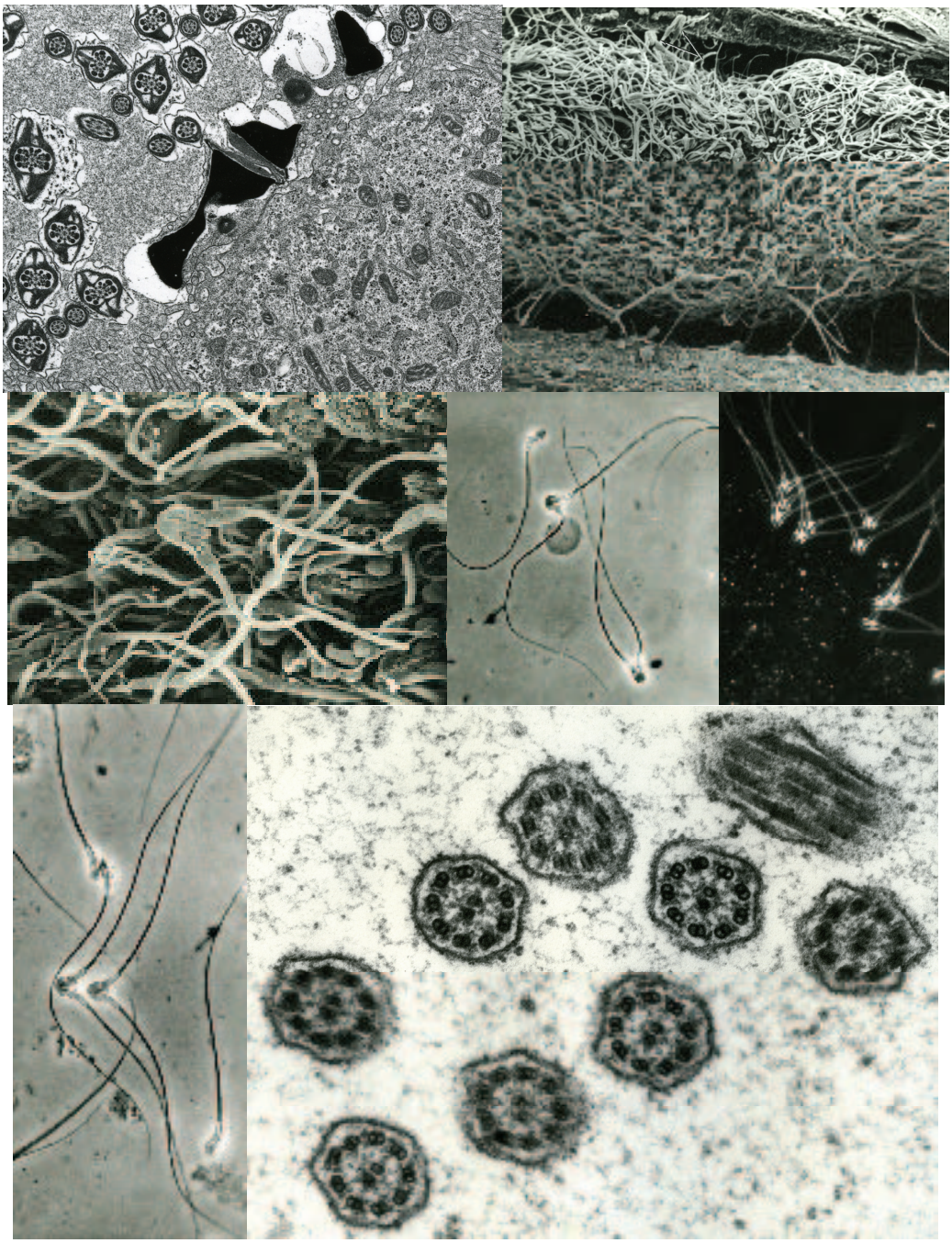

Fig. 10. (*Above left*). The sperm pair united acrosome to acrosome have a close relationship with an adjacent principal epididymal cell. TEM X 12,000. (*Above right*). A region of the caudal epididymal duct reveals the large concentration of spermatozoa within the lumen. SEM X 50. (*Center left*). Increased magnification of the previous figure reveals a sperm pair. SEM X 600. (*Center*). Two sperm pairs and an unpaired spermatozoon as viewed by phase contrast microscopy. LM X 400. (*Center right*). A preparation of paired spermatozoa from the caudal epididymis examined using dark field microscopy. LM X 400. (*Below left*). Phase contrast microscopy illustrating two sperm pairs near the center. LM X 400. (*Below right*). Sections of tails (end pieces) from paired spermatozoa within the caudal epididymis. TEM X 60,000.

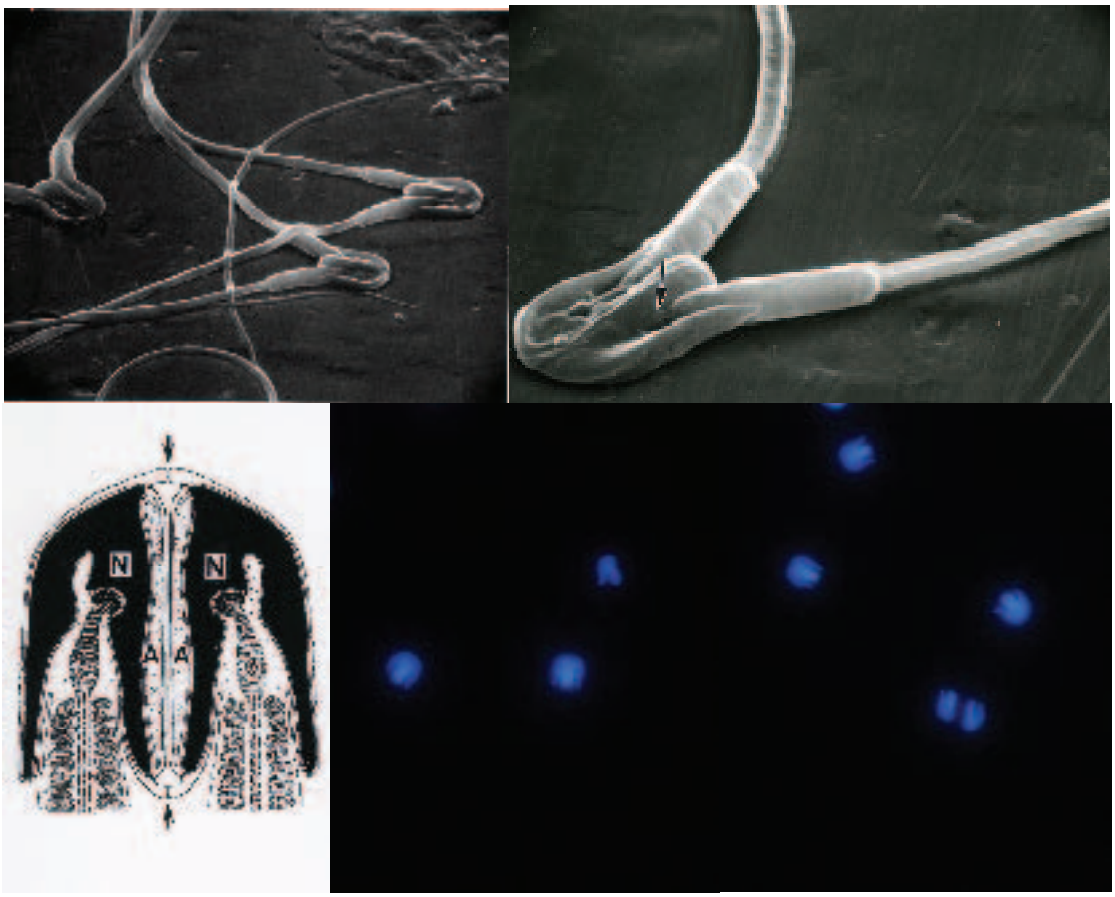

Fig. 11. (*Above left*). Three pairs of spermatozoa isolated from the caudal region of the epididymis. Observe that only the flat surface of the large nuclear arm together with its overlying acrosome participates in the union to form a pair. SEM X 2,000. (*Above right*). A sperm pair from the caudal epididymis viewed at increased magnification illustrates the connecting piece of one (arrow), that lies between the large (central) and small (peripheral) nuclear arms, unites the head and tail regions. SEM X 5,000. (*Below left*). A line drawing of a sperm pair illustrates that the acrosome (A) associated with each spermatozoon is oriented toward the other and is separated only by the cell membranes that occupy a central compartment formed by junctional complexes (arrows). (*Below right*). Spermatozoa treated with DAPI (which binds to DNA) and subsequently examined by ultraviolet light emit a blue fluorescence. These observations demonstrate that the primary subcomponent of the head region of both mature paired and unpaired spermatozoa is DNA. LM X 600.

Chapter 2. Female Reproductive System/Gamete Production

Synopsis:

The adult female reproductive system consists of paired ovaries, oviducts, uteri, cervices, a median vaginal apparatus (fused vaginal culs-de-sac), two lateral vaginal canals, a urogenital sinus and a urogenital strand. Two distinct phases of the reproductive cycle occur during the year. A breeding period extends from February to June and an anestrus period extends from July to January. Females are polyestrous with each cycle lasting about 28 days. The ovaries are typically mammalian in structure and the paired oviducts are lined by a simple ciliated columnar epithelium. Like the oviducts, the uteri and cervices are completely separate. The cervix of each side opens into a median vaginal cul-de-sac. The cul-de-sac of one side is joined to the cul-de-sac of the other forming the median vaginal apparatus. Usually the culs-de-sac are separated by a medium septum. The paired vaginal canals consist of two regions: a lateral loop, which extends from the median cul-de-sac to the urogenital strand, and a median portion, which lies within the urogenital strand. Midway within the urogenital strand the median portions of the vaginal canals open posteriorly into the urogenital sinus. The urogenital strand is a column of connective tissue that envelops the urethra, the vaginal culs-de-sac, the median portions of the lateral vaginal canals, a portion of the loop of the lateral vaginal canals, the pseudovaginal passageway, and is continuous with tissue forming the outer wall of the urogenital sinus. Bartholin's glands represent the only accessory sex glands in the female.

At birth, the connective tissue between the urethra and median portions of the lateral vaginal canals separates and forms a median passageway (pseudo-vaginal canal) that extends from the caudal end of the median-vaginal cul-de-sac to the cephalic end of the urogenital sinus. During parturition the caudal end of the median vaginal cul-de-sac ruptures and a separation occurs within the connective tissue of the urogenital strand positioned between the urethra and the median portions of the lateral vaginal canals is followed by a rupture of the anterior wall of the urogenital sinus. The pseudo-vaginal canal does not remain a permanent passageway in *Didelphis* as in some marsupials, but disappears soon after the young are born. Thus, in the opossum occurs the unusual circumstance that following coitus spermatozoa pass through two separate lateral vaginae, cervices and uteri to the proximal region of the paired oviducts where fertilization takes place. At parturition, fetuses follow a different route to the urogenital sinus. Rather than passing through the lateral vaginal canals, the fetuses pass through the single, centrally located birth canal, the median or pseudovaginal canal. This temporary passageway is a separation of the connective tissue between the vaginal culs-de-sac and the anterior end of the urogenital sinus and at birth may contain fragments of fetal membranes, maternal blood clots, and leukocytes. In *Didelphis* this cleft in the connective tissue disappears soon after birth and reopens with the birth of each litter. In several Australian marsupials (macropodidae) the median vaginal canal may persist following its formation.

The structure of the ovary is similar to that of eutherian mammals as are the growth patterns of the follicle and oocyte. The oocyte, oocyte nucleus and follicle of *Didelphis* are significantly larger in comparison to those of eutherian mammals. In addition, primordial oocytes contain a spherical yolk nucleus, numerous mitochondria and lipid droplets. The yolk nucleus consists of RNA, protein and lipoprotein. The lipid droplets are primarily phospholipids. Two types of yolk, compound yolk and lipid yolk have been demonstrated in

the growing oocytes. The more abundant compound yolk consists of a carbohydrate-protein complex; lipid yolk consists primarily of phospholipids. Completion of the first meiotic division and extrusion of the first polar body occurs in the mature Graffin follicle whereas the second meiotic division is not completed until after ovulation at fertilization. Ova are discharged from both ovaries at the same time. The number of follicles that ovulate varies considerably with as many as 60 being reported and about 16-20 being the average. Following ovulation, granulosa cells quickly luteinize to from corpora lutea. Luteal cells of the corpora lutea are derived only from granulosa cells in *Didelphis* and reach maximum size by day seven. Relaxin, oxytocin, and prolactin have been identified immunohistochemically in opossum corpora lutein cells. The luteal phase occupies less than 60% of the estrus cycle and is followed by a follicular phase leading to the next estrus and ovulation. At ovulation the mature oocyte lacks a corona radiata and is surrounded only by a thin zona pellucida. The zona pellucida is 2.4-3.3 μM in thickness and consists of proteins and glycosaminoglycans. Ova are large measuring about 135 μM in diameter and their cytoplasm remains characterized by yolk granules, lipid droplets and numerous filamentous mitochondria.

Acknowledgments:

Fig.1, courtesy of and from: McCrady, E. Jr. (1938). The embryology of the opossum. Am. Anat. Mem. 16: 1-223.

Fig. 2 (bottom), courtesy of and from: Krause, W.J. (1998) A review of histogenesis/organogenesis in the developing North American opossum (*Didelphis virginiana*). Adv. Anat. Embryol. Cell Biol. 143 (II): Springer Verlag, Berlin, pp 120.

Figs. 3 (bottom) and 4 (top), courtesy of and from: Krause, W.J. and D.M. Sherman (1992). Immunohistochemical localization of relaxin in the reproductive tract of the female opossum (*Didelphis virginiana*). Ann. Anat. 174:341-344.

Figs. 4 (bottom) and 5, courtesy of and from: Krause, W.J. (1993) Ultrastructural observations on the opossum corpus luteum late in pregnancy. Zool. Anz. 230:249-255.

Fig. 10 (bottom), courtesy of and from: Kumano, A., M. Sasaki, T. Budipitojo, N. Kitamura, W.J. Krause, and J. Yamada. (2005). Immunohistochemical localization of gastrin-releasing peptide, neuronal nitric oxide synthase and neuron specific enolase in the uterus of the North American opossum, *Didelphis virginiana*. Anat. Histol. Embryol. 34: 225-231.

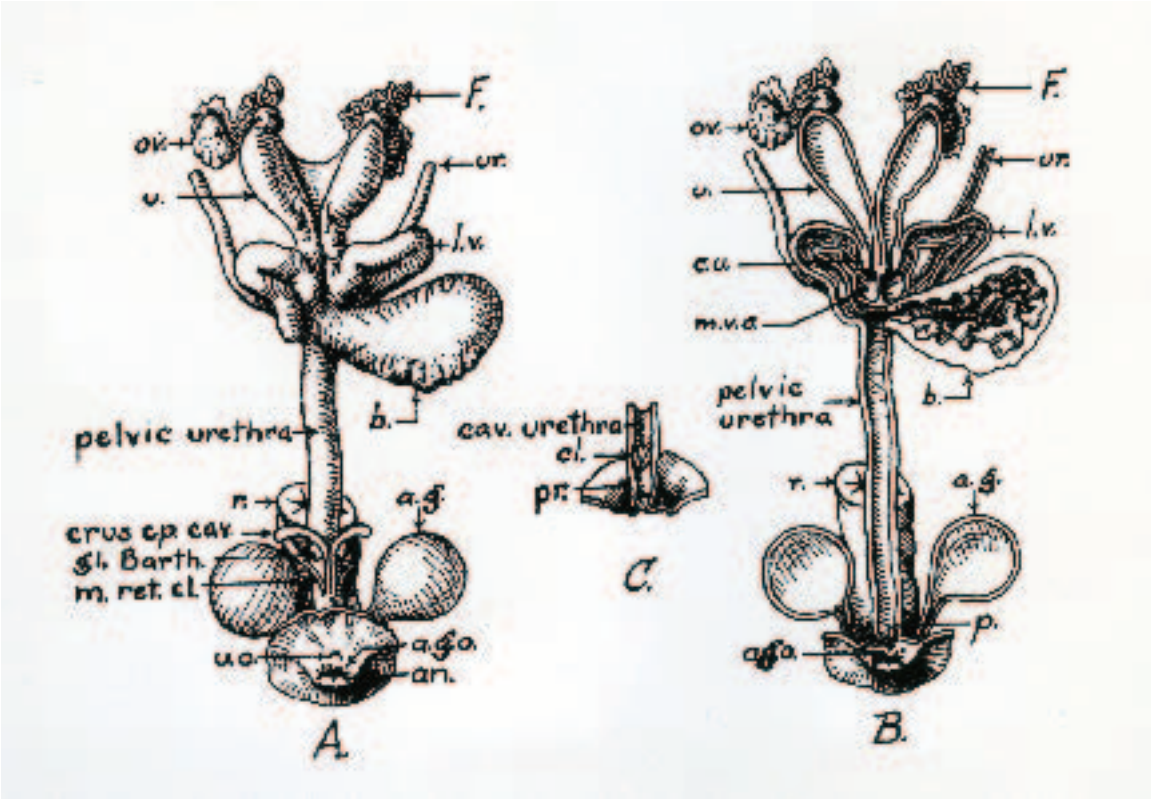

Fig. 1. Line drawings illustrate the exterior (**A**) and interior (**B**) of the urogenital system of an adult female opossum. Ovary (ov), oviduct or Fallopian tube (F), ureter (ur), uterus (u), lateral vaginal canal (lv), median vaginal cul-de-sac (mcv), cervical uterus (cu), urinary bladder (b), pelvic urethra, rectum (r), crus of corpus cavernosus (crus cp. Cav.), Bartholin's gland (gl. Barth), anal gland (ag), urethral orifice (uo), anal gland orifice (ago), and anus (an). Line drawing (**C)** (*center*) illustrates the cavernosus urethra (cav. urethra), the bifurcate glans clitoridis (cl) and prepuce (p).

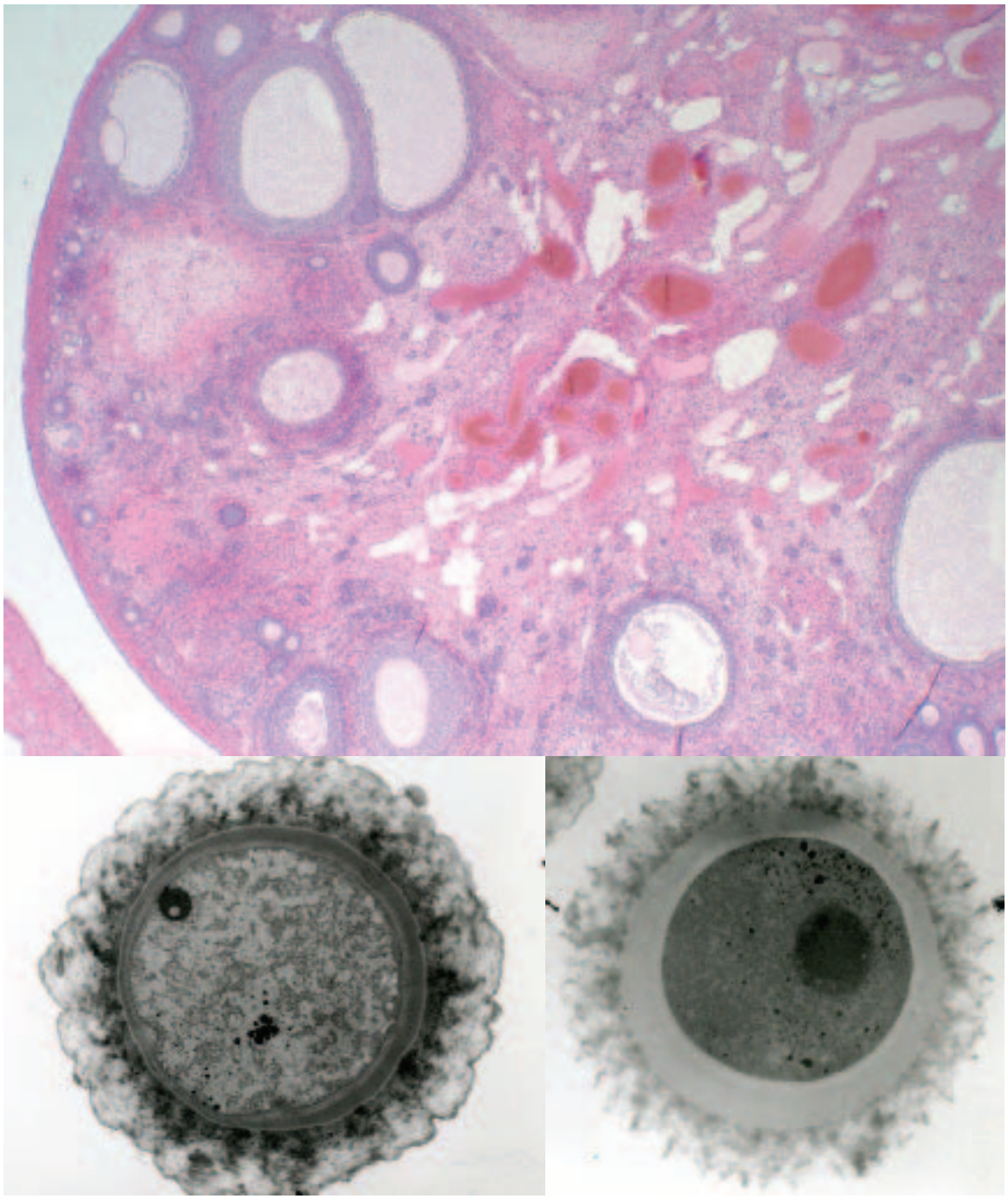

Fig. 2. (*Above*). A section through the ovary of an adult female opossum illustrates the cortex and vascular medulla near the center of the specimen. Note the number of follicles at various stages of development in the surrounding cortex. LM X 40. (*Below*). Two unfertilized oocytes flushed from oviduct after administration of 70 IU of PMSG followed by 50 IU of hCG four days later. The ova were collected two days after the last injection. Note that the oocytes are surrounding by an envelope of mucoid material. A tangential section through the right oocyte demonstrates the surrounding zona pellucida. LM X 500.

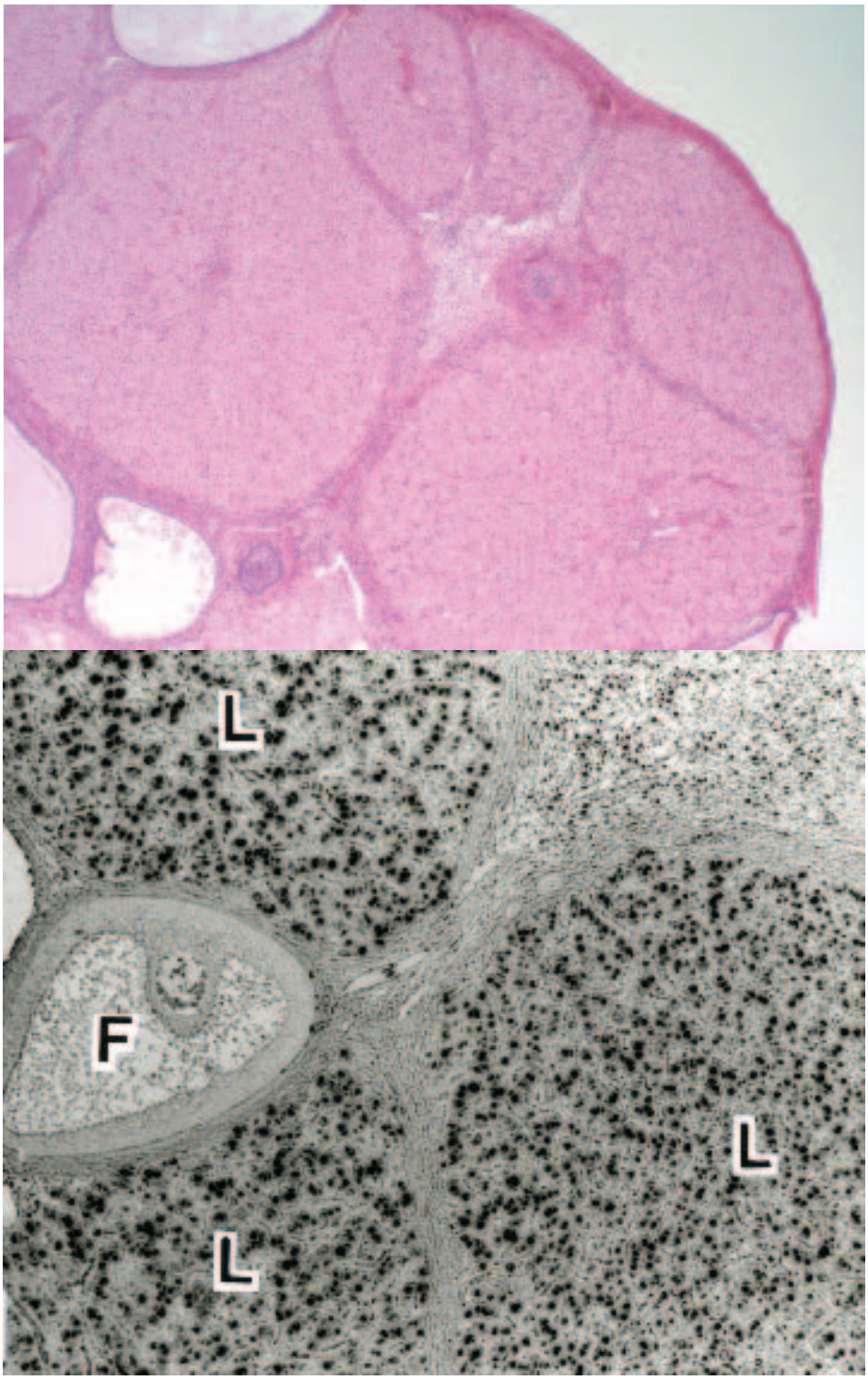

Fig. 3. (*Above*). A region of opossum ovary gathered during the 11.5 day of pregnancy illustrates several large corpora lutea within the cortex. LM X 40. (*Below*). Portions of three corpora lutea (L) and a tertiary follicle (F) from the ovary of an opossum examined during the 11.5 day of pregnancy and stained immunohistochemically for porcine relaxin. The intense immunoreactive staining for relaxin (appears dark) is restricted to luteal cells and is absent in the adjacent follicle and other regions of the ovary. LM X 100.

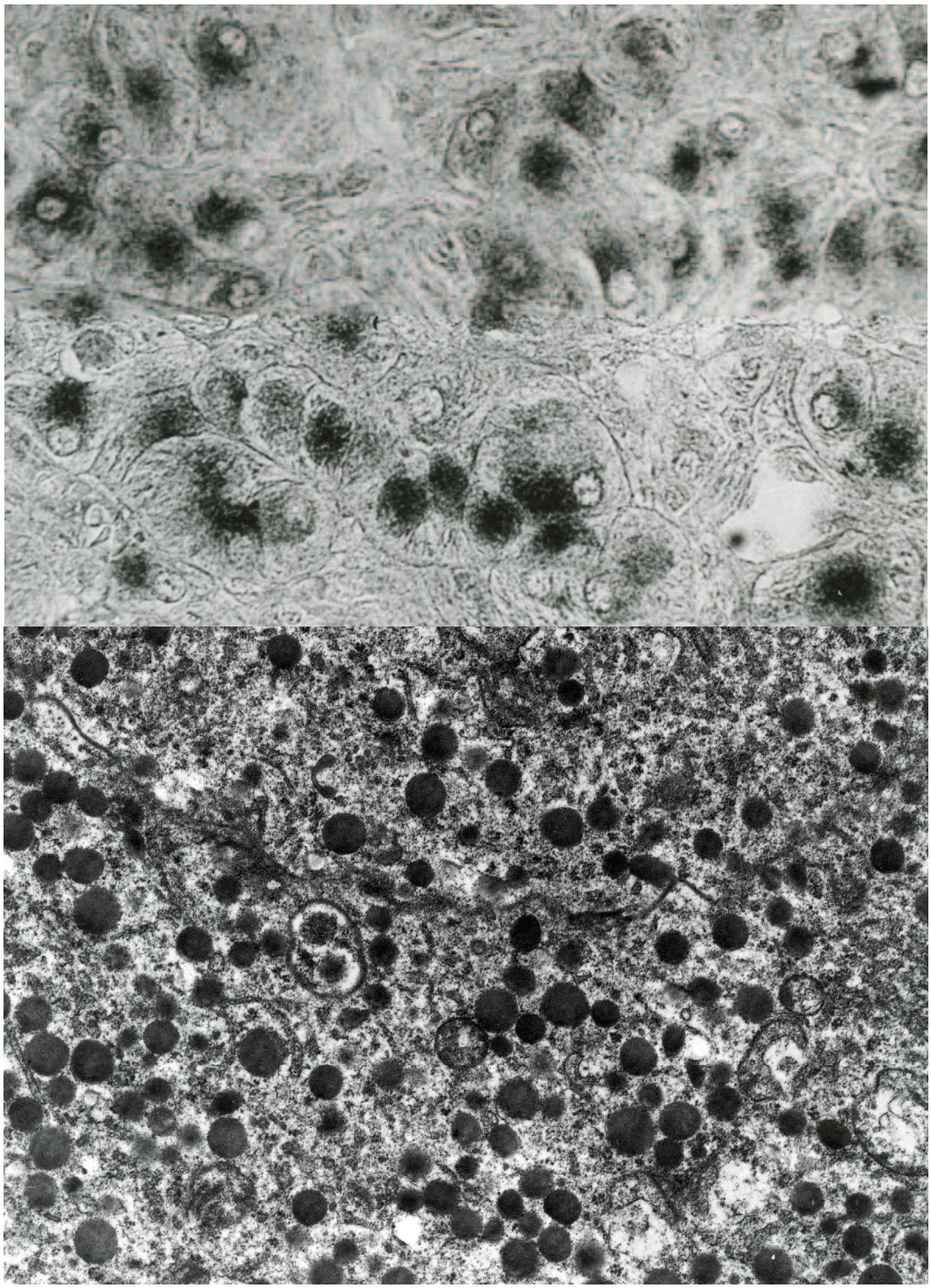

Fig. 4. (*Above*). Increased magnification of the previous specimen illustrates that the majority but not all luteal cells exhibit intense immunoreactive staining for porcine relaxin. Opossum 11.5 days into pregnancy. LM X 350. (*Below*). A transmission electron micrograph of the cytoplasm from a corpora lutein cell demonstrates cluster of electron dense granules. The granules vary in size, show subtle differences in electron density, and most show a round profile although some are elongate in outline. Opossum 11.5 days into pregnancy. TEM X 21, 300.

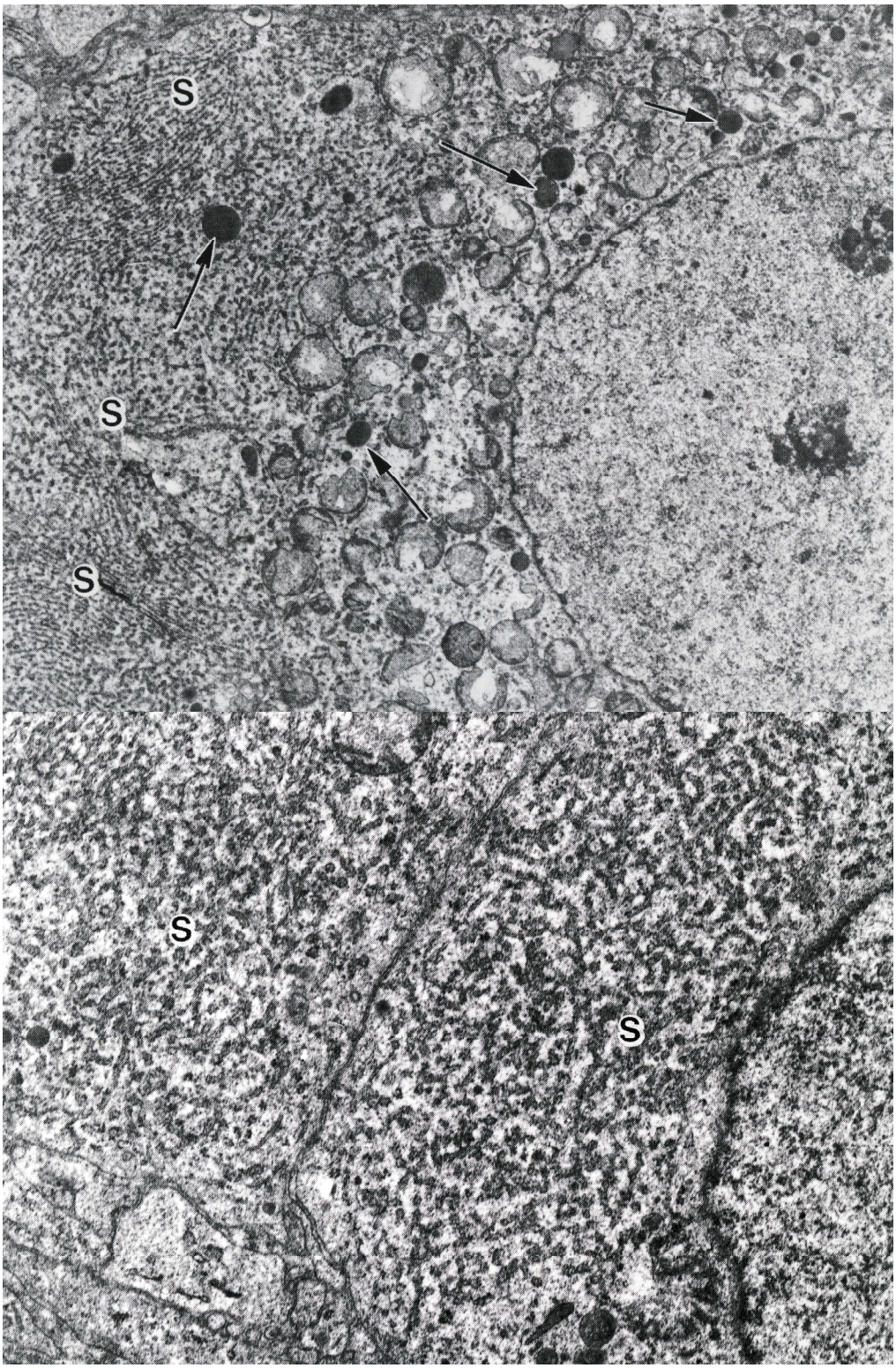

Fig. 5. (*Above*). In addition to electron dense granules (arrows) in the perinuclear cytoplasm, a corpora lutein cell contains abundant profiles of smooth endoplasmic reticulum (S). TEM X 7,500. (*Below*). Portions of two adjacent corpora lutein cells filled primarily by smooth endoplasmic reticulum (S). Opossum ovary 11.5 days into pregnancy. TEM X 17,750.

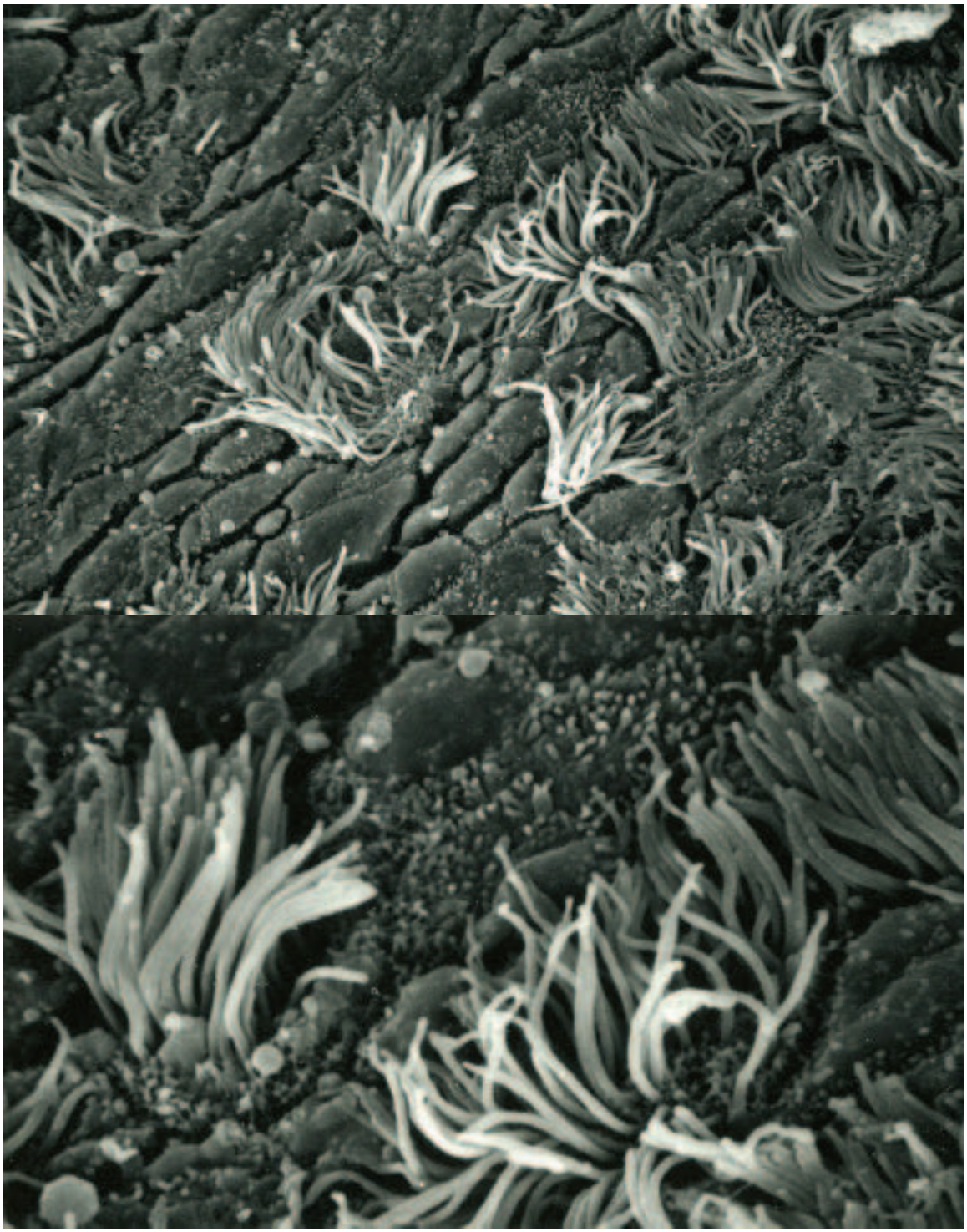

Fig. 6. (*Above*). The mucosal surface of an oviduct from an adult female opossum illustrates numerous, scattered ciliated cells. SEM X 3,000. (*Below*). Increased magnification of this mucosal surface details the surface features of the non-ciliated epithelial cells. SEM X 6,000.

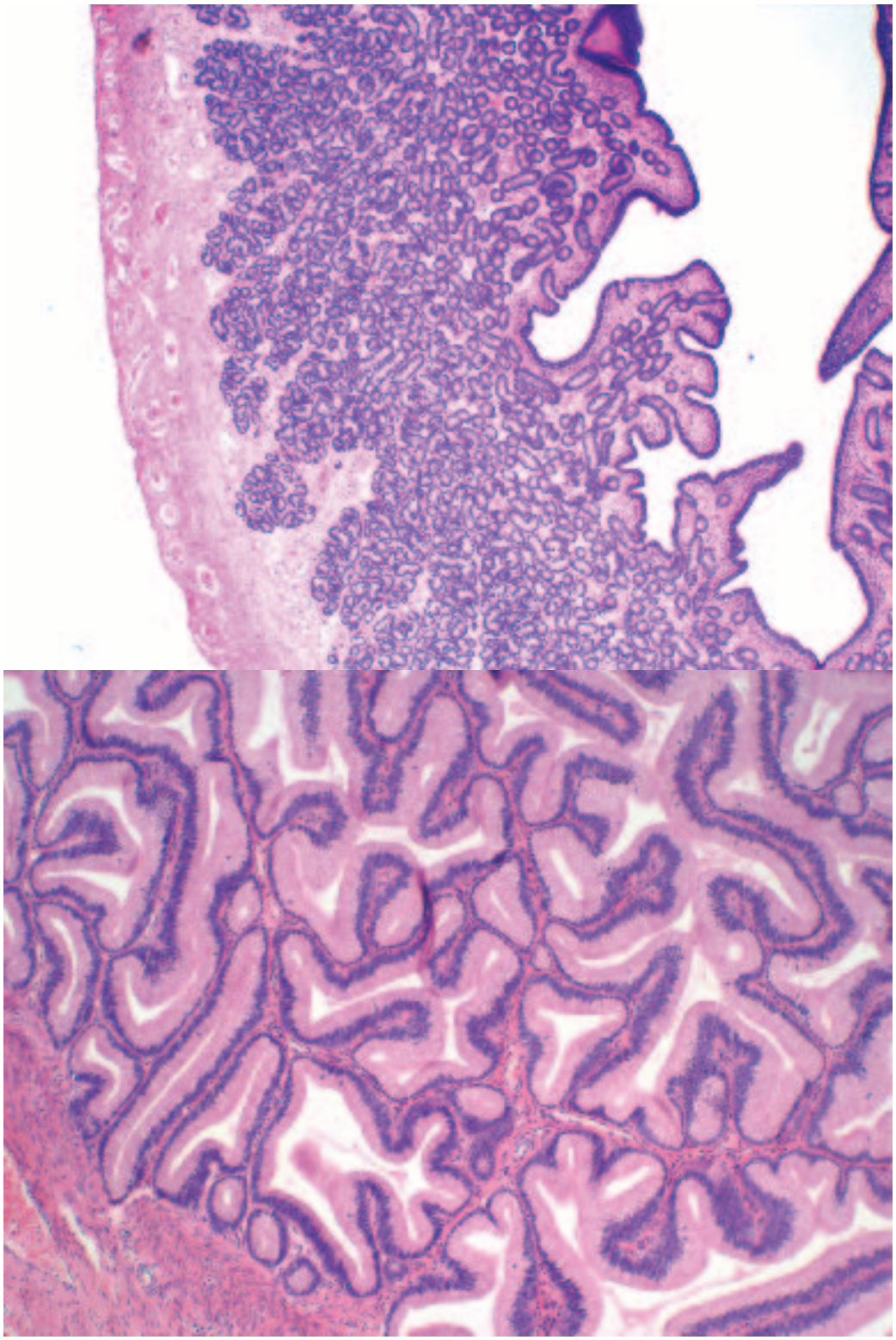

Fig. 7. (*Above*). A section through a region of an adult opossum uterus illustrates the abundance of uterine glands. Note the vascular nature of the myometrium at the extreme left. LM X 40. (*Below*). A region through the cervical portion of the uterus shows the complex folded nature of its interior. The mucosal surface is lined by a tall columnar, mucin producing epithelium. LM X 100.

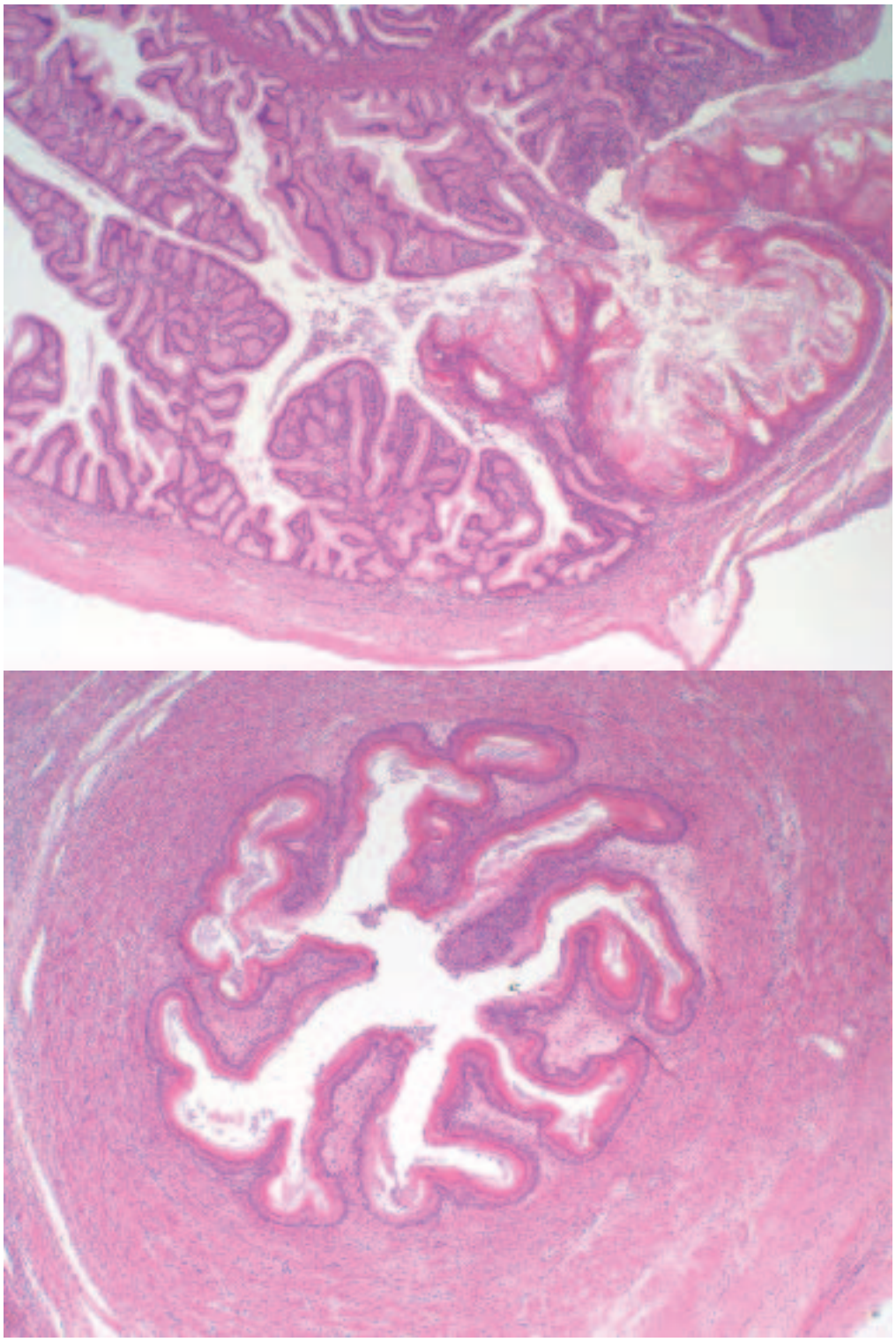

Fig. 8. (*Above*). A histological section illustrates the junction between cervical uterus (at left) and the median vaginal cul-de-sac (at right). Note the abrupt change from tall simple columnar to stratified squamous epithelium. LM X 40. (*Below*). A cross-section through a lateral vaginal canal illustrated its cornified stratified squamous epithelial lining and limiting wall of smooth muscle. LM X 40.

Fig. 9. (*Above*). The mucosal surface of a lateral vaginal canal is extensively folded and forms numerous rugae. SEM. X 30. (*Below*). When the mucosa of the lateral vaginal canals is viewed at increased magnification individual cell boundaries of surface cells can be observed. Note also the scattered distribution of short microvilli on the luminal surface of the surface lining cells. SEM X 3000.

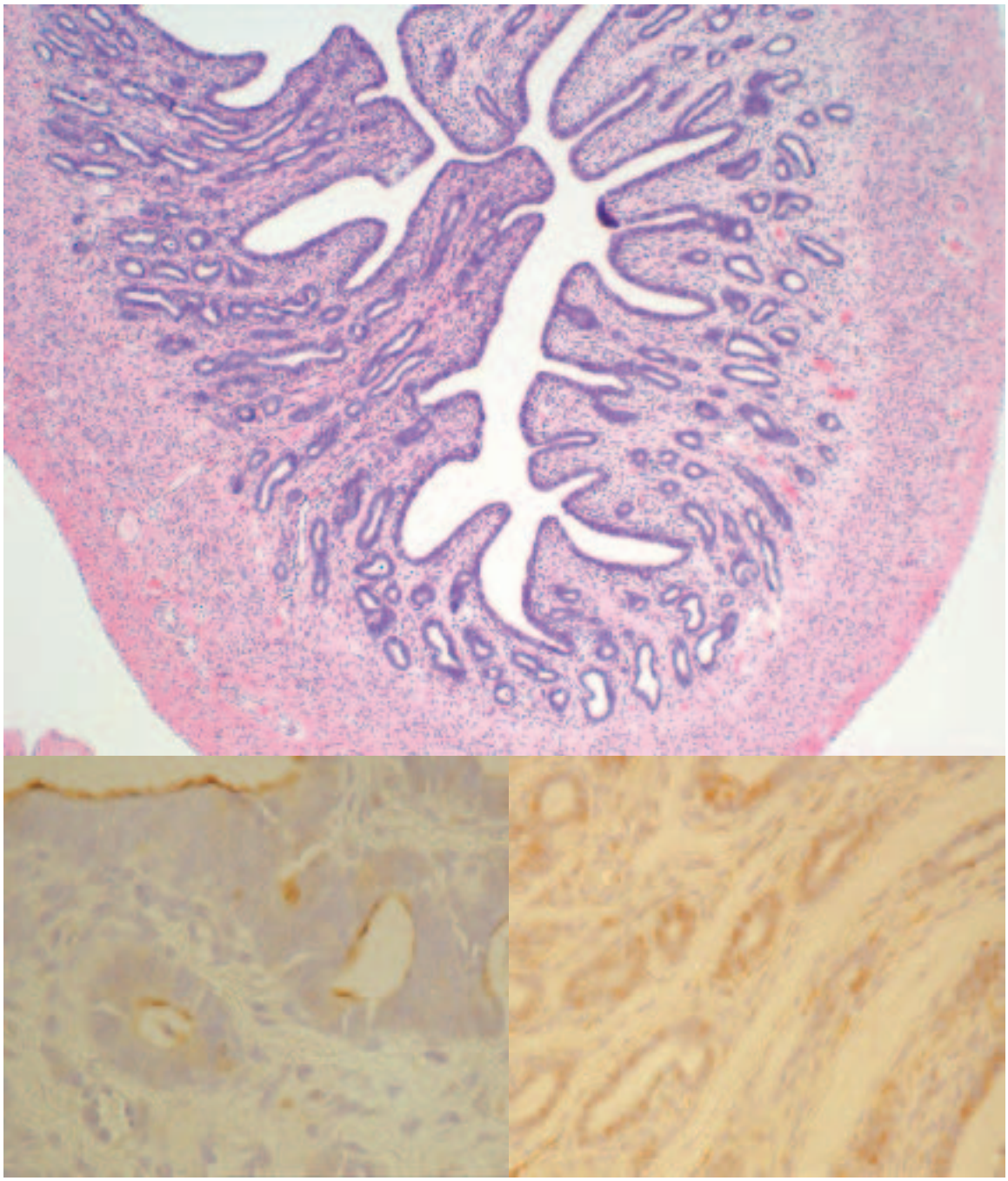

Fig.10. (*Above*). A histological section illustrates the uterus of a juvenile opossum. Note the rudimentary nature of the developing tubular shaped uterine glands. LM X 40. (*Below left*). A histological section demonstrates positive immunohistochemical staining for neuronal nitric oxide synthase (nNOS) in the epithelium of the uterine glands near the bottom of the endometrium of a juvenile opossum. LM X 250. (*Below right*). Neurone-specific enolase (NSE) positive immunoreactive staining is observed within the epithelium throughout the length of the forming uterine glands of a juvenile opossum. LM X 250.

Chapter 3. Shell Membrane

Synopsis:

Fertilized oocytes reach the uterus between 12 and 24 hours following ovulation. The zygote at this time is enveloped by a zona pellucida, a thick mucoid layer, and an outer limiting shell membrane. Non-ciliated secretory cells within the epithelial lining of the oviduct produce the mucoid material. The oocyte together with its oviductal mucoid covering may reach a diameter of 0.75 millimeters. The shell membrane consists of a disulfide-rich ovokeratin structural protein and is thought to be the secretory product of non-ciliated secretory cells within the distal oviduct and/or cells within the uterine glands located near the junction of oviduct and uterus. Morphologically, this tough, transparent membrane consists of a dense mat of closely interwoven fibers. The shell membrane acts as a physical barrier separating maternal and embryonic tissues during the first nine days of the 12.5 day gestation period. However, it is porous enough to allow nutrients (primarily albumins, pre-albumins, β-globulins) found in uterine secretions to make their way to the embryo for absorption.

Acknowledgments:

Figs. 1 and 3, courtesy of and taken from: Krause, W.J. and J.H. Cutts (1983) Ultrastructural observations on the shell membrane of the North American opossum (*Didelphis virginiana*). Anat. Rec. 207:335-338.

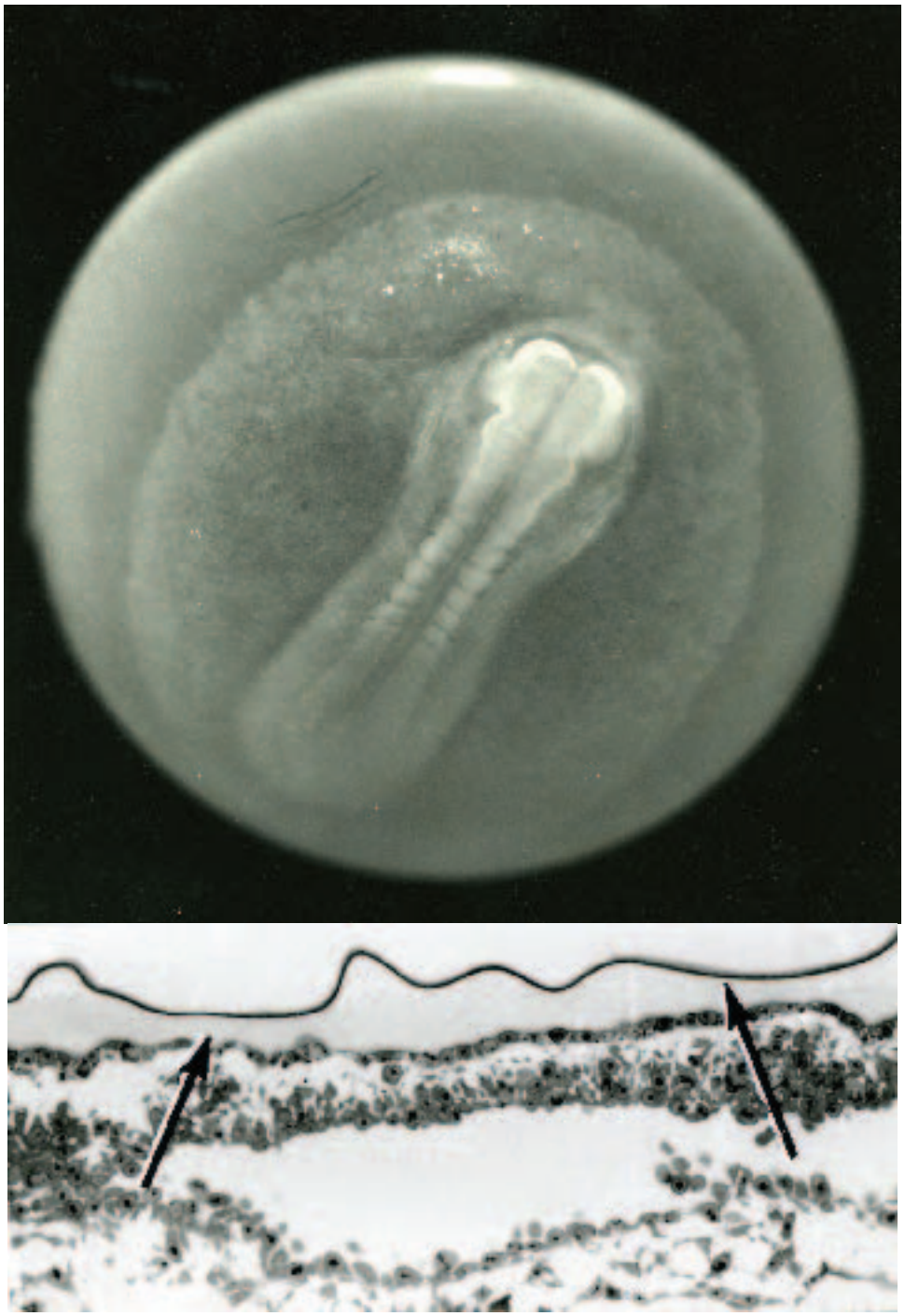

Fig. 1. (*Above*). The nine-day opossum embryo is part of an embryonic sphere, which is surrounded by a transparent shell membrane. A wrinkle in the shell membrane can be visualized near the top of the photomicrograph just beyond the extent of the extra-embryonic mesoderm that appears rough in texture. The embryo proper exhibits a forming brain, spinal cord, and somites. X 50. (*Below*). When sectioned and viewed under the light microscope the shell membrane appears as a thin homogeneous membrane (arrows). A portion of the forming nine-day old opossum embryo lies beneath the shell membrane. LM X 350.

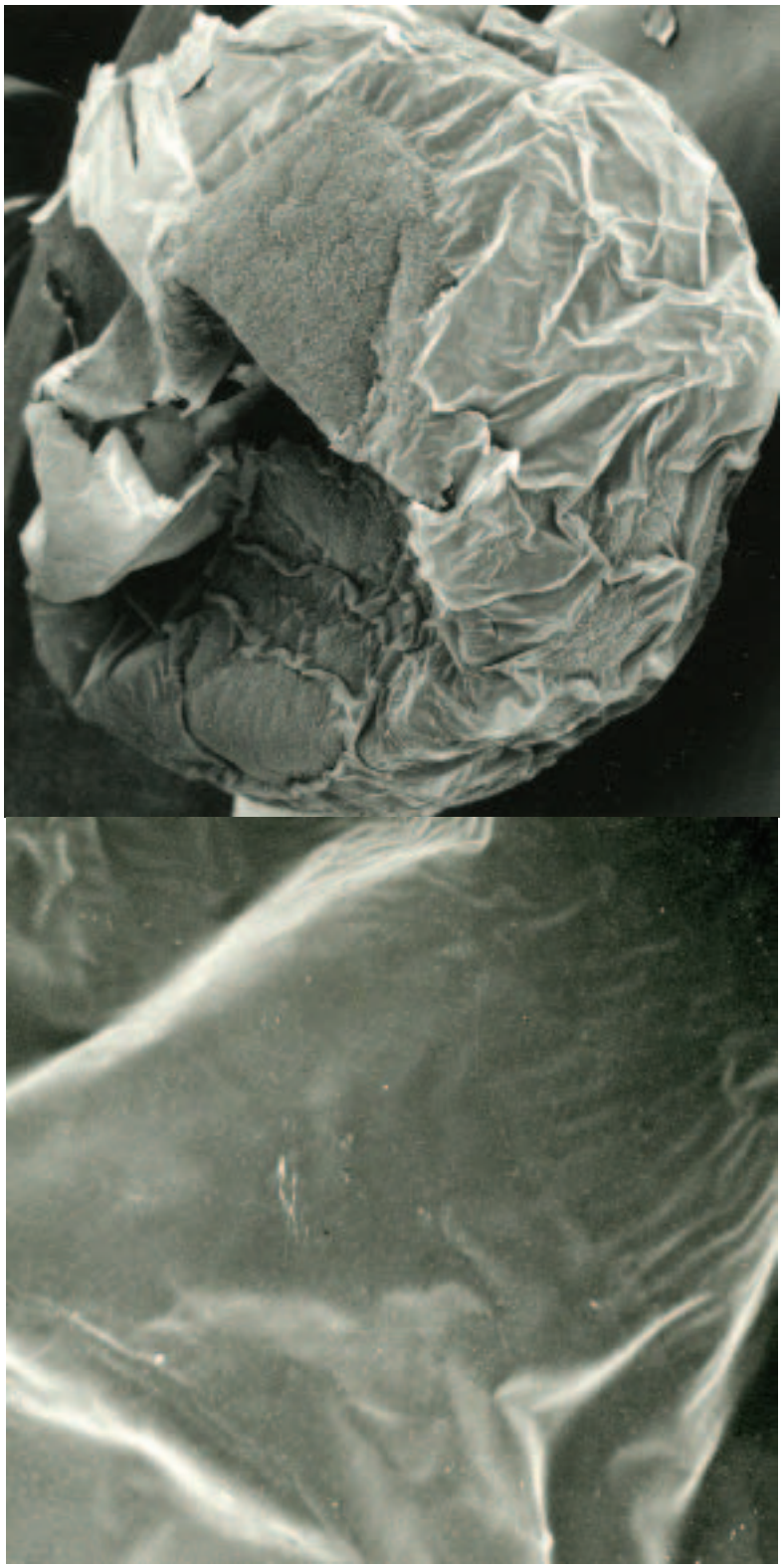

Fig. 2. (*Above*). A scanning electron micrograph illustrates the embryonic sphere and surrounding shell membrane of a nine-day opossum embryo. SEM X 30. (*Below*). When viewed at a slight increase in magnification the external surface of the shell membrane appears smooth. Nine-day opossum embryo. SEM X 150.

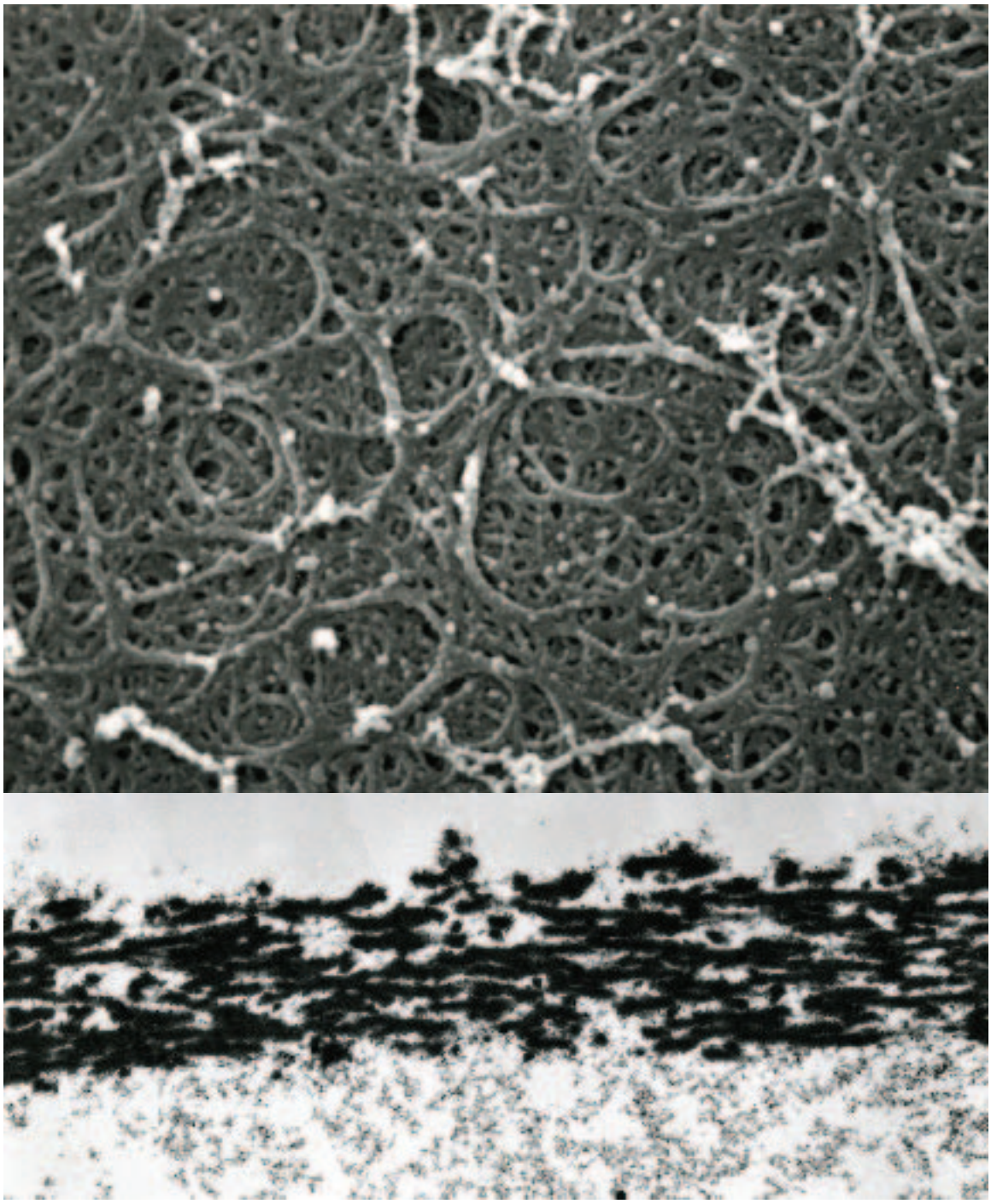

Fig. 3. (*Above*). The external surface of the shell membrane when viewed at a much higher magnification demonstrates that it consists of a mat of interwoven fibers that vary considerable in diameter and shape. Nine-day opossum embryo. SEM X 11,000. (*Below*). When viewed in section with the transmission electron microscope the shell membrane is seen to consist of numerous electron-dense fibers without apparent substructure. The external surface of the shell membrane lies at the top of the photomicrograph. TEM X 16,000.

Chapter 4. Placentation

Synopsis:

The extra-embryonic mesoderm splits into splanchnic and somatic layers by the tenth day of gestation. With the appearance of blood vessels within the extra-embryonic splanchnic mesoderm the forming placenta can be divided into three regions: a small chorion (consisting of somatic mesoderm and ectoderm), a vascular yolk sac placenta (formed by endoderm, mesoderm, and trophectoderm), and a non-vascular yolk-sac placenta (that consists only of trophectoderm and endoderm). The non-vascular region of the yolk-sac placenta represents that region of the original embryonic vesicle never invaded by mesoderm. As small blood vessels are established within the extra-embryonic (splanchnic) mesodermal layer, a distinct sinus terminalis forms at the most distal extent. This large blood vessel (the sinus terminalis) courses around the equator of the embryonic vesicle and forms a distinct boundary that separates the vascular from the non-vascular region of the yolk sac placenta. Cells forming the trophectoderm that cover both regions continue to exhibit morphological features (numerous elongated microvilli, an apical endocytic complex, and vacuoles) indicative of a cell type actively involved in absorption.

The extra-embryonic mesoderm does not invade the region of the proamnion. As a result, the proamnion region of the expanding embryonic vesicle lacks a mesodermal layer and consists only of ectoderm and endoderm. Early in gestational day ten, the proximal (head) region of the embryo elongates, and due to a flexure in the region of the midbrain, the proximal portion of the embryo extends into the central space of the original embryonic sphere. The forming amnion courses with and surrounds the cranial half of the embryo as it enters the embryonic vesicle. Like the original proamnion, this region of the amnion consists only of ectoderm and endoderm. The remainder of the amnion develops as a result of folding. Lateral and caudal amniotic folds originate from somatic mesoderm and extra-embryonic ectoderm. The amniotic folds meet and fuse dorsal to the embryo forming the remainder of the amniotic sac as well as a small, avascular region of true chorion during the tenth prenatal day. As a result of the formation of the amnion in this fashion, the opossum embryo descends into and becomes enveloped by it as well as the outer, surrounding yolk sac placenta. The surrounding shell membrane breaks down by the end of the tenth prenatal day and as a result the yolk sac placenta rapidly expands, the vascular portion of which establishes an intimate relationship with the uterine epithelium. Once established, the relationship between the vascular yolk sac placenta and the uterine mucosa remains relatively unchanged until term.

The uterine mucosa during the first nine days of gestation contains numerous glands and is lined by a thick, ciliated pseudostratified columnar epithelium. Most ciliated cells have disappeared by the eleventh day of gestation and the uterine epithelium becomes simple columnar. The number of uterine glands begins to decrease at mid-gestation, whereas the total uterine volume continues to increase. The uterine glands are thought to be the primary source of nutrients early in gestation, whereas the nutritive role is taken over by the uterine lining epithelium during the last three to four days of the 12.5 day gestation period. Both uterine lining epithelial cells and cells of the trophoblast exhibit morphological features suggesting involvement in the transport and exchange of materials.

Acknowledgments:

Figs. 1, 2, 3 (top), 4 (bottom), 6, 7, 9, 10, 11, 12 (bottom), 14 (bottom), 15, 16, 17, 18, 19, and 20, courtesy of and from: Krause, W.J. and J.H. Cutts (1985) Placentation in the opossum (*Didelphis virginiana*). Acta Anat. 123:156-171.

Figs. 3 (bottom) and 13, courtesy of and from: Krause, W.J. (1998) A review of histogenesis/organogenesis in the developing North American opossum (*Didelphis virginiana*). Adv. Anat. Embryol. Cell Biol. Vol 143 (I): Springer Verlag, Berlin, pp 143.

Figs. 8 (bottom) and 21, courtesy of and from: Kumano, A., M. Sasaki, T. Budipitojo, N. Kitamura, W.J. Krause, and J. Yamada. (2005). Immunohistochemical localization of gastrin-releasing peptide, neuronal nitric oxide synthase and neuron specific enolase in the uterus of the North American opossum, *Didelphis virginiana*. Anat. Histol. Embryol. 34: 225-231.

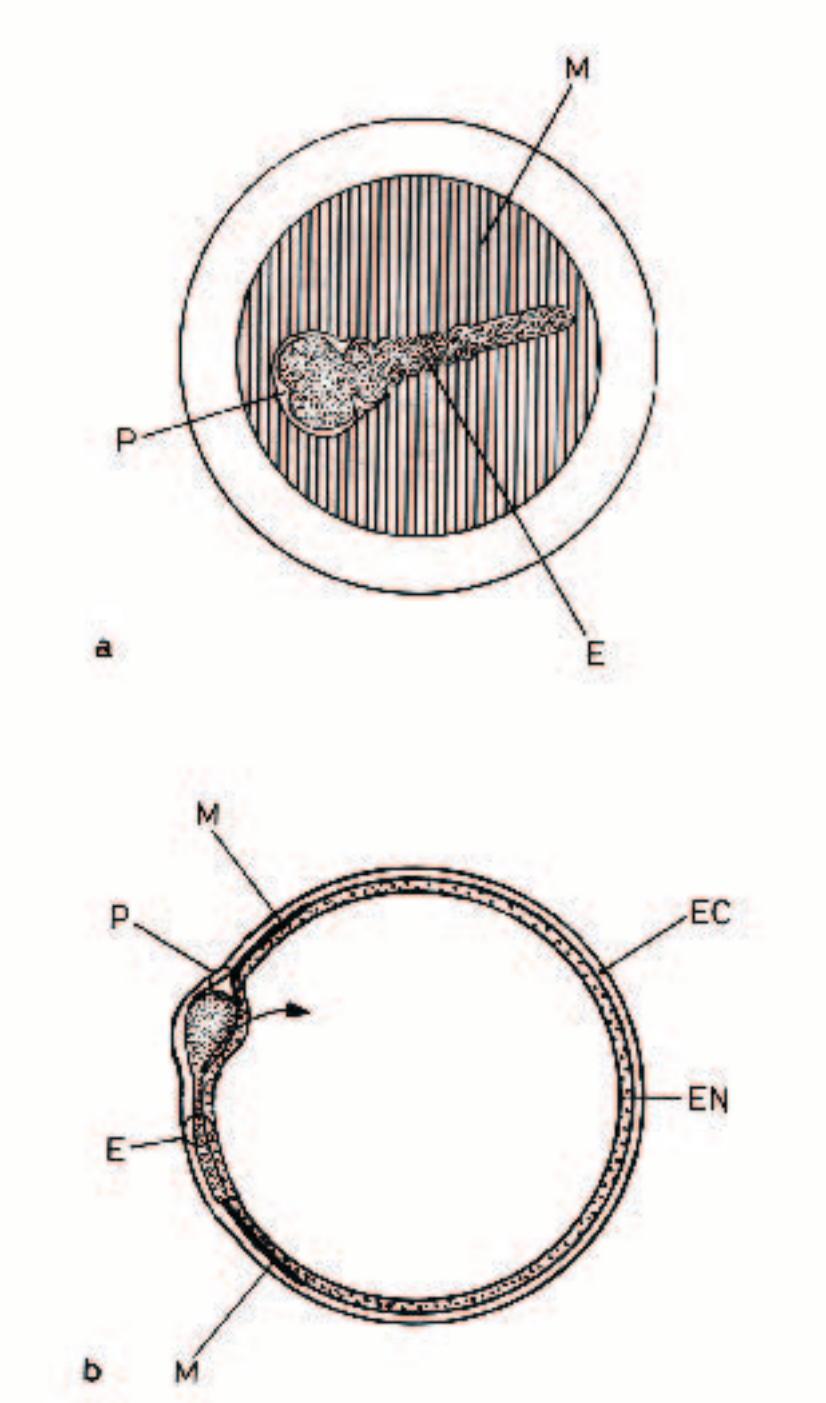

Fig.1. (**a**). A line drawing illustrates the extent of the extra-embryonic mesoderm (M) within the embryonic sphere of an opossum at nine days gestation. The position of the embryo (E) and proamnion (P) also are shown. (**b**). A line drawing of a section through the embryonic sphere of a nine-day opossum embryo illustrates the position of the embryo (E) and proamnion (P). The proamnion lacks a mesodermal layer (M) and consists only of ectoderm (EC) and endoderm (EN), as does that portion of the embryonic sphere on the side opposite the forming embryo. The head region of the embryo will, as development continues, extend ventrally into the embryonic sphere as a result of the cervical flexure (arrow).

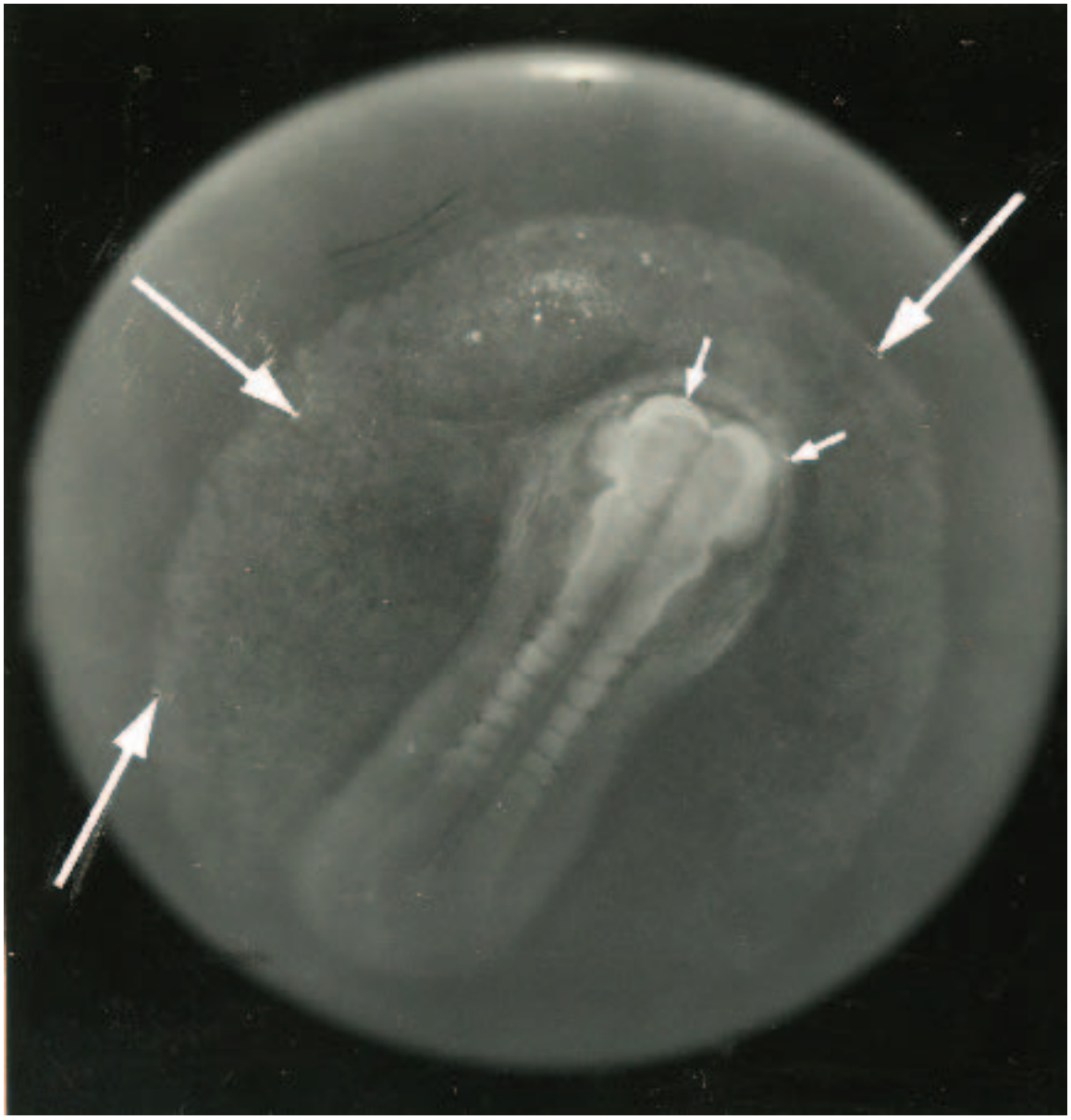

Fig. 2. The nine-day opossum embryo floats freely within uterine secretions separated from maternal tissues only by a thin, transparent shell membrane. The lateral extent of the extra-embryonic mesoderm (large arrows) is visible within the wall of the embryonic sphere. The position of the proamnion (small arrows) is visible around the forming head region of the opossum embryo. The somites within the embryo are clearly visible. Compare this specimen with the line drawing depicted in figure 1a. X 40.

Fig. 3. (*Above*). A scanning electron micrograph of the nine-day blastocyst illustrates that the developing opossum embryo is part of the embryonic sphere. SEM X 50. (*Below*). The head region of the forming nine-day opossum embryo is surrounded by the proamnion (arrows). SEM X100.

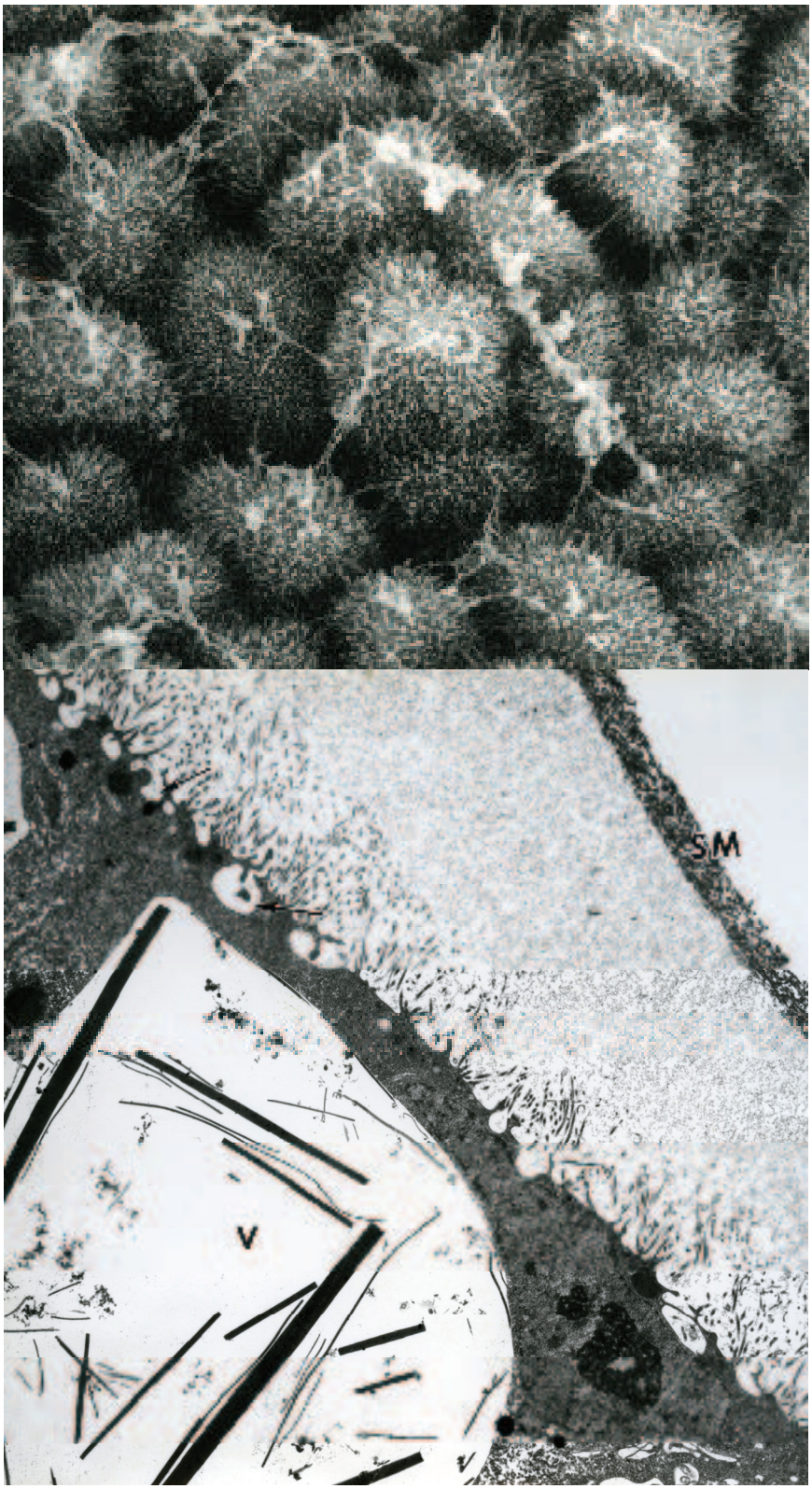

Fig. 4. (*Above*). The external (apical) surface of cells forming the trophectoderm of a nine-day opossum embryo exhibits numerous elongate microvilli. SEM X 2,000. (*Below*). When viewed in section, in addition to elongate microvilli, cells of the trophectoderm exhibit numerous invaginations of the apical cell membrane (arrows) and a large central vacuole (V). The shell membrane (SM) is shown at the upper right. Nine-day opossum embryo. TEM X 12,500.

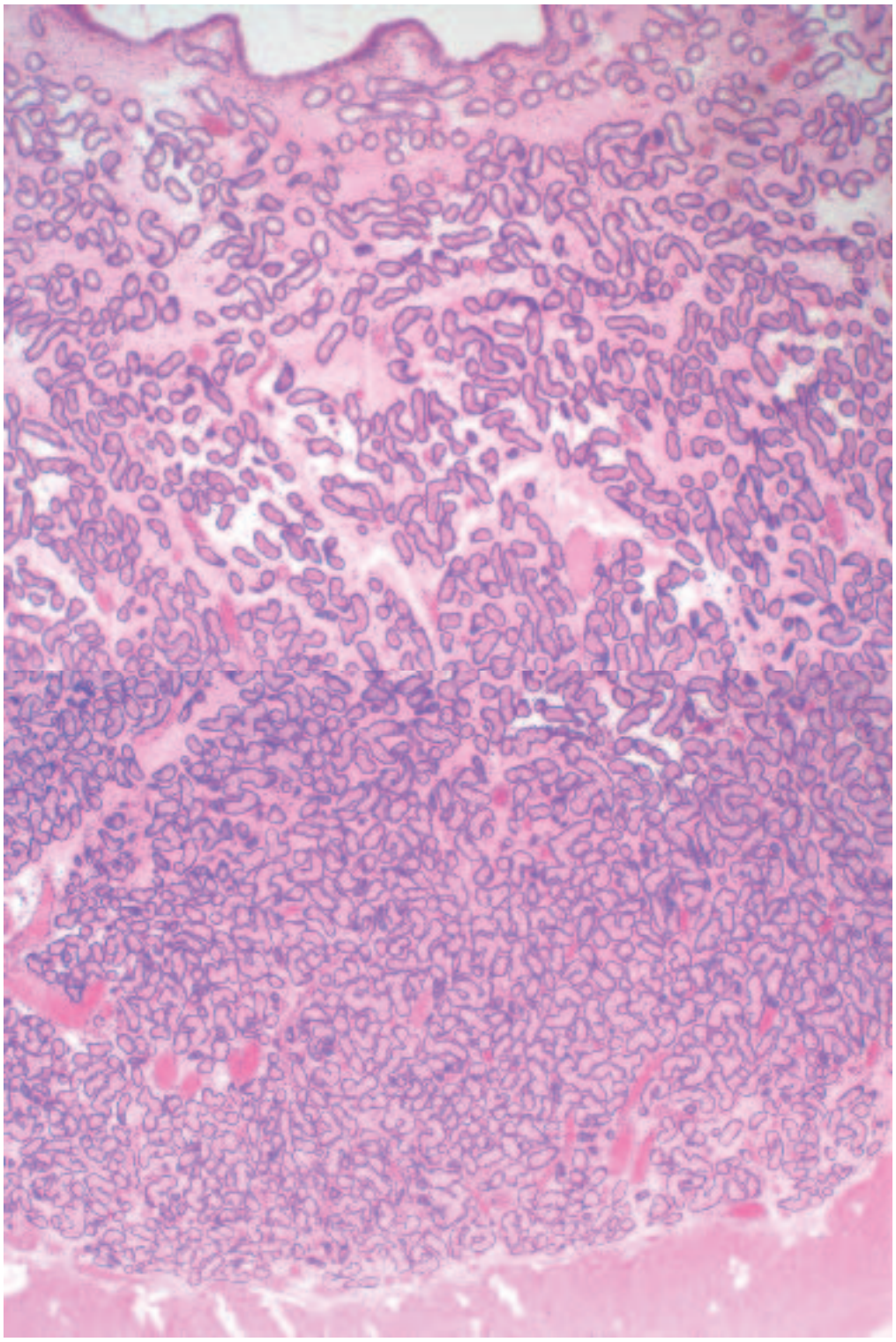

Fig. 5. (*Above*). A micrograph illustrates a region of the uterine mucosa taken near the lumen of the uterus during the ninth day of gestation. Note the abundance of ground substance within the stroma separating uterine glands and vascular elements. LM X 100. (*Below*). A region of uterine mucosa taken adjacent to the myometrium (bottom of light micrograph) during the ninth day of gestation illustrates the more compact nature of uterine glands with less intervening ground substance. Numerous vascular elements also are present. LM X 100.

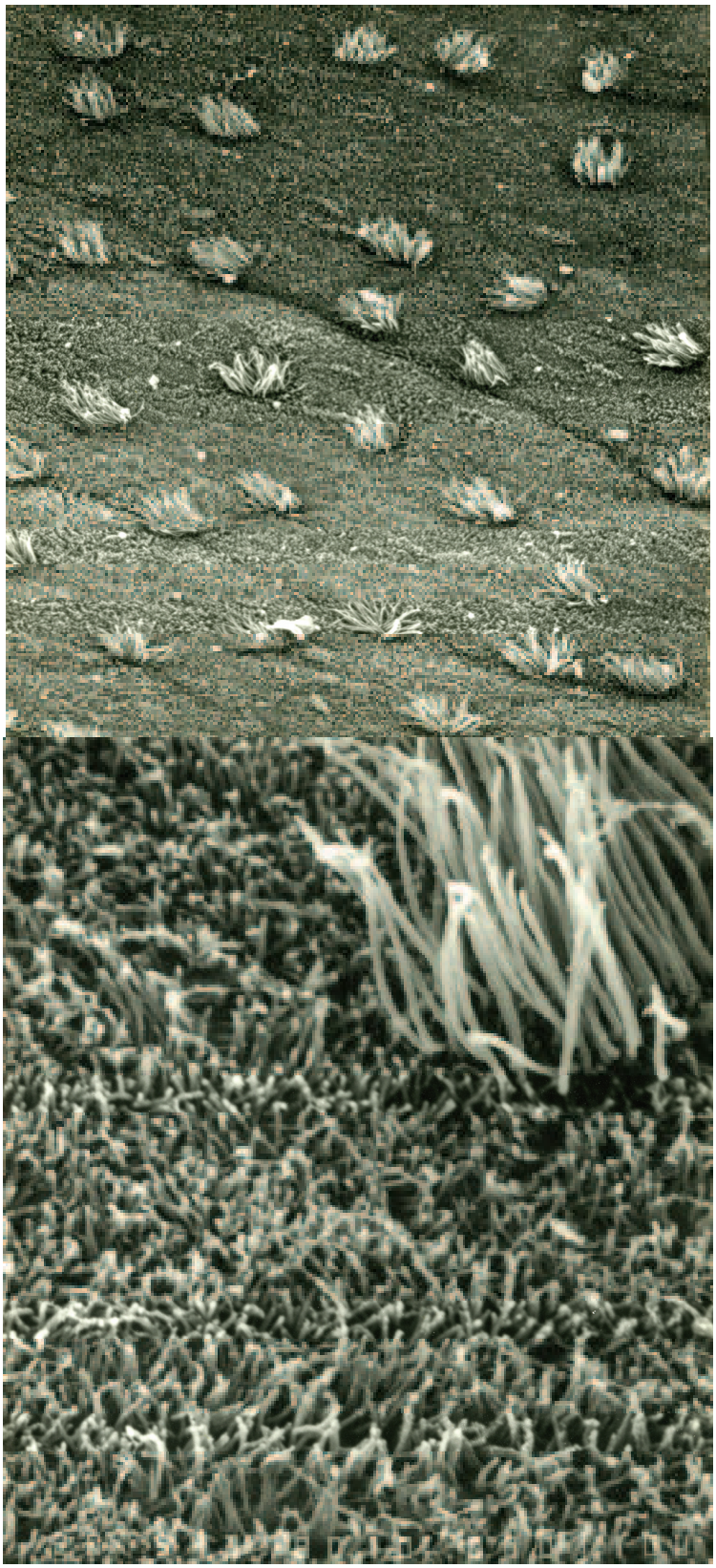

Fig. 6. (*Above*). A micrograph depicts the luminal surface of uterine epithelium taken from an adult opossum at the ninth day of gestation. SEM X 600. (*Below*). When the above specimen is viewed at increased magnification the non-ciliated cells within the uterine epithelium are observed to have abundant elongate microvilli that extend from their apical surface. TEM X 3,400.

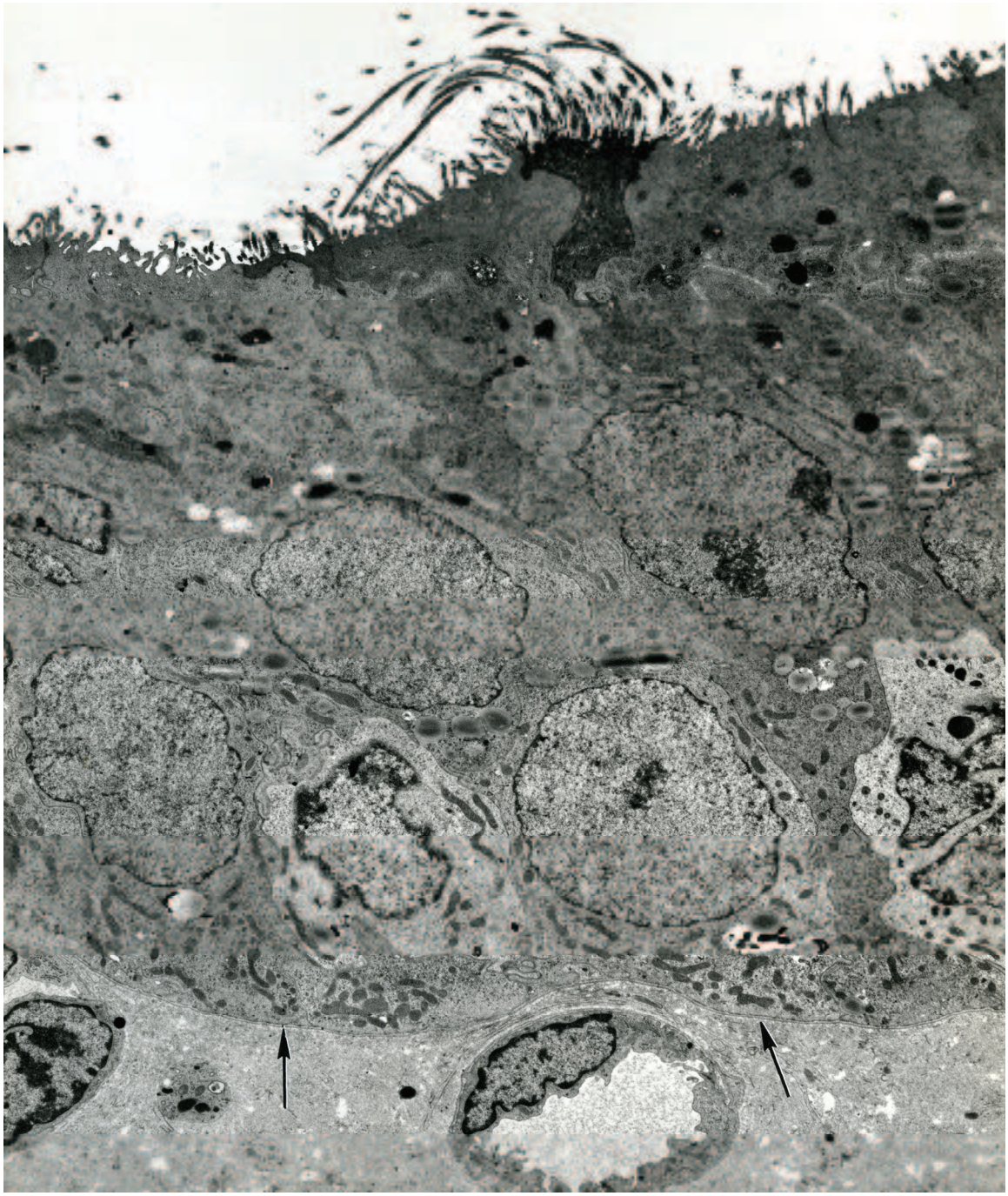

Fig. 7. The uterine epithelium during the ninth day of gestation is pseudostratified columnar in character and lies on a distinct basal lamina (arrows). Numerous electron-lucent and electron-dense granules are present within the cytoplasm of component cells. The electron-lucent granules often exhibit a core with slightly greater electron-dense. Mitochondria appear to be in greater abundance in the basal cytoplasm and the basolateral plasmalemma is relatively smooth with few infoldings. Note the ciliated cell at the luminal surface, which appears degenerate and in the process of being sloughed. Note also the abundant ground substance present within the stroma and adjacent to a capillary shown at the bottom center of the electron micrograph. TEM X 5,500.

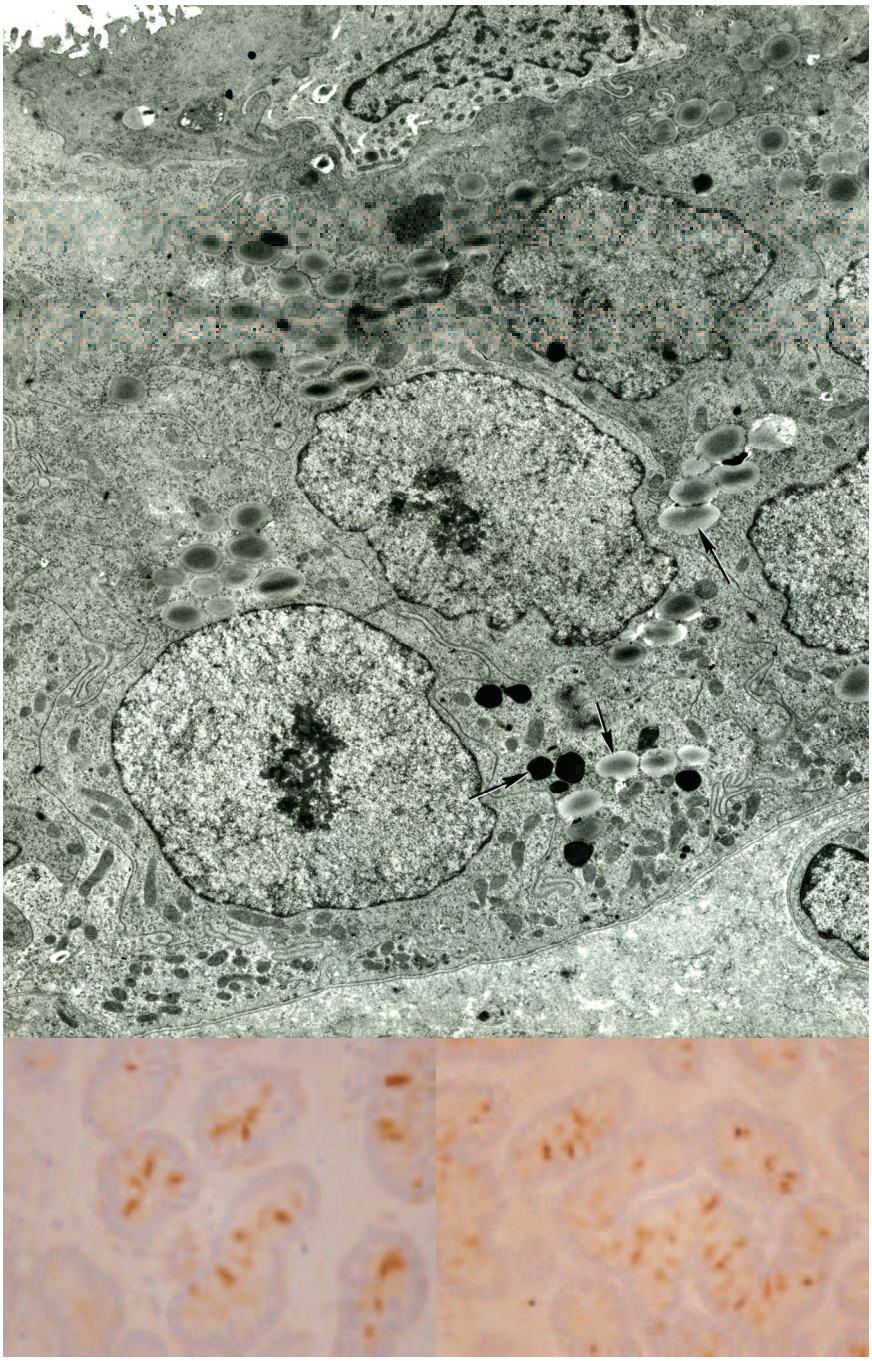

Fig. 8. (*Above*). A micrograph at increased magnification illustrates the electron-lucent and electron-dense granules (arrows) within uterine lining epithelial cells at nine days gestation. Note the concentration of mitochondria near the basal plasmalemma. TEM X 12,500. (*Below left*). A micrograph illustrates immunohistochemical staining that demonstrates neuronal nitric oxide synthase (nNOS) in the uterine glands of a female opossum at nine days gestation. Positive immunoreactive cells are confined to uterine glands in the basal region of the mucosa (endometrium). LM X 350. (*Below right*). A micrograph illustrates immunohistochemical staining that demonstrates neurone-specific enolase (NSE) positive cells in the uterine glands of a female opossum at nine days gestation. Positive immunoreactive cells are restricted to uterine glands within the middle and basal regions of the mucosa (endometrium). LM X 350.

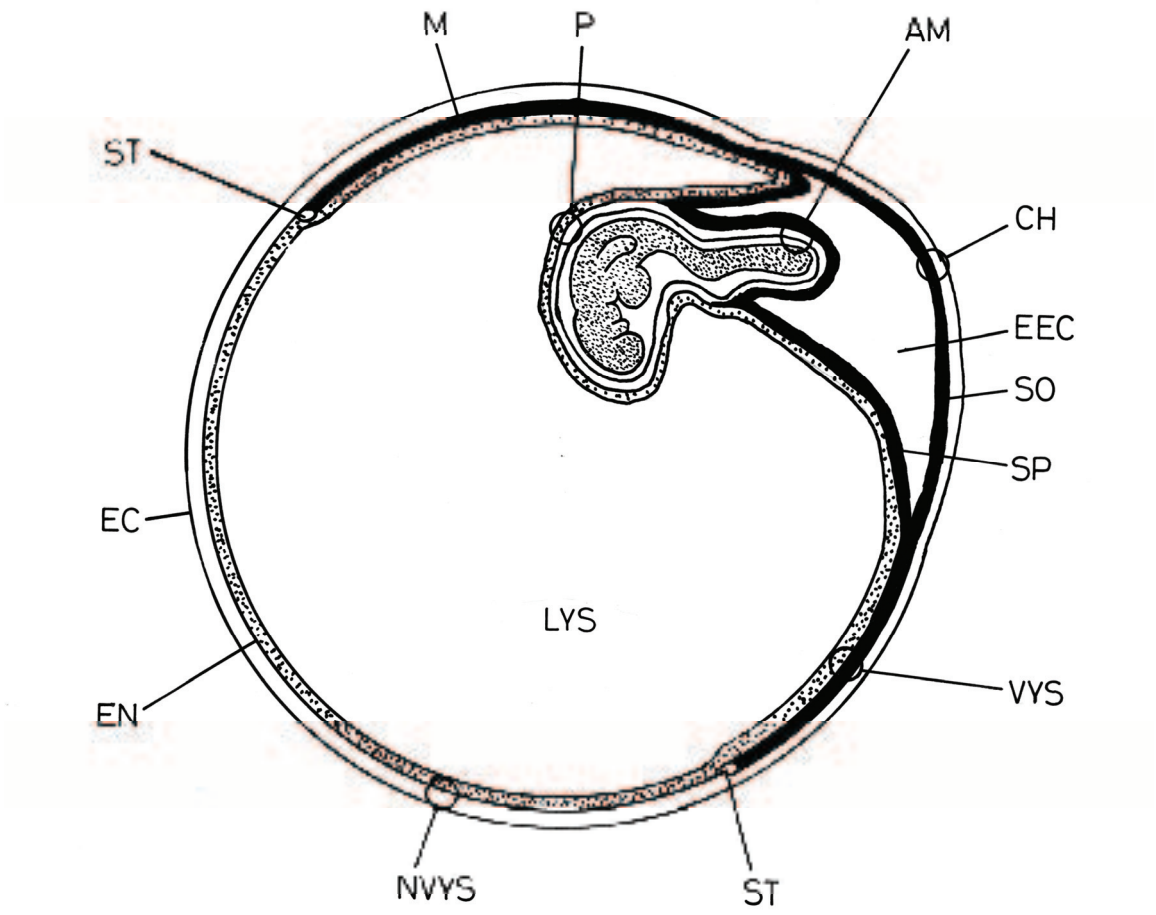

Fig. 9. The opossum embryo enters the embryonic sphere and becomes enveloped by the amnion as well as the yolk-sac placenta during the tenth day of gestation. The proamnion/amnion (P) that surrounds the cranial half of the embryo consists only of ectoderm and endoderm, whereas the caudal half of the amnion (AM) consists of ectoderm and splanchnic mesoderm. The position of the extra-embryonic mesoderm (M), splanchnic mesoderm (SP), somatic mesoderm (SO), sinus terminalis (ST), extra-embryonic coelom (EEC), chorion (CH), vascular yolk-sac placenta (VYS), non-vascular yolk-sac placenta (NVYS), ectoderm/trophectoderm (EC), endoderm (EN), and lumen of the yolk-sac (LYS) are illustrated at this stage of development.

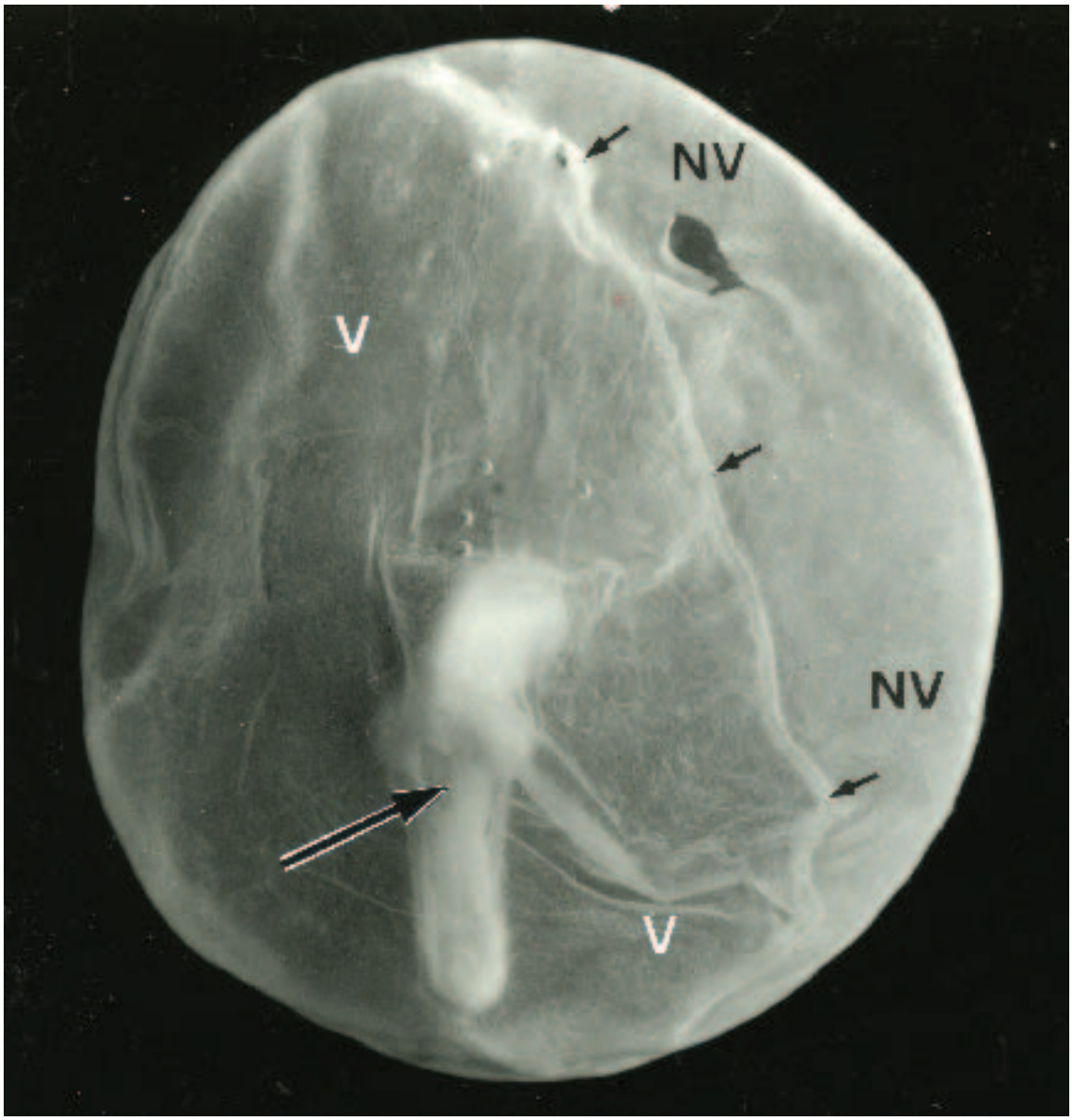

Fig. 10. Fetal membranes envelop the opossum embryo late during the tenth prenatal day. A distinct sinus terminalis (small arrows) can be observed separating the yolk-sac placenta into distinct vascular (V) and non-vascular (NV) regions at this time. The closing amniotic pore (large arrow) also can be seen at this time. X 25.

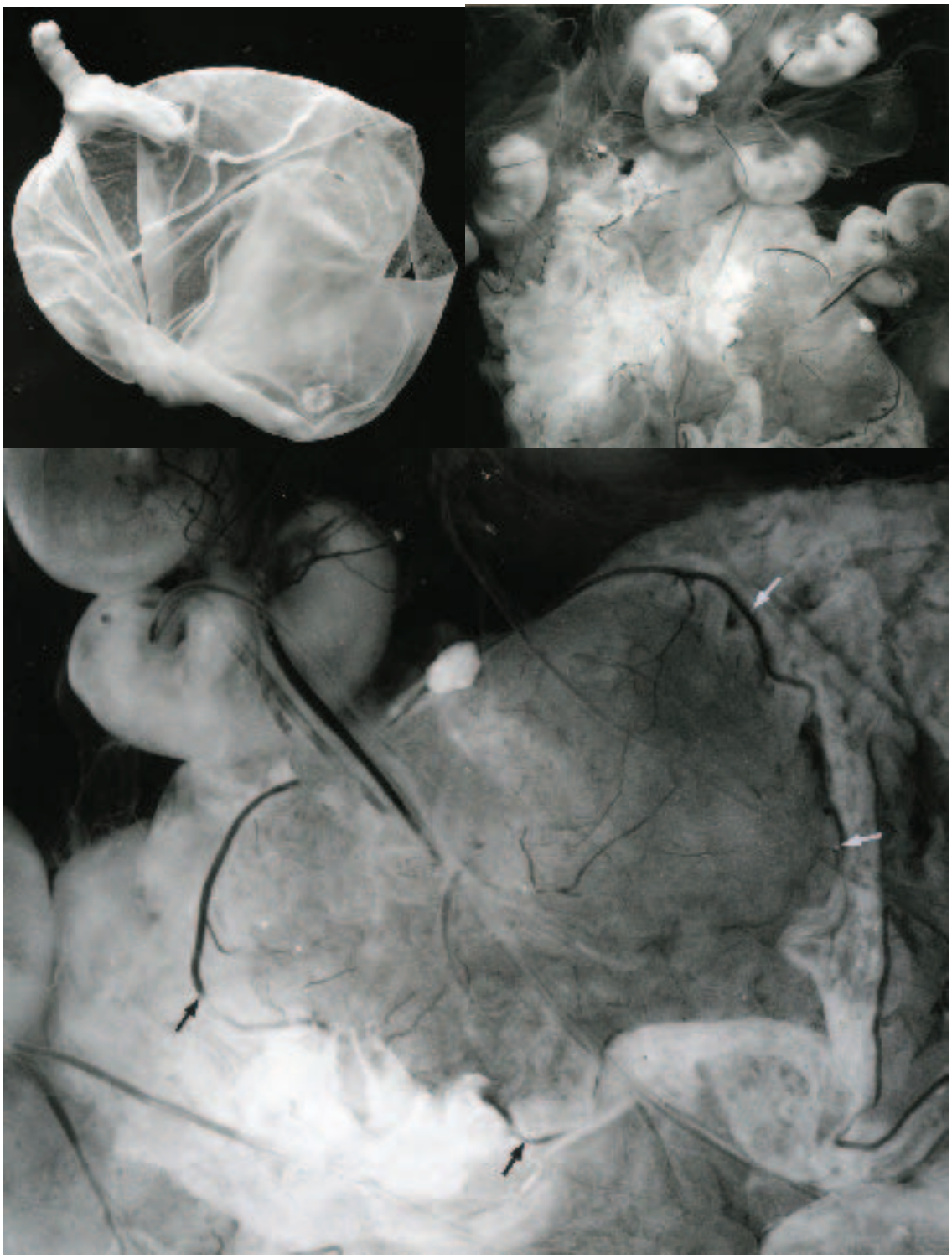

Fig. 11. (*Above left*). A specimen in which the yolk sac placenta has been opened exposes the contained opossum embryo at the tenth day gestation X 8. (*Above right*). Several exposed opossum embryos at the twelfth day of gestation. The vascular portion of the yolk-sac placenta is intimately associated with the uterine mucosa. X 2. (*Below*). Increased magnification of the above right figure illustrates that the sinus terminalis (arrows) continues to define the limits of the vascular yolk-sac placenta. Each placental unit is connected to a single embryo by two vitelline veins and a vitelline artery. X 8.

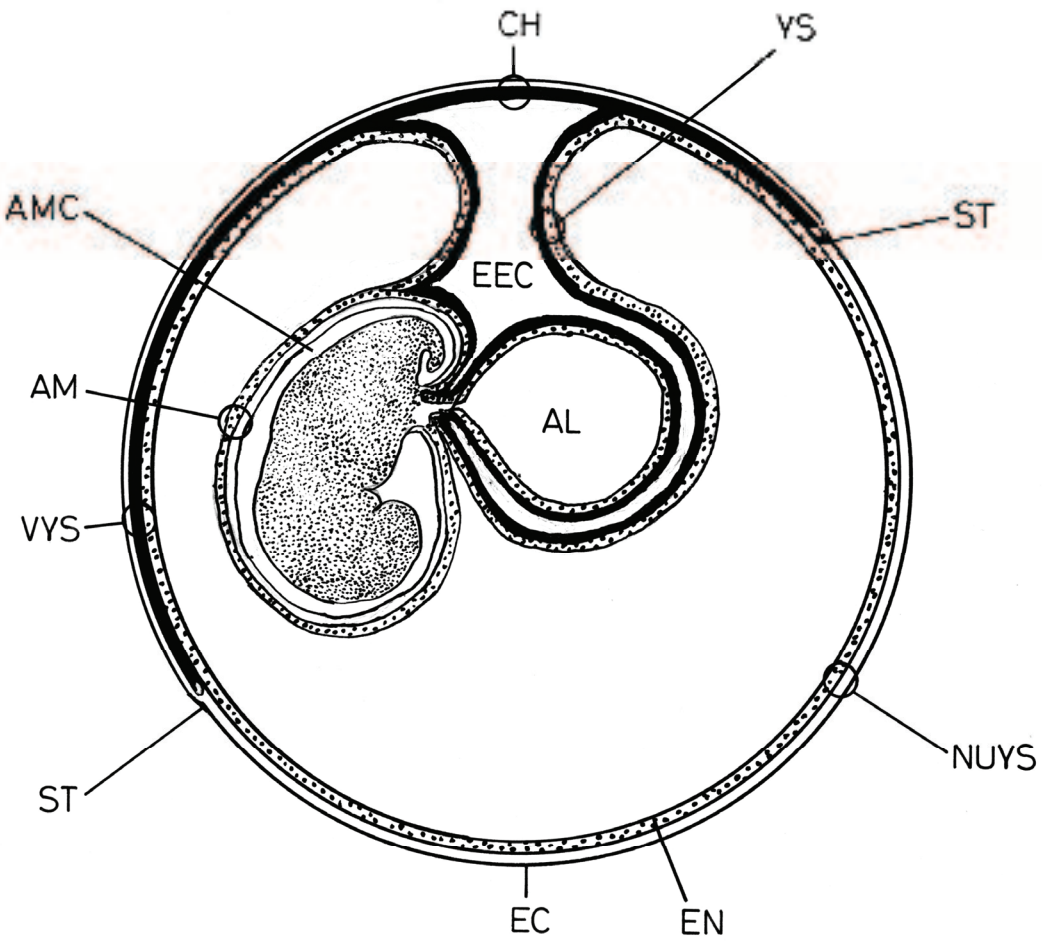

Fig.12. The allantois (AL) is well established by the eleventh prenatal day and lies within the extra-embryonic coelom (EEC) separated by folds of the yolk sac (YS) from the adjacent chorion (CH). The position of the amnion (AM), amnionic cavity (AMC), sinus terminalis (ST), vascular yolk-sac placenta (VYS), non-vascular yolk-sac placenta (NUYS), ectoderm (EC), and endoderm (EN) also are shown in this line drawing.

Fig. 13. An opossum embryo eleven days prenatal enshrouded in its amniotic sac. The surrounding yolk-sac placenta has been removed. Compare the development of the forelimbs with that of the hind limbs. Note the open mouth with protruding tongue, the pigmentation of the retina, and the heart shadow in the thorax. X 45.

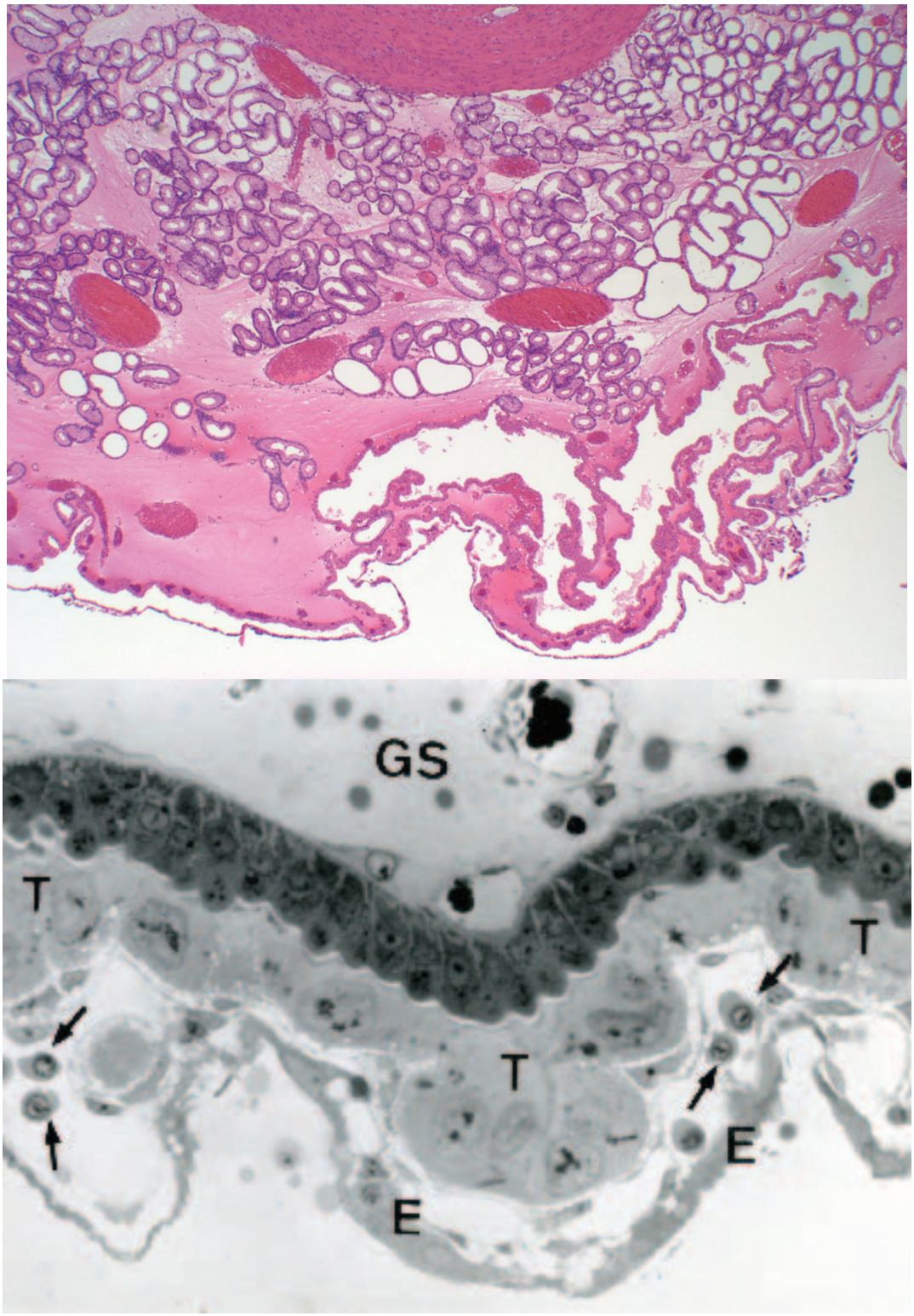

Fig. 14. (*Above*). The mucosa of the opossum uterus at the twelfth day of gestation shows scattered uterine glands separated by an abundant ground substance in the stroma. A portion of myometrium is seen at the top of the figure; the uterine lumen is at the bottom. Note the relationship between the uterine lining epithelium and the trophoblast. LM X 100. (*Below*). A region of the endometrium associated with the vascular yolk-sac placenta illustrates the intimate relationship between cells of the trophoblast (T) and the uterine epithelium. Nucleated erythrocytes (arrows) lie within thin walled vessels positioned between cells of the yolk-sac endoderm (E) and the cells of the trophoblast. Note the abundant ground substance (GS) beneath the uterine epithelium. LM X 400.

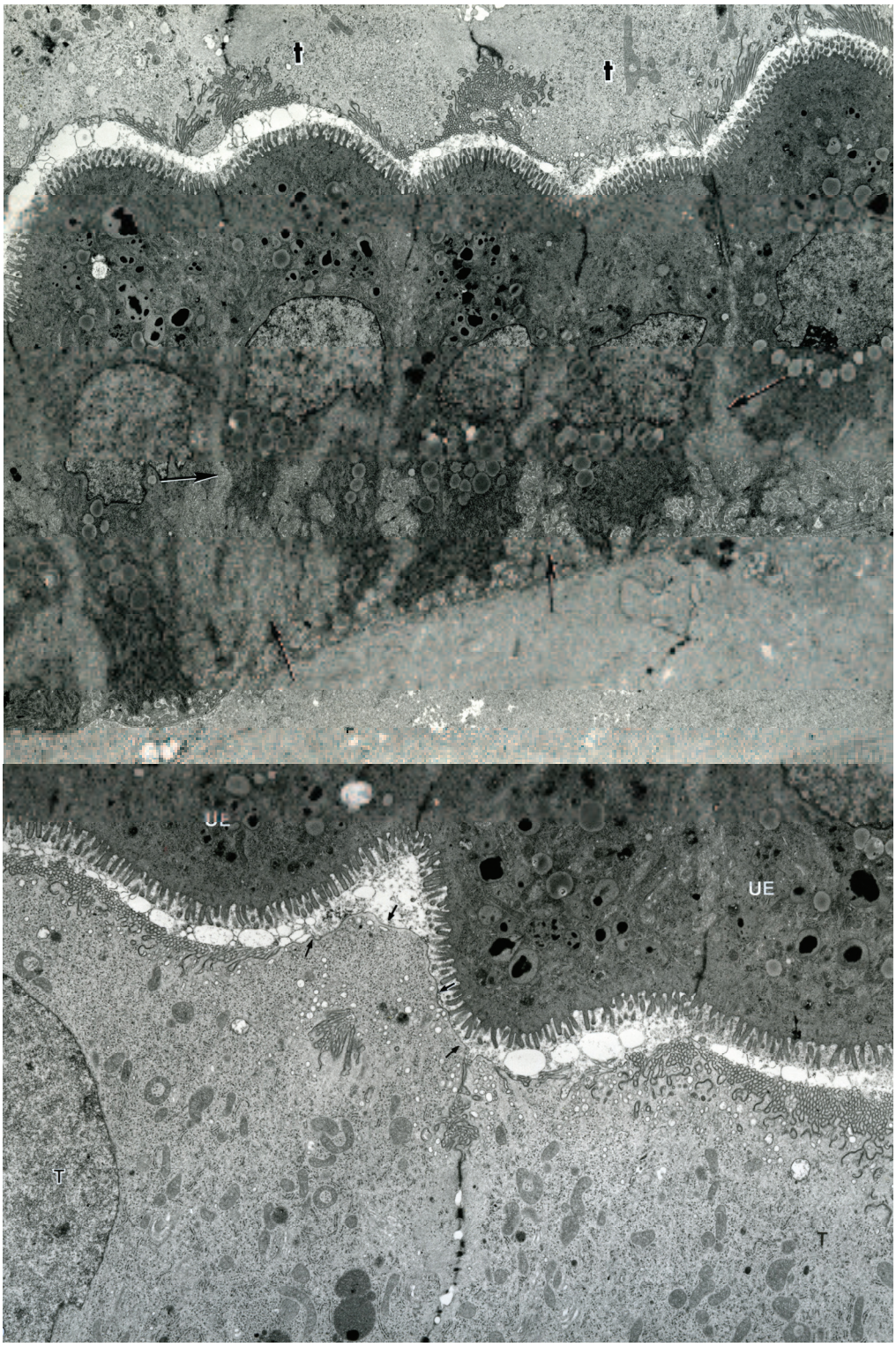

Fig. 15. (*Above*). The uterine epithelium at the twelfth day of gestation is simple columnar, lacks cilia, and exhibits elaborate infoldings of the basolateral plasmalemma (arrows). The cytoplasm contains numerous inclusions and mitochondria appear to be concentrated in the basal half of the cells. Cells of the trophectoderm (t) are shown at the top of the micrograph. TEM X 3,000. (*Below*). Increased magnification illustrates the relationship between the uterine epithelium (UE) and cells of the trophoblast (T). The luminal surface of the latter shows regions where the cell membrane is relatively smooth (arrows). Note the well-developed apical endocytic complex in cells of the trophoblast. TEM X 8,000.

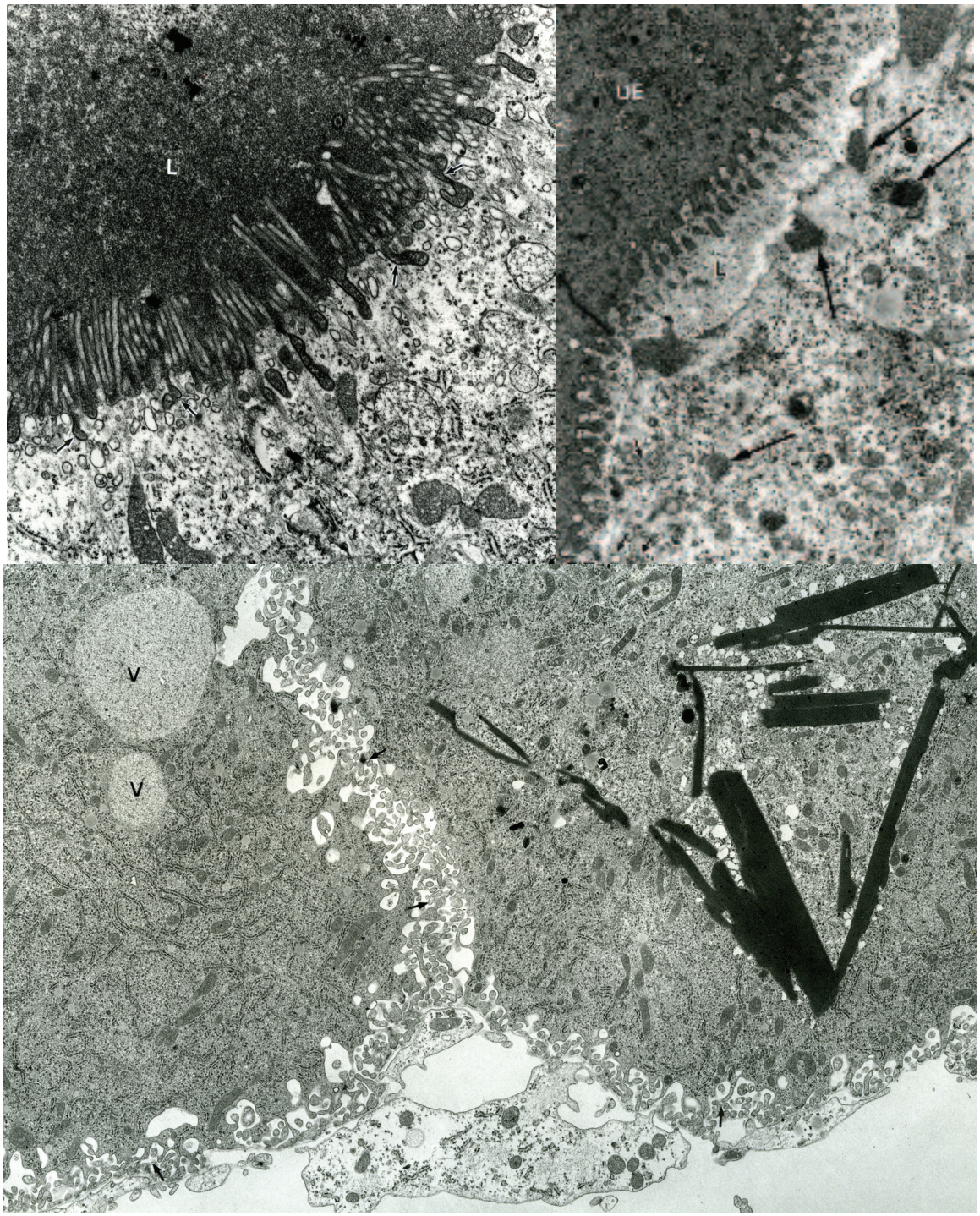

Fig. 16. (*Above left*). The apical endocytic complex (arrows) within cells of the trophoblast appears to be actively involved in sequestering material from the uterine lumen (L). Note the presence of elongate microvilli projecting into the lumen. TEM X 10,000. (*Above right*). Trophoblast cells devoid of apical microvilli also show numerous invaginations and the formation of small vesicles (small arrows). Larger invaginations form vacuoles (large arrows) that contain an electron-dense material acquired from the uterine lumen (L). The apices of two uterine lining epithelial cells (UE) are shown at the upper left. TEM X 12,800. (*Below*). The basolateral plasmalemma of trophoblast cells usually exhibits elaborate infoldings (arrows). Vacuoles (V) and electron-dense crystalline structures in the basal cytoplasm also are a common observation. TEM X 8,000. All illustrations are from the twelfth day of gestation.

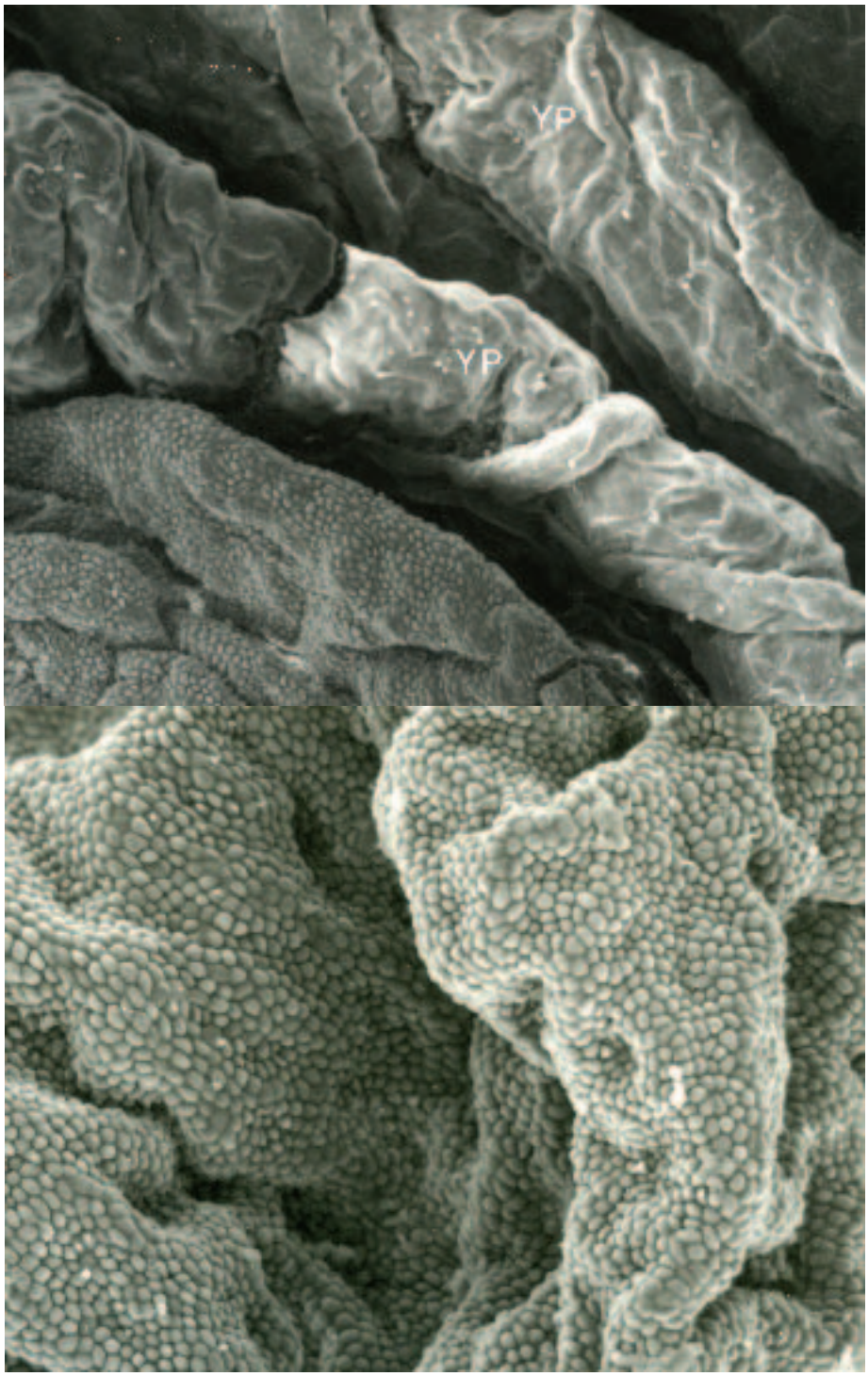

Fig. 17. (*Above*). Large folds are characteristic of the uterine mucosa at the twelfth day of gestation. The upper right region of the uterine mucosa in this preparation of uterus gathered at the twelfth day of gestation is covered by the vascular component of the yolk-sac placenta (YS). SEM X 70. (*Below*). The apices of uterine lining epithelial cells at the twelfth day of gestation are devoid of cilia. SEM X 150.

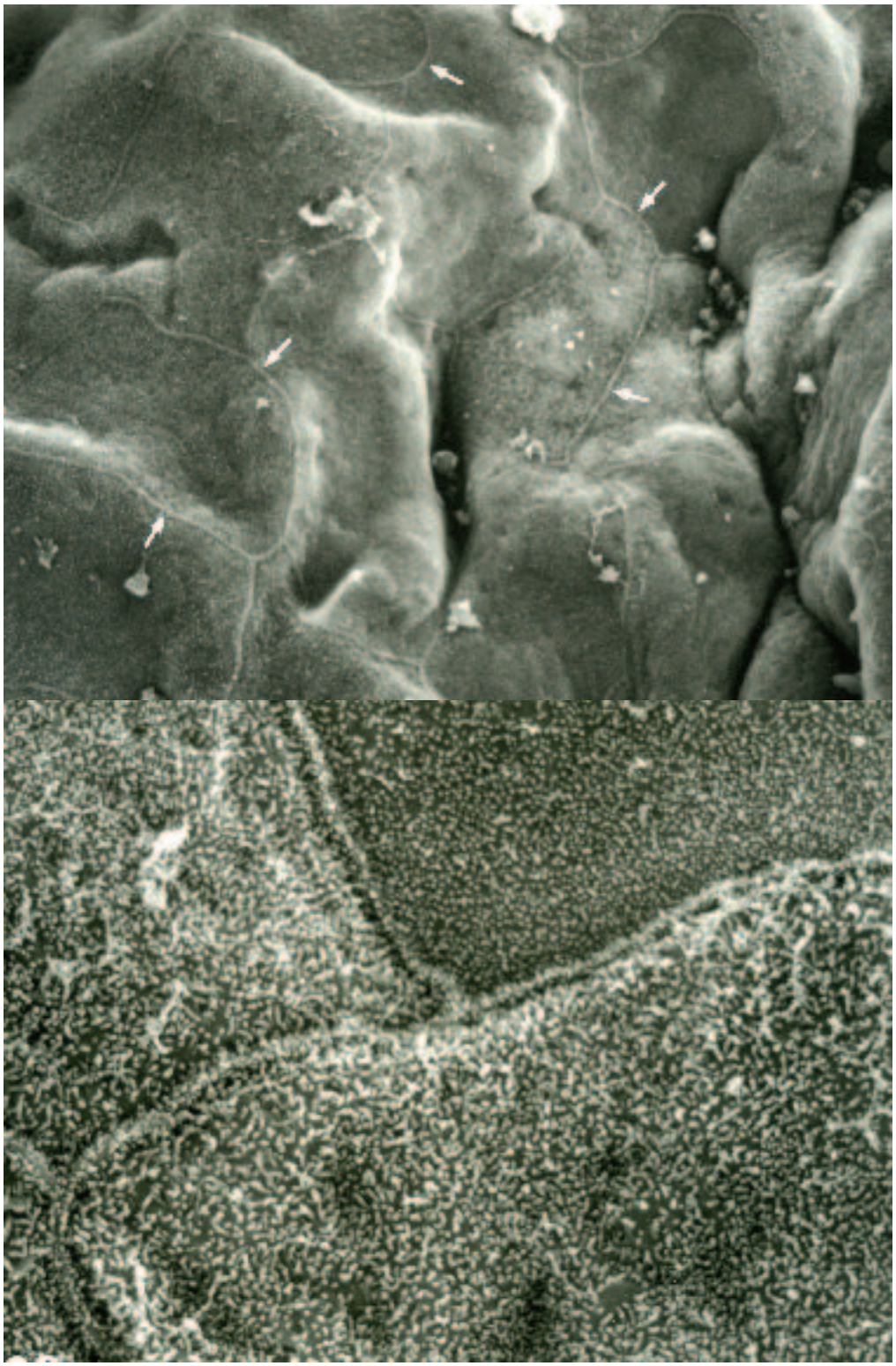

Fig. 18. (*Above*). The interior surface of the yolk-sac placenta taken from region where it covered uterine folds is lined by large, irregular shaped, endodermal cells with distinct boundaries (arrows). Twelve-day opossum embryo. SEM X 800. (*Below*). Increased magnification of portions of four adjacent endodermal cells details the cell boundaries and the nature of the short microvilli on their luminal surface. Twelve-day opossum embryo. SEM X 3,000.

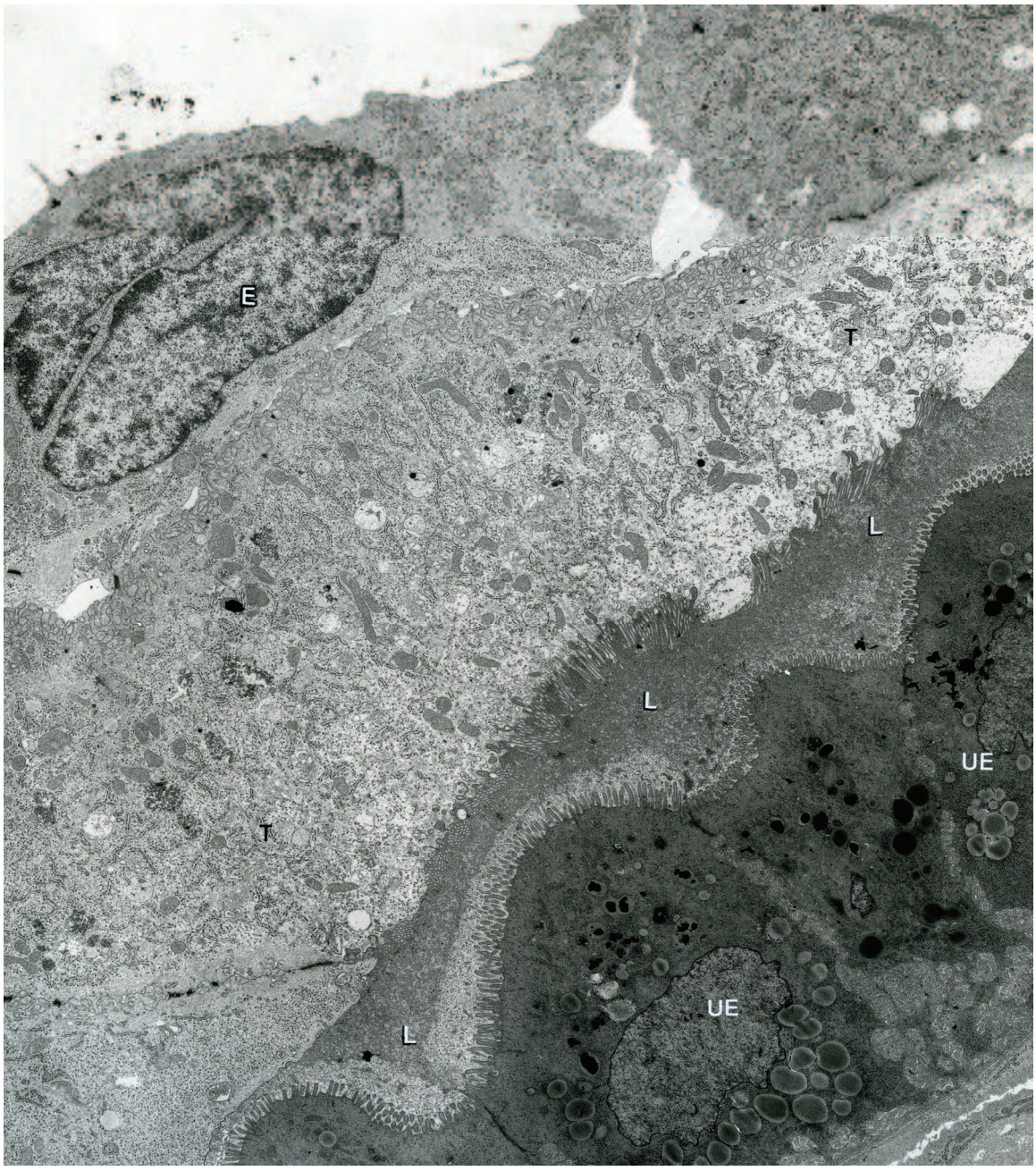

Fig. 19. A region of the non-vascular yolk-sac placenta just beyond the sinus terminalis illustrates endodermal cells (E) lining the lumen of the yolk sac positioned immediately adjacent to cells forming the trophoblast (T). Intervening mesodermal derivatives are absent. An electron-dense material is present within the uterine lumen (L). The uterine lining epithelium (UE) is shown at the lower right. Note the abundance of vacuolar material of varying density within the cytoplasm of the uterine lining epithelial cells. Note also the elaborate basolateral infoldings of the plasmalemma associated with the uterine lining epithelial cells. TEM X 3,000.

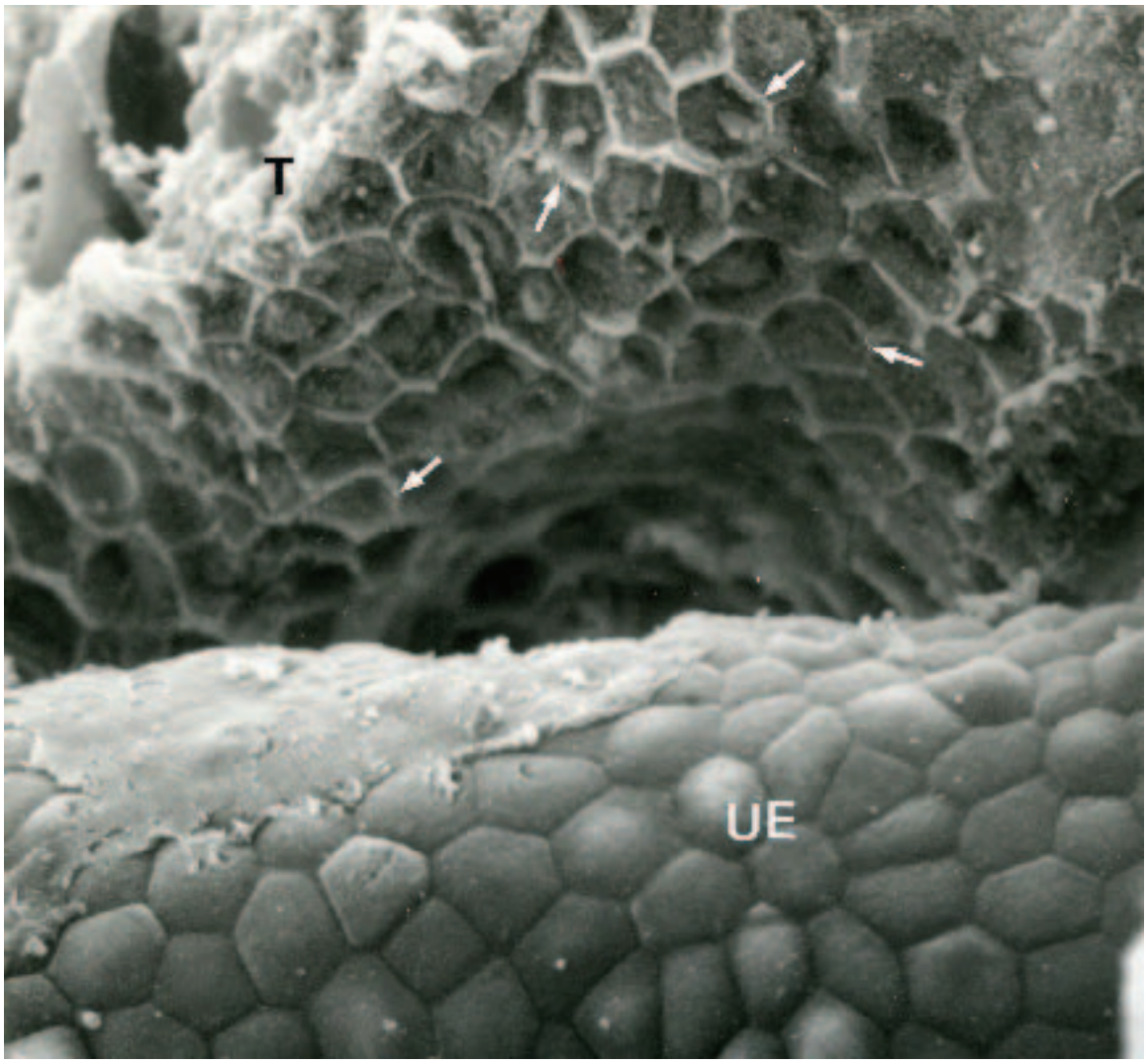

Fig. 20. (*Above*). A micrograph illustrates a region of uterine mucosa from an opossum at the twelfth day of gestation where the vascular yolk-sac placenta has been teased away from the uterine epithelium (UE). Note the honeycombed appearance (arrows) of the associated trophoblast (T). This appearance is thought to represent the presence of individual boundaries between cells of the trophoblast. SEM X 900

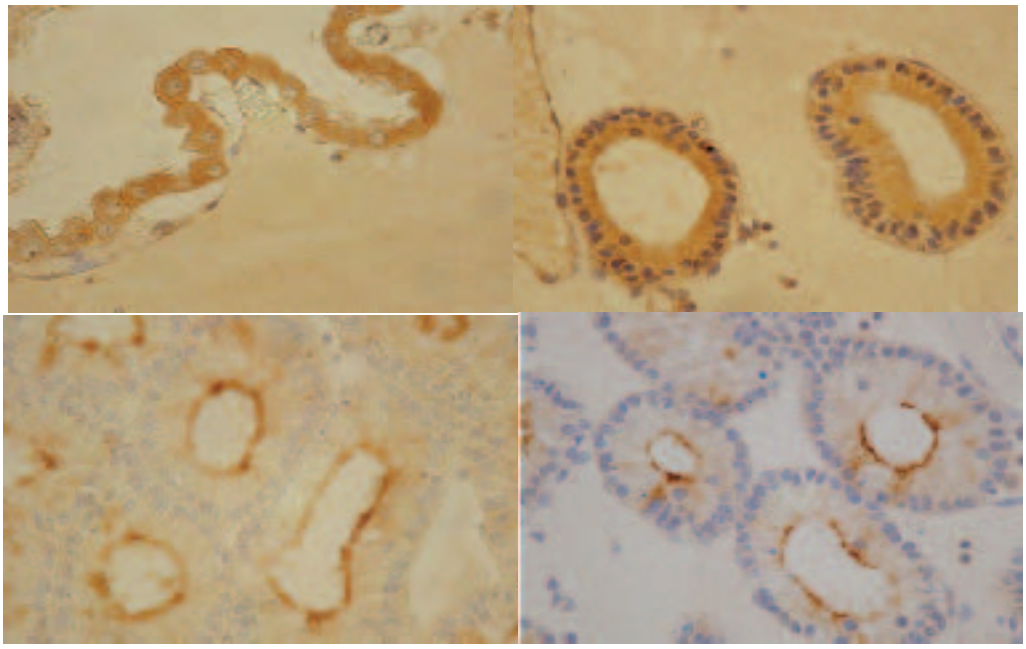

Fig. 21. Positive immunohistochemical staining for gastrin-releasing peptide (GRP) is observed in the uterine surface lining epithelium (*Above left*) and uterine glands (*Above right*) during the eleventh day of gestation. LM X 250. (*Below left*). Positive immunohistochemical staining for neuronal nitric oxide synthase (nNOS) is observed throughout the uterine glands during the eleventh day of gestation. LM X 250. (*Below right*). Neurone-specific enolase (NSE) positive immunohistochemical staining also is observed throughout the length of the uterine glands during the later days of pregnancy (eleven days plus) in the opossum. LM X 250.

Chapter 5. Allantois

Synopsis:

The allantois forms as a ventral outgrowth of the hindgut during the middle of the tenth day of gestation and extends into and remains trapped within the extraembryonic coelom. It never establishes a firm relationship with either the serosal chorion or the yolk sac placenta as occurs in other species. With continued development, the allantois expands away from the embryo and its distal portion accumulates fluid resulting in a balloon-like vesicle, the allantoic sac. The short, narrow proximal portion retaining a connection to the embryo is referred to as the allantoic stalk. The allantois increases in size due to the accumulation of fluid and reaches its maximum development by gestational day twelve. The accumulating fluid, which is light amber in color, is produced by the mesonephric kidneys which begin to function late during the tenth day of gestation. Structurally, the allantois consists of an endodermally derived epithelium that lines the interior; a mesothelium that covers the external surface and a delicate, vascularized connective tissue positioned between these two epithelial sheets.

Acknowledgments:

Figs. 1, 2, 3, 4, 5, 6 and 7 courtesy of and from: Krause, W.J. and J.H. Cutts (1985) The allantois of the North American opossum (*Didelphis virginiana*) with preliminary observations on the yolk sac endoderm and trophectoderm. Anat. Rec. 211:166-173.

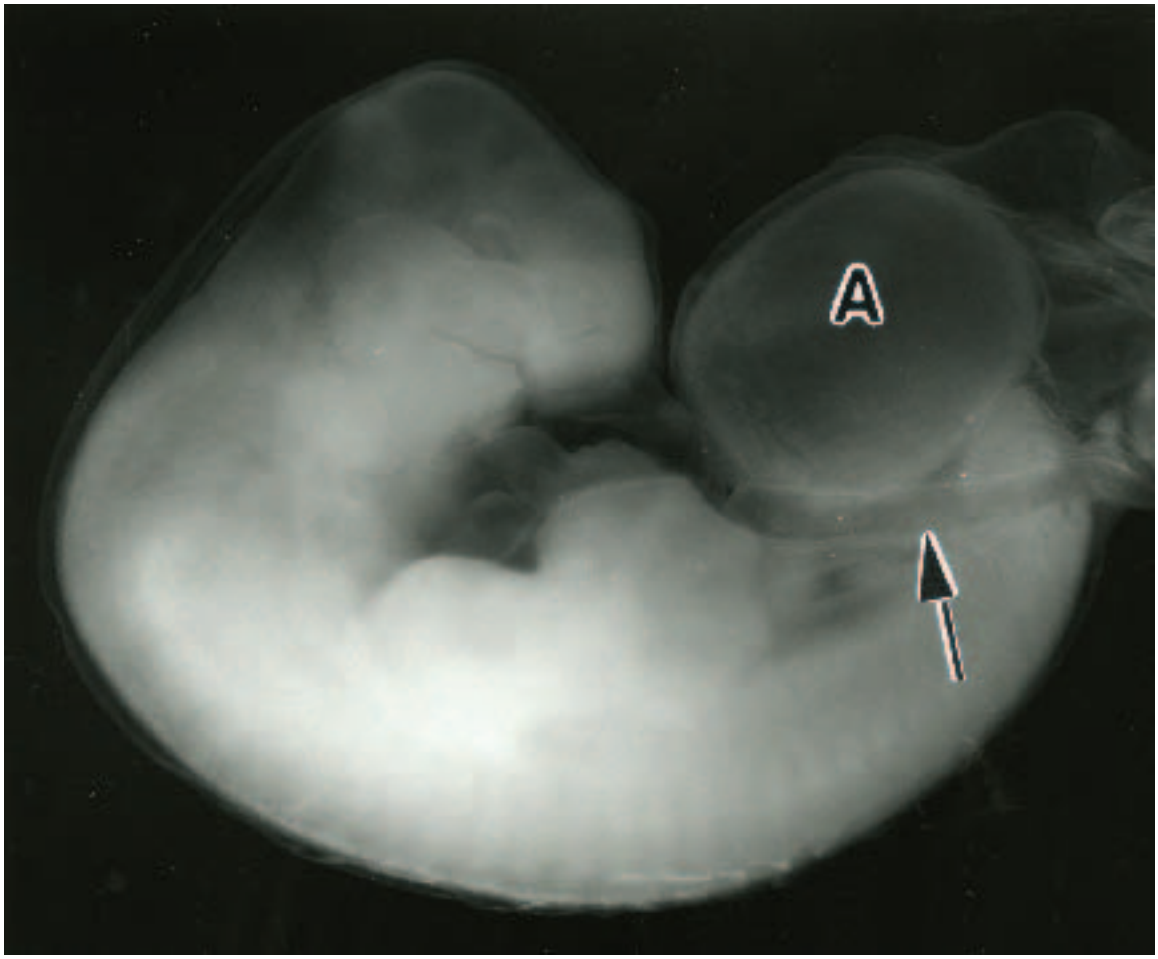

Fig. 1. The allantois (A) of a ten-day opossum embryo. A thin membrane, the amnion, envelops the embryo proper. A vitelline vessel (arrow) united to a portion of dissected yolk sac placenta at the far right also can be seen. Note that morphological features such as the developing forelimb, remnants of the pharyngeal arches, and forming eye can be visualized in the embryo proper. X 20.

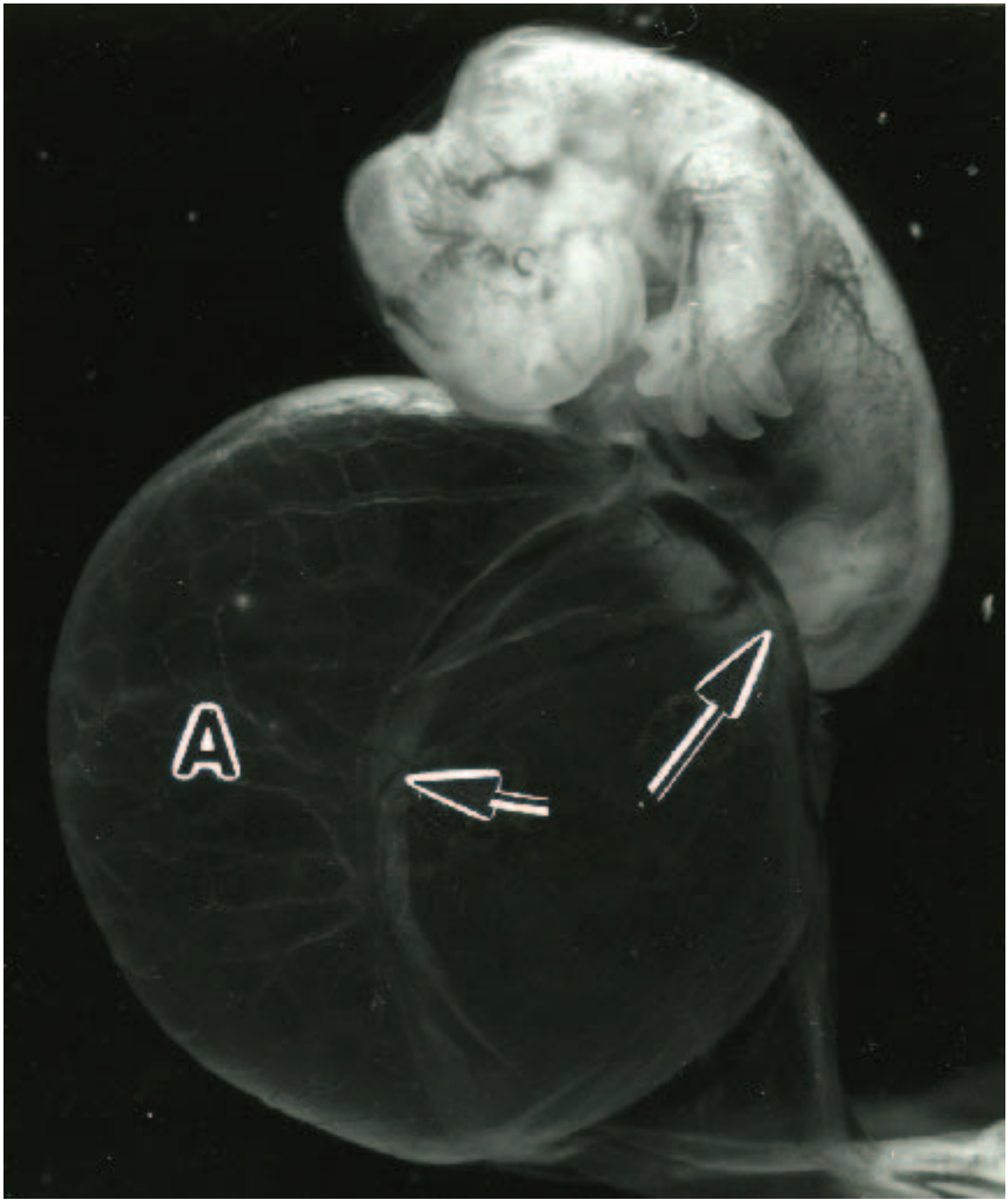

Fig. 2. The allantois (A) of an eleven-day opossum embryo. Observe the vitelline vessels (arrows) that course around the allantois to supply the vascular portion of the yolk sac placenta (not shown). Note the numerous small vessels present within the thin wall of the allantois. The digits of the forelimb are clearly visible as is the development of the hind limb. Note that the pigmented portion of the retina and numerous small vessels can be visualized within the embryo proper beneath the integument. X 20.

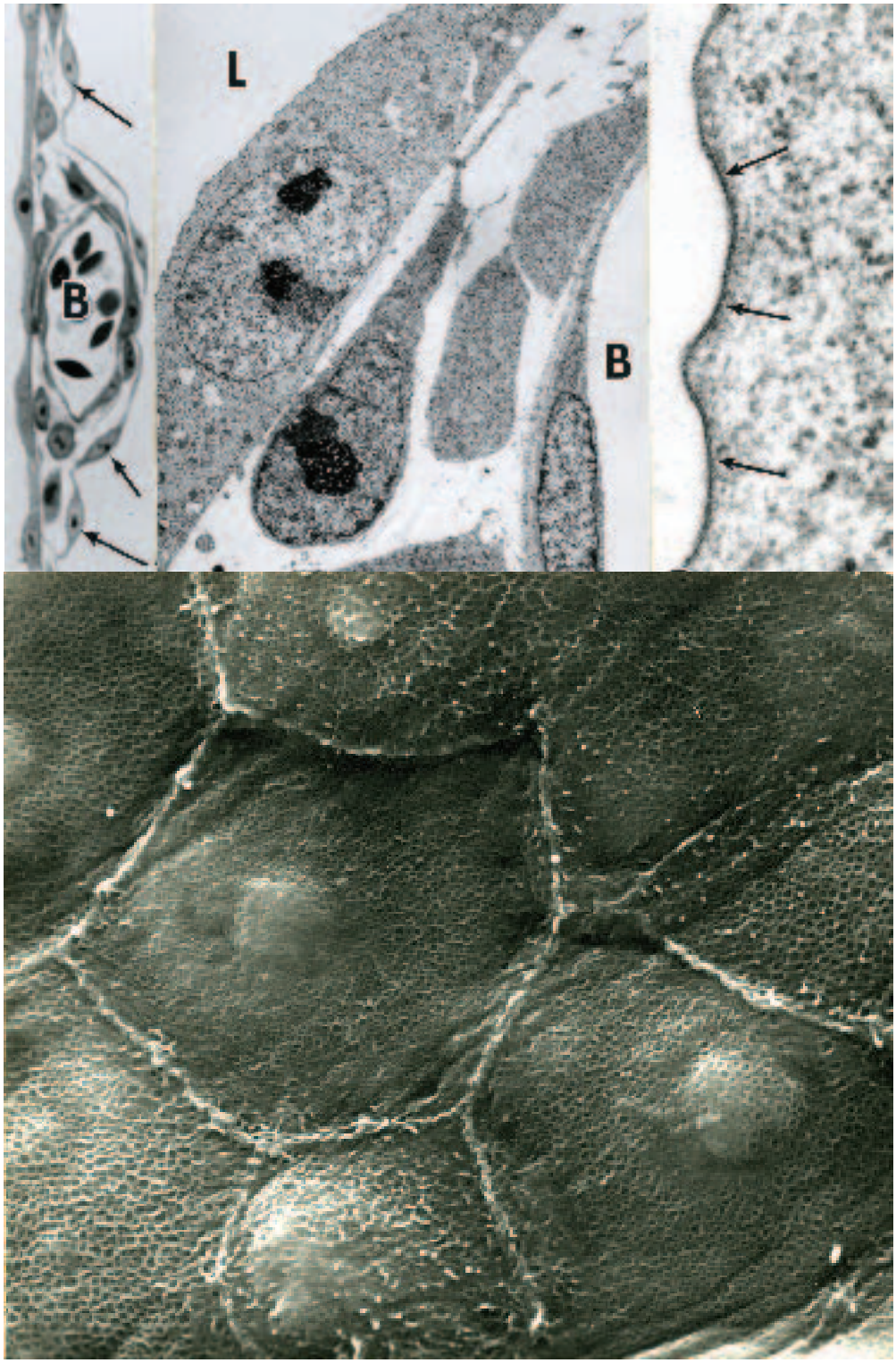

Fig. 3. (*Above left).* A section through the wall of the allantois illustrates a region that contains a blood vessel (B). The lumen lined by allantoic epithelium is to the extreme left; the allantoic mesothelium is to the right (arrows). LM X 250. (*Above center*). The lumen (L) of the allantois is lined by a flattened epithelium. Scattered mesenchymal cells and collagen fibers are observed between the epithelium and the endothelium lining the blood vessel (B) at the right. TEM X 1,500. (*Above right*). The luminal plasmalemma of an epithelial cell lining the allantois appears thickened and presents a scalloped appearance (arrows). TEM X 64,000. (*Bottom*). A micrograph illustrates the surface features of epithelial cells lining the allantoic lumen as well as their nuclear profiles. SEM X 3,750.

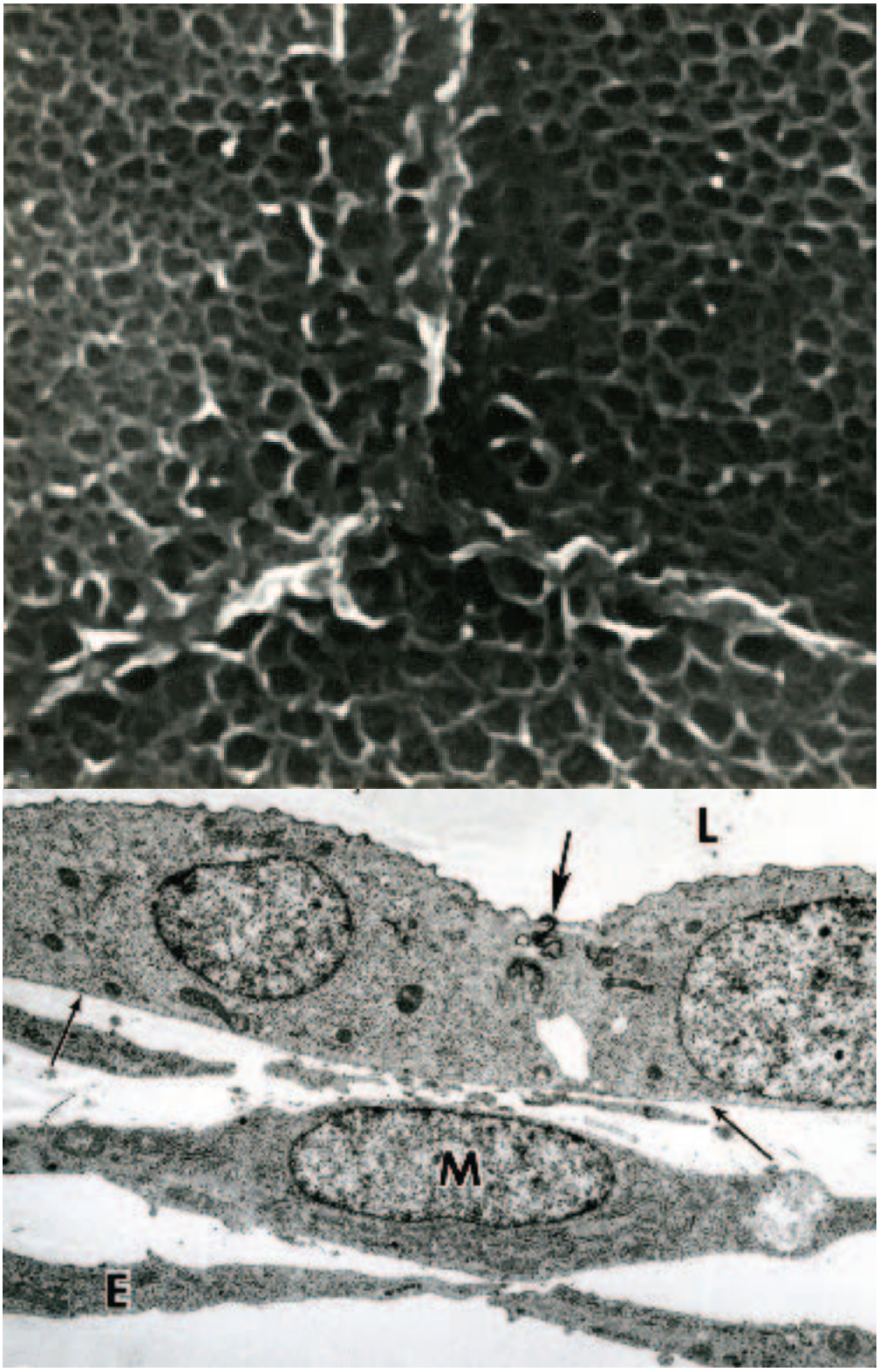

Fig. 4. (*Above*). Increased magnification of the luminal plasmalemma of three epithelial cells lining the allantois details its scalloped appearance. Compare this illustration with those presented in figure 3. SEM X 12,600. (*Below*). The epithelial cells lining the allantoic wall are united at their apices by junctional complexes (large arrows) and lie on a thin basal lamina (small arrows). The mesothelium covering the external surface (E) of the allantois is thin and attenuated. Mesenchymal cells (M) and scattered collagen fibers occur between the two epithelial sheets. The lumen of the allantois (L) is shown at the top of the figure. TEM X 2,300.

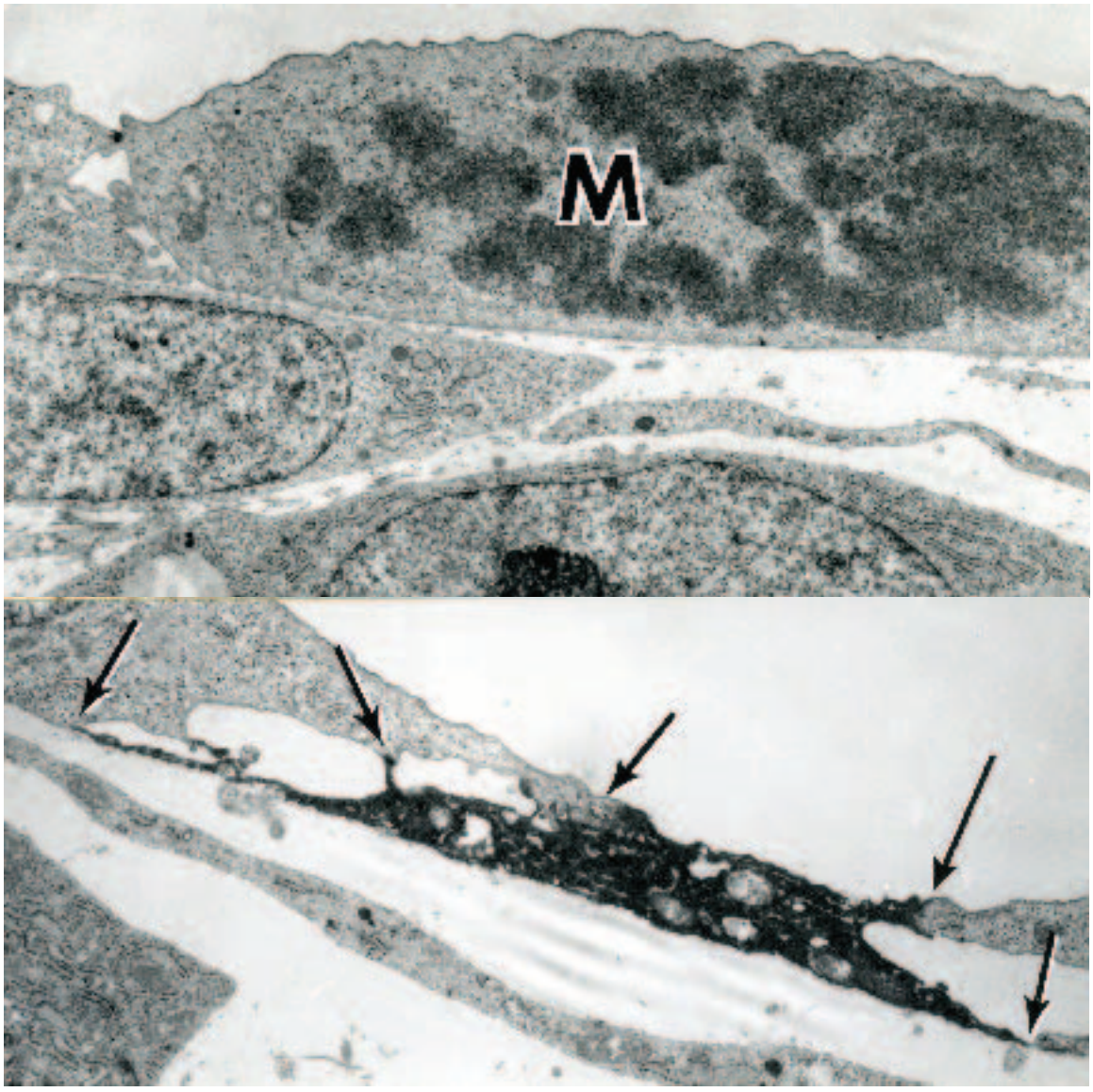

Fig. 5. (*Above*). Occasional mitotic figures (M) are observed within the allantoic lining epithelium. Two mesenchymal cells within the allantoic wall are shown near the bottom of the figure. Twelve-day opossum embryo. TEM X 3,000. (*Below*). In addition to proliferating cells within the lining epithelium of the allantois, what appear to be dead or dying cells also occur. The cytoplasm of these cells appears electron dense, the organelles disrupted, and the nuclei pyknotic. These shrunken cells often are observed to maintain contact (arrows) with adjacent, apparently healthy, epithelial lining cells. TEM X 2,000.

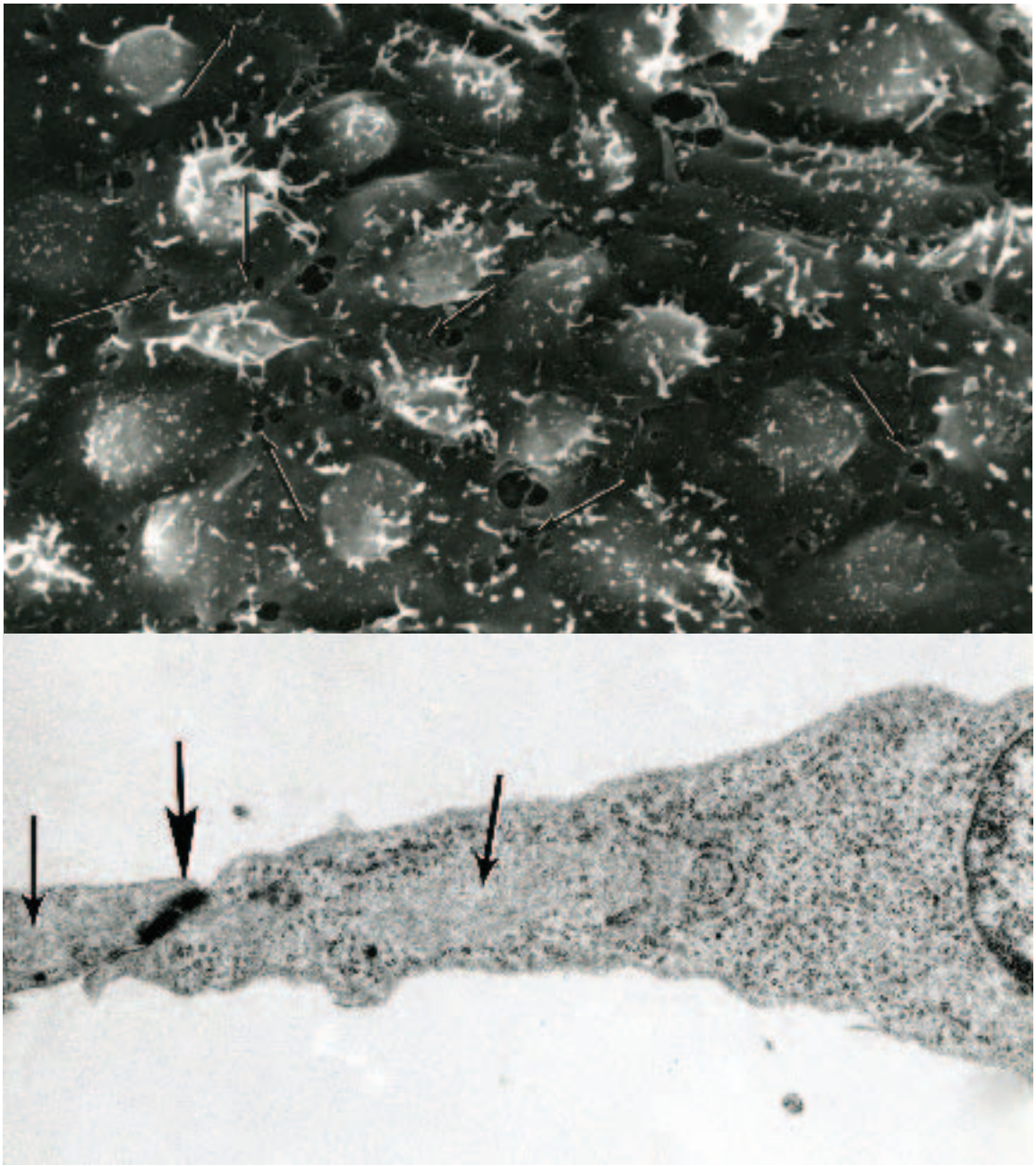

Fig. 6. (*Above*). The mesothelium covering exo-coelomic surface of the allantois differs considerably in structure from the epithelial lining. Mesothelial cells are more irregular in shape and the lateral cell membrane of adjacent cells appears serrated and interdigitate with one another (arrows). Scattered microvilli project from their external surfaces. Eleven-day opossum embryo. TEM X 1,400. (*Below*). A micrograph illustrates an attachment point (large arrow) between two mesothelial cells covering the external surface of the allantois. Bundles of intermediate (cytokeratin) filaments (small arrows) occur in the cytoplasm that are associated with the desmosomes. Twelve-day opossum embryo. TEM X 8,000.

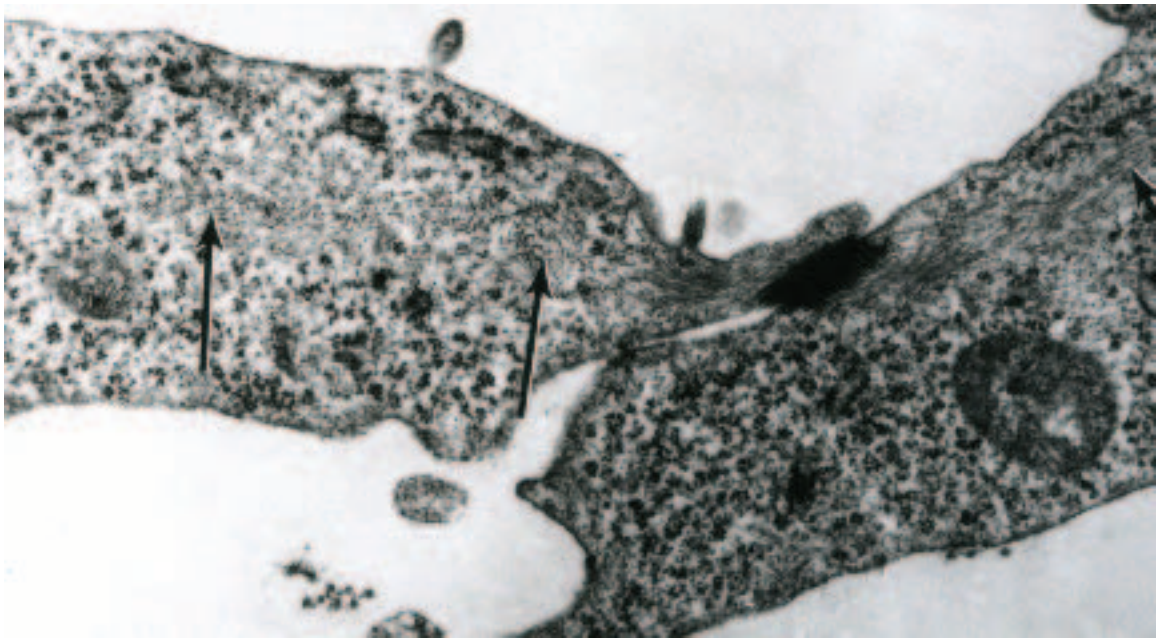

Fig. 7. An additional micrograph illustrates at increased magnification a junctional complex between two mesothelial cells covering the allantois. Note that the intermediate (cytokeratin) filaments seen in a transverse profile (arrows) also are observed coursing towards and uniting with attachment plaques of a desmosome. Twelve-day opossum embryo. TEM X 20,000.

Chapter 6. Embryo Formation

Synopsis:

Mono spermatic fertilization occurs in the oviduct shortly after ovulation and the fertilized oocyte or zygote enters the uterus 12-24 hours later. The zygote usually measures 0.4-0.5 mm in diameter after its arrival in the uterus. The very short gestation period of *Didelphis* can be subdivided into five categories: cleavage, unilaminar blastocysts, bilaminar blastocysts, trilaminar blastocysts, and early organogenesis.

The first cleavage occurs on the second day followed by the second, third, and fourth cleavages on the third day of gestation. The resulting blastomeres become arranged around a presumptive blastocoele and lie separately against the inner surface of the zona pellucida. The blastomeres flatten and spread, and with continued mitotic activity a unilaminar blastocyst is established by the fourth day of gestation. The unilaminar blastocyst generally measures about 0.11 mm in diameter and consists of 32 cells. Endodermal cells first appear in blastocysts measuring 0.11 to 0.34 mm in diameter, which consist of 50 to 60 cells. Enlarged cells, endodermal mother cells, appear between unilaminar protodermal cells at one hemisphere of the unilaminar blastocyst about 12 hours following its formation. The endodermal mother cells migrate into the blastocyst interior and then flatten against the cells forming the wall of the unilaminar blastocyst. These cells eventually come to line the entire blastocyst interior and establish the definitive endoderm transforming the unilaminar blastocyst into a bilaminar blastocyst.

The bilaminar blastocyst measures about 0.75 mm in diameter and occurs midway during the gestation period (about the sixth prenatal day). The zona pellucida and the surrounding mucoid layer disappear with the formation of the bilaminar blastocyst. As endodermal cells proliferate, differences between what will become the embryonic and extra-embryonic areas of the blastocyst wall become more pronounced. Protodermal cells in the region of the blastocyst wall where the mother endodermal cells originated, appear taller, more closely packed together and the cytoplasm is more granular. Protodermal cells at this location form the presumptive medullary plate and identify the position of the embryo. The embryonic area occupies a specific position in the wall of the blastocyst vesicle. A morula stage does not occur nor is an inner cell mass observed during development in *Didelphis*.

The trilaminar blastocyst stage begins with the appearance of mesodermal cells at about the sixth day of gestation and ends with the appearance of somites and the neural plate. Trilaminar blastocysts measuring 1.4 mm in diameter are present by the seventh day of gestation. The formation of the primitive streak at this time marks the beginning of the migration of mesodermal cells between the endoderm and ectoderm and forms the third primary embryonic germ layer of the blastocyst. By gestational day eight, mesoderm extends beyond the region of the forming embryo but is confined to one pole of the embryonic vesicle and lies between the extra-embryonic ectoderm and endoderm. The ventral one-third of the embryonic sphere is never invaded by mesoderm and represents a persistent portion of the original bilaminar vesicle. This region of the embryonic vesicle will become the non-vascular portion of the definitive yolk-sac placenta. The region of the embryonic vesicle where extra-embryonic mesoderm is positioned between endoderm and ectoderm will become the vascular component of the yolk-sac placenta. Thus, by the ninth day of gestation the embryo proper consists of all three germ layers and exhibits the initial development of some of their derivatives. The extra-embryonic region of the vesicle may show two or three

germ layers. Numerous, elongate microvilli, a well-developed endocytic complex and large intracellular vacuoles characterize cells of the extra-embryonic ectoderm or trophectoderm. These morphological features suggest a cell type actively involved in the absorption of macromolecules. Prior to and during the ninth day of gestation the embryonic vesicles float freely in uterine secretions and obtain their nutrition from secretions produced by the uterine mucosa. These secretions are rich in proteins, particularly albumins and pre-albumins.

Early organogenesis, the last stage of gestation, occupies that period of time between the appearance of the notochord and birth, and occurs during the last four days of gestation. With the loss of the shell membrane and the establishment of a non-invasive yolk sac (choriovitelline) placenta, organogenesis of the embryo proceeds at an incredible rate and results in a viable fetus capable of independent migration to the pouch and survival in an external environment.

Acknowledgments:

Figs. 1 and 2, courtesy of and from: Krause, W.J. (1998) A review of histogenesis/organogenesis in the developing North American opossum (*Didelphis virginiana*). Adv. Anat. Embryol. Cell Biol. Vol 143 (I): Springer Verlag, Berlin, pp 143.

Figs. 3, 4, 5 and 6, courtesy of and from: Krause, W.J. and J.H. Cutts (1985) Morphological observations on the mesodermal cells in the eight day opossum embryo. Anat. Anz. 158:273-278.

Figs. 7, 8 (top), 11, 12 and 13 (bottom), courtesy of and from: Krause, W.J. and J.H. Cutts (1985) Placentation in the opossum (*Didelphis virginiana*). Acta Anat. 123:156-171.

Figs. 10 (top), 11 (top) and 14, courtesy of and from: Krause, W.J. and J.H. Cutts (1984) Scanning electron microscopic observations on the nine-day opossum embryo. Acta Anat. 120:93-97.

Figs. 15 (upper left), 16 (bottom), 18, 22 (top), 24, 25 and 26, courtesy of and from: Krause, W.J. and J.H. Cutts (1986) Scanning electron microscopic observations on developing opossum embryos: days nine through twelve. Anat. Anz. 161:11-21.

Fig. 17 (top), courtesy of and from: Krause, W.J. and J.H. Cutts (1984) Scanning electron microscopic observations on the opossum yolk sac chorion immediately prior to uterine attachment. J. Anat. 138:189-191.

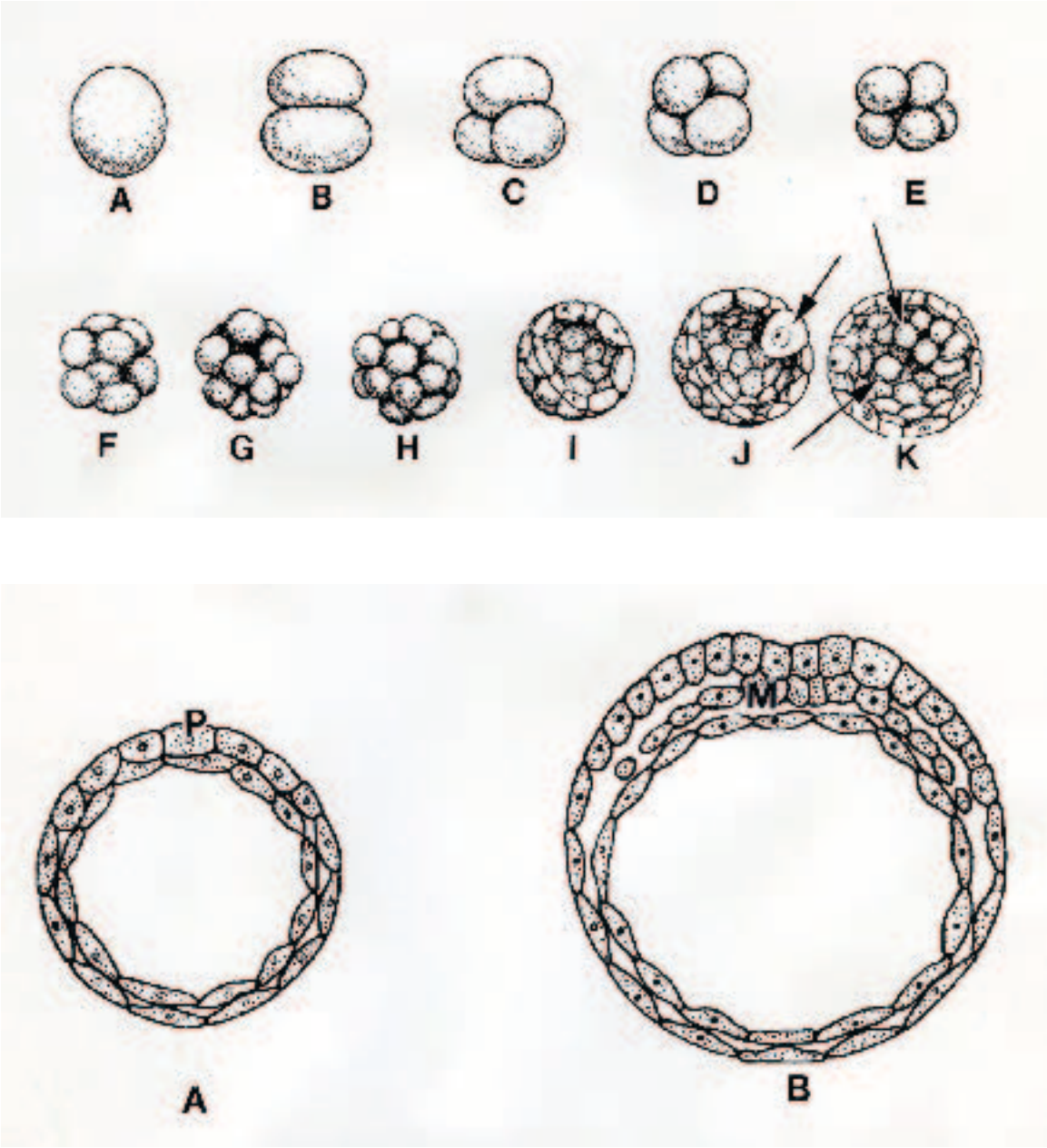

Fig. 1. (*Above*). Line drawings illustrate cleavage and the establishment of the unilaminar blastocyst in the opossum. ***A*** one-cell stage, ***B*** two-cell stage, ***C*** three-cell stage, ***D*** four-cell stage, ***E*** six-cell stage, ***F*** eight-cell stage, ***G*** twelve-cell stage, ***H*** sixteen-cell stage, I thirty-two-cell stage unilaminar blastocyst, ***J*** initial appearance of endodermal mother cells (arrow), ***K*** the spread of endodermal mother cells (arrows) under the region of ectoderm destined to become the medullary plate of the embryo. (*Below*). ***A*** A line drawing illustrates an opossum bilaminar blastocyst. The position of the medullary plate (P) is established in the outer lying ectoderm by this stage of development. Note that a complete layer of endodermal cells now lines the interior of the blastocyst. ***B*** With the appearance of mesodermal cells (M) between the outer layer of ectoderm and inner layer of endoderm, a trilaminar opossum blastocyst is established. Note that the region of the forming medullary plate continues to differentiate.

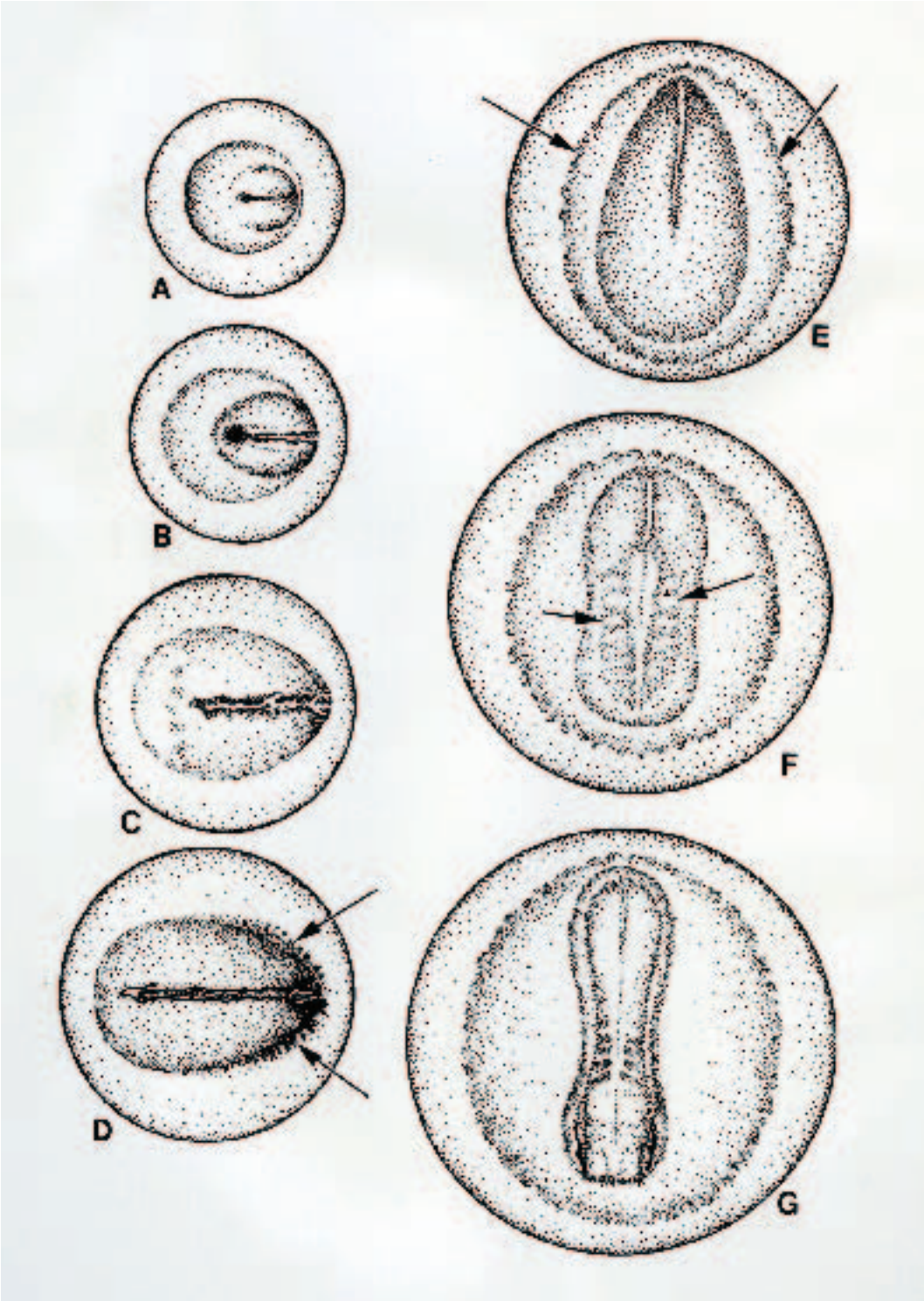

Fig. 2. A series of embryonic stages of the opossum illustrates: ***A*** the primitive streak with mesodermal crescents, ***B*** Hensen's node, ***C*** the primitive groove (note that mesodermal cells occur only beneath the medullary plate), ***D*** and ***E*** mesoderm is beginning to extend beyond the medullary plate (arrows), ***F*** the notochord is longer than the primitive groove. Note the appearance of forming somites (arrows) in this eight-day blastocyst. ***G*** The initial appearance of coelomic rudiments occurs in the nine-day opossum blastocyst.

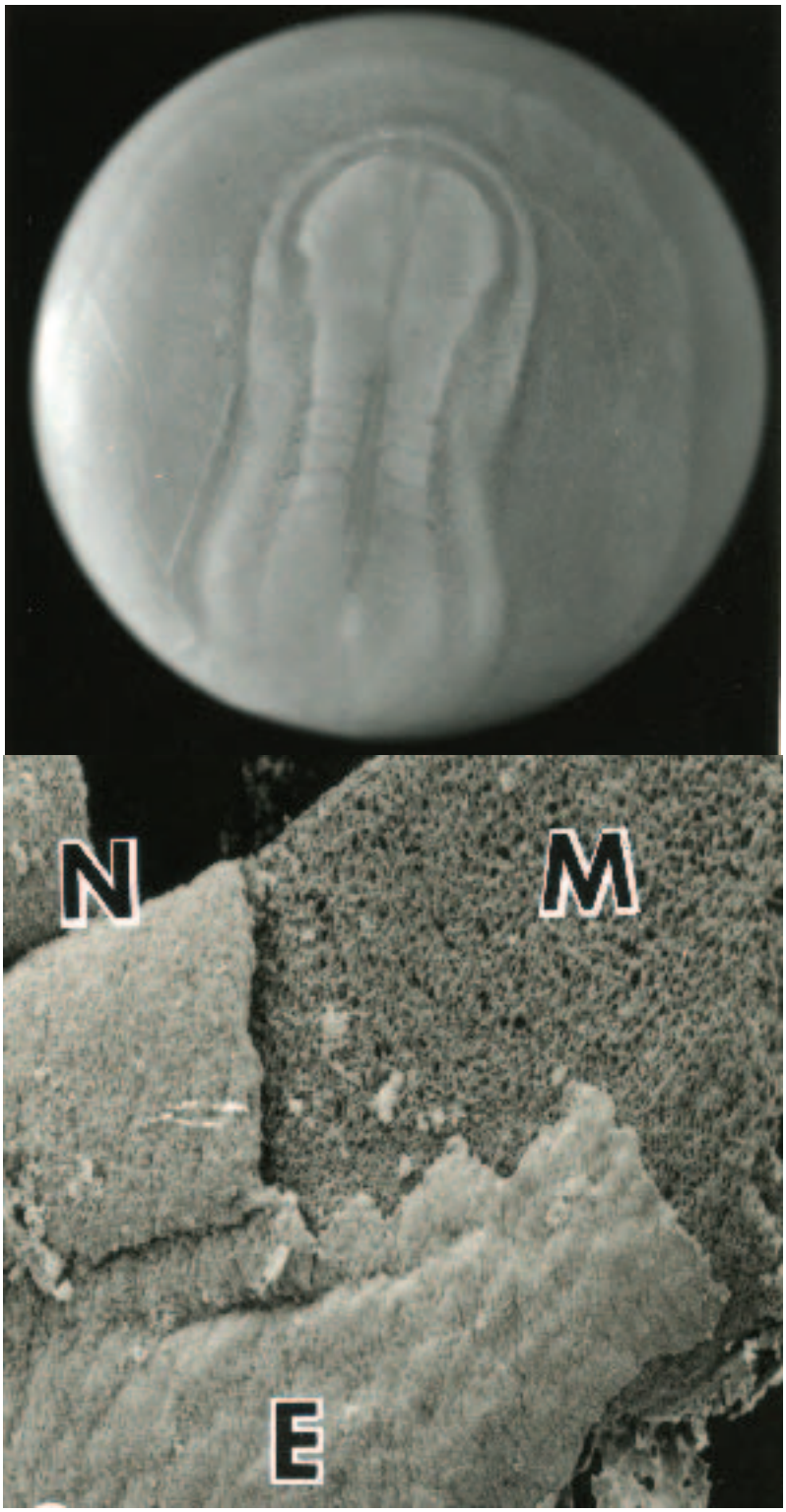

Fig. 3. (*Above*). An opossum embryo from late in prenatal day eight photographed floating free in a phosphate buffer. Somites as well as the position of the developing brain and spinal cord are clearly evident. Note that the embryo is part of an embryonic sphere. X 80. (*Below*). A partially dissected opossum embryo of the same age illustrates the neural groove (N) and adjacent ectoderm (E). A region of ectoderm has been removed to expose the underlying mesodermal layer (M). SEM X 110.

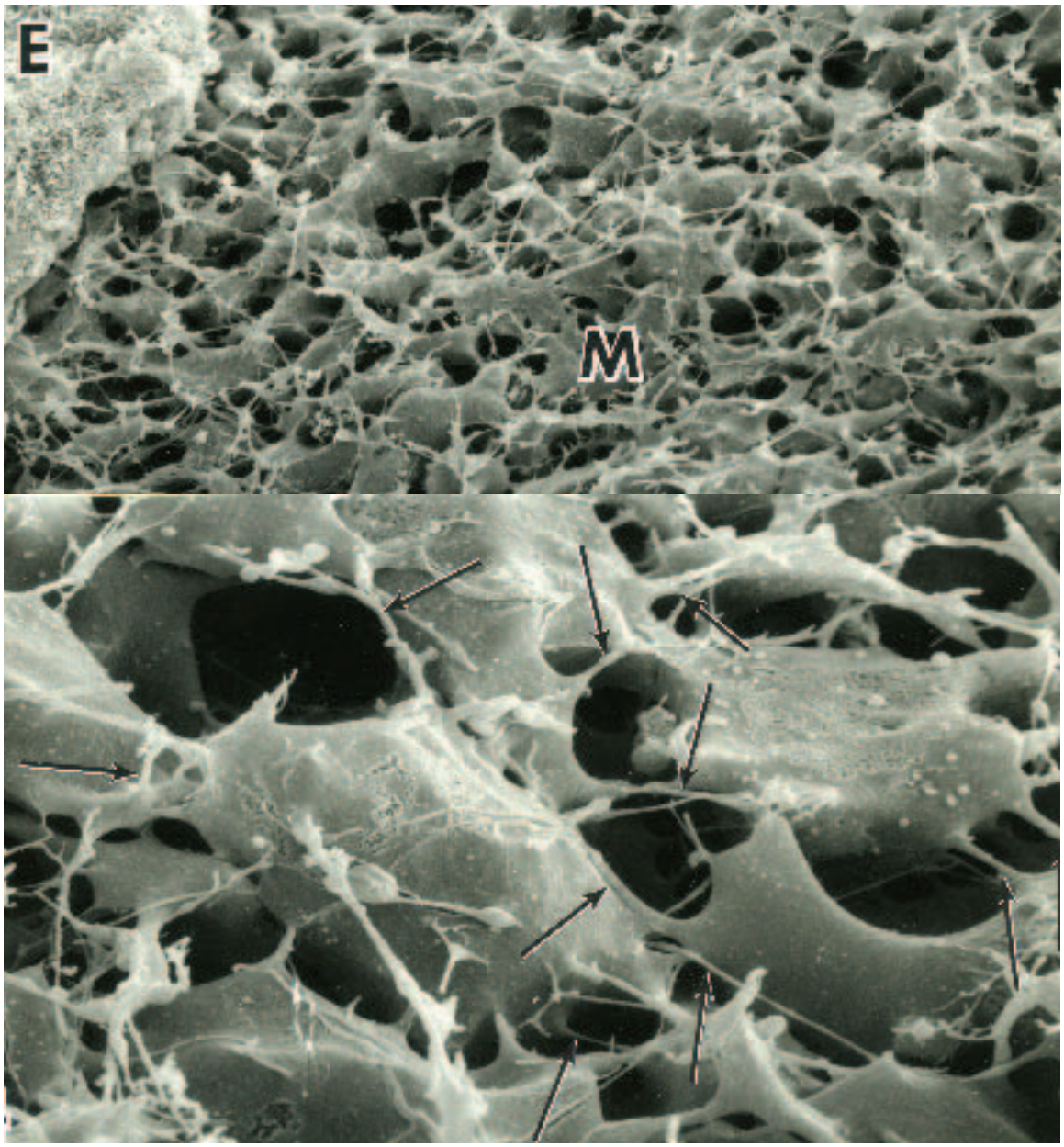

Fig. 4. (*Above*). When viewed at increased magnification the mesodermal layer (M) is observed to consist of a multilayered network of large, flattened, stellate-shaped cells. Note that the broad surface of individual mesodermal cells lies parallel to the external surface of the embryo. A portion of overlying ectoderm (E) is shown at the upper left. Eight-day opossum embryo. SEM X 500. (*Below*). Numerous, thin, thread-like cytoplasmic processes (arrows) extend from the mesodermal cells. The cytoplasmic processes may extend to adjacent mesodermal cells or course considerable distances to contact more distant mesodermal cells. Eight-day opossum embryo. SEM X 3,000.

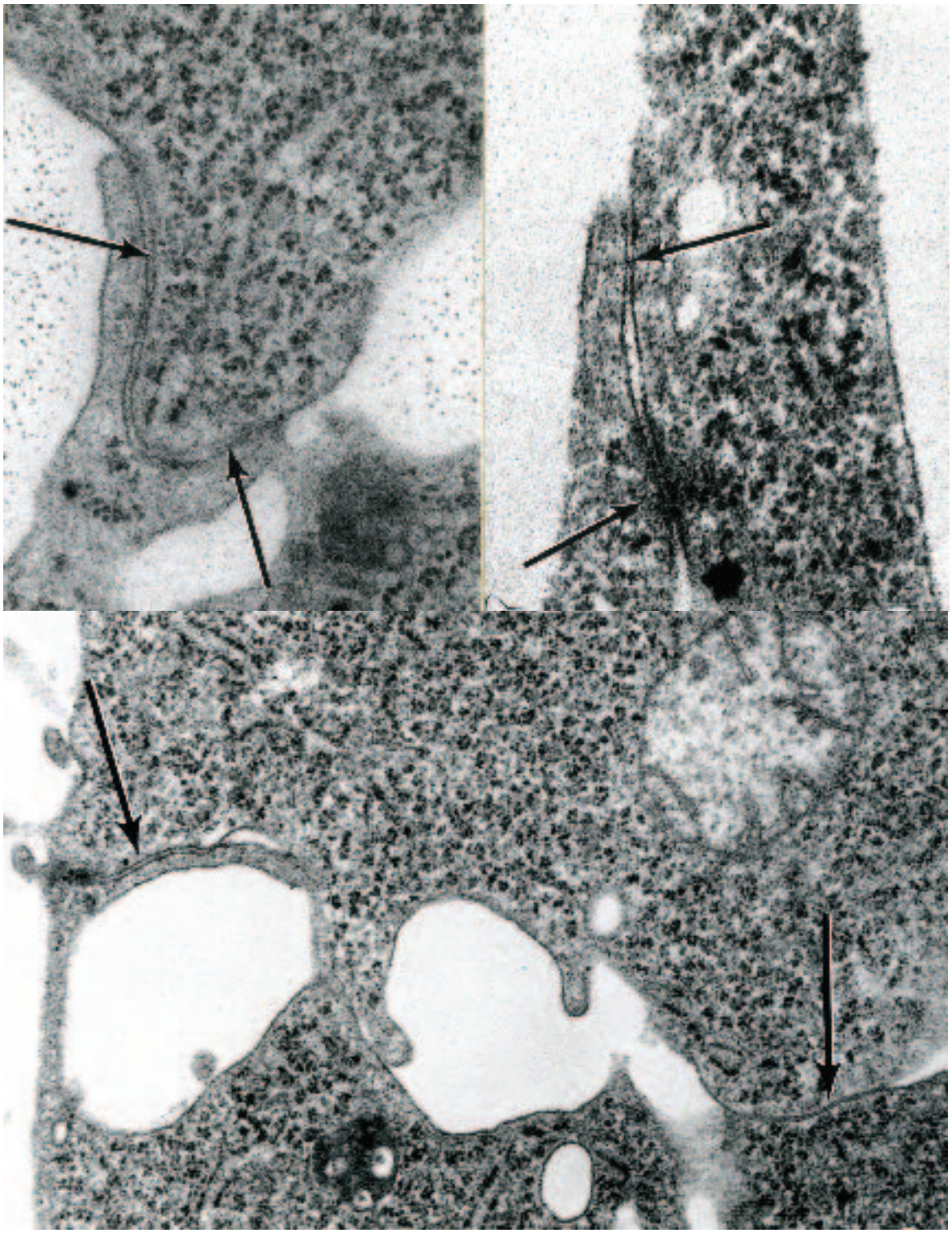

Fig. 5. (*Above left*). A micrograph illustrates a junctional complex (arrows) between a cytoplasmic process and the cell body of two adjacent mesodermal cells. TEM X 38,000. (*Above right*). A micrograph illustrates a junctional complex between two cytoplasmic processes of adjacent mesodermal cells. TEM X 50,000. (*Below*). A micrograph illustrates a junctional complex (arrows) between cell bodies of two adjacent mesodermal cells. TEM X 20,000.

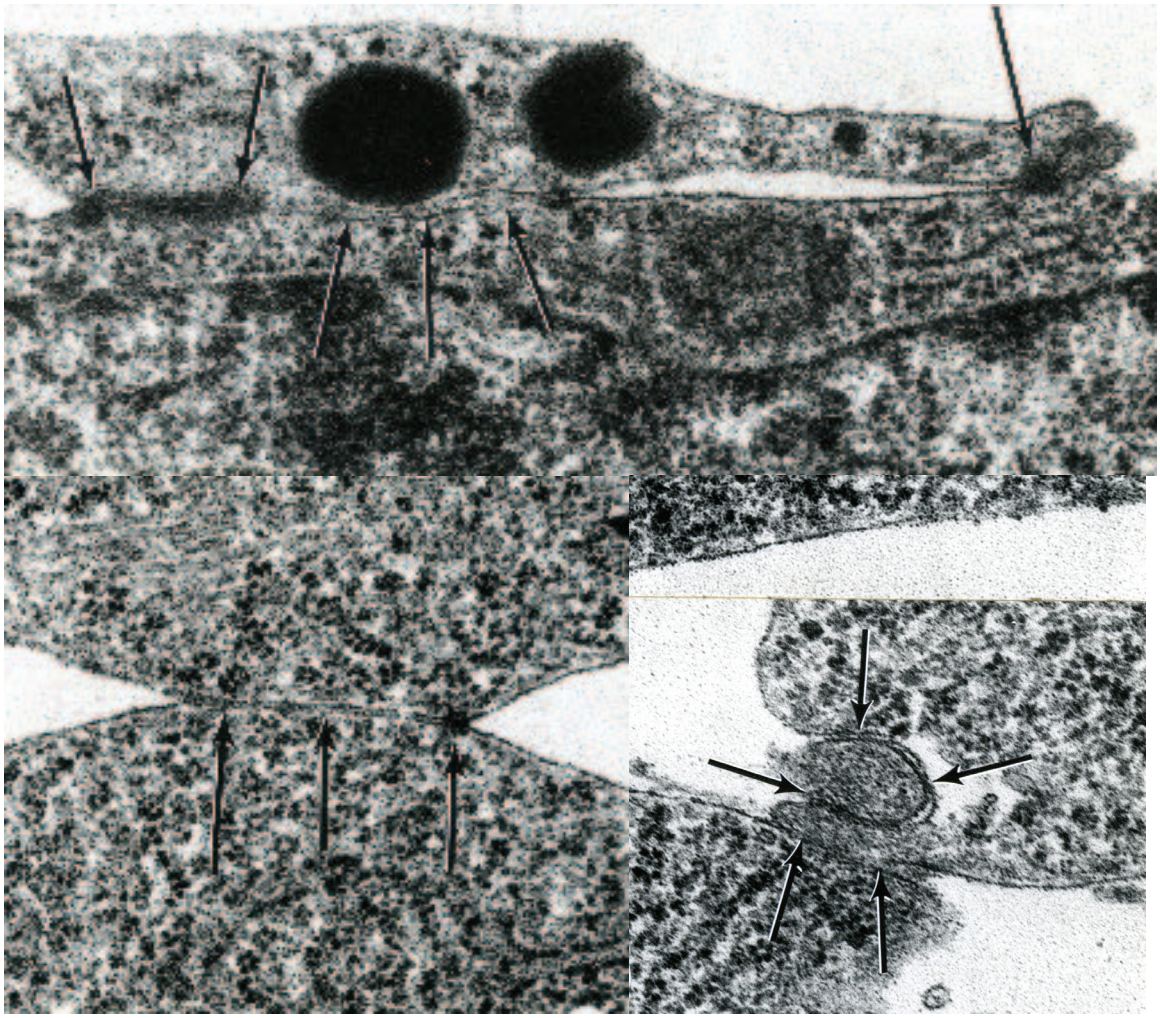

Fig. 6. (*Above*). A micrograph illustrates junctional complexes (arrows) between the cell body and a large cytoplasmic process of adjacent mesodermal cells. Note that the junctional complexes to the extreme right and left in the photomicrograph show an increase in electron density that appears similar to attachment plaques associated with desmosomes. TEM X 50,000. (*Below left*). A micrograph illustrates a junctional complex (arrows) between the cell bodies of two adjacent mesodermal cells. TEM X 50,000. (*Below right*). A junctional complex (arrows) unites a thin cytoplasmic process and the cell body of a mesodermal cell. Note that the cytoplasmic process lies within a groove on the external surface of the mesodermal cell. Note also the junctional complex between the two adjacent mesodermal cells (bottom arrows). TEM X 50,000.

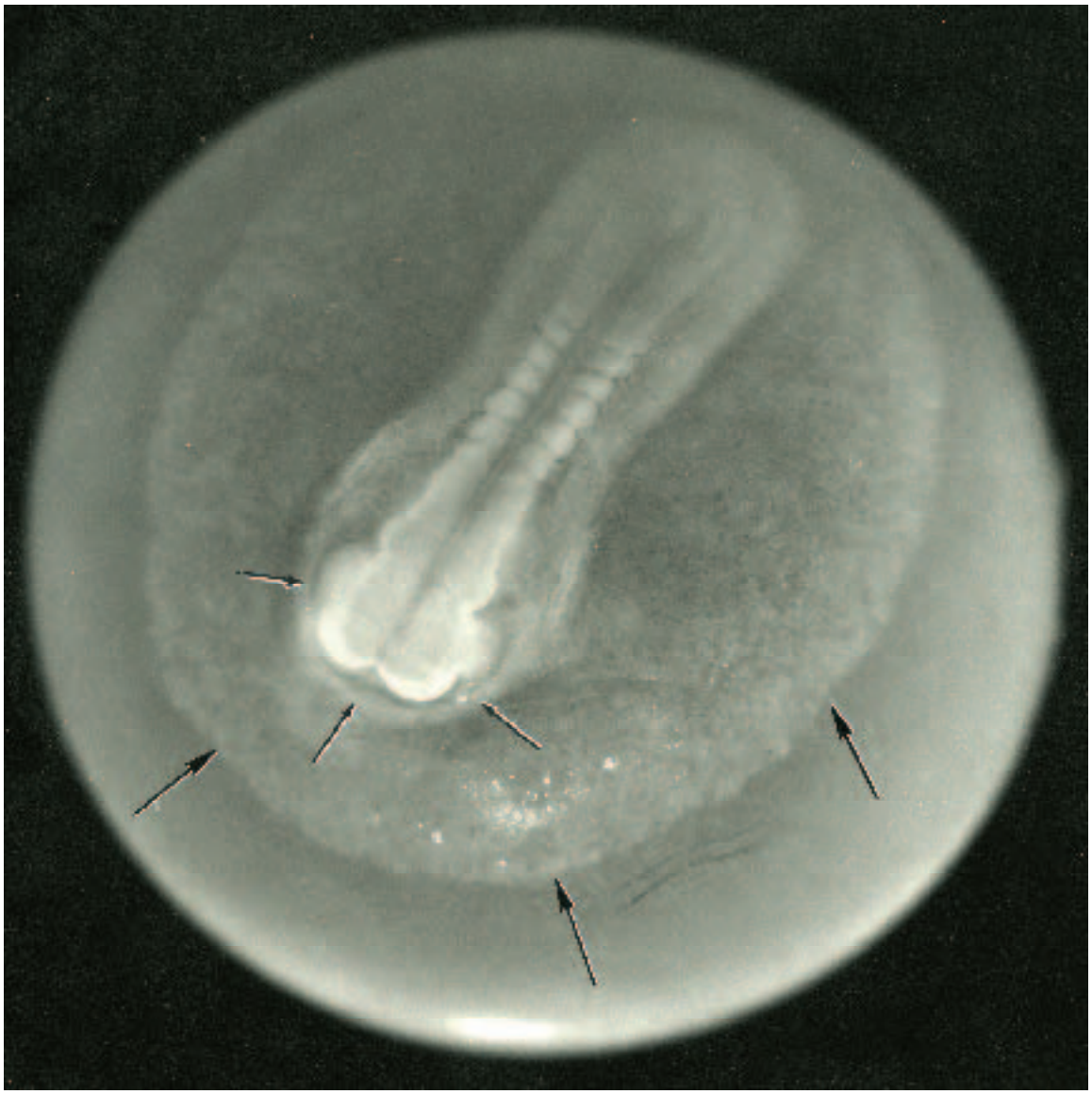

Fig. 7. The nine-day opossum embryo is a component of the blastocyst wall, which floats freely in uterine secretions during this period of gestation. The blastocyst is separated from surrounding maternal tissues by a transparent shell membrane that envelops the blastocyst. The shell membrane of this specimen can be visualized by a wrinkle found between the two arrows at the lower right. The lateral extent of the mesoderm in the embryonic sphere can be observed in this specimen (large arrows). Somites and the developing nervous system can be visualized also. Note the formation of the proamniotic folds (small arrows) around the head region of the developing embryo. X 60.

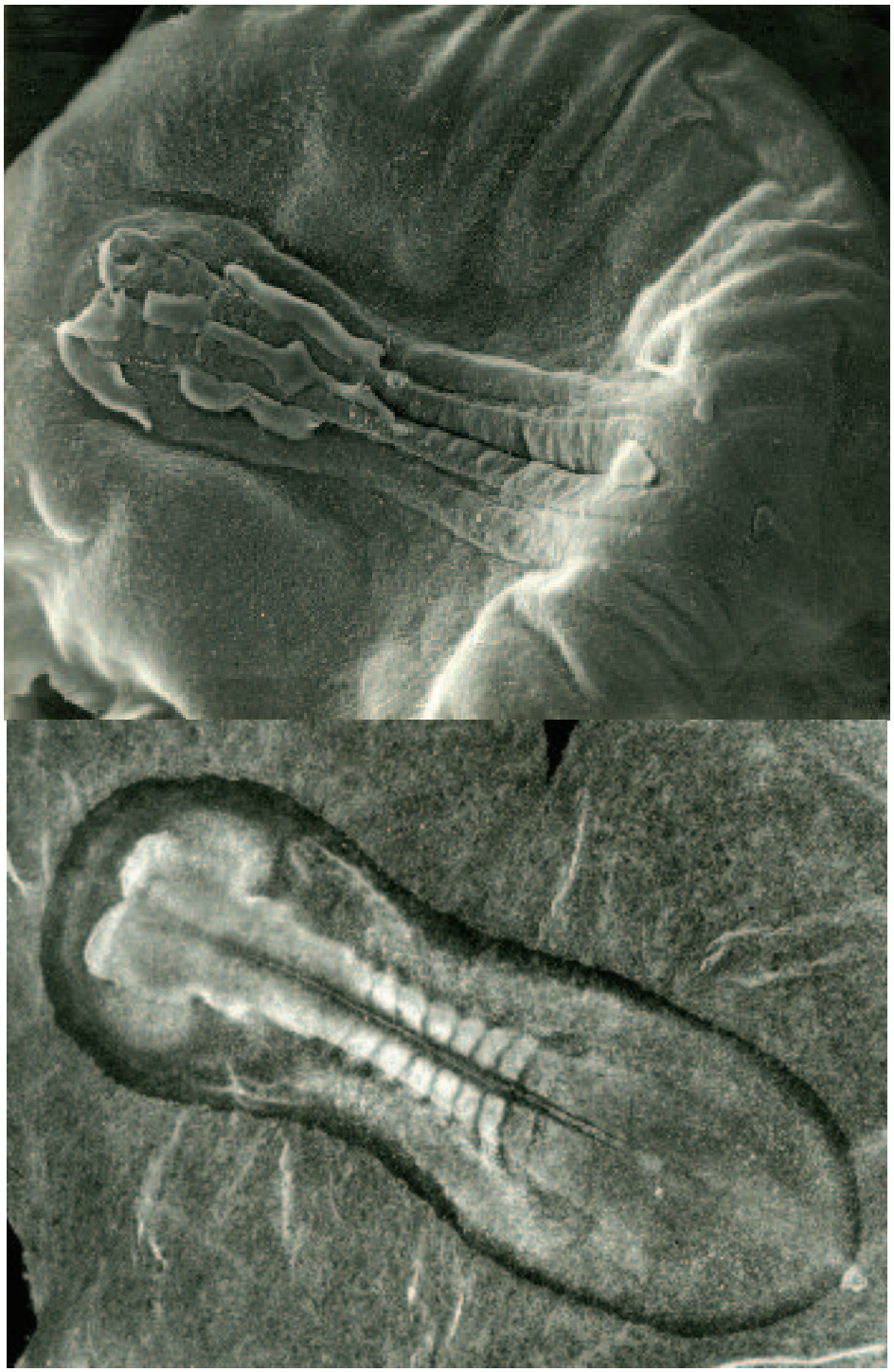

Fig. 8. (*Above*). A nine-day opossum blastocyst examined following the removal of the surrounding shell membrane illustrates that the opossum embryo is continuous with and a component of the embryonic sphere (blastocyst wall). SEM X 50. (*Below*). An air-dried nine-day blastocyst photographed with direct light illustrates in greater detail subcomponents and the extent of the forming opossum embryo. X 50.

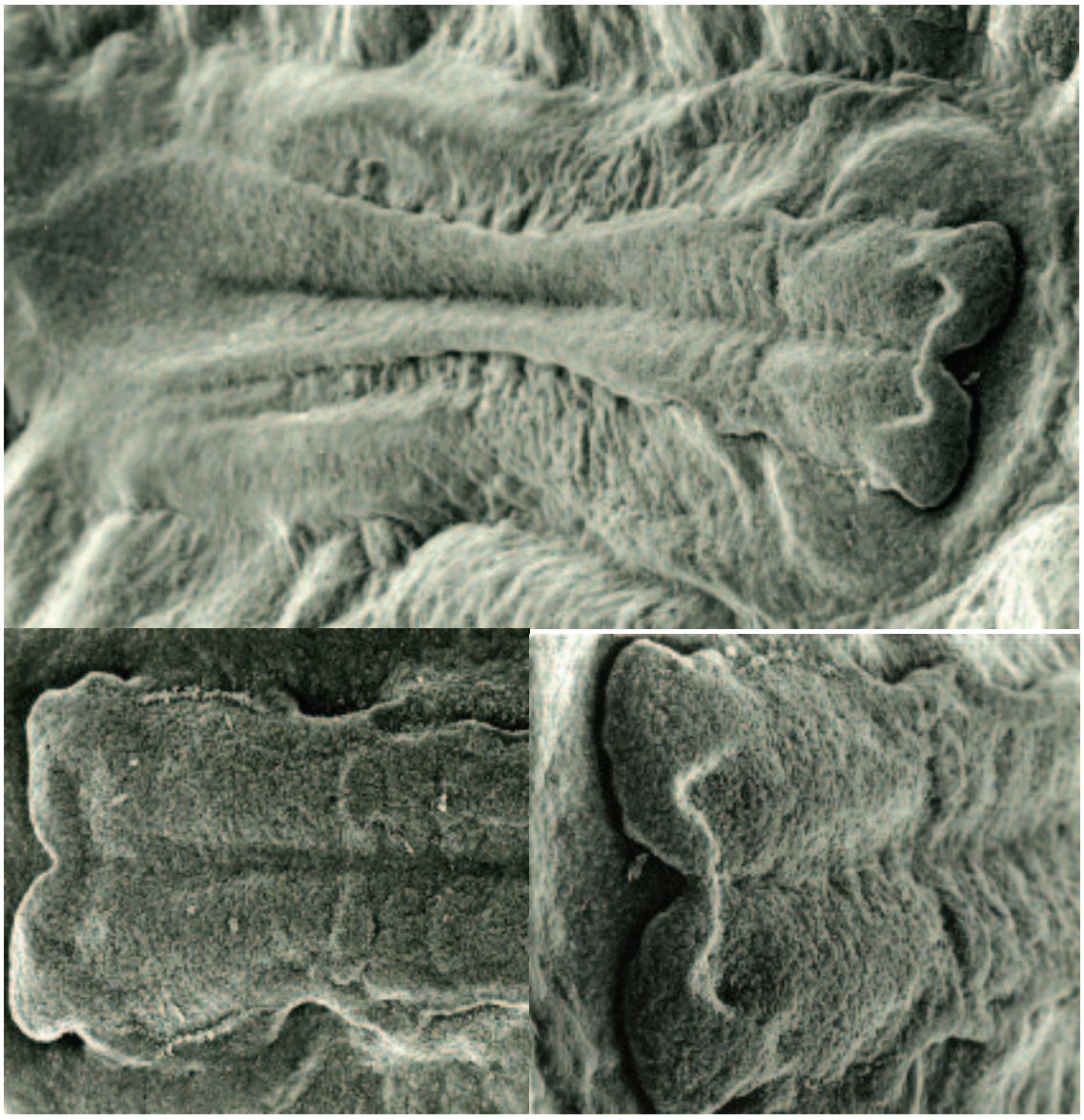

Fig. 9. (*Above*). A micrograph illustrates the surface features of an opossum embryo growing within the wall of a nine-day old blastocyst. The surrounding shell membrane has been removed. The ectodermal cells of the forming embryo have differentiated into and established the initial pattern for the central nervous system. The developing brain can be observed at the extreme right. The developing spinal cord, which appears as a deep groove, courses horizontally along the length of the embryo toward the caudal end at the left. SEM X 75. (*Below left*). A micrograph illustrates the developing forebrain (left) and midbrain (right) regions of the nine-day opossum embryo. SEM X 100. (*Below right*). When the nine-day opossum embryo is viewed from an angle in front and toward the embryo, the forming brain region appears somewhat elevated in comparison to the remainder of the embryo. SEM X 100.

Fig. 10. (*Above left*). When the forming spinal cord region of the nine-day opossum embryo is viewed at increased magnification details of the surface structure of the neural folds (NF) as well as the neural groove can be observed. SEM X 200. (*Above right*). A slightly older nine-day opossum embryo illustrates a continued expansion of the neural folds (NF) to establish a much deeper and narrower neural groove. Note the continuity between the ectoderm forming the neural folds and ectoderm covering the parietal mesoderm (M). SEM X 120. (*Below*). The forming tail region of a nine-day opossum embryo. The neural groove can be observed at the extreme left. SEM X 200.

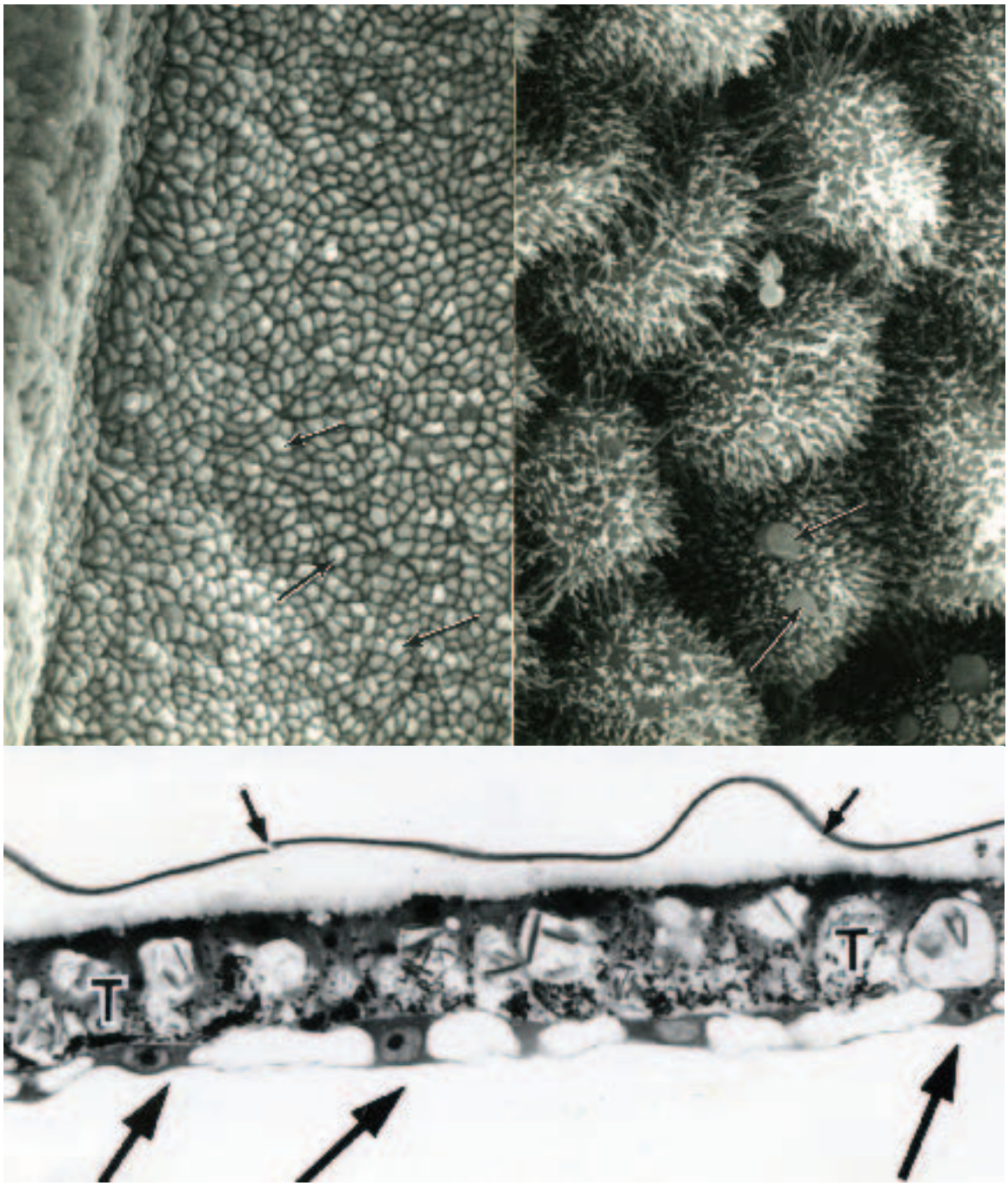

Fig. 11. (*Above left*). A micrograph illustrates a region of the nine-day opossum embryo where the ectoderm overlying the parietal mesoderm becomes continuous with that covering the yolk-sac chorion. Note that the apices of the latter (arrows) bulge from the surface clearly defining individual ectodermal cells. SEM X 225. (*Above right*). The bulging ectodermal cell apices that lie away from the embryo proper when viewed at increased magnification exhibit numerous, elongate microvilli and occasional cytoplasmic blebs (arrows). SEM X 3,200. (*Below*). A section through a portion of the embryonic sphere on the side opposite the embryo exhibits an overlying shell membrane (small arrows). The wall of the embryonic sphere at this location consists of trophectoderm (T) and cells of endoderm (large arrows). Nine-day opossum embryo. LM X 700.

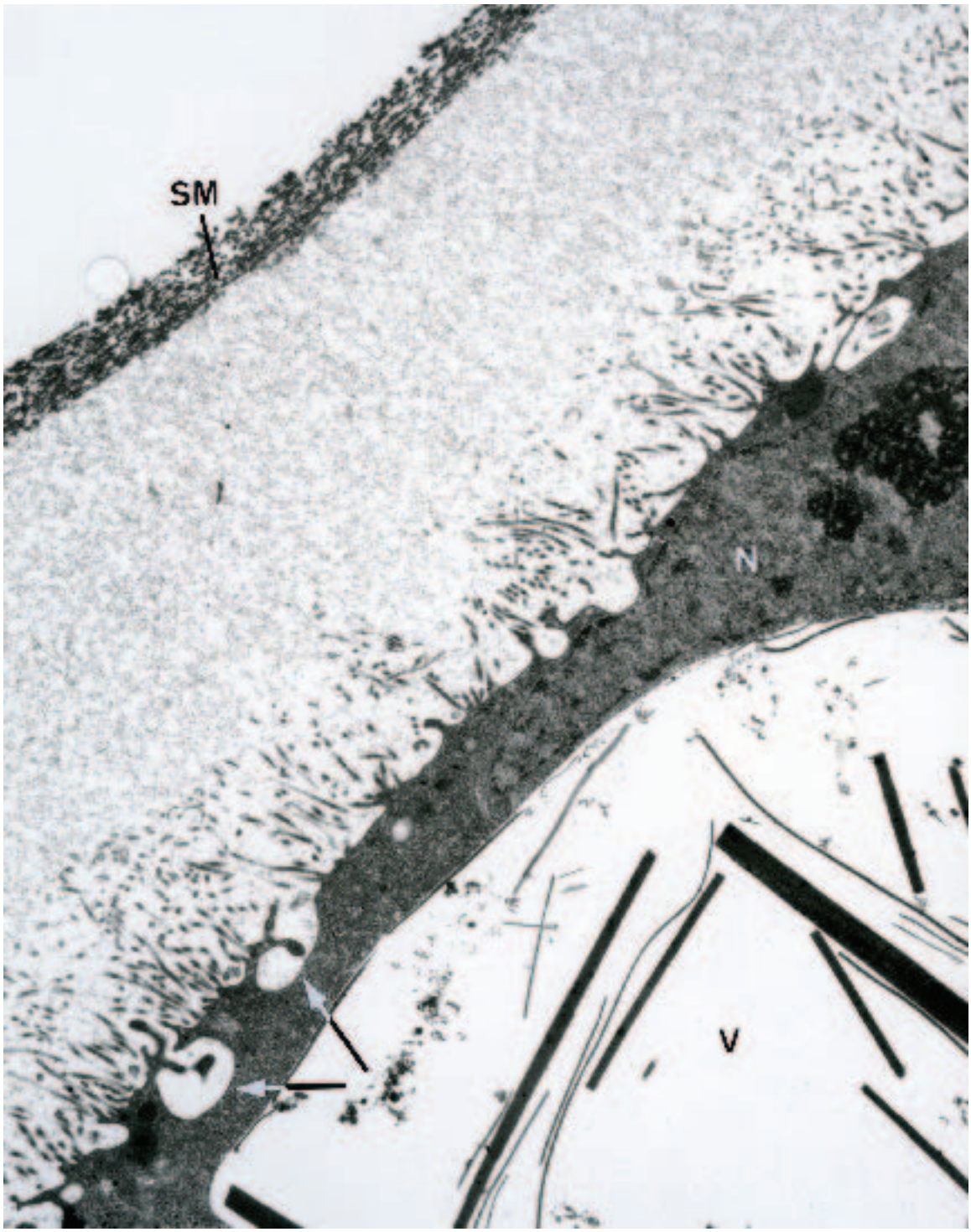

Fig. 12. Cells comprising the trophectoderm of the nine-day opossum embryo exhibit a well-developed system of invaginations from the apical plasmalemma (arrows). Note the concentration of elongate microvilli extending from the apical region of the cell. A large central vacuole (V) is present in the majority of cells that contains electron-dense crystals and/or a flocculent amorphous material. The nucleus (N) is shown in the upper right portion of the cell. Note the shell membrane (SM) located at the upper left and the amorphous material that lies between the shell membrane and the apical plasmalemma of the trophectodermal cell. TEM X 13,000.

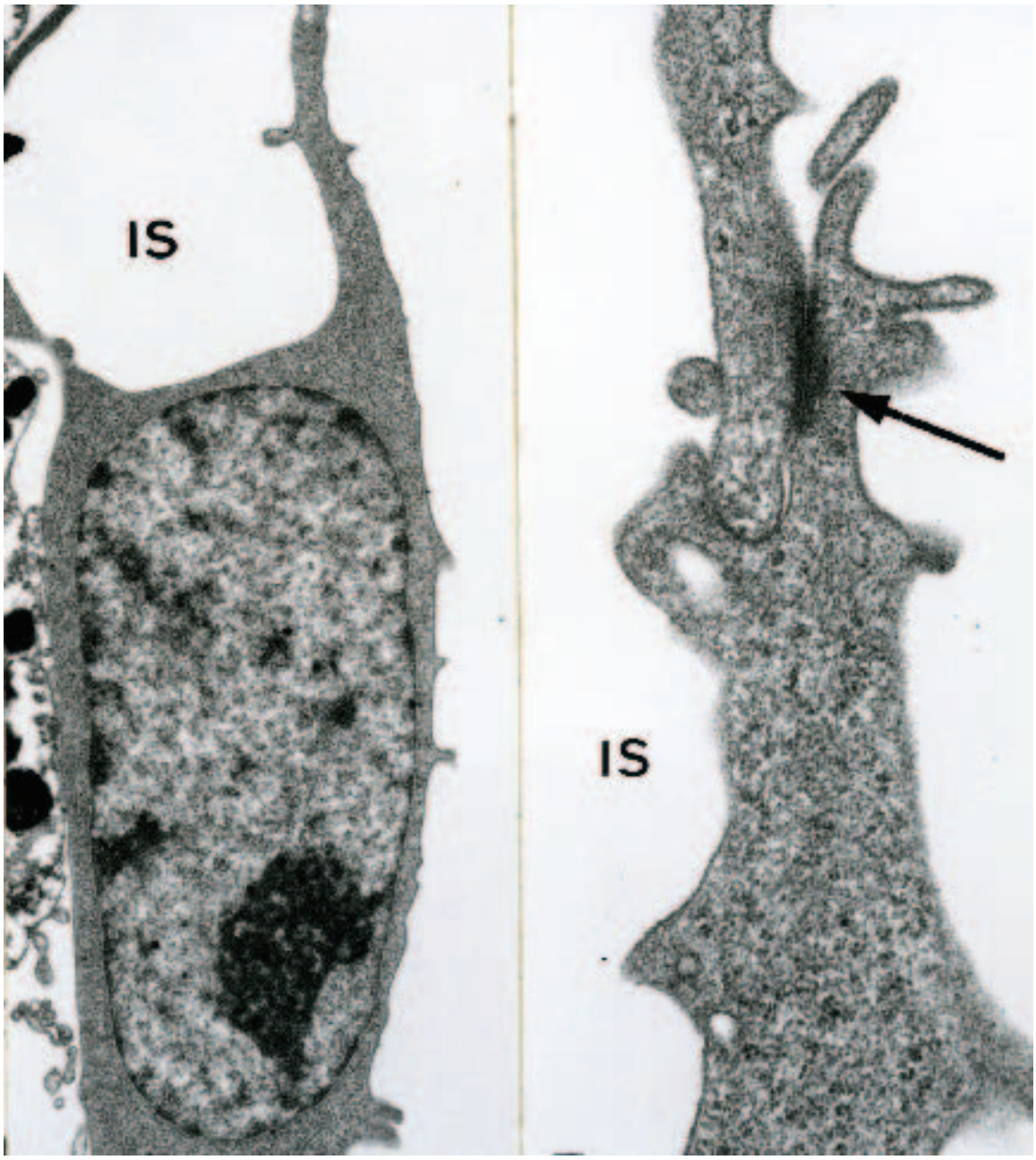

Fig. 13. (*Left*). A micrograph illustrates a segment of an endodermal cell from that region of the embryonic sphere opposite the embryo of a nine-day blastocyst. Compare this endodermal cell with those shown in figure 11. Note the large intercellular space (IS). TEM X 8,000. (*Right*). A micrograph illustrates a junctional complex (arrow) that links cytoplasmic processes of two adjacent endodermal cells. These thin processes unite with those of adjacent endodermal cells to bound large intercellular spaces (IS). Note similar thin endodermal cell processes also shown in figure 11. TEM X 24,000.

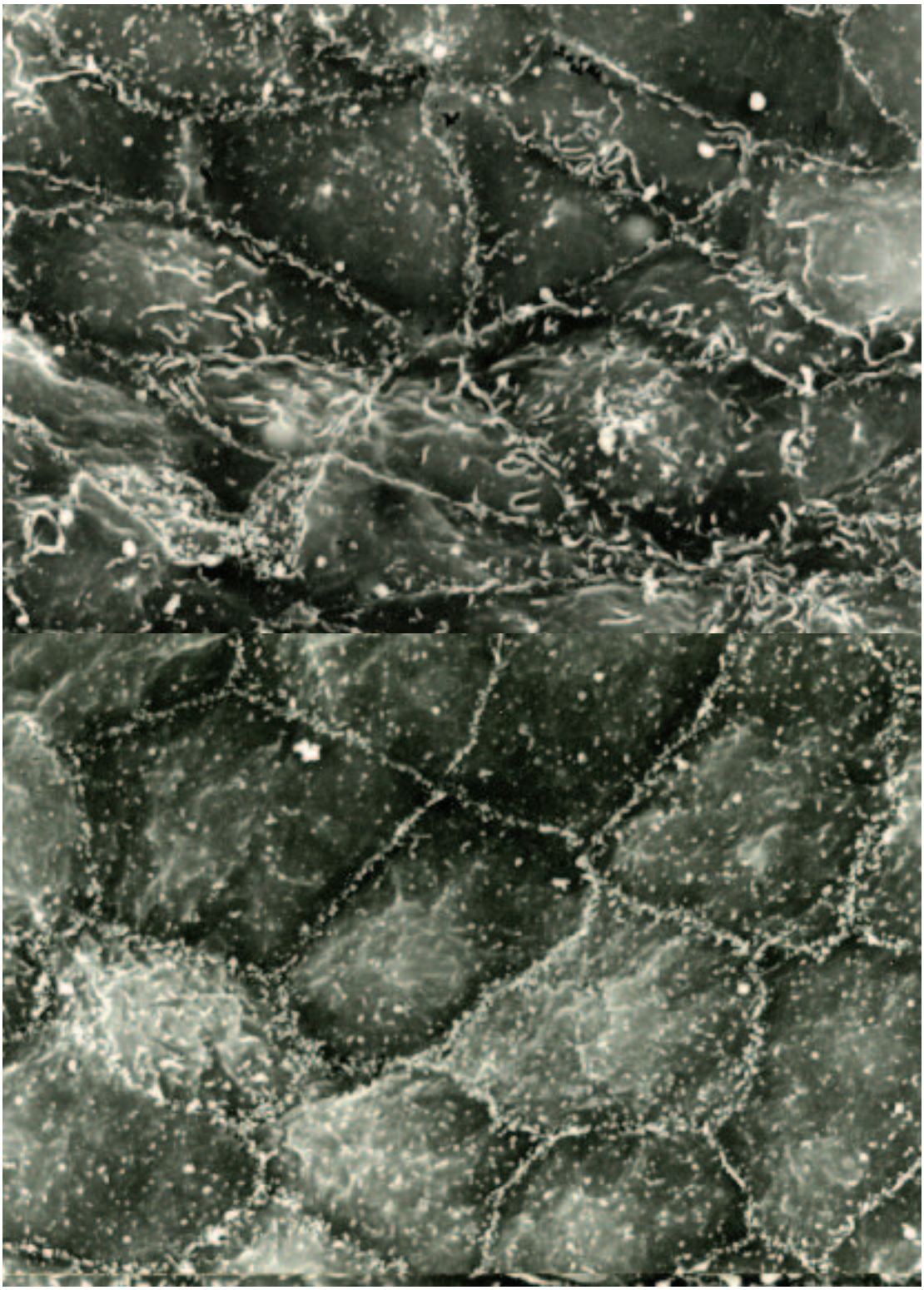

Fig. 14. (*Above*). Endodermal cells that line the internal surface of the nine-day opossum embryo exhibit distinct cell boundaries but only scattered and poorly developed microvilli and microplicae. SEM X 4,000. (*Below*). Endodermal cells also line the interior wall of the yolk-sac placenta from the side of the embryonic sphere opposite the embryo. These cells also are clearly delineated by distinct cell boundaries. The associated microvilli on their luminal surface are short and scattered but tend to be concentrated at cell junctions. SEM X 4,000.

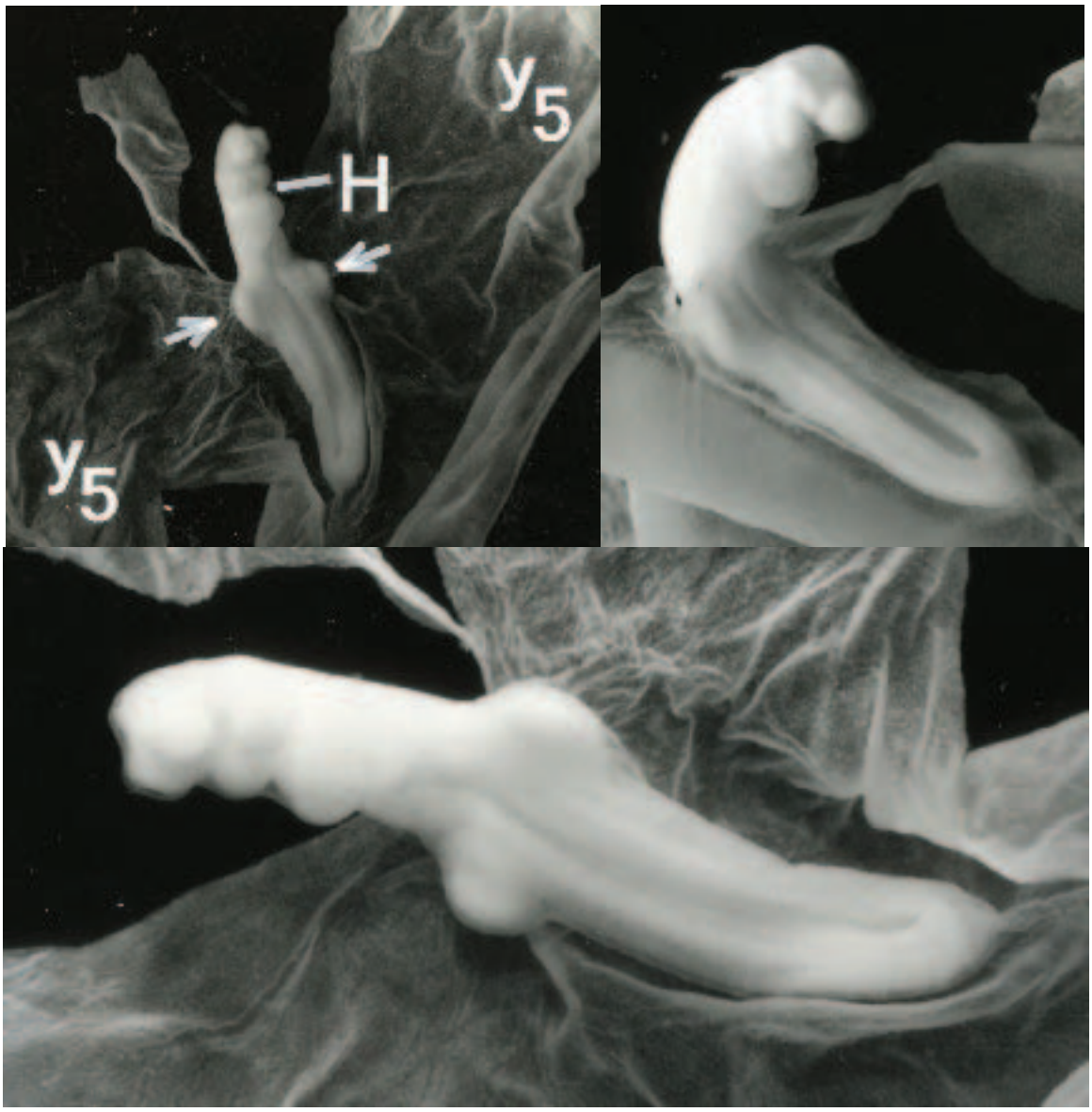

Fig. 15. *(Above left)*. The yolk sac placenta (Y5) of an opossum early in the tenth day of gestation opened and reflected to expose the embryo. The developing forelimbs (arrows) and forming heart (H) have been labeled. X 20. (*Above right*). Another fixed early ten-day opossum embryo photographed while floating in a saline buffer. X 40. (*Below*). At increased magnification and when examine at a slightly different angle external details of the forming early ten-day opossum embryo can be observed. Note the appearance of the pharyngeal arches, the bulge of the developing heart, and the state of the developing forelimbs as well as the trunk of the embryo. The hind limbs have yet to appear. The embryo is contained within a thin, transparent amniotic membrane visible along the edge of the embryo in the region of the pharyngeal arches and heart. X 80.

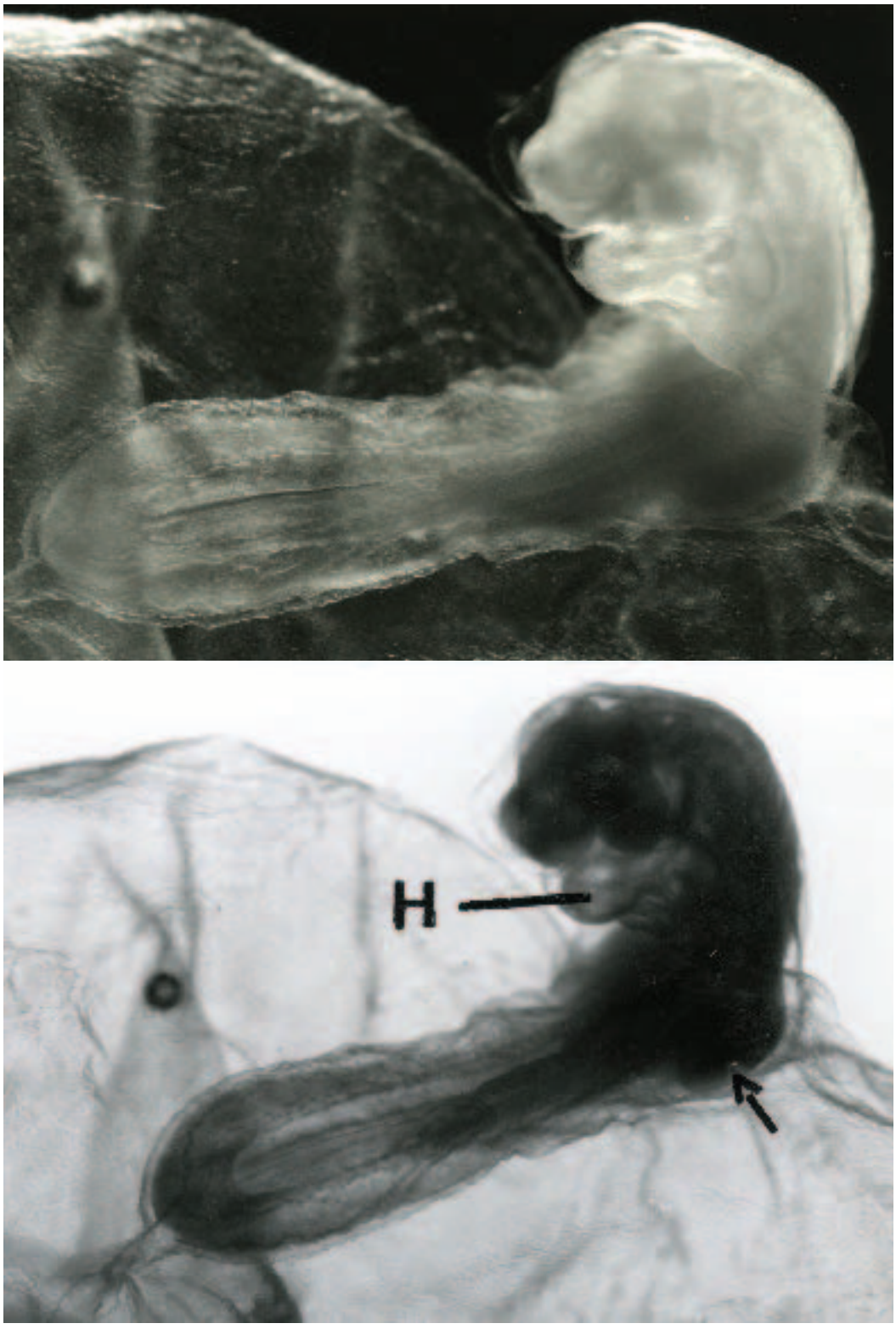

Fig.16. (*Above*). An early ten-day opossum embryo dissected free of the surrounding yolk sac placenta and photographed with direct light. X 75. (*Below*). A same opossum embryo as above but photographed using transilluminated lighting. Note the developing heart (H) and forelimb (arrow). X 75.

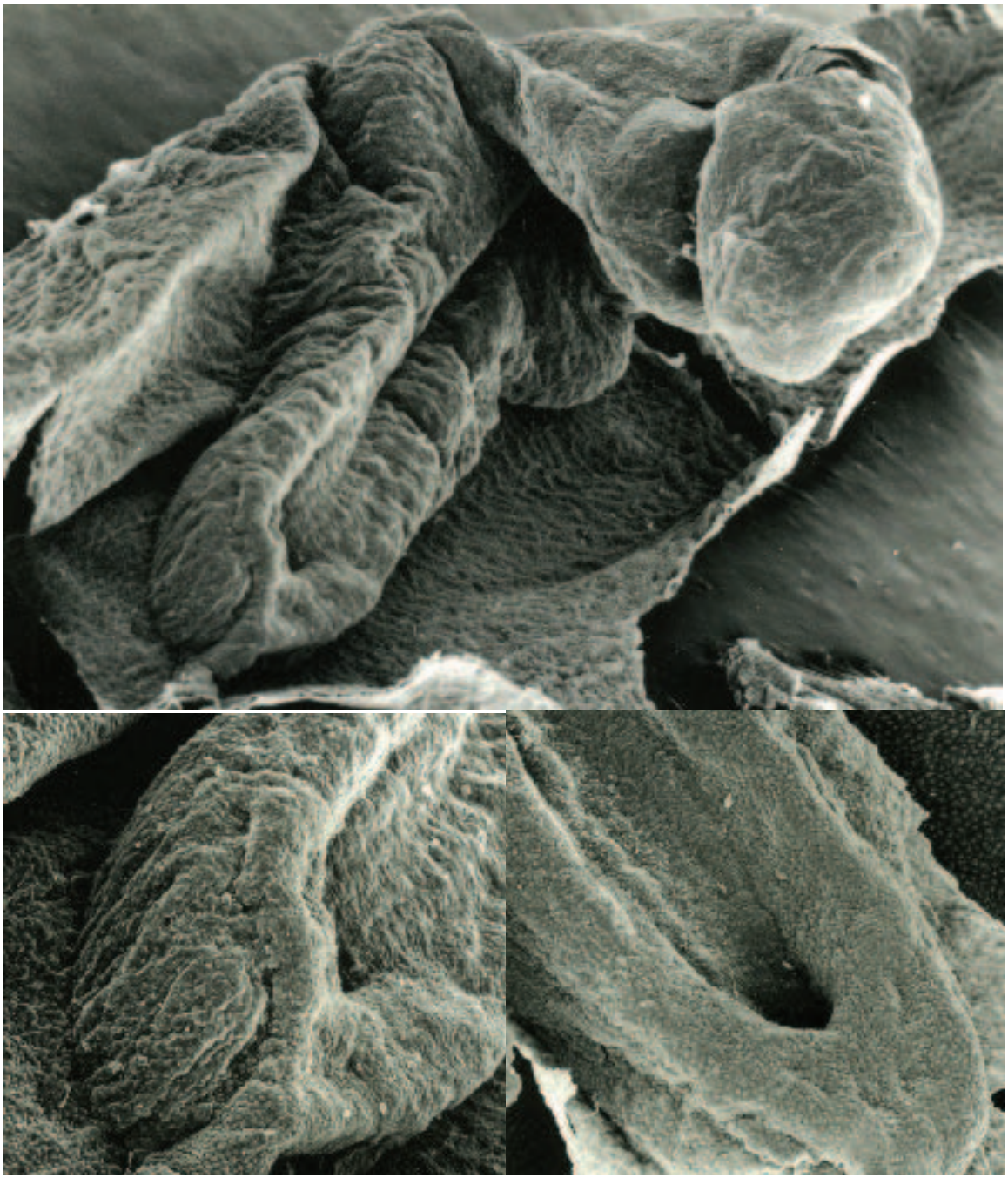

Fig. 17. (*Above*). The surrounding yolk-sac placenta has been opened to reveal an opossum embryo early during the tenth day of gestation. It remains enshrouded by the amniotic sac; however, the position of the developing forelimbs is clearly evident. SEM X 40. (*Below left*). A micrograph illustrates the developing caudal end of the early ten-day opossum embryo. SEM X 120. (*Below right*). The developing caudal end of the early ten-day opossum embryo but viewed to show its ventral surface. The amnion has been removed. SEM X 100.

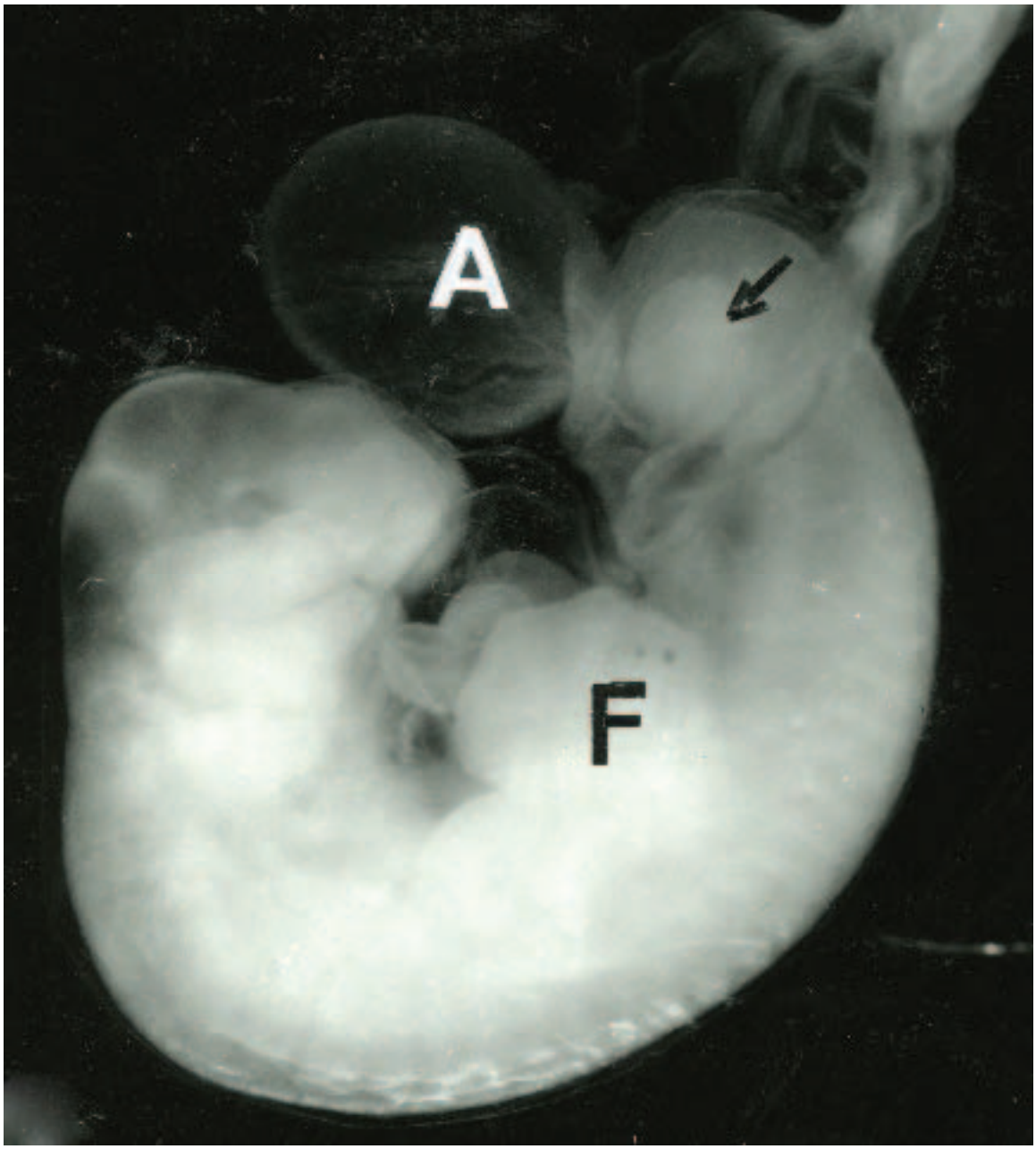

Fig. 18. By late in prenatal day ten the external features of the opossum embryo have changed dramatically. The allantoic sac (A) is apparent for the first time, as is the initial external evidence for the appearance of the hind limb (arrow). Compare the bud-like structure of the hind limb with the developing forelimb (F), which at this time shows the initial formation of digits. Note the continued development and expansion of the head region, which now exhibits mandibular and hyoid arches. Note also what appears to be the initial position of the eye. Opossum embryo photographed with direct light while floating in buffer. The surrounding yolk-sac placenta was dissected away exposing the embryo for examination. X 300.

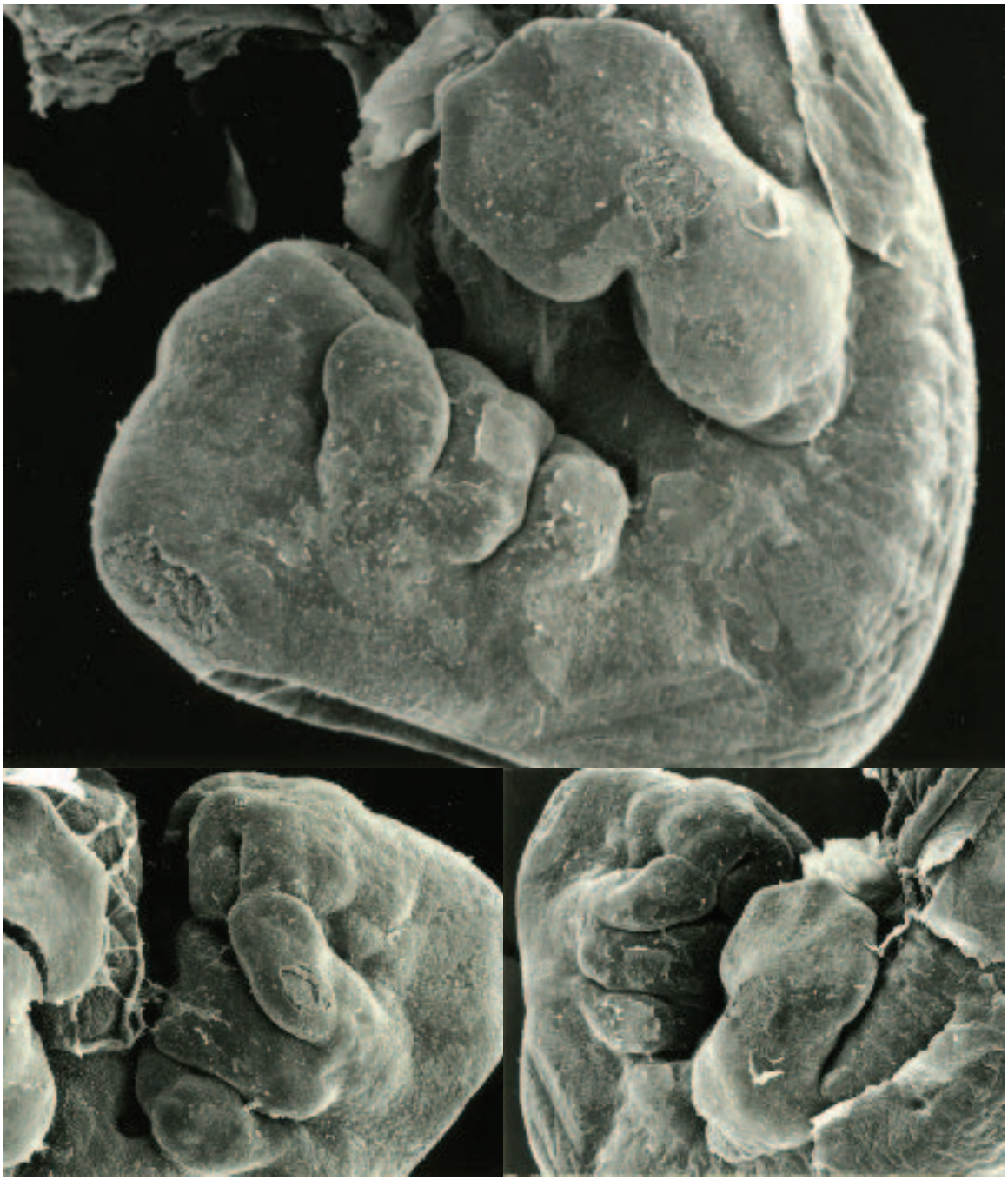

Fig. 19. (*Above*). The external features of the developing head and forelimb of an opossum embryo examined late in prenatal day ten. Compare this illustration with figure 18. SEM X 50. (*Below left*). The forming head of the opossum embryo in the above illustration but viewed from an inferior lateral angle demonstrates more clearly the mandibular and hyoid arches, the forming external nares, and what appears to be position of the forming eye. SEM X 40. (*Below right*). The head of an opossum embryo (late in prenatal day ten) viewed from an inferior angle details these structures (mandibular and hyoid arches, external nares, forming eye, and developing forepaw) again, but from a different angle. The thin membrane covering portions of this embryo as well as the embryo in the top figure is the amnion. SEM X 40.

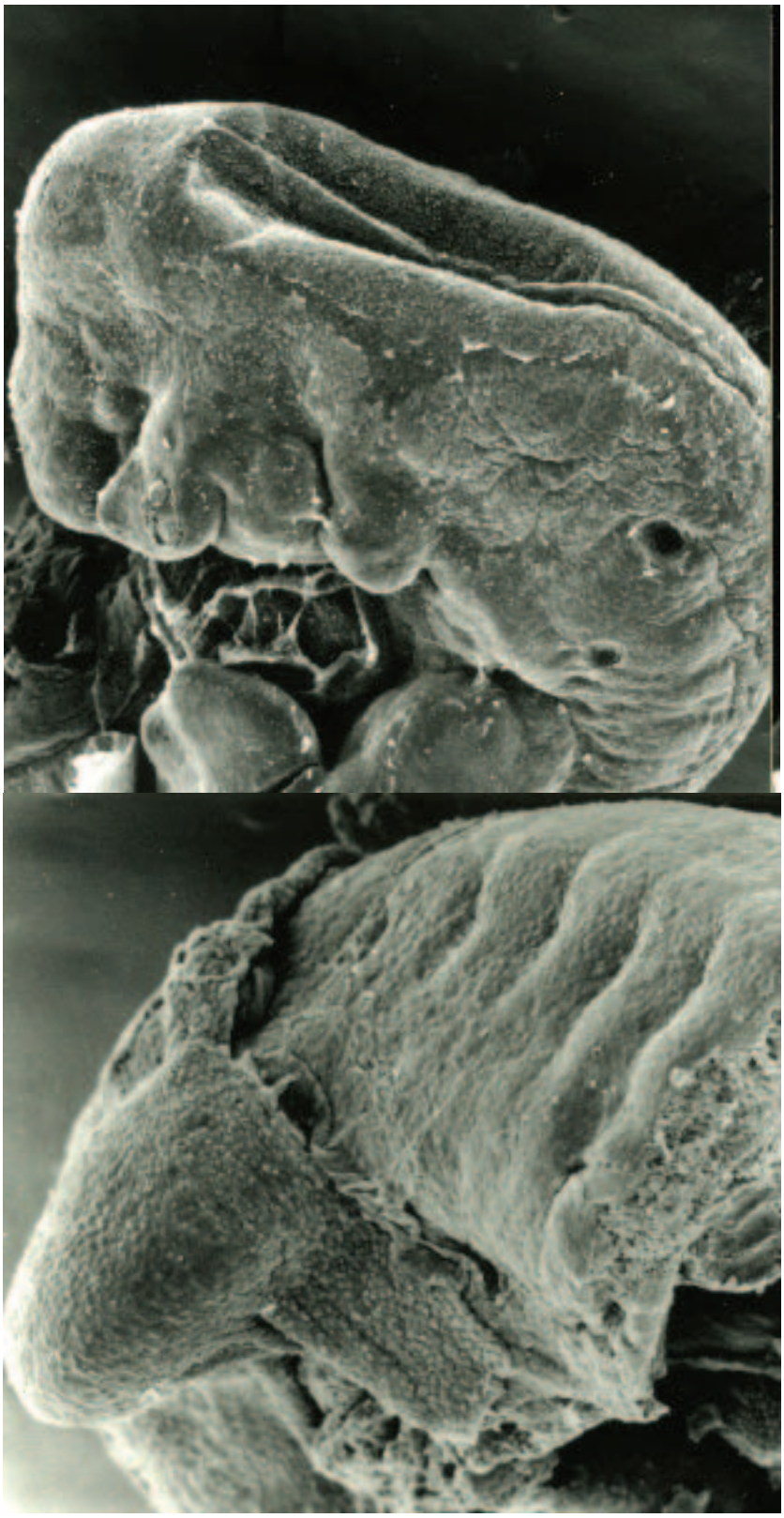

Fig. 20. (*Above*). The forming eye is better defined in the opossum embryo late in day ten when viewed from a superior dorsal angle. The cervical flexure also is quite obvious from this angle as well as in ten-day opossum specimens viewed in figure 19. SEM X 40. (*Below*). A micrograph illustrates the developing hind limb of an opossum embryo late in prenatal day ten. SEM X 80.

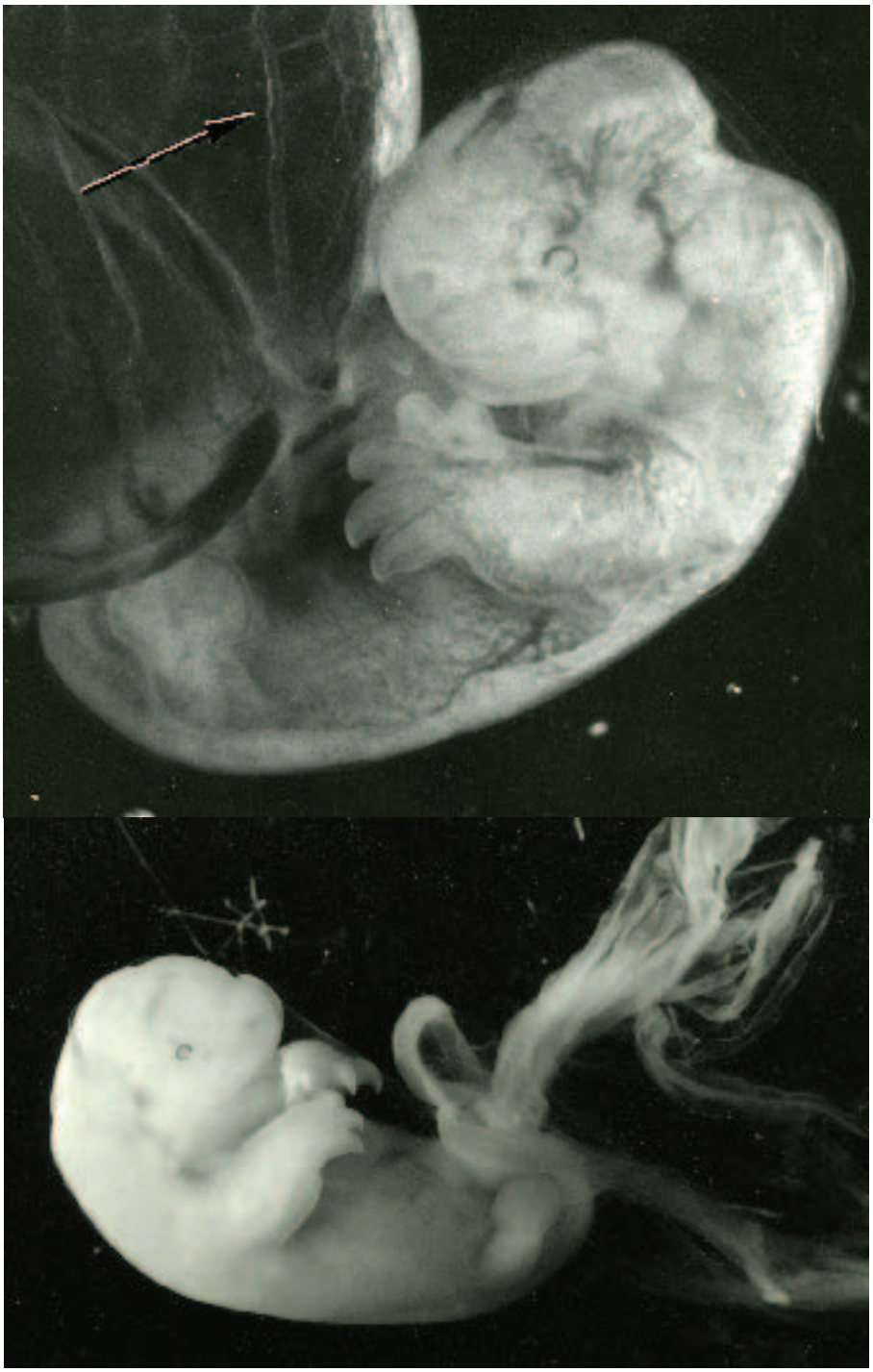

Fig. 21. (*Above*). An opossum embryo (eleventh prenatal day) photographed floating in buffer following removal of the surrounding yolk sac placenta. The large allantoic sac is to the left and crossed by the arrow. Note the vasculature associated with the forelimb and developing hind limb. The latter is only in the paddle stage of development whereas digits are now well established on the forepaw. The pigmented portion of the eye is visible beneath the transparent integument. X 60. (*Below*). An opossum embryo late in the eleventh prenatal day shows continued development of the forelimbs and the hind limb. Note that the features of the head (mouth, external nares, tongue, and pigmentation of eye) are clearly established by this stage of development. X 24.

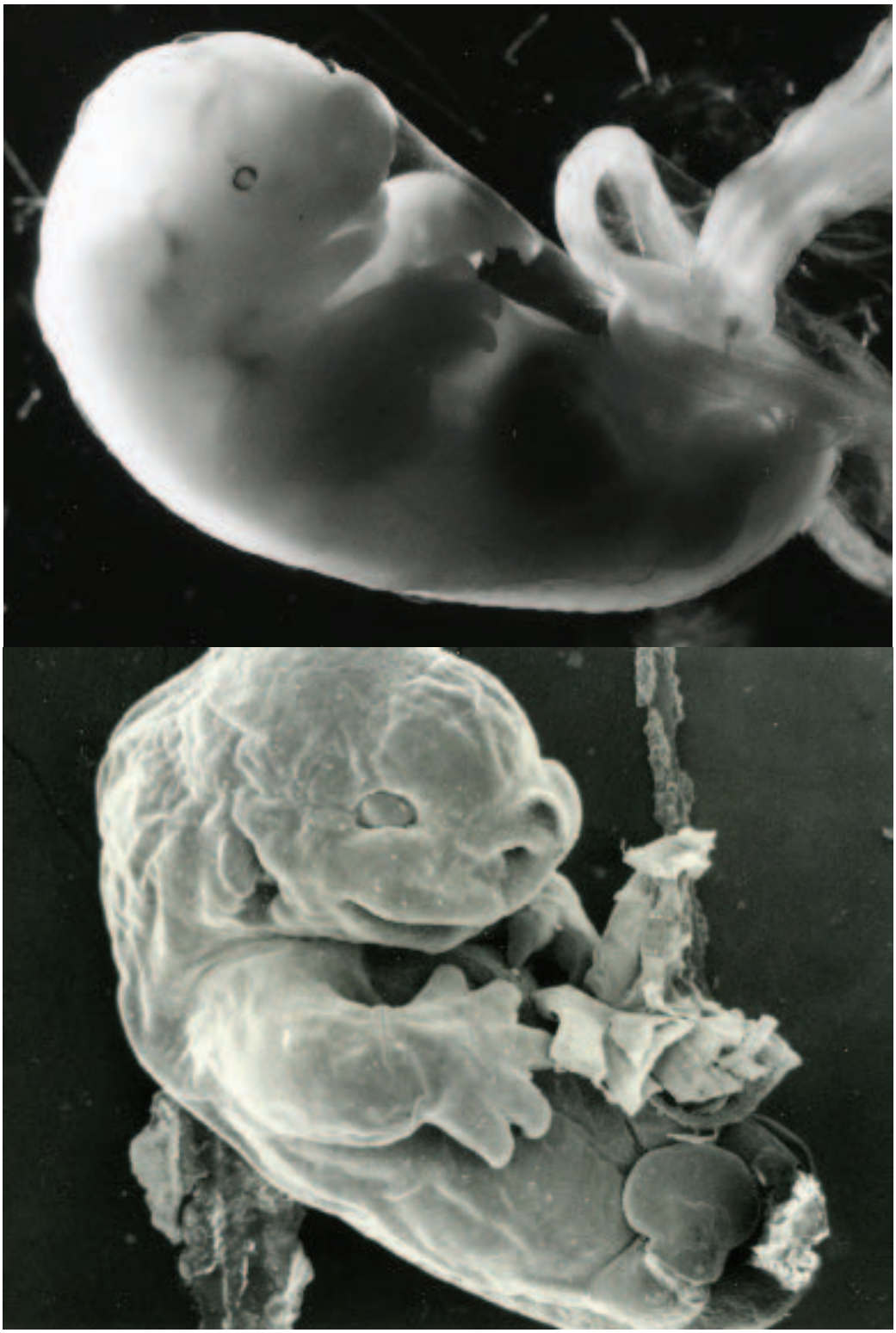

Fig. 22. (*Above*). The same opossum embryo shown in figure 21 (bottom) but photographed using transilluminated light illustrates the size and position of the liver at this time. The embryo remains enshrouded in its amniotic sac. X 50. (*Below*). When viewed by scanning electron microscopy the details of the head (external nares, mouth, eye, and ear) are features clearly established at this time. Compare and contrast the forelimb and hind limb. SEM X 50.

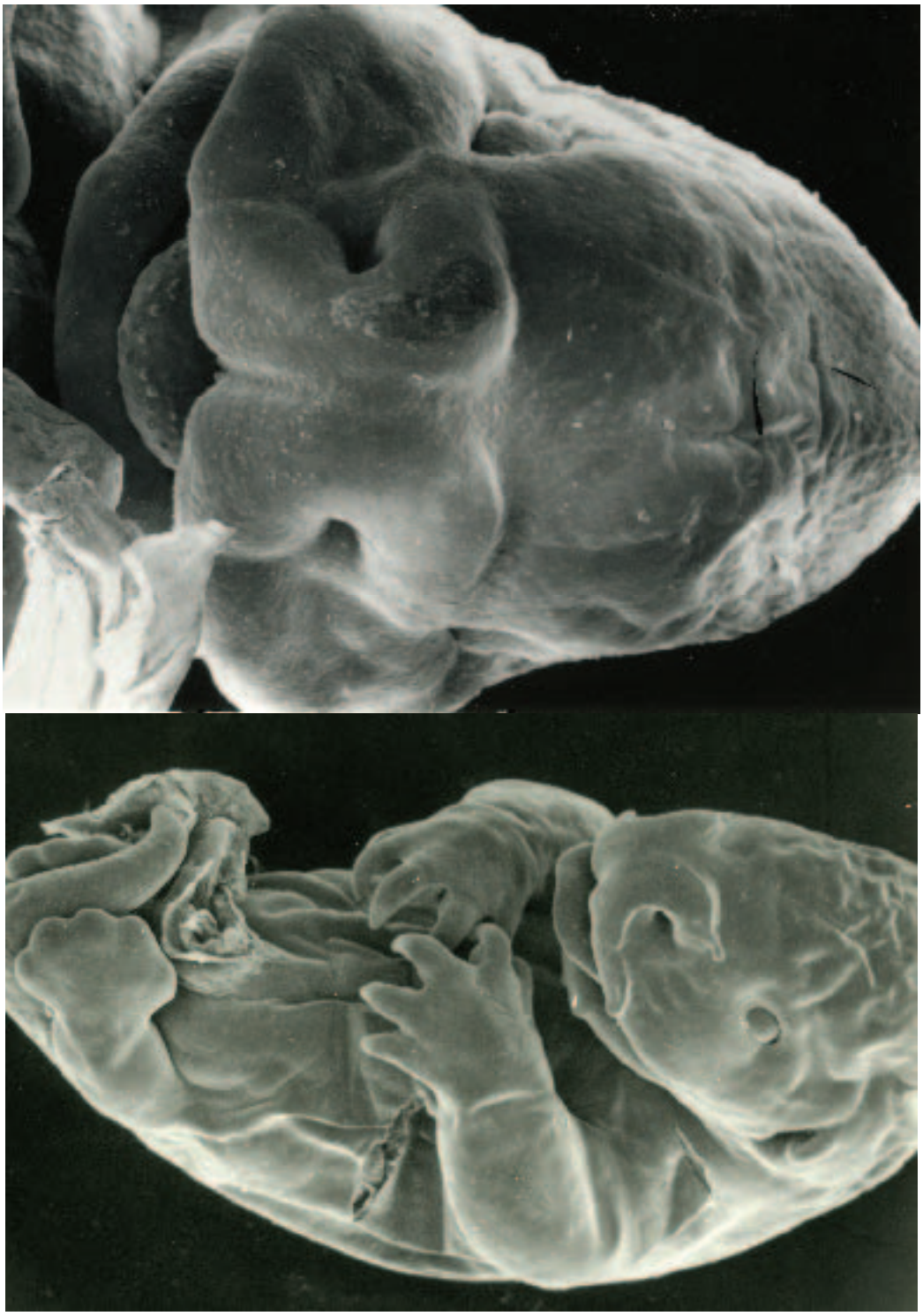

Fig. 23. (*Above*). The head of the eleven day opossum embryo when viewed at increased magnification from the front details the features of the forming snout as well as a developing mouth, a protruding tongue, the eyes and external nares. SEM X 50. (*Below*). A slightly older eleven-day opossum embryo exhibits the initial formation of digital ridges on the hind limb. Note the appearance of the developing eye and external ear and that the tongue is protruding further out of the oral cavity. Note also the initial development of the oral shield. SEM X 30.

Fig. 24. (*Above*). The head of the eleven-day opossum embryo shown in the previous figure viewed at increased magnification. Note the developing ear, eye, oral shield and tongue protruding from the oral cavity. Note also the angle of the mouth, which in this specimen remains open. SEM X 50. (*Below*). A micrograph illustrates an opossum embryo just prior to birth (approximately 12.5 days gestation). The pigmented portion of the eye, the external nares, oral shield, and open mouth with protruding tongue are well established. Digits of the forepaws are now equipped with deciduous claws. The hind limb remains paddle-like but does exhibit well-formed digital ridges. X 30.

Fig. 25. (*Above*). An opossum embryo at about 12.5 days gestation (just prior to birth) exhibits well-developed forelimbs the digits of which are equipped with deciduous claws. The mouth is large and surrounded by an oral shield. It contains a well-developed tongue. The hind limb is paddle-like but does show the differentiation of digital ridges. A periderm (epitrichium) covers the pinnae of the ears and the eyes prior to birth. Compare this figure with the bottom illustration of figure 24. SEM X 20. (*Below left*). The deciduous claws of the forepaws are essential for the migration from the birth canal to the pouch immediately after birth. SEM X 25. (*Below right*). The hind limb of a 12.5 day opossum embryo shows continued differentiation of the digits. SEM X 30.

Fig. 26. (*Above*). A micrograph illustrates the mouth and oral shield of an opossum embryo at 12.5 days gestation. Note the wide orifice of the external nares and the tongue protruding from the oral cavity. SEM X 45. (*Below*). Surface features of the periderm that covers the entire embryo at this time. Note the central nuclear profile within each cell and the distinct cell boundaries (arrows). SEM X 860.

Chapter 7. Limb Formation

Synopsis:

Initial limb development occurs during the first portion of the tenth prenatal day with the appearance of the forelimbs. Hind limb development begins late in prenatal day ten and lags behind the development of the forelimbs until about tenth week of postnatal life. Little if any independent movement occurs in the hind limbs during the first postnatal week. In contrast to the hind limbs, the forelimbs of the newborn opossum are functional at birth and the forepaws capable of digital-palmar prehension. Shortly before birth a thickening of the epitrichium (periderm) at the leading edge of the digits on the forepaws occurs that extends beyond the terminal ends to form pointed deciduous claws. The deciduous claws lack a nail matrix and are shed by the second postnatal week to eventually be replaced by true nails. Following birth, the deciduous claws gather and tightly lock onto hairs of the mother's fur by digital-palmar prehension of the forepaw. Thus, the minute forepaws are capable of grasping and with the clawed digits grasp the fur of the mother allowing the newborn to crawl (unaided by the mother) from the birth canal to the pouch. The young exhibits a swimming (overhand stroke) motion where the head and neck are flexed laterally followed by the forward motion of the ipsilateral foreleg. The head and neck are then flexed in the opposite direction while the deciduous claws of the forepaw clasp the abdominal fur of the mother. As the forepaw is moved backward the newborn is pushed forward. Movement does occur in the hind limbs during the second postnatal week, but such movements are not coordinated with each other or with the forelimbs. At nine weeks postnatal, young opossums are capable of walking and supporting their own weight, but it is not until about eleven weeks that the young opossums are capable of running and climbing.

Acknowledgments:

Figs. 1 (top), 2, 4 (bottom), 6 (top), 7 (top), 8, 9 and 10 (top), courtesy of and from: Krause, W.J. and J.H. Cutts (1986) Scanning electron microscopic observations on developing opossum embryos: days nine through twelve. Anat. Anz. 161:11-21.

Figs. 11, 12 (bottom) and 13, courtesy of and from: Cutts, J.H., Krause, W.J., and C.R. Leeson (1978) General observations on the growth and development of the pouch young opossum, *Didelphis virginiana*. Biol. Neonate 33:264-272.

Figs. 14 and 15 (top), courtesy of and from: Cutts, J.H. and W.J. Krause (1983) Structure of the paws in *Didelphis virginiana*. Anat. Anz. 154:329-335.

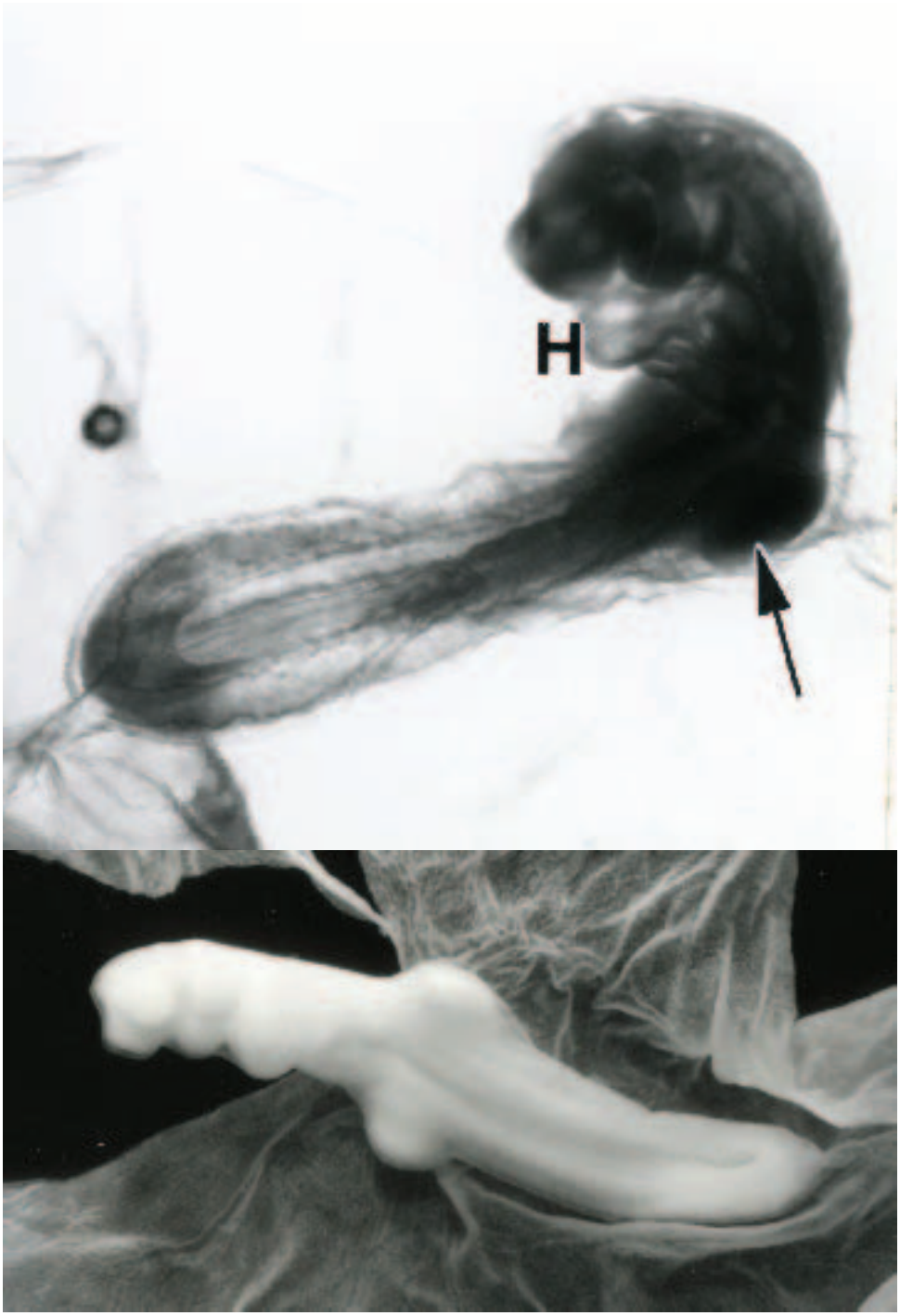

Fig. 1. (*Above*). The forelimb (arrow) and heart (H) of a non-fixed ten-day opossum embryo photographed using transilluminated lighting. The embryo was dissected free of the surrounding yolk sac placenta. X 30. (*Below*). A fixed ten-day opossum embryo illustrates somewhat better not only the developmental status of the forelimb, but also the general conformation of the head and trunk at this stage of development. The membrane surrounding the opossum embryo is the interior surface of the yolk sac placenta. X 20.

Fig. 2. (*Above*). By late in the tenth prenatal day digital ridges are present on the developing forepaw and the hind limb is present as a bud-like structure. X 40. (*Below*). A micrograph illustrates details of the opossum forepaw late in prenatal day ten. SEM X 100.

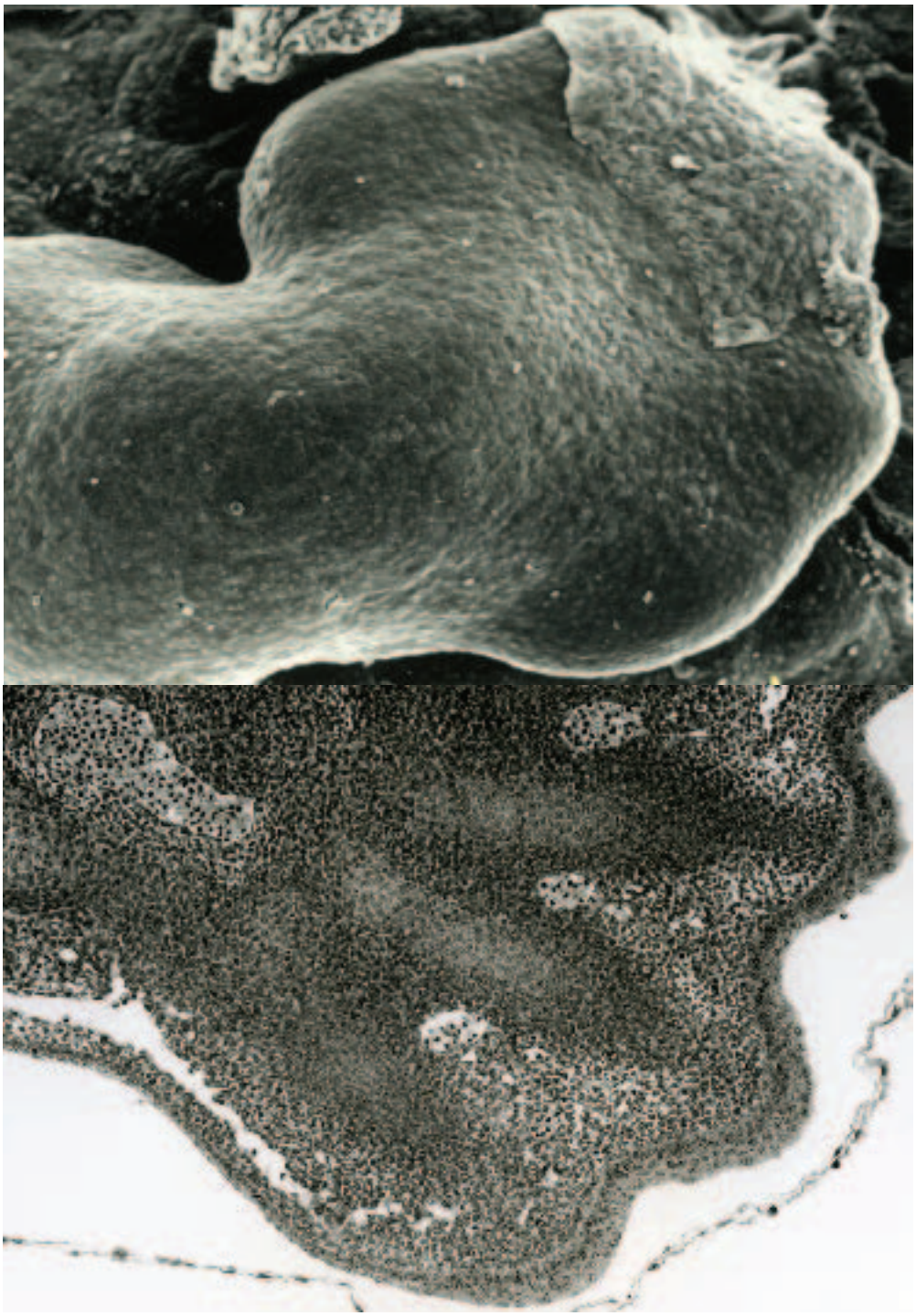

Fig. 3. (*Above*). A micrograph illustrates the forelimb and developing forepaw of an opossum embryo late in prenatal ten. The membrane covering the region of the developing digits is the amniotic membrane. SEM X 80. (*Below*). A histological section though a region of the developing forepaw of an opossum embryo late in prenatal day ten. Compare this histological section with the scanning electron micrograph shown above. Note the thin membrane at the bottom of the illustration, which is a region of the amniotic sac surrounding the embryo at this time. LM X 100.

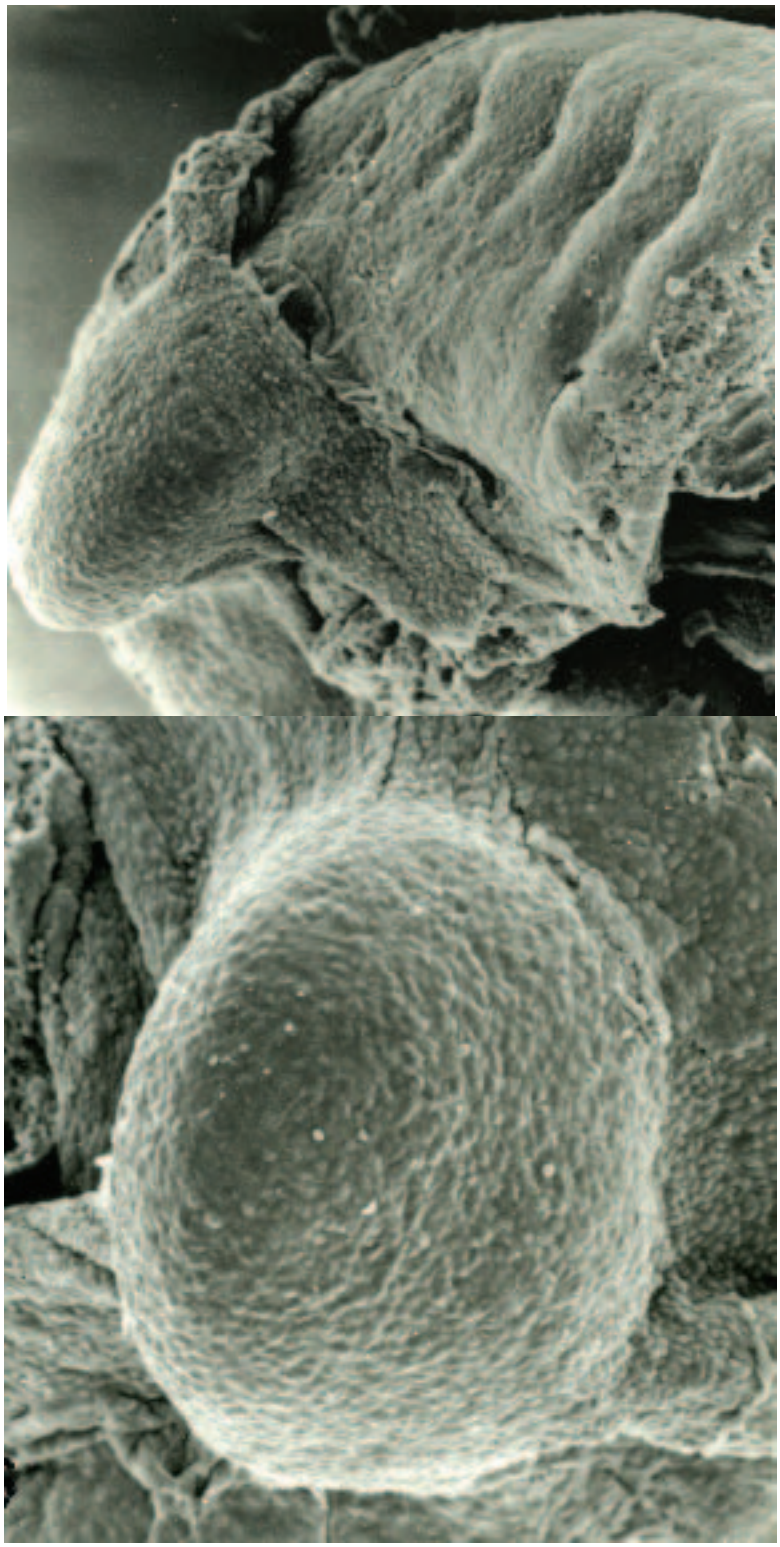

Fig. 4. (*Above*). A micrograph illustrates the distal trunk of an opossum late in prenatal day ten shows the initial appearance of the hind limb. SEM X 75. (*Below*). A micrograph illustrates the initial bud-like appearance of the developing hind limb from an opossum embryo late in prenatal day ten. SEM X 150.

Fig. 5. (*Above*). By prenatal day eleven digits of the forepaw are well delineated and the hind limb appears paddle-like. X 75. (*Below*). A scanning electron micrograph illustrates an eleven-day opossum embryo. Compare the fore- and hind limbs shown here with those in the above figure. SEM X 24.

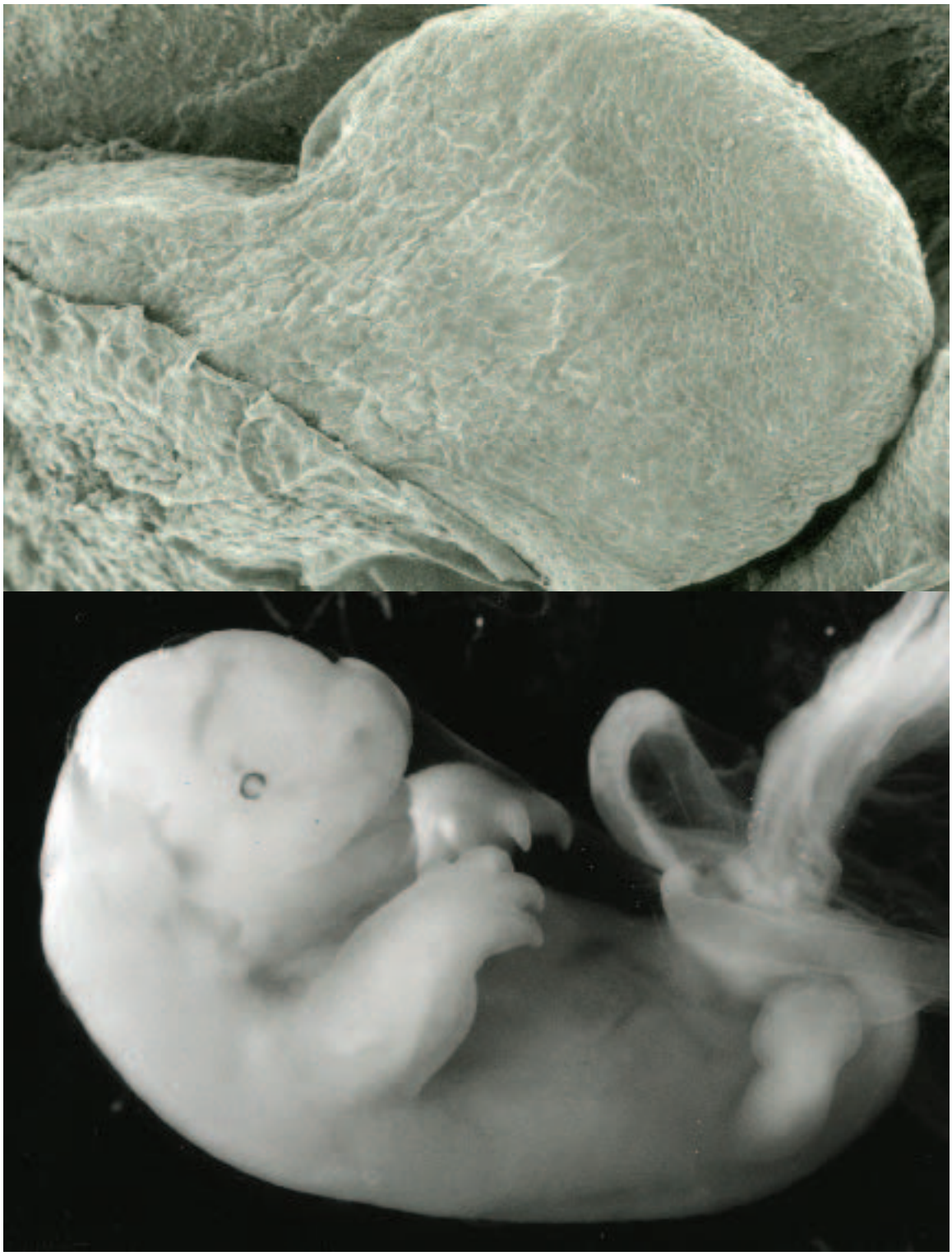

Fig. 6. (*Above*). A micrograph illustrates the external features of a hind limb from an eleven-day opossum embryo. SEM X 100. (*Below*). A slightly older eleven-day opossum embryo shows continued rapid growth of the limbs. Compare the developmental status of the forelimb with that of the hind limb. Note that the hind limb in a matter of hours now exhibits proximal and distal regions. X 25.

Fig. 7. (*Above*). Slightly later in day eleven both the proximal and distal regions of the hind limb of the opossum embryo are clearly evident. SEM X 100. (*Below*). The hind limb of an opossum embryo early in prenatal day twelve shows the initial formation of the digits. Compare and contrast the development of the forelimb with that of the hind limb at this stage of development. SEM X 20.

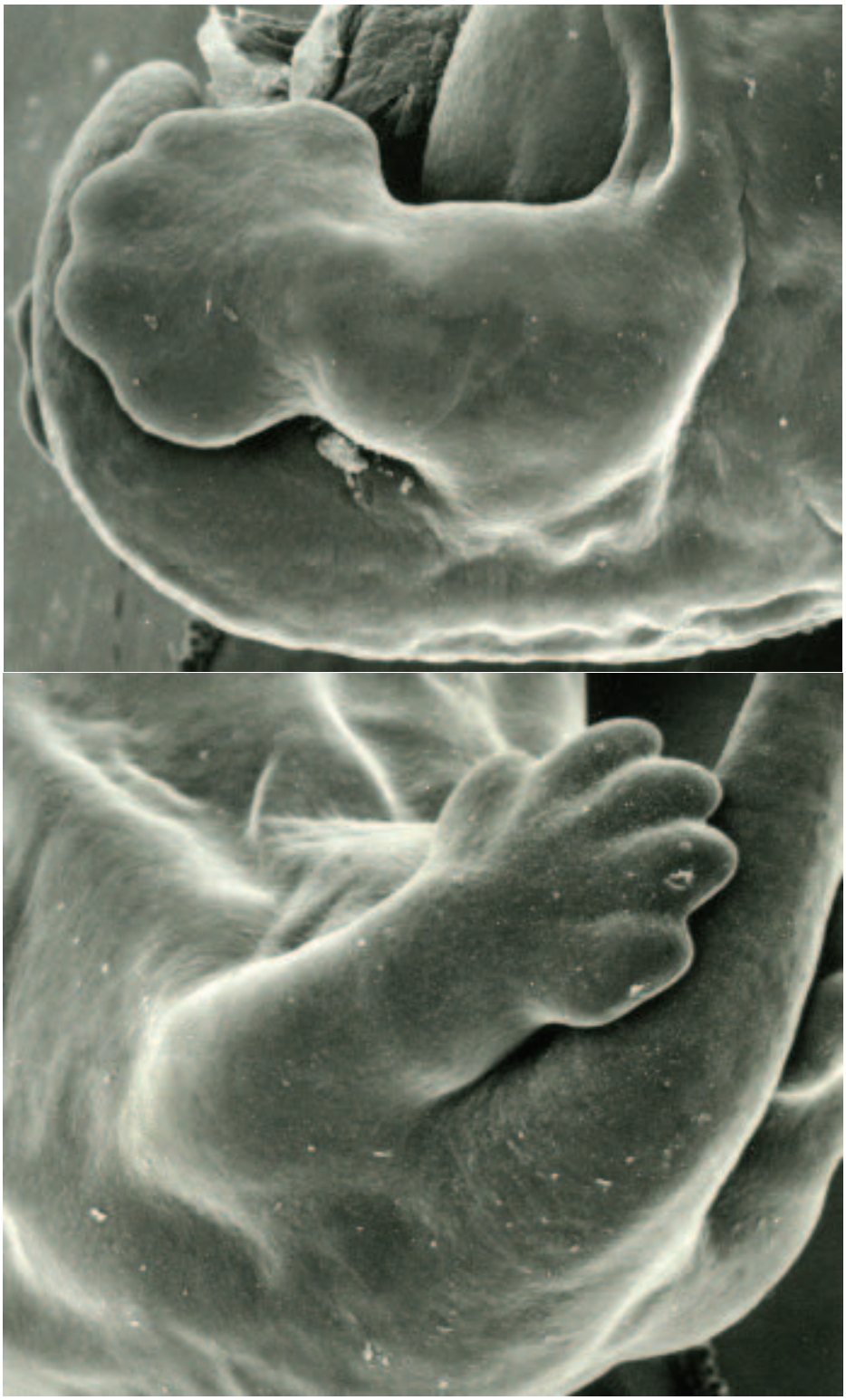

Fig. 8. (*Above*). A micrograph illustrates the lateral view of the developing hind limb of an opossum embryo early in prenatal day twelve. SEM X 60. (*Below*). A micrograph illustrates features of the hind limb of an opossum embryo later in prenatal day twelve. Note the rapid formation of digits. Compare this illustration with the above figure. SEM X 60.

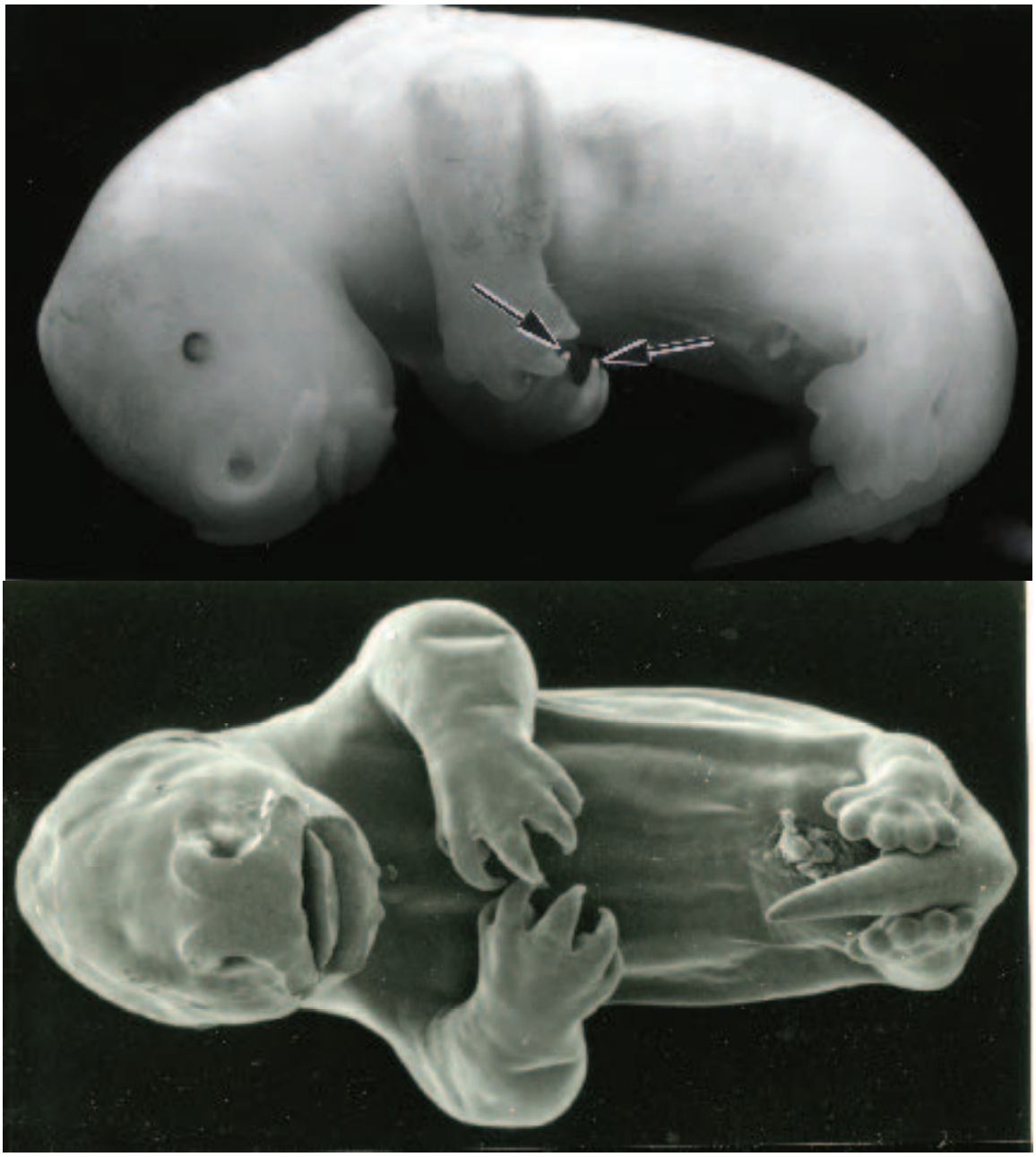

Fig. 9. (*Above*). The forepaws of the opossum embryo late in prenatal day twelve (just prior to birth) exhibit deciduous claws (arrows) essential for grasping fur and together with the mobile forelimb enables the newborn opossum to crawl from the birth canal to the pouch. The migration of the newborn opossum from the birth canal to the pouch for teat attachment is unaided by the mother. Note that even though the hind limb exhibits the formation of digits, it still remains paddle-like and is immobile. X 20. (*Below*). A scanning electron micrograph illustrates an opossum embryo late in prenatal day twelve. Compare the well-developed mobile forelimbs with the immobile hind limbs, which remain paddle-like in appearance. SEM X 18.

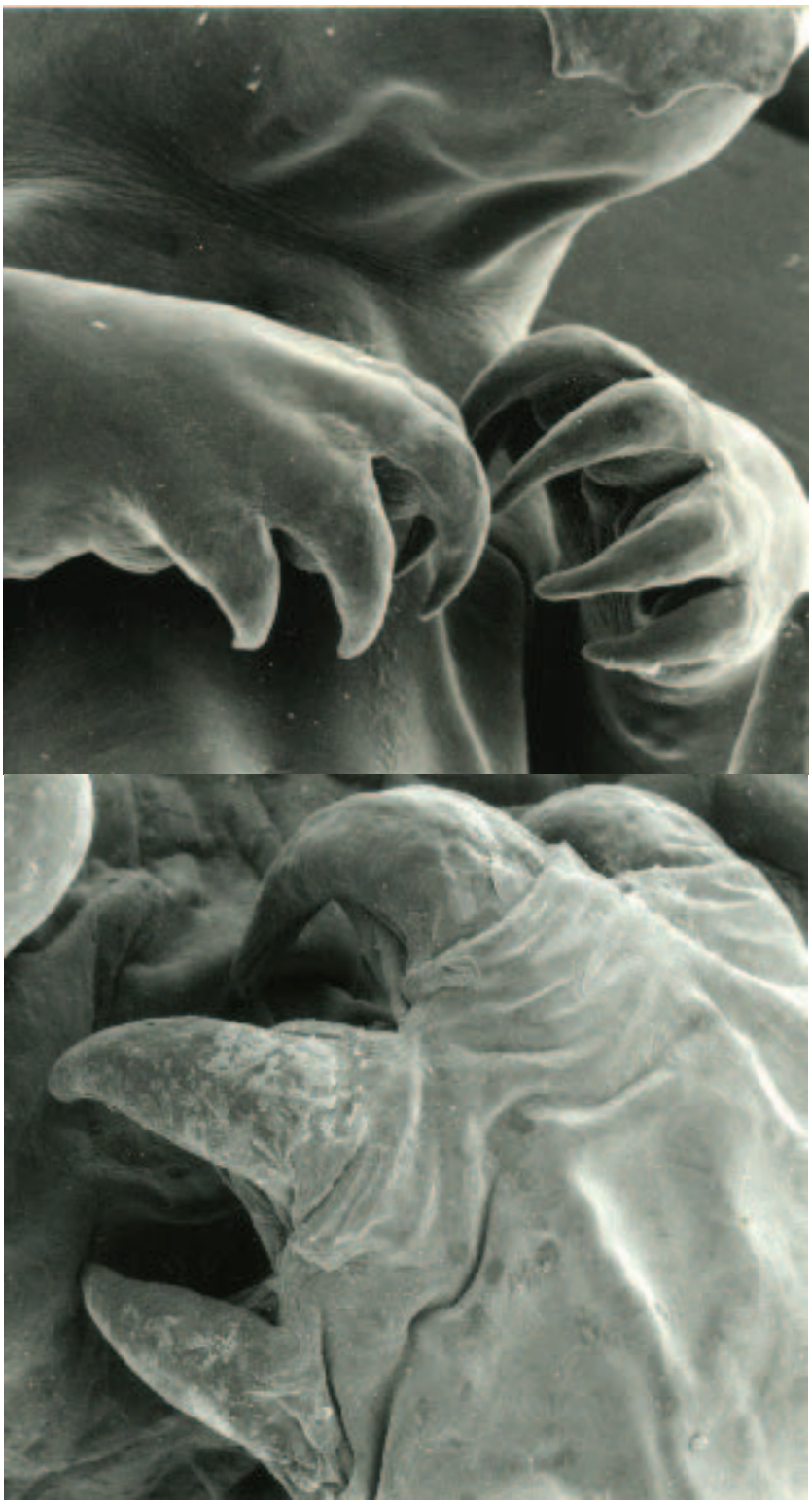

Fig. 10. (*Above*). Well-developed forepaws with deciduous claws characterize the opossum embryo late in day twelve. SEM X 40. (*Below*). The deciduous claws of an opossum forepaw late in prenatal day twelve viewed at increased magnification. SEM X 100.

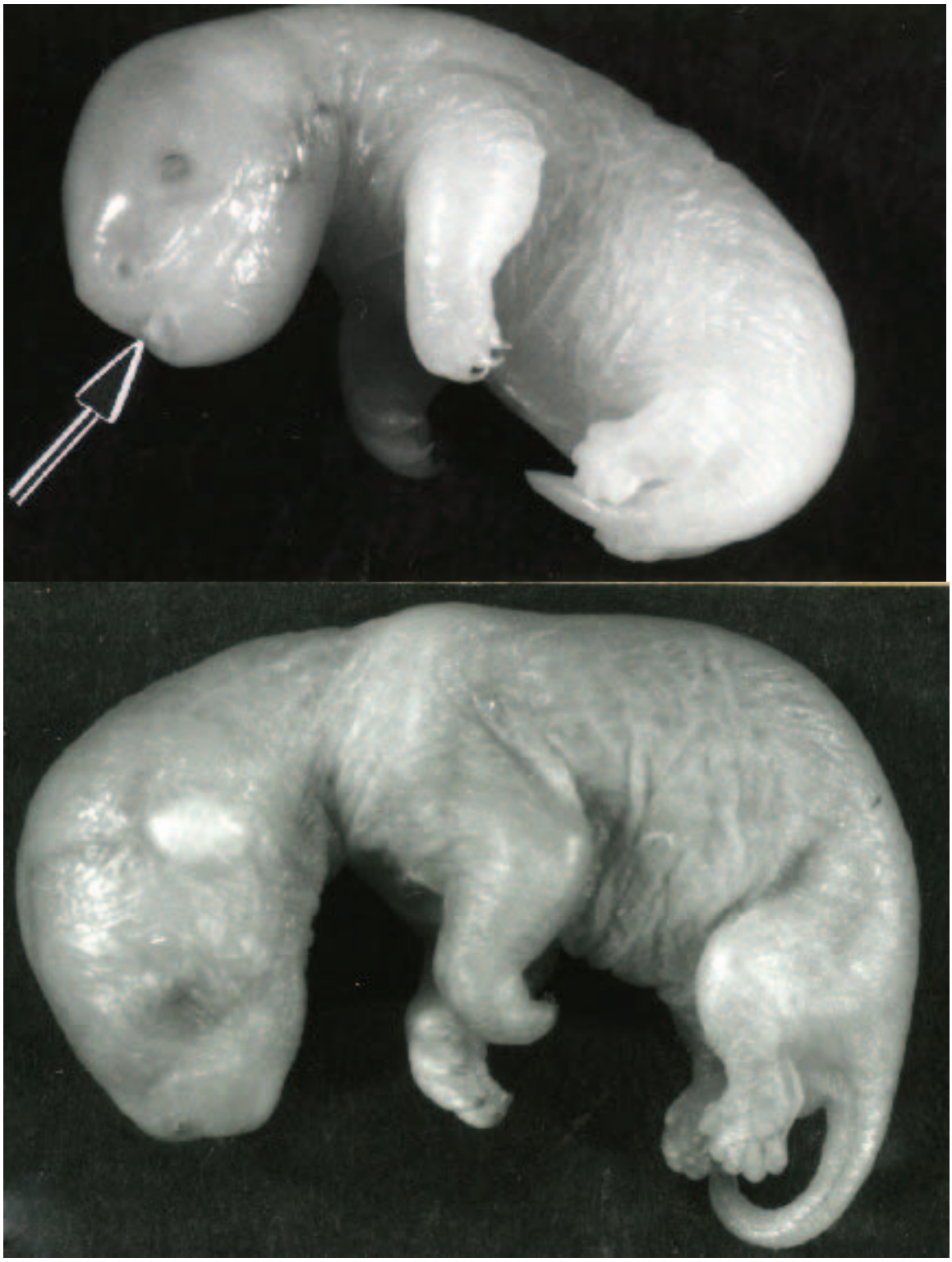

Fig. 11. (*Above*). The hind limbs of a pouch young opossum one week postnatal show little additional development in comparison to specimens examined just prior to birth (figure nine). Note that the lips are fused except for a small anterior opening (arrow) for the teat. Snout-rump length 25 mm. (*Below*). Development of the hind limbs in a pouch young opossum two weeks postnatal, although advanced in comparison to previous ages, lags behind that of the forelimbs. The deciduous claws have been shed and nails are now beginning to emerge from the digits of the forepaws. Snout-rump length 35 mm.

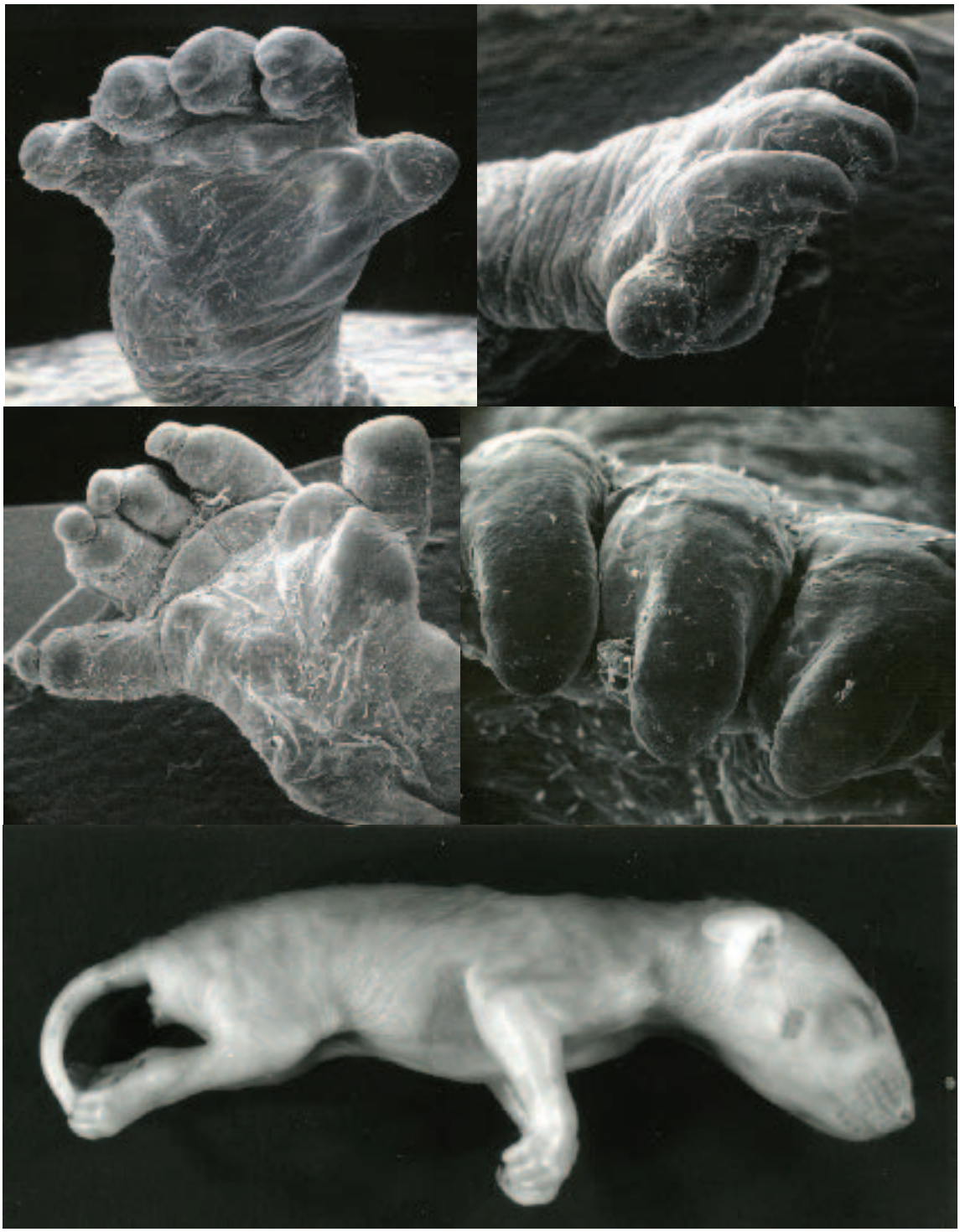

Fig. 12. (*Above left*). A micrograph illustrates the volar surface of a hind paw from a pouch young opossum two weeks postnatal. Snout-rump length 35 mm. SEM X 20. (*Above right*). The dorsal surface of the hind paw from a pouch young opossum two weeks postnatal. Snout-rump length 35 mm. SEM X 20. (*Center left*). The volar surface of the hind paw from a pouch young opossum three weeks postnatal. Snout-rump length 45mm. SEM X 20. (*Center right*). Increased magnification of three digits from the previous specimen details the status of the forming nails. SEM X 60. (*Bottom*). The forelimbs remain considerably more advanced in development than the hind limbs even in opossums well into the sixth week of postnatal life. Snout-rump length 80 mm.

Fig. 13. (*Above*). By the tenth postnatal week hind limb development of the opossum is now similar to that of the forelimb. Both limbs are mobile but the forelimbs continue to be the stronger. Prior to this time, the locomotion observed is by a dragging action of the forelimbs, with the hind limbs being relatively immotile. Length 115 mm. (*Below*). By the eleventh week postnatal pouch young opossums freely leave and re-enter the pouch to explore their surroundings. Length 140 mm.

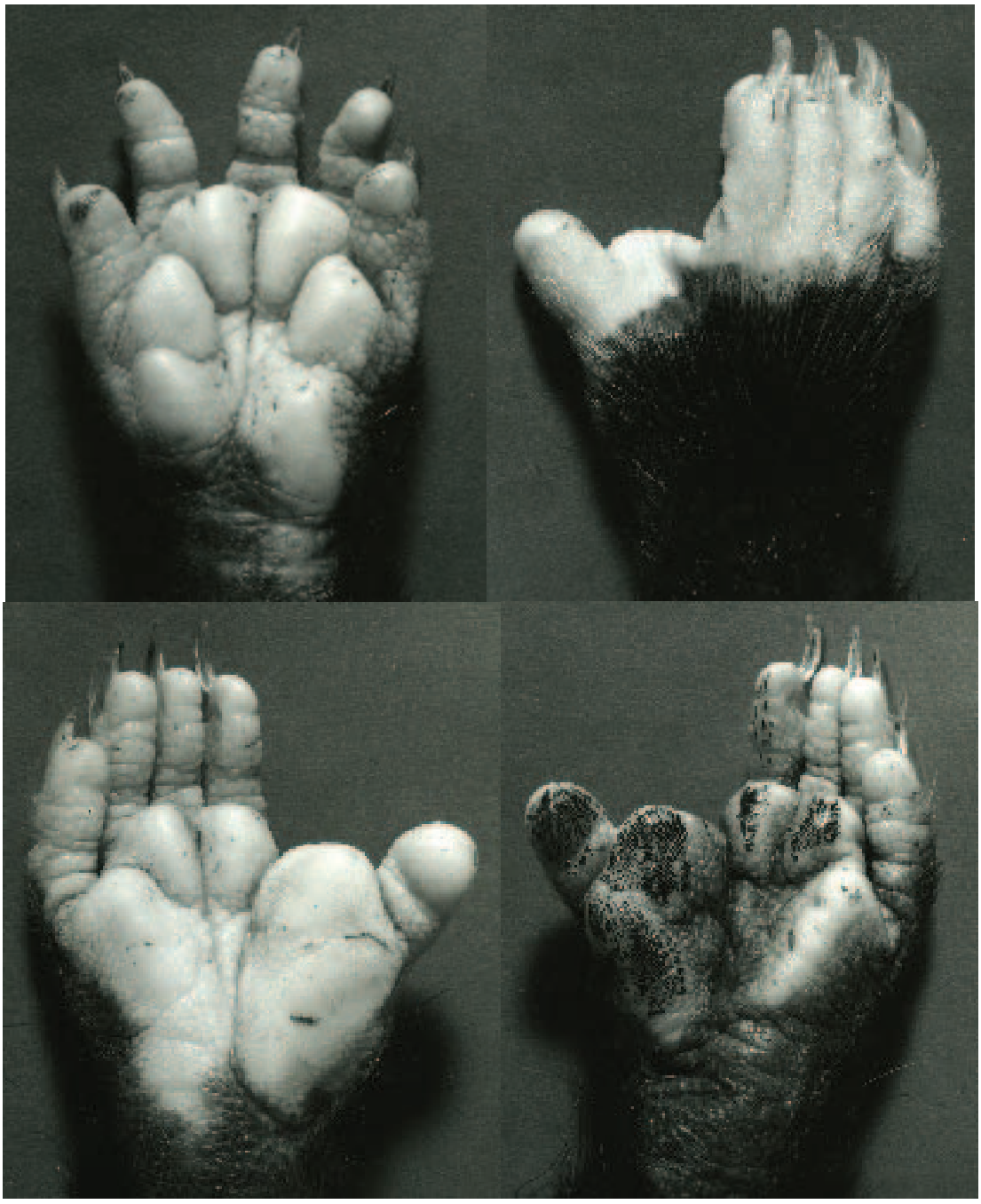

Fig. 14. (*Above left*). A photograph illustrates the volar surface of a forepaw, its tori, digital pads, and deep midline groove. All digits have nails. X 1.5. (*Above right*). The dorsum of the hind paw exhibits a sharply divergent Pollex that lacks a nail. X 1.5. (*Below left*). The volar surface of a hind paw has prominent tori and digital pads, each bearing a distinct pattern of grooves and ridges. X 1.5. (*Below right*). A photograph of the volar surface of a hind paw inked to demonstrate the pattern of ridges on the tori and digital ridges. X 1.5.

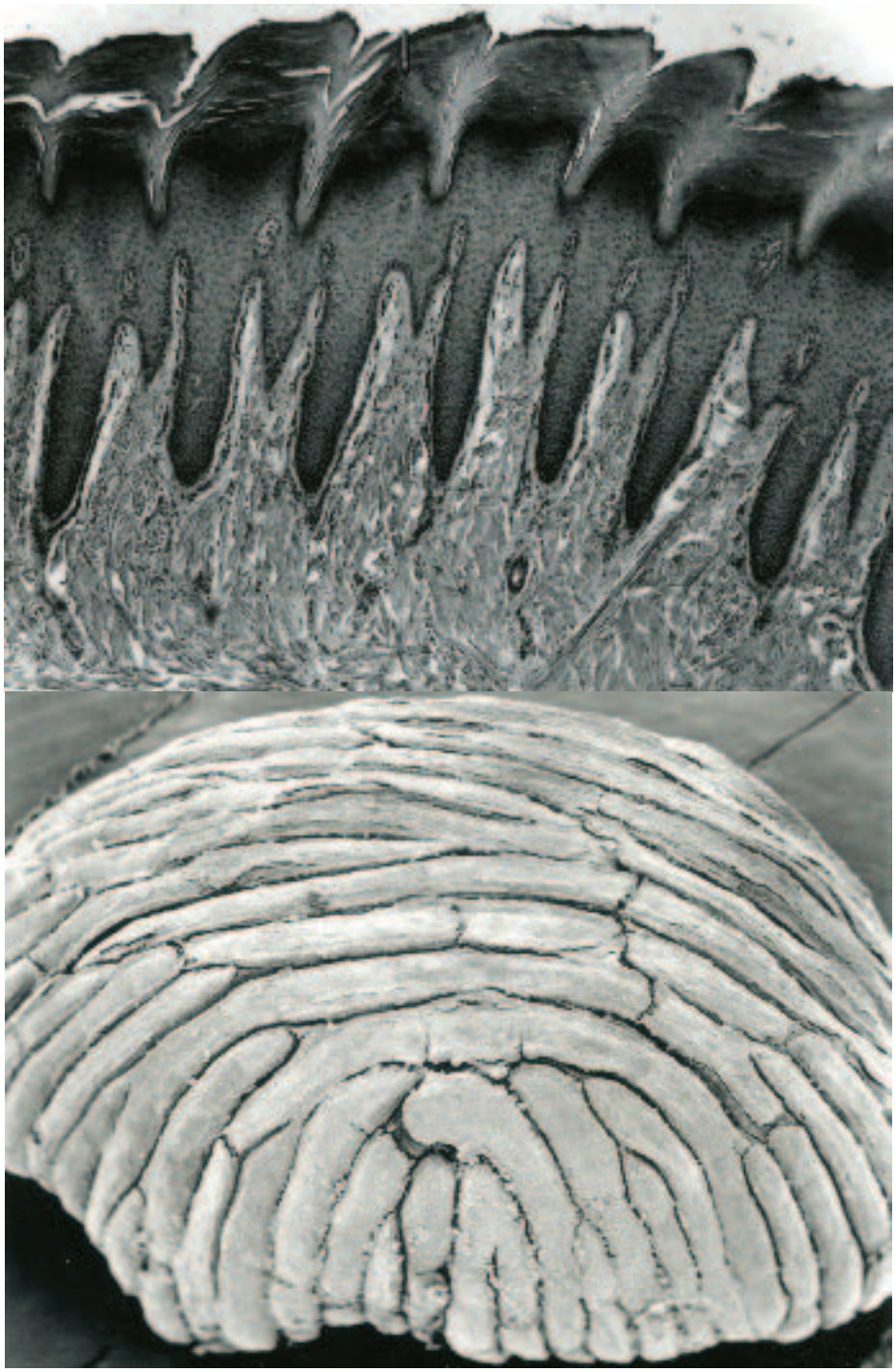

Fig. 15. (*Above*). The epidermal ridges on the digits are longer, narrower and more closely packed than those found on the tori. The overlying keratin exhibits a regular scalloping that corresponds to the epidermal down growths. Each ridge (epidermal down growth) is associated with an arteriolar complex of blood vessels. LM X 40. (*Below*). A scanning electron micrograph illustrates the character of the epidermal ridges on the digital pad of the Pollex. Male opossum. SEM X 25.

Chapter 8. Musculoskeletal Development

Synopsis:

Mesodermal cells make their initial appearance early during the seventh prenatal day and the notochord and first somites appear later the same day. The notochord at first is in the form of a slender rod, appears quite cellular and resembles a loose mucoid connective tissue. With continued development, it comes to resemble cartilage. The notochordal tissue of the 7.5-8.0 mm opossum embryo consists of a network of cells separated by large vacuoles filled with a mucopolysaccharide type of material and is limited externally by a thin sheath. In the 11.0 mm opossum embryo the notochord becomes segmented with large amounts of notochordal tissue being present in regions of the intervertebral thickenings. With chondrification of the forming vertebrae, notochordal tissue within the vertebral centra decreases in amount with a corresponding increase of this tissue occurring in the intervertebral regions. The intervertebral enlargements of notochordal tissue assume a diamond-shaped appearance in the 12 mm embryo. The notochord of newborn opossum is avascular and the diamond-shaped enlargements continue to occupy the central regions of the developing intervertebral discs. In the developing centra, the notochordal tissue is attenuated in appearance and continues to appear as a thin cylinder of material. In intervertebral regions the notochordal tissue is more cellular than within developing centra. The cellular component of the notochordal tissue at birth consists of light and dark cells. Dark cells are characterized by dense nuclei and an electron-dense cytoplasm and often appear attenuated. In contrast, light cells contain euchromatic nuclei and exhibit an abundant, light staining cytoplasm. Both cell types exhibit large accumulations glycogen, contain intracellular vacuoles filled with mucopolysaccharide and have thin cytoplasmic processes that extend to the periphery of the notochordal mass. By the end of the first postnatal week notochordal tissue continues to be reduced in amount in the centra of the vertebral bodies and the regions of the intervertebral discs continue to expand. Most thoracic vertebrae show signs of replacement of notochordal tissue and hyaline cartilage by bone at the end of the third postnatal week. In later developmental stages notochordal tissue within the centra of vertebrae can be recognized only as a thin cylindrical homogeneous region containing debris. Notochordal tissue of the intervertebral regions shows increased expansion and contributes to the formation of the nucleus pulposus in the forming intervertebral discs as development continues.

Ossification centers are present within the cartilaginous skeleton of newborn opossum in the humerus, clavicle, scapula, radius, ulna, ribs, mandible, premaxilla, maxilla, lacrimal, nasal, palatine, pterygoid, and tympanic ring. Epiphysial union in the opossum is often delayed and may not be completed. It occurs first in the elbow region, then sequentially in the following regions: shoulder, wrist, hip, ankle, and knee. Epiphysial union begins near the end of the first year and the process continues throughout the second and third years. It may not be completed even in the oldest opossums.

Skeletal muscle tissue of the limbs and trunk of the opossum develops from myotomal mesenchyme, and that associated with the head and neck from mesenchyme associated with the branchial arches. The majority of myocytes associated with the musculature of the shoulder region and cranial end of the opossum just prior to and after birth are in the form of early and late myotubes characterized by chains of centrally positioned nuclei. Myofibrils within the differentiating myotubes show prominent cross-

striations. During the first week of postnatal life nuclei begin to move from the center of these differentiating cells to the periphery to form true myocytes. These cells are now filled with myofibrils. Development of myocytes is not a synchronous event along their length and the same skeletal muscle cell may show features of both a myotube and a myocyte. The most mature portion of a skeletal myocyte during this period of development is in the mid-region along the length of the cell where the fusion of myoblasts first occurred. In contrast to developing skeletal muscle tissue associated with shoulder and forelimb, that of the caudal region and hind limb of the newborn opossum are at a much earlier state of differentiation and consist primarily of spindle shaped myoblasts. Some myoblasts of this region have fused with one another, end to end, to form primitive myotubes. Different cell types can be recognized early in development and the proportions of type I and type II myocytes show a distinct cranial/caudal gradation in the distribution of type II muscle cells through the trunk musculature. Type II muscle cells are more prominent near the surface of individual muscles taken from the forelimb and hind limb of *Didelphis*. In the limbs, type I myocytes tend to be located centrally within individual muscles.

Acknowledgments:

Fig. 1 (top), courtesy of and from: Williams, L.W. (1908). The later development of the notochord in mammals. Am. J. Anat. 8: 251-284.

Figs. Figs. 1 (bottom), 2, 3, 4, and 5, courtesy of and from: Krause, W.J. and J.H. Cutts (1982) The notochord of the newborn opossum and its fate during postnatal development. Arch. Histol. Jap. 45:155-165.

Figs. 6, 7, 8 and 9, courtesy of and from: Nesslinger, C.L. (1955). Osteogenesis and ossification in the postnatal Virginia opossum, *Didelphis marsupialis virginiana* Kerr. PhD Dissertation, Cornell University, Ithaca, New York, pp 55.

Fig. 10, courtesy of and from: Krause, W.J. (1998) A review of histogenesis/organogenesis in the developing North American opossum (*Didelphis virginiana*). Adv. Anat. Embryol. Cell Biol. 143 (I): Springer Verlag, Berlin, pp 143.

Fig. 11, courtesy of and from: Hansen, S.E., J.H. Cutts, W.J. Krause and J.H. Cutts III. (1987). The distribution of fiber types in thirty-seven muscles of the opossum, *Didelphis virginiana*. Anat. Anz. 164:153-158.

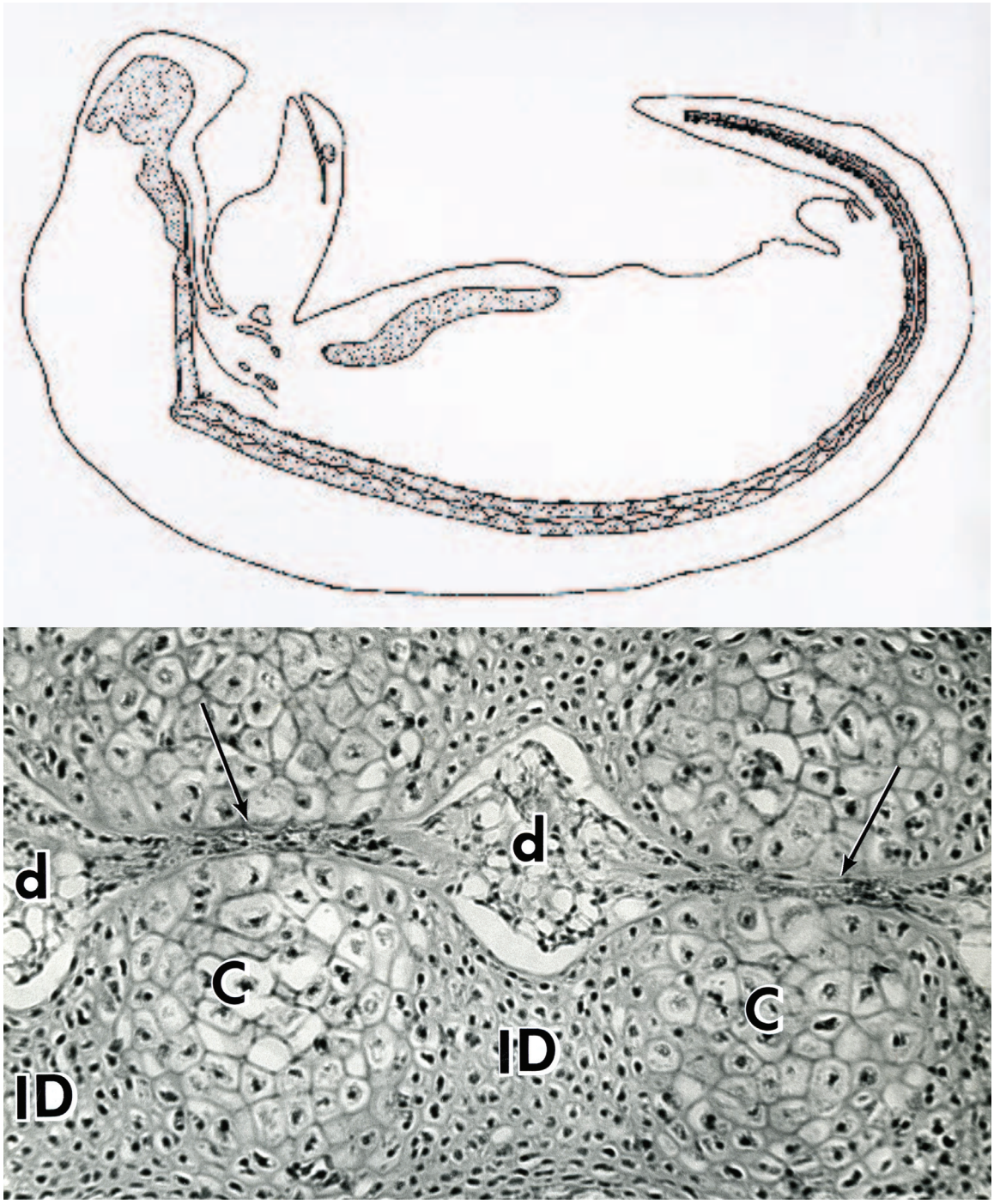

Fig. 1. (*Above*). A line drawing illustrates the notochord within an opossum embryo that measured 12 mm in length (approximately eleven days gestation). (*Below*). A micrograph illustrates a region of notochord within the developing vertebral column from the thoracic region of a newborn opossum. The notochord appears as diamond-shaped intervertebral expansions (d) within the regions of forming intervertebral discs (ID) and intravertebral constrictions (arrows) within the developing vertebral centra (C). LM X 125.

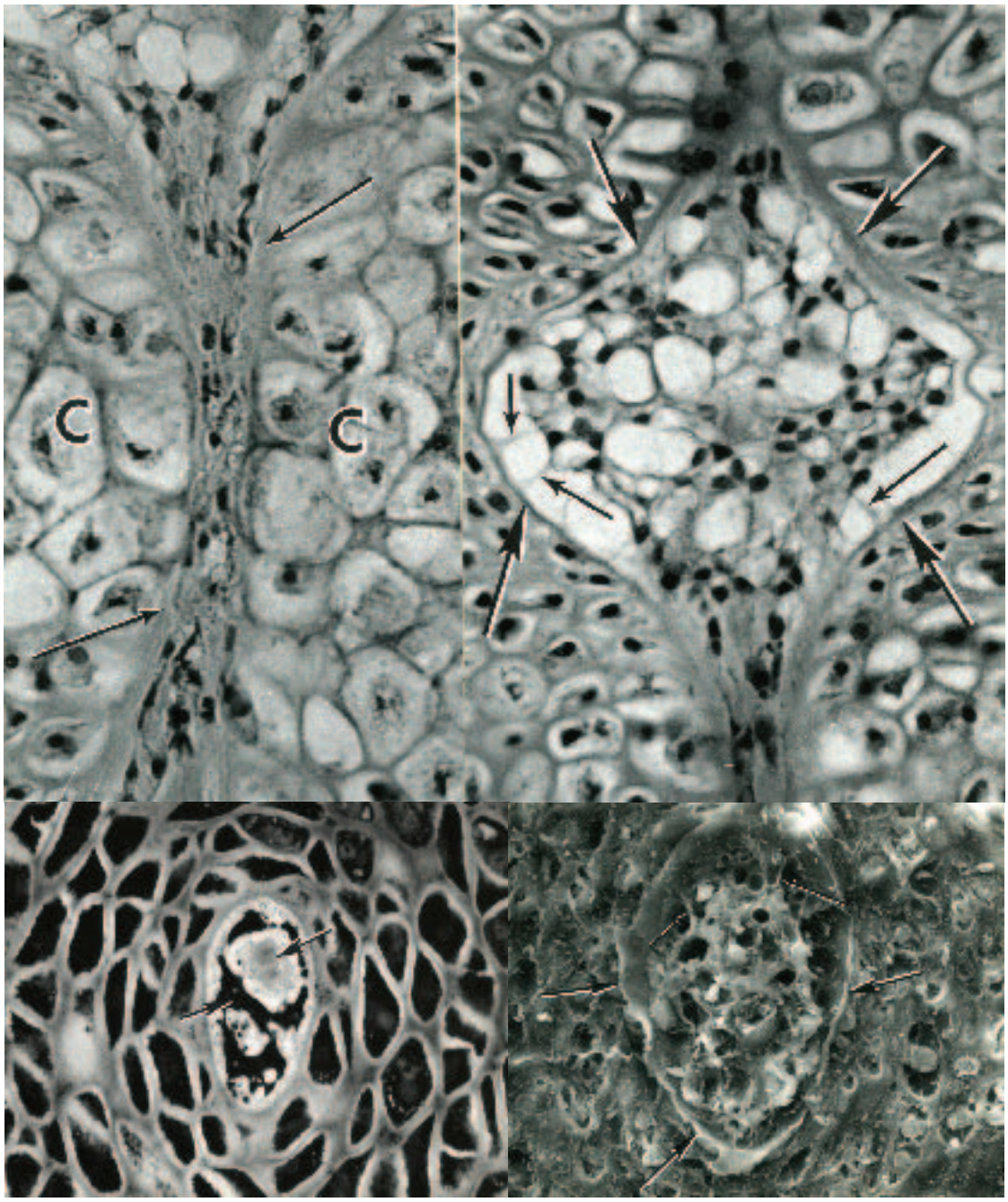

Fig. 2. (*Above left*). Increased magnification of an intravertebral constriction (arrows) shows scattered cells and cellular debris within a dense eosinophilic matrix. Surrounding chondrocytes (C) within developing vertebral centra show signs of hypertrophy. LM X 300. (*Above right*). In areas of the intervertebral expansions, notochordal cells appear loosely arranged and resemble mesenchymal tissue. Thin cytoplasmic processes (small arrows) extend from the notochordal cells and contribute to a limiting notochordal sheath (large arrows) at the periphery. Intra- and intercellular vacuoles are associated with notochordal cells. Newborn opossum. LM X 300. (*Below left*). A transverse section through a developing vertebral centrum from the thoracic region of a newborn opossum illustrates light and dark cells (arrows) in the notochordal tissue. LM X 400. (*Below right*). Thin cytoplasmic processes (small arrows) extend from the notochordal cells and contribute to the interior of the limiting notochordal membrane (large arrows) are evident in this scanning electron micrograph. SEM X 500.

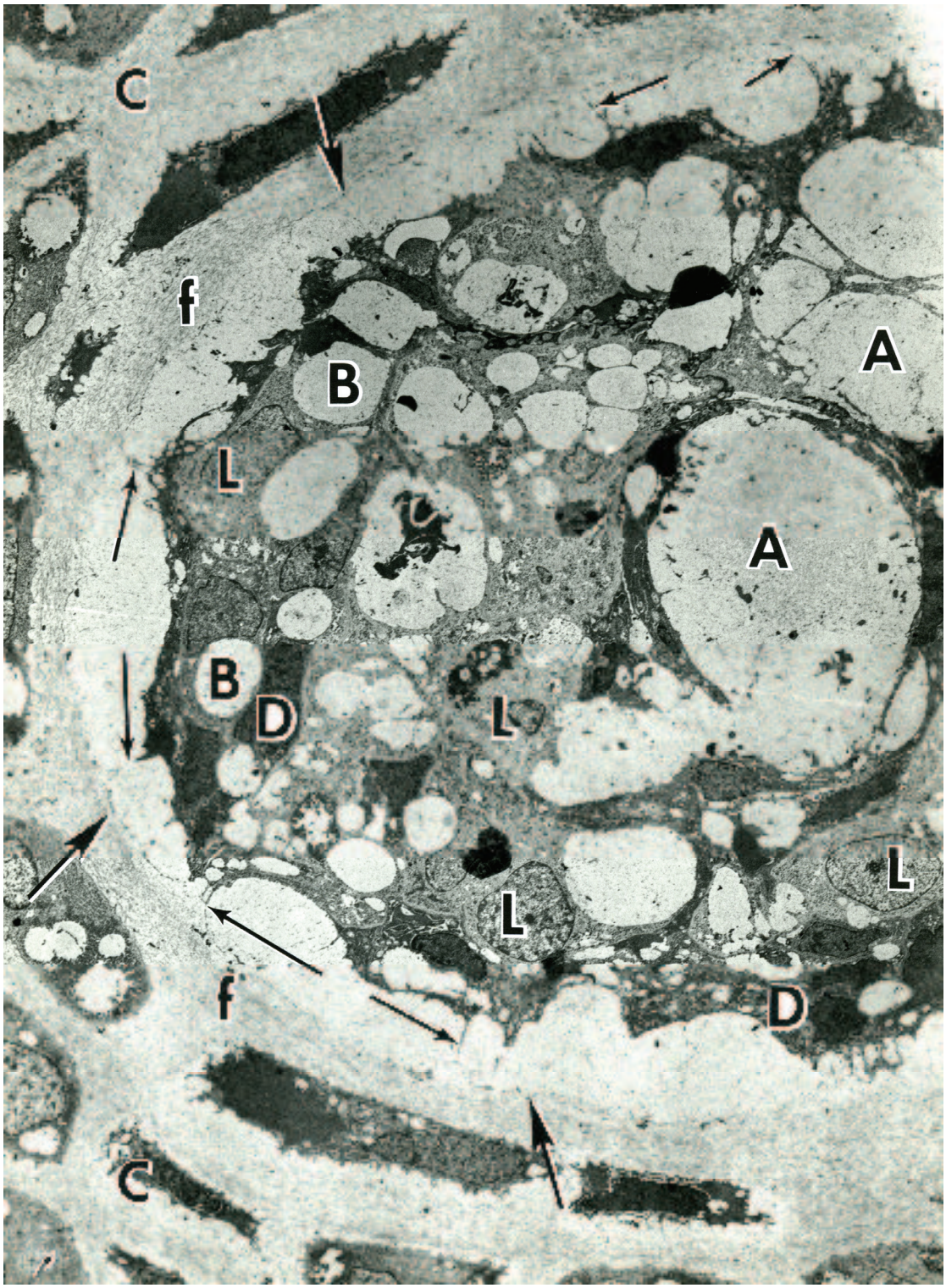

Fig. 3. A micrograph illustrates a region of notochord from the newborn opossum that depicts light (L) and dark (D) notochordal cells. Both intercellular (A) and intracellular (B) vacuoles are observed. Numerous, thin cytoplasmic processes (small arrows) extend from the periphery of the cylindrical mass of notochordal cells, cross a perinotochordal space, and contribute to a thin cytoplasmic limiting sheath (large arrows). A layer of cartilage matrix that contains a larger concentration of microfibrils (f) than observed in surrounding cartilage matrix (C) immediately surrounds the cytoplasmic sheath. TEM X 1,500.

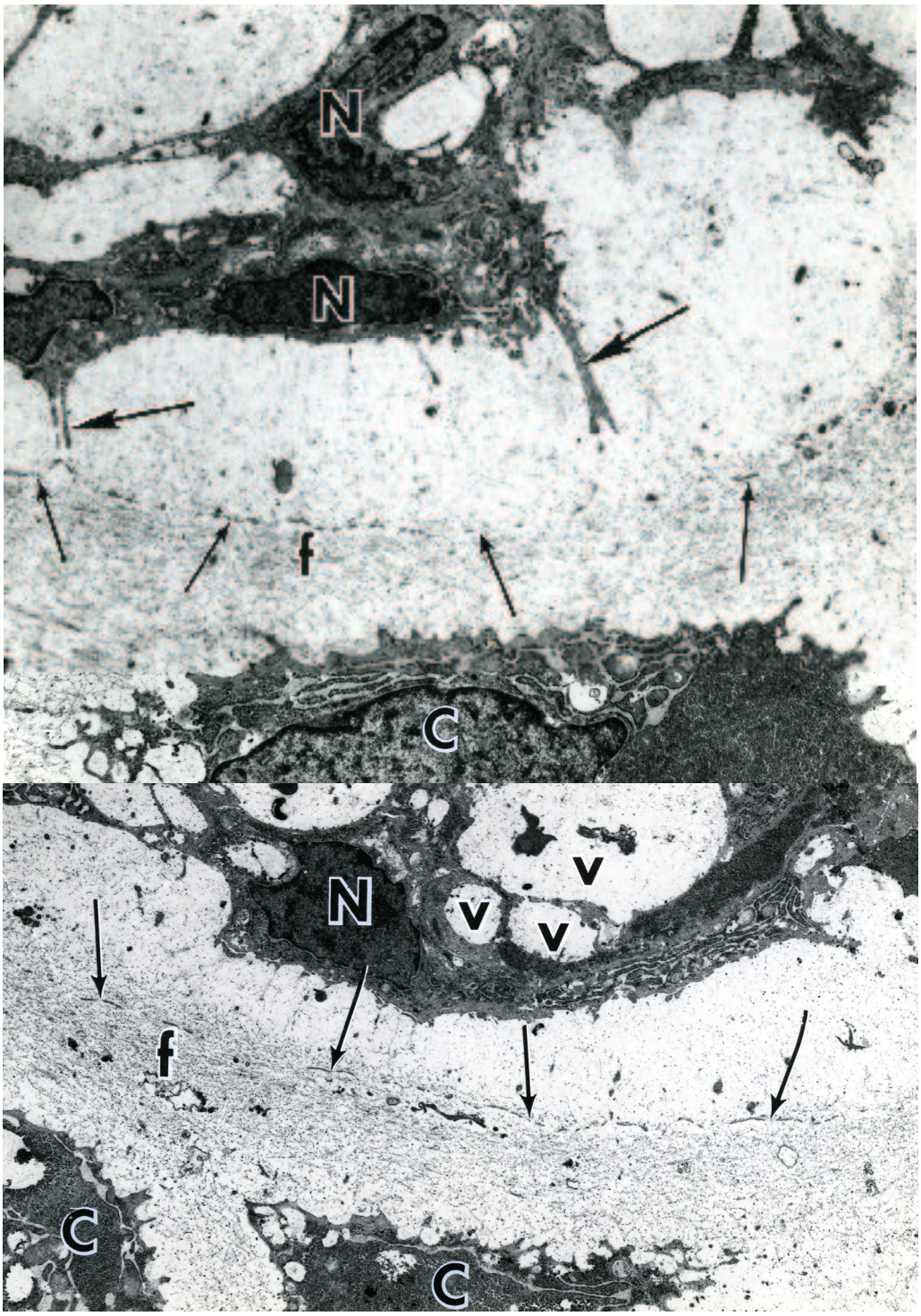

Fig. 4. (*Above*). Increased magnification of notochordal cells (N) at the periphery of the notochord illustrates the cytoplasmic processes (large arrows) that contribute to the surrounding cytoplasmic sheath (small arrows). Microfilaments (f) in the surrounding cartilaginous matrix and a neighboring chondrocyte (C) containing glycogen also are shown. Newborn opossum. TEM X 5,000. (*Below*). A notochordal cell (N) with intracellular vacuoles (v), the sheath of cytoplasmic processes (arrows), microfilaments (f) within the cartilaginous matrix, and portions of two chondrocytes (C) are demonstrated in this region of developing vertebral column. Newborn opossum. TEM X 5,000.

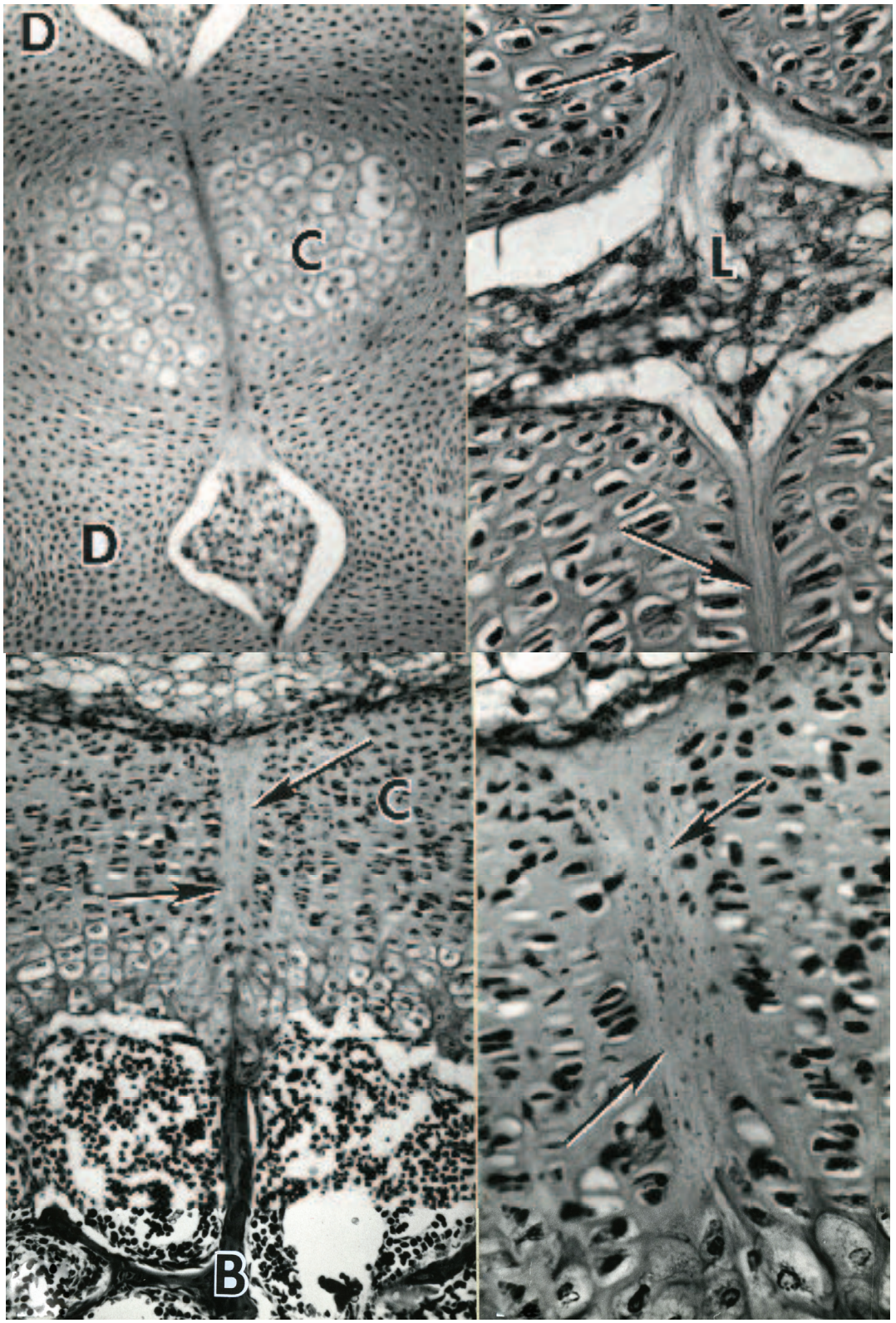

Fig. 5. (*Above left*). Vertebral bodies show a loss of most notochordal tissue in the centra (C) by the end of the first postnatal week. Most of the remaining notochordal tissue occupies a diamond-shaped space within developing intervertebral discs (D). LM X 100. (*Above right*). At two weeks postnatal, only a cylinder of mucopolysaccharide is found in developing centra (arrows) with most notochordal tissue occupying the intervertebral region (L). LM X 250. (*Below left*). Most vertebral bodies exhibit bone formation by the third postnatal week with a replacement of cartilage (C) and notochordal tissue (arrows) by bone (B). LM X 150. (*Below right*). The cylinder of intravertebral notochordal tissue (arrows) consists only of polysaccharide and cell debris by three weeks postnatal. LM X 250.

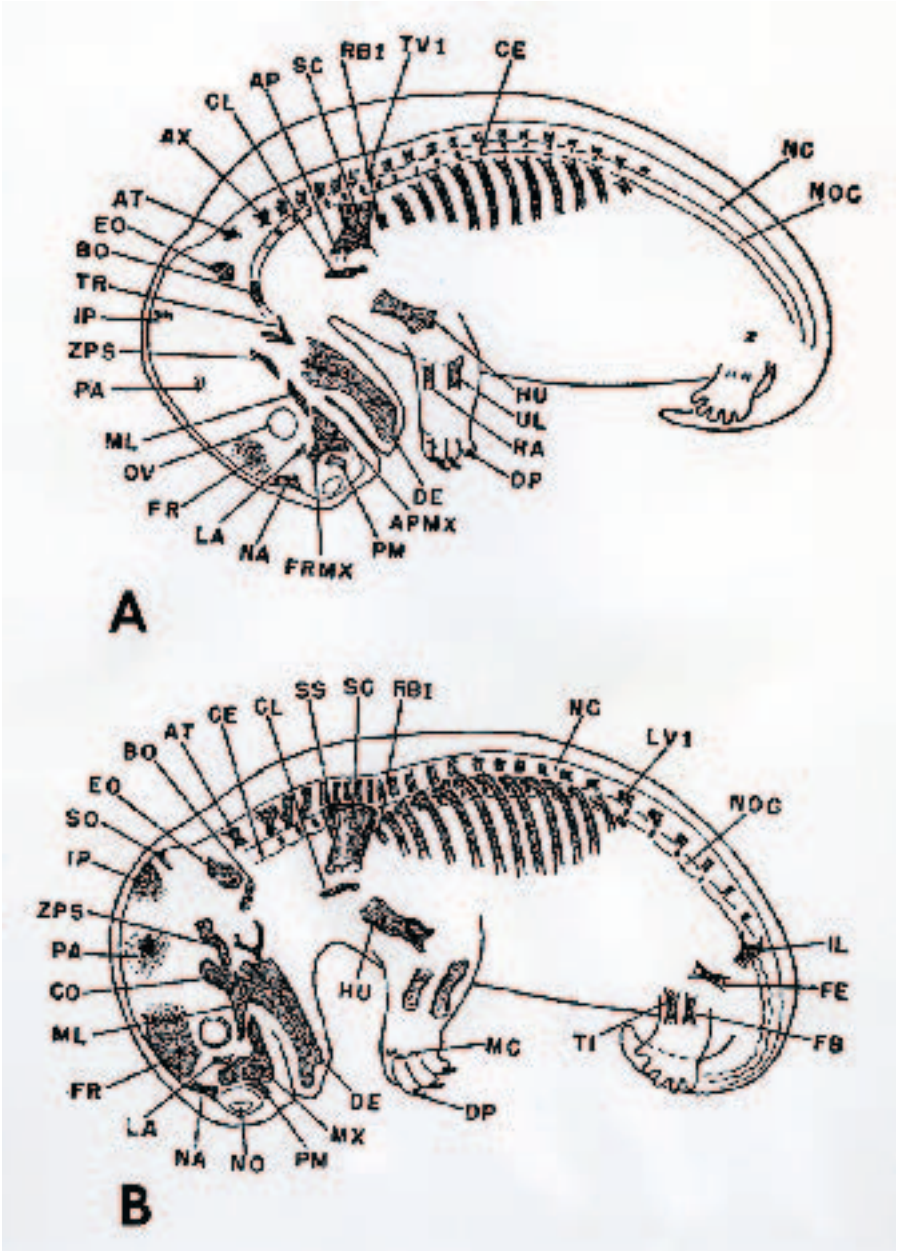

Fig. 6. (**A**). A line drawing depicts the developmental status of the skeleton from a pouch young opossum measuring 15 mm in length (approximately one week postnatal). (**B**). A line drawing depicts the developmental status of the skeleton from a pouch young opossum measuring 20 mm in length (approximately two weeks postnatal).
Humerus, *HU*, ulna, *UL*, radius, *RA*, distal phalanx, *DP*, dentary, *DE*, alveolar process of maxillary, *APMX*, premaxilla, *PM*, frontal process of maxillary, *FRMX*, nasal, *NA*, lacrimal, *LA*, frontal, *FR*, optic vesicle, *OV*, malar, *ML*, parietal, *PA*, zygomatic process of squamosal, *ZPS*, interparietal, *IP*, tympanic ring, *TR*, basioccipital, *BO*, exoccipital, *EO*, atlas, *AT*, axis, *AX*, clavicle, *CL*, acromion process, *AP*, scapula, *SC*, first rib, *RB1*, first thoracic vertebra, *TV1*, centrum, *CE*, spinal cord, *NC*, notochord, *NOC*, first lumbar vertebra, *LV1*, maxilla, *MX*, narial opening, *NO*, coronoid process, *CO*, supraoccipital, *SO*, scapular spine, *SS*, ilium, *IL*, femur, *FE*, fibula, *FB*, tibia, *TI*, and metacarpal, *MC*.

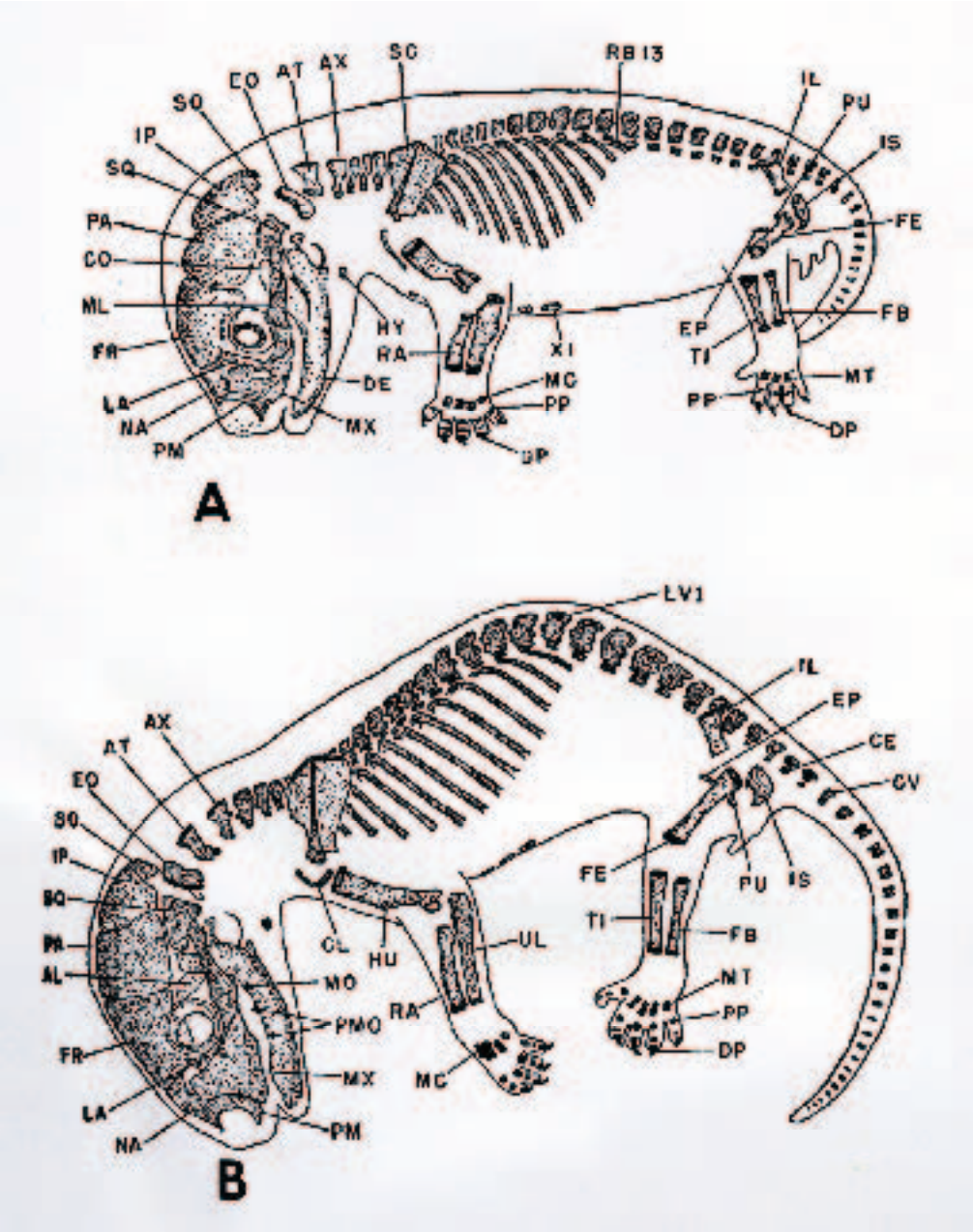

Fig. 7. (**A**). A line drawing depicts the developmental status of the skeleton from a pouch young opossum measuring 30 mm in length (approximately three weeks postnatal). (**B**). A line drawing depicts the developmental status of the skeleton from a pouch young opossum measuring 45 mm in length (approximately four weeks postnatal).
Thyrohyal, *HY*, dentary, *DE*, maxilla, *MX*, premaxilla, *PM*, nasal, *NA*, lacrimal, *LA*, frontal, *FR*, malar, *ML*, condyle, *CO*, parietal, *PA*, squamosal, *SQ*, interparietal, IP, supraoccipital, *SO*, exoccipital, *EO*, atlas, *AT*, axis, *AX*, scapula, *SC*, thirteenth rib, *RB13*, ilium, *IL*, pubic bone, *PU*, ischium, *IS*, femur, *FE*, fibula, *FB*, metatarsal, *MT*, distal phalanx, *DP*, proximal phalanx, *PP*, tibia, *TI*, epipubic bone, *EP*, xiphoid process, *XI*, metacarpal, *MC*, radius, *RA*, clavicle, *CL*, molar, *MO*, premolar, PMO, alisphenoid, *AL*, first lumbar vertebra, *LV1*, centrum, *CE*, caudal vertebra, *CV*, humerus, *HU*, and ulna, *UL*.

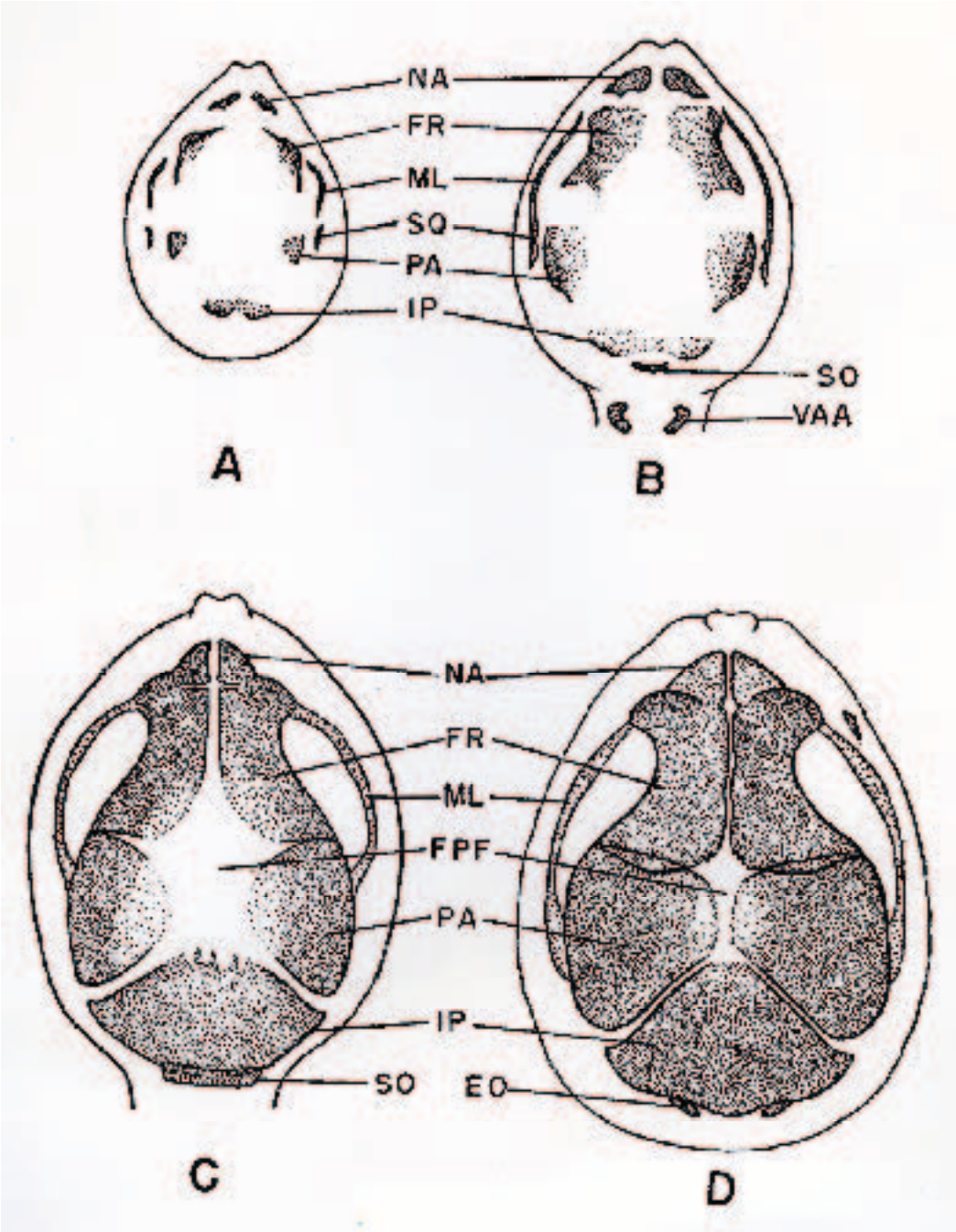

Fig. 8. (**A**). Ossification of the skull from an opossum approximately one week postnatal. Viewed from the dorsal surface. (**B**). Ossification of the skull from an opossum approximately two weeks postnatal. Viewed from the dorsal surface. (**C**). Ossification of the skull from an opossum approximately three weeks postnatal. Viewed from the dorsal surface. (**D**). Ossification of the skull from an opossum approximately four weeks postnatal. Viewed from the dorsal surface.
Nasal, *NA*, frontal, *FR*, malar, *ML*, squamosal, *SQ*, parietal, *PA*, interparietal, *IP*, supraoccipital, *SO*, vertebral arch of atlas, *VAA*, fronto-parietal fontanelle, *FPF*, and exoccipital, *EO*.

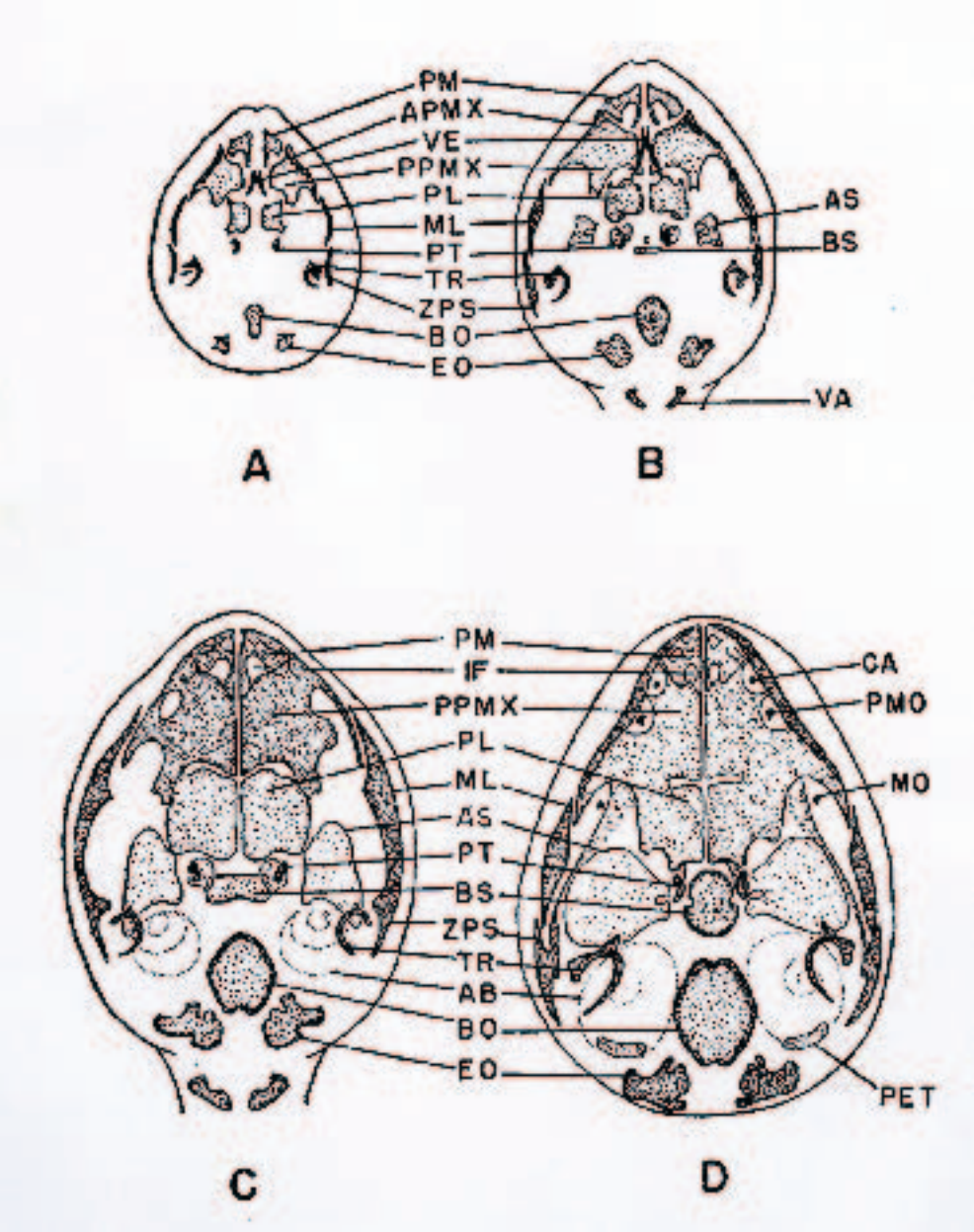

Fig. 9. (**A**). Ossification of the base of the skull from an opossum approximately one week postnatal. Viewed from the ventral surface. *(***B**). Ossification of the base of the skull from an opossum approximately two weeks postnatal. Viewed from the ventral surface. (**C**). Ossification of the base of the skull from an opossum approximately three weeks postnatal. Viewed from the ventral surface. *(***D**). Ossification of the base of the skull from an opossum approximately four weeks postnatal. Viewed from the ventral surface.
Premaxilla, *PM*, alveolar process of maxillary, *APMX*, vomer-ethmoid, *VE*, palatine process of maxillary, *PPMX*, palatine, *PL*, malar, *ML*, pterygoid, *PT*, alisphenoid, *AS*, basisphenoid, *BS*, tympanic ring, *TR*, zygomatic process of squamosal, *ZPS*, basioccipital, *BO*, exoccipital, *EO*, vertebral arch of atlas, *VA*, incisive foramen, *IF*, canine, *CA*, premolar, *PMO*, molar, *MO*, auditory bulla, *AB*, and petromastoid, *PET*.

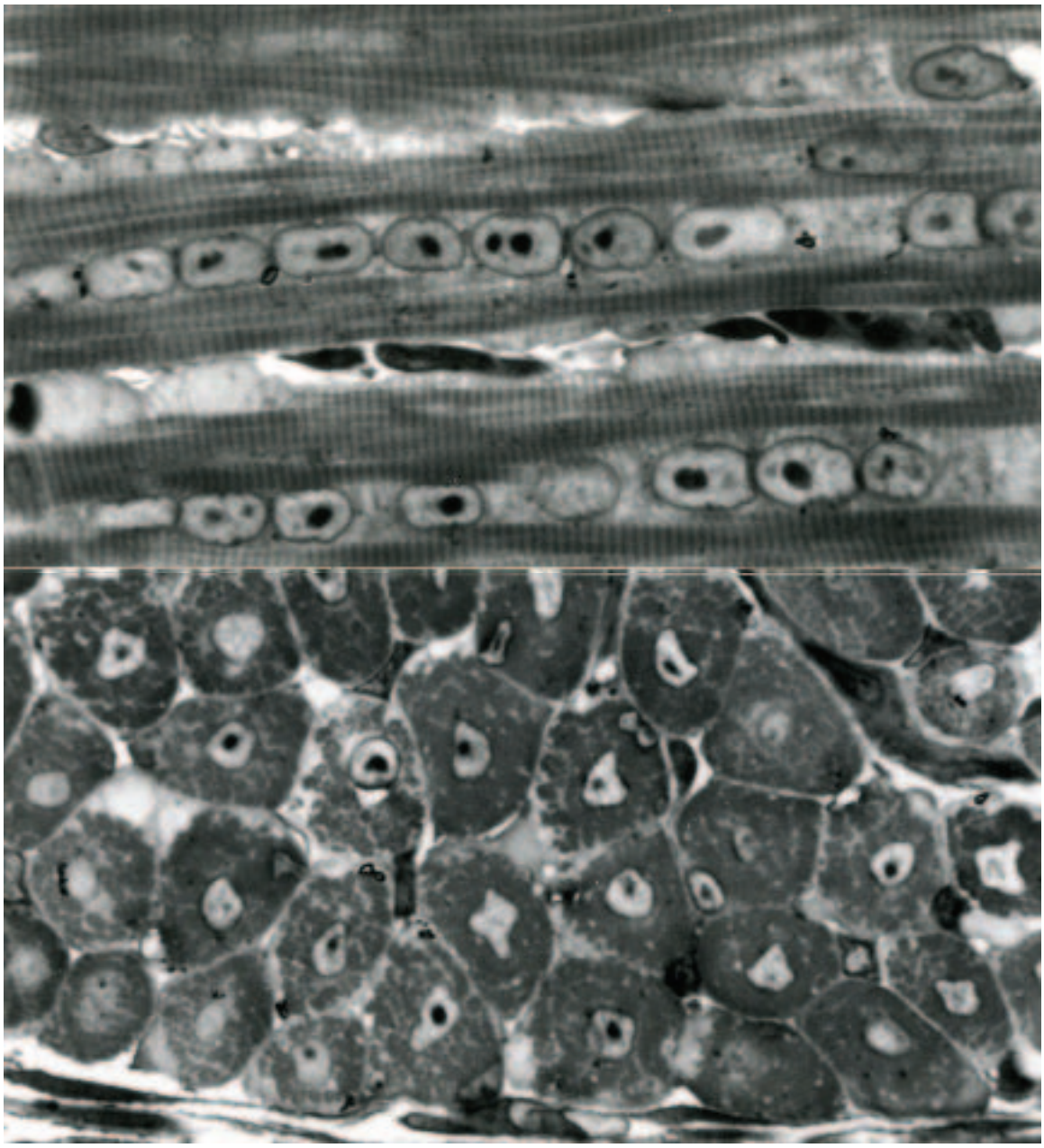

Fig. 10. (*Above*). A micrograph illustrates a longitudinal profile of myotubes within differentiating skeletal muscle tissue taken from the forelimb of an opossum embryo just prior to birth (12.5 days gestation). LM X 800. (*Below*). A micrograph illustrates a transverse profile through myotubes within differentiating skeletal muscle tissue taken from the forelimb of an opossum embryo just prior to birth (12.5 days gestation). LM X 800.

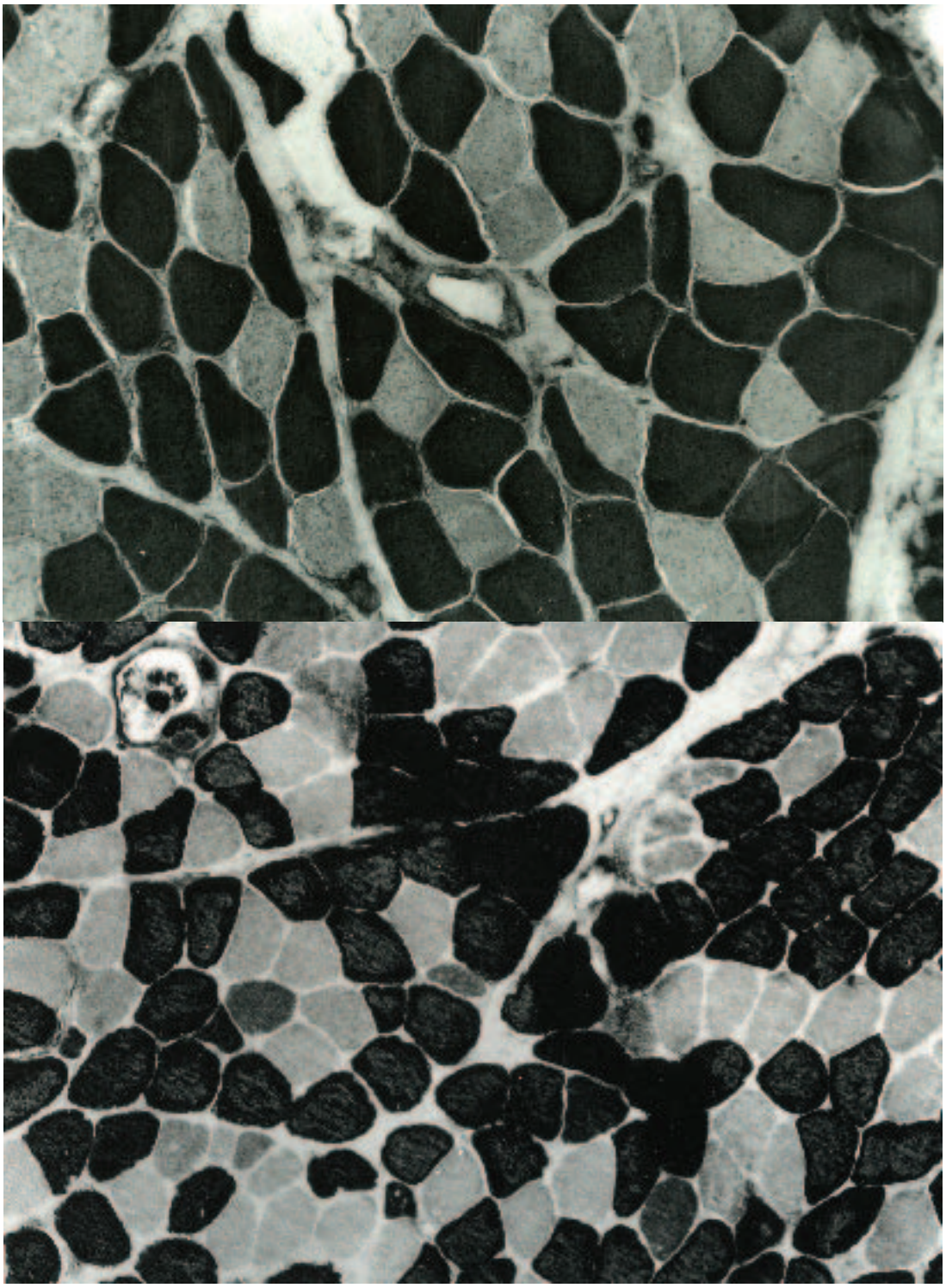

Fig. 11. (*Above*). A transverse section through a region of the sternohyoid muscle of a juvenile opossum illustrates Type I (light) and Type II (dark) muscle fibers (cells). Stained for adenosine triphosphatase (ATPase). LM X 150. (*Below*). A transverse section through the musculature of the tail, mid dorsal region, of a juvenile opossum illustrates Type I (light) and Type II (dark) muscle fibers (cells). Note the muscle spindle in the upper left corner of the illustration. Intrafusal fibers (cells) stain darkly. Stained for adenosine triphosphatase (ATPase). LM X 150.

Chapter 9. Pouch

Synopsis:

The panniculus carnosus that lies just beneath the ventral skin of the opossum can be subdivided into three regions: pars dorsalis, pars thoracoabdominalis, and pars pudenda. The pars pudenda lies at the abdominal midline and in the female passes around the pouch. Some of its skeletal muscle fibers pass into the fascia over the pubis and others unite posterior to the orifice of the pouch to form the sphincter marsupii. Other skeletal muscle fibers lie between the folds of skin forming the pouch wall and insert into the margin of the pouch that borders the opening. The female opossum can voluntarily close the orifice to the pouch by contracting the muscle fibers forming the pars pudenda. The pars pudenda is not well developed in the male and a pouch is lacking.

The first indications of pouch formation in the opossum are epidermal invaginations that form plates lateral and posterior to the developing mammary gland region. These epidermal ridges will become the future margins of the pouch and are present by the end of the second postnatal week. The margin of the pouch forms as a result of the epithelial ridges remaining stationary while the expanding mammary area pushes the skin into a double-walled fold. The double fold of skin forms the margin of the pouch. Skeletal muscle fibers of the pars pudenda differentiate in the connective tissue between the two layers of skin forming the margin of the developing pouch. As this occurs, a space is formed between the edge of the developing mammary gland area and the expanding margin of the pouch. The area occupied by the pouch expands with the first litter to accommodate the growth of the young. This expansion is temporary however, and after weaning becomes much reduced in size but never returns to the original dimensions prior to the first litter.

Between birth of a litter and weaning, sudoriferous (apocrine sweat) glands within the integument lining the pouch produce an amber colored, musky exudate. The secretions of these glands are thought to contain odoriferous cues that facilitate maternal-young recognition. It also has been suggested that the secretions of the pouch sudoriferous glands may have bactericidal properties.

Lactation in the opossum is separated into two phases: a teat attachment and the fixation phase, and a nest phase. The former phase occurs for about the first nine weeks of postnatal life when the young are fixed to a teat, which cannot be released voluntarily. During the nest phase, which occurs late in lactation, young can release the teat and are often left in a den (nest) as the mother forages for food. Young are not weaned until about 100 days postnatal.

Mammary gland primordia appear as small oval thickenings of the epidermis in the newborn opossum. As these solid oval thickenings expand into the underlying dermis they acquire a flask shape. The mammary anlagen occur in pairs arranged in two lines each of which forms a semicircular pattern inside the forming pouch. Usually six such pairs are present in each line with a single unpaired median mammary gland occurring between the two groups. The mammary gland primordia of the female show signs of branching by the seventh postnatal week and by twelve weeks the position of the ducts are clearly established. The solid epithelial invaginations of the mammary anlagen become tubular and eventually ducts and a few scattered secretory alveoli are established. Sebaceous glands are present in the overlying integument. The same general pattern of development occurs in the male but

components appear less well developed and smaller. Considerable development and expansion of the mammary glands occurs during pregnancy and lactation.

Acknowledgments:

Fig. 1, courtesy of and from: Krause, W.J. and W. A. Krause (2004) The Opossum: Its Amazing Story. Walsworth Publishing Company, Marceline, Missouri, pp. 71

Fig. 2 (bottom), courtesy of and from: Krause, W.J. (1998) A review of histogenesis/organogenesis in the developing North American opossum (*Didelphis virginiana*). Adv. Anat. Embryol. Cell Biol. 143 (II): Springer Verlag, Berlin, pp 120.

Fig. 3, courtesy of and from: Enders, R.K. (1937). Panniculus carnosus and formation of the pouch in Didelphids. J. Morphol. 61: 1-26.

Fig. 1. (*Above*). The pouch of a young female opossum opened with gentle finger pressure to reveal the pouch young that are about four weeks old. (*Below*). A photograph illustrates at increased magnification the lips or margins of the pouch opening. Note the amber colored hair associated with the pouch. The color of the stained fur is thought to be the result of sudoriferous (apocrine sweat) glands located in the integument lining the pouch interior.

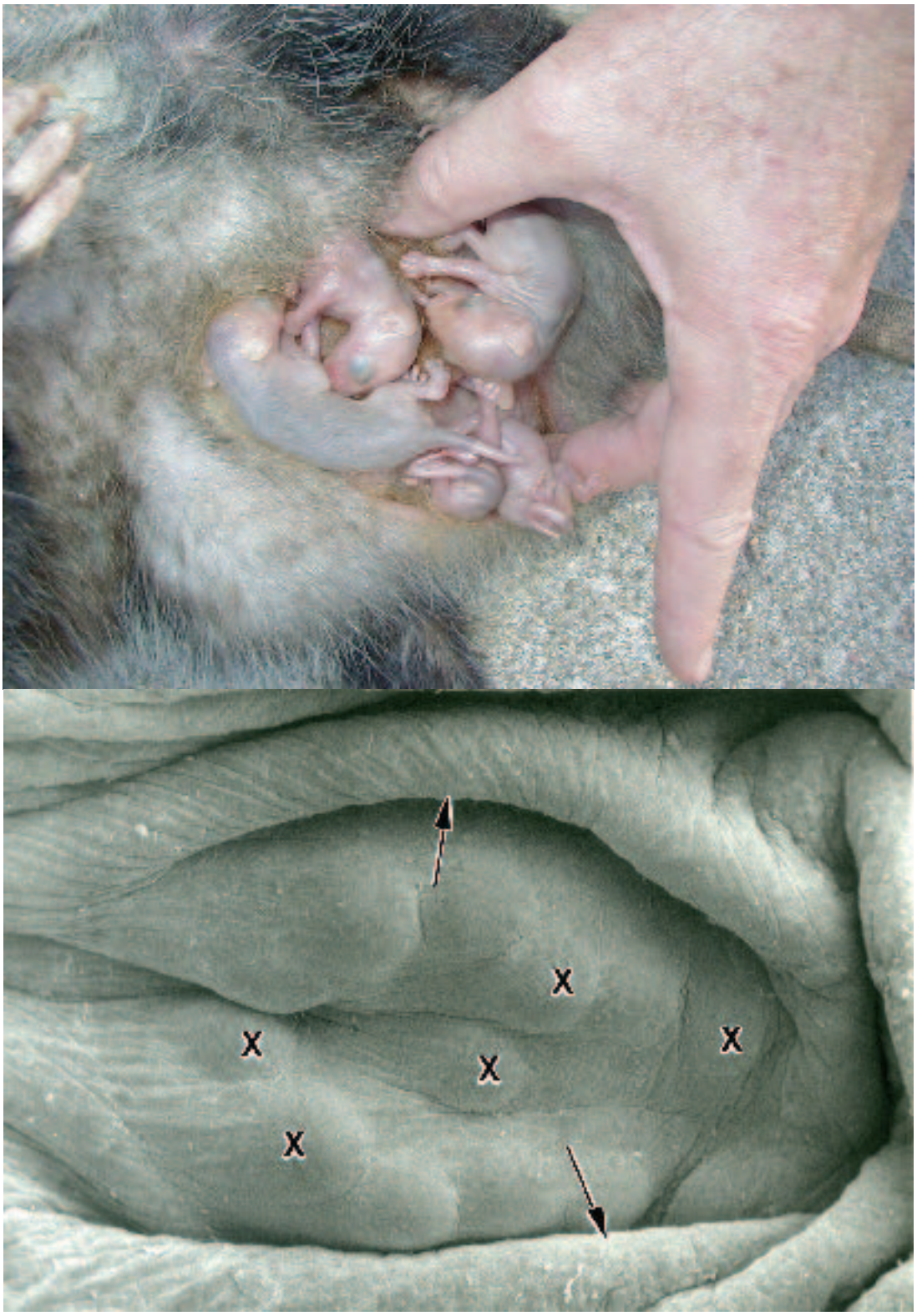

Fig. 2. (*Above*). The opossum pouch expands to accommodate the growth of the young. (*Below*). The developing pouch of an opossum twenty-five days postnatal. The developing lateral folds (arrows) of the presumptive pouch as well as the primordia for several of the mammary glands (X) can be observed. The developing mammary glands are organized into two lateral lines each of which forms a semicircular pattern within the forming pouch. Usually there are six mammary glands in each lateral line separated by a single median mammary gland. Pouch young female opossum, snout rump length 50 mm. SEM X 25.

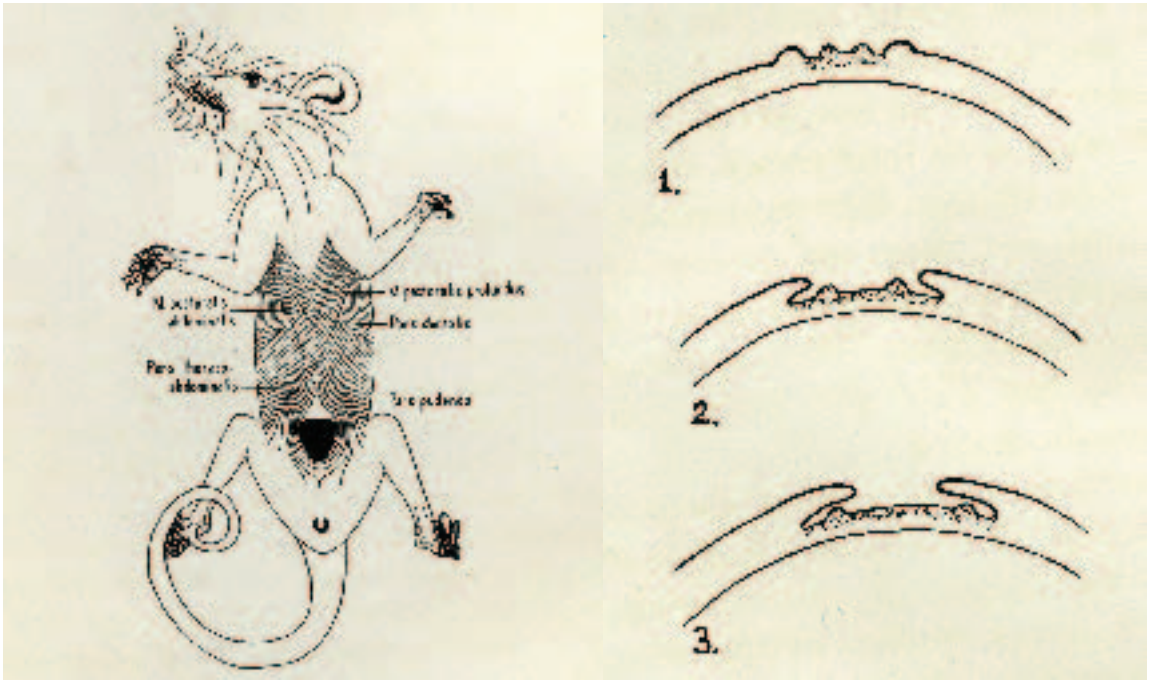

Fig. 3. (*Left*). A line drawing of the panniculus carnosus of a closely related species, *Didelphis marsupialis*, illustrates the three subcomponents of this cutaneous muscle: pars dorsalis, pars thoracoabdominalis, and pars pudenda. The skeletal muscle fibers of the pars pudenda are well developed and pass around the pouch forming the sphincter marsupii. Some short skeletal muscle fibers that arise immediately anterior to the pouch opening (not shown) course between the folds of skin forming the pouch and insert into the skin at the pouch margin (lips of the pouch). Muscle fibers of the panniculus carnosus do not extend into the mammary gland area. (*Right*). A schematic drawing illustrates pouch formation in Didelphids. Initially, epidermal ridges appear around the region of forming mammary glands. These ridges will ultimately form the lips of the pouch and are visible macroscopically by the end of the second postnatal week in *Didelphis virginiana*. A pouch forms as a result of the epidermal ridges remaining stationary during growth as the area of the developing mammary glands expands. As a consequence of this growth pattern, the surrounding skin expands into a double-walled fold around the expanding mammary gland area.

Chapter 10. General Postnatal Features

Synopsis:

The most notable feature of the newborn opossum and early pouch young is their overall embryonic appearance. The newborn exhibits a well-developed shoulder girdle and forelimbs and the digits of the forepaws bear deciduous claws. These features are in marked contrast to the clawless hind limbs that are only at the paddle stage of development. The advanced development of the cranial half of the newborn is directly related to the unaided migration of the newborn to the pouch at birth. The coordinated crawling movement of the forepaws, the precocious appearance of functional olfactory epithelium in the snout, the presence of hair cells within the macula of the utricle, together with a large mouth containing a well developed tongue all are essential features for pouch and teat location as well as initial teat attachment and suckling. After nipple attachment the lateral margins of the mouth fuse and only the apex of the forming snout remains open to permit an entrance for the teat. Although the epithelium lining the oral cavity and that covering the teat are in close approximation for about the next 60 days (the fixation period when the opossum remains attached to the same teat for this period), fusion of maternal to fetal tissues does not occur. The epiglottis at birth projects into the nasopharynx so that following teat attachment, milk is channeled laterally to enter the esophagus. Air coming from the nasal cavity passes medially into the trachea. This arrangement ensures simultaneous patency of the digestive and respiratory passageways. The most prominent features of the head during the first postnatal days are the oral shield and widely flared external nares. The external ears (pinnae) are unformed and together with the fused eyelids are covered by an epitrichium, as is the remainder of the body surface. By the end of the second postnatal week the pinnae are visible as swellings on the lateral sides of the head, the hind limb is more advanced in development, the deciduous claws of the forepaws have been shed, and the mouth and eyes remain tightly closed. By the end of the seventh week of postnatal life, the upper and lower lips remain fused but are more clearly defined. The eyelids remain closed. Vibrissae (tricholith hairs) are clearly visible around the mouth and in a patch located posterior and inferior to the eye. The pinnae have formed and a light downy hair covers the dorsal body surface. Development of the forelimbs remains in advance of the hind limbs and even at nine weeks postnatal locomotion is by a crawling motion of the forelimbs with the hind limbs being relatively immobile. Pouch young opossums can detach from the nipple, are freely mobile and can leave and return to the pouch by the end of the tenth postnatal week. The young are fully furred except for the ventral surface and the forelimbs and hind limbs show a similar degree of development. Lips remain fused at the corners and the eyes have yet to open completely. By the end of the eleventh postnatal week the opossum is completely furred and coarse guard hairs are a prominent feature. The eyes are now fully open and the lips completely separated.

Acknowledgments:

Figs. 2, 6 (top) and 10 (top), courtesy of and from: Cutts, J.H., Krause, W.J., and C.R. Leeson (1978) General observations on the growth and development of the pouch young opossum, *Didelphis virginiana*. Biol. Neonate 33:264-272

Fig. 1 (top), courtesy of and from: Krause, W.J. and W. A. Krause (2004) The Opossum: It's Amazing Story. Walsworth Publishing Company, Marceline, Missouri, pp. 71

Fig.1. (*Above*). The newborn opossum has an overall embryonic appearance but does exhibit a well-formed shoulder girdle and forelimbs. In contrast, the hind limbs are at the paddle stage of development. Note the deciduous claws on the forepaws. Snout-rump length 14 mm. (*Below*). At three days postnatal the lateral margins of mouth are fused and only anteriorly are the lips separated to permit the entrance of a nipple. Like the newborn, the external ears are unformed; the eyelids are fused with the most prominent facial feature being the widely flared nostrils. Pouch young opossum, snout-rump length 17 mm.

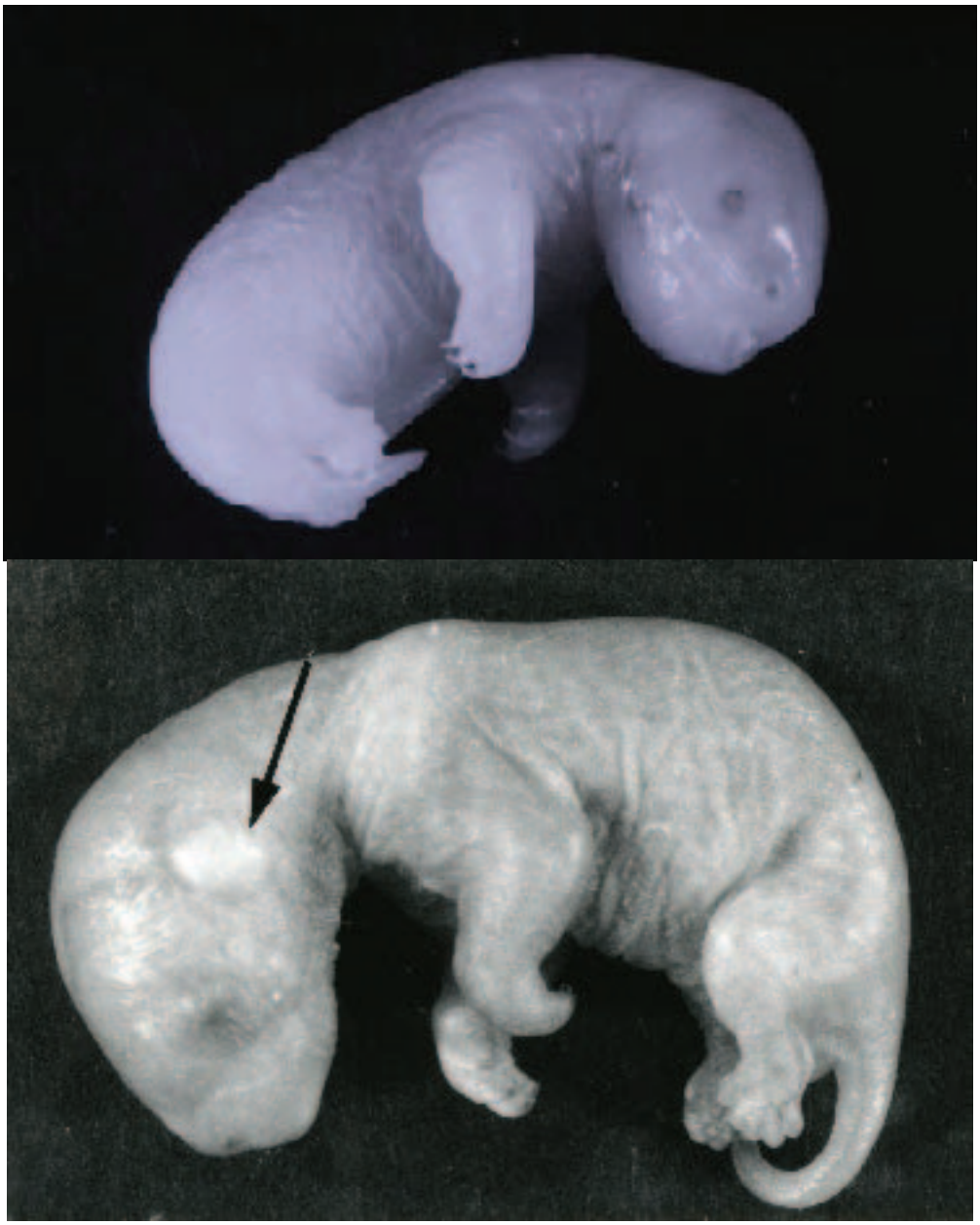

Fig. 2. (*Above*). Even at one week postnatal the opossum is markedly immature in appearance. The lips remain closed except for the small anterior opening for the teat. The eyes also remain closed but their position is well defined due to the pigmented retina that can be visualized through the transparent overlying skin. Deciduous claws continue to be observed on the digits of the forelimb. Compare the overall development of the forelimb with that of the hind limb. Pouch young opossum, snout-rump length 25 mm. (*Below*). A swelling (arrow) on the lateral surface of the head indicates the pinna of the external ear at the end of the second postnatal week. The deciduous claws have been shed and new nails are beginning to emerge on the digits of the forepaws. Development of the hind limb has progressed markedly in one week but continues to lag behind the development of the forelimbs. The integument appears more opaque in comparison to earlier developmental stages. Pouch young female opossum, snout rump length 35 mm.

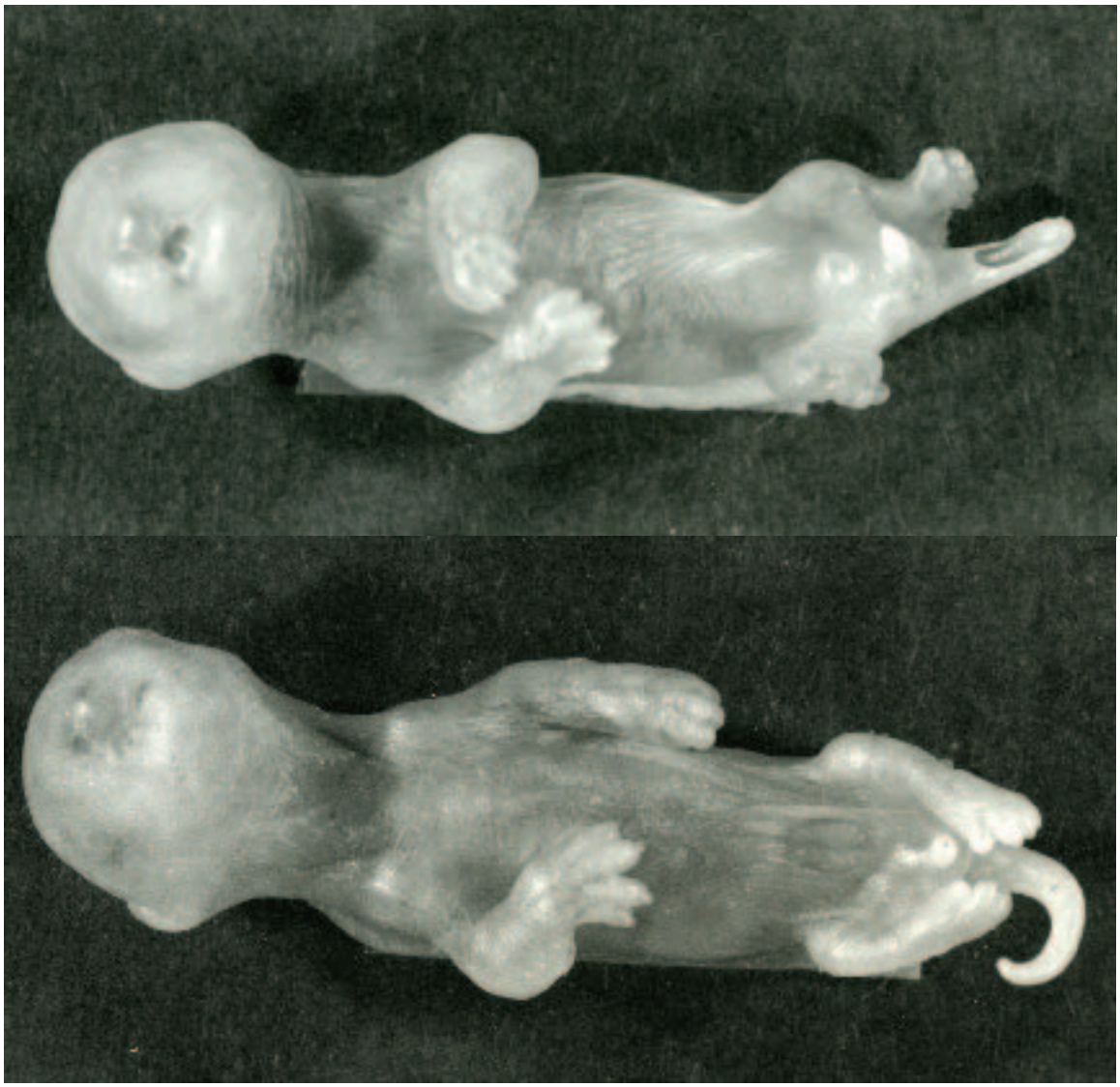

Fig. 3. (*Above*). The ventral aspect of an opossum two weeks postnatal exhibits more obvious development as compared to earlier ages. The lips and eyelids remain tightly fused. This pouch young male opossum can be identified by the appearance of a scrotum. Snout-rump length 35 mm. (*Below*). An obvious pouch located along the caudal aspect of the ventral surface identifies this pouch young opossum as a female. Snout-rump length 35 mm.

Fig. 4. (*Above*). A photograph illustrates the lateral aspect of a pouch young female opossum three weeks postnatal. Note the appearance of the external ear (pinna) and the continued rapid development of the hind limb. (*Below*). A photograph illustrates the ventral surface of the opossum shown in the above figure. Note the developing pouch and the appearance two milk lines. The eyelids and lips (although well defined) remain tightly fused at this stage of postnatal life. Pouch young opossum, snout-rump length 45 mm.

Fig. 5. (*Above*). A photograph illustrates the lateral aspect of a pouch young male opossum at three weeks postnatal. In addition to the appearance of the external ear, note the development of the Pollex extending from the hind paw and the appearance of the phallus. (*Below*). The ventral surface of the male opossum shown in the above figure illustrates the continued development of the scrotum and decent of the testes located in the inguinal region adjacent to the scrotum. The testes are enveloped by a heavily pigmented tunica vaginalis, which can be observed through the transparent integument. Pouch young opossum, snout-rump length 45 mm.

Fig. 6. (*Above*). A considerable advance in development is apparent by the end of the seventh week of postnatal life. Facial development includes the appearance of vibrissae around the mouth and in a patch inferior and posterior to the eye. The external ear continues to develop and expand. The dorsolateral surface of the trunk is lightly covered with fur and is most prominent over the back. The forelimbs remain considerably more advanced in development than the hind limbs. (*Below*). A photograph illustrates the ventral surface of the pouch young opossum shown above reveals that it is a male (note the scrotal sac). Note also the appearance of a cluster of vibrissae that have formed in the integument covering the ventral surface of the lower jaw. The lips, though still closed, continue to be more clearly defined. A light, downy hair that is more prominent along the spine also is observed. However, it should be noted that the initial emergence of hair occurs earlier at about four weeks postnatal (snout-rump length of 55 mm). Pouch young male opossum, snout-rump length 80 mm.

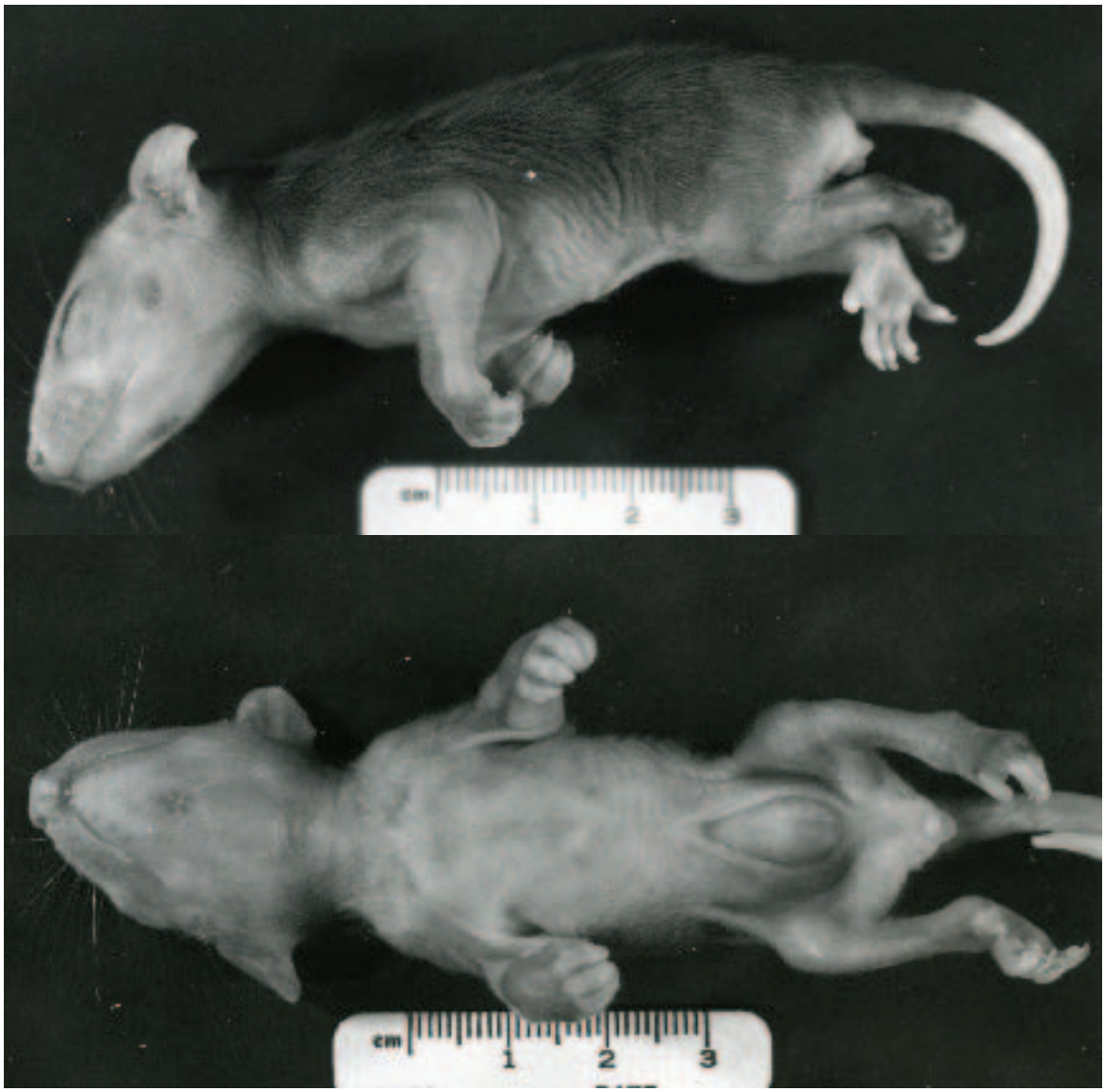

Fig. 7. (*Above).* A photograph illustrates the external (lateral) features of a pouch young female opossum eight weeks postnatal. (*Below*). A photograph illustrates the ventral surface of the female opossum shown in the above illustration. Note the continued development of a well-defined pouch. Hair continues to grow being most prominent on the dorsal surface. Development of the forelimbs remains in advance of the hind limbs. Pouch young female opossum, snout-rump length 95 mm.

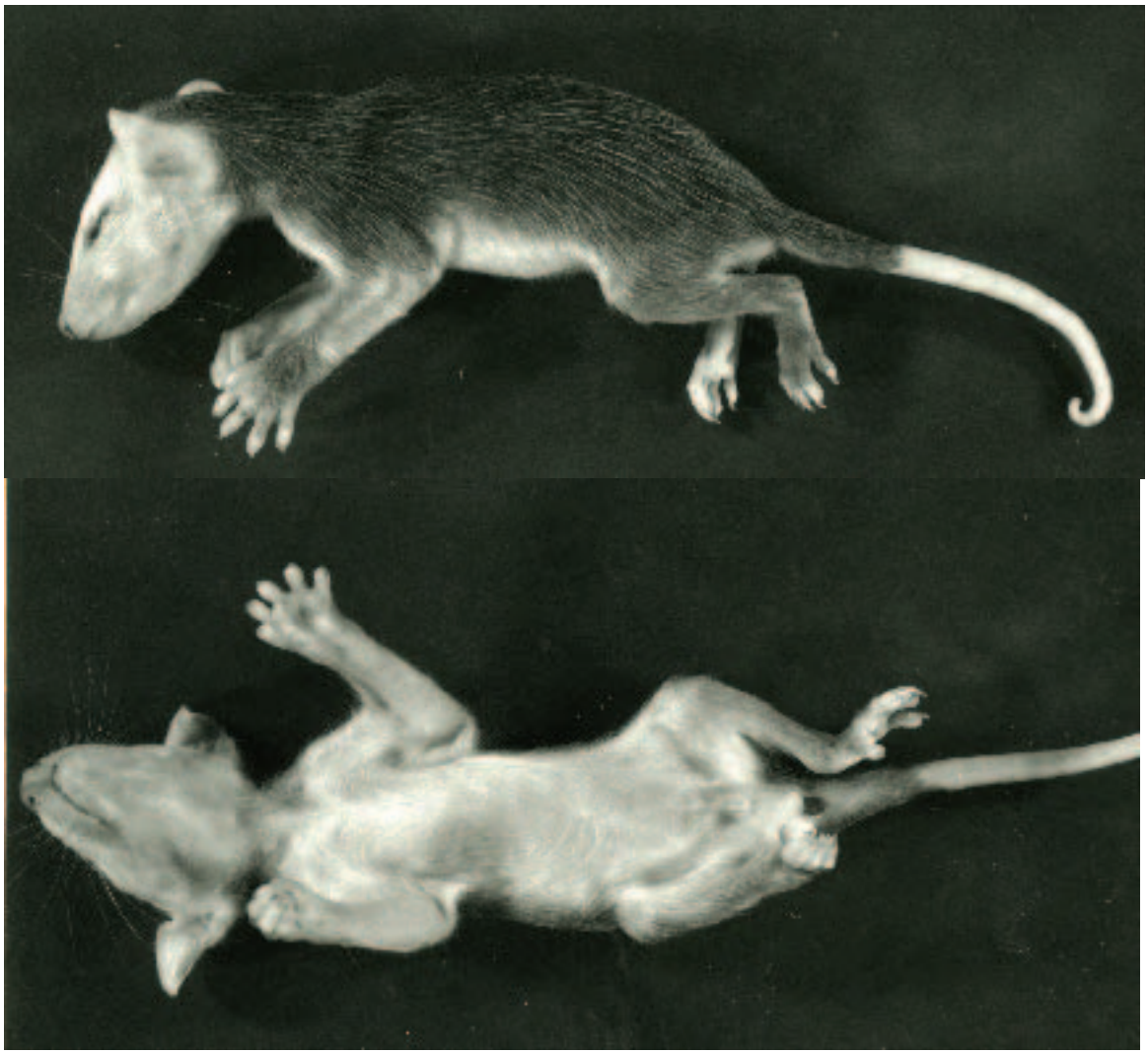

Fig. 8. (*Above).* A photograph illustrates the external features of a pouch young male opossum ten weeks postnatal. Pouch young at this age can detach from the nipple, are freely mobile, and are able to leave and re-enter the pouch at will. (*Below*). A photograph illustrates the ventral surface of the male opossum shown in the above illustration. Except for some sparseness along its ventral surface, the opossum is covered with fur. Pouch young male opossum, snout-rump length 120 mm.

Fig. 9. (*Above*). A photograph illustrates the external features of a pouch young female opossum ten weeks postnatal. The eyes are not fully opened at this stage of postnatal life and the lips remain fused at the corners of the mouth. (*Below*). A photograph illustrates the ventral surface of the female opossum shown in the above illustration. Pouch young female opossum, snout-rump length 120 mm.

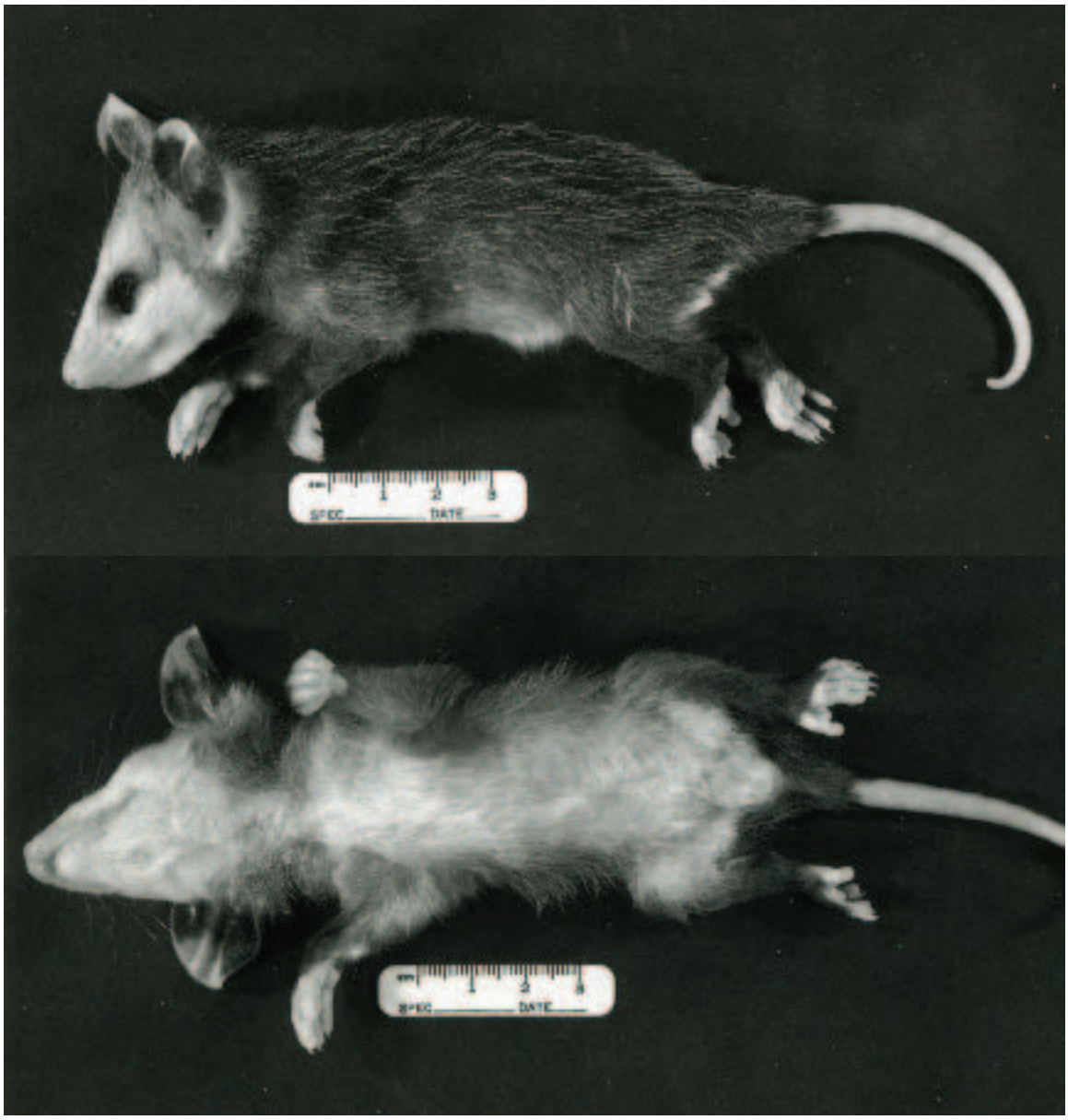

Fig. 10. (*Above*). A photograph illustrates the dorsolateral surface of a pouch young male opossum eleven weeks postnatal. The mouth and eyes are fully open and a luxuriant coat of fur with light guard hairs covers the dorsal and lateral surfaces of the trunk and limbs. The external ears (pinnae) appear large and well developed. (*Below*). The ventral surface of the pouch young male opossum eleven weeks postnatal shown above. Note that a luxuriant fur also covers the ventral surface and the presence of a small fur covered scrotal sac. Pouch young opossum, snout-rump length 140 mm.

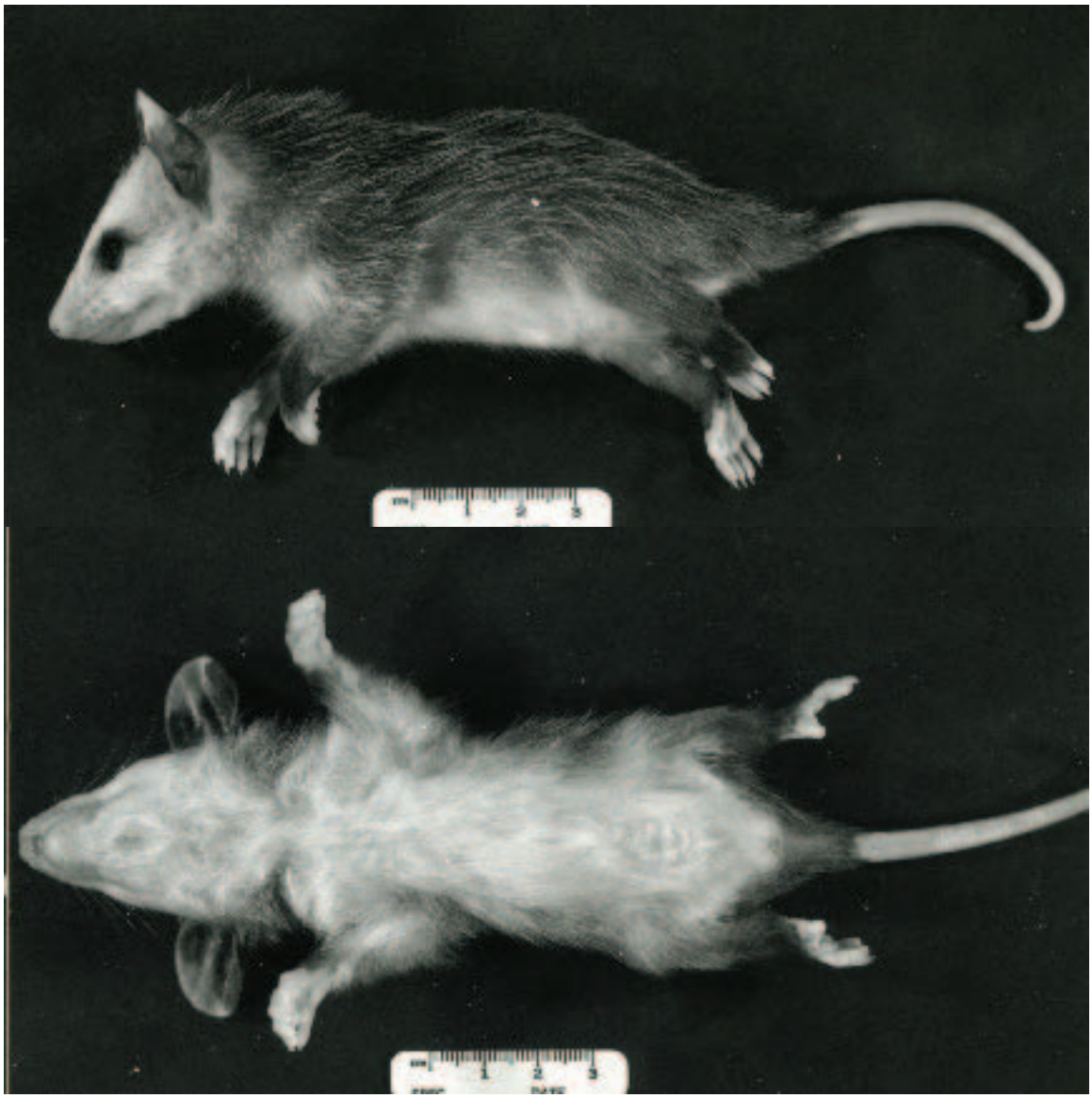

Fig. 11. (*Above*). A photograph illustrates the dorsolateral surface of a pouch young female opossum eleven weeks postnatal. (*Below*). A photograph illustrates the ventral surface of the pouch young female opossum eleven weeks postnatal shown above. Note that a luxuriant fur also covers the ventral surface and the presence of a small fur lined pouch on the caudal-ventral surface. Although opossums of this age freely leave and re-enter the pouch, they are still dependent on the mother for nutrition. Pouch young opossum, snout-rump length 140 mm.

Chapter 11. Integument

Synopsis:

Initially, a single layer of cube shaped cells derived from ectoderm covers the external surface of the late nine-day embryo. By the eleventh prenatal day, a surface layer of flattened cells called the periderm or epitrichium is present and with continued proliferation by underlying cells within the basal layer a stratum spinosum is formed. The opossum embryo (just prior to birth) and the newborn are completely covered by peridermal cells with the exception of the orifices to the external nares and the oral cavity. Distinct cell boundaries and nuclear profiles characterize individual cells of the periderm. The epidermis of the newborn opossum is about 43 μM thick and consists of a basal layer of cuboidal cells and a spinosal layer of fusiform shaped cells covered by peridermal cells. The epidermis is thicker in the snout region than on the trunk. Dermal papillae, hair follicles and glands are absent along the lateral and dorsal body wall; however, developing vibrissae (tricholith hairs) are present in the snout region. They begin their development on the day prior to birth.

The epidermis increases in thickness during the first postnatal week and the initial development of hair follicles is observed in areas covering the lateral and dorsal body wall. Cells of the periderm are lost and cells filled with bundles of cytokeratin filaments then appear to form a keratinized layer. Cytokeratin intermediate filaments are now prominent in cells forming the spinosa and germinal layers and membrane-coating granules appear in cells forming the stratum spinosum and granulosum for the first time. The epidermis attains its greatest depth (58 μM) by the end of the third postnatal week and hair follicles continue to differentiate and develop. Langerhans cells also are observed with greater frequency at this time. Hair shafts begin to emerge from hair follicles by the end of the fourth postnatal week and by the sixth postnatal week hairs are well established. At this time the epidermis decreases in thickness due primarily to a decrease in depth of the stratum spinosum. By ten weeks postnatal the epidermis is only about 20 μM thick. The epidermis continues to thin postnatally and in the adult is about 14 μM in thickness and consists of a germinal layer, a thin spinosal layer, a granular layer with prominent keratohyalin granules, and a keratinized layer.

Hair follicles make their initial appearance within the epidermis covering the body wall by the end of the first postnatal week. The first population of hair follicles develops during the rapid increase in epidermal thickness (the first three postnatal weeks); later follicles develop as the epidermis decreases in thickness.

A vascular bed of thin-walled, large bore vessels lies beneath the developing epidermis prior to birth. These vessels become less obvious postnatally and it may be that the thickness of the adult epidermis represents the maximum depth that can be maintained by the underlying dermis, which becomes less vascular with age. Although the epidermal-dermal interface appears irregular, true dermal papillae do not develop in association with the epidermis covering the trunk. The periderm may provide a protective barrier that prevents desiccation during the first few days of postnatal life.

Papillary ridges do develop during the postnatal period on the volar pads of both the fore- and hind paws. Dermal papillae begin to form by the end of the fourth postnatal week and are well established by the eighty days postnatal. It is the thick, keratinized epidermis that exhibits the exaggerated scalloped appearance on the pads and tori of both the forepaws and hind paws in the adult. The papillary layer of the dermis in this region is especially thick

and vascular where it abuts the epidermis. It is believed that the blood vessels of this region play a role in temperature regulation in the opossum. Typical eccrine sweat glands are found in the region of the paws and begin their development around the end of the third postnatal week. They occur elsewhere in the skin but are much fewer in number. Sudoriferous (apocrine sweat) glands also occur in the deep layers of the dermis within the footpads. Suprasternal and paracloacal glands develop in association with the integument and are thought to function as scent glands in *Didelphis*. The suprasternal gland region of the male opossum is readily identified by a diamond-shaped patch of amber/orange stained fur located between the neck and the sternum of the adult. The suprasternal gland region consists of both well-developed sebaceous and sudoriferous glands. Functional development and secretion of the glands in this region does not occur until puberty with the onset of androgen secretion. The glands are poorly developed in the female. In contrast, the paracloacal glands are equally developed in both sexes and consist of paired structures located along the walls of the cloaca. Each consists of two components: simple coiled tubular sudoriferous glands and a central storage vesicle. A single, elongated duct unites the storage vesicle to the integument near the cloacal orifice. Secretion of the paracloacal glands is pea green in color and has a strong musk odor. Development of the paracloacal gland unit begins early arising from the epithelium immediately beyond the opening of the cloaca. These glands are capable of elaborating a secretion by the end of the third postnatal week.

Acknowledgments:

Figs. 11 (top), 13 (top) and 16 (bottom), courtesy of and from: Cutts, J.H., Krause, W.J., and C.R. Leeson (1978) General observations on the growth and development of the pouch young opossum, *Didelphis virginiana*. Biol. Neonate 33:264-272.

Figs. 1, 2, 3, 4, 5, 6, 10, (bottom), 11 (bottom), 14 (bottom) and 15, courtesy of and from: Krause, W.J., J.H. Cutts and C.R. Leeson (1978) Postnatal development of the epidermis in a marsupial, *Didelphis virginiana*. J. Anat. 125:85-99.

Figs. 17 (bottom) and 18, courtesy of and from: Krause, W.J. (1992). Histological observations on the suprasternal gland region of the North American opossum (*Didelphis virginiana*). Zool. Anz. 227:286-294.

Fig. 17 (top), courtesy of and from: Krause, W.J. and Winifred A. Krause (2004) The Opossum: It's Amazing Story. Walsworth Publishing Company, Marceline, Missouri, pp. 71

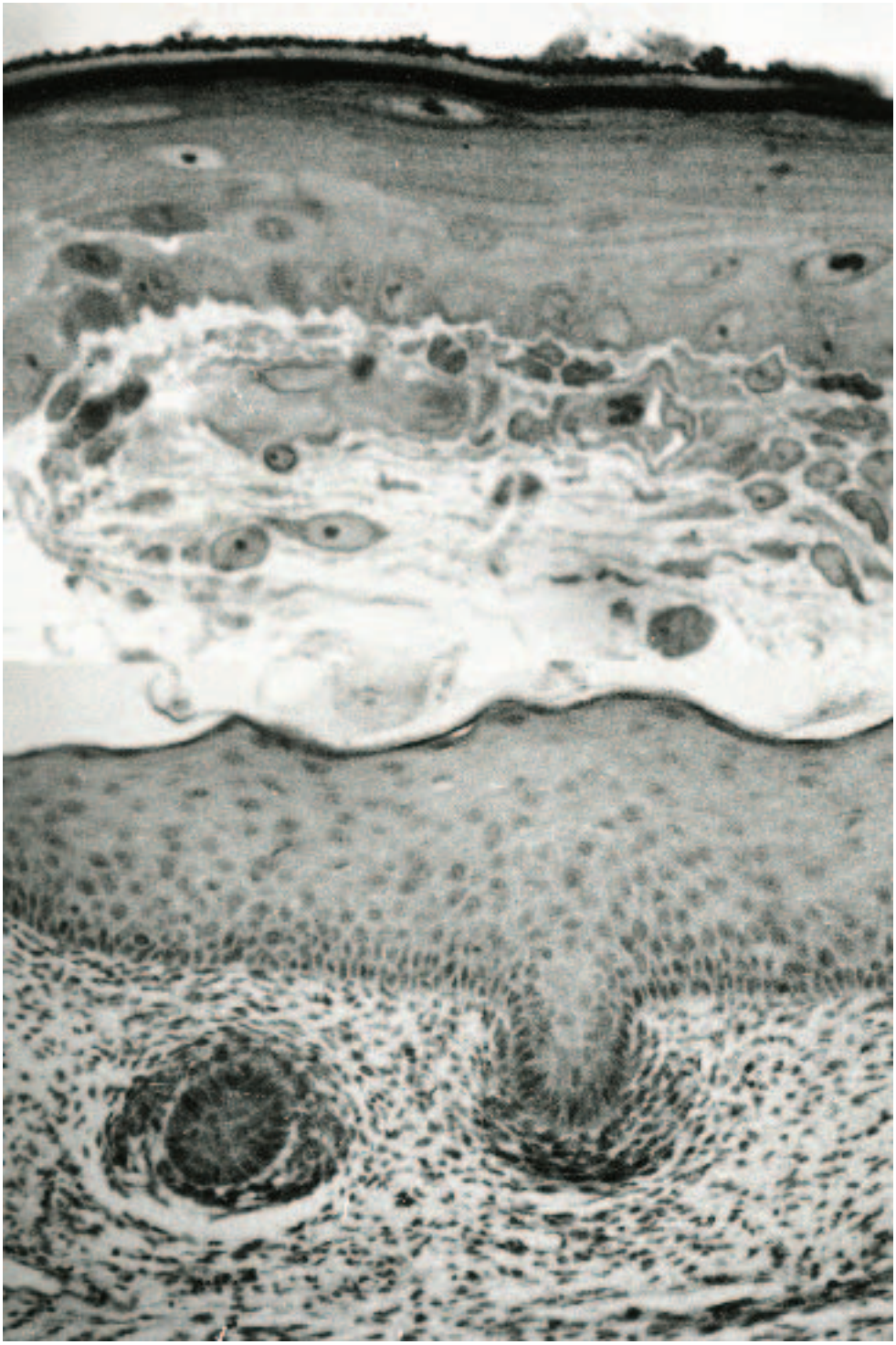

Fig.1. (*Above*). A micrograph illustrates a section of skin taken from the back of a newborn opossum. The epidermal-dermal interphase appears irregular. Cells constituting stratum basale, spinosum, and granulosum are clearly evident. A light staining periderm lies immediately above the forming keratinizing layer. LM X 600. (*Below*). A section of integument taken from the snout region of a newborn opossum illustrates the precocious development of vibrissae. The integument covering other regions of the body surface is devoid of hair follicles. LM X 200.

Fig. 2. (*Above*). The external surface of the newborn opossum epidermis is covered by a thin periderm. Squamous cells of the periderm are characterized by distinct cell boundaries and discrete, centrally positioned nuclei. SEM X 300. (*Below*). Occasional small colonies of bacteria are observed on the external surface of the periderm when it is examined at increased magnification. SEM X 700.

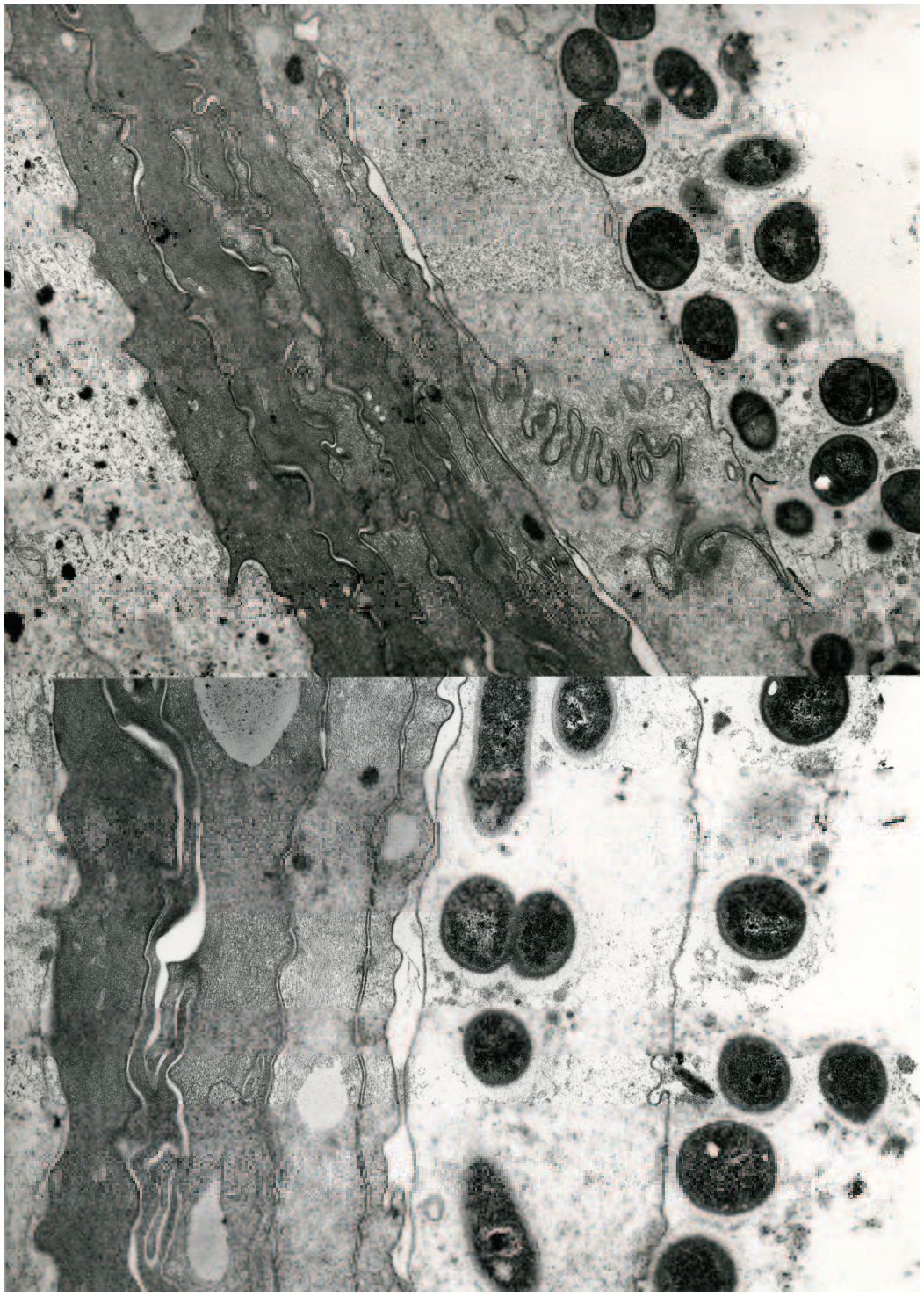

Fig. 3. (*Above*). The junction between two light staining cells of the periderm exhibits extensive implication of the adjacent cell membranes. Note that numerous bacteria lie on the external surface of the periderm. The forming keratinized layer of the epidermis is electron-dense and lies immediately subjacent to cells of the periderm. A portion of a cell from the stratum granulosum that contains keratohyalin granules is shown at the bottom left. TEM X 15,000. (*Below*). Bacteria are occasionally observed lying within the cytoplasm of cells forming the periderm. Keratinized cells of the stratum corneum are seen at the left. Both illustrations are from a newborn opossum. TEM X 25,000.

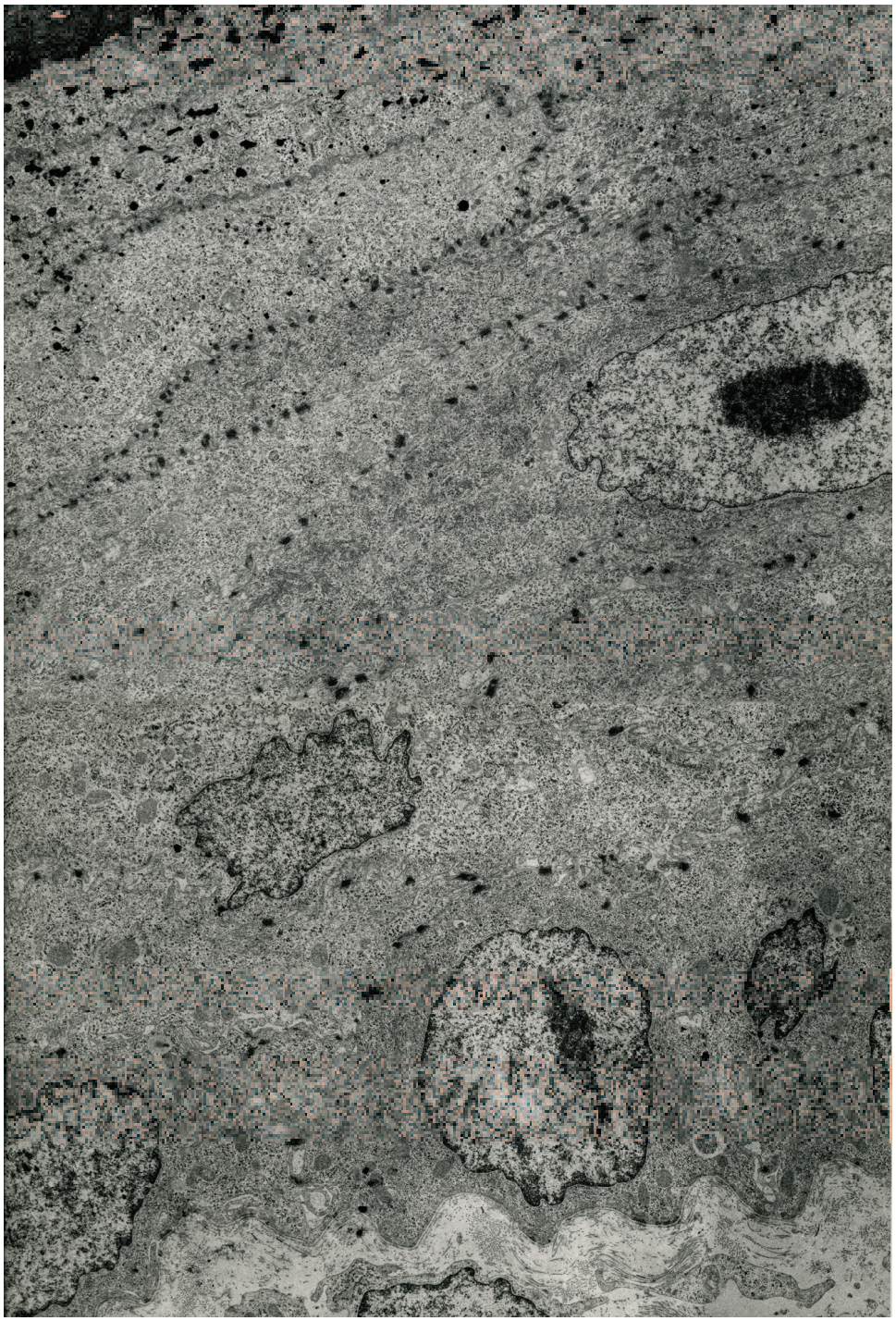

Fig. 4. An electron micrograph illustrates the depth of newborn opossum epidermis. The basal cell membrane of the stratum basale exhibits scattered hemidesmosomes and lies on a thin basal lamina. Note its irregular undulating course at the interphase with the underlying dermis. Cells of the stratum spinosum exhibit abundant free polyribosomes, scattered cytokeratin intermediate filaments and numerous desmosomes. Cell of stratum granulosum (top left) exhibit dense, irregular keratohyalin granules. A portion of stratum corneum also is shown in the upper left corner. TEM X 1,500.

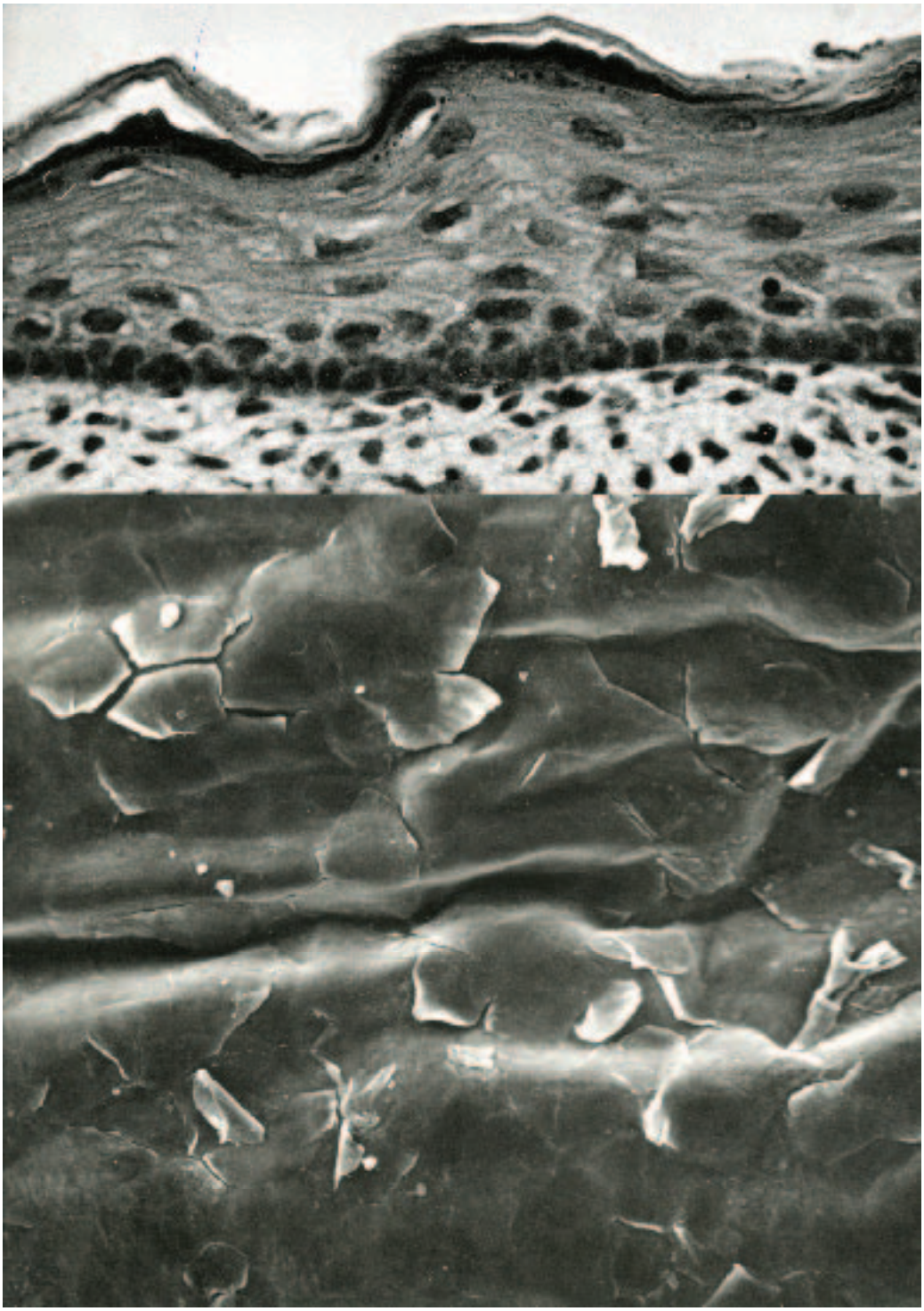

Fig. 5. (*Above*). The epidermis of an opossum one week postnatal exhibits an increase in depth of the stratum spinosum. Note that dermal papillae are absent. LM X 500. (*Below*). The external surface of the epidermis one week into the postnatal period exhibits what appear to be sloughing squames. SEM X 250.

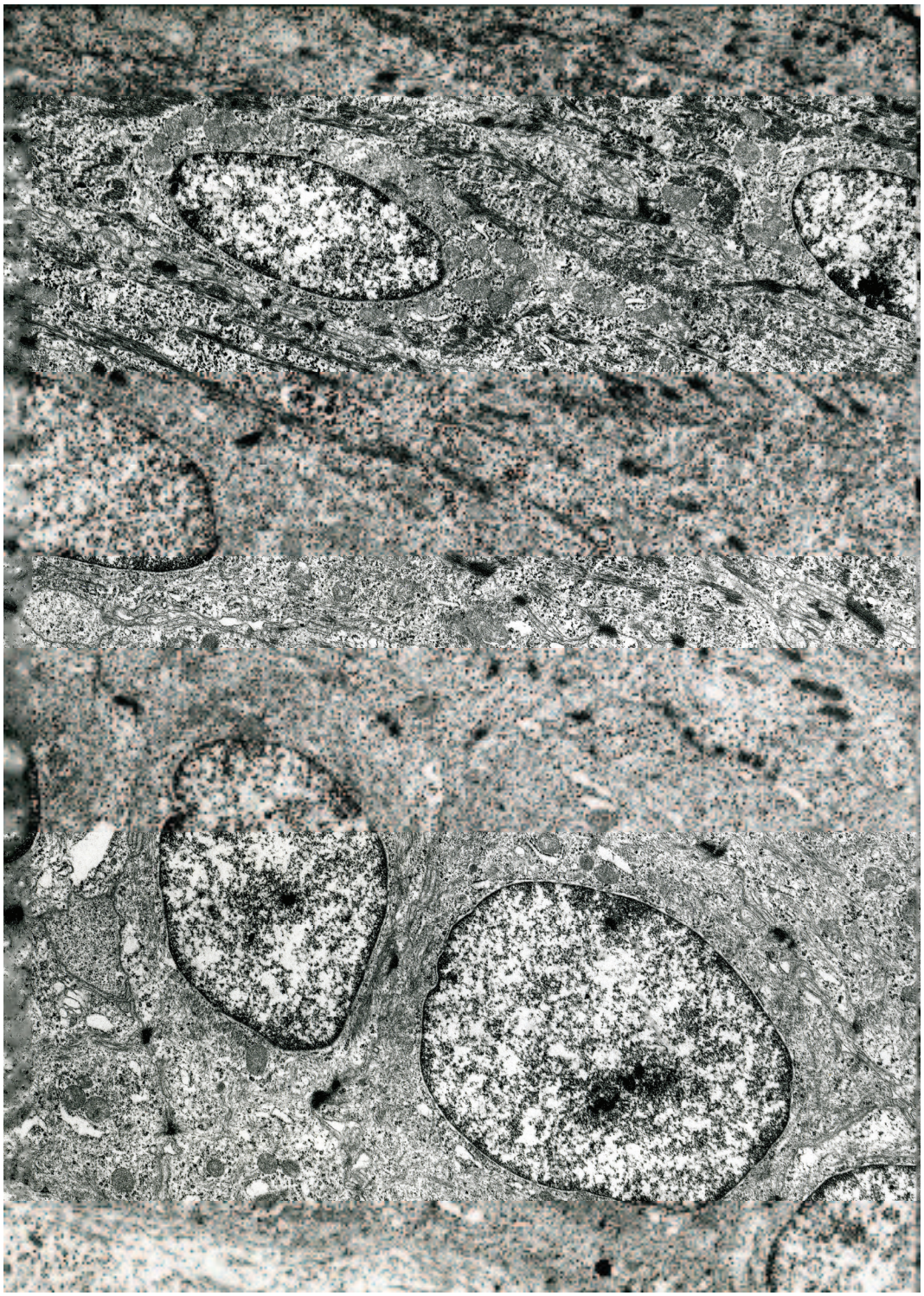

Fig. 6. Cells comprising stratum basale and the lower regions of the stratum spinosum show an increase in the number of bundles of intermediate filaments (cytokeratin) and numerous polyribosomes by the end of the first postnatal week. TEM X 7,500.

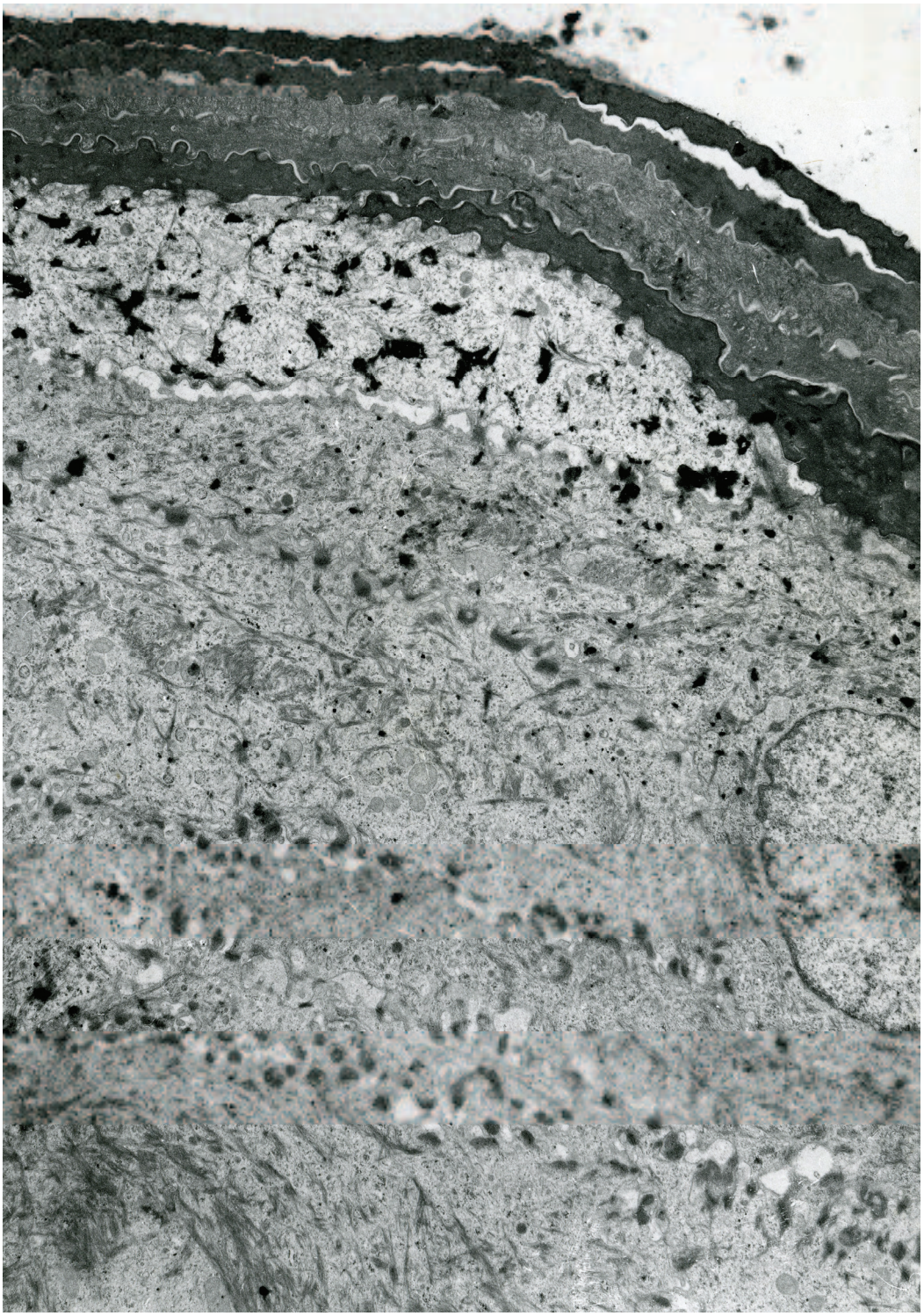

Fig. 7. A micrograph illustrates cells comprising the stratum corneum (the keratinized layer at the top), the stratum granulosum, and the upper layers of stratum spinosum from the epidermis of an opossum one week postnatal. The portion of a light-staining cell from the stratum granulosum is characterized by electron-dense, irregularly shaped keratohyalin granules within the cytoplasm. Cells from the upper region of the spinosal layer show an increase in the number of bundles of intermediate (cytokeratin) filaments. TEM X 3,500.

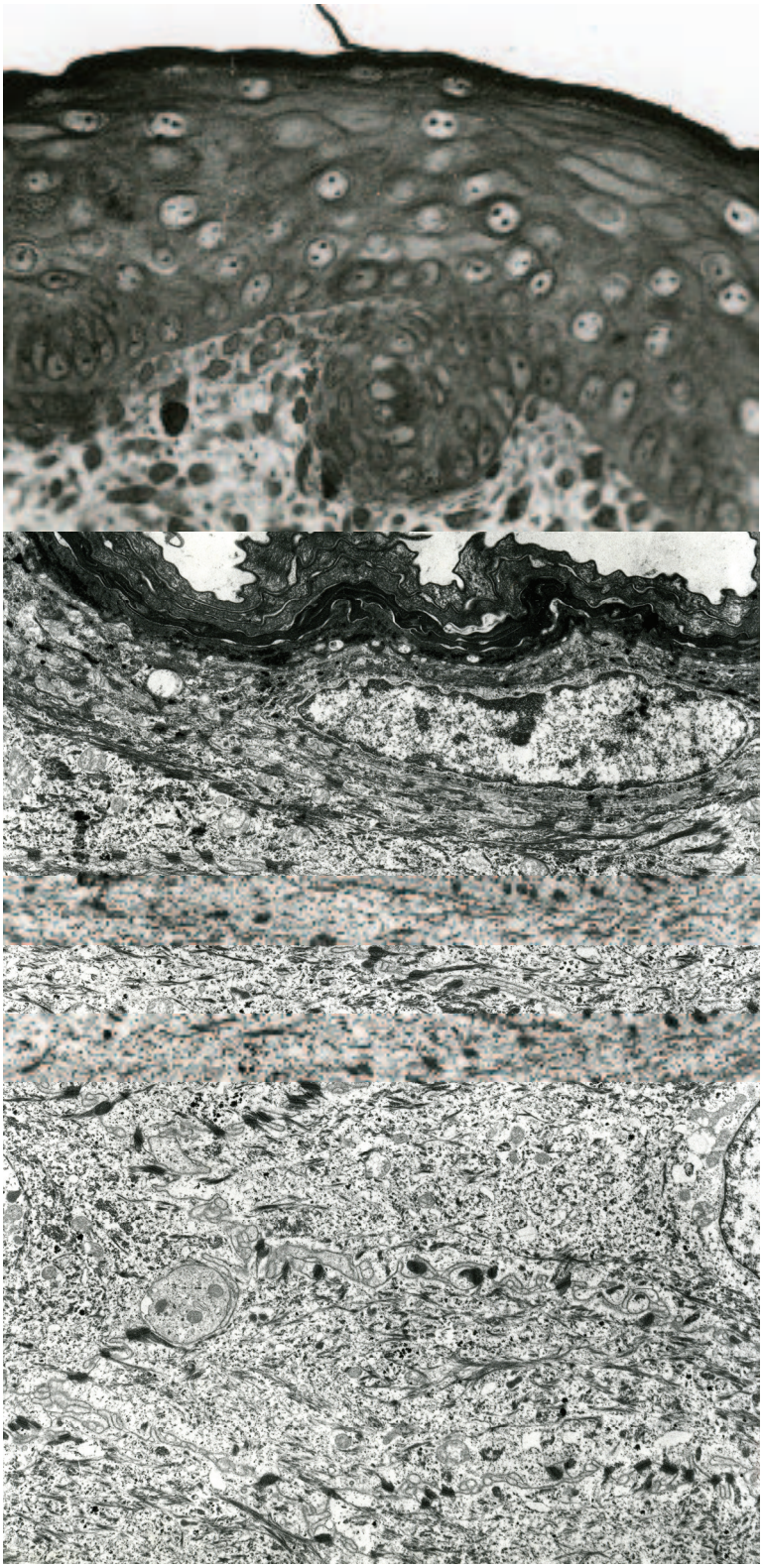

Fig. 8. (*Above*). The epidermis of an opossum 2.5 weeks into the postnatal period shows a continued increase in depth of the stratum spinosum. Note the development of hair follicles at this time. LM X 400. (*Below*). Observe the ultrastructural appearance of cells comprising the stratum corneum (the keratinized layer at top), stratum granulosum, and cells from the upper layers of the stratum spinosum. An opossum 2.5 weeks postnatal. TEM X 2,000.

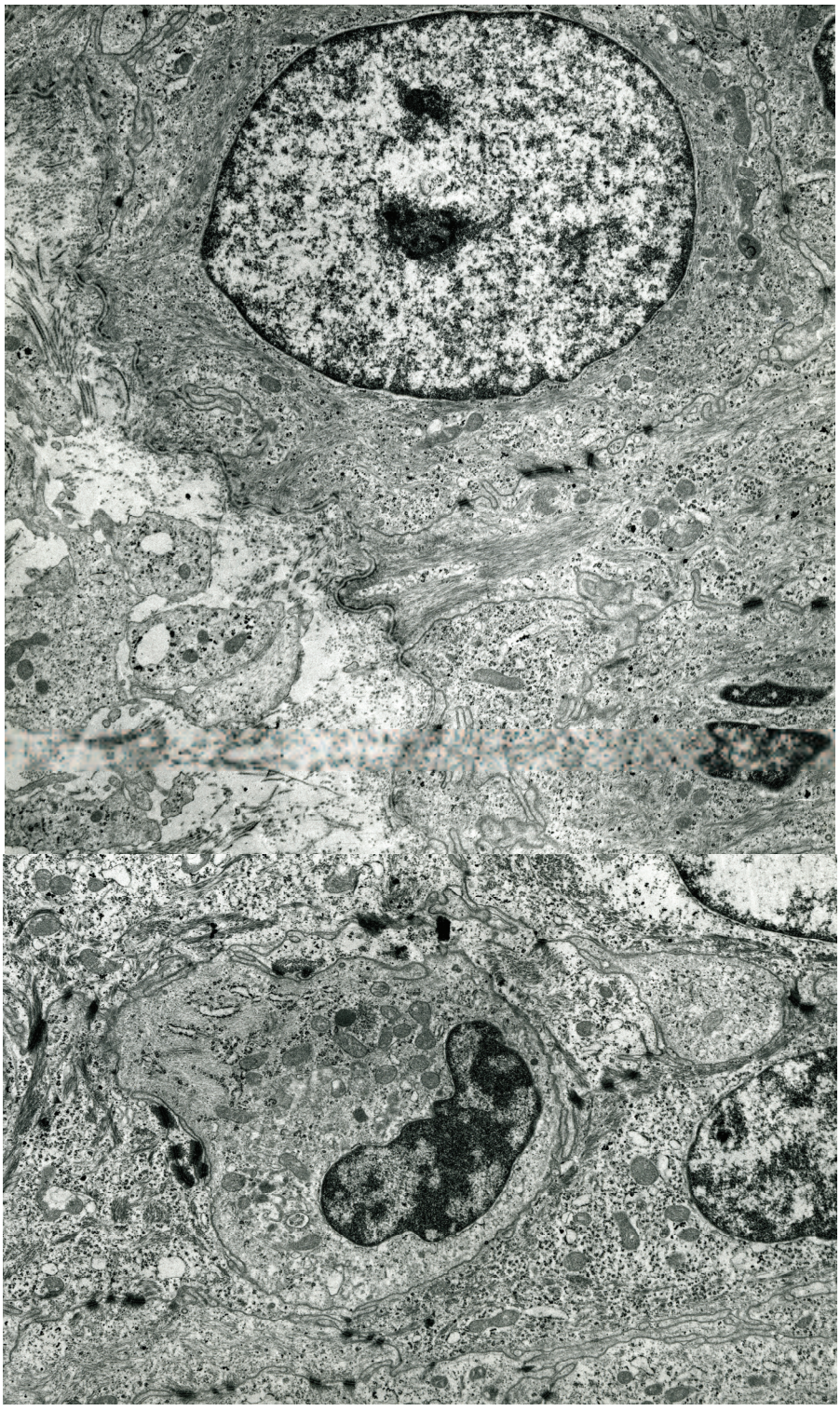

Fig. 9. (*Above*). The dermal-epidermal interface remains irregular in the opossum 2.5 weeks postnatal. Cells of the stratum basale continue to show an increase in intermediate (cytokeratin) filaments. Note the presence of numerous hemidesmosomes along the basal plasmalemma. TEM X 8,000. (*Below*). A micrograph illustrates a Langerhans cell (an antigen presenting cell) migrating between keratinocytes of the stratum spinosum. An opossum 2.5 weeks postnatal. TEM X 10,000.

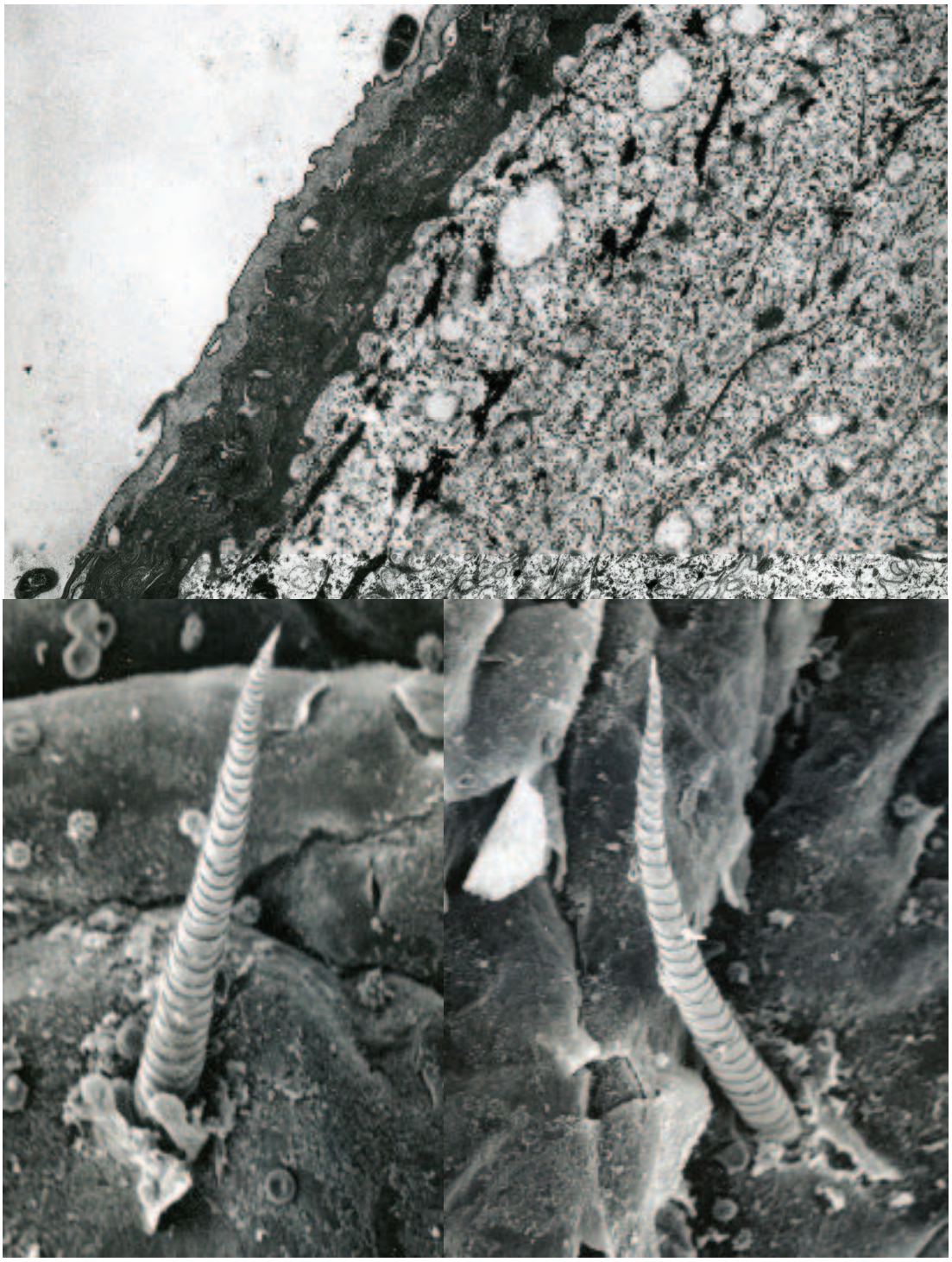

Fig. 10. (*Above*). Occasional bacteria (located on the extreme upper and lower surface of stratum corneum) continue to be encountered on the epidermal surface of the opossum 2.5 weeks postnatal. Note the keratohyalin granules present within the cytoplasm of a cell from the stratum granulosum. TEM X 8,000. (*Below left and right*). Micrographs illustrate the appearance of emerging hairs from the external surface of the epidermis of an opossum four weeks postnatal. SEM X 700; SEM X 600.

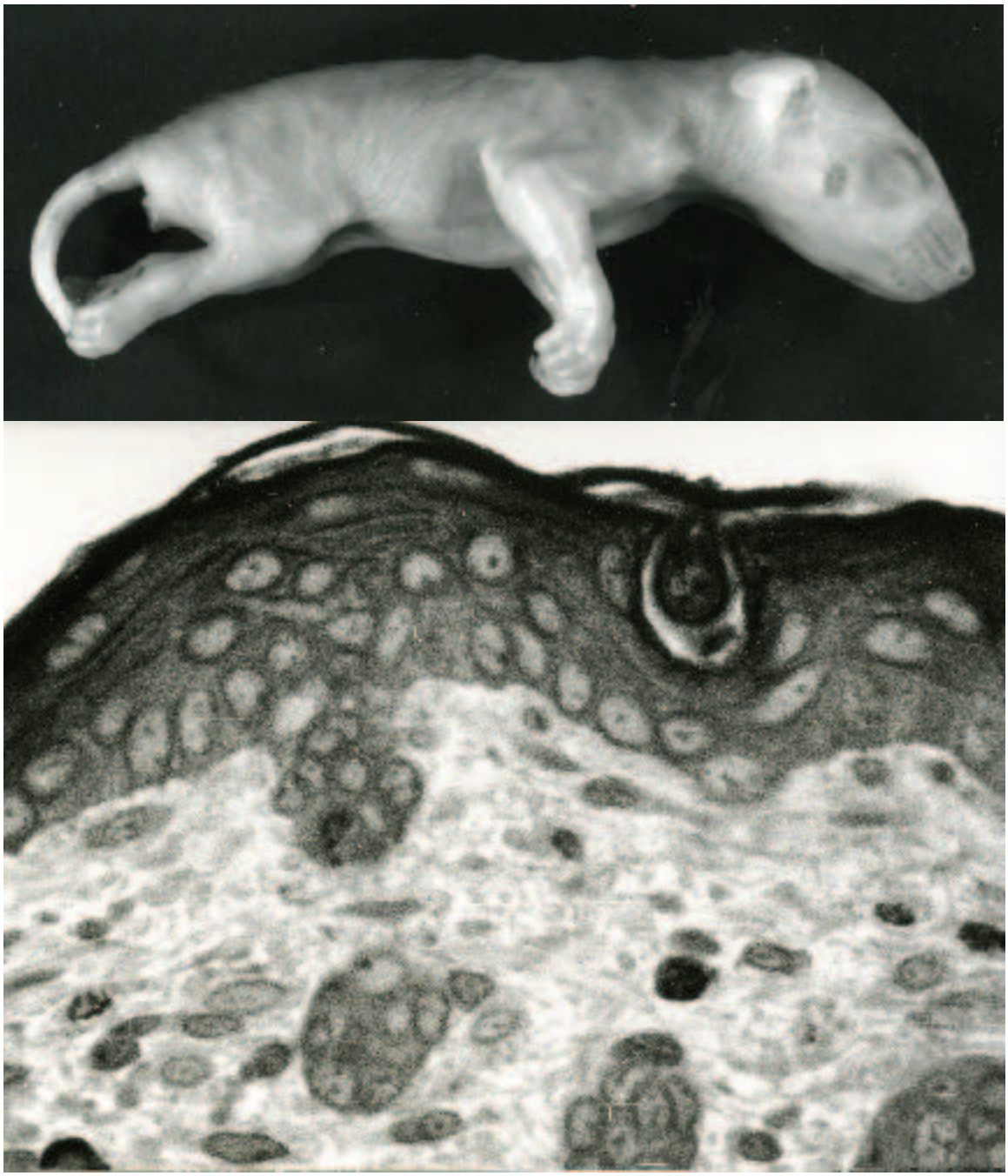

Fig. 11. (*Above*). By the seventh week of postnatal life a light downy hair, that is more prominent dorsally along the spine, covers the opossum. Note the development of vibrissae about the mouth and in a patch inferior and posterior to the eye. Pouch young opossum, snout-rump length 80mm. (*Below*). A micrograph illustrates a section through the integument of a pouch young opossum seven weeks postnatal. Note the appearance of an eccrine sweat gland coursing through the dermis at this time. LM X 650.

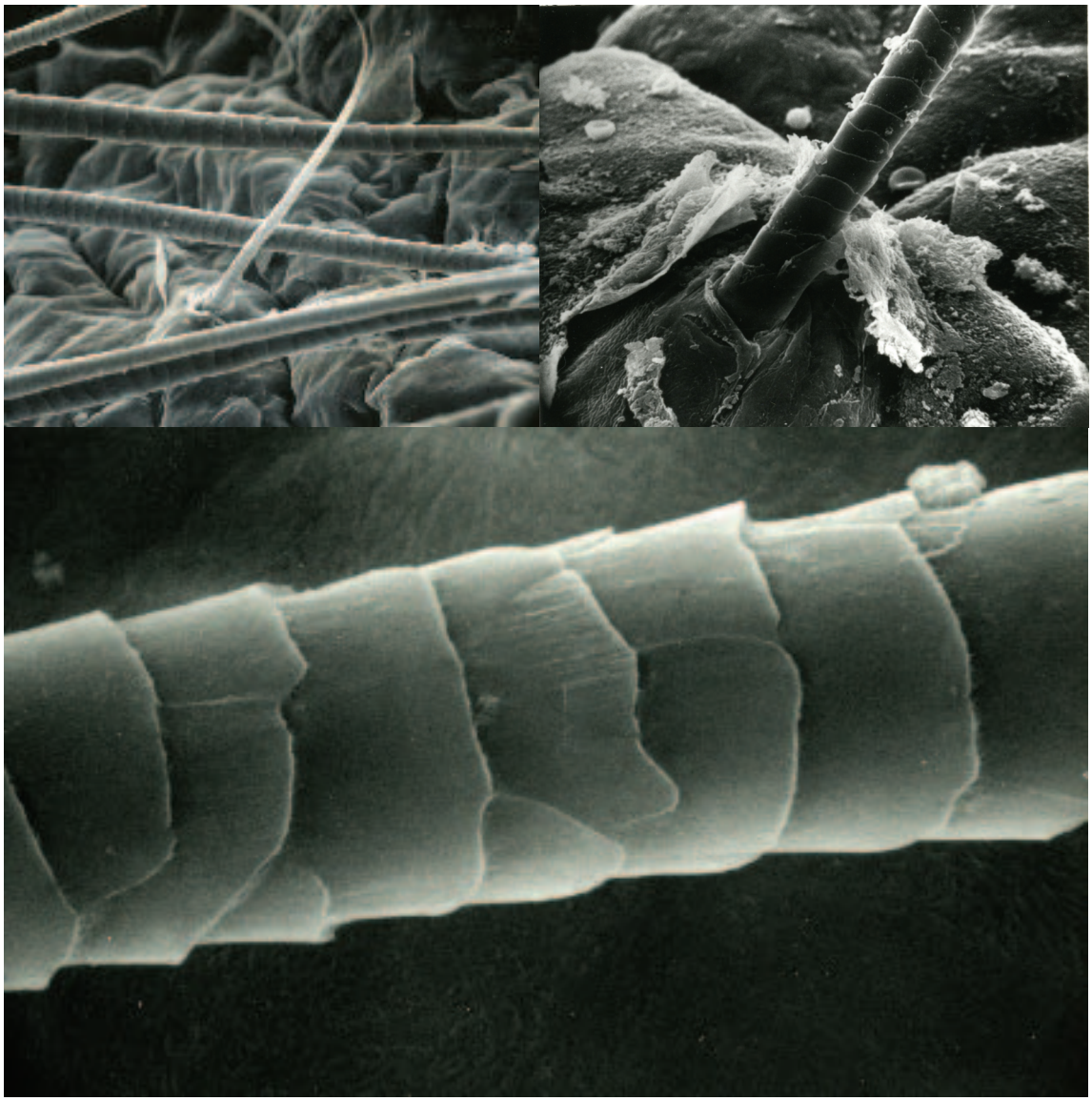

Fig.12. (*Above left*). A micrograph illustrates the epidermal surface of the dorsal integument from an opossum seven weeks postnatal. Several hairs can be observed lining parallel to the epidermal surface. Note that one hair (found near the center of the micrograph) is emerging from a hair follicle. SEM X 250. (*Above right*). A micrograph illustrates at increased magnification a hair shaft emerging from a hair follicle. Note the adjacent sloughing squame. Opossum seven weeks postnatal. SEM X 800. (*Below*). A segment of a hair shaft from an opossum seven weeks postnatal illustrates the pattern of squames forming its external (cuticular) surface. SEM X 2,500.

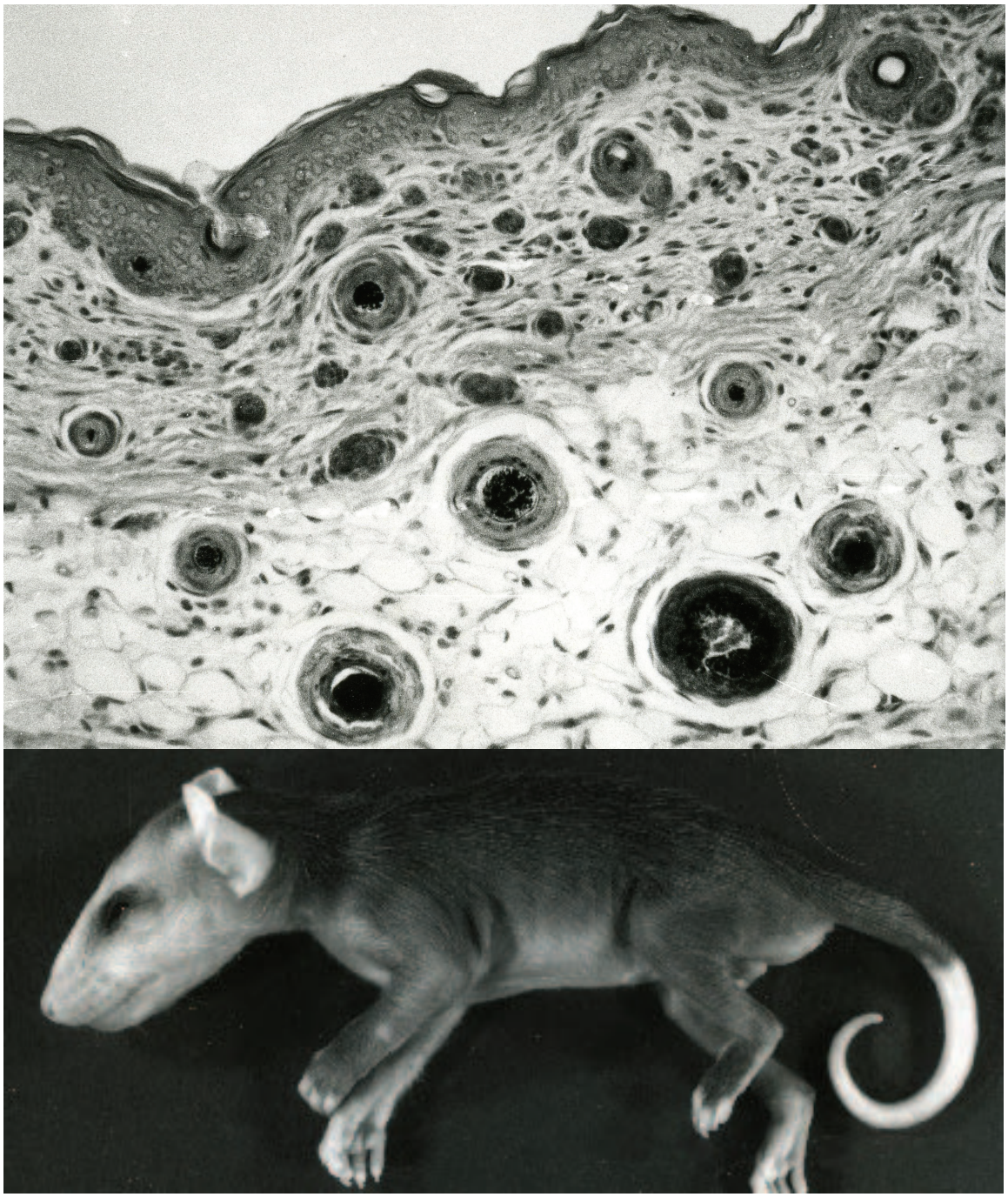

Fig. 13. (*Above*). A micrograph illustrates a section of developing integument from a pouch young opossum nine weeks postnatal. Note the abundance of developing hair follicles. LM X 500. (*Below*). Except for some sparseness along the ventral surface, the opossum is well furred by the end of the tenth postnatal week. Pouch young opossum, snout-rump length 115 mm.

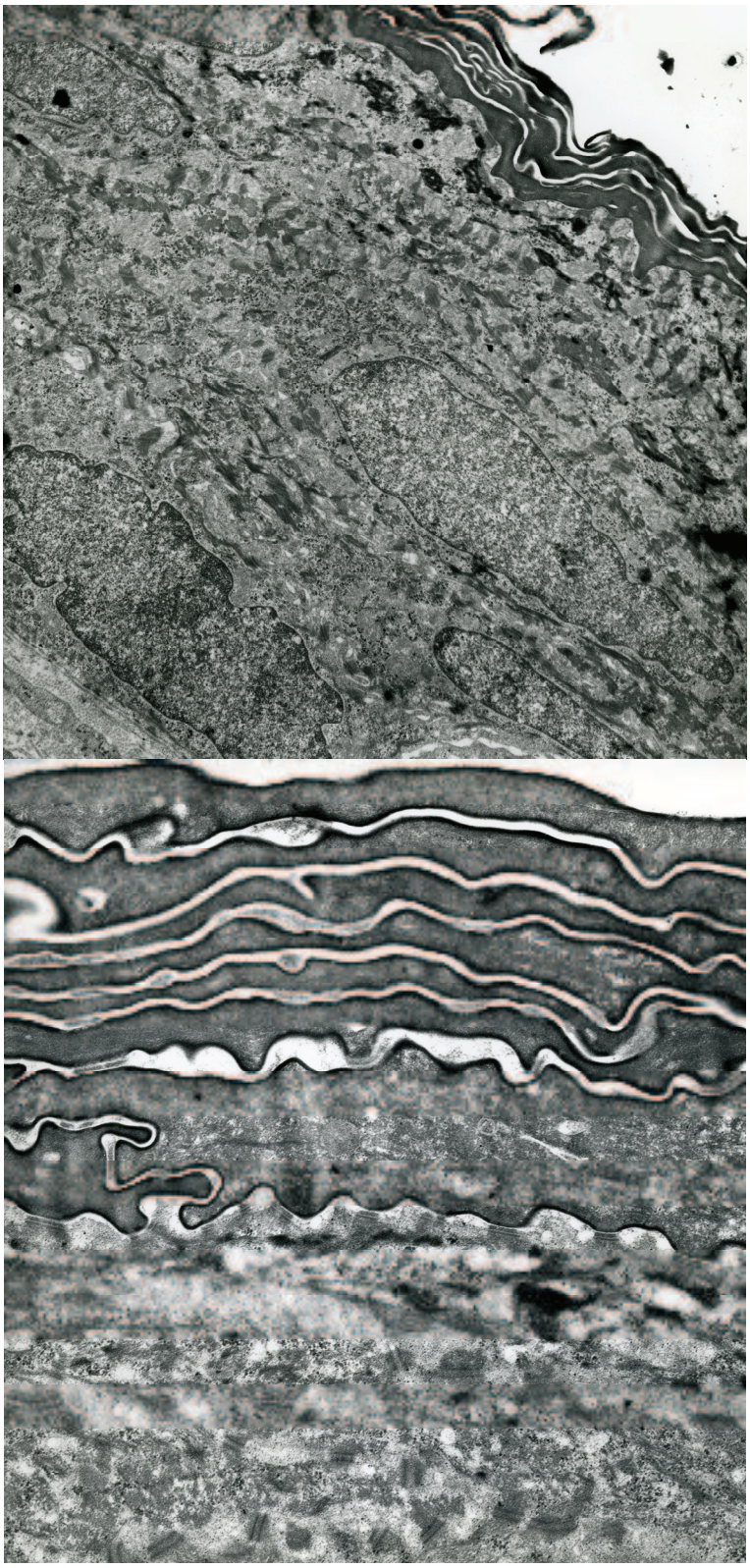

Fig. 14. (*Above*). A transmission electron micrograph illustrates the depth of the epidermis from the dorsal surface of an opossum ten weeks postnatal. TEM X 2000. (*Below*). A micrograph illustrates the stratum corneum and portions of cells forming the stratum granulosum and spinosum of an opossum 11.5 weeks postnatal. What appear to be degenerate desmosomes occur between elements of the keratinizing layer. TEM X 19,000.

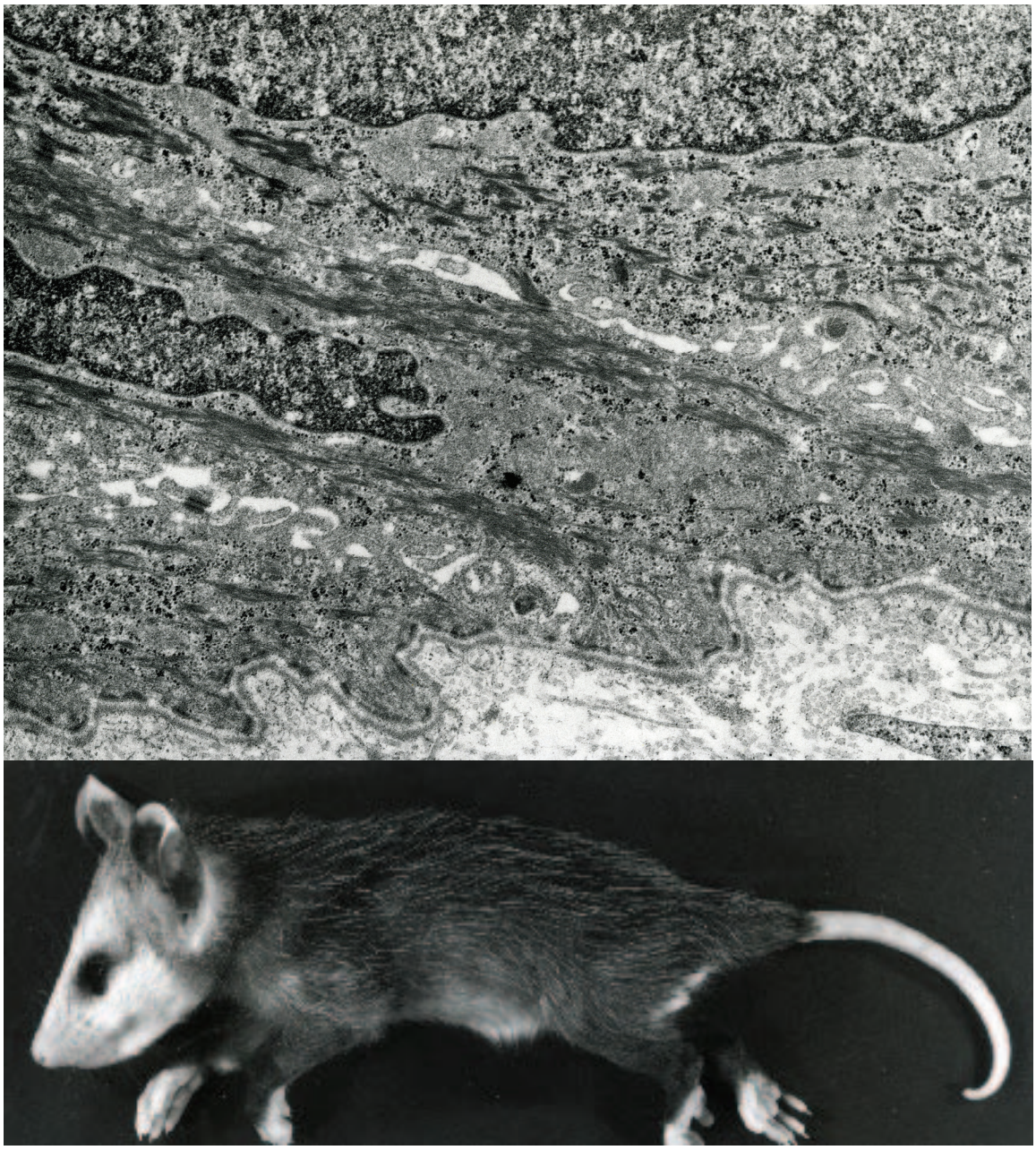

Fig. 15. (*Above*). A micrograph illustrates the interphase of the stratum basale of the epidermis with the underlying dermis of an opossum 11.5 weeks postnatal. Note the prominent basal lamina and the numerous hemidesmosomes associated with the basal plasmalemma of cells forming the stratum basale. Note also the abundance of cytokeratin intermediate filaments within the cytoplasm of these cells. TEM X 15,000. (*Below*). By eleven weeks postnatal a luxuriant coat of fur with prominent guard hairs covers the opossum and extends onto its ventral surface. Pouch young opossum, snout-rump length 140 mm.

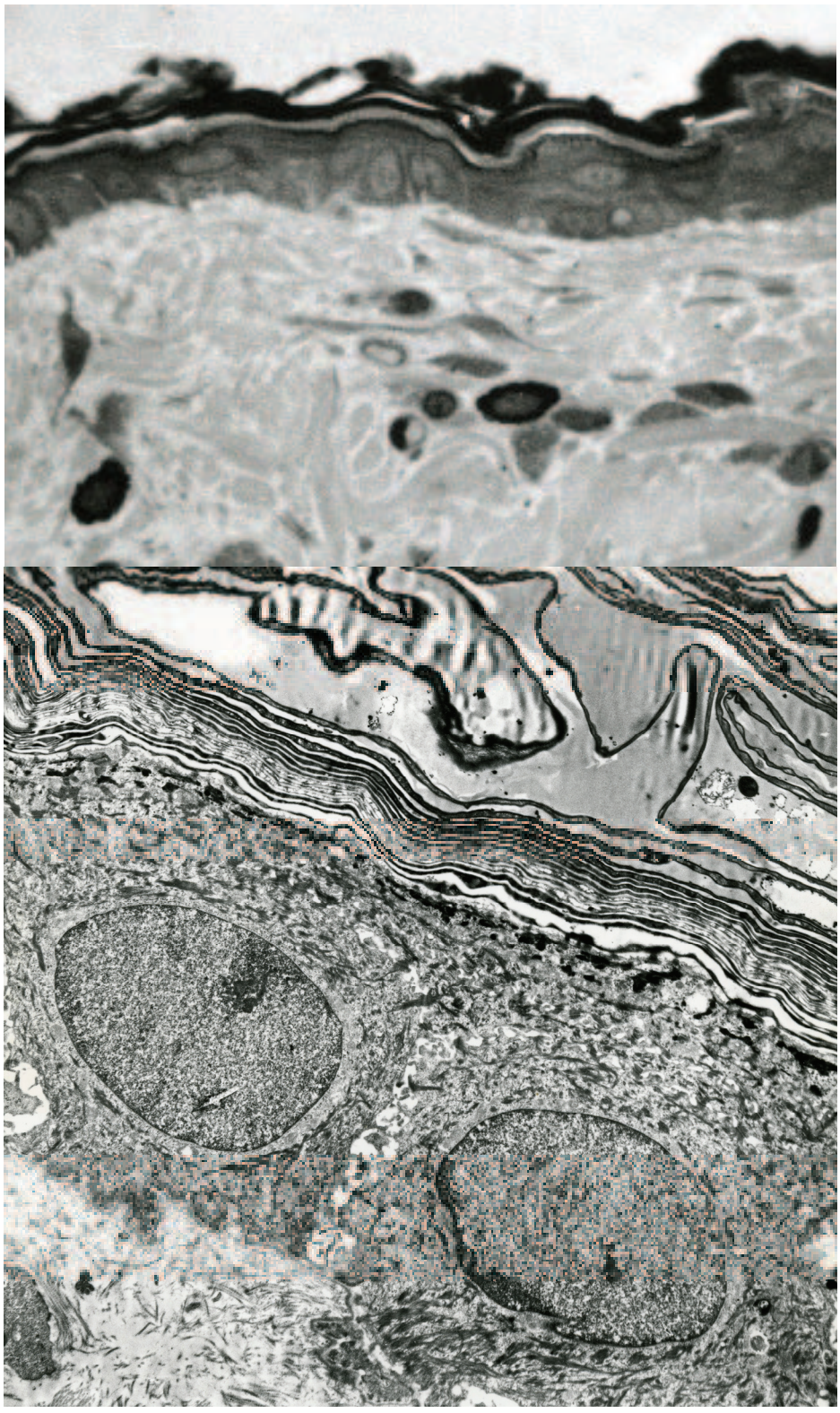

Fig. 16. (*Above*). A micrograph illustrates the epidermis from the body wall of an adult opossum. Note that it is much thinner when compared to that of opossums three and four weeks postnatal. LM X 700. (*Below*). The epidermis of the adult opossum consists of a stratum basale, a very thin stratum spinosum, a stratum granulosum, and a desquamating keratinized layer. Note the presence keratohyalin granules in the cell of the stratum granulosum. TEM X 6,000.

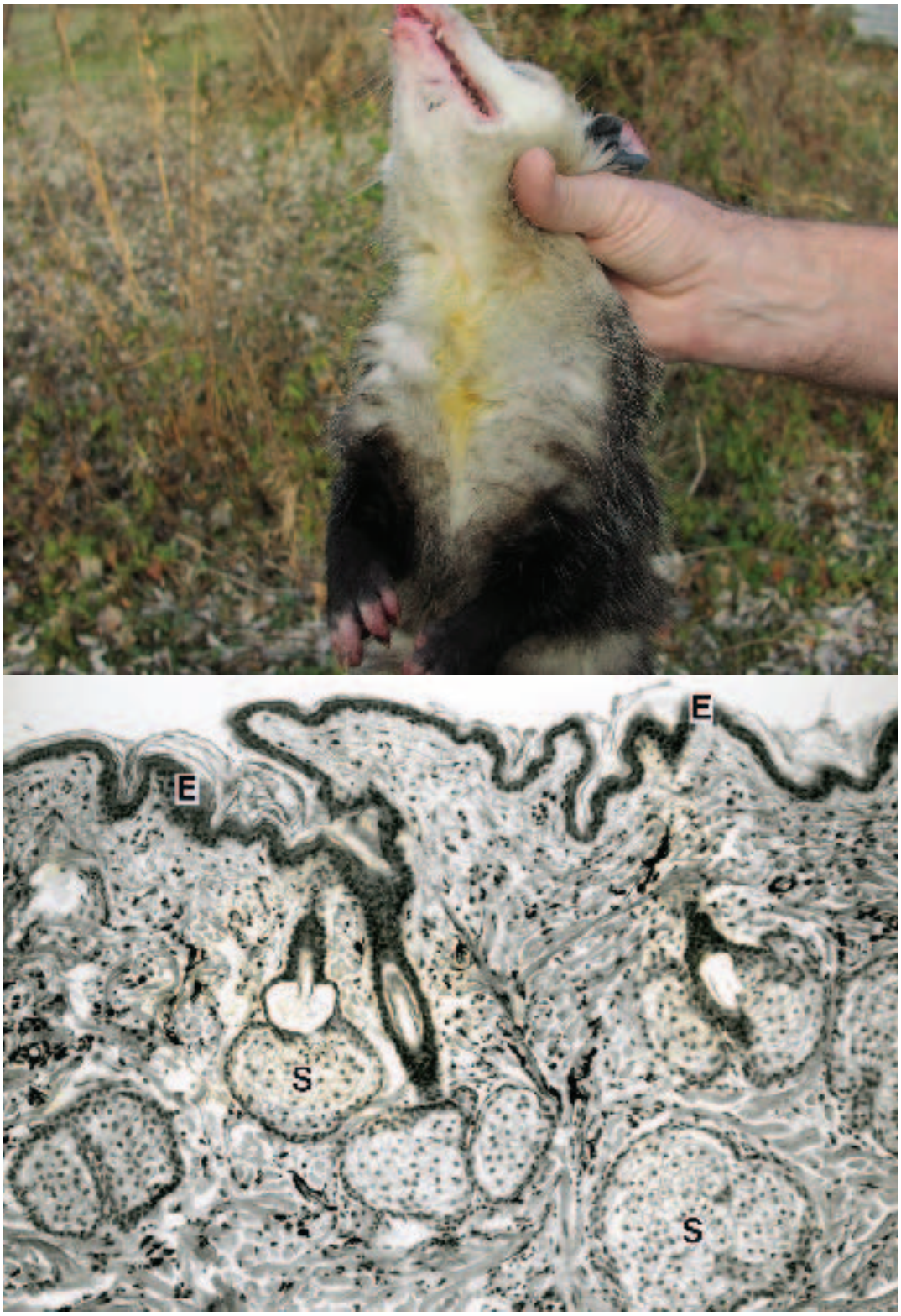

Fig. 17. (*Above*). The distribution of suprasternal glands is readily identified in the adult male opossum by a diamond-shaped patch of fur stained a yellow-amber color by secretion of the underlying glands. (*Below*). A histological section through the superficial aspect of the suprasternal gland region illustrates the appearance of the epidermis (E) and sebaceous glands (S) found in this region. LM X 100.

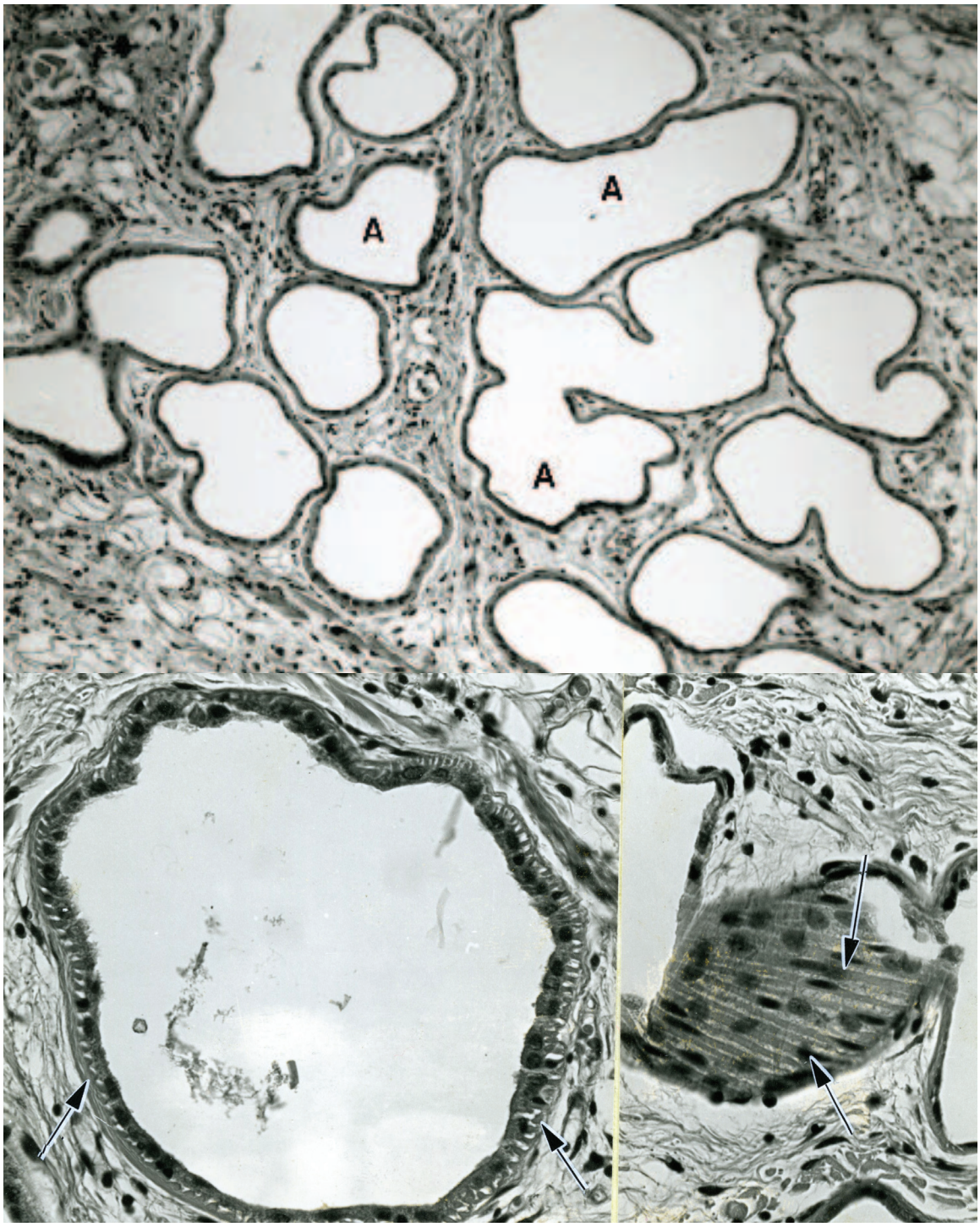

Fig. 18. (*Above*). A histological section through an area of the deep dermis of the suprasternal gland region illustrates a portion of a sudoriferous gland (A). LM X 100. (*Below left*). A transverse section through a secretory unit of a sudoriferous gland illustrates the variable nature of the lining epithelium. Note the abundance of myoepithelial cells (arrows). LM X 275. (*Below right*). A tangential section through the peripheral edge of a secretory tubule illustrates in greater detail the abundance and nature of the myoepithelial cells (arrows). LM X 275. All illustrations comprising figure eighteen were from an adult male opossum.

Chapter 12. Mesonephros

Synopsis:

The mesonephros is first apparent as an enlargement of the nephrogenic ridge near the eleventh somite of the nine-day opossum embryo. At the time of birth the mesonephros is a large well-developed structure consisting of differentiated nephron units separated by a delicate connective tissue. Four segments of the mesonephric nephron can be identified: a renal corpuscle, a proximal tubule, a distal tubule, and a collecting tubule. Mesonephric nephrons lack a loop of Henle. Between 35 and 45 large renal corpuscles are found within each mesonephros arranged along its ventromedial surface. Renal corpuscles located nearest the caudal pole appear slightly larger. A single mesonephric tubule originates from each renal corpuscle, forms a double loop, and then joins the mesonephric duct that courses along the lateral surface of the mesonephros. Each mesonephric renal corpuscle consists of a glomerulus and a surrounding renal (Bowman's) capsule. Cells forming the parietal layer of the renal capsule are simple squamous in nature but assume a cuboidal shape near the urinary pole and are continuous with cells forming the proximal mesonephric tubule. Podocytes constitute the visceral layer of Bowman's capsule. A well-developed basal lamina separates the layer of podocytes from the underlying fenestrated glomerular endothelium. Large, pyramidal-shaped cells the apices of which are united by tight junctions line proximal mesonephric tubules. A well-developed microvillus border characterizes the apical surface and basolateral infoldings are a prominent feature of the basal half of proximal tubular cells. Large supranuclear vacuoles and a well-established apical endocytic complex further characterize cells of the proximal tubule. In contrast, columnar cells of the distal mesonephric tubule are smaller in size than those of the proximal tubule and lack the microvillus border and apical endocytic complex as well as supranuclear vacuoles. The basolateral plasmalemma of cells forming the distal tubule does show extensive infoldings. A heterogeneous population of light and dark cells forms the mesonephric collecting tubule. Dark cells exhibit an electron-dense cytoplasm filled with many small membrane-bound vesicles and numerous mitochondria. Light cells exhibit a light staining cytoplasm that contains scattered polyribosomes and mitochondria. The mesonephric duct is lined by a simple cuboidal to low-columnar epithelium the apical plasmalemma of which shows scattered, stubby microvilli. The basal cell membrane is relatively smooth whereas the lateral plasmalemma shows extensive infoldings that interdigitate with those of adjacent cells. The cytoplasm contains free ribosomes, scattered profiles of rough endoplasmic reticulum and mitochondria.

The morphological features of the mesonephroi remain relatively unchanged during the first four postnatal days; however, by the end of the first postnatal week some nephrons located within the cranial pole do exhibit varying degrees of degeneration. In contrast, mesonephric nephrons within the caudal pole appear normal and continue to function. Thus, the mesonephroi of the opossum persist, in an apparent functional state, for most of the first postnatal week. Near the end of the second week postnatal the mesonephric nephrons are reduced is size and appear shrunken. Although the caudal pole continues to show intact nephrons, the majority show signs of degeneration. By the end of the third postnatal week the mesonephroi consist only of fragments of nephron units scattered within a surrounding connective tissue mass.

Acknowledgments:

Figs. 1, 2, 6 (bottom), 12 (top), 14 and17 (bottom), courtesy of and from: Krause, W.J., J.H. Cutts, and C.R. Leeson. (1979) Morphological observations on the mesonephros in the postnatal opossum, *Didelphis virginiana*. J. Anat. 129:377-397.

Fig. 7 (top), courtesy of and from: Krause, W.J. (1998) A review of histogenesis/organogenesis in the developing North American opossum (*Didelphis virginiana*). Adv. Anat. Embryol. Cell Biol. 143: (II): Springer Verlag, Berlin, pp 120.

Fig. 12 (bottom), courtesy of and from: Krause, W.J., R.H. Freeman and L.R. Forte. (1990) Autoradiographic demonstration of specific binding sites for *E. coli* enterotoxin in various epithelia of the North American opossum. Cell Tissue Res. 260:387-394.

Fig. 1. (*Above*). A micrograph illustrates the external features of the mesonephroi from a newborn opossum. The mesonephric duct courses along the lateral surface of these structures whereas the developing gonad lies along their medial surface. The urinary bladder is at the bottom. SEM X 50. (*Below*). A longitudinal section through a newborn mesonephros demonstrates the position of renal corpuscles (C) along the ventromedial surface. The mesonephric duct is shown at the arrow. LM X 45.

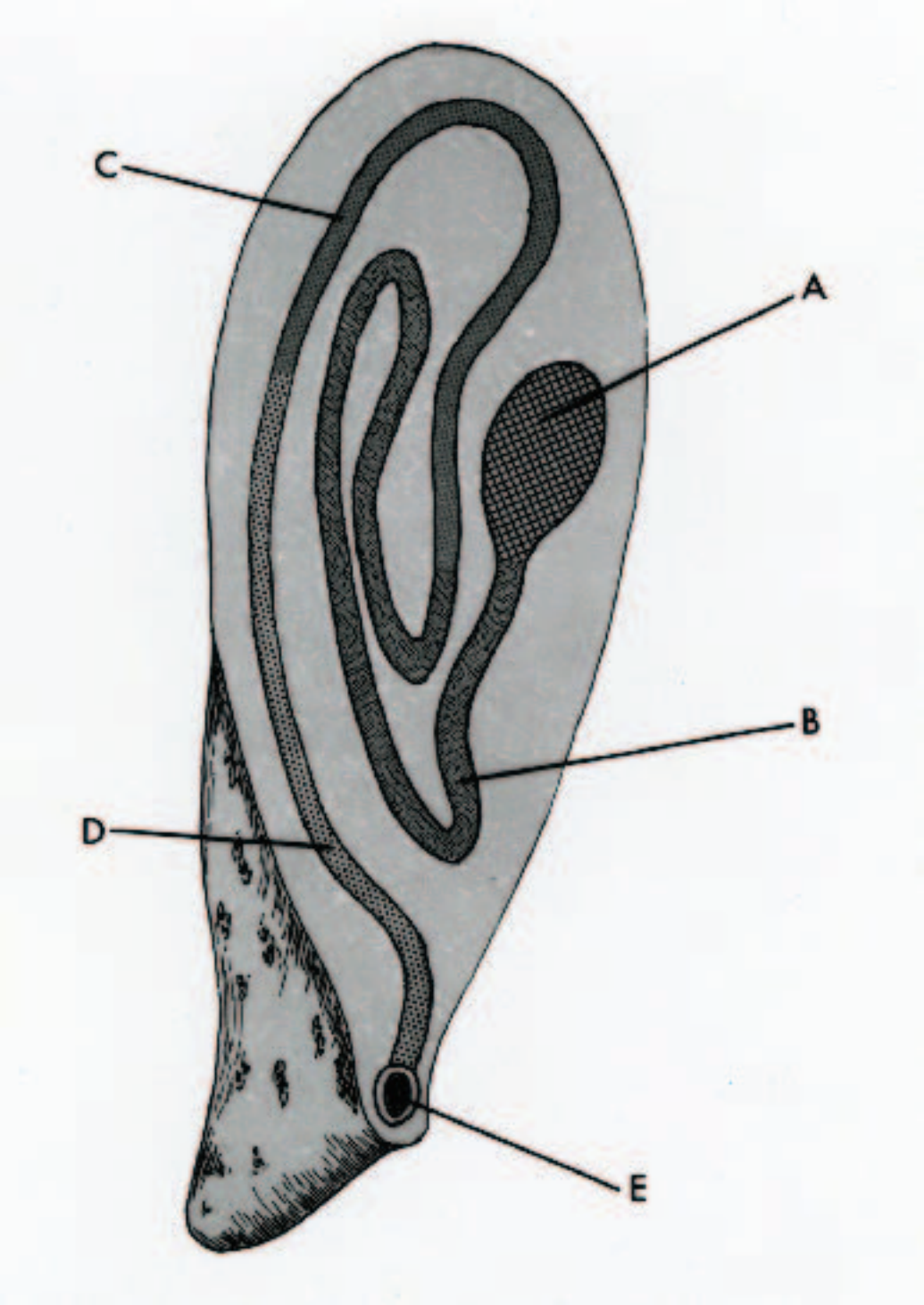

Fig. 2. A line drawing illustrates an opossum mesonephric nephron. The renal corpuscle (A) is linked to the proximal tubule (B) that after coursing through the mesonephros eventually loops back to lie adjacent to the parent renal corpuscle. At this location there is an abrupt transition from the proximal mesonephric tubule to the distal mesonephric tubule (C). After a short course beneath the surface of the mesonephros, the distal mesonephric tubule gradually merges into a collecting tubule (D). The mesonephric collecting tubule eventually unites with the mesonephric duct (E). A thin segment is absent in mesonephric nephrons.

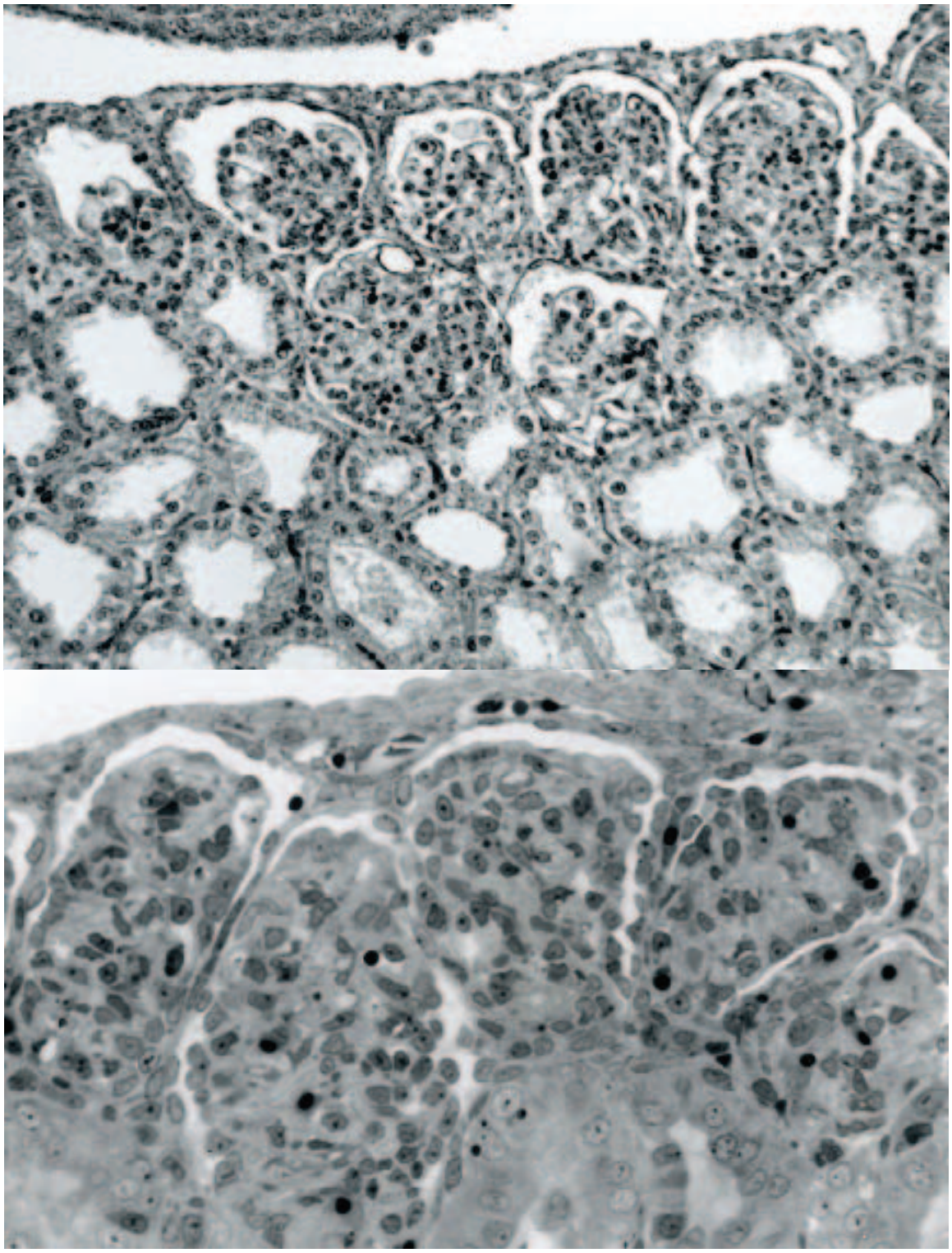

Fig. 3. (*Above*). The ventromedial region of the newborn opossum mesonephros illustrates two strata of renal corpuscles and adjacent mesonephric tubules. LM X 150. (*Below*). When viewed at increased magnification it can be demonstrated that each mesonephric renal corpuscle consist of centrally positioned glomerulus and a surrounding renal capsule (Bowman's capsule). LM X 400.

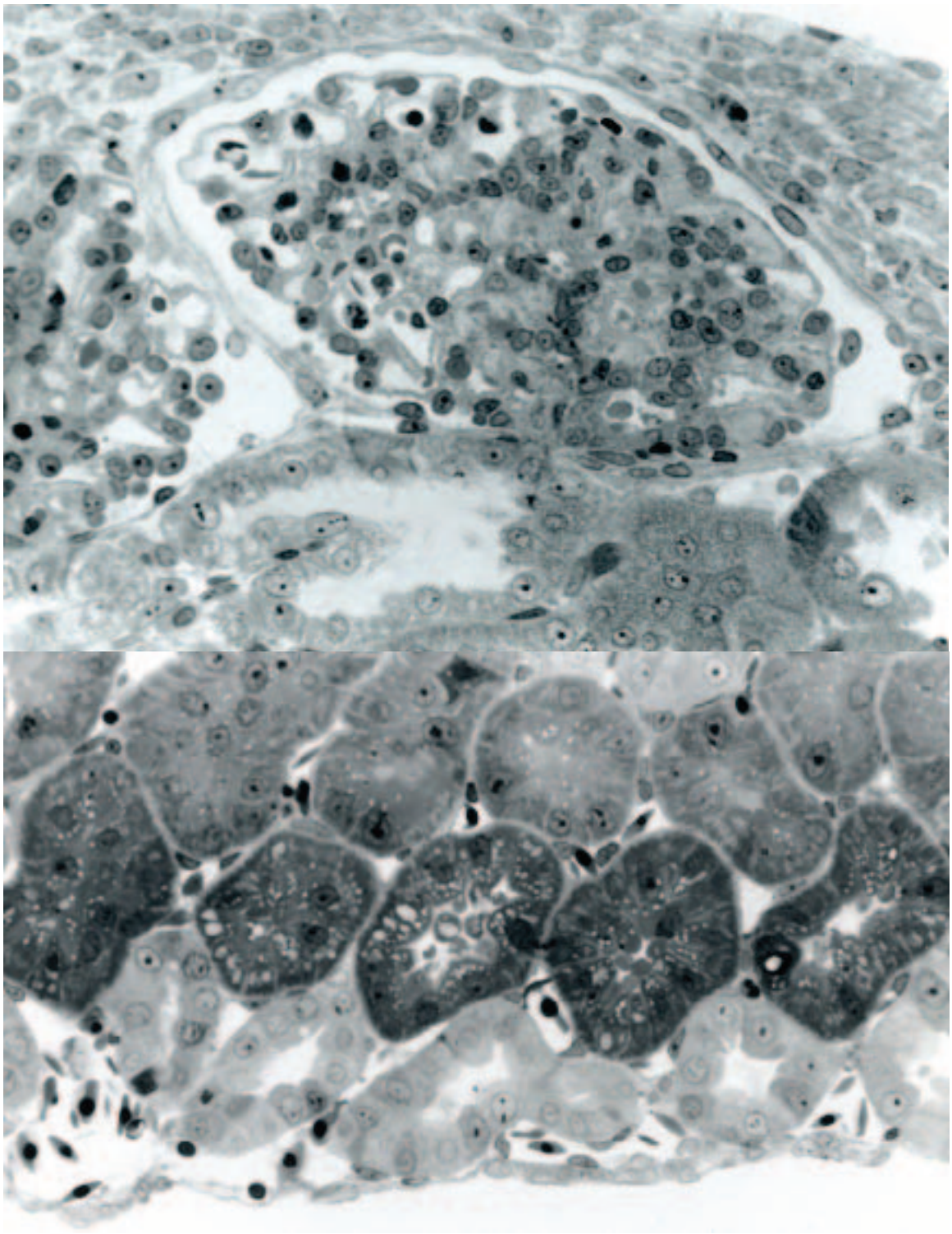

Fig. 4. (*Above*). A micrograph illustrates a mesonephric renal corpuscle from a newborn opossum. The simple squamous epithelium forming the parietal layer of the glomerular capsule is well defined and separated from the visceral layer of the by a well-established capsular space. The capillary loops comprising the glomerulus are clearly evident. LM X 500. (*Below*). A lateral region of the newborn mesonephros illustrates two strata of dark staining proximal mesonephric tubules characterized by pyramidal shaped cells filled with vacuoles. Cells comprising the distal mesonephric tubules are light staining and are shown near the bottom of the illustration. LM X 500.

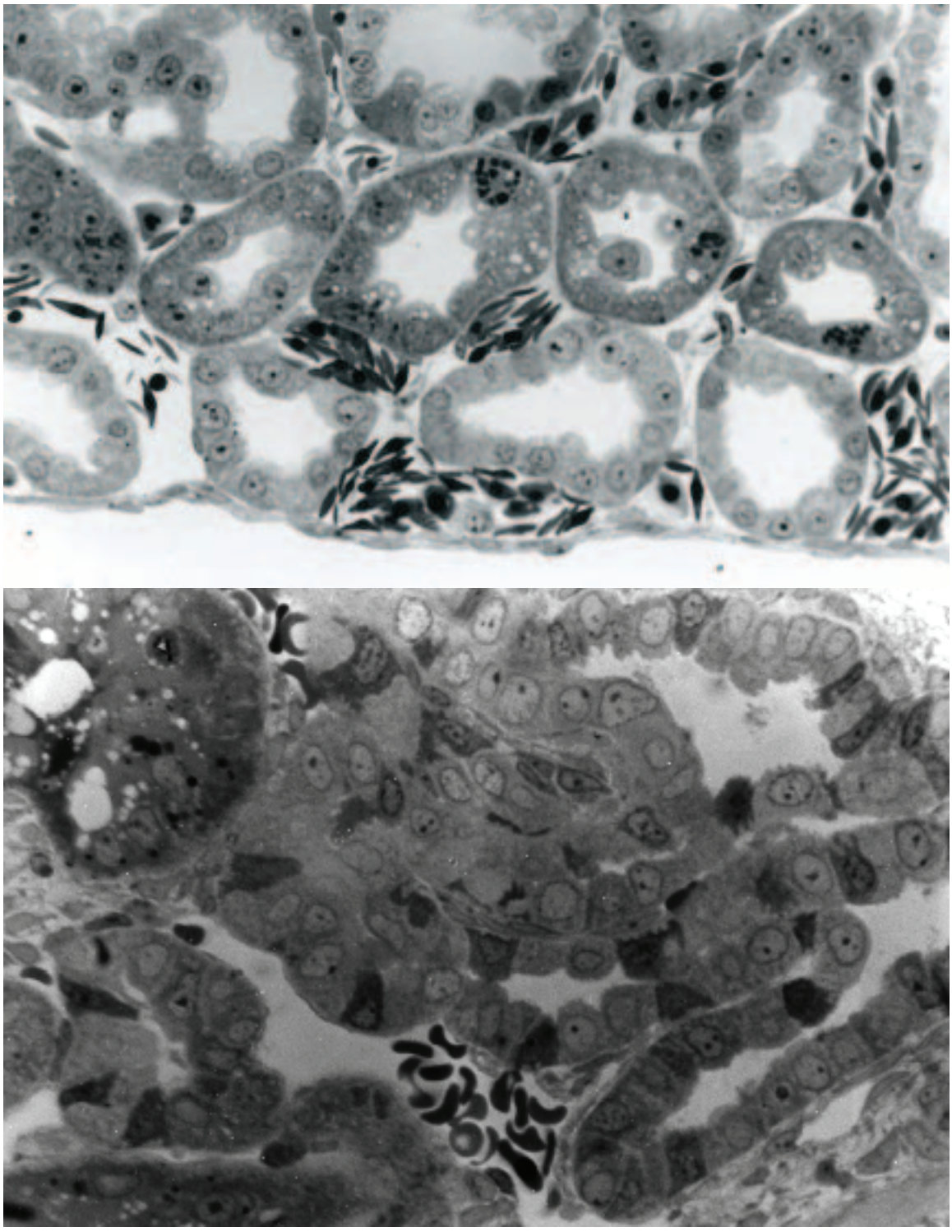

Fig. 5. (*Above*). A peripheral region of newborn mesonephros illustrates the darker staining proximal tubules (the top and center rows of tubules) and the distal tubules at the bottom of the photomicrograph. Note the surrounding vascular elements filled with erythrocytes, which are nucleated at this time in development. LM X 500. (*Below*). A lateral region of newborn opossum mesonephros illustrates collecting tubules. Note that the collecting tubules consist of a heterogeneous population of dark and light cells. LM X 500.

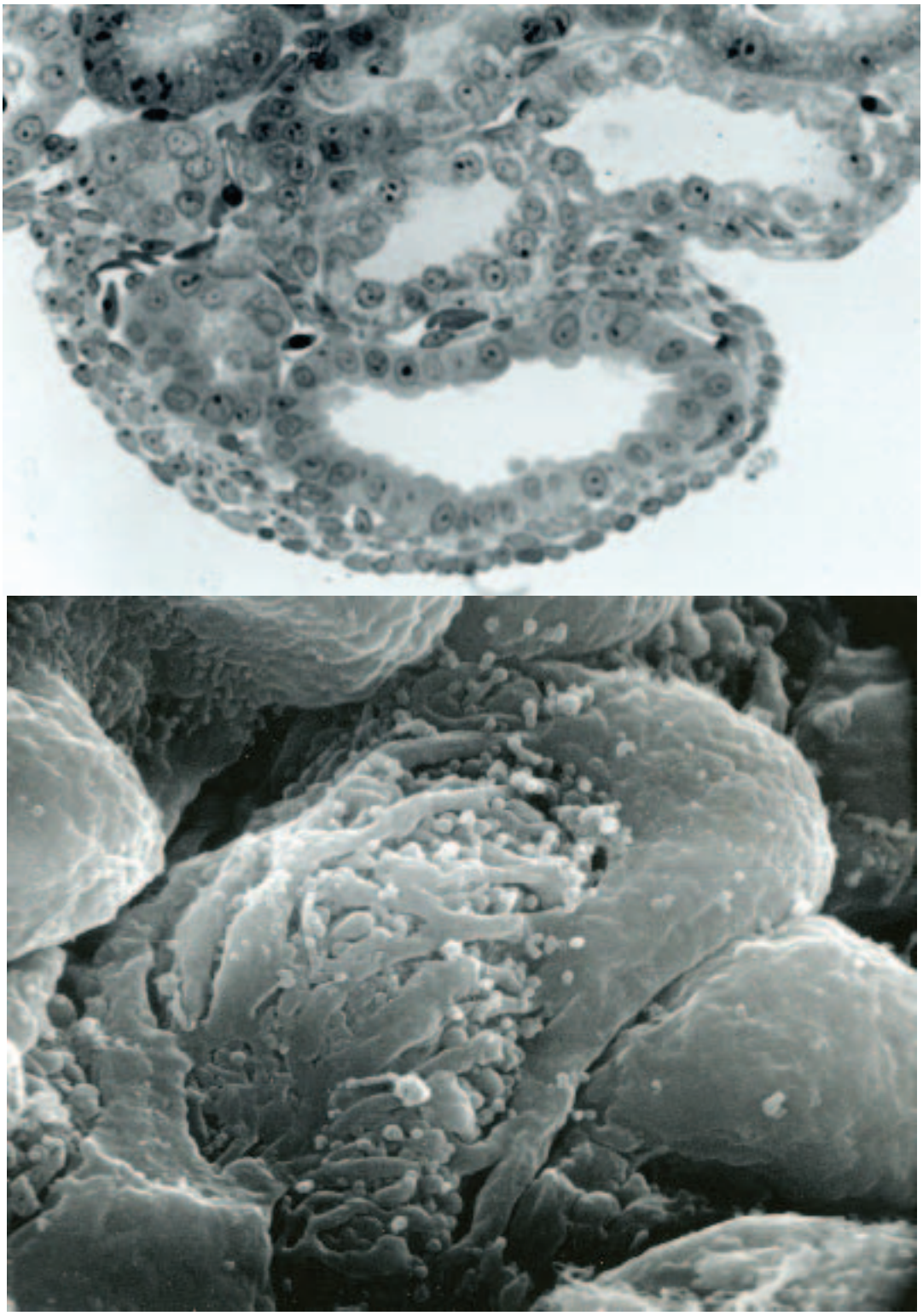

Fig. 6. (*Above*). A section through the lateral edge of a newborn mesonephros illustrates a profile of the mesonephric duct (at bottom of photomicrograph). It is lined by s light staining, simple columnar epithelium. LM X 500. (*Below*). A scanning micrograph illustrates surface features of podocytes comprising the glomerular epithelium (the visceral layer of Bowman's capsule) of a mesonephric renal corpuscle. Note the interdigitating foot processes (pedicles). Newborn opossum. SEM X 15,000.

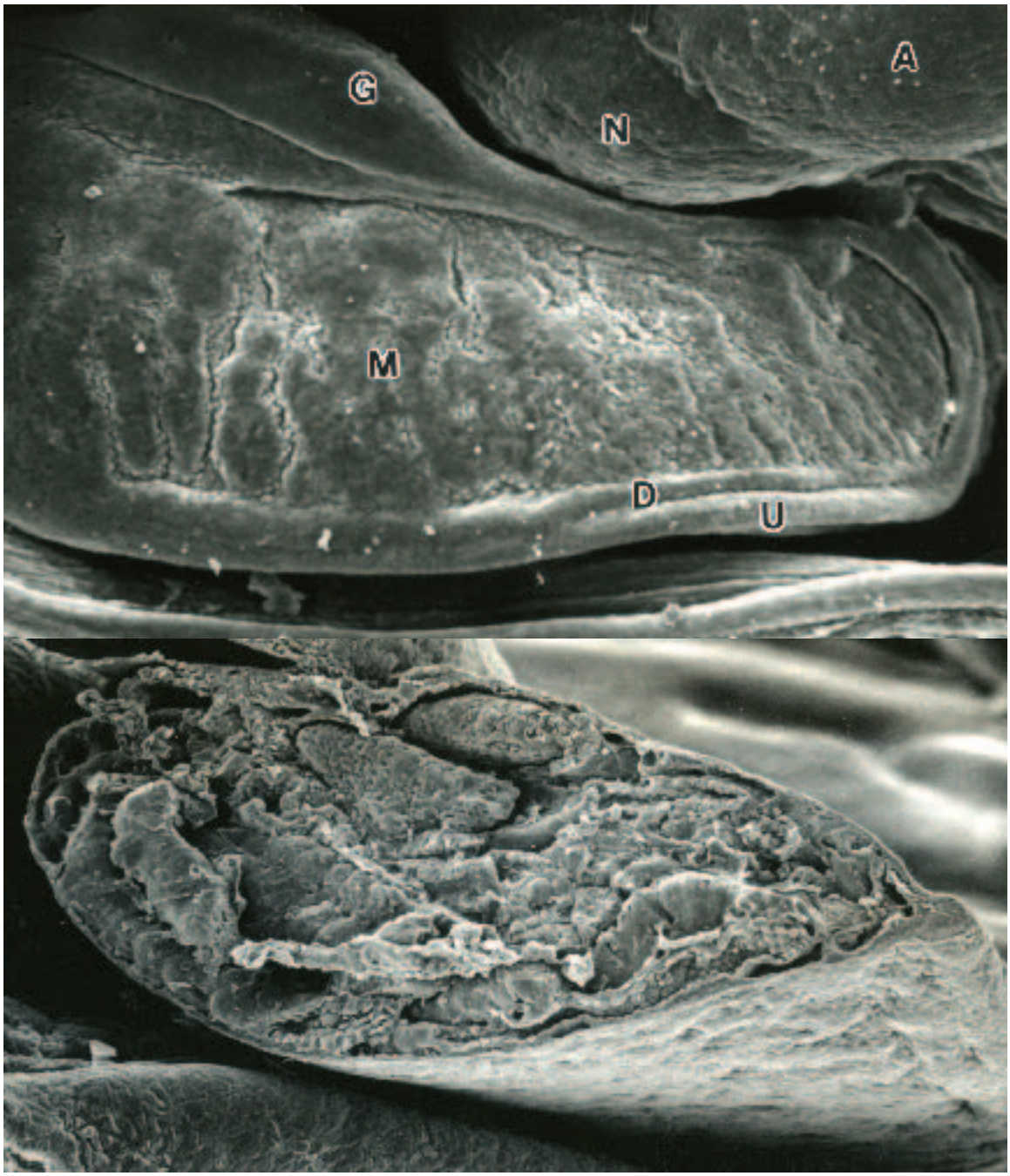

Fig.7. (*Above*). A micrograph illustrates surface features of a mesonephros (M) from an opossum four days postnatal. Note the continued presence of the mesonephric duct (D) as well as the Müllerian duct (U) in this preparation. The developing gonad (G) lies near the medial surface of the mesonephros. The surface of the differentiating metanephros (N) and adrenal gland (A) also can be observed. SEM X 100. (*Below*). A fractured region through the center of the four-day postnatal opossum mesonephros illustrates two glomeruli (top center), the torturous nature of mesonephric tubules, and the position of the mesonephric duct shown at the extreme center right. SEM X 200.

Fig. 8. A micrograph illustrates surface features of the urinary system of a male opossum one week into the postnatal period. Note the development of the mesonephric duct as it courses along the lateral surface of the mesonephros to terminate near the base of the urinary bladder (bottom right). The developing testis lies on the medial surface of the mesonephros and appears closely related to its cranial region that appears shrunken at this stage of development. The gubernaculum extends from the caudal surface of the testis. The continued development of the metanephroi and adrenal glands along their superior/medial borders is quite evident. SEM X 60.

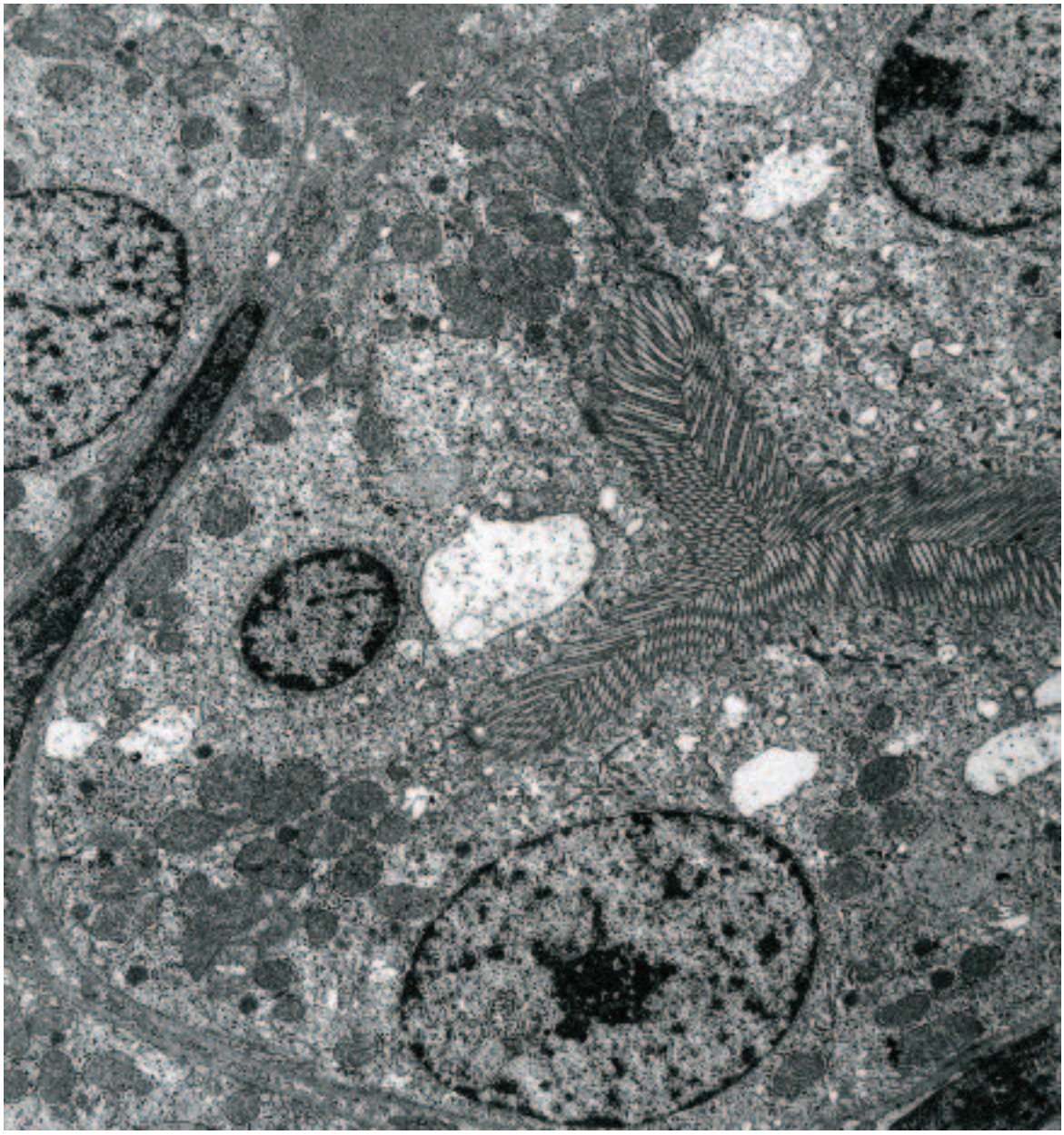

Fig. 9. A section through a proximal mesonephric tubule taken from an opossum one week into the postnatal period illustrates a viable, functional mesonephric tubule during this period of development. Note the well-developed microvillus border that occludes the lumen of the proximal tubule and the underlying apical endocytic complex and supranuclear vacuoles. Numerous mitochondria appear concentrated in the cytoplasm of basolateral regions of the proximal mesonephric tubule cells. TEM X 2,000.

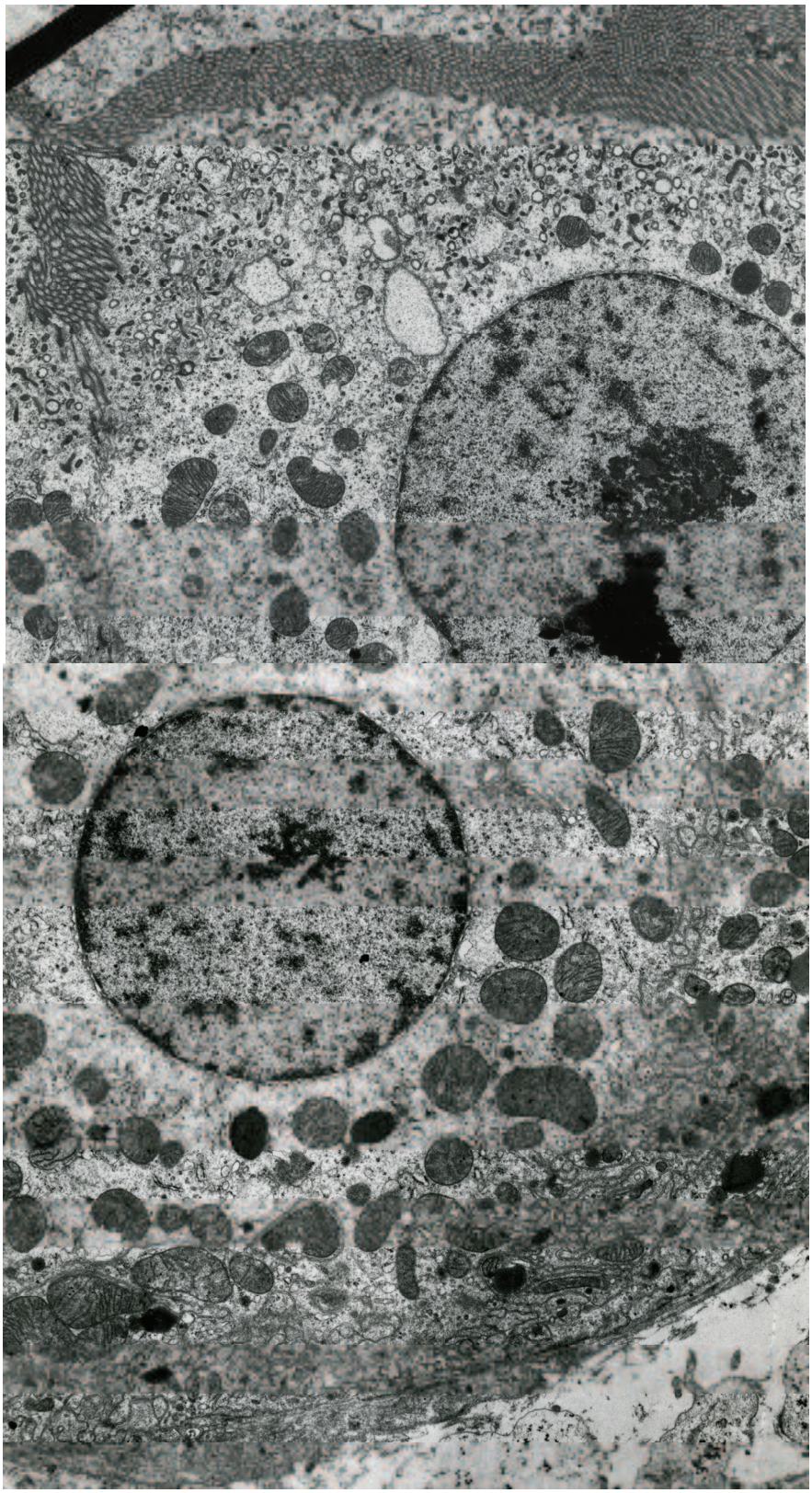

Fig. 10. (*Above*). The apical and supranuclear regions of a cell from a proximal mesonephric tubule illustrates in greater detail the endocytic complex of anastomosing tubules and vesicles positioned immediately beneath the microvillus border. Opossum one week postnatal. TEM X 3,000. (*Below*). The base of a proximal mesonephric cell illustrates the well developed basolateral infoldings of the plasmalemma. TEM X 3,000.

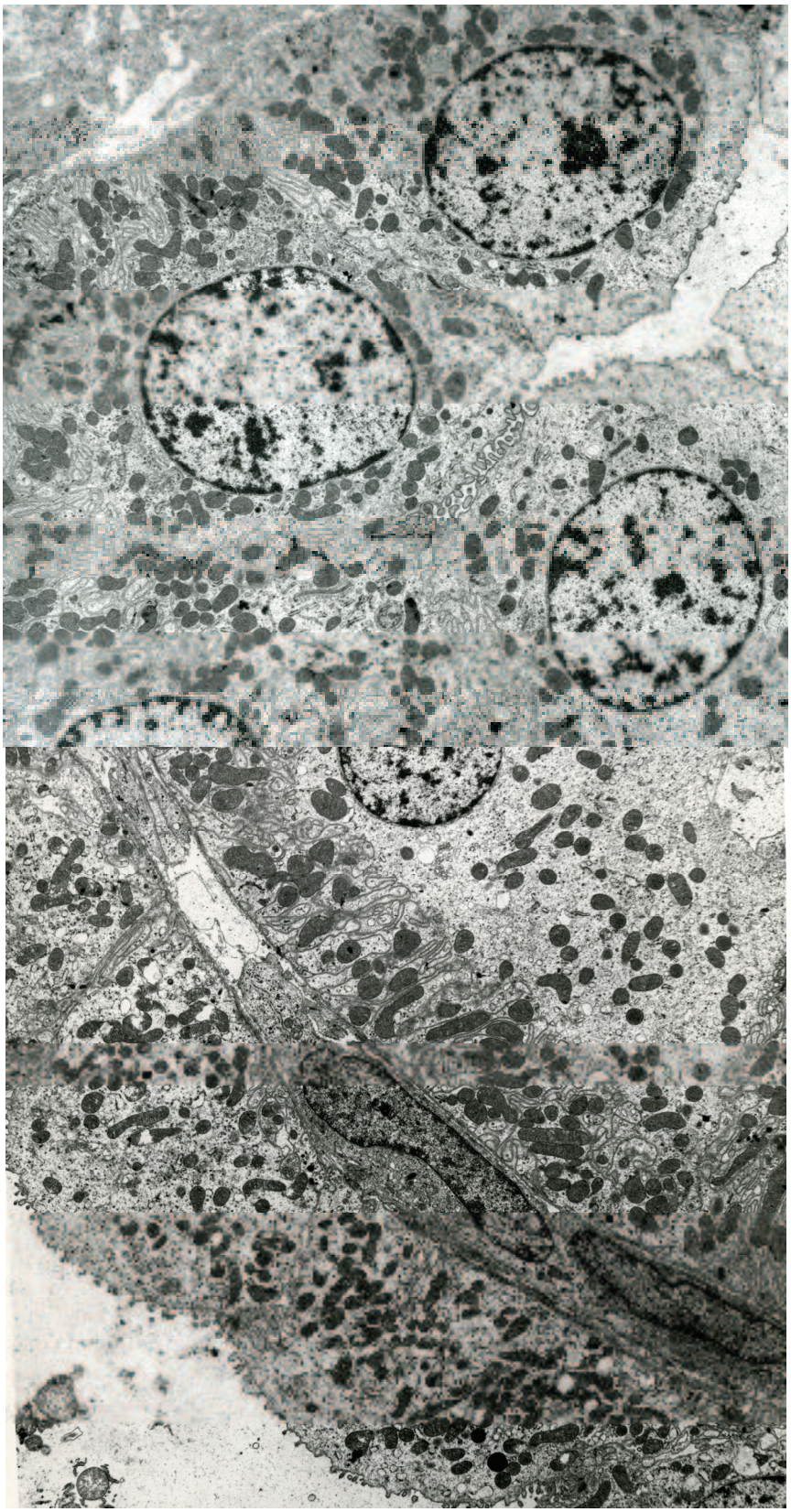

Fig. 11. (*Above*). Mitochondria fill the apical and basal cytoplasm of cells forming a distal mesonephric tubule of a week old opossum. The cells lack a microvillus border. TEM X 2,000. (*Below*). A micrograph illustrates a region of mesonephros illustrating a distal tubule (upper right) and a collecting tubule (lower left). Note the well-developed basolateral infoldings of cells forming the distal mesonephric tubule. TEM X 2,000.

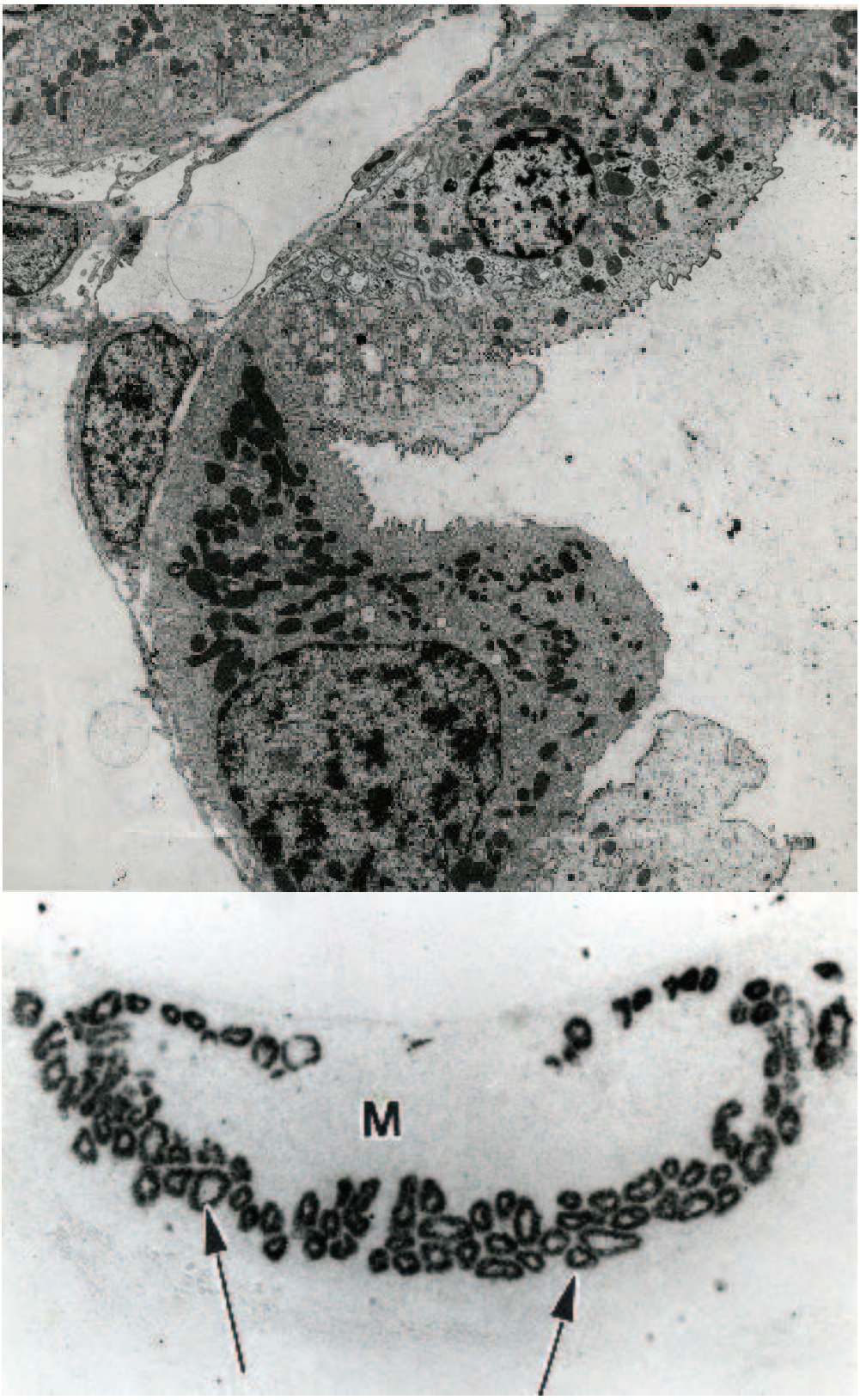

Fig. 12. (*Above*). A micrograph illustrates a region of a mesonephric collecting tubule containing both light and dark cells. The latter contains an abundance of mitochondria. Note the endothelial cell of a capillary immediately adjacent to the base of the tubule. Opossum one week old. TEM X 2,500. (*Below*). A portion of a week old opossum mesonephros incubated with ^{125}I-ST enterotoxin shows that specific binding sites are confined primarily to proximal tubules (arrows). The position of the medulla (M) also is shown. Autoradiograph. X 100.

Fig. 13. The mesonephros degenerates considerably following the first postnatal week and by the end of the second postnatal week begins to appear shrunken and collapsed. The gonads (ovaries) continue to develop and expand along the ventromedial surface of the mesonephroi. The urinary bladder is shown at the top left of the photomicrograph. Female opossum two weeks postnatal. SEM X 25.

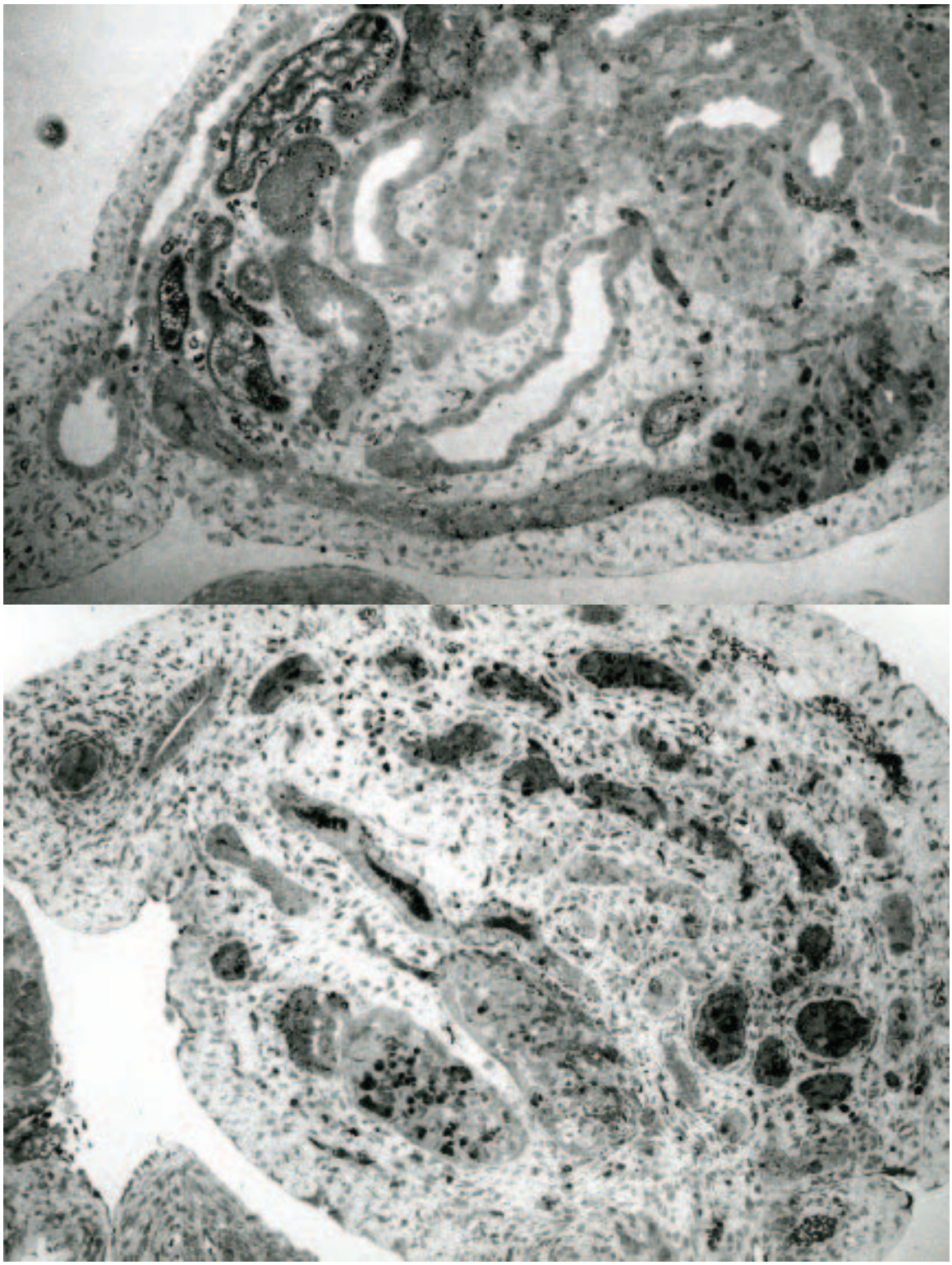

Fig. 14. (*Above*). A transverse section through the caudal region of a mesonephros two weeks into the postnatal period illustrates intact nephrons that appear to be in the initial phases of involution (degeneration). A renal corpuscle is shown at the lower right. The mesonephric duct is depicted at the lower left. LM X 125. (*Below*). A transverse section through the cranial region of the same mesonephros shown above illustrates a more advanced regression of mesonephric nephrons. A viable mesonephric duct is shown at the top left just medial to a degenerate Müllerian duct. LM X 125.

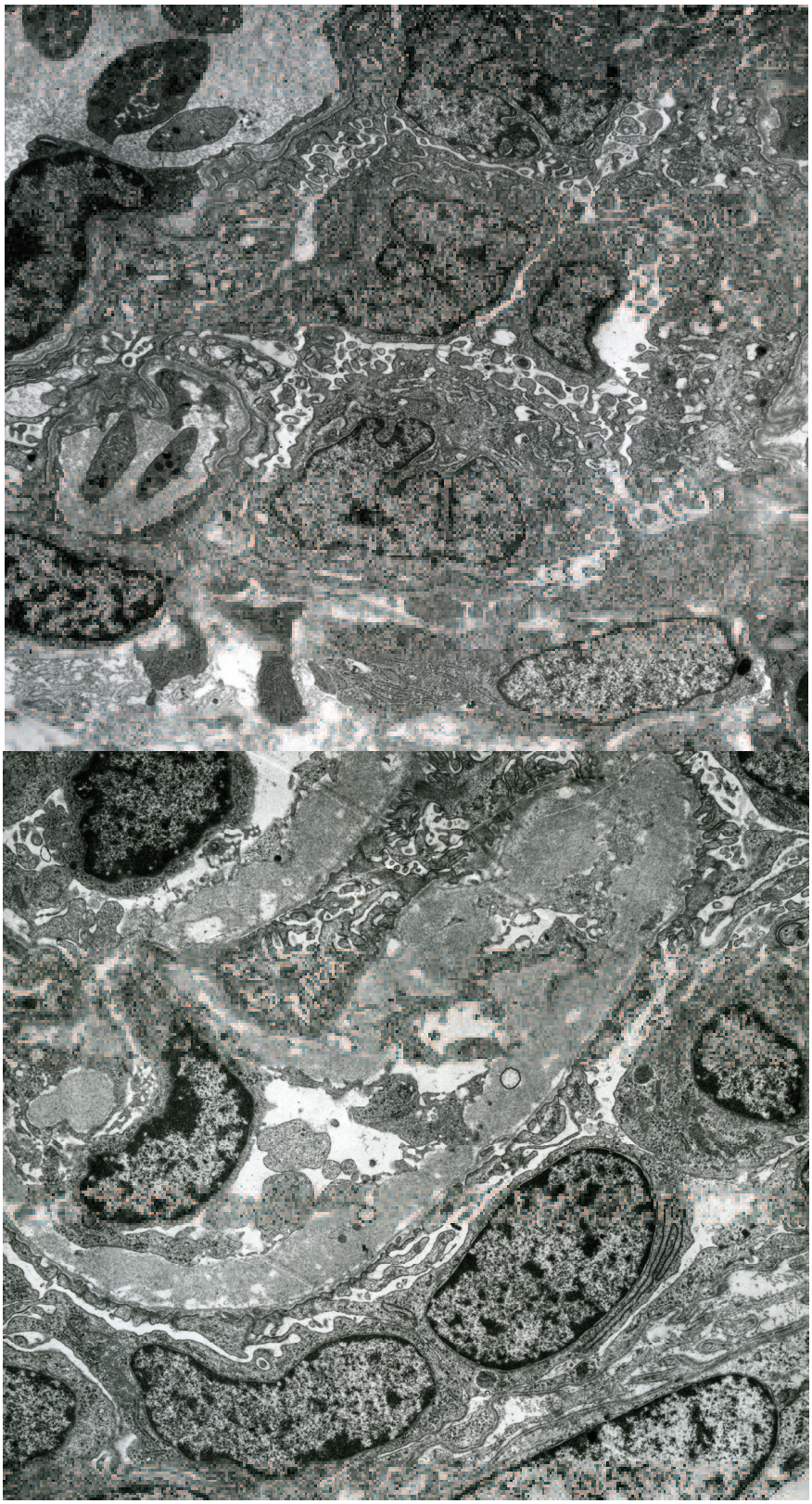

Fig. 15. (*Above*). A degenerating renal corpuscle taken from the caudal region of a mesonephros illustrates podocytes in the initial stages of involution. Opossum two weeks postnatal. TEM X 1,500. (*Below*). A micrograph illustrates a degenerating renal corpuscle from a more cranial region of the mesonephros of a two-week-old opossum. Note the thickened glomerular basement membrane. TEM X 1,500.

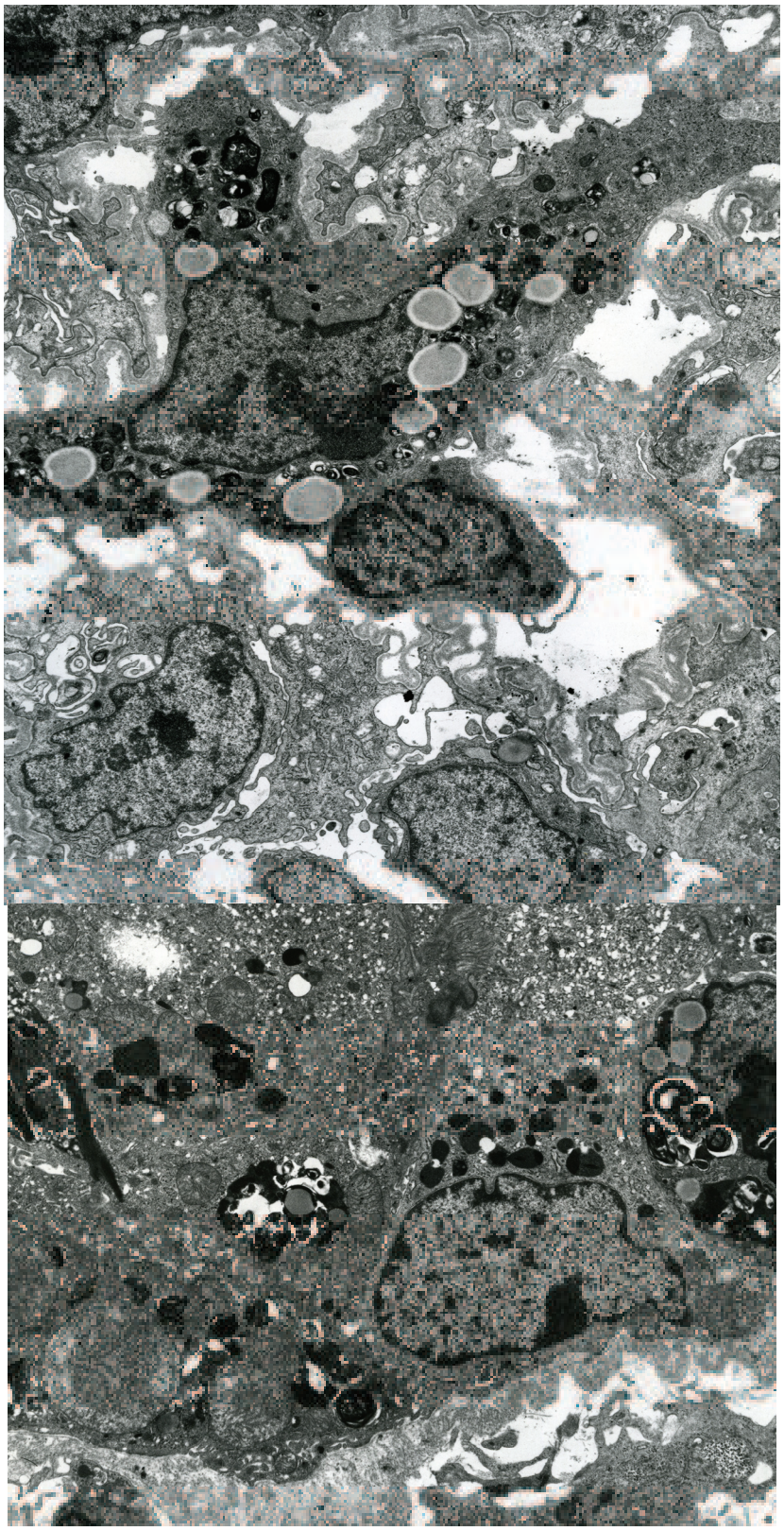

Fig. 16. (*Above*). A macrophage within a regressing mesonephros, surrounded by remnants of a renal corpuscle, contains numerous lipid droplets and myelin figures. Two-week-old opossum. TEM X 1,000. (*Below*). Cells of a regressing proximal mesonephric tubule exhibit large accumulations of electron dense material and mitochondria often become enlarged. Two-week-old opossum. TEM X 1,000.

Fig.17. (*Above*). Cells from a regressing distal mesonephric tubule also show accumulations of electron dense material within their cytoplasm. Note the accumulation of filamentous material surrounding the mesonephric tubule. Opossum three weeks old. TEM X 1,000. (*Below*). The mesonephros at three weeks postnatal exhibits only scattered remnants of tubules. In this male opossum the mesonephric duct persists as a viable duct (left center). The differentiating testis is shown at the upper left. LM X 150.

Fig. 18. A cell from the epithelial lining of a mesonephric duct illustrates scattered stubby microvilli at its apical surface and a smooth basal plasmalemma lying on a delicate basal lamina. Scattered ribosomes, mitochondria, multivesicular bodies, and profiles of granular endoplasmic reticulum are found within the cytoplasm. Male opossum three weeks postnatal. TEM X 3,000.

Chapter 13. Metanephros

Synopsis:

The ureteric bud begins as a small outgrowth from the mesonephric duct near where it joins the cloaca during the eleventh prenatal day. Prior to birth it grows dorsally and medially and is intimately associated with condensing mesenchyme, the metanephric blastema. This region of condensing mesenchyme is continuous with the same nephrogenic mass of mesenchyme in which the mesonephric nephrons formed. By the time of birth, the first generation of metanephric nephrons has begun to differentiate. The metanephros at this time consists primarily of collecting tubules that divide dichotomously near the developing renal capsule. Adjacent differentiating nephrons within this area are separated by a scant connective tissue. The nephronogenic zone lies immediately subjacent to the renal capsule and is formed by two to three layers of irregularly shaped mesenchymal cells. The metanephric nephrons vary in the degree of maturation but all follow the same pattern of differentiation and development. Initially, the mesenchymal cells near the terminal branches of the collecting tubules coalesce into solid, oval shaped masses. With time, a central cavity develops within the tear drop shaped mass and component cells form a single layer of columnar shaped cells whose long axes lie perpendicular to the lumen. As these cells proliferate the renal vesicle is transformed into a renal tubule. As this formed tubule elongates, two indentations appear, resulting in an S-shaped tubule. That portion of the tubule furthest from the collecting tubule will differentiate into a renal corpuscle. That portion immediately adjacent to the collecting tubule will form the distal tubule, and that portion positioned between will become the proximal tubule. Simultaneous with these events, small vascular sprouts enter the region between the distal and middle portions of the S-shaped tubule. These ultimately will form the vascular component of the differentiating renal corpuscle. As the invading vasculature becomes intimately associated with the columnar cells on one side of the tubule the latter begin to differentiate into podocytes and establish the visceral layer of Bowman's capsule. Cells on the opposite side of the tubule transform into the simple squamous epithelium of the parietal layer of Bowman's capsule.

Cell forming the proximal tubular component of the nephron in the newborn opossum are columnar in shape, moderately electron dense, and contain numerous polyribosomes. Scattered microvilli occur at the apical surface. Cells characterized by numerous mitochondria and infoldings of the basal cell membrane form the distal component of the developing nephron. The cytoplasm is of moderate electron density and contains abundant polyribosomes. The collecting tubules at this time are formed by cuboidal to columnar shaped cells, the cell membrane of which is relatively smooth in appearance. The cytoplasm contains numerous free ribosomes and small, scattered mitochondria. Clusters of small electron-dense granules are seen on occasion and are thought to contain factors that induce nephronogensis in the adjacent nephrogenic zone of mesenchymal cells.
The metanephros increases considerably in size during the first week and by the end of the third postnatal week its internal architecture and general conformation are well established. Continued nephronogenesis occurs until about ninth week of postnatal life. The pattern of differentiation and development of nephrons later in the postnatal period appears identical to that observed in earlier ages. Newly differentiated nephrons continue to form from the subcapsular nephronogenic layer of mesodermal cells. Likewise, further expansion and differentiation of formed nephrons continues to occur. Cells forming the proximal tubules

of corticomedullary nephrons are characterized by a microvillus border, a well developed apical endocytic complex and basolateral infoldings by the end of the first postnatal week. Proximal tubules, like the renal corpuscles, are less well differentiated in nephrons nearer the renal capsule. Loops of Henle are initially observed at the end of the second postnatal week, but are much more evident in the medulla by the end of week four. Cells of the distal tubules at this time, as in earlier ages, show basolateral infoldings with associated mitochondria. The epithelium of collecting tubules increases in height is light staining and contains scattered ribosomes, small mitochondria and small electron-dense granules in the supranuclear region adjacent to Golgi complexes.

The metanephros continues to increase in weight and size throughout the remainder of the postnatal period due primarily to the continued growth of established nephrons. The renal corpuscles increase in size and the tubular component increases in length, resulting in the convolution of both the proximal and distal tubules.

Thus, development of the opossum metanephros occurs primarily during the postnatal period and can be subdivided into two distinct phases: an initial phase during the first nine weeks that is concerned primarily with nephronogenesis and the differentiation of nephrons; and a second phase concerned primarily with further differentiation and growth of established nephrons. It is during the second phase that the tubular portion of the nephron increases markedly in length. Some metanephric nephrons are capable of function near the end of the first postnatal week. Thus, during the first postnatal week there is functional overlap between mesonephric and metanephric nephrons.

Acknowledgments:

Figs. 1, 2, 3, 15 (top), 16, courtesy of and from: Krause, W.J., J.H. Cutts, and C.R. Leeson (1979) Morphological observations on the metanephros in the postnatal opossum, *Didelphis virginiana*. J. Anat. 129:459-477.

Figs. 4, 6, 7, courtesy of and from: Krause, W.J. and J.H. Cutts (1980) Transitory cell attachments in the differentiating glomerular epithelium of the opossum metanephros. Acta Anat. 106:281-289.

Fig. 10 (bottom right), 11, courtesy of and from: Krause, W.J. (1998) A review of histogenesis/organogenesis in the developing North American opossum (*Didelphis virginiana*). Adv. Anat. Embryol. Cell Biol. 143 (II): Springer Verlag, Berlin, pp 120.

Fig. 17, courtesy of and from: Krause, W.J., R.M. London, R.H. Freeman, and L.R. Forte. (1997) The guanylin and uroguanylin peptide hormones and their receptors. Acta Anat. 160:213-231.

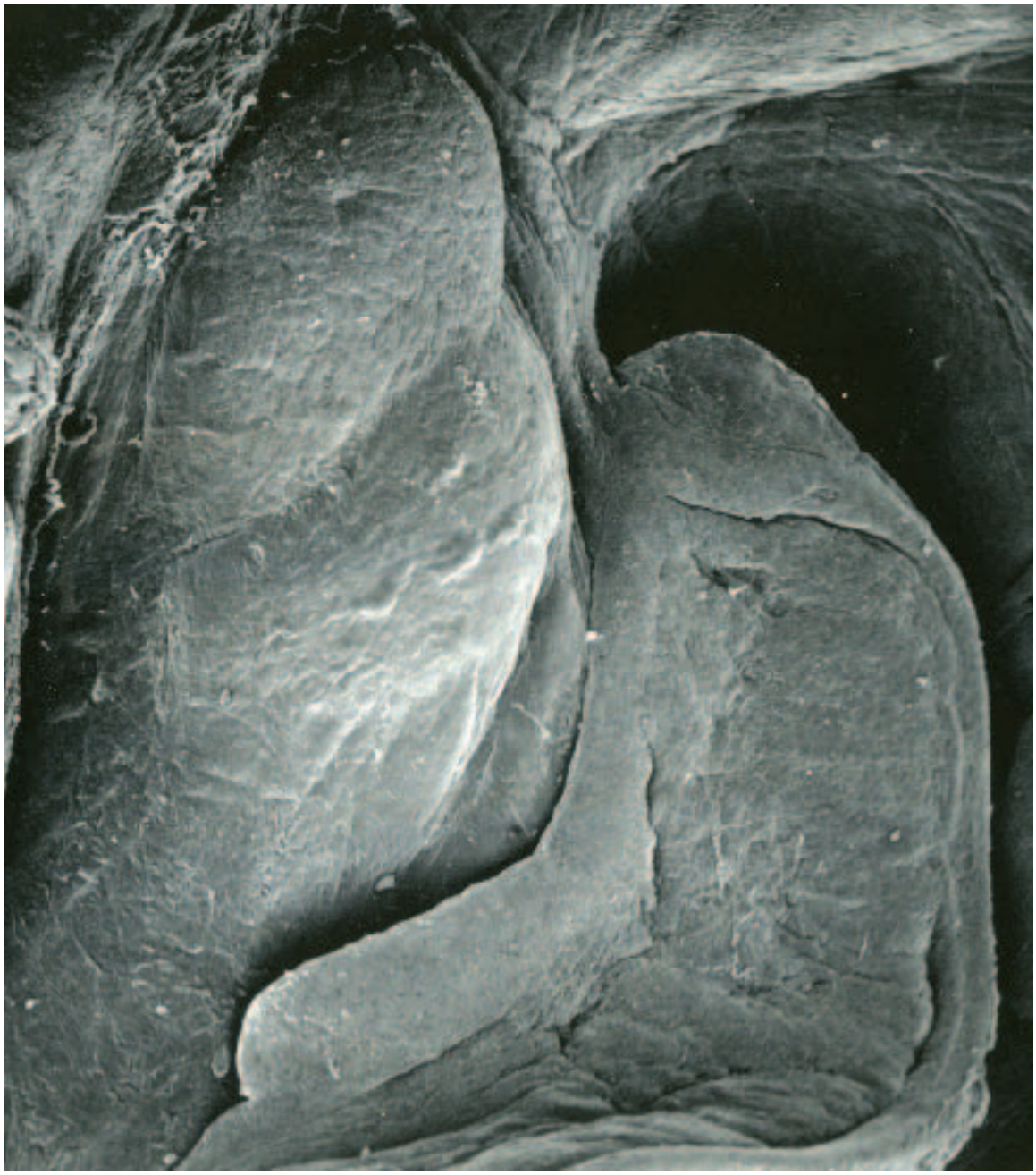

Fig. 1. A region of the posterior abdominal wall from a newborn opossum illustrates the position of the mesonephros with the mesonephric and Müllerian ducts coursing along its lateral surface (right) and a developing gonad, which lies along the medial surface. The position of the metanephros and the overlying adrenal gland at its superior pole are shown at the upper left of the field. SEM X 150.

Fig. 2. A line drawing summarizes early nephronogenesis and formation of the renal corpuscle in the developing metanephros of the opossum. (**A**). Initially, primitive mesenchymal cells envelope terminal branches of a collecting tubule in the nephronogenic zone located beneath the renal capsule. (**B**). Groups of mesenchymal cells organize into loose, oval aggregates that lie between a collecting tubule and one of its branches. (**C**). The mesenchymal cells coalesce to form a presumptive tubule, the component cells of which become arranged so that the long axis of each cell lies perpendicular to a forming lumen that appears within the interior. (**D**). As this tubular structure elongates, two indentations appear transforming it into a blind-ended, S-shaped tubule. (**E**-**G**). The region of the primitive tubule furthest from the collecting tubule will become the renal corpuscle; the middle portion will form the proximal tubule; and the region closest to the collecting tubule will form the loop of Henle and the distal tubule. As the S-shaped configuration is established, a vascular bud of forming capillaries enters the region between the middle and distal portions of the elongating tubule. Tubular cells intimately associated with the forming capillaries remain cuboidal or columnar in shape, whereas cells on the opposite side of the tubule flatten to form the parietal layer of Bowman's capsule. Simultaneous with these events, the proximal end of the differentiating nephron joins with the collecting tubule. (**G**, **H**). The parietal layer expands and constricts around the entry point of the vascular bud forming the vascular pole. The morphology of the tubular epithelium associated with the forming glomerular capillaries changes markedly at this time and differentiates into podocytes forming the visceral layer of Bowman's capsule.

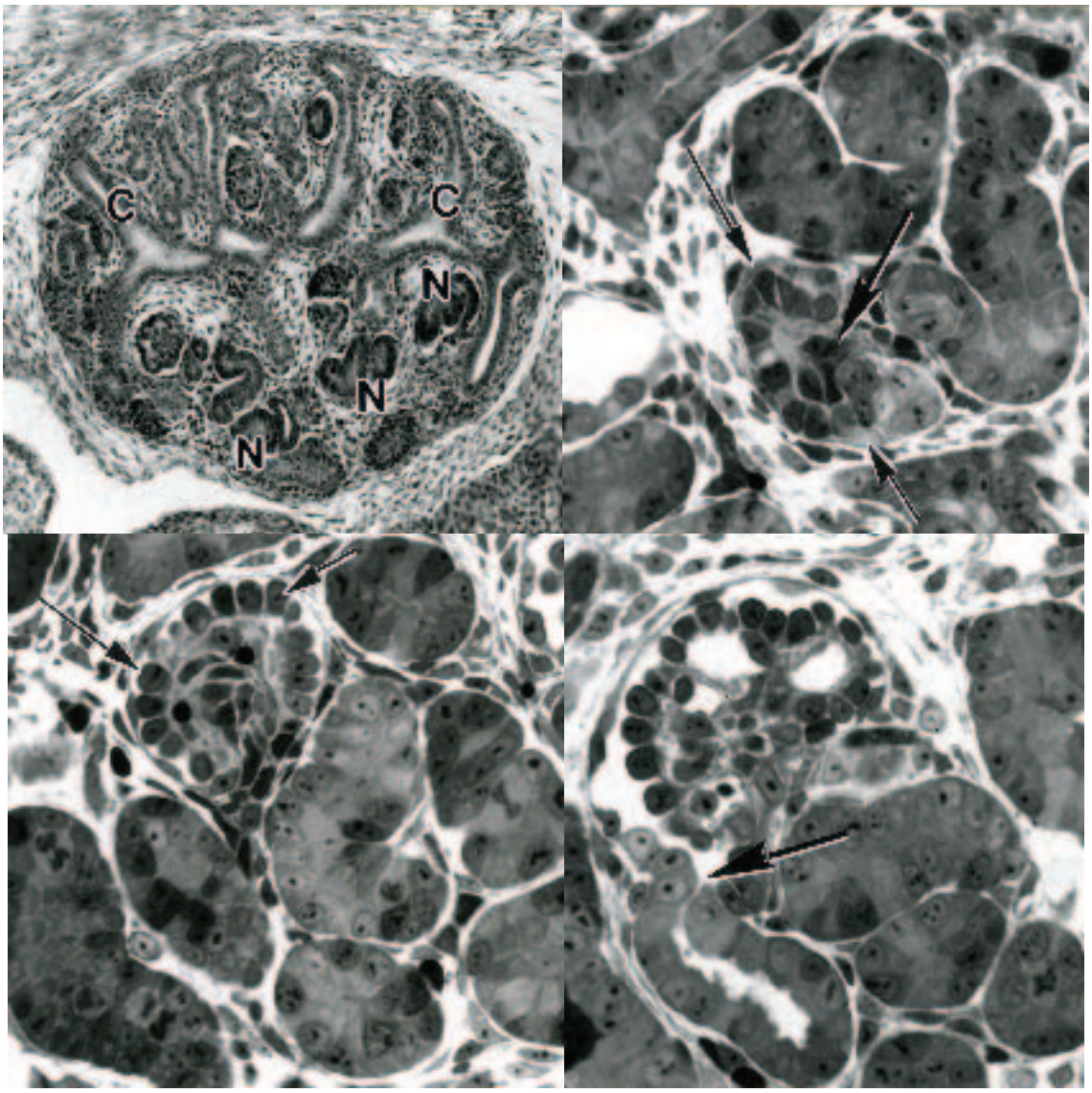

Fig. 3. (*Above left*). A section through a newborn opossum metanephros cut near the pelvis illustrates numerous collecting tubules (C) and closely associated differentiating nephrons (N). LM X 100. (*Above right*). A renal corpuscle in the initial stages of differentiation in which flattened peripheral cells (small arrows) forms the parietal layer of Bowman's capsule and a vascular bud (large arrow) of the future glomerular capillaries can be visualized. The layer of dark cuboidal cells positioned between these two entities will differentiate in the visceral (podocytic) layer of Bowman's capsule. The tubular component of the differentiating nephron is at the upper right. LM X 400. (*Below left*). A renal corpuscle more fully differentiated than the one in the upper right illustration shows a clearly defined layer of cube shaped podocytes forming the visceral layer of Bowman's capsule (arrows). The differentiating podocytes lie upon a vascular bud of differentiating glomerular capillaries. The tubular component of the nephron continues its development at the lower right. LM X 400. (*Below right*). This illustration of a more fully differentiated renal corpuscle clearly shows the establishment of glomerular capillaries and the surrounding layer of podocytes, the simple squamous epithelium of the parietal layer, and a well-defined capsular space. Note the continuity of the capsular space with the lumen of the proximal convoluted tubule (arrow). LM X 400.

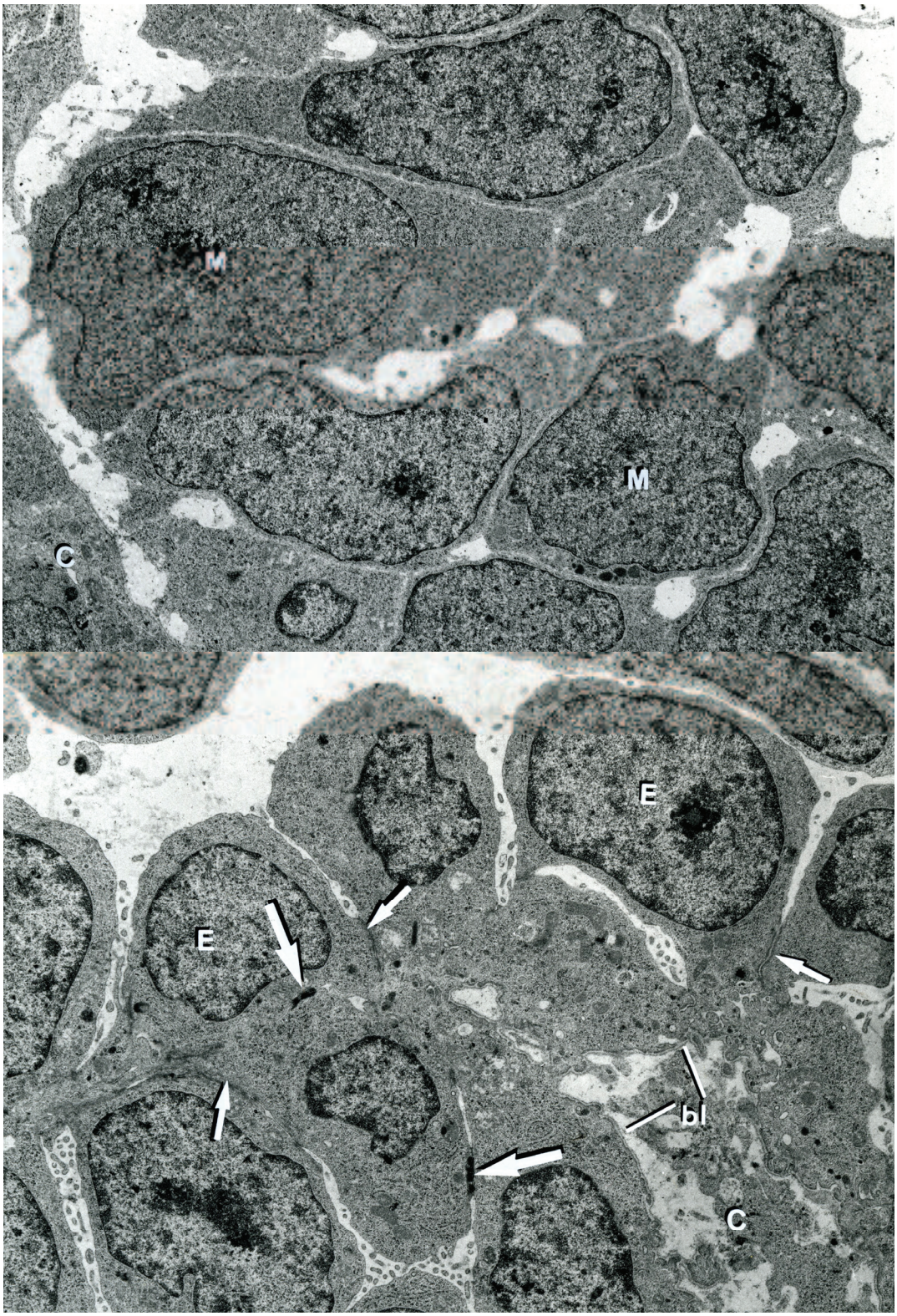

Fig. 4. (*Above*). Mesenchymal cells (M) of a forming renal vesicle from a newborn opossum metanephros exhibit considerable electron density, are irregular in shape, and lack any apparent organization. The position of a collecting tubule (C) is shown at the extreme lower left. TEM X 4,500. (*Below*). An electron micrograph illustrates differentiating glomerular epithelial cells (E) (podocytes) in a forming renal corpuscle. They lie on a distinct basal lamina (bl), and show adherens-like attachments (small arrows) as well as scattered desmosomes (large arrows). A portion of a glomerular capillary (C) lies at the lower right. TEM X 4,000.

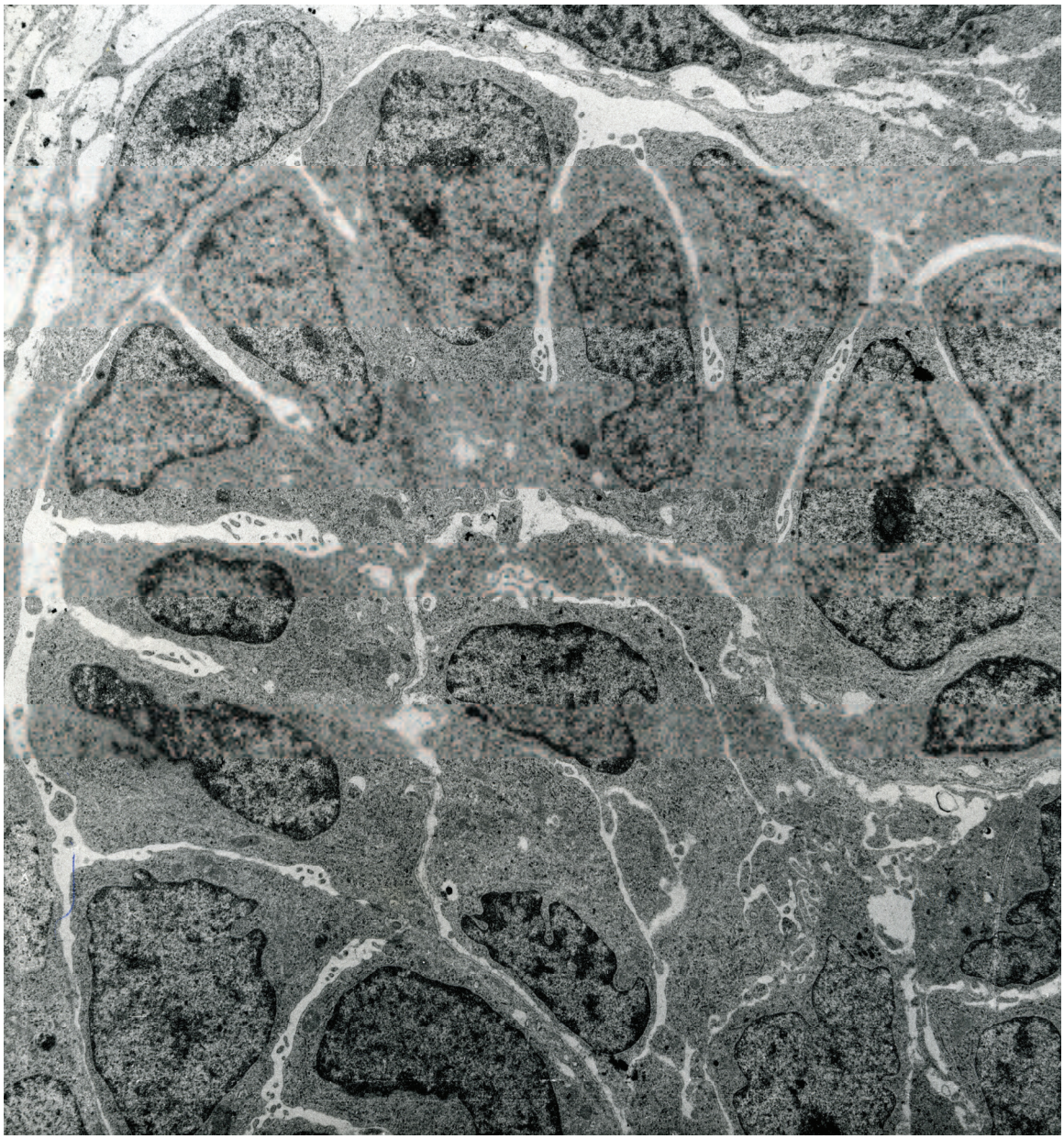

Fig. 5. A micrograph illustrates a section through the length of a differentiating renal corpuscle from the metanephros of a newborn opossum. The single layer of flattened epithelial cells at the extreme left comprises the parietal layer of Bowman's capsule (the glomerular capsule) and is separated by a narrow capsular space from a layer of differentiating podocytes that arch over and around two centrally positioned endothelial cells of a forming glomerular capillary. TEM X 2,000.

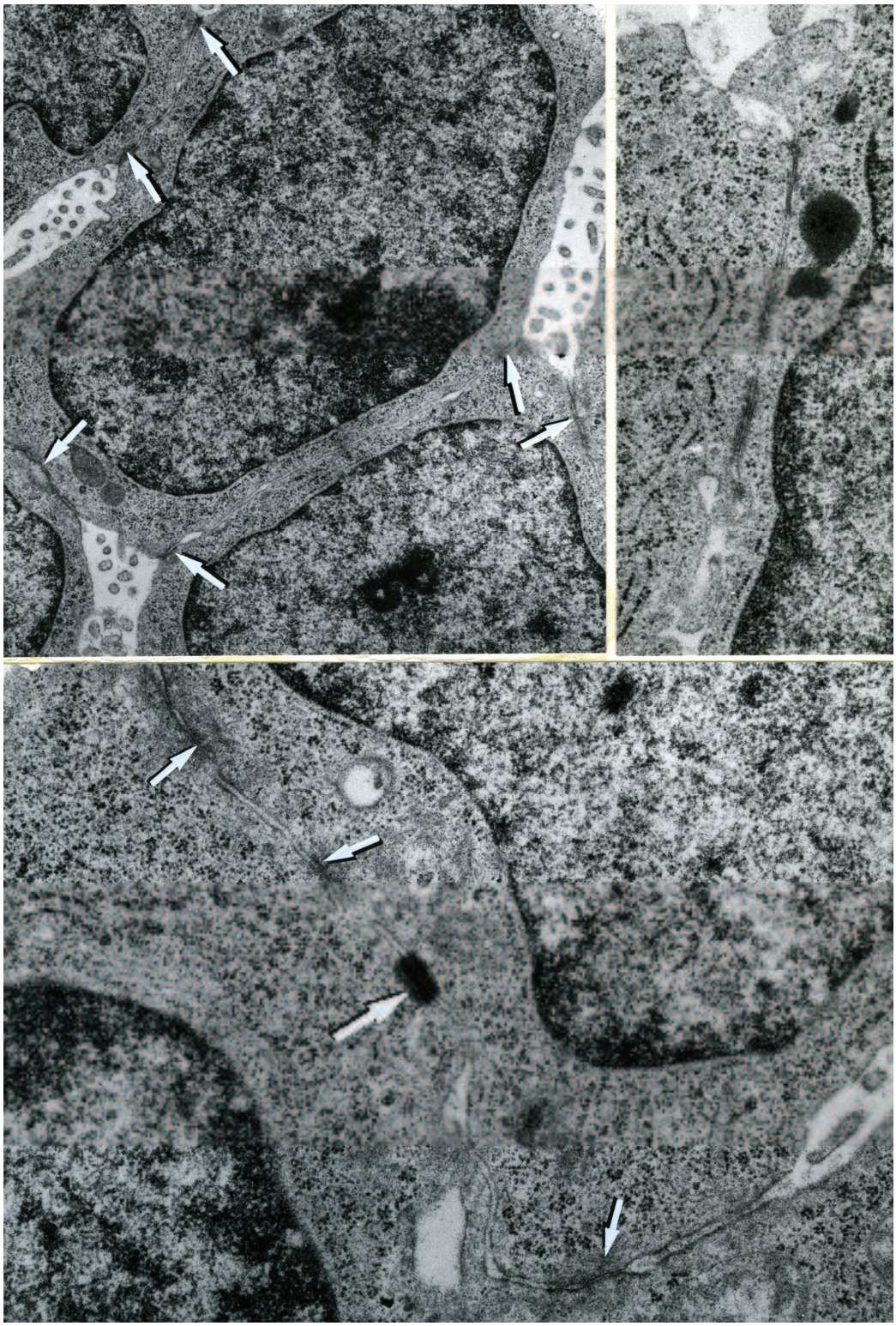

Fig. 6. (*Above left*). A micrograph illustrates cell attachments uniting four differentiating podocytes (arrows). Newborn opossum. TEM X 10,400. (*Above right*). A micrograph at increased magnification illustrates a cell attachment between adjacent differentiating podocytes. Newborn opossum. TEM X 26,500. (*Below*). A complex of intercellular attachments between podocytes illustrates several adherens-like structures (small arrows) and a macula adherens (desmosome) (large arrow). Newborn opossum. TEM X 26,500.

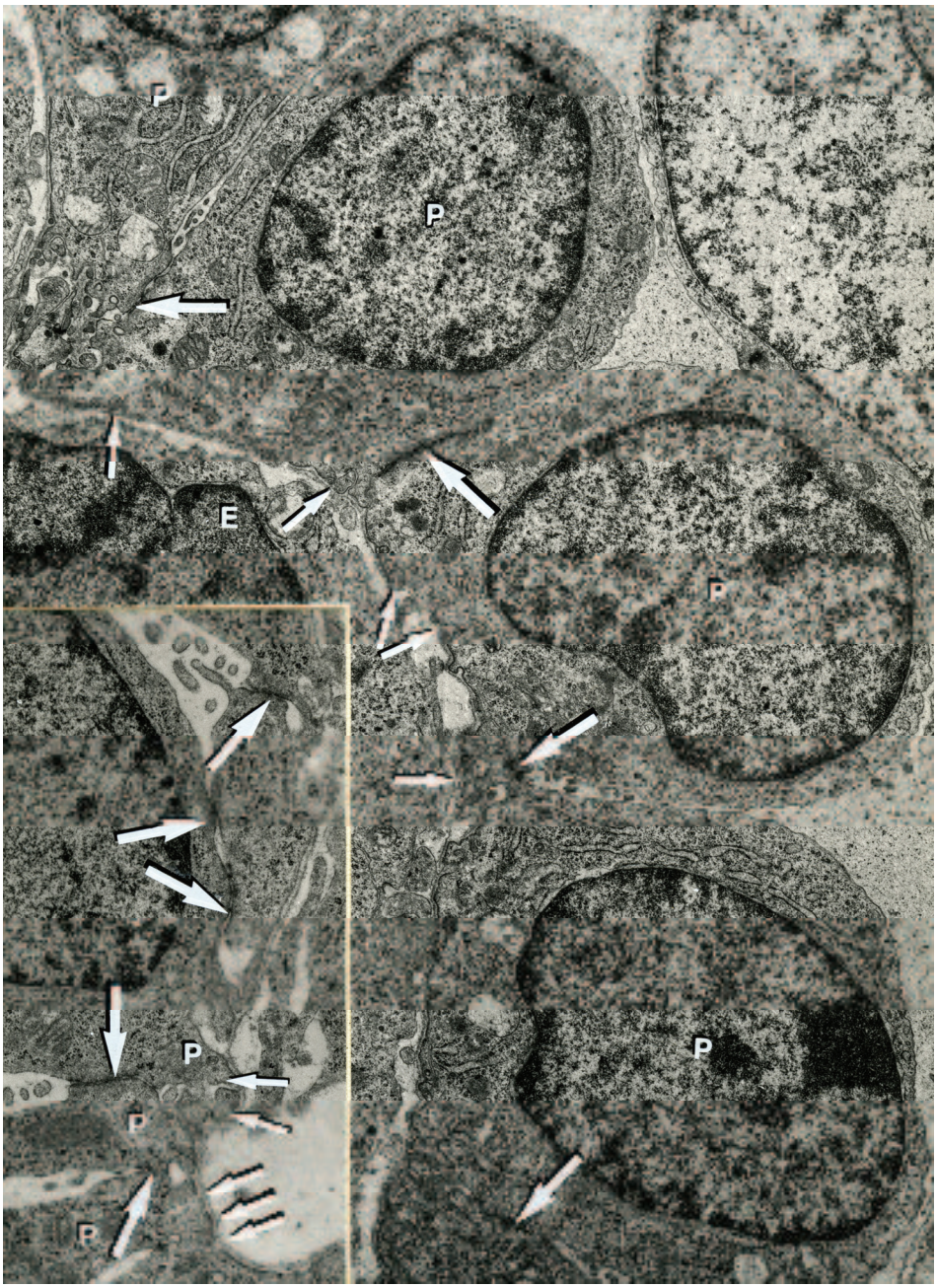

Fig. 7. A micrograph illustrates a region of a more completely differentiated renal corpuscle from the metanephros of a newborn opossum. The podocytes (P) show a definite organization into a monolayer adjacent to an endothelial cell (E) of a developing glomerular capillary. Most cell attachments are lost except for those located in the basal region near the endothelial cell of a glomerular capillary (large arrows). Note the differentiating foot processes (pedicles) of the podocytes (small arrows) immediately adjacent to the basal lamina. TEM X 7,000. (*Inset*). Podocytes from a more completely differentiated renal corpuscle show continued development of the foot processes (small arrows) and the initial appearance of secondary processes (P). Persistent cell attachments (large arrows) continue to unite the bases of adjacent podocytes. One-week-old opossum. TEM X 16,500.

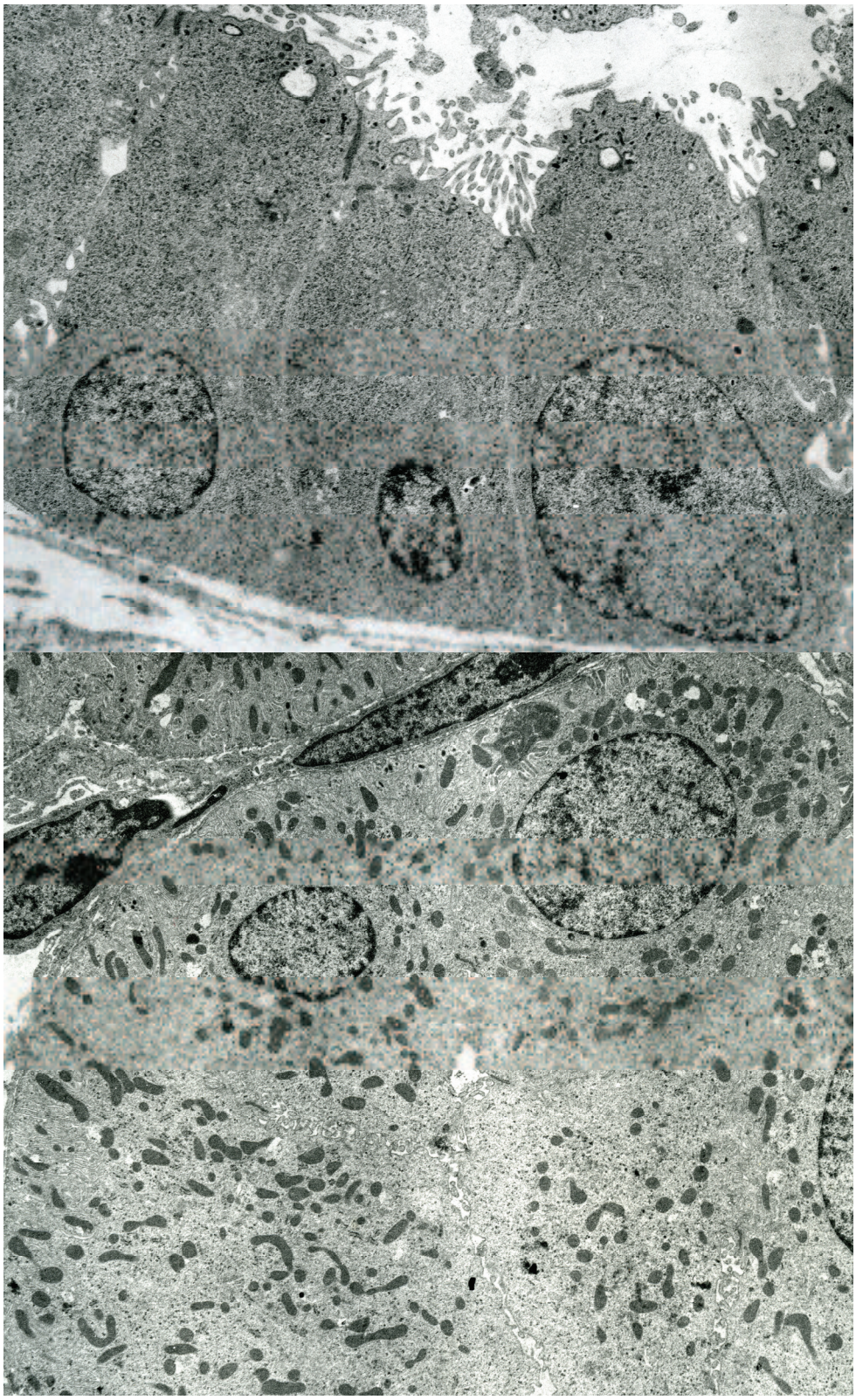

Fig. 8. (*Above*). Epithelial cells comprising the proximal tubule of a newborn metanephros are characterized by numerous polyribosomes, exhibit a poorly developed microvillus border and underlying endocytic complex, and lack basal infoldings. TEM X 2,000. (*Below*). Epithelial cells forming the distal metanephric tubule are characterized by basolateral infoldings of the plasmalemma and numerous mitochondria. Newborn opossum. TEM X 2,000.

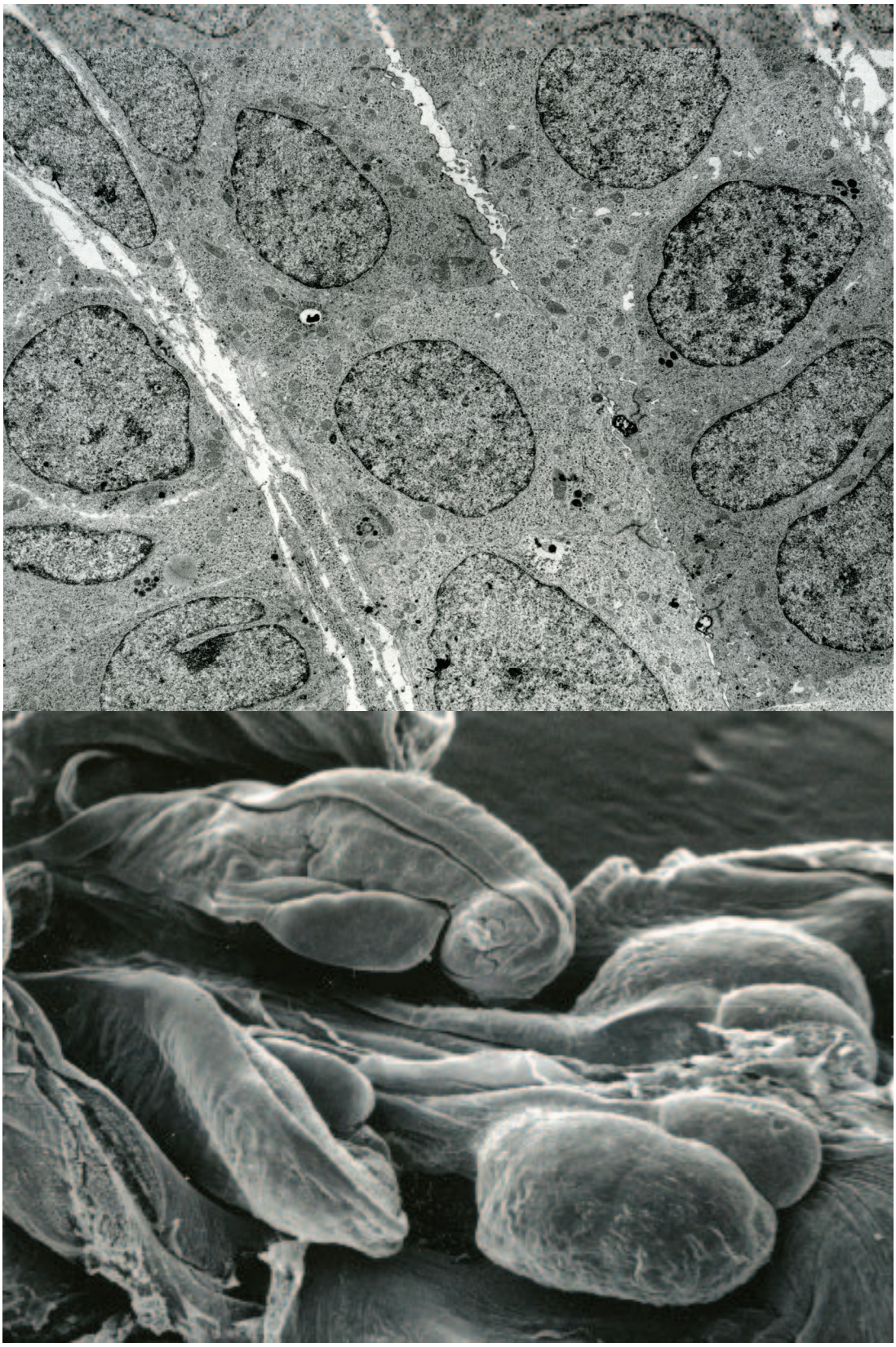

Fig. 9. (*Above*). A segment of a collecting tubule located near the renal capsule of a newborn opossum. A portion of a proximal tubule is seen at the lower left. TEM X 2,000. (*Below*). The urogenital system of an opossum one week postnatal illustrates the continued development of the metanephroi and adrenal glands (right). Developing gonads lie medial to the involuting mesonephroi (left). SEM X 60.

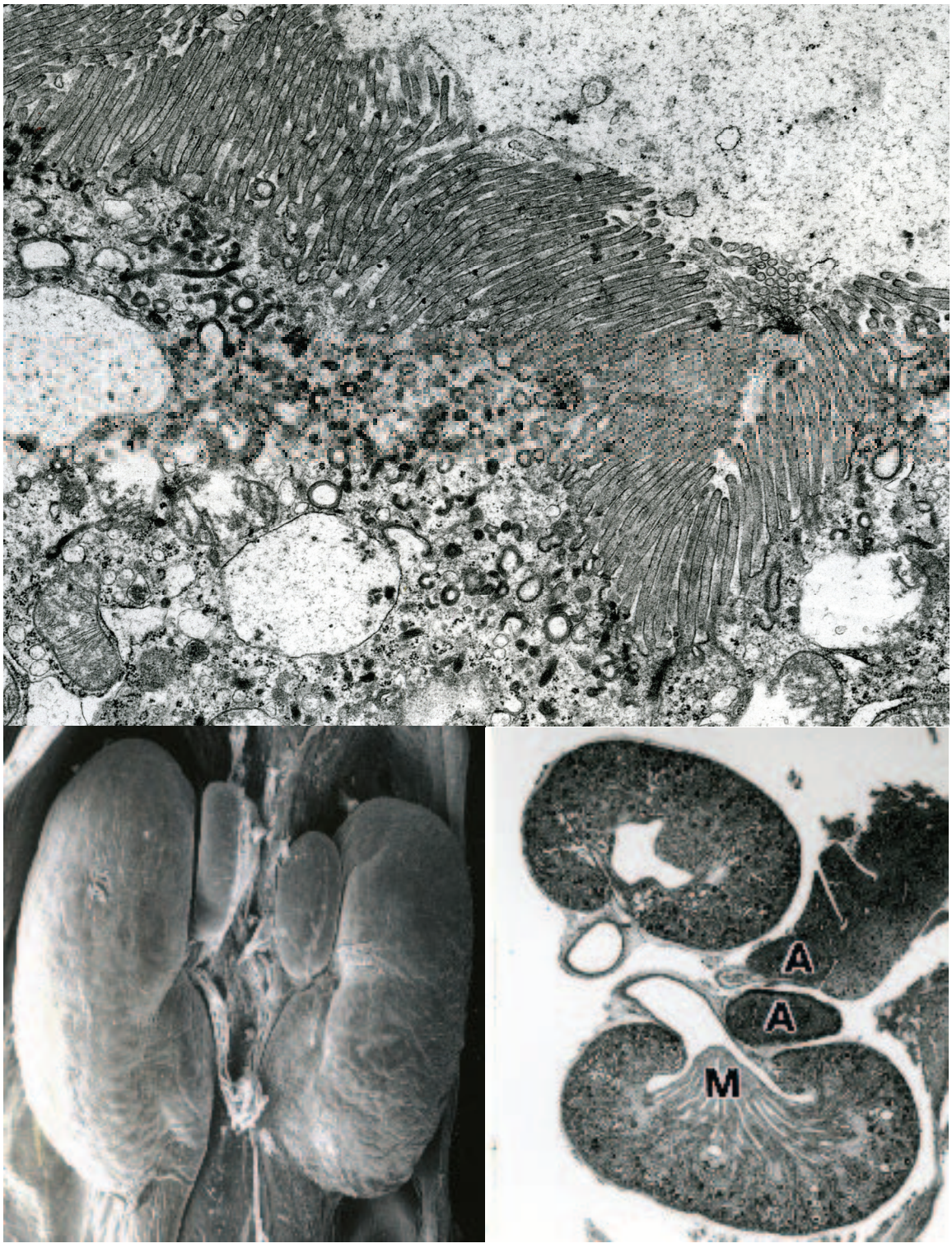

Fig. 10. (*Above*). The apical region of an epithelial cell from the proximal tubule of a week old opossum is characterized by a well-developed microvillus border and endocytic complex. TEM X 11,000. (*Below left*). A micrograph illustrates the metanephroi and adrenal glands of an opossum two weeks postnatal. SEM X 30. (*Below right*). A histological section through the metanephroi of an opossum eighteen days postnatal illustrates their general internal architecture at this period of development. Cortical and medullary regions (M) are clearly evident. The adrenal glands (A) also are shown. LM X 15.

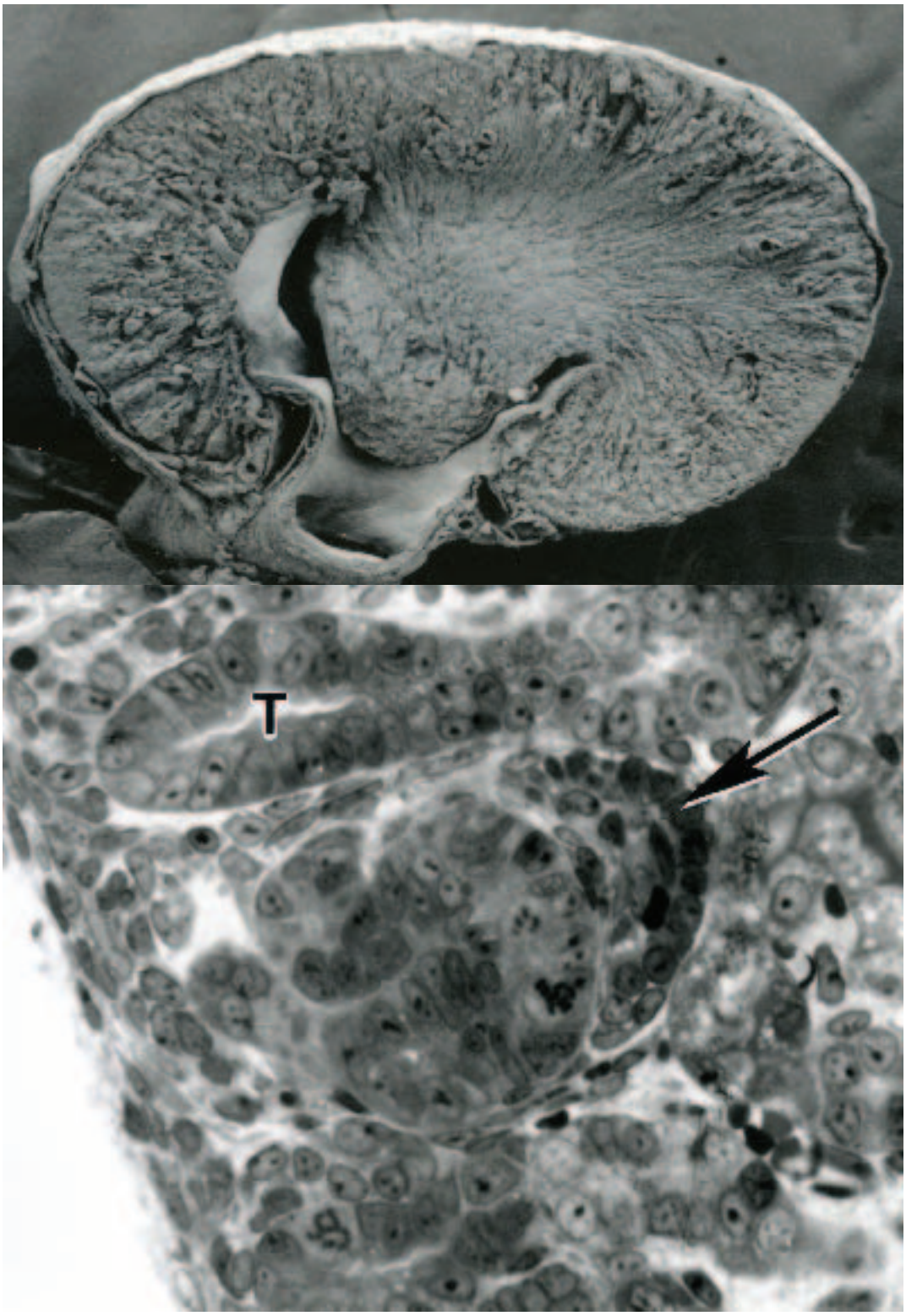

Fig. 11. (*Above*). A micrograph illustrates the interior of an opossum metanephros four week postnatal. Note that the opossum metanephros is a unilobular kidney. SEM X 20. (*Below*). A micrograph illustrates a differentiating nephron (arrow) within the nephronogenic zone near the renal capsule (left) of a four-week-old opossum. A portion of the associated collecting tubule (T) lies immediately adjacent to the differentiating nephron unit. LM X 400.

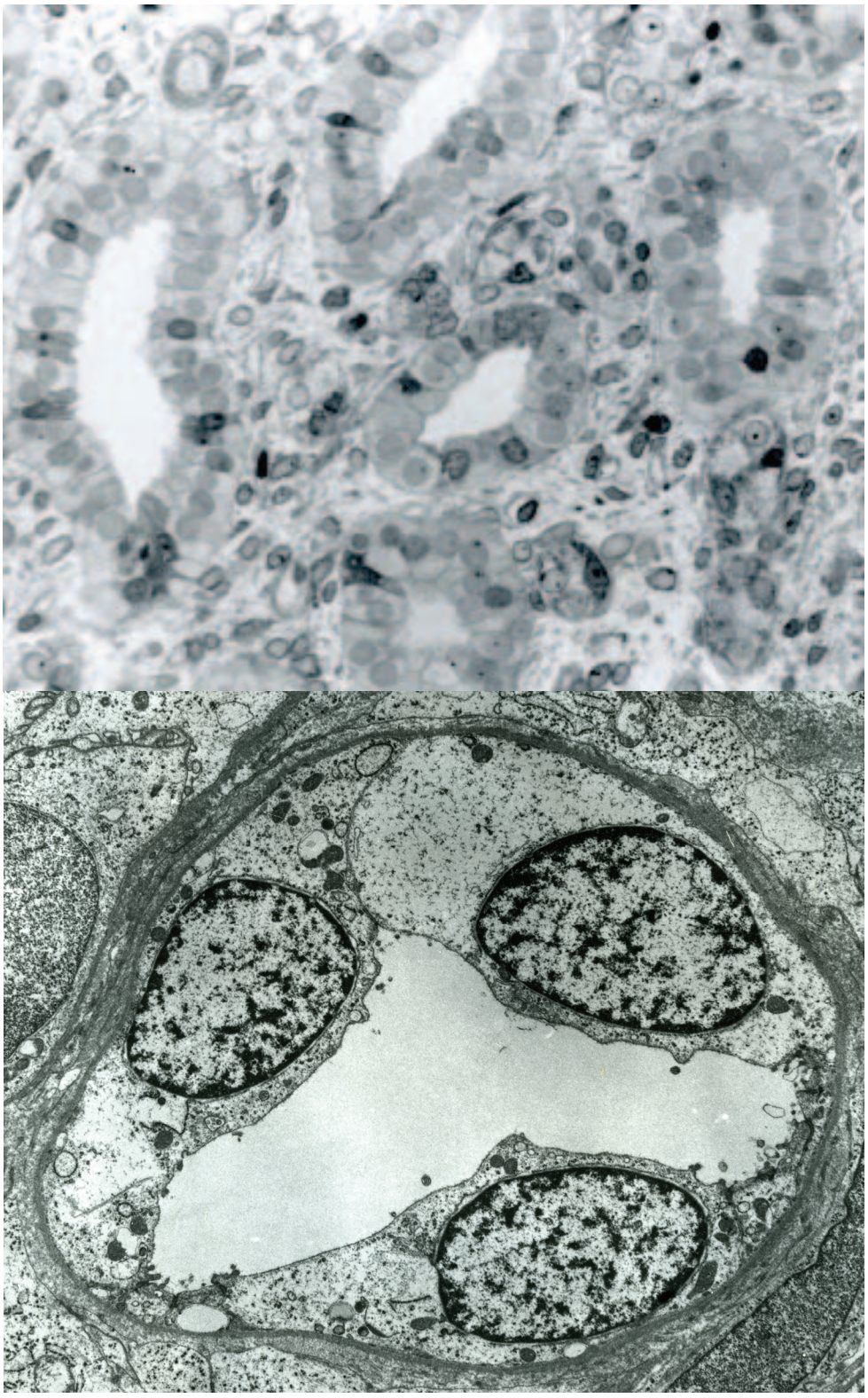

Fig. 12. (*Above*). A region of the medulla from a four-week-old opossum shows well developed collecting tubules and loops of Henle scattered within the diffuse interstitial connective tissue. LM X 350. (*Below*). Epithelial cells forming a thin segment of the loop of Henle are characterized by an electron lucent cytoplasm that shows a paucity of organelles. Opossum four weeks postnatal. TEM X 3,000.

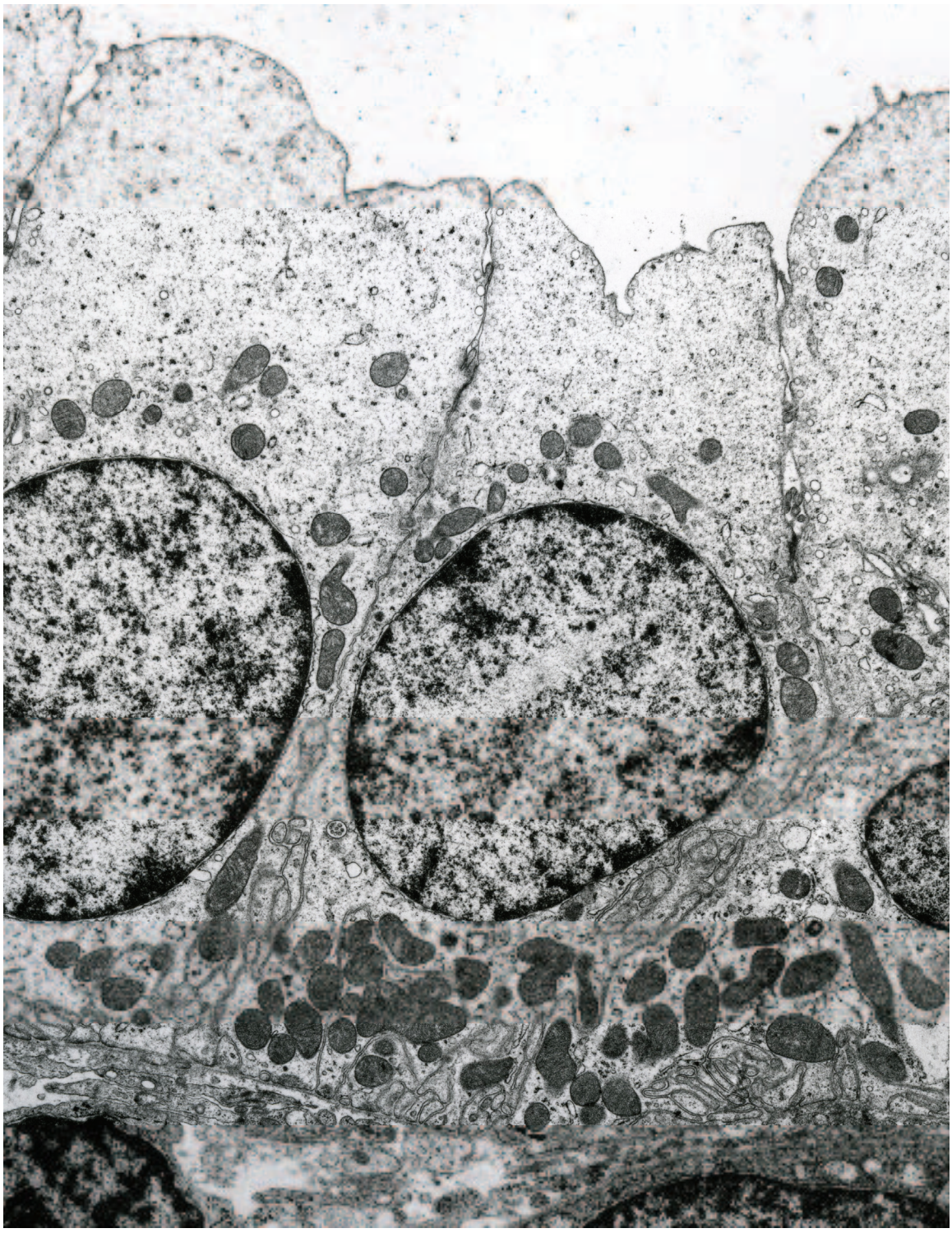

Fig. 13. Epithelial cells lining the terminal region of the distal tubule are columnar in shape and exhibit an electron lucent cytoplasm. The luminal plasmalemma is relatively smooth whereas the basal plasmalemma shows well-established basolateral infoldings. Note the intimate relationship between the basal concentration of mitochondria and the basolateral infoldings. TEM X 3,000.

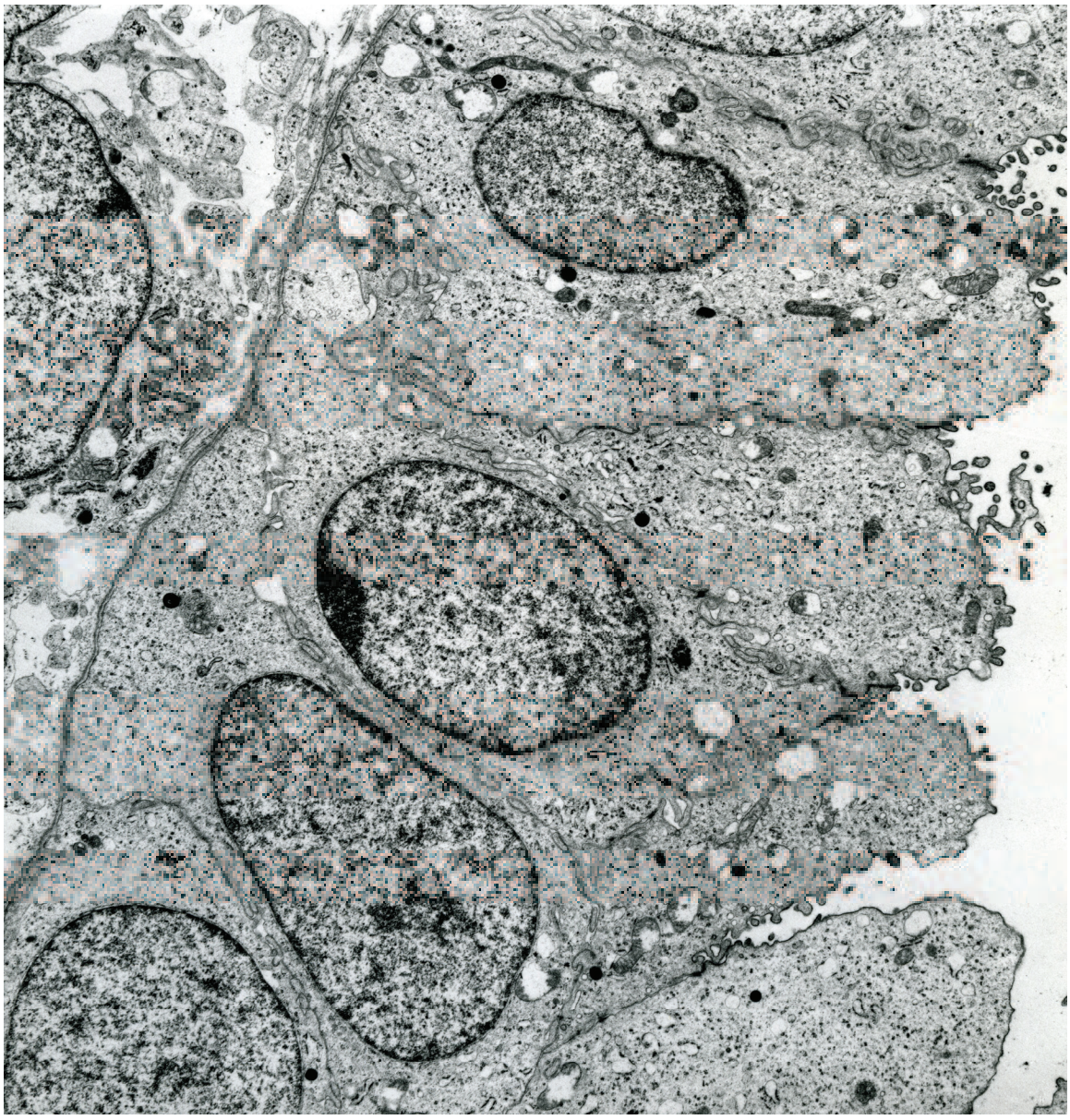

Fig. 14. A photograph illustrates a collecting tubule from the medulla of a metanephros of an opossum four weeks into the postnatal period. The cytoplasm of the tall columnar lining epithelial cells is electron lucent and contains scattered mitochondria and polyribosomes. Small, scattered electron-dense granules also are observed. The apical and basal cell membranes are relatively smooth. The lateral cell membranes show implications and apical tight junctions. The epithelial cells lie on distinct basal lamina. TEM X 3,500.

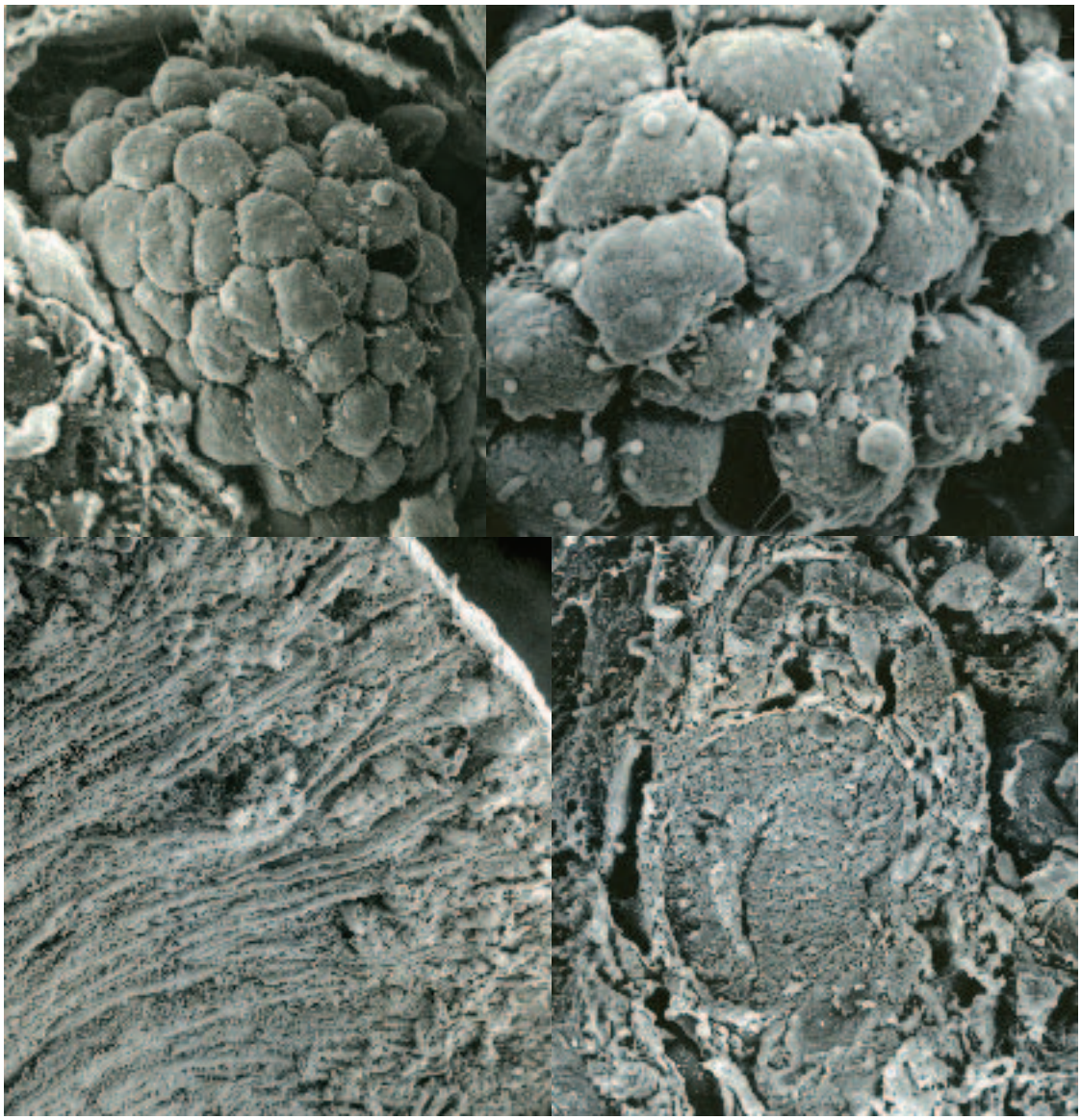

Fig. 15. (*Above left*). A scanning electron micrograph illustrates the dome shaped external surfaces of differentiating podocytes forming the visceral layer of Bowman's capsule from a developing renal corpuscle located near the renal capsule of six-week-old opossum. SEM X 2,000. (*Above right*). Pedicles (foot processes), which appear as narrow cytoplasmic processes extending from cell body, can be visualized extending from the cell body of individual podocytes when examined at increased magnification. SEM X 5,000. (*Below left*). A fracture through the cortical region of a metanephros from a seven-week-old opossum illustrates the depth of the forming cortex at this period of development. SEM X 100. (*Below right*). A scanning electron micrograph illustrates a fracture through a differentiating nephron unit found in the outer cortex of a metanephros from an opossum seven weeks postnatal. SEM X 300. Compare this figure with figure 11 (bottom) and figure 16 (top).

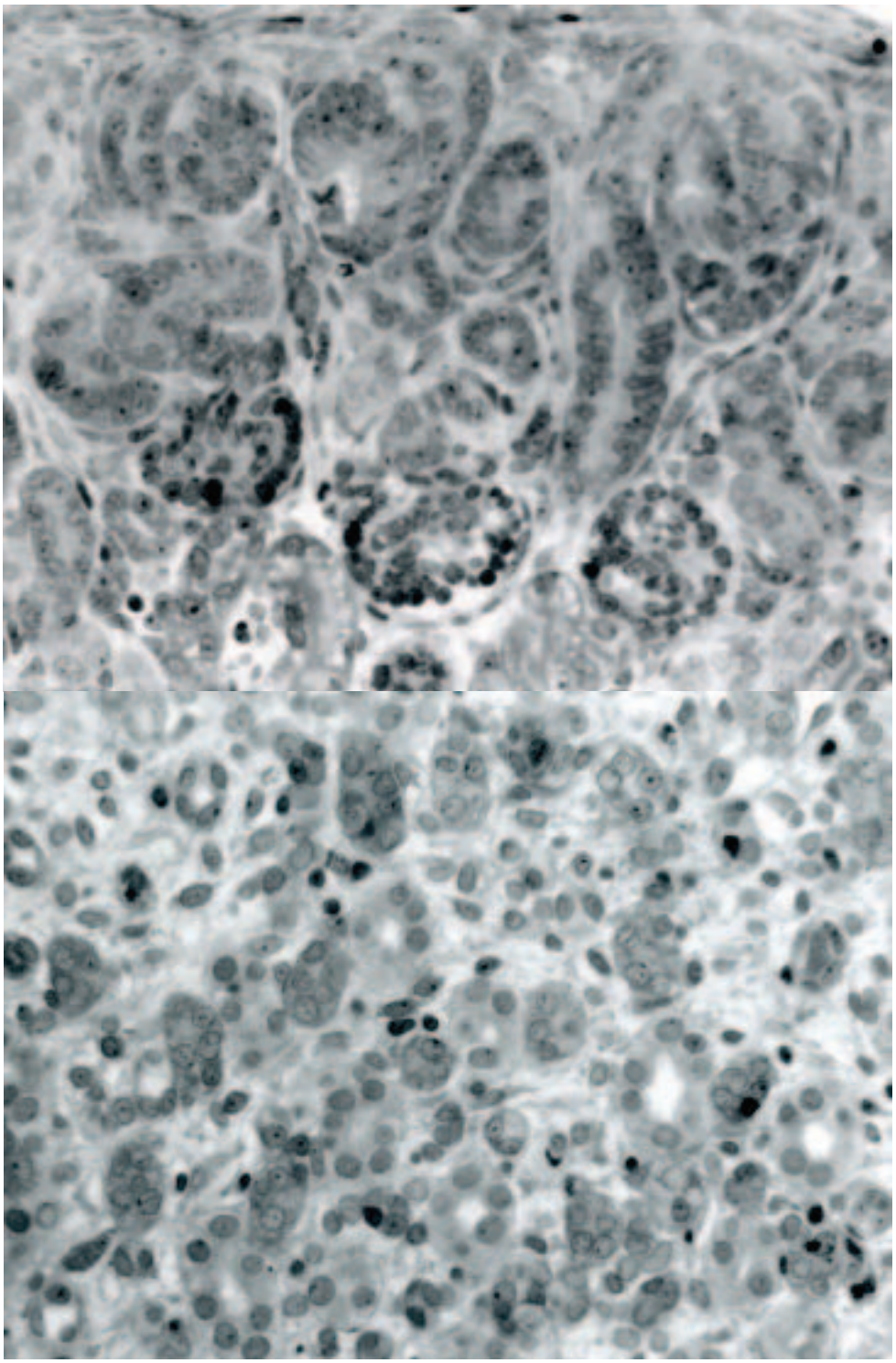

Fig. 16. (*Above*). New generations of differentiating nephron units continue to be found in the subcapsular region of a metanephros from a 7.5 week-old opossum. Note the dichotomous branching of the collecting tubules. LM X 350. (*Below*). A region of medulla from a 7.5 week-old opossum illustrates that the collecting tubules and loops of Henle are in greater numbers and positioned closer together when compared to younger ages. LM X 350.

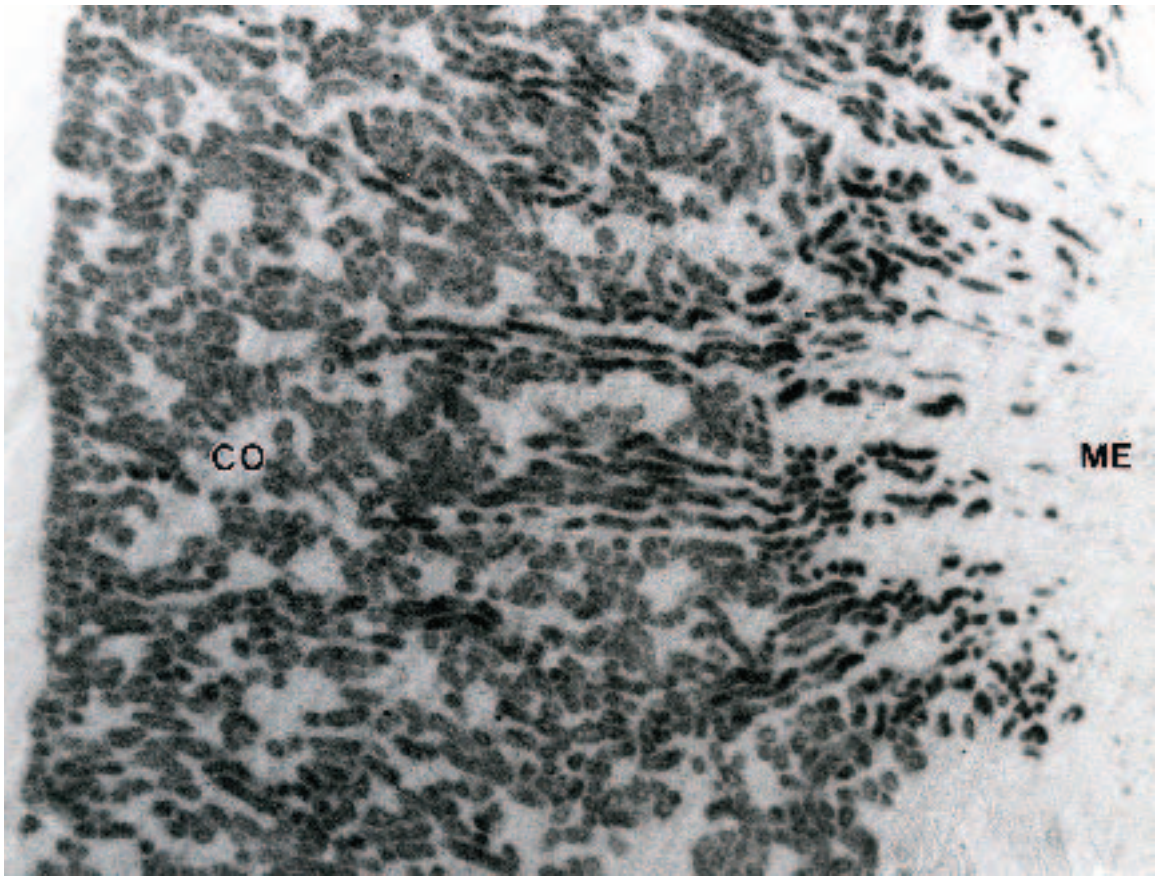

Fig. 17. The metanephros of an adult opossum labeled with ^{125}I-ST enterotoxin illustrates that specific binding is restricted primarily to the proximal convoluted tubule of the cortex (CO). Little if any specific binding occurs in the tubules comprising the medulla (ME) of the kidney. Autoradiograph X75.

Chapter 14. Nasal Cavity

Synopsis:

The head and snout of the opossum are established during the last three prenatal days. Maxillary and mandibular swellings as well as the olfactory placodes are apparent early in the tenth prenatal day and by prenatal day eleven the lateral and medial nasal processes fuse to form the nasal pits. The lateral palatine processes come together and unite at the midline to form the hard palate early in prenatal day twelve as the nasal septum grows downward to unite with the anterior one-third of the forming palate. By the end of prenatal day twelve, the palate separates nasal and oral cavities and the snout and external nares are clearly defined. The external nares just prior to and after birth are large and flared and open into the nasal cavity. Immediately interior to the orifice of the external nares, cells of the epitrichium (which cover the entire opossum at this time) are abruptly replaced by surface cells of another form of stratified squamous epithelium. Surface cells associated with this epithelium are of less diameter and have numerous, short microvilli extending from their luminal surface. The area occupied by this form of epithelium is narrow and abruptly changes to olfactory epithelium. The olfactory epithelium also is restricted in distribution during this period of development to the dorsal-rostral-most region of the nasal cavity. The olfactory epithelium consists primarily of olfactory bipolar neurons, sustentacular cells, and basal cells.

The olfactory bipolar neurons are in various stages of maturation with mature neurons being characterized by a spindle shape and centrally positioned round or oval nuclei. Numerous microtubules fill the dendritic processes that terminate as large olfactory knobs that extend above the surface of the olfactory epithelium. Olfactory cilia originate from basal bodies within the olfactory knobs and form a thick mat that lies parallel to the surface of the olfactory epithelium. The formed mat of olfactory cilia occurs along the dorsal-rostral-most extent of the nasal cavity just interior to the entrance of the nares. Olfactory receptor neurons within this region synthesize olfactory marker protein (OMP), a protein considered unique for mature olfactory neurons. Its presence suggests that the olfactory receptor neurons of this region have established synaptic contact with other neurons within the forming brain. OMP-positive axons that extend from olfactory bipolar neurons into the presumptive olfactory bulb region of the brain one day prior to birth suggests that synaptic contact is established extremely early in the opossum. The olfactory epithelium found in the dorsal-caudal region of the nasal cavity is less well differentiated and immature in appearance.

Scattered cells with dense pyknotic nuclei and/or vacuolated cytoplasm are seen within the rostral olfactory epithelium late during the first postnatal week. The majority of the nasal cavity including the turbinates, which begin to form shortly after birth, is covered by a differentiating respiratory epithelium at this time. By the end of the second postnatal week the snout has elongated considerably and the expanding turbinates provide greater surface area to the interior of the nasal cavity. The majority of the nasal cavity continues to be lined by respiratory epithelium consisting of ciliated and non-ciliated cells. Non-ciliated cells characterized by numerous microvilli are particularly prominent in regions of respiratory epithelium associated with the turbinates. The majority of olfactory epithelium is now confined to the more dorsal-medial and caudal regions of the nasal cavity. The olfactory epithelium, previously located in the dorsal-rostral-most extent of the nasal cavity, disappears

after the first few weeks of postnatal life. This apparent loss of mature olfactory epithelium may be due, in part, to differential growth. As the snout and nasal cavity elongate with continued growth and the turbinates expand into the nasal cavity, the olfactory epithelium becomes localized in the more protected dorsal-caudal regions of the nasal cavity. It is hypothesized that the olfactory epithelium develops precociously in the dorsal-rostral area of the nasal cavity just interior to the nares to specifically guide the newborn opossum to the pouch. Following the migration to the pouch, the olfactory epithelium found in this area is lost and replaced by a stratified squamous epithelium. Olfactory epithelium then differentiates in the more protected dorsal-caudal regions of nasal cavity and will eventually occupy extensive regions of the nasal septum, turbinates, and roof of the nasal cavity.

Acknowledgments:

Figs. 1 (bottom), 2, 3, 4 (top), 5 (top right), 6, 7 (top), 9 (top right and bottom), 11 (bottom) and 12, courtesy of and from: Krause, W. J. (1992) A scanning electron microscopic study of the opossum nasal cavity prior to and shortly after birth. Anat Embryol. 185:281-289.

Figs. 4 (bottom), 5 (top left), 7 (bottom), 8, 9 (top left), and 13, courtesy of and from: Lin, J.J.P., C. Phelix and W.J. Krause. (1988). An immunohistochemical study of olfactory epithelium in the opossum before and after birth. Zeit. mikrosk. anat. Forsch. 102:272-282.

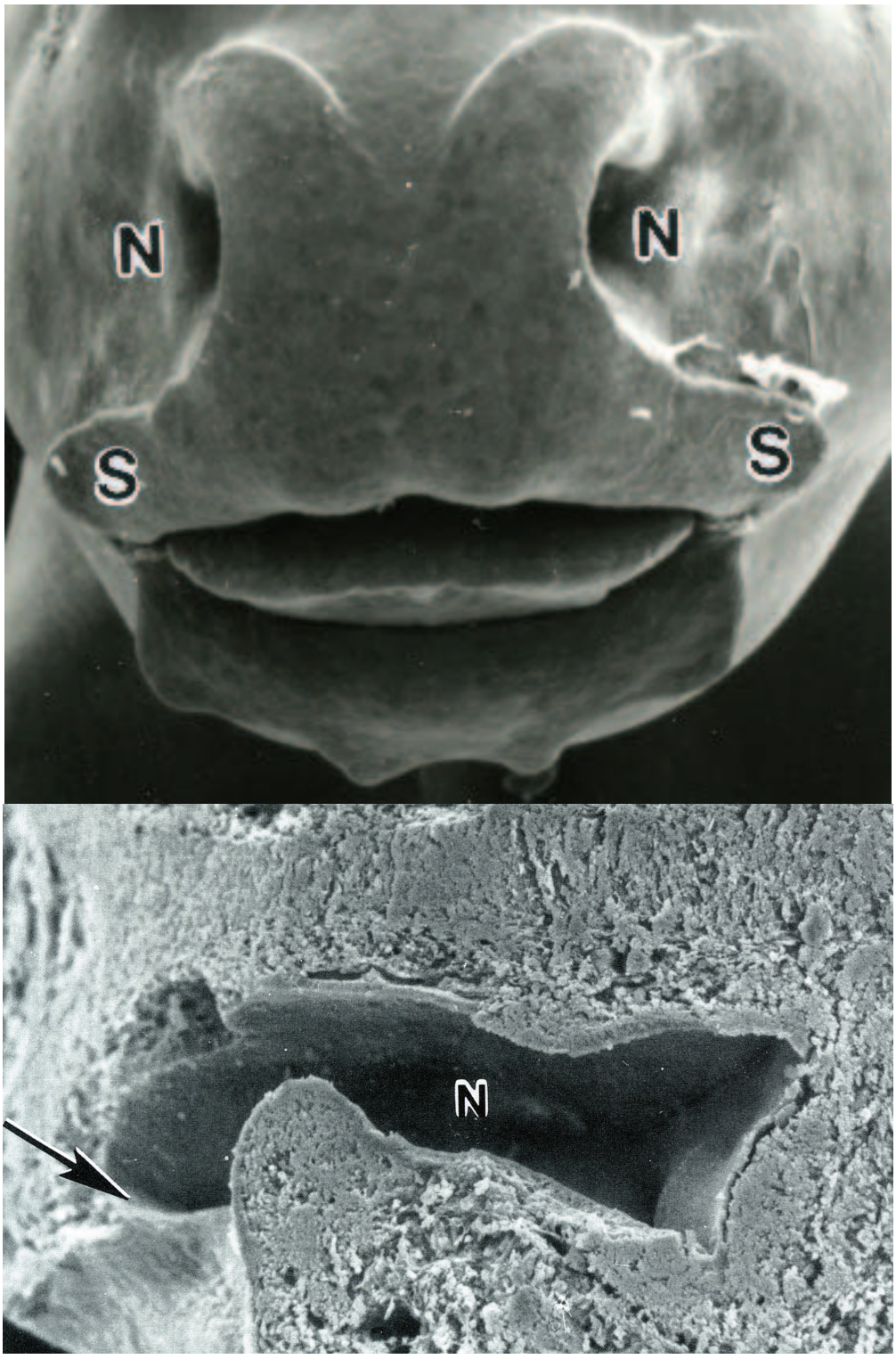

Fig. 1. (*Above*). The snout of an 11.5 day opossum embryo as viewed from the front illustrates the large, open external nares (N) and the oral shield (S) that develops around the opening to the oral cavity. Note the large, well-developed tongue within the oral cavity. SEM X 50. (*Below*). A dissected region of the snout illustrates the entrance of the external nares (arrow) into the open chamber of the nasal cavity (N). SEM X 60.

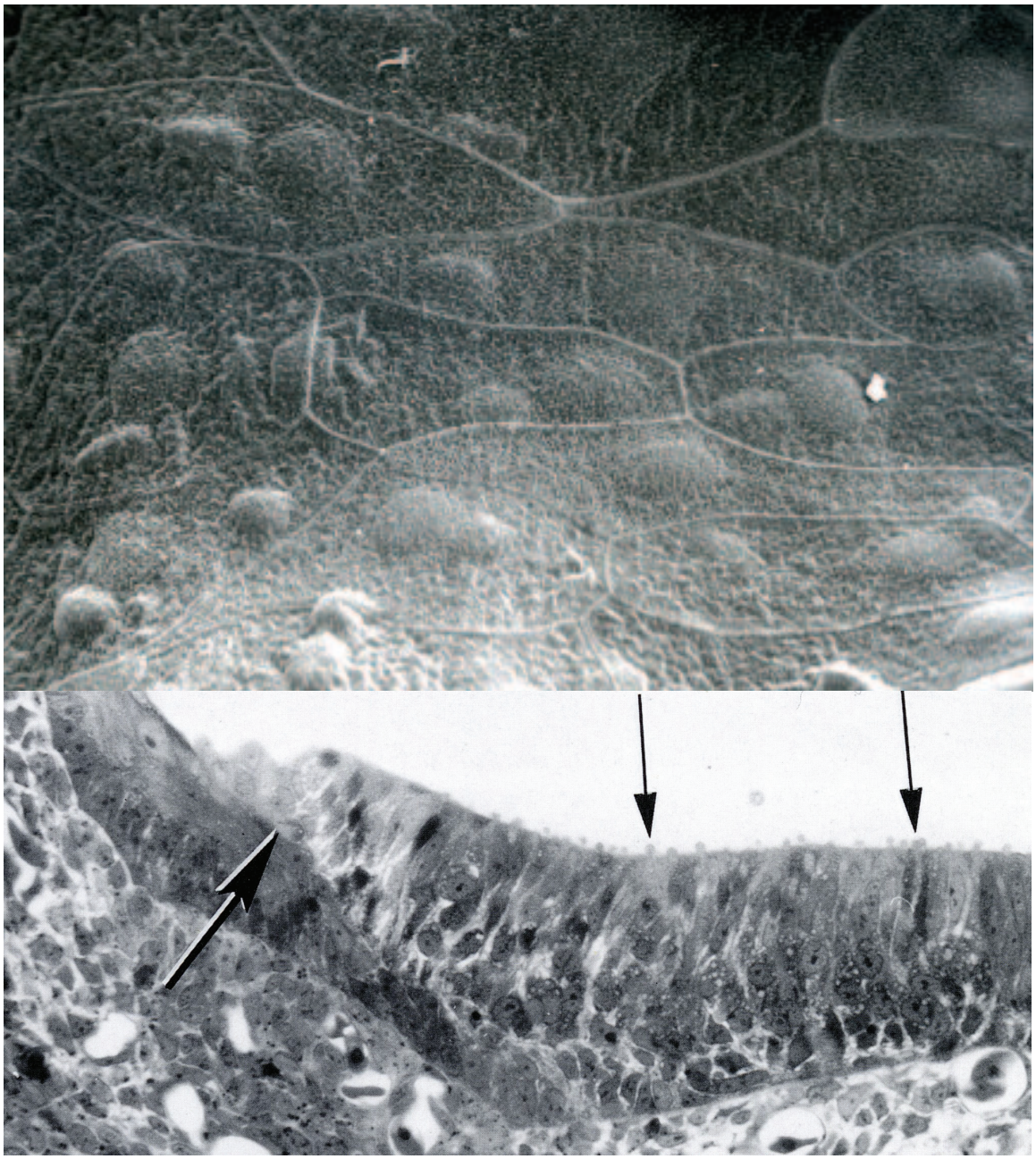

Fig. 2. (*Above*). The stratified squamous epithelium lining the entrance to the external nares is covered by a periderm (epitrichium). Note the distinct cell boundaries and nuclear profiles of the epitrichial cells. 11.5 day opossum embryo. SEM X 1000. (*Below*). A micrograph illustrates the abrupt junction between the transition zone of stratified squamous epithelium and olfactory epithelium (large arrow). Numerous olfactory knobs (small arrows) can be visualized on the surface of the olfactory epithelium. LM X 500.

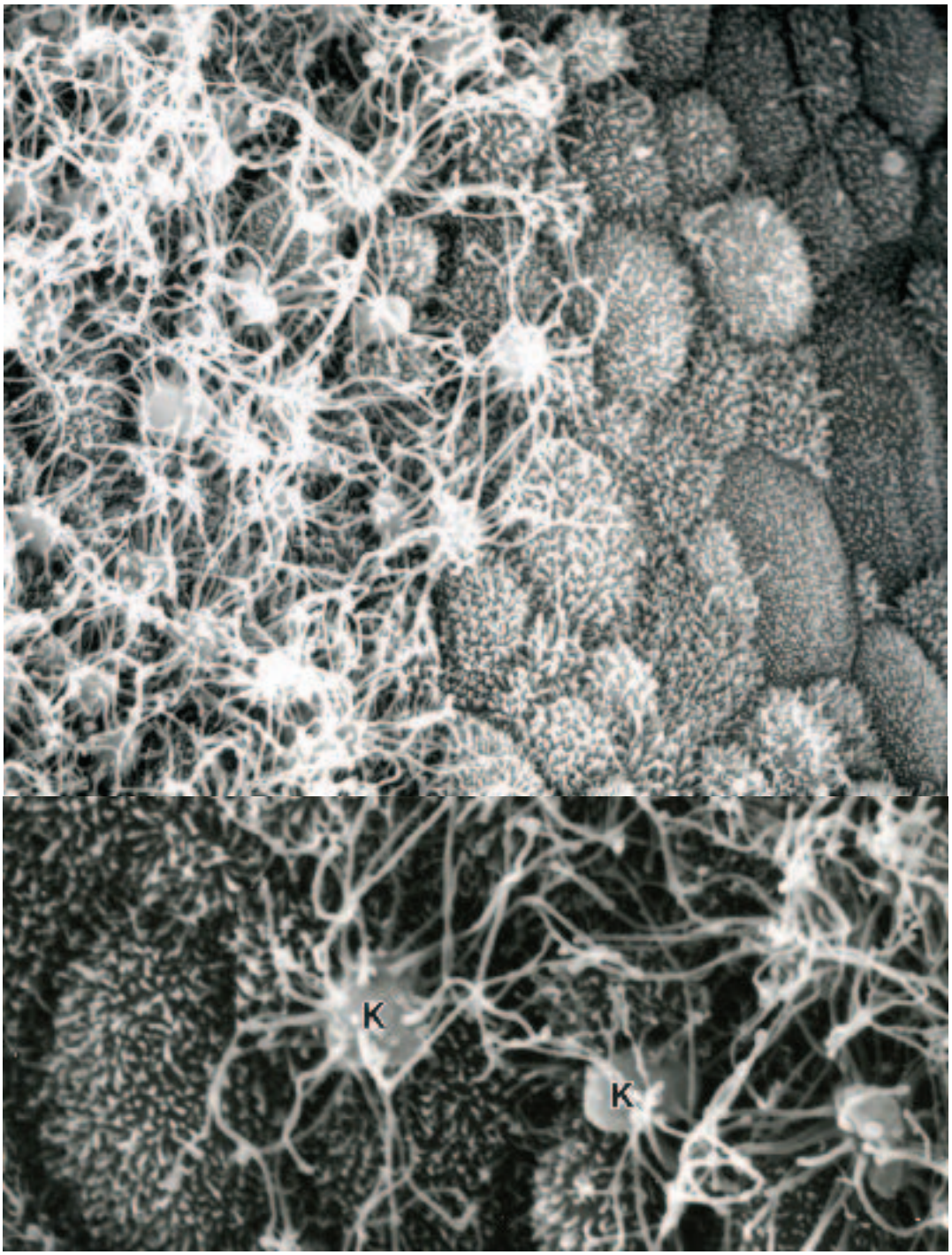

Fig. 3. (*Above*). A micrograph illustrates surface features of the epithelia on either side of the junction between the transition zone lining the external nares and the olfactory epithelium of an 11.5 day opossum embryo. The surface of the olfactory epithelium is to the left. Surface cells of the transition zone exhibit numerous microvilli whereas olfactory knobs characterize the surface of the olfactory epithelium. SEM X 5,000. (*Below*). Several olfactory knobs (K) and associated olfactory cilia extend from the surface of the olfactory epithelium. 11.5 day opossum embryo. SEM X 12,000.

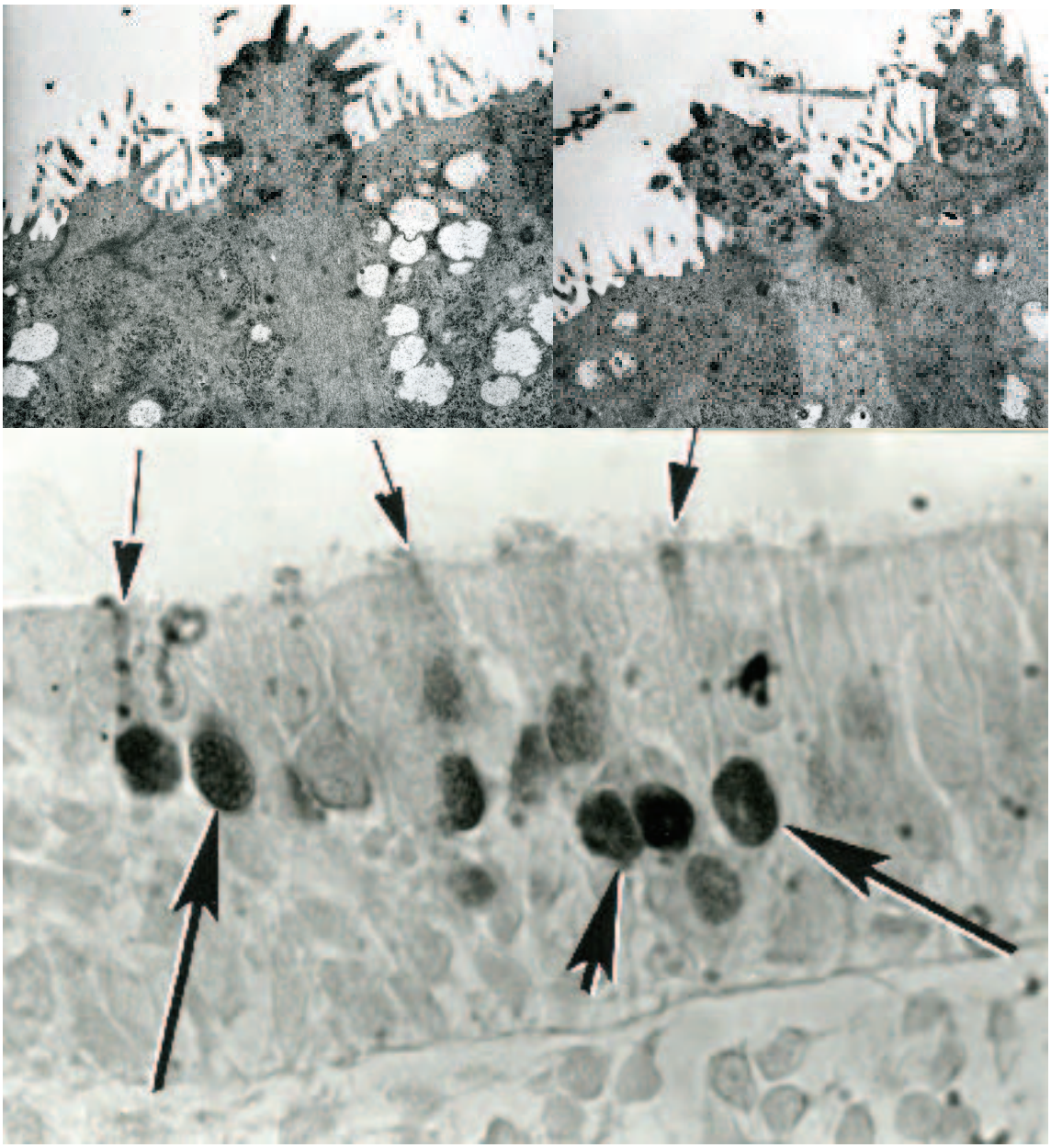

Fig. 4. (*Above*). Two photomicrographs illustrate olfactory knobs that extend above the surface of the olfactory epithelium and contain the basal bodies each of which is associated with an olfactory cilium. The apices of the olfactory bipolar neurons are separated by sustentacular cells. 11.5 day opossum embryo. TEM X 18,000. (*Below*). The olfactory epithelium of a twelve-day opossum embryo stained with olfactory marker protein (OMP) illustrates several positive olfactory bipolar neurons (large arrows). The majority of the most intense OMP immunoreactivity occurs in the nucleoplasm and the perinuclear cytoplasm. Several apical dendrites terminating in olfactory knobs also can be observed that show light immunoreactive staining with olfactory marker protein (small arrows). LM X 800.

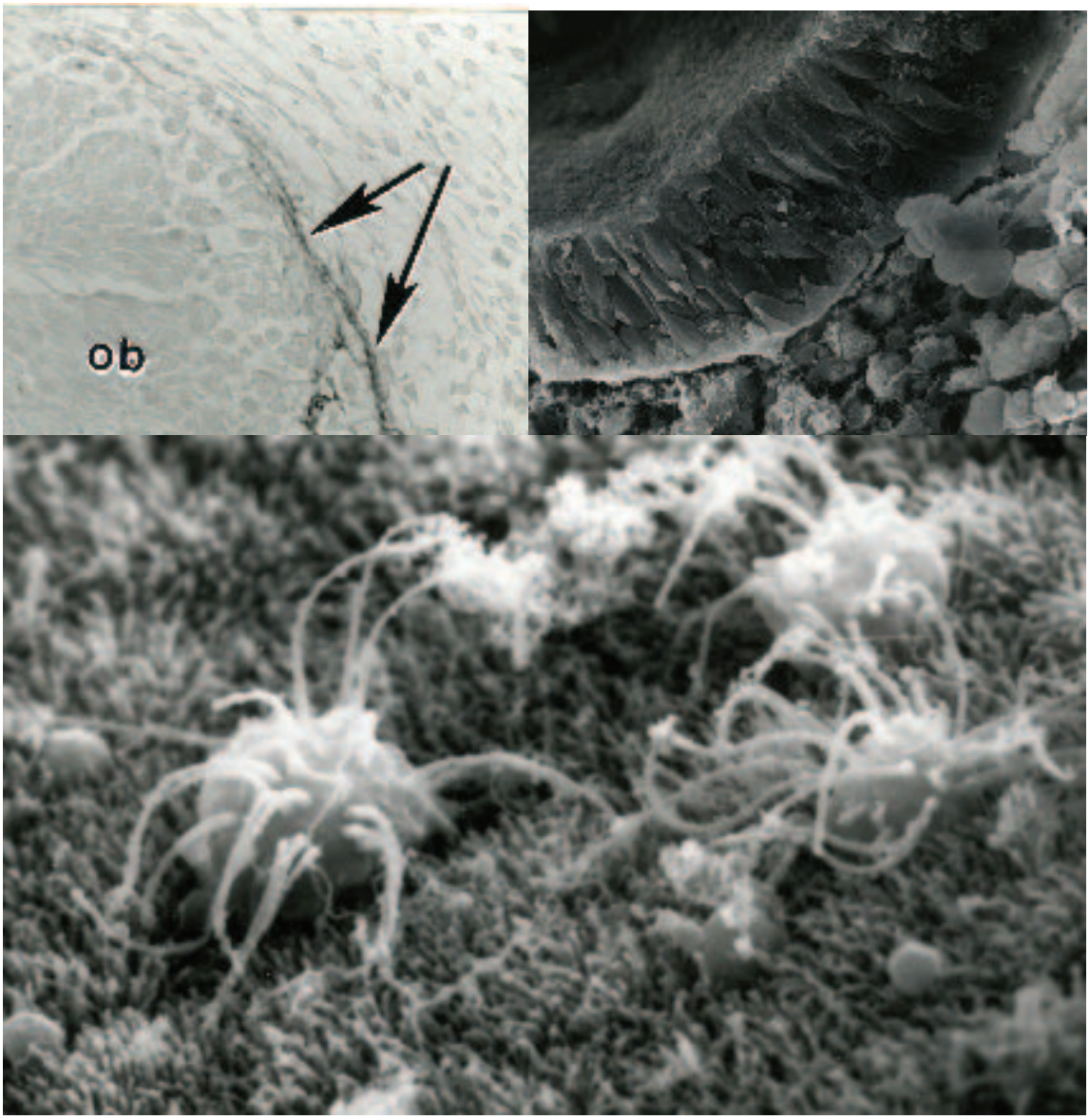

Fig. 5. (*Above left*). The presumptive olfactory bulb region (ob) shows a direct association with OMP-immunoreactive axons (arrows) originating from olfactory bipolar neurons within the olfactory epithelium of a twelve-day opossum embryo. LM X400. (*Above right*). A fractured region through differentiating olfactory epithelium gathered from the dorsal-medial region of the nasal cavity of an 11.5 day opossum embryo illustrates an absence of olfactory cilia at this time. SEM X 950. (*Below*). A region of olfactory epithelium from the medial wall of the nasal cavity but further rostral to the specimen shown at the above right illustrates developing olfactory knobs and olfactory cilia. The apices of surrounding sustentacular cells have numerous microvilli that carpet the adjacent surface of the olfactory epithelium. SEM X 15,000.

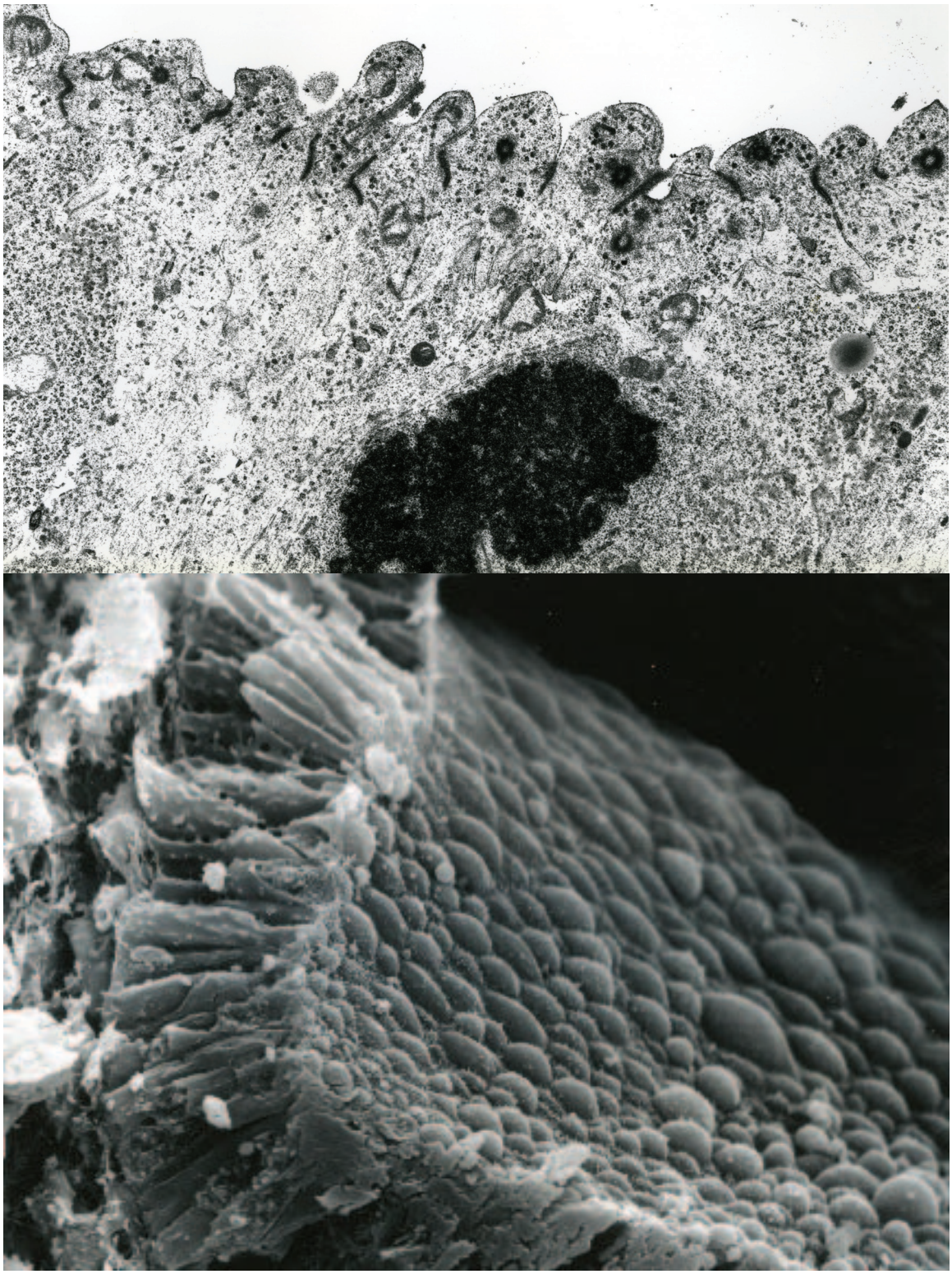

Fig. 6. (*Above*). A region of differentiating olfactory epithelium illustrates the apices of several dendritic processes of olfactory bipolar neurons. The developing olfactory knobs extend above the surface and contain centrioles and numerous fibrous granules. Apices of adjacent sustentacular also are observed. 11.5 day opossum embryo. TEM X 18,000. (*Below*). A micrograph illustrates a region of undifferentiated respiratory epithelium from the floor of the nasal cavity of an eleven-day opossum embryo. Cilia and microvilli are absent. SEM X 2,000.

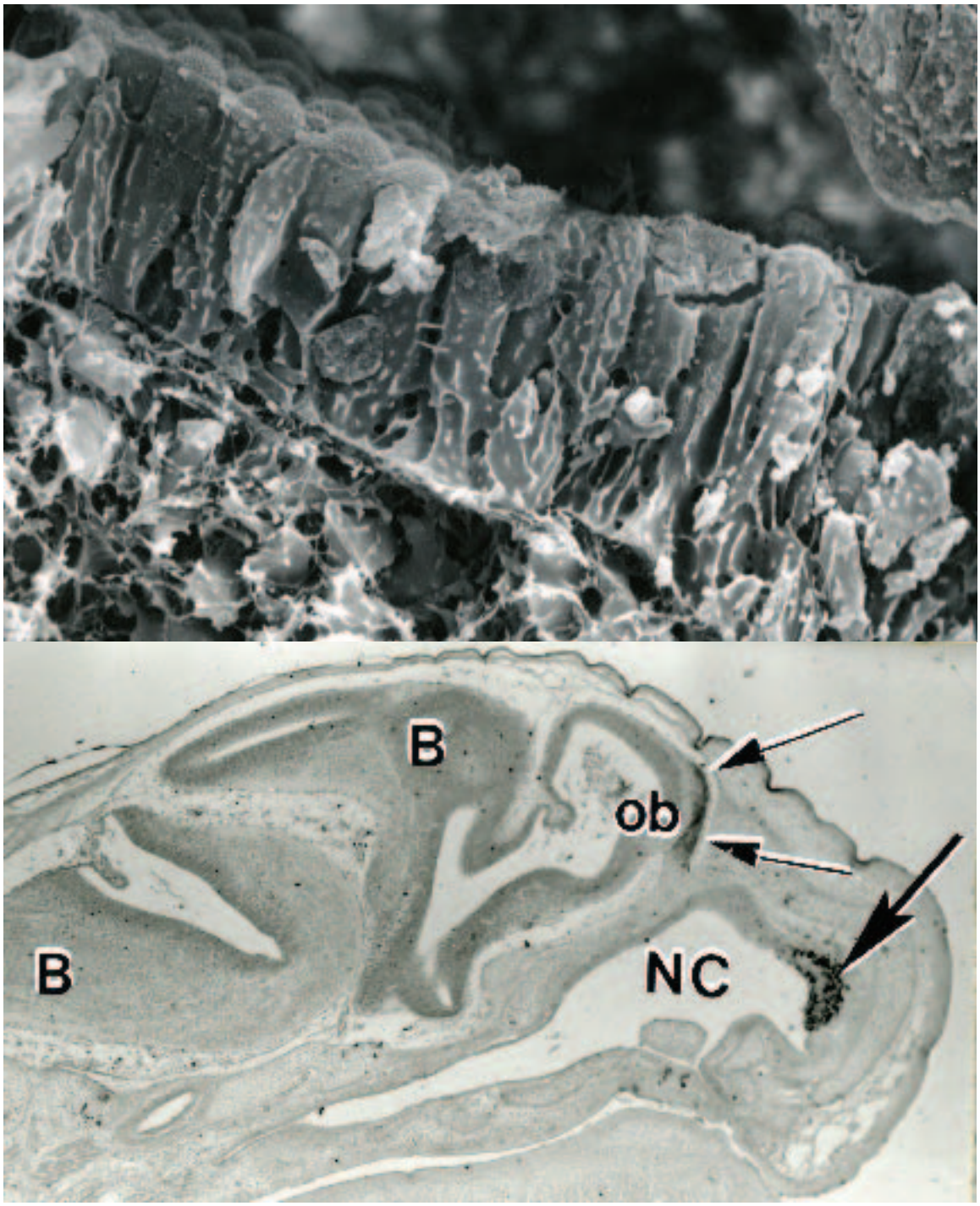

Fig. 7. (*Above*). Cell apices of differentiating respiratory epithelium from the nasal septum of an 11.5 day embryo are dome shaped and exhibit short microvilli. Lateral cell membranes of component cells have short microplicae that interdigitate with one another and the basal plasmalemma expands slightly to rest on a basement membrane supported by underlying mesenchymal cells. SEM X 2,500. (*Below*). A section through the head of a newborn opossum illustrates the continued relationship between the developing brain (B), the presumptive olfactory bulb (ob) area of the brain, OMP-positive axons (small arrows), and the intense concentration of OMP-positive olfactory bipolar neurons (large arrow) in the nasal cavity (NC) just inside the opening of the external nares. LM X 75.

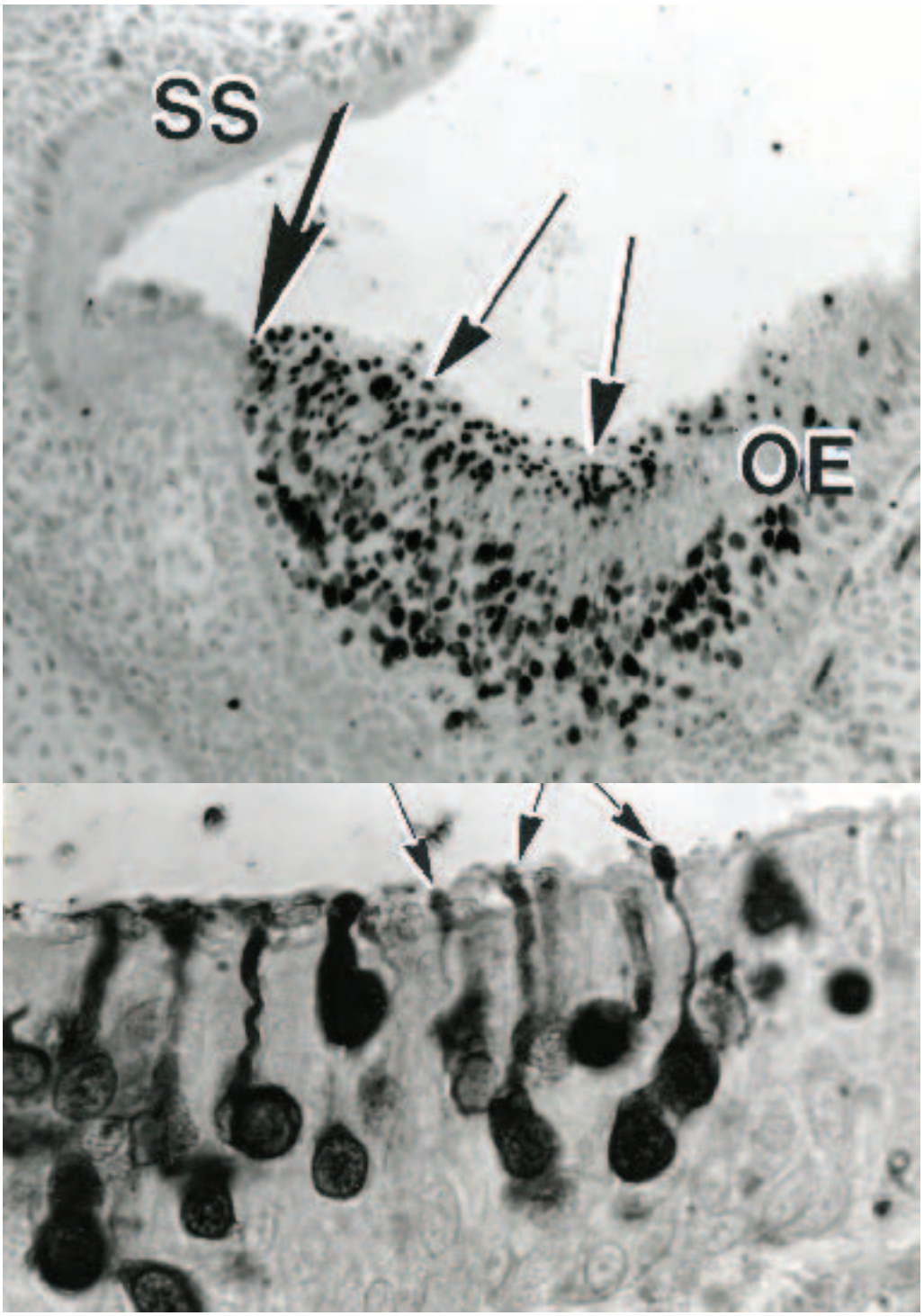

Fig. 8. (*Above*). A micrograph illustrates the abrupt junction (large arrow) between the stratified squamous epithelium (SS) lining the external nares and the olfactory epithelium (OE) of the nasal cavity. Note the abundance of olfactory knobs in this tangential section (small arrows). Newborn opossum. LM X 500. (*Below*). The bipolar neurons within the olfactory epithelium of the newborn opossum exhibit intense olfactory marker protein (OMP) immunoreactivity. Note the prominent dendritic processes terminating in olfactory knobs (arrows). LM X 1,200.

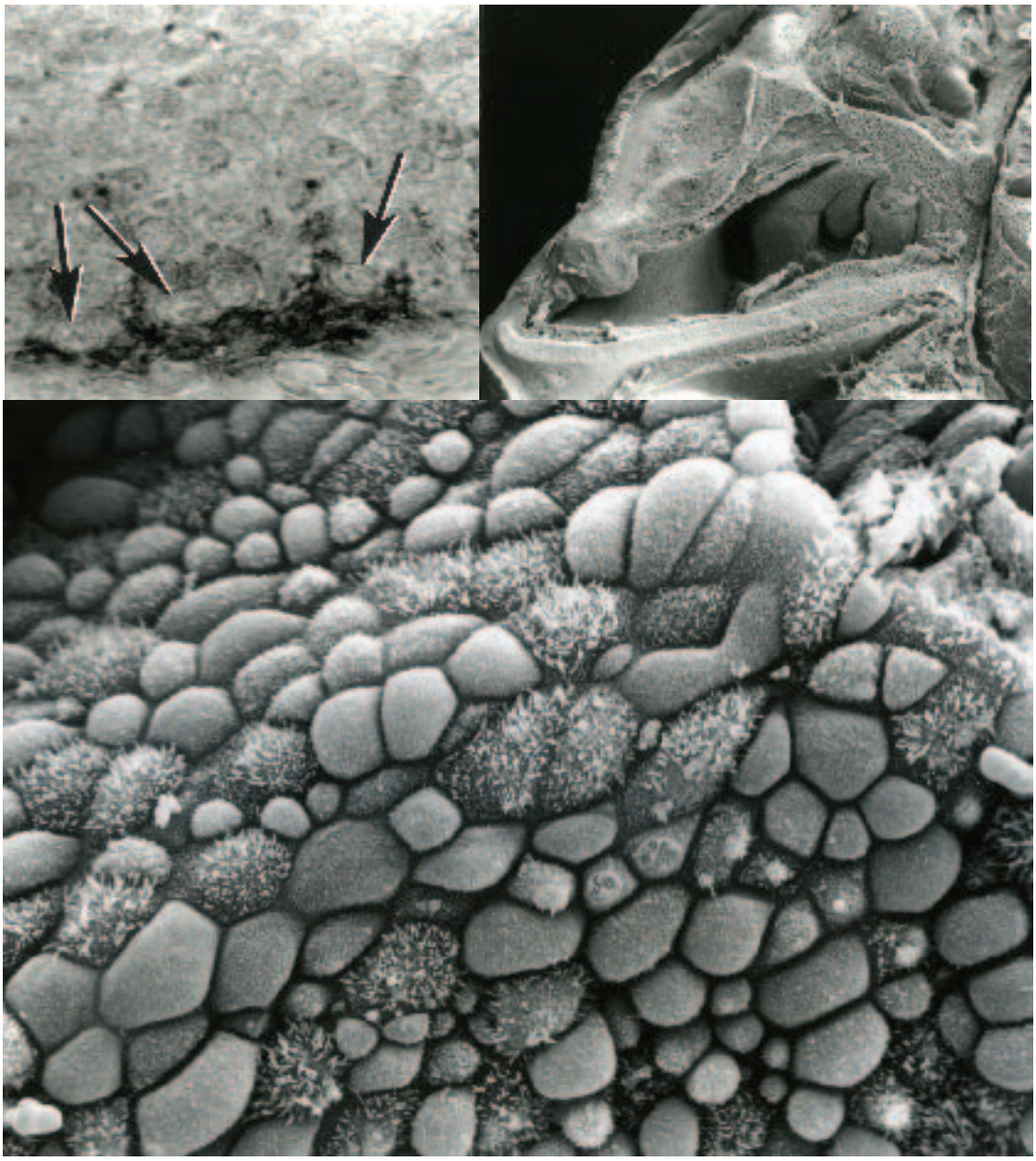

Fig. 9. (*Above left*). OMP-positive axons within the developing olfactory bulb of a newborn opossum show an increase in number as compared to embryonic stages. Note the close relationship between the large neurons (arrows) found in this region of the developing brain and the OMP-positive axons. LM X 600. (*Above right*). A fractured region of the newborn opossum snout illustrates the expansion of the external nares into the nasal cavity and the position of the developing turbinates. SEM X 45. (*Below*). Surface features of differentiating respiratory epithelium from the region covering the nasal turbinates illustrate several cell apices with developing respiratory cilia. Adjacent cell apices appear relatively smooth. Newborn opossum. SEM X 2,000.

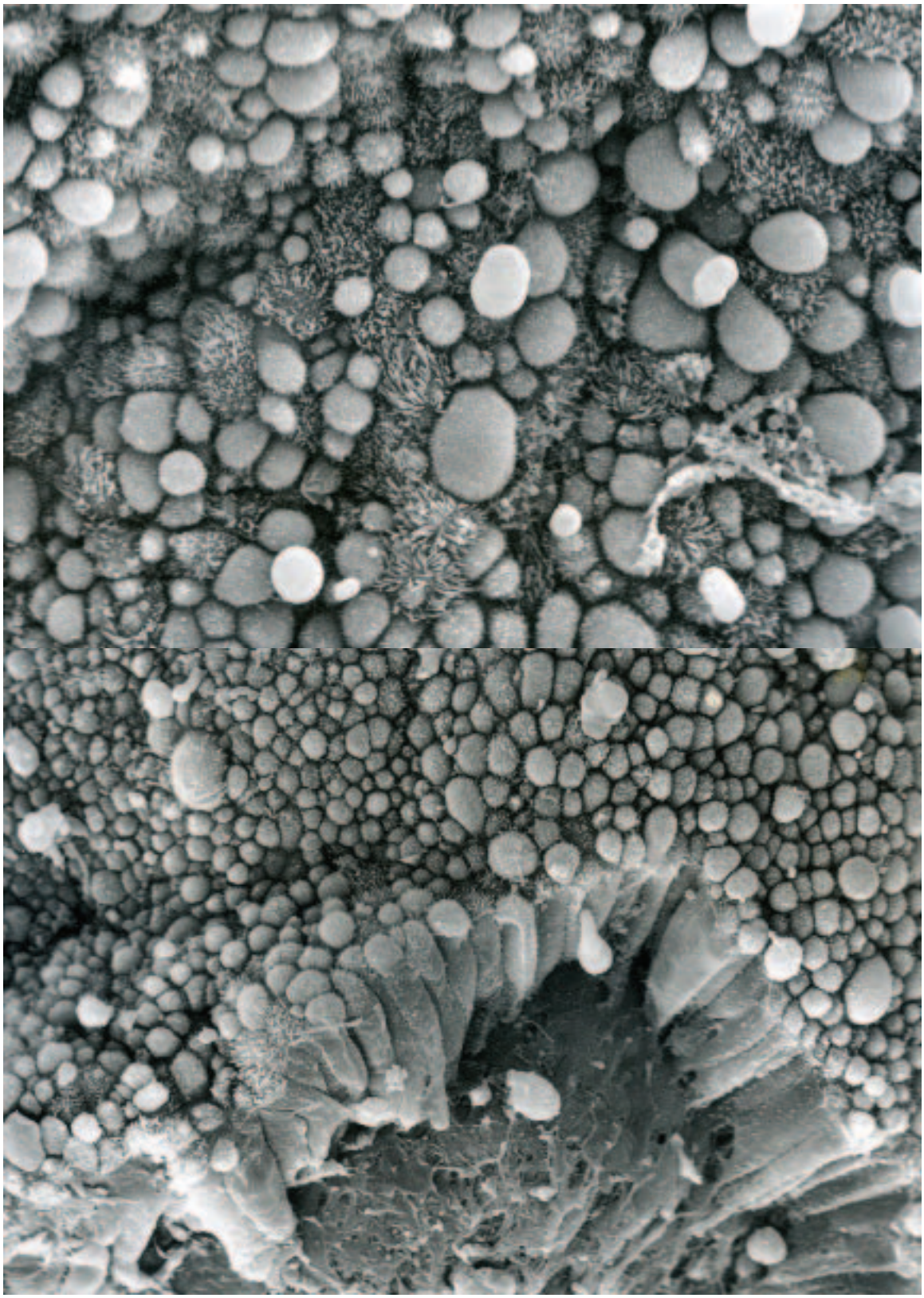

Fig. 10. (*Above*). Surface features of respiratory epithelium deep within the nasal cavity one week postnatal show continued differentiation as cilia continue to elongate. SEM X 2,000. (*Below*). A fractured preparation of differentiating respiratory epithelium from a more caudal region of the nasal cavity illustrates both surface and lateral features of component cells. Opossum one week postnatal. SEM X 2,000.

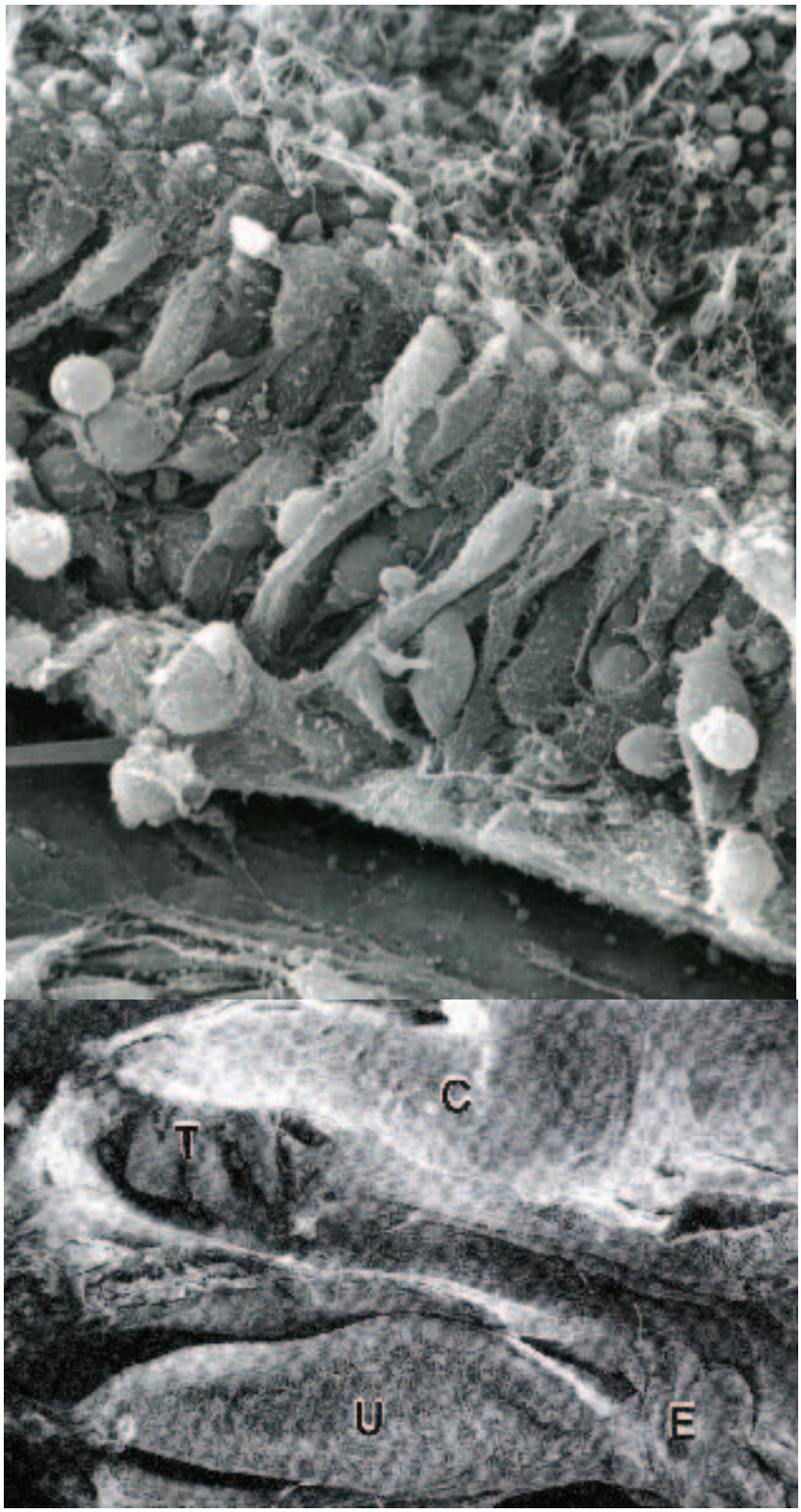

Fig. 11. (*Above*). A fractured region through the olfactory epithelium of an opossum one week postnatal illustrates its morphological features. Note the olfactory cilia, axons of the bipolar neurons, and basal cells. SEM X 2,000. (*Below*). The snout of a twelve-day opossum as seen in a mid-sagittal view illustrates the continued development of the turbinates (T), tongue (U), epiglottis (E) and the region of the cranial cavity (C) that contains the olfactory bulb. SEM X 25.

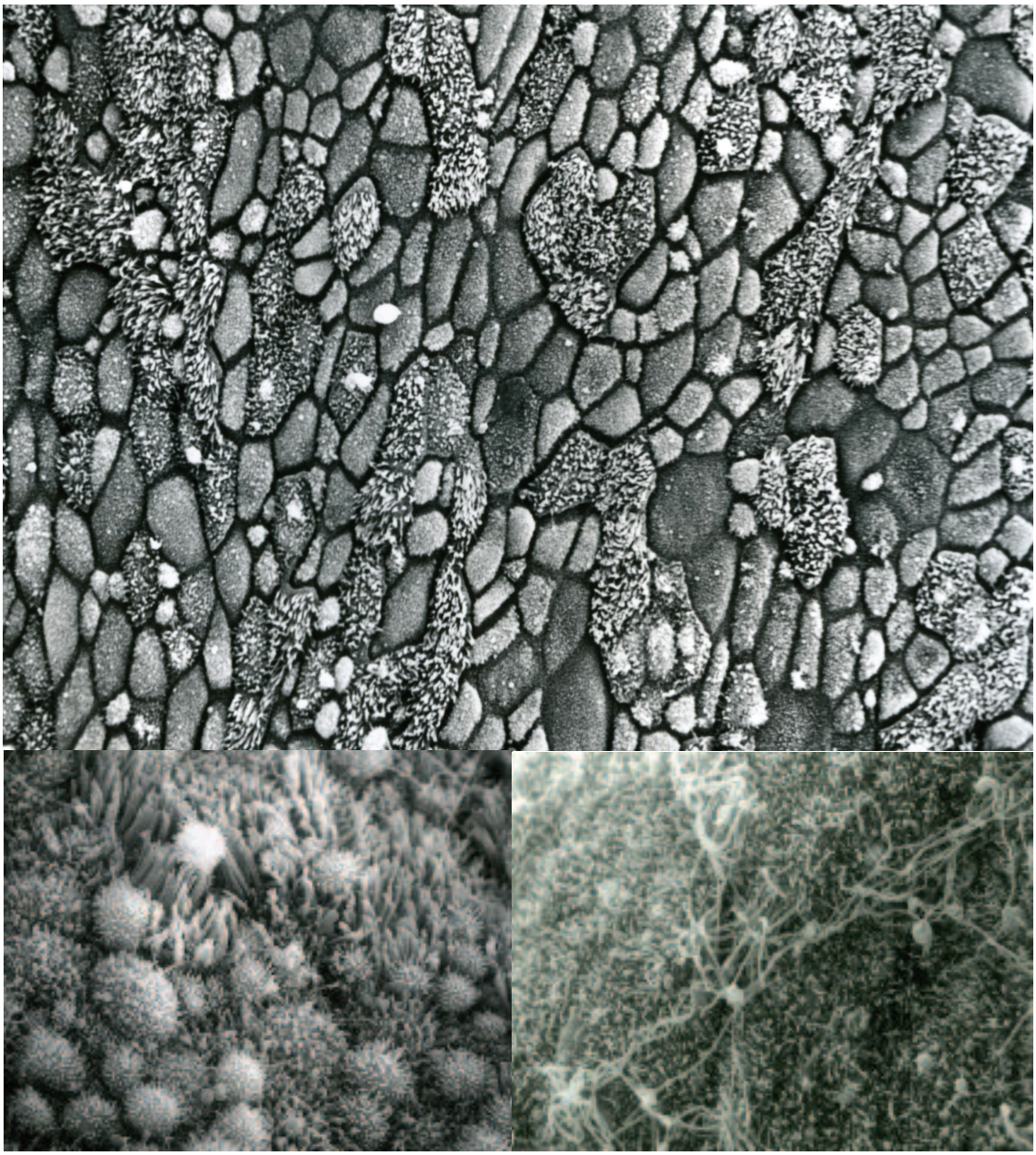

Fig. 12. (*Above*). The floor of the nasal cavity of a twelve-day-old opossum is lined by respiratory epithelium comprised of ciliated cells separated by small clusters of non-ciliated cells. SEM X 2,000. (*Below left*). A well-differentiated respiratory epithelium covers the exposed regions of turbinates of the opossum by the twelfth postnatal day. The majority of non-ciliated cells now exhibit short but well defined microvilli. SEM X 3,000. (*Below right*). The caudal region of the superior turbinate from the twelve-day-old opossum now exhibits scattered olfactory knobs and olfactory cilia. The latter lie upon a carpet of microvilli extending from underlying sustentacular cells. SEM X 3,000.

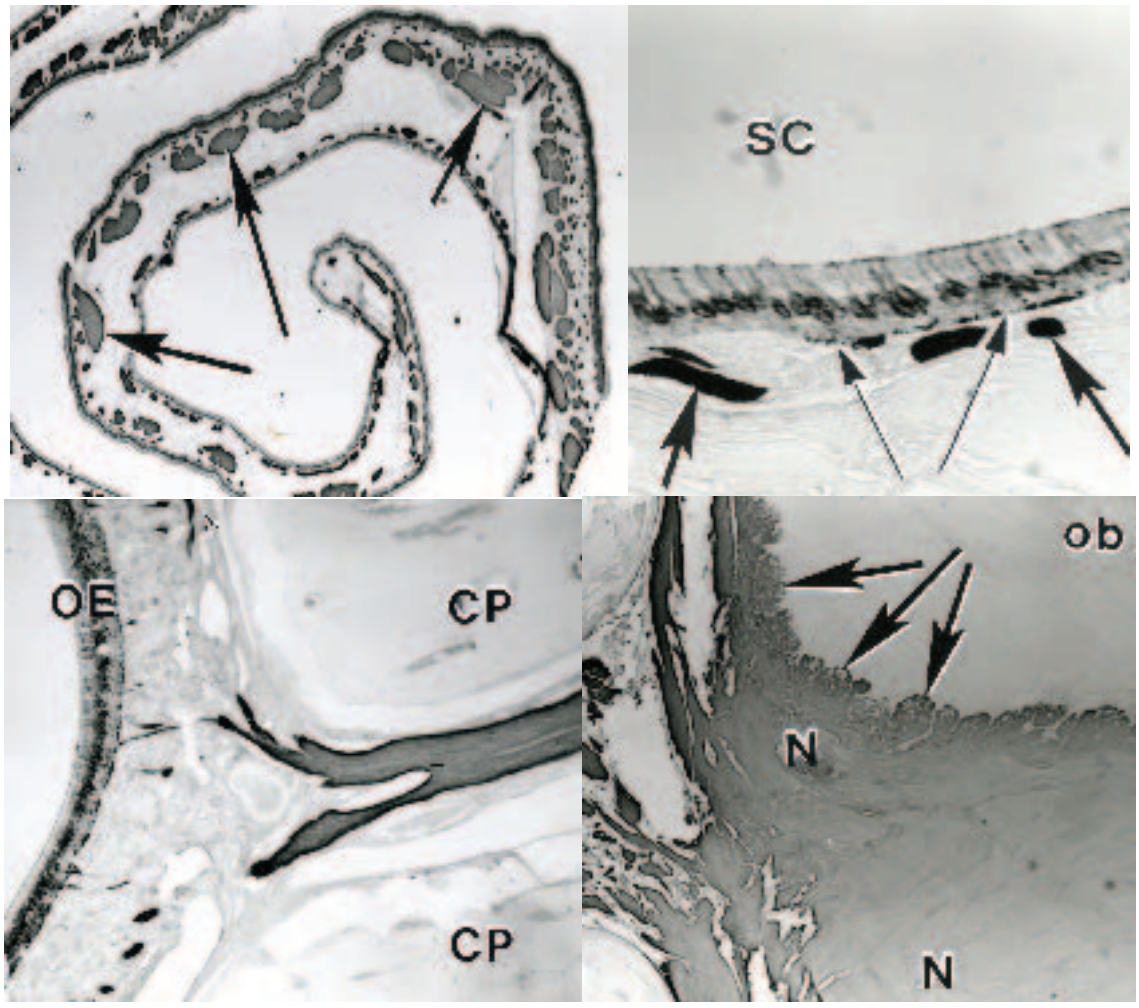

Fig. 13. (*Above left*). A transverse section through the superior conchae of an adult opossum demonstrates the intense olfactory masker protein (OMP) immunoreactivity in the axons comprising the fila olfactoria (arrows). LM X 8. (*Above right*). Increased magnification of the olfactory epithelium covering the superior conchae of an adult opossum illustrates numerous OMP positive bipolar neurons within the epithelium. Note the OMP positive axons (small arrows), dendrites, and fila olfactoria (large arrows). The lumen of the superior conchae (SC) is at the top of the photomicrograph. LM X 250. (*Below left*). A section through the roof of the nasal cavity of an adult opossum illustrates the relationship between olfactory epithelium (OE) and collections of OMP positive axons, fila olfactoria, and nerve bundles that pass through the cribriform plate (CP) of the ethmoid bone. LM X 100. (*Below right*). A section through the olfactory bulb (ob) of an adult opossum illustrates the enveloping thick layer of OMP positive nerve fibers (N) extending from the olfactory epithelium. Even at this low magnification numerous glomeruli (arrows) can be visualized within the olfactory bulb. LM X 6.

Chapter 15. Trachea and Lungs

Synopsis:

Anlagen of the opossum lungs begin as endodermal outpocketings from paired longitudinal branchial furrows in the nine-day opossum embryo. These paired dorsal-lateral structures move ventrally and by the eleventh prenatal day are united to the pharynx by a single, ventral tube, the provisional trachea. The lining epithelium of the larynx is derived from endoderm; the supporting wall of connective tissue, cartilage, and muscle is derived from mesoderm of the branchial arches. The epiglottis of the opossum becomes intranarial with continued development projecting into the posterior nares. It is positioned so that milk can pass around it on either side during nursing without interrupting breathing. The intranarial epiglottis persists into adulthood.

Each lung bud elongates to form a stem bronchus from which secondary bronchial buds arise during the remainder of the prenatal period. Mesoderm surrounding the expanding lung forms the visceral and parietal pleura. At birth the lung consists primarily of the conducting portion of the respiratory system. This system of simple, branching airways ends in a number of large terminal respiratory chambers. These chambers are lined by a thin, attenuated squamous epithelium within which are scattered cuboidal cells. The squamous cells are type I pneumocytes; the cuboidal cells are type II pneumocytes. The cytoplasm of the latter is characterized by lamellated (surfactant containing) bodies. Mesenchymal cells form the chamber wall and with delicate reticular fibers support a well-established capillary bed. Nearer the bronchi the chamber wall often contains differentiating smooth muscle cells. Thus, the large respiratory chambers constitute large expansions of the conducting portion of the lung that are modified for gaseous exchange. The trachea and bronchi of the newborn are lined by a non-ciliated columnar epithelium that lacks goblet cells. The bronchial epithelium immediately adjacent to the large chambers assumes a cuboidal appearance and it is at this location where most mitotic activity is observed.

Ciliated cells appear scattered throughout the epithelial lining of the trachea and bronchi by the end of first postnatal week and the respiratory chambers continue to make up a major portion of the lung at this time. The conducting portion of the lung increases in complexity by the end of the second week postnatal and a distinct band of smooth muscle is present beneath the bronchial mucosa, which now begins to show some folding. The large respiratory chambers continue to be present but are observed chiefly in the peripheral areas of the lung. The terminal respiratory chambers are in a constant state of change as they eventually become incorporated into the expanding bronchial system. By the end of the third postnatal week there is a marked increase in the cellularity of the lung stroma, the bronchial system has increased in complexity, and the terminal respiratory chambers appear more irregular in outline. The initial nine weeks of organogenesis in the respiratory system emphasizes the development and expansion of the conducting portion of the lung. The large terminal respiratory chambers lined by respiratory epithelium represent those portions of the conducting system that are modified for gaseous exchange during this period of development. As lung development continues, the regions of the terminal respiratory chambers immediately adjacent to established bronchi differentiate and become incorporated into the expanding bronchial tree. Simultaneously, new regions of the terminal chambers expand at the distal extremes of this system to form new areas for gaseous exchange. The continuous process of bronchial tree expansion and formation of peripheral

respiratory chambers continues until well into the twelfth week of postnatal life. The differentiation of bronchioles from the large terminal respiratory chambers involves two major events. Initially, the type I and type II pneumocytes lining the proximal regions of the terminal respiratory chambers are replaced by a simple cuboidal epithelium. This epithelium differentiates from those portions of the terminal chamber that immediately transition into the bronchial tree and it is this region of the epithelium where mitotic activity is highest. Secondly, as these changes occur, smooth muscle cells differentiate from mesenchymal cells within the respiratory chamber wall to initially establish bronchial musculature. In some instances the establishment of smooth muscle cells from mesenchyme in the respiratory chamber wall may precede the differentiation of bronchial epithelium, as scattered smooth muscle cells can found in regions of the respiratory chambers lined by type I and type II pneumocytes. True alveoli do not form a significant portion of the opossum lung until after the twelfth postnatal week when young begin to leave the pouch for brief periods of time. Although alveoli are initially observed by about the seventh postnatal week, their most rapid development is after the twelfth postnatal week. Neuroepithelial bodies are present in the conducting portion of the opossum lung by the fourth postnatal week. What substances they produce and what role they play in the organogenesis of the respiratory system is unknown.

With the appearance of alveoli, submucosal glands develop both within the trachea and bronchi. Bronchial glands initially develop from the bronchial epithelium lining the bottoms of bronchial folds. The ductal system of the tracheal and bronchial glands shows considerable development by twelfth postnatal week and in juvenile opossums extends beyond the bronchial musculature into the submucosa. The forming secretory tubules of the tracheal glands consist of mucous cells and clumps of serous cells. The bronchial glands consist of mucous tubules that are capped with an unusual type of serous cell referred to as a hydropic cell. Myoepithelial cells differentiate around the forming secretory units of the glands. Goblet cells do not appear in significant numbers within the lining epithelium of the conducting portion of the lung until after weaning. The large number of goblet cells appears restricted in distribution to the ducts of the tracheal glands and to the depths of the bronchial folds. A lamina of collagen and elastin forms subjacent to the visceral pleural mesothelium early in development and shows continued growth throughout the postnatal period into adulthood.

Acknowledgments:

Figs.1 (bottom right), 2 (top left), 6 (top), 7, 10 (bottom), 13 (top), courtesy of and from: Krause, W.J. and C.R. Leeson (1973) The postnatal development of the respiratory system of the opossum. I. Light and scanning electron microscopy. Am. J. Anat. 137:337-356.

Figs. 1 (bottom left), 6 (center and bottom), 11 (bottom), 12 (top), courtesy of and from: Krause, W.J. and C.R. Leeson (1975) The postnatal development of the respiratory system of the opossum. II. Electron microscopy of the epithelium and pleura. Acta Anat. 92:28-44.

Figs. 3 (top), 4, 5 (top), courtesy of and from: Krause, W.J., J.H. Cutts and C.R. Leeson (1976) Type II pulmonary epithelial cells of the newborn opossum lung. Am. J. Anat. 46:181-188.

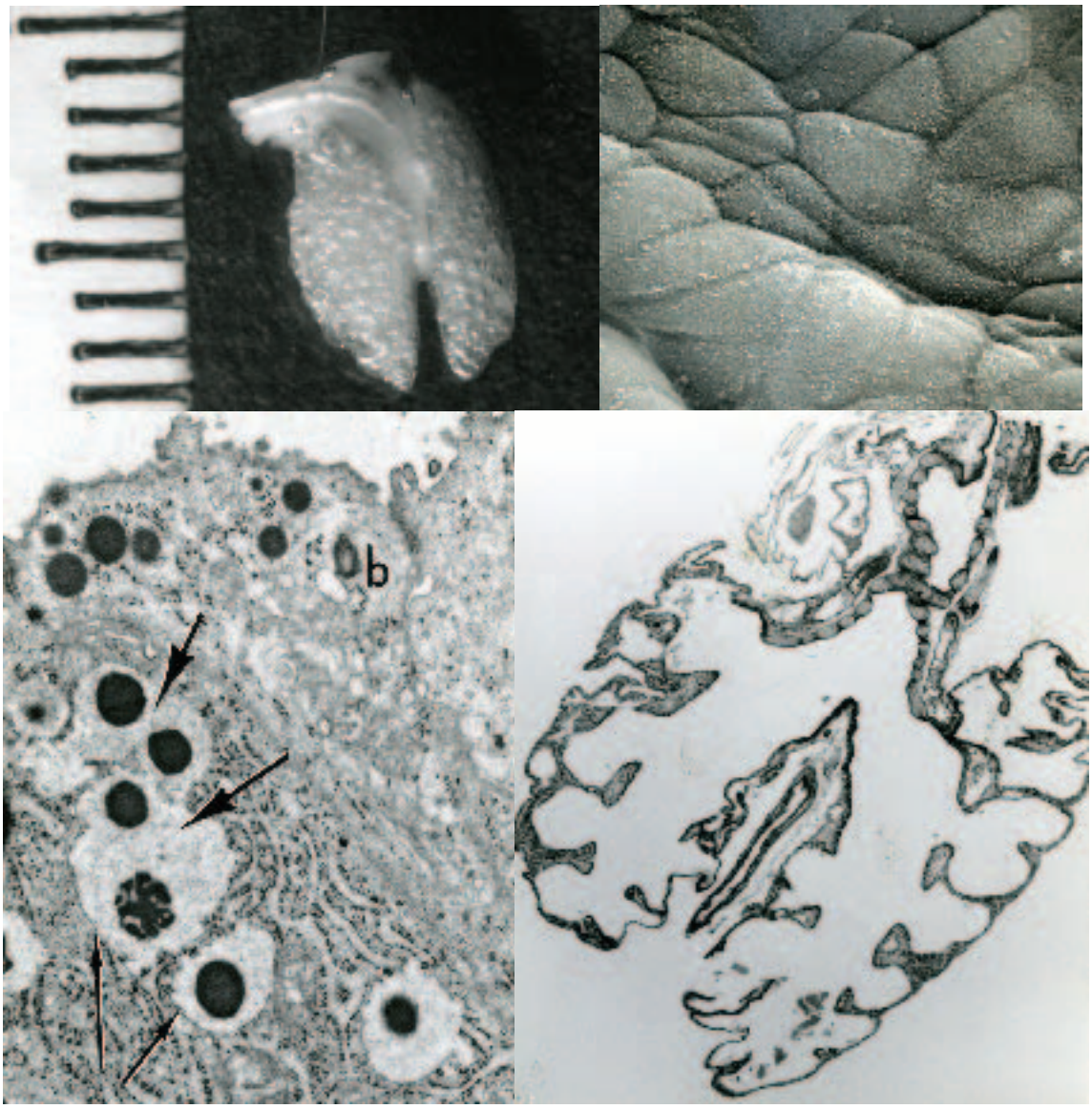

Fig. 1. (*Above left*). Terminal respiratory chambers appear as clear bubbles within newborn opossum lungs. X10. (*Above right).* A micrograph illustrates surface features of the epithelial lining of a newborn opossum trachea. Boundaries of individual epithelial lining cells are apparent. Ciliated cells are absent. SEM X 800. (*Below left*). The apical region of two adjacent epithelial cells lining the newborn trachea exhibit secretory granules that appear to be at different stages of maturation. Those located nearest the supranuclear region contain an electron-dense core surrounded by a halo of flocculent material. These granules are bound by a membrane (small arrows) and tend to coalesce into irregularly shaped complexes (large arrows). Mature, small, dense granules lie in the cytoplasm just beneath the apical plasmalemma. A basal body (b) also is observed. TEM X 12,000. (*Below right*). A section through the trachea of the newborn opossum as it divides into the primary bronchi. Note that the large terminal respiratory chambers open directly into the primary bronchi. LM X 35.

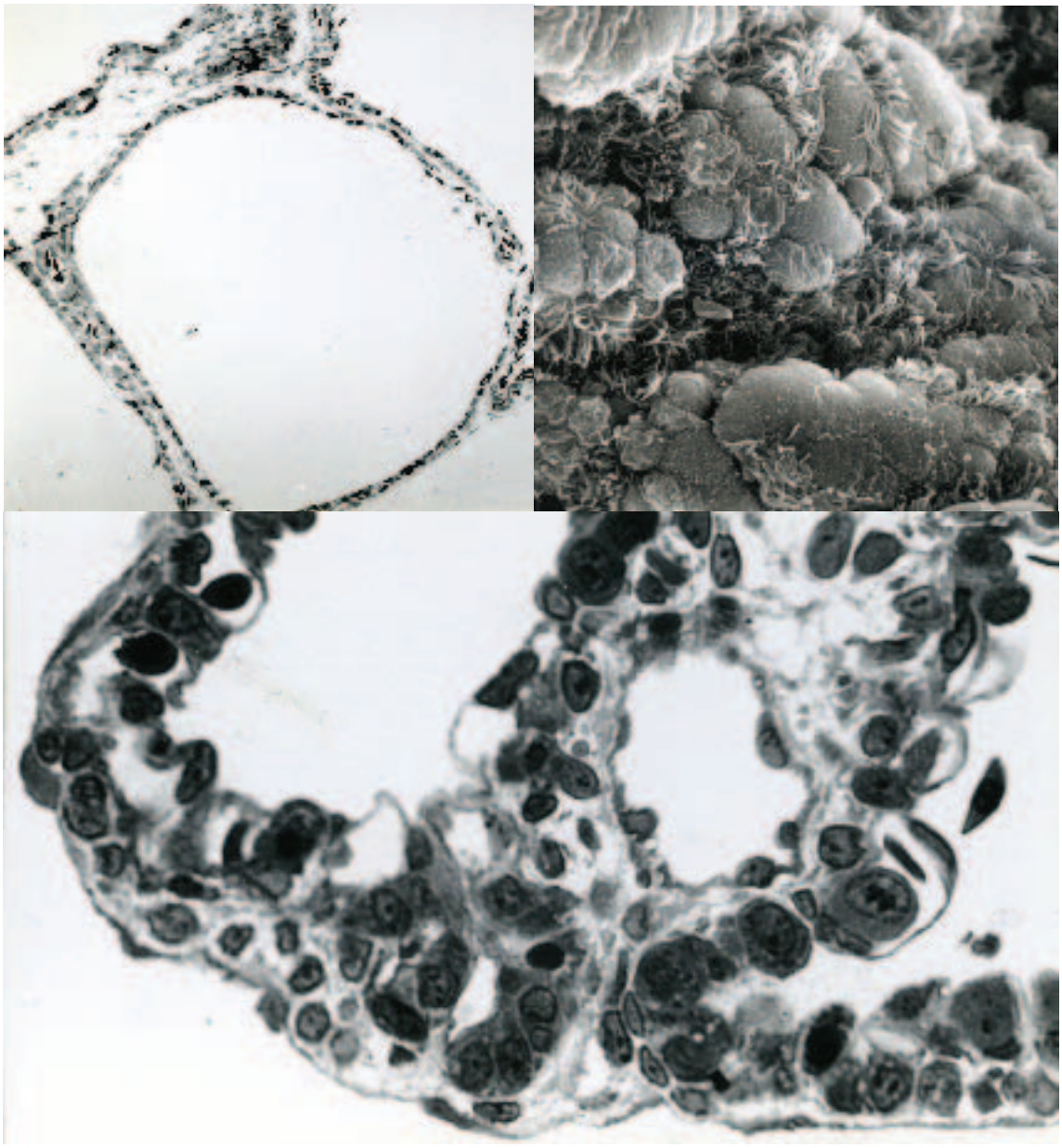

Fig. 2. (*Above left*). A capillary network lies under the epithelial lining of a terminal respiratory chamber from a newborn opossum lung. LM X 100. (*Above right*). The bronchial epithelium of an opossum four days postnatal contains groups of ciliated cells scattered between groups of non-ciliated cells. SEM X 2,000. (*Below*). The periphery of the lung illustrates the covering visceral pleural layer of mesothelium and portions of two large terminal respiratory chambers. Note the delicate stroma of the lung tissue and the network of capillaries underlying the epithelial lining of the respiratory chambers. The epithelial lining of the large terminal respiratory chambers consists of both squamous (type I pneumocytes) and cuboidal (type II pneumocytes) cells. Newborn opossum. LM X 500.

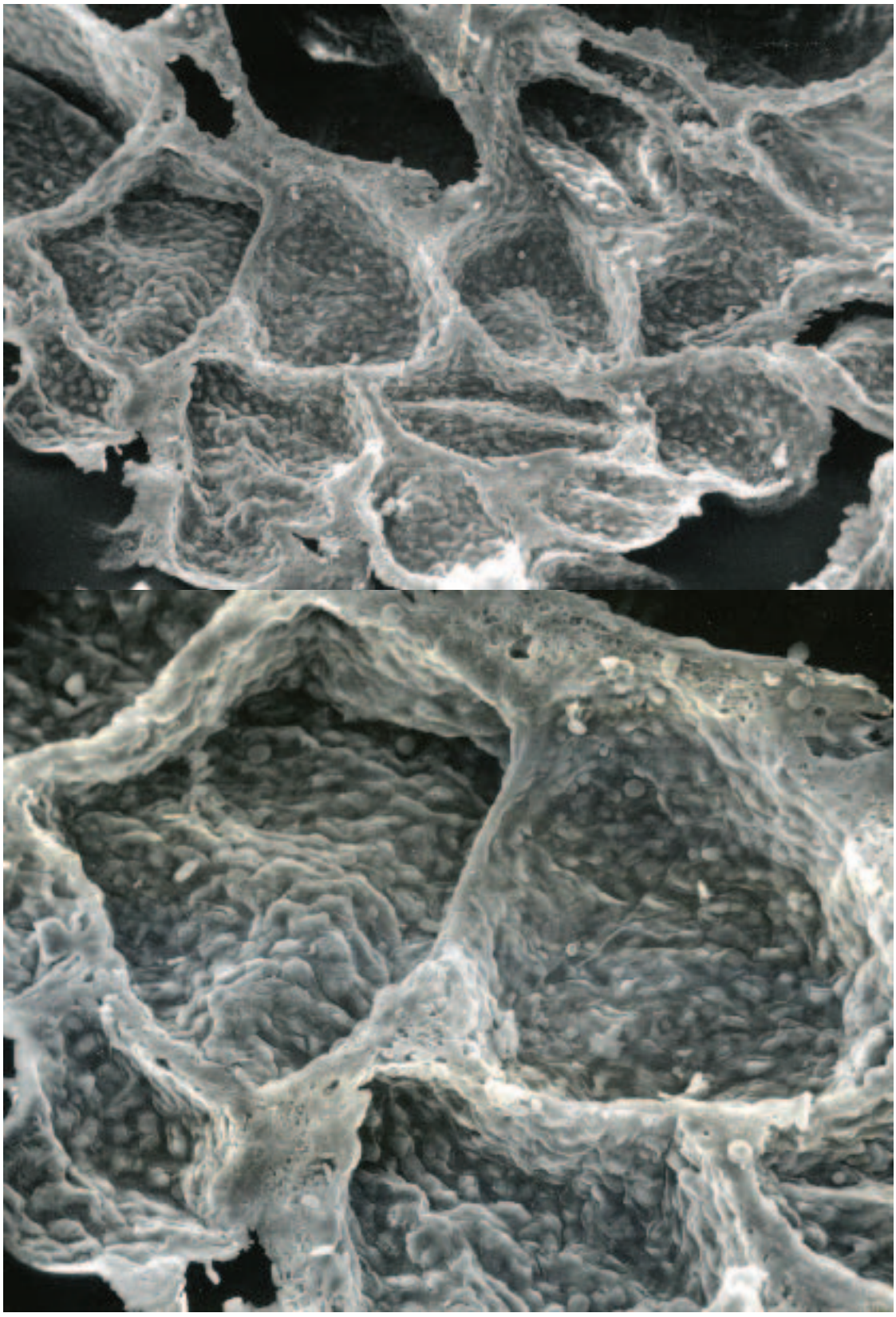

Fig. 3. (*Above*). The interior (epithelial) surface of the right lung illustrates the peripheral portions of several large terminal respiratory chambers. A major bronchus is shown at the top of the figure. Newborn opossum. SEM X 200. (*Below*). The epithelial lining of four terminal respiratory chambers as viewed from the interior. Newborn opossum. SEM X 400.

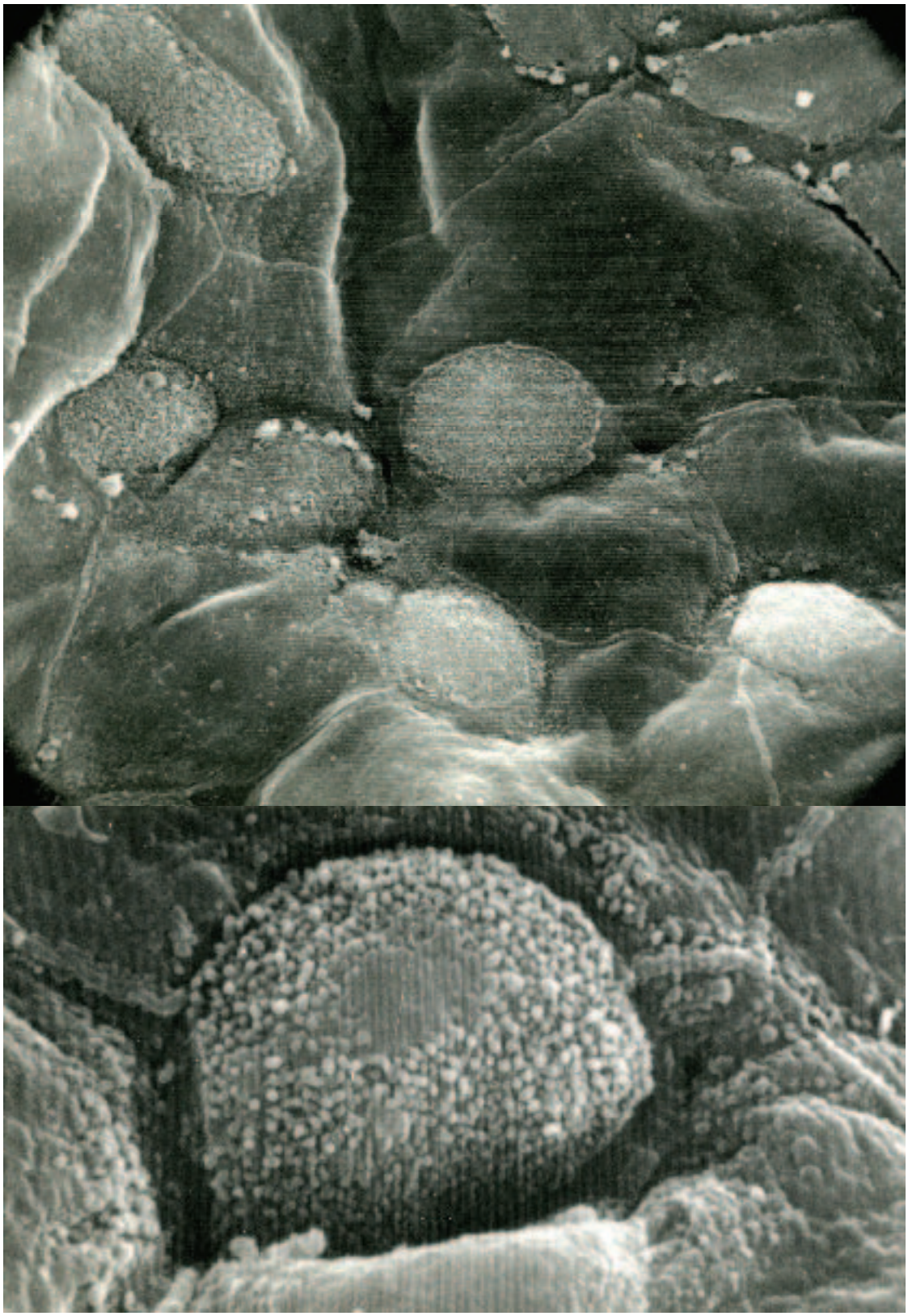

Fig. 4. (*Above*). The epithelial lining of a terminal respiratory chamber consist of type I pneumocytes identified by their smooth surface and type II pneumocytes characterized by round apices covered by numerous, stubby microvilli. Note the distinct cell boundaries between individual cells. Newborn opossum. SEM X 4,000. (*Below*). A micrograph illustrates the apex of a type II pneumocyte. SEM X 10,000.

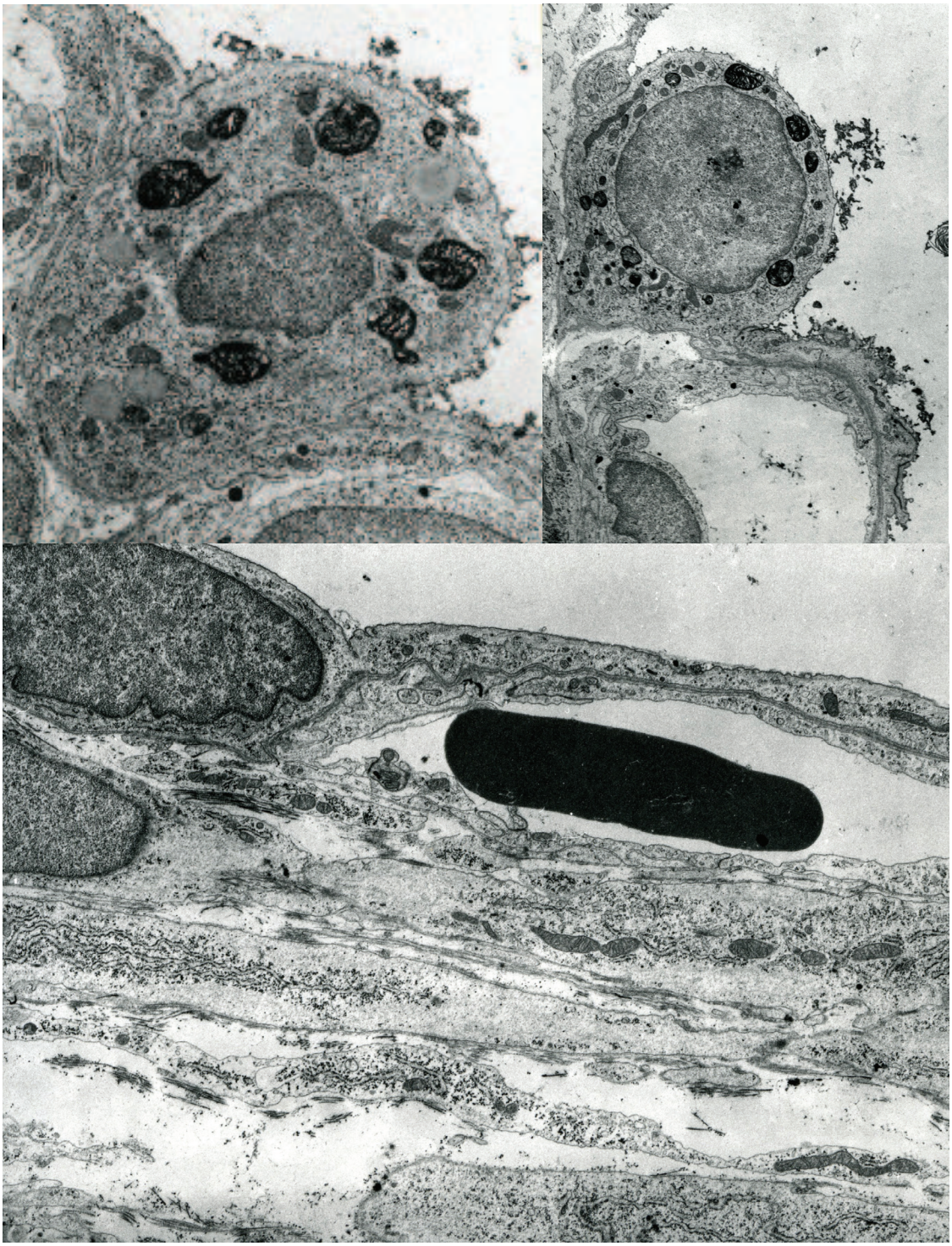

Fig. 5. (*Above left*). A micrograph illustrates a type II pneumocyte, from a terminal respiratory chamber of a newborn opossum, characterized by a roughly cuboidal shape and several osmiophilic lamellae (myelin bodies). Scattered lipid droplets also are observed within the cytoplasm. TEM X 4.500. (*Above right*). A type II and type I pneumocyte (overlying the endothelial cell of a capillary) lining a terminal respiratory chamber of a newborn opossum lung. TEM X 3,000. (*Below*). A portion of a type I pneumocyte observed near its nuclear profile covers an endothelial cell of an underlying capillary. The latter contains an erythrocyte. Note the fused basal laminae between the two epithelial cell types. Terminal respiratory chamber of a newborn opossum. TEM X 5,000.

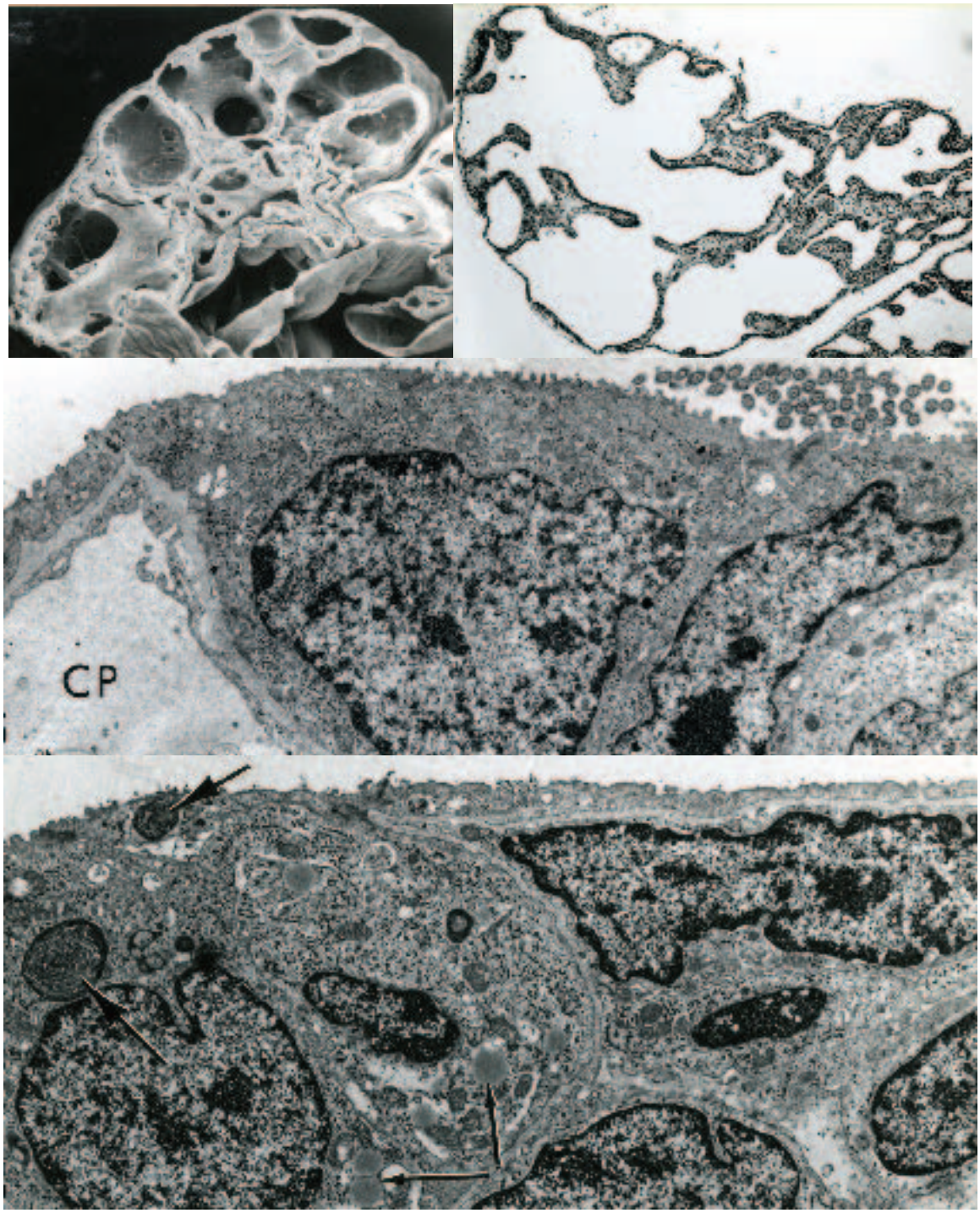

Fig. 6. (*Above left*). The interior of a week old opossum lung continues to exhibit terminal respiratory chambers two of which communicate with a major bronchus as it enters at mid-center. SEM X 45. (*Above right*). A section of week old lung illustrates a major bronchus centrally communicating with peripheral respiratory chambers. LM X 40. (*Center*). A micrograph illustrates the point of transition between bronchiolar epithelium (right) and the epithelial lining of a respiratory chamber (left). Note the capillary (CP) within the chamber wall. Opossum one week postnatal. TEM X 6,000. (*Bottom*). A type II pneumocyte contains lamellated bodies (large arrows) and lipid droplets (small arrows) lining a respiratory chamber of an opossum one week after birth. A portion of an attenuated type I pneumocyte covering three mesenchymal cells can be seen at the right. TEM X 6,000.

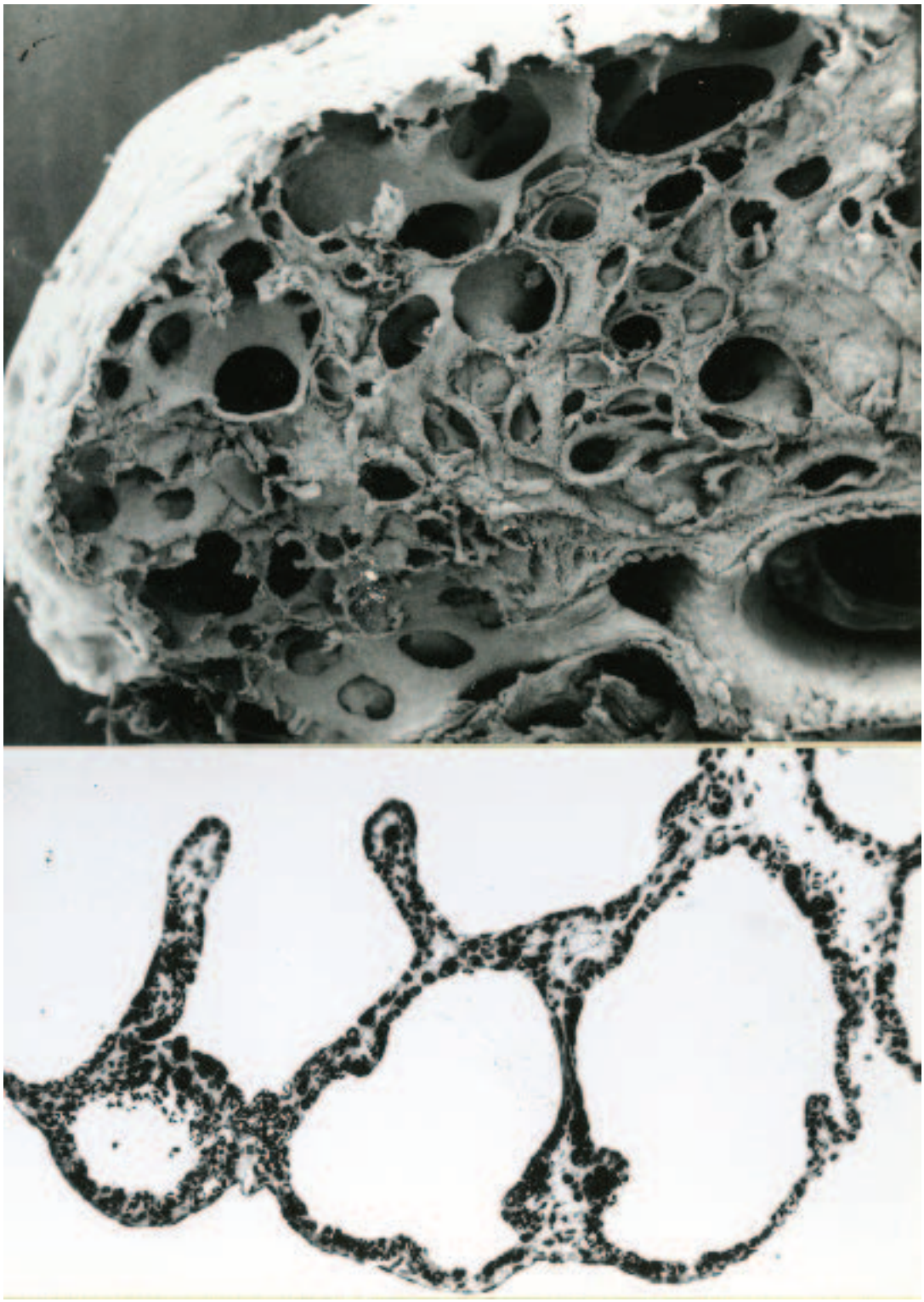

Fig. 7. (*Above*). At two weeks of age the bronchial system has expanded markedly. At the lower right note the continuity of epithelium from the primary bronchus to the secondary bronchus to what will become bronchioles (the proximal portions of the respiratory chamber walls). The large terminal respiratory chambers remain at the periphery of the developing lung. SEM X 75. (*Below*). Terminal respiratory chambers at the periphery of a lung from an opossum two weeks postnatal. Note the differentiating smooth muscle cells seen between two chambers near the center of the field. These regions of the respiratory chambers are destined to differentiate and become incorporated into the conducting portion of the lung. LM X 200.

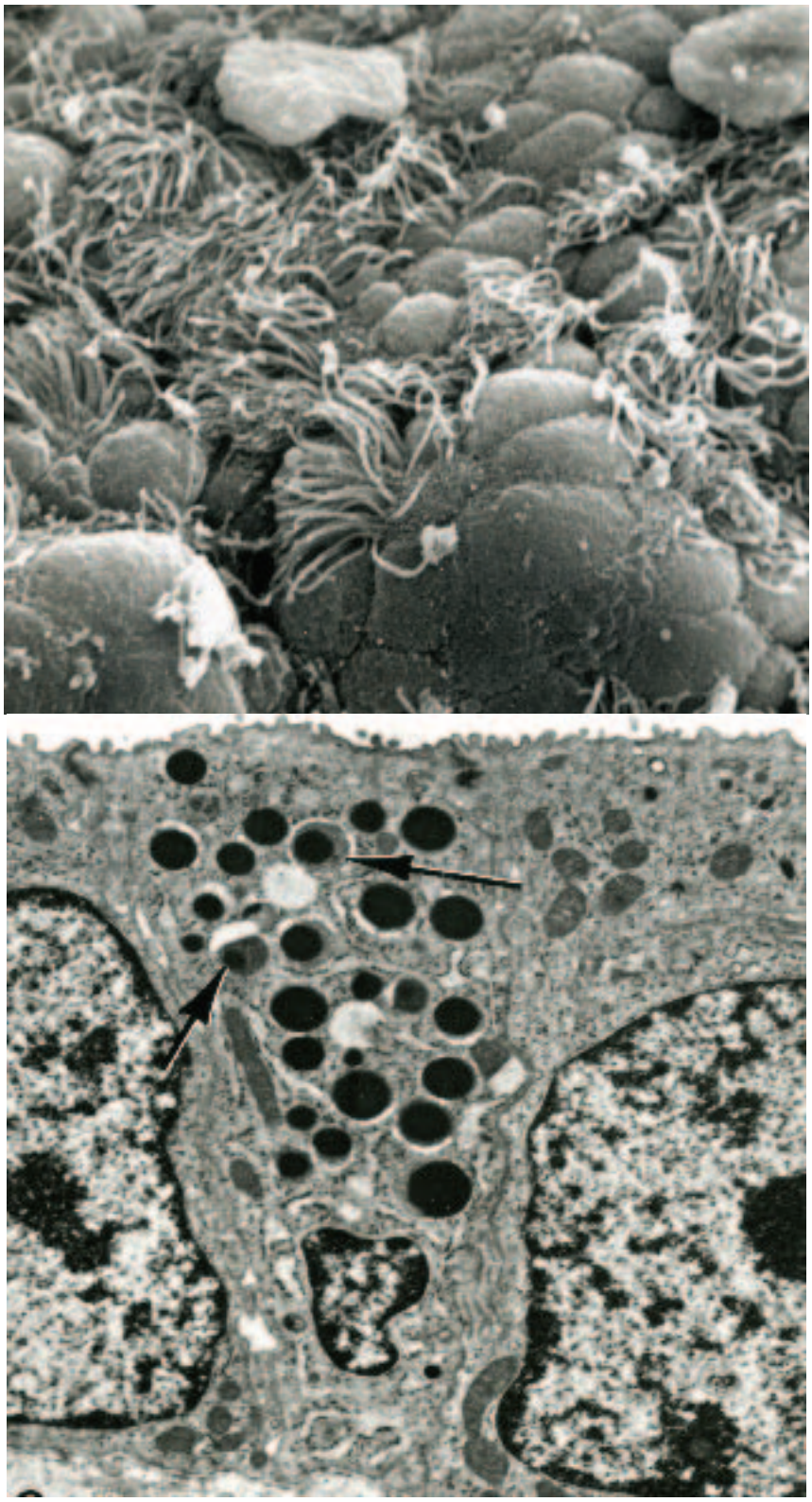

Fig. 8. (*Above*). A micrograph illustrates surface features of the epithelium lining the bronchial tree of an opossum two weeks postnatal. Note the continued differentiation of ciliated cells. SEM X 3,000. (*Below*). Three non-ciliated cells line, in part, the trachea of an opossum three weeks postnatal. The central cell contains numerous electron-dense granules, a few of which are enveloped by halo of light-staining amorphous material (arrows). TEM X 10,000.

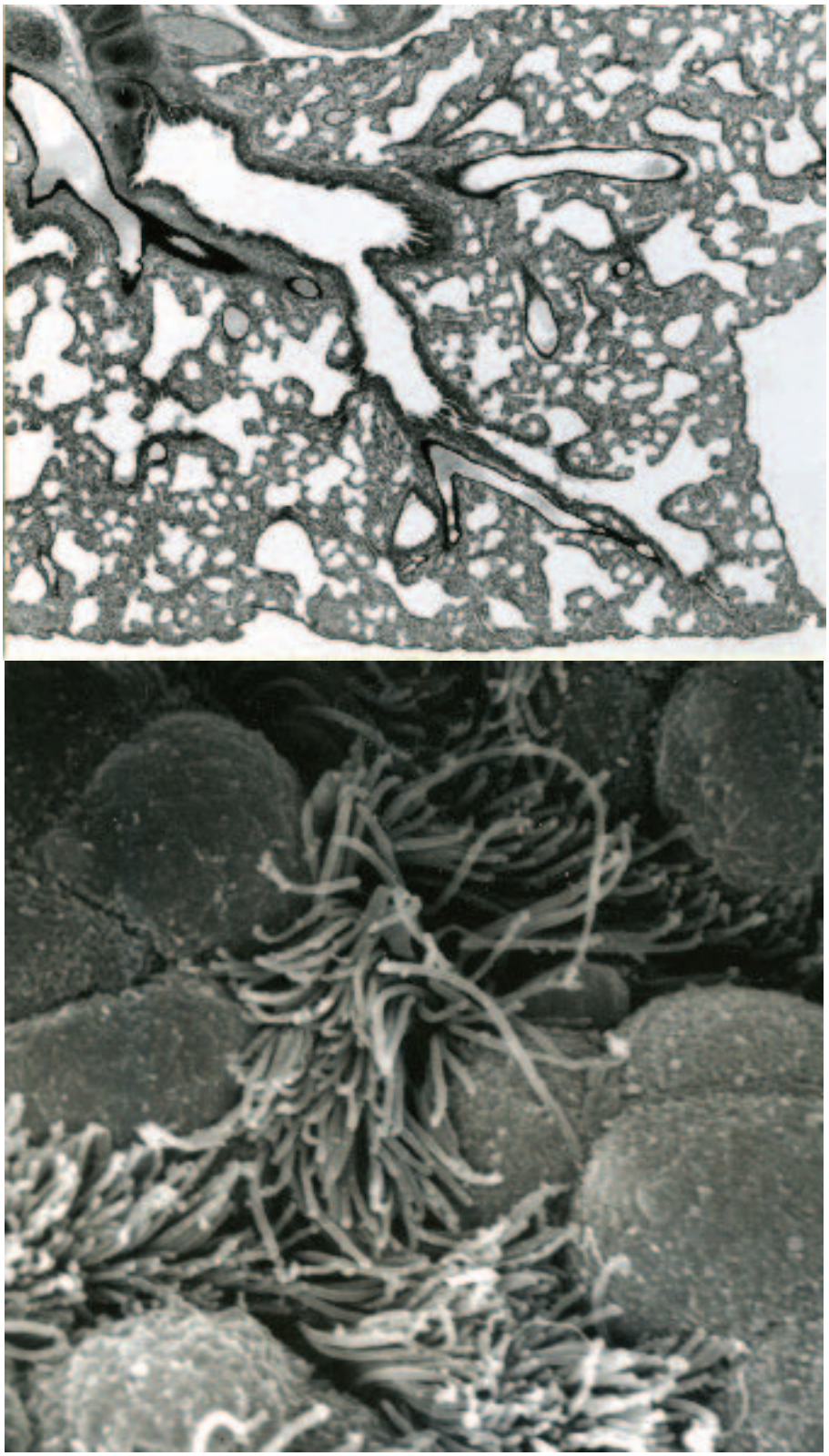

Fig. 9. (*Above*). The lung of an opossum three weeks postnatal shows an increase in cellularity. A primary bronchus enters at the upper left and courses to the lower right to ultimately terminate in terminal respiratory chambers. LM X 50. (*Below*). Surface features of ciliated and non-ciliated cells from an established bronchus of an opossum three weeks postnatal. SEM X 9,000.

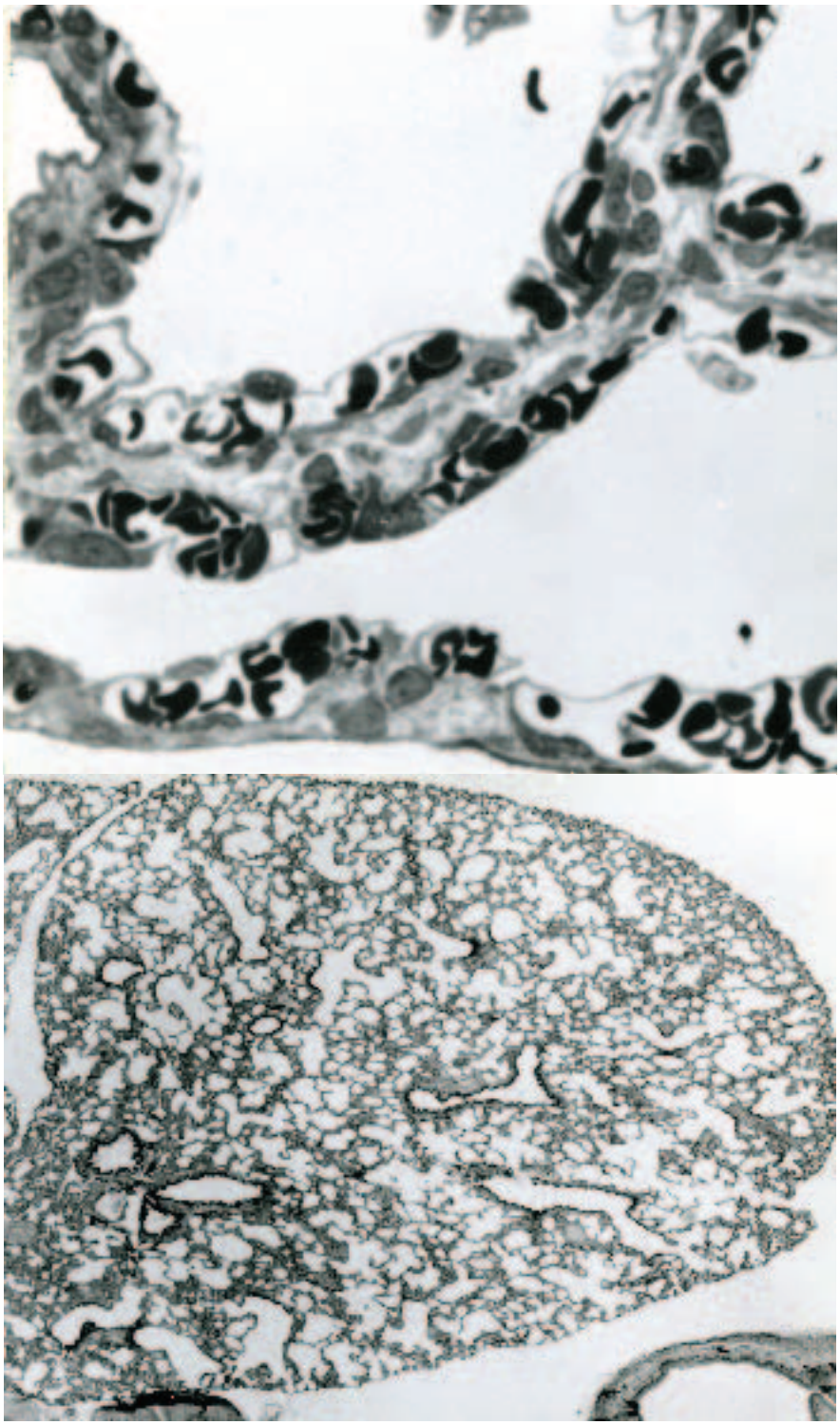

Fig. 10. (*Above*). A micrograph illustrates portions of two terminal respiratory chambers adjacent to the pleura (bottom of photomicrograph) of an opossum three weeks postnatal. A well-established capillary bed continues to underlie the respiratory epithelium. LM X 600. (*Below*). The cranial half of a lung from a six-week-old opossum exhibits primitive alveoli differentiating in the parenchyma. Bronchi remain a dominant feature at this stage of organogenesis being concentrated toward the hilum. LM X 25.

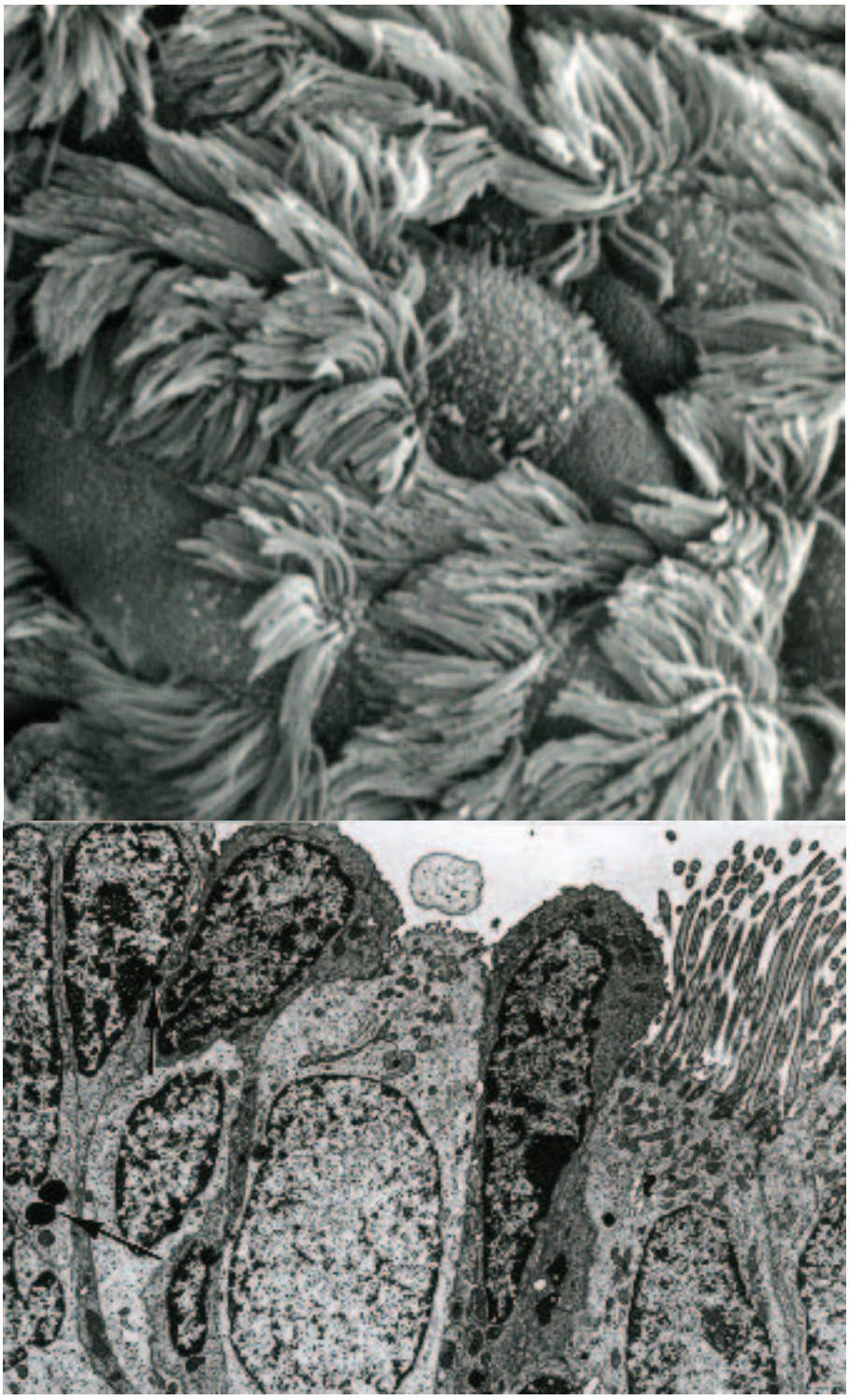

Fig. 11. (*Above*). Surface features of ciliated and non-ciliated cells lining the trachea of an opossum nine weeks postnatal. SEM X 6,000. (*Below*). A micrograph illustrates a region of epithelium from a bronchiole of an opossum nine weeks postnatal. Both dark and light staining non-ciliated cells show scattered electron dense granules (arrows). A ciliated cell is shown at the far right. TEM X 6,000.

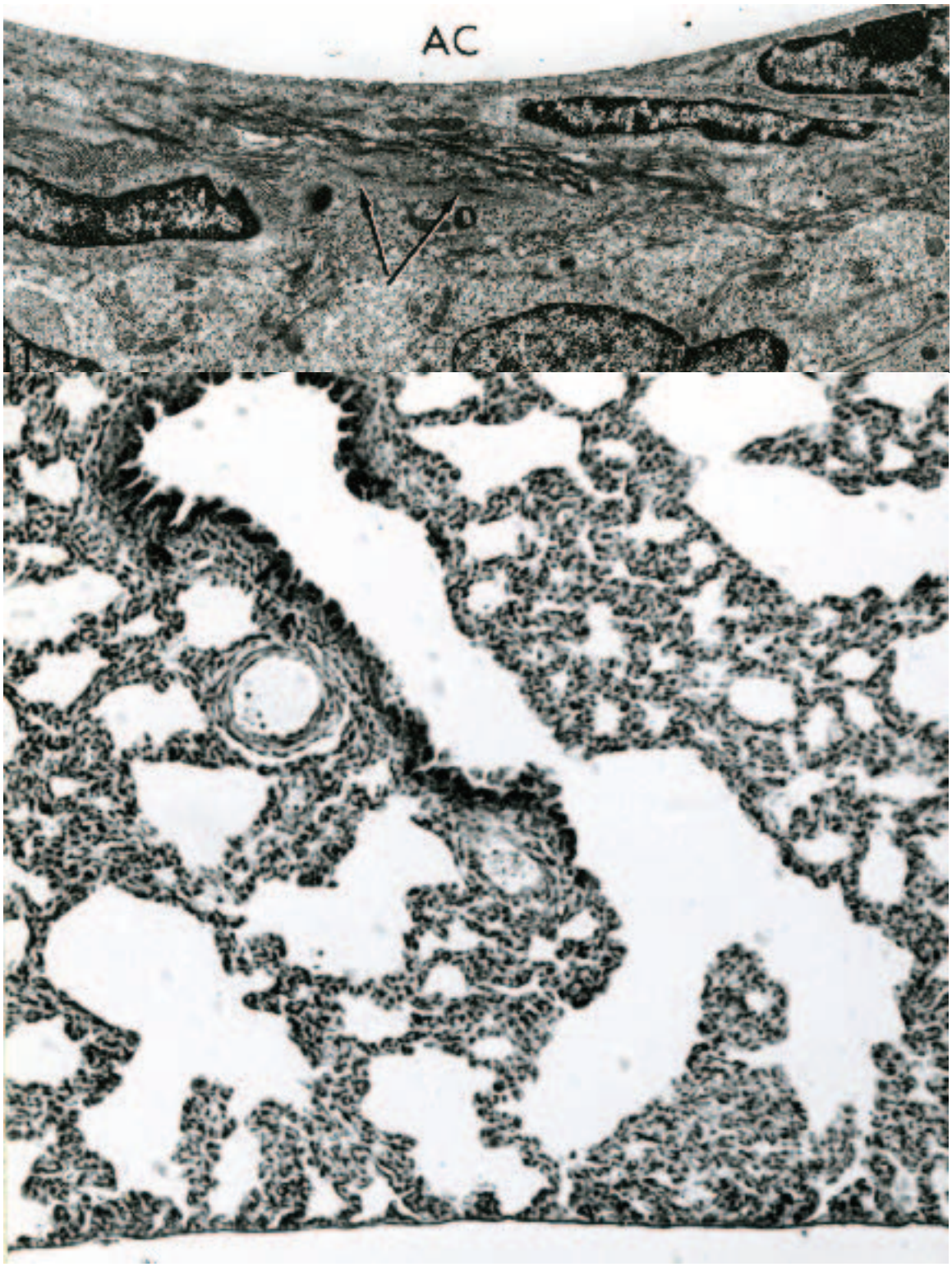

Fig. 12. (*Above*). A region of a terminal respiratory chamber (AC) that contains differentiating smooth muscle cells in its wall (arrows) that underlies a type I pneumocyte. This region of the chamber wall is destined to become incorporated into the bronchial tree. Opossum nine weeks postnatal. TEM X 6,000. (*Below*). A bronchus transitions into a differentiating bronchiole and respiratory bronchioles in this section of lung tissue from nine-week opossum. The parenchyma around the bronchi appears less compact in comparison to earlier ages. LM X 250.

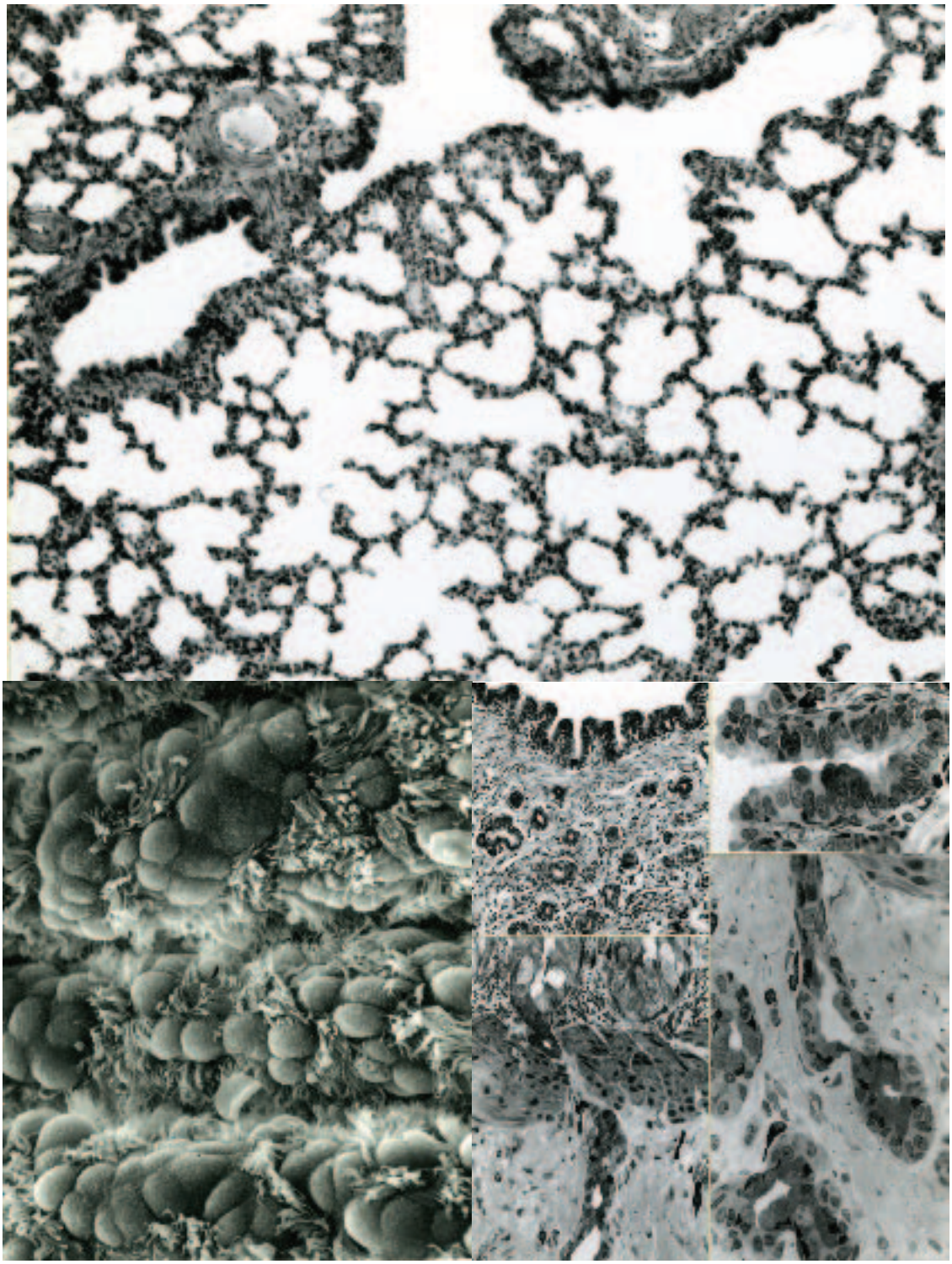

Fig. 13. (*Above*). A portion of lung from a juvenile opossum illustrates bronchioles, respiratory bronchioles, and numerous alveoli, LM X 200. (*Below left*). Surface features of bronchial epithelium from a twelve week opossum appears adult like and exhibits ridges of non-ciliated cells that appear separated by ciliated cells within intervening bronchial folds. SEM X 1,500. (*Below right*). A composite of illustrations depicts the bronchial glands of a juvenile opossum. The upper right illustrates a bronchial fold from which they originate. The lower left shows a duct piercing bronchial smooth muscle to drain into a bronchial fold. At the lower right terminal secretory tubules are capped with light-staining hydropic cells. LM X 200, 400, 400, 400.

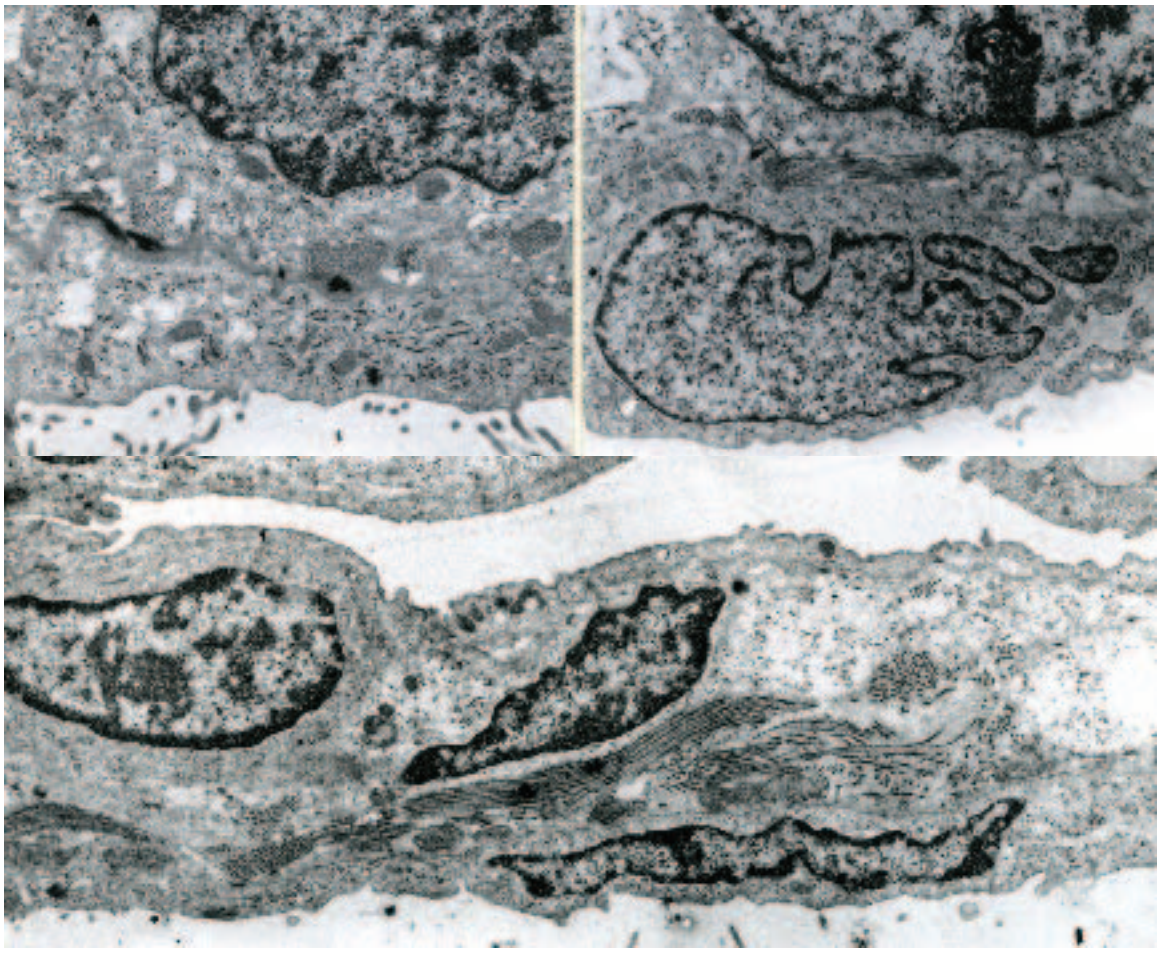

Fig. 14. (*Above left*). The pleural mesothelium of a newborn opossum exhibits only scattered microvilli and lies on a thin basal lamina. An incomplete layer of collagen unit fibrils lies interposed between the basal lamina and a nucleated mesenchymal cell. TEM X 4,500. (*Above right*). At one week postnatal the pleura shows an increase in connective tissue elements. TEM X 4,500. (*Below*). The subpleural connective tissue continues to expand as illustrated in this specimen from an eight-week opossum. A pleural mesothelial cell is shown at the bottom of the photomicrograph and is separated by collagen unit fibrils from an adjacent fibroblast. TEM X 5,000.

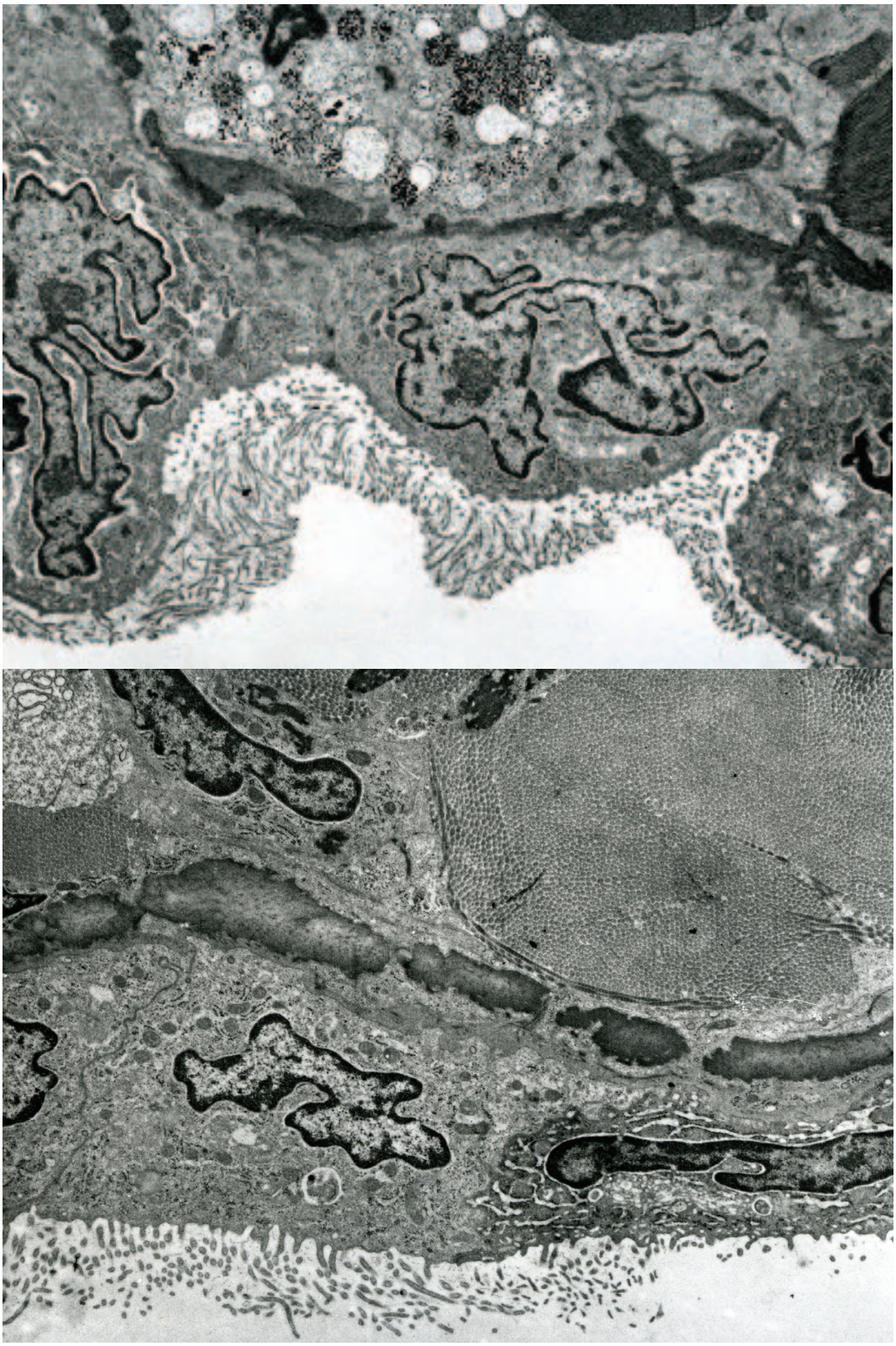

Fig. 15. (*Above*). The luxuriant border of microvilli characteristic of mesothelial cells of the opossum pleura is present in the juvenile opossum. Secretory granules within a nearby mast cell are shown at the top of the micrograph. TEM X 6,000. (*Below*). A region of adult pleura illustrates a band of elastin separating the mesothelial lining from adjacent bundles of collagen. TEM X 6,000.

Chapter 16. Tongue

Synopsis:

Initial formation of the tongue begins early during the tenth prenatal day in *Didelphis* arising from two lateral and a single medial lingual swelling. The tongue is a prominent structure late in day ten and due to its rapid growth protrudes from the oral cavity by the eleventh prenatal day. The dorsal surface of the tongue is relatively smooth at this period of development and lacks papillae. The epithelium covering the tongue is stratified squamous, which is thickest on the dorsal surface. The intrinsic musculature of the tongue interior is characterized by myotubes with chains of centrally positioned nuclei and peripherally positioned myofibrils at this stage of organogenesis. The majority of myotubes are orientated perpendicular to the long axis of the tongue. At about one week after birth typical skeletal myocytes characterize the intrinsic musculature of the tongue, which remains divided into left and right halves by an incomplete lingual septum. The tongue is richly innervated during this period of development. Filiform, fungiform, and three circumvallate papillae are present on the dorsum of the tongue by end of the fourth postnatal week. Taste buds also are present by this time and are associated primarily with the fungiform papillae. Taste buds are not associated with the circumvallate papillae until later in development and will be the primary location for the majority of taste buds in the adult. The adult tongue of the opossum is elongate and exhibits five forms of papillae: filiform, fungiform, conical, compound filiform, and circumvallate.

The large, open mouth with the well-developed tongue of the newborn opossum are essential features for nipple attachment and suckling. Once secured, the nipple occupies a shallow grove on the dorsal aspect of the tongue and the lips fuse together during the first week of postnatal life to form a tight seal around the entrance of the nipple into the oral cavity. During suckling the tongue is lowered by the contraction of the vertically oriented skeletal muscle fibers within the tongue musculature. As a result, a negative pressure is created within the oral cavity and milk is drawn from the nipple and into the oral cavity and is swallowed.

Acknowledgments:

Figs. 3 (center and bottom), 4, 5, 6 (top) and 7, Krause, W.J. and J.H. Cutts (1982) Morphological observations on the papillae of the opossum tongue. Acta Anat. 113:159-168.

Figs. 1 (bottom), 2 and 3 (top), Krause, W.J. and J.H. Cutts (1992) Development of the Digestive System in the North American Opossum (*Didelphis virginiana*). Adv. Anat. Embryol. Cell Biol. 125:1-148.

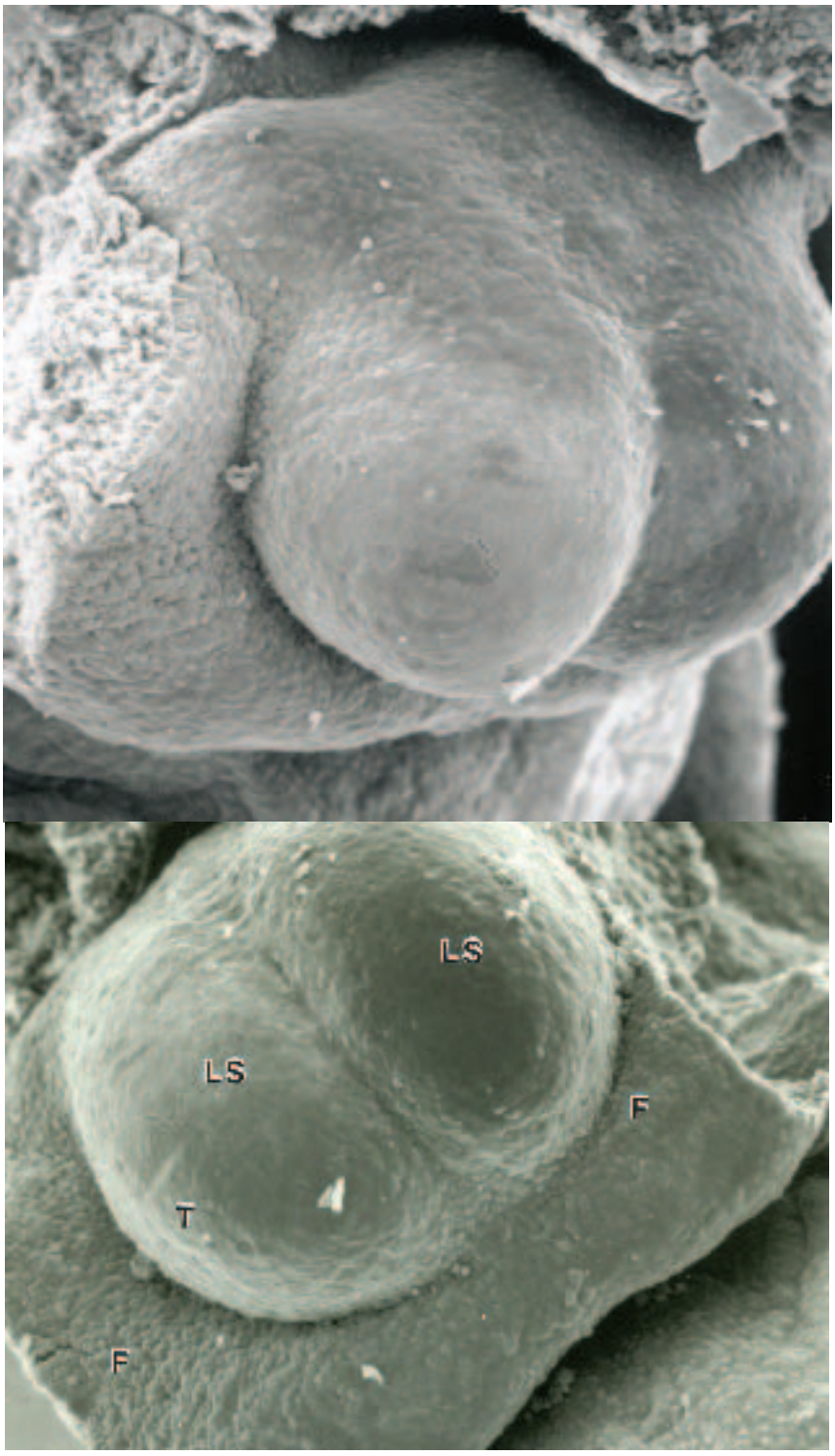

Fig. 1. (*Above*). The developing tongue (center) extends from the floor of the oral cavity early in prenatal day ten. SEM X 160. (*Below*). The two lateral lingual swellings (LS) of the developing tongue (T) are clearly visible extending from the floor (F) of the oral cavity in the ten-day-old opossum embryo. SEM X 130.

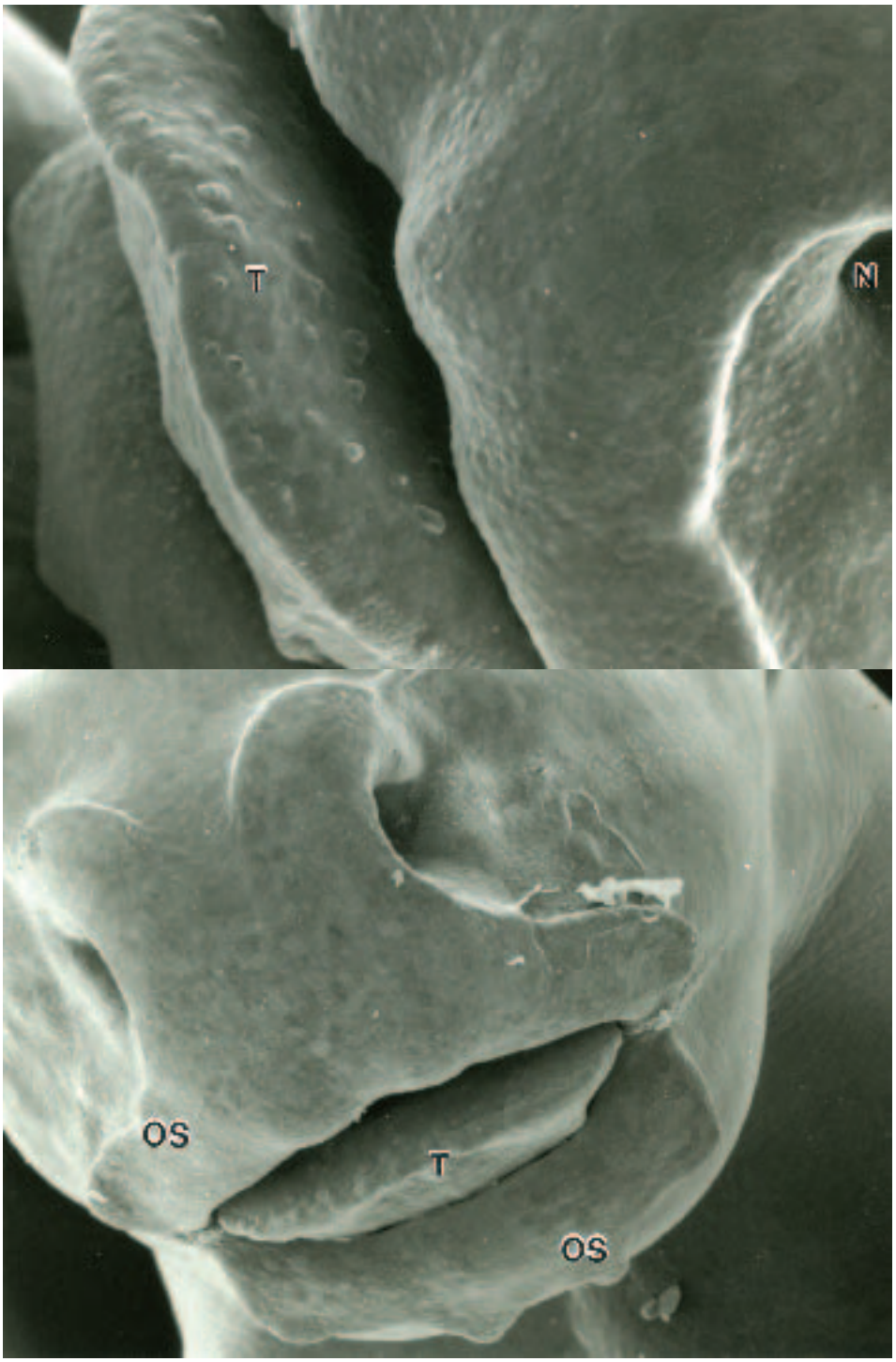

Fig. 2. (*Above*). A large protruding tongue (T) extends form the open oral cavity of an eleven-day opossum embryo. The opening to one of the external nares (N) can be seen at the extreme right. SEM X 100. (*Below*). The protruding tongue (T) continues to extend from the forming mouth of the twelve-day-old opossum embryo. Note the extensive development of an oral shield (OS) that surrounds the opening to the mouth at this stage of development. SEM X 50.

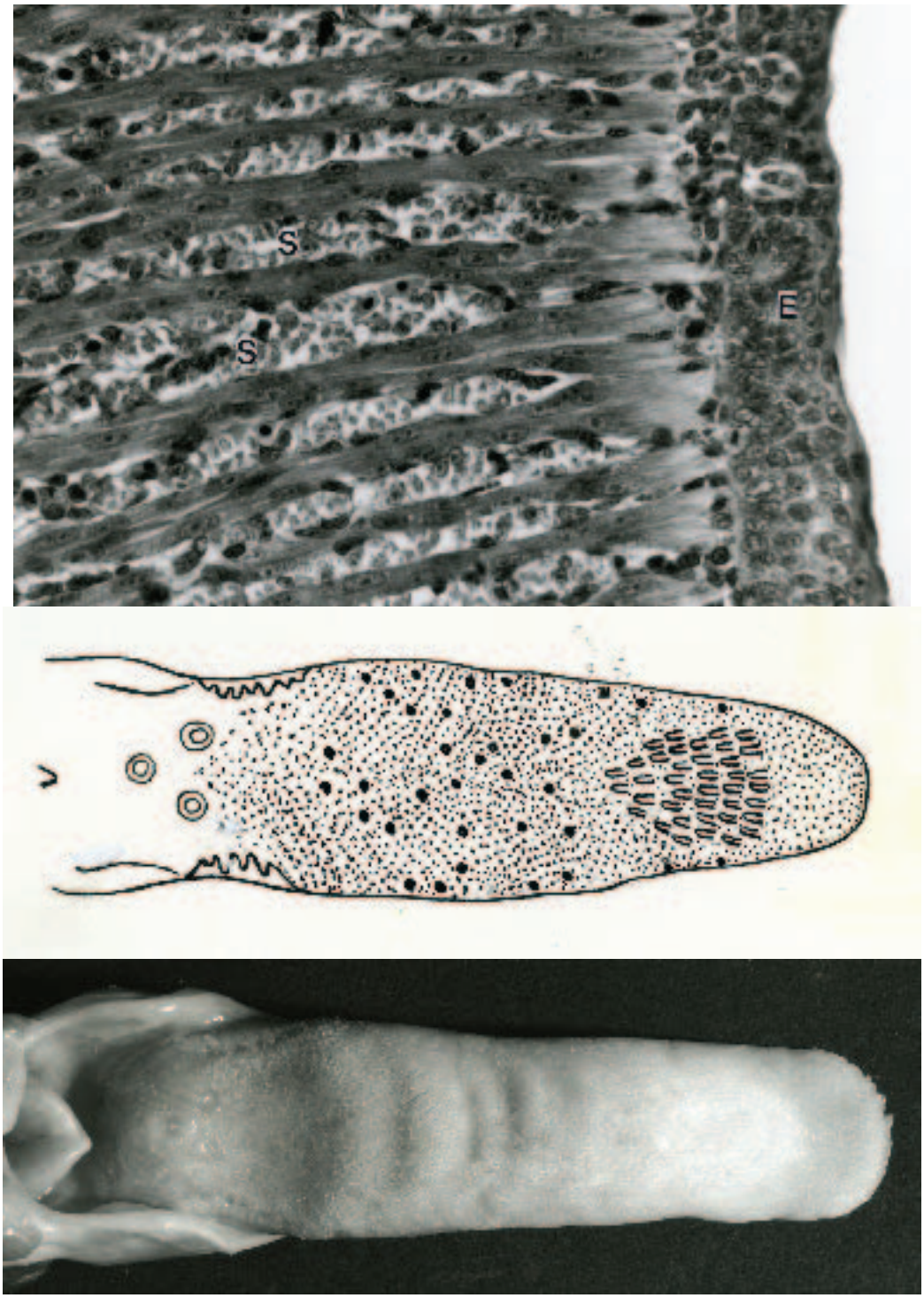

Fig. 3. (*Above*). A portion of tongue from an eleven-day-old opossum embryo illustrates the developing skeletal muscle cells (seen in both transverse (S) and longitudinal profiles) of the tongue musculature. Note depth of epithelium (E) covering the dorsal surface of the tongue at this stage of development. LM X 300. (*Center*). A line drawing of the adult opossum tongue illustrates the location of scattered fungiform (black), three posterior circumvallate, and a patch of conical papillae near the tip. The posterior lateral mucosal folds also are illustrated. (*Bottom*). A photograph illustrates the tongue of an adult opossum. Compare the features observed with those depicted in the line drawing. The three circumvallate papillae are clearly visible at the left. X 3.

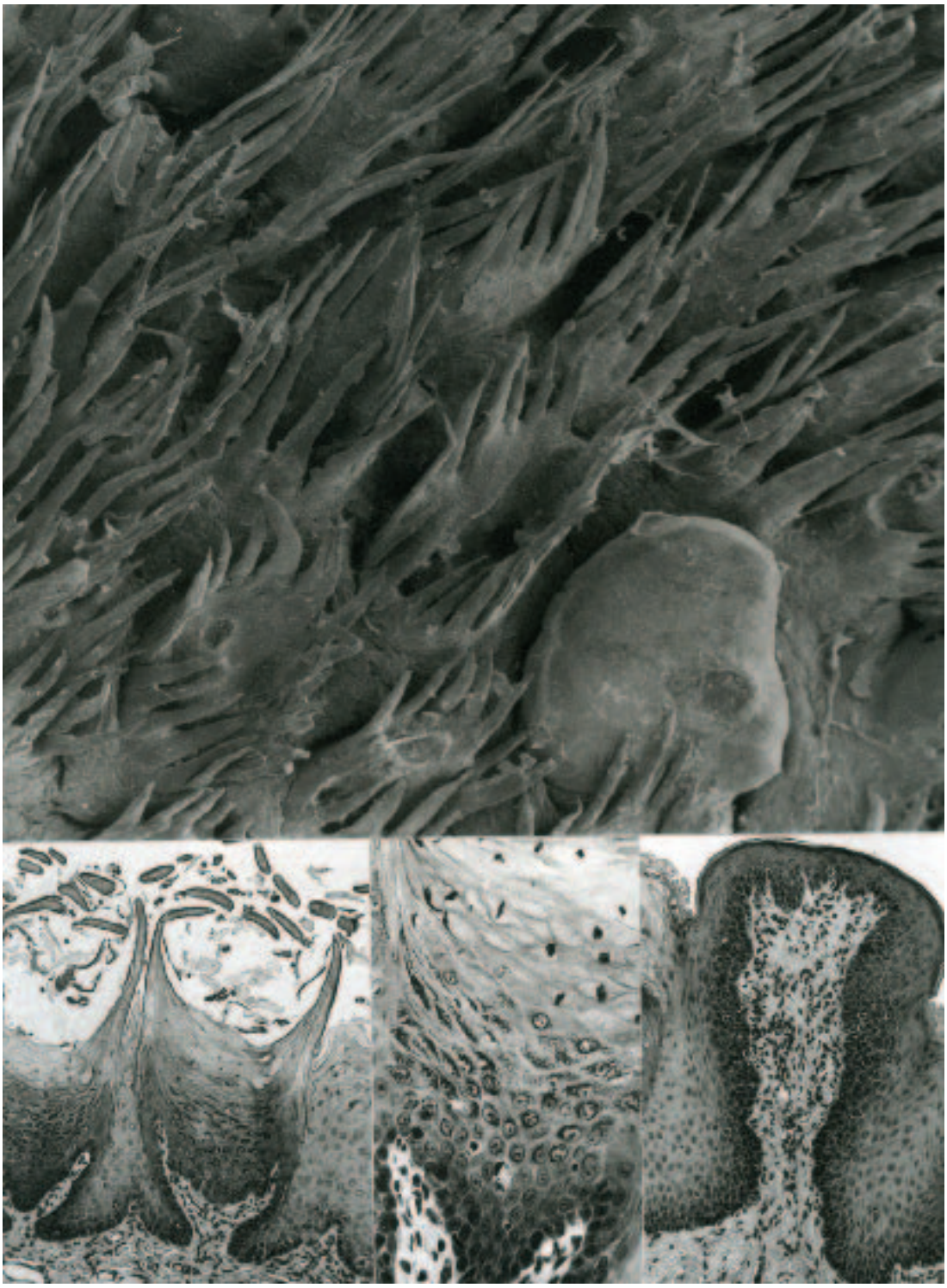

Fig. 4. (*Above*). The compound filiform type of papillae exhibits a fringe of keratinized projections around the top of each papilla. A smooth appearing fungiform papilla is shown at the lower right. SEM X 100. (*Below left*). A micrograph illustrates the appearance of compound filiform papillae when viewed in histological section. LM X 100. (*Below middle*). When viewed at increased magnification the central epithelial region of a compound filiform papilla is seen to exhibit several layers of cells comprising the stratum granulosum. LM X 250. (*Below right*). A section through a fungiform papilla shows only limited cornification of the covering epithelium. LM X 100.

Fig. 5. (*Above left*). The smooth surface of stratified squamous epithelium covering the posterior aspect of the tongue surrounds a single circumvallate papilla but is separated from it by an intervening moat. Note the abrupt transition to compound filiform papillae. SEM X 20. (*Above right*). A micrograph illustrates the appearance of compound filiform papillae (CF) taken just anterior to the smooth area of the tongue surrounding the vallate papillae. SEM X 85. (*Below*). The appearance of the conical papillae taken from the anterior patch of papillae located on the dorsal surface of the tongue. Compound filiform papillae often lie immediately adjacent to the large conical papillae. SEM X 50.

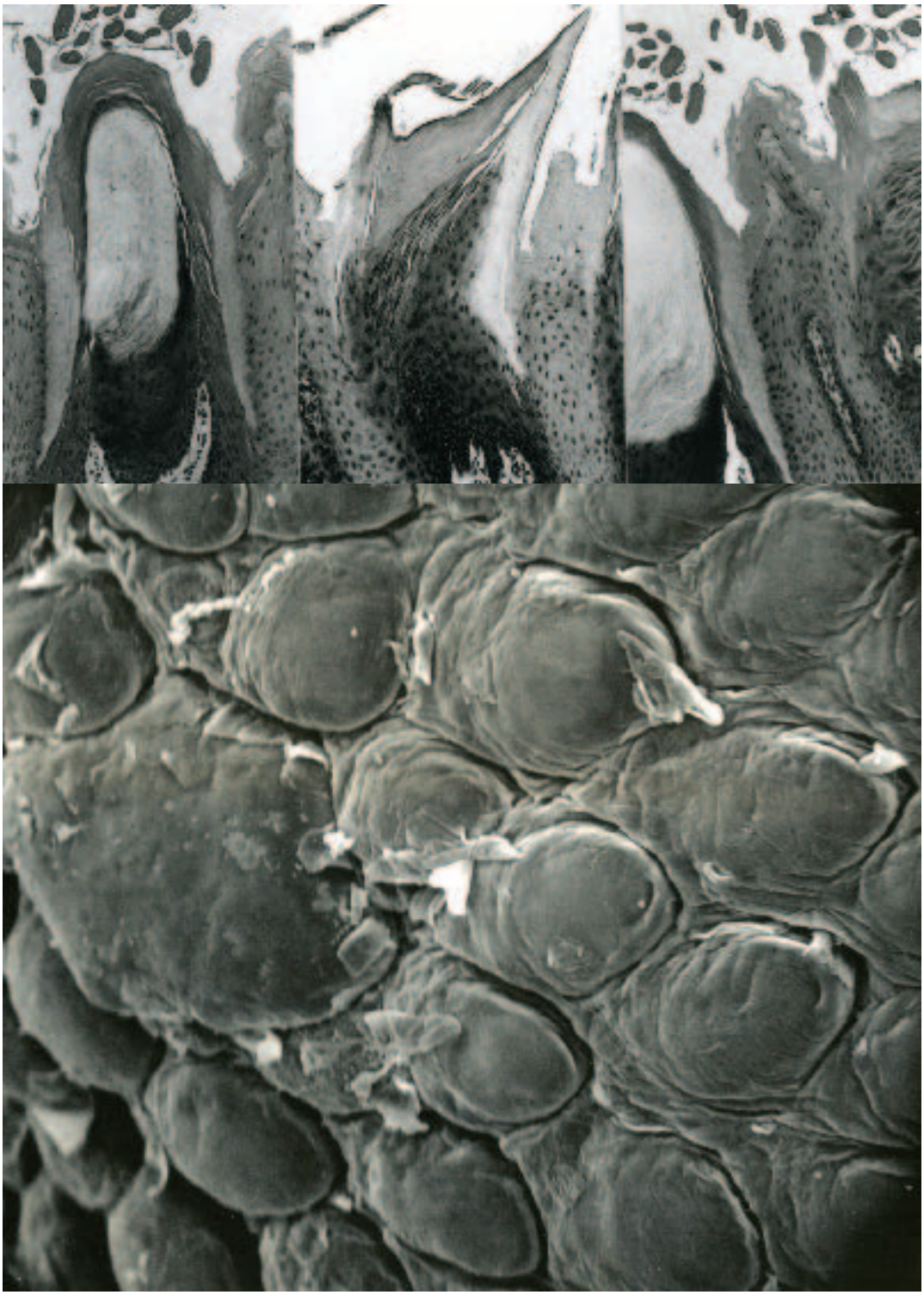

Fig. 6. (*Above left*). A section demonstrating the large amount of keratin associated with the conical form of papillae. Projections from adjacent compound filiform overly the latter. LM X 100. (*Above center*). The tapered point of a conical papilla directed towards the pharynx. LM X 100. (*Above right*). A region of tongue illustrates portions of adjacent conical and compound filiform papillae. LM X 100. (*Below*). A region of the dorsal tongue surface posterior to the patch of conical papillae illustrates numerous smaller, conical-shaped papillae. A fungiform papilla is located at the extreme left. SEM X 70.

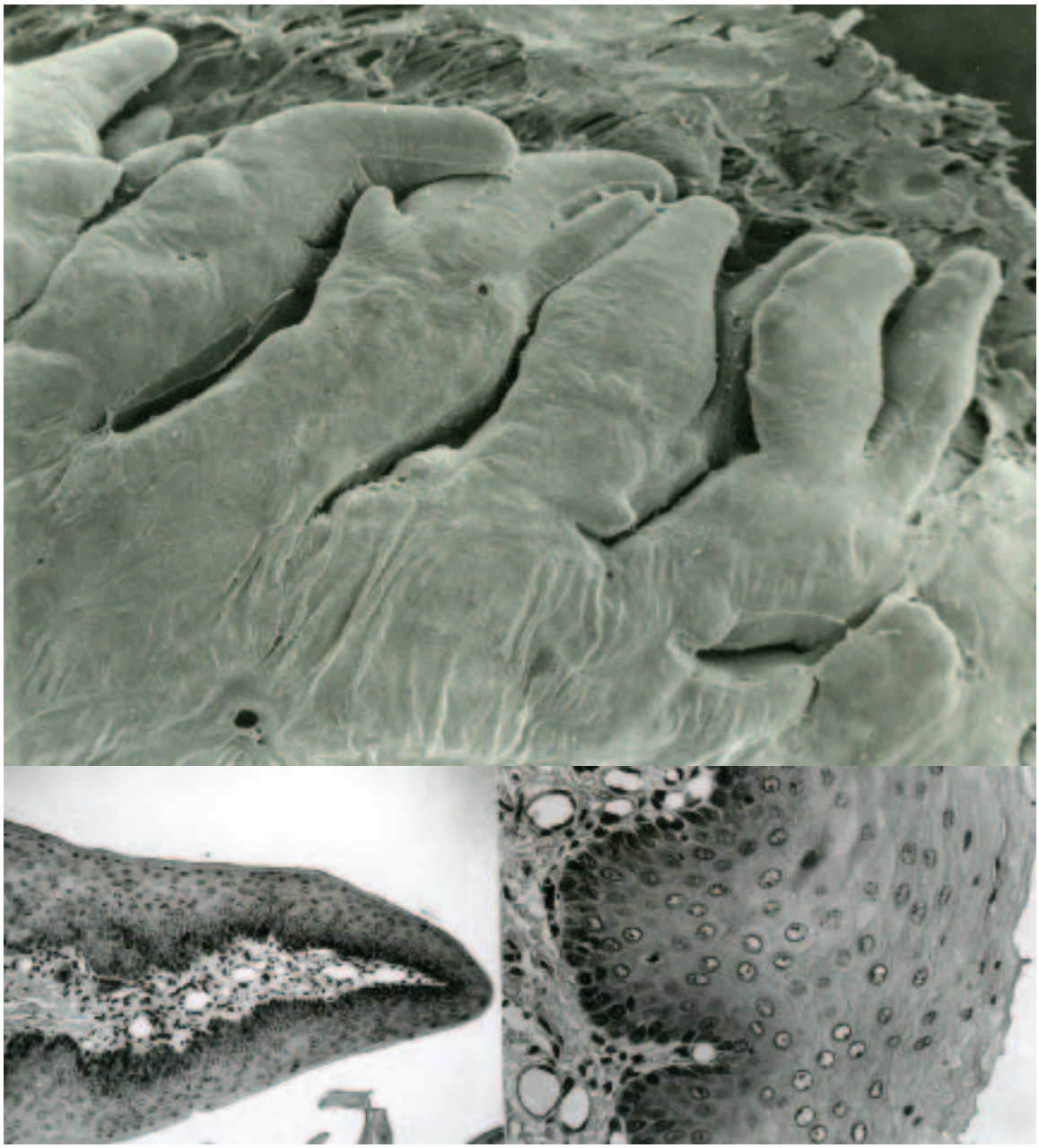

Fig. 7. (*Above*). A region of the posterior lateral lingual folds illustrates in greater detail the numerous smooth finger-like projections shown in figure 3. SEM X 50. (*Below left*). A section through the tip of one the finger-like projections illustrates that it contains a vascularized connective tissue core. LM X 100. (*Below right*). A section through the epithelium covering a posterior lateral fold illustrates that it is less keratinized when compared to the epithelium covering the remainder of the dorsum of the tongue. LM X 250.

Chapter 17. Submandibular Gland

Synopsis:

The parotid, submandibular, molar, and greater and lesser sublingual glands constitute the major salivary glands of *Didelphis virginiana*. Of these, the submandibular gland is the most prominent. The submandibular glands originate early during prenatal day twelve as epithelial outgrowths from the floor of the oral cavity. An expanding primitive ductal system branches repeatedly during its early growth and at birth terminates in end-pieces formed by proacinar cells. During its period of early growth the expanding ductal system is enveloped in, and organized by, a delicate connective tissue rich in ground substance. The submandibular glands show progressive growth throughout the postnatal period but it is not until after weaning that the glands assume an adult appearance. The postnatal growth of the submandibular glands can be subdivided into two major periods. The first period is concerned with the development of the ductal system and occurs primarily during the first four weeks of postnatal life. The second period lasts for the remainder of the postnatal period and is concerned with the establishment of secretory tubules and end-pieces. Prior to eleven weeks postnatal, the secretory units consist primarily of proacinar cells. Thereafter, the secretory units elongate and form a branching network of tubules consisting of mucous cells with proacinar cells remaining at the ends of the tubules. Special serous cells in older, weaned juveniles eventually replace the proacinar cells. The special serous cells are organized into serous demilunes and are characterized by two types of secretory granule. It is thought that both the mucous and special serous cells arise from proacinar cells rather than ductal cells. Myoepithelial cells envelope the intercalated ducts and secretory units throughout the postnatal period and are positioned between the epithelial components and their limiting basal lamina. No histological differences have been demonstrated between female and male opossum submandibular glands either during postnatal development or in the adult.

Numerous inclusions bodies (unusual minute granules) are observed in the lumina of the intralobular ducts and mucous tubules of the opossum submandibular gland. The inclusions bodies occur in all postnatal opossums examined (except newborn) as well as in adults. These particles are often observed to clump into irregular shaped aggregates. Similar appearing particles are not found in the cytoplasm or nuclei of cells comprising the submandibular glands. For the most part the particles are spherical in outline, of uniform size, and exhibit a distinct, centrally positioned electron dense core. The particles range from 100 nm to 150 nm in diameter with the central core measuring from 50 nm to 100 nm in diameter. A distinct membrane limits the particles. Whether these particles represent a secretory factor of some type (epidermal or nerve growth factor) or some form of pathogen is unknown.

Acknowledgments:

Figs. 1 (top right), 2, 7 (bottom), 8 and 9 (bottom), courtesy of and from: Leeson, C.R., J.H. Cutts and W.J. Krause (1978) Postnatal development of the submandibular gland in the opossum (*Didelphis virginiana*). J. Anat.126:329-351.

Figs. 4 (bottom), 5 (top), 6, courtesy of and from: Krause, W.J. and J.H. Cutts (1992) Development of the Digestive System in the North American Opossum (*Didelphis virginiana*). Adv. Anat. Embryol. Cell Biology, 125:1-148

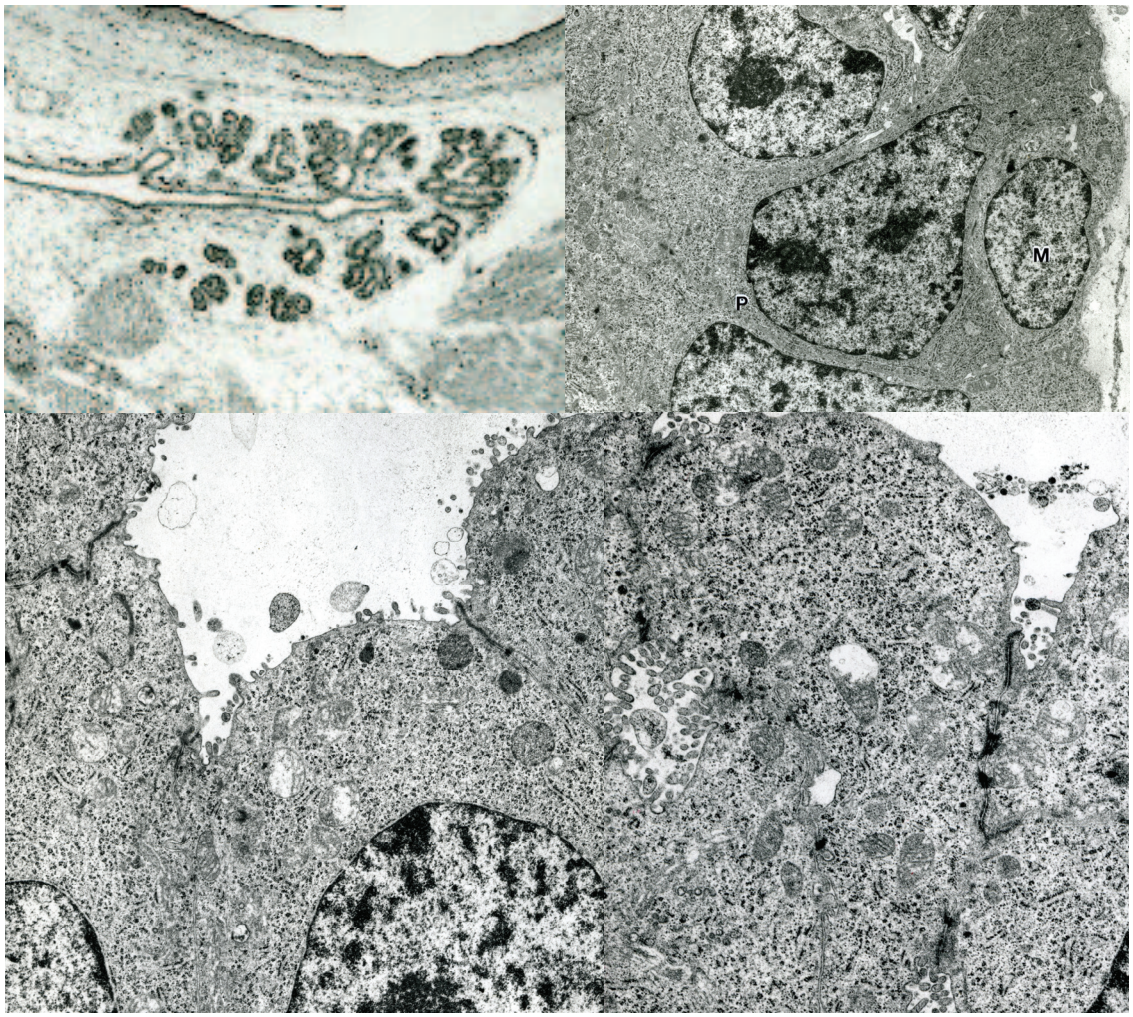

Fig. 1. (*Above left*). A section of a newborn opossum submandibular gland illustrates the two epithelial components present at this time, ducts and end-pieces. LM X 40. (*Above right*). A micrograph illustrates a proacinar cell (P) and a differentiating myoepithelial cell (M) from the end-piece of a newborn opossum submandibular gland. TEM X 6000. (*Below*). This electron micrograph details the apical cytoplasm of several proacinar cells from a newborn opossum submandibular gland. Intercellular canaliculi, limited by junctional complexes, occur between neighboring cells. TEM X 10,000.

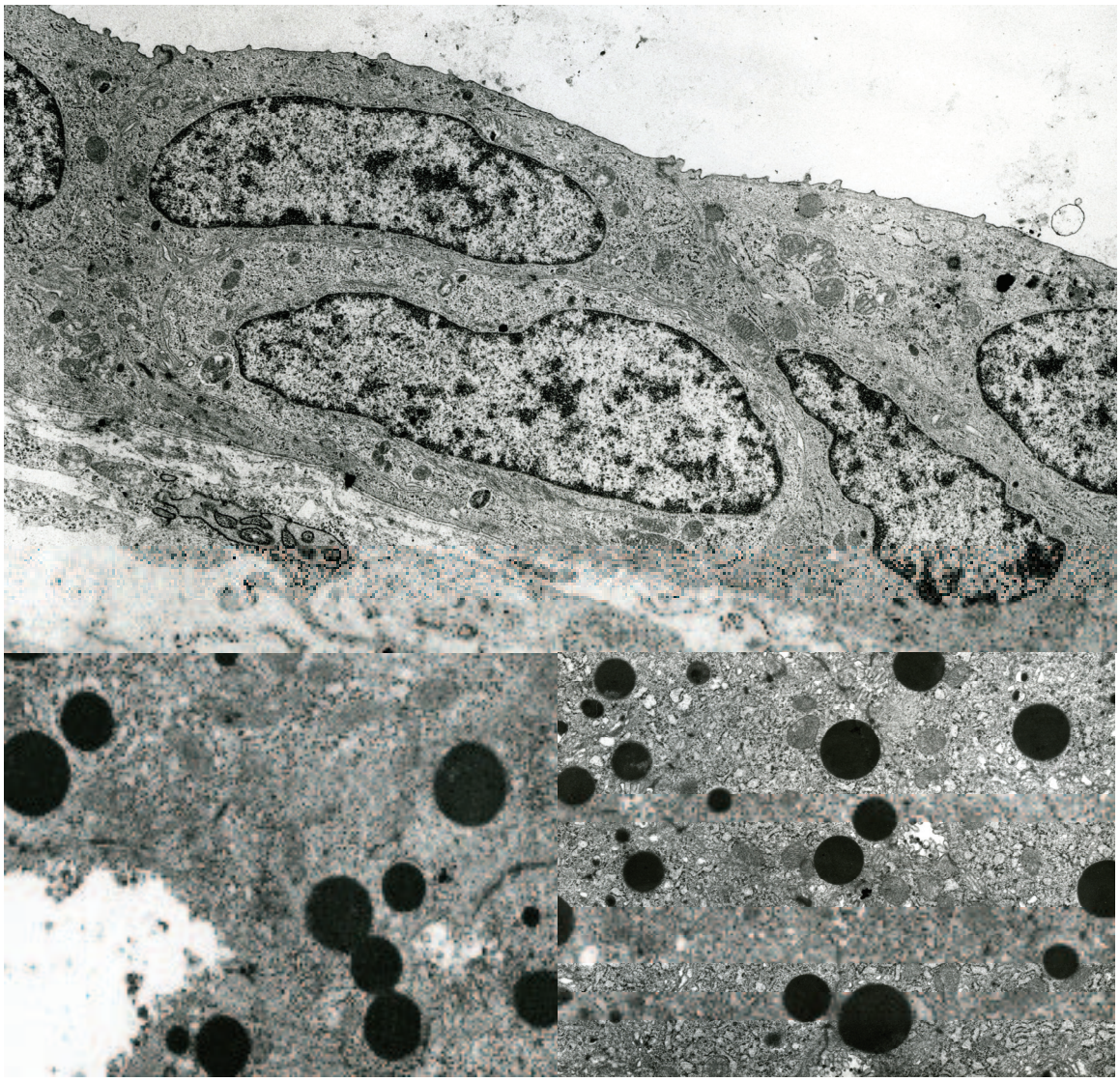

Fig. 2. (*Above*). An electron micrograph illustrates the epithelium forming a portion of the ductal system in the submandibular gland of a newborn opossum. The epithelium lies on a delicate basal lamina and consists of two layers of flattened cells without apparent specialization. TEM X 8,000. (*Below left*). This electron micrograph depicts the apices of submandibular proacinar cells from an opossum one week postnatal. Note the presence of electron dense granules in relation to the apical plasmalemma and to intercellular canaliculi. TEM X 9,000. (*Below right*). A micrograph of the apical region of adjacent proacinar cells depicts an additional example of the relationship between secretory granules and intercellular canaliculi. TEM X 9,000.

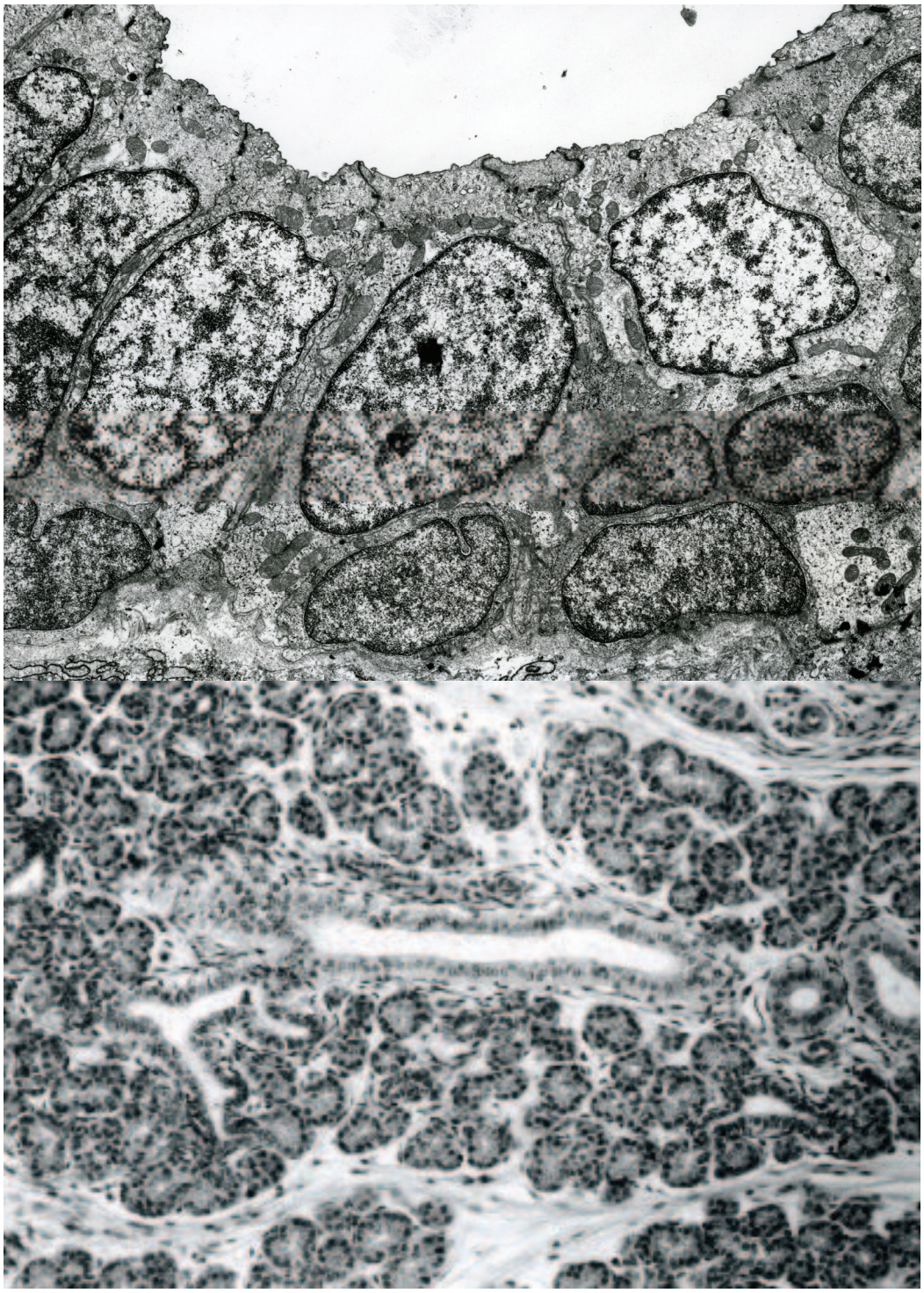

Fig. 3. (*Above*). The epithelium lining an intralobular duct of a week old opossum submandibular gland consists of two distinct cell types. Tall columnar cells border the lumen, small cells with dark nuclei and dense cytoplasm lie in relation to the basal lamina. TEM X 10,000. (*Below*). A photomicrograph illustrates a portion of a submandibular gland from an opossum three weeks postnatal. Note the development of the interlobular and intralobular portions of the ductal system as well as secretory tubules. LM X 250.

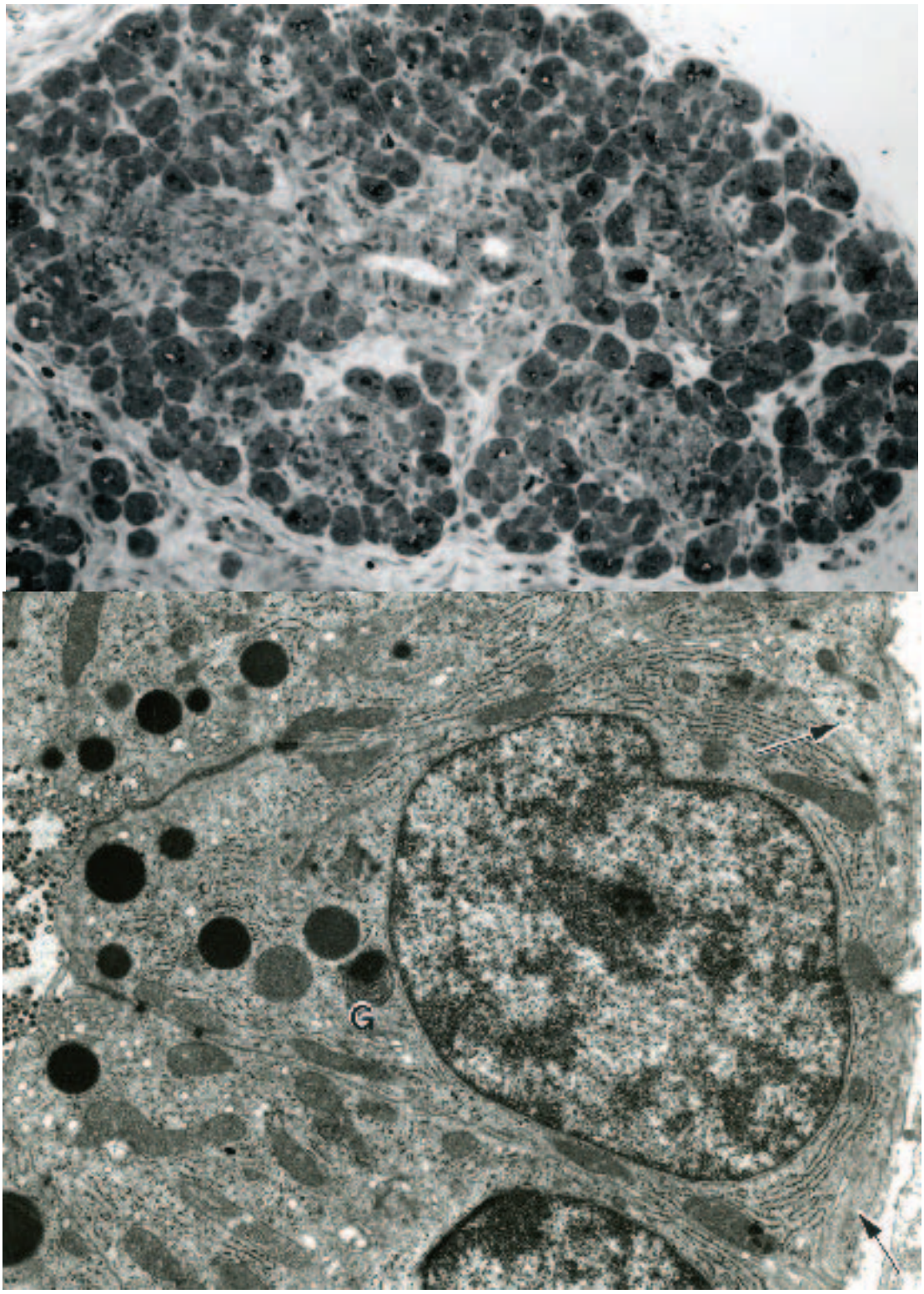

Fig. 4. (*Above*). A micrograph illustrates a portion of a lobe from the submandibular gland of a five-week-old male opossum. Interlobular ducts are central in position and lined by columnar epithelium. LM X 200. (*Below*). Proacinar cells, taken from the above specimen, are filled with profiles of granular endoplasmic reticulum, electron-dense secretory granules, and Golgi complexes (G). Myoepithelial cell processes (arrows) are shown at the extreme right. TEM X 7000.

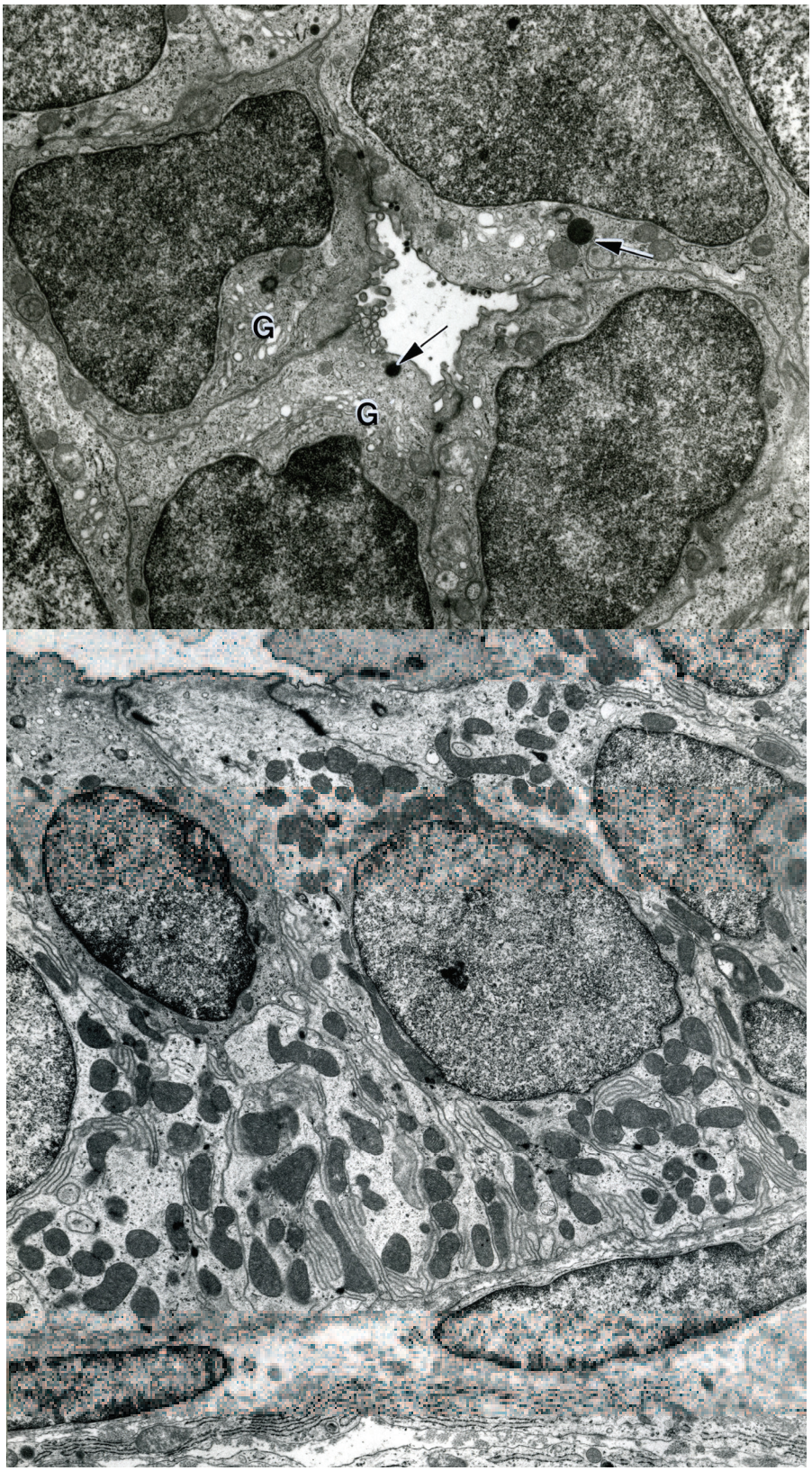

Fig. 5. (*Above*). The apical cytoplasm of an intercalated duct from a five-week-old male opossum contains occasional secretory granules (arrows) and Golgi complexes (G). TEM X 6,000. (*Below*). A portion of an intralobular duct from the same specimen illustrates a dark cell (upper left) and tall light cells. The latter exhibit numerous infoldings of the basolateral plasmalemma closely associated with mitochondria. TEM X 4,500.

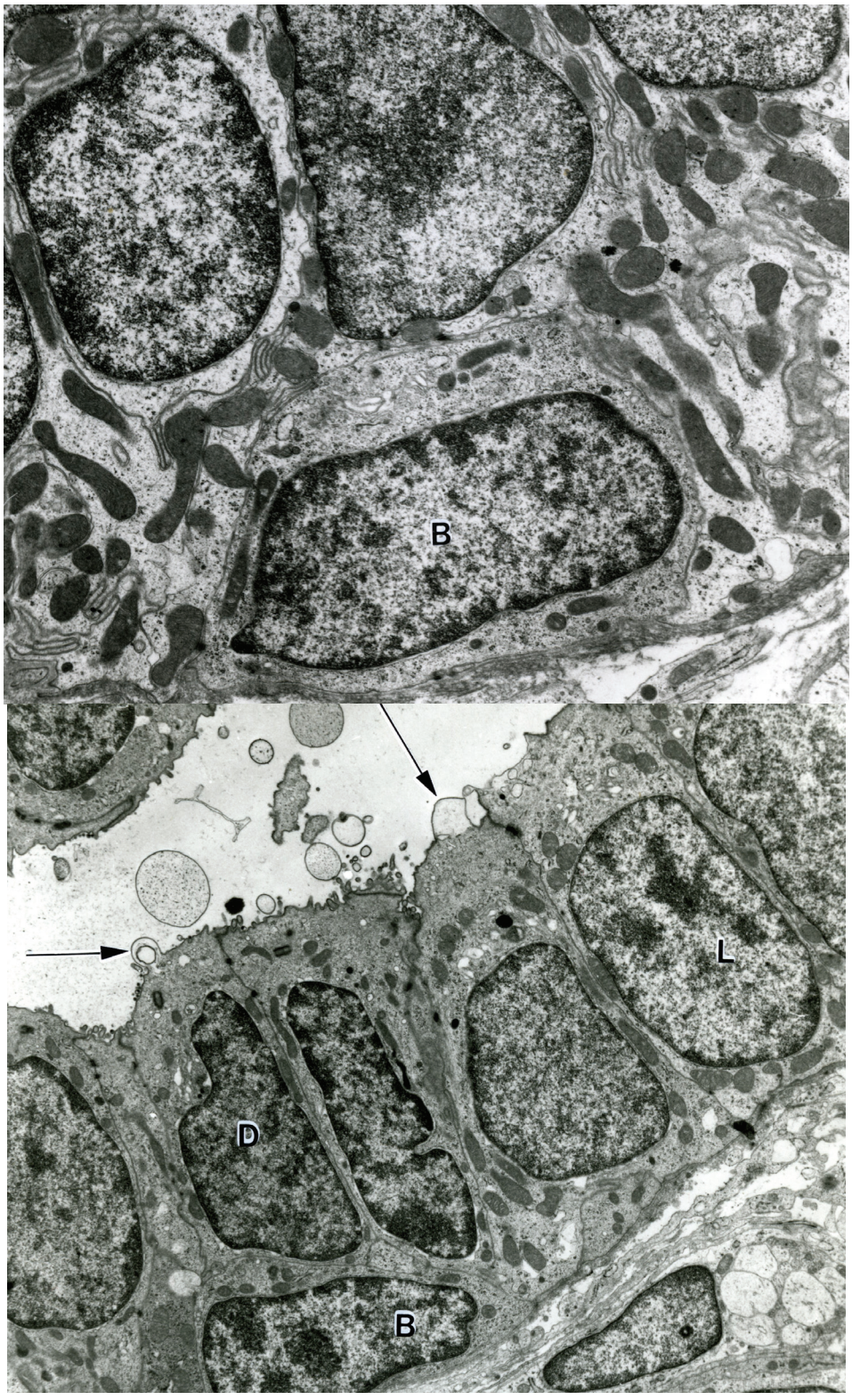

Fig. 6. (*Above*). The basal region of an intralobular duct from a five-week-old male opossum illustrates a basal cell (B), which lies on the inner aspect of the basal lamina. TEM X 6,000. (*Below*). A region of an interlobular duct from the same specimen as above illustrates tall light cells (L), dark cells (D), and a basal cell (B). Apical blebbing (arrows) is observed on some cells. TEM X 6,000.

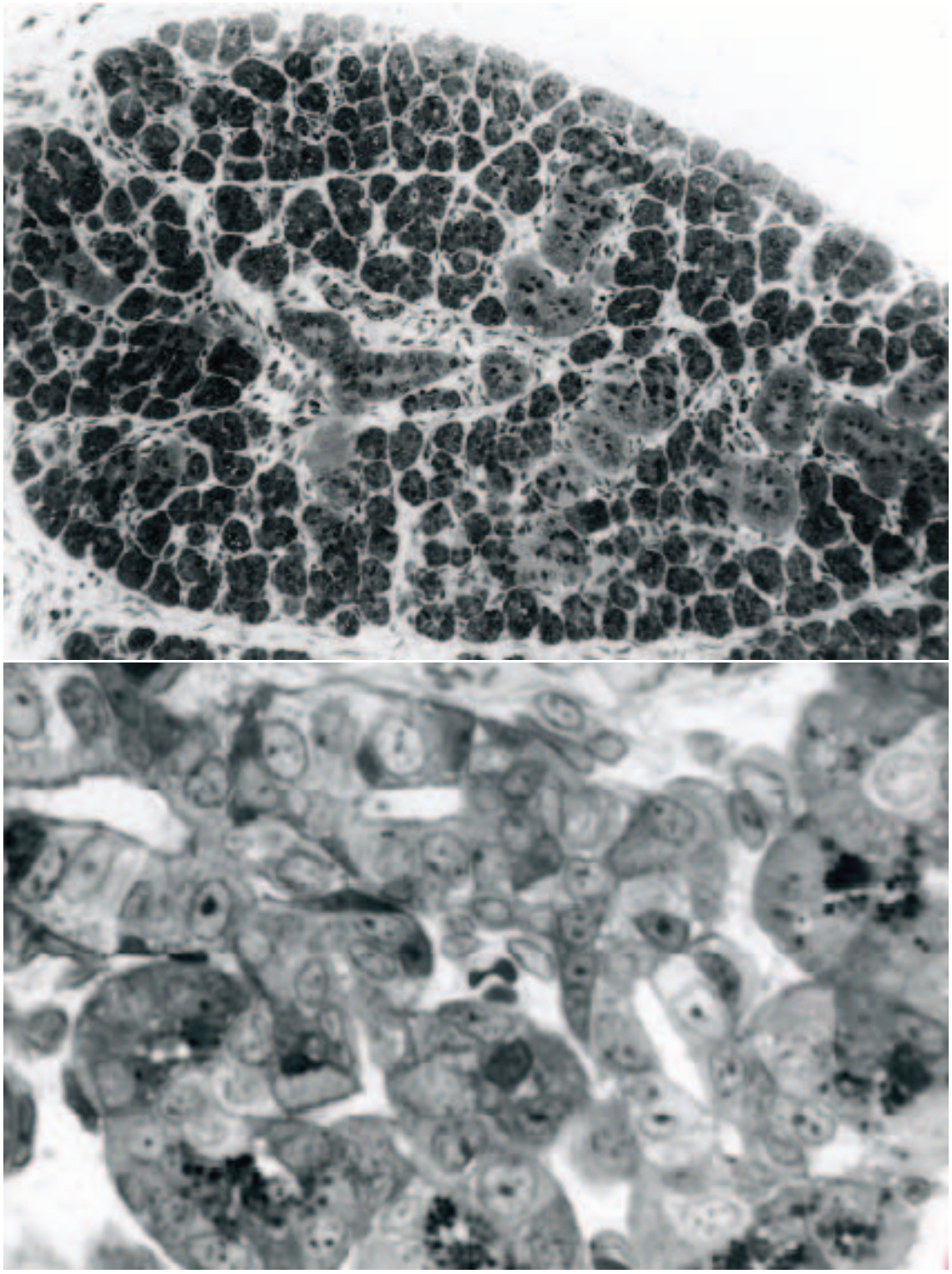

Fig. 7. (*Above*). A photograph illustrates the appearance of the submandibular gland from a nine-week-old female opossum. LM X 200. (*Below*). When viewed at increased magnification an intralobular duct (left center), divides into several branching intercalated ducts that ultimately terminate in secretory units. Dense secretory granules fill the apical cytoplasm of the proacinar cells forming the secretory units. LM X 500.

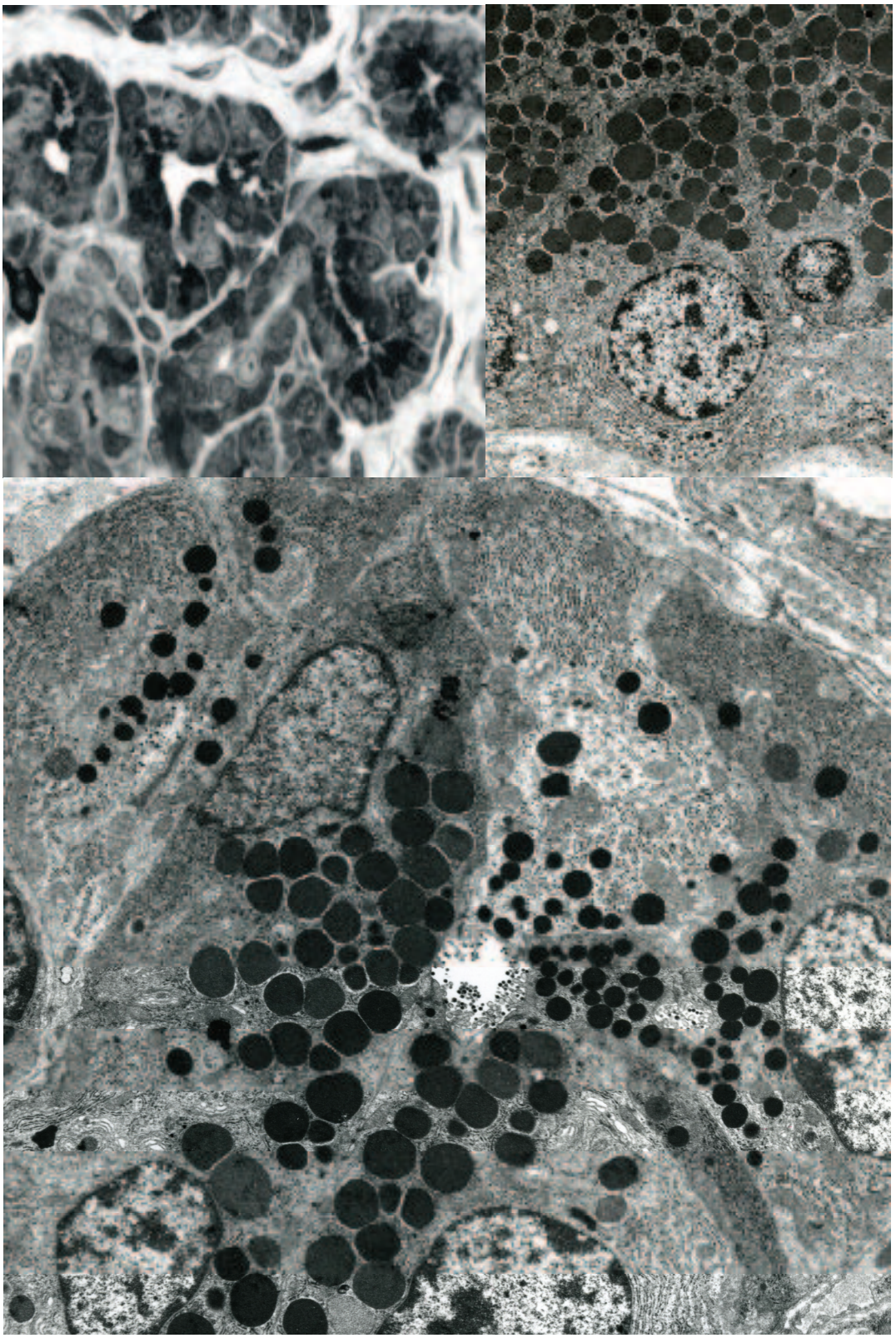

Fig. 8. (*Above Left*). In the twelve-week-old opossum submandibular gland the secretory units are more elongated and dense secretory granules fill the apices of most component cells. LM X 375. (*Above right*). Cells from a region of a secretory tubule. TEM X 3,000. (*Below*). Cells forming the majority of secretory tubules from the juvenile opossum contain large secretory granules and intracellular canaliculi are absent. Cells at the periphery of a secretory unit may contain small dense granules in relation to either to the tubular lumen or intercellular canaliculi. TEM X 5,000.

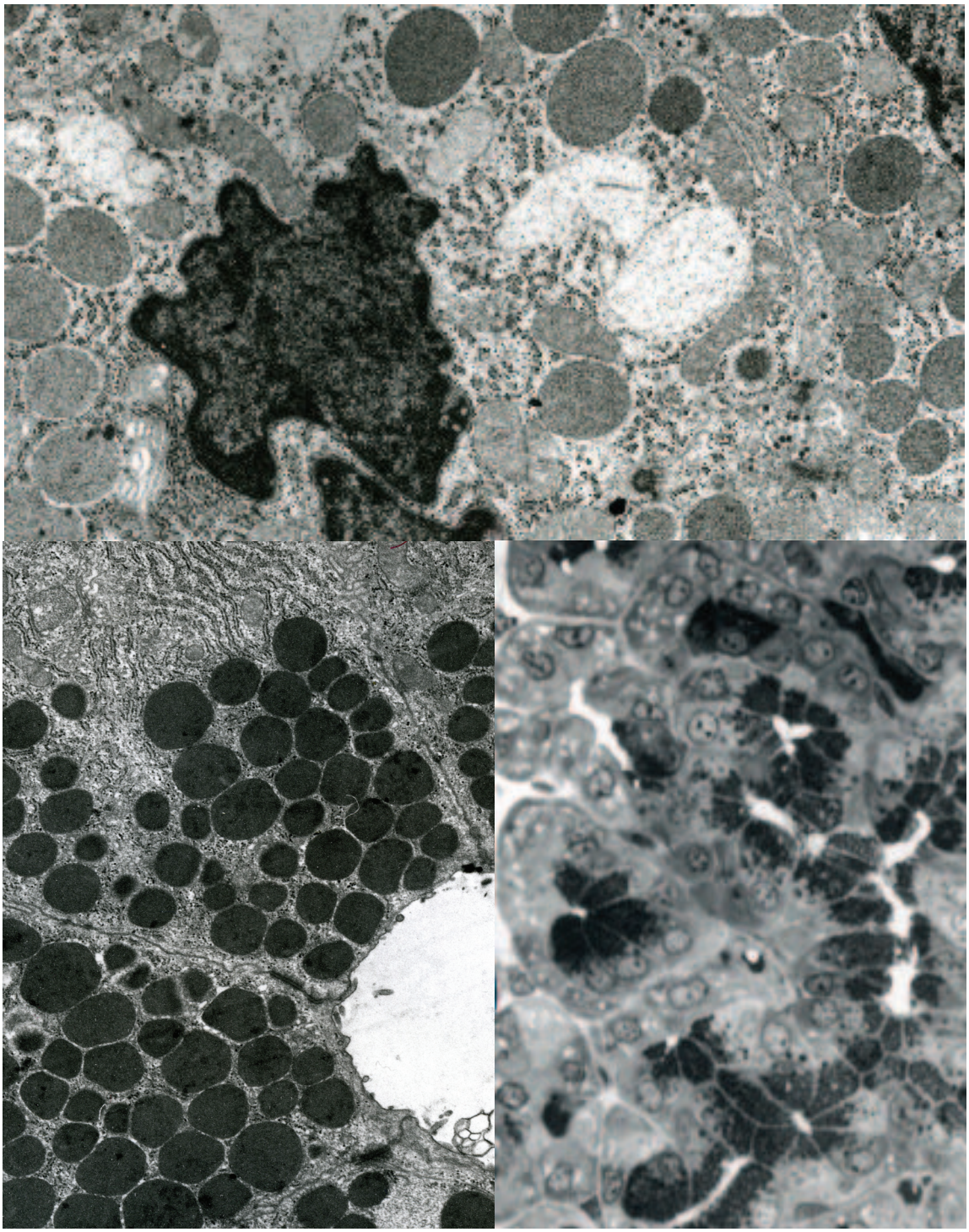

Fig.9. (*Above*). A micrograph illustrates portions of two special serous cells from a juvenile opossum. Note the dense irregular nuclear profile and the variation in electron density of the secretory granules. TEM X 8,000. (*Below Left*). Apices of several mucous cells forming a secretory tubule are filled with dense secretory granules. Juvenile opossum. TEM X 6,000. (*Below right*). Branching tubules lined by mucous cells filled with dense secretory granules terminate as bulbous endings made up of special serous cells. The latter exhibit a pale, flocculent cytoplasm. Adult opossum. LM X 375.

Chapter 18. Tooth Eruption

Synopsis:

The development of teeth in the opossum occurs primarily during the postnatal period. Initial tooth development is from the free edge of the dental lamina and then proceeds through cap and bell stages of development. The majority of tooth germs are well established in the mandible and maxilla by the end of the forth week postnatal. Although epithelial down growths occur on the lingual side of each formed enamel organ, these do not differentiate into tooth germs for the permanent teeth as is the case for eutherian species. The exception is the third premolar. Thus, tooth replacement in *Didelphis* involves only one tooth, the deciduous third premolar. Tooth eruption begins at about twelve weeks and commences as a small crater in the gingival mucosa covering the tooth prior to its actual emergence. As the tooth enters the oral cavity the crater expands to accommodate the tooth. It is believed that the gingival layer degenerates prior to the emergence of the tooth into the formed defect rather than by actively pushing through and rupturing the gingival covering. Crater development is thought to be the result of enzymes released by dental and/or oral epithelium or may be the result of focal pressure necrosis. The dental formula for the opossum is: incisors 5/4, canines 1/1, premolars 3/3, molars 4/4 x2, and totals fifty teeth.

Acknowledgments:

Fig. 1, courtesy of and from: Krause, W.J., and J.H. Cutts (1980) Scanning electron microscopic observations on the tooth eruption of primary teeth in the opossum. Arch. histol. Jap. 43:281 285.

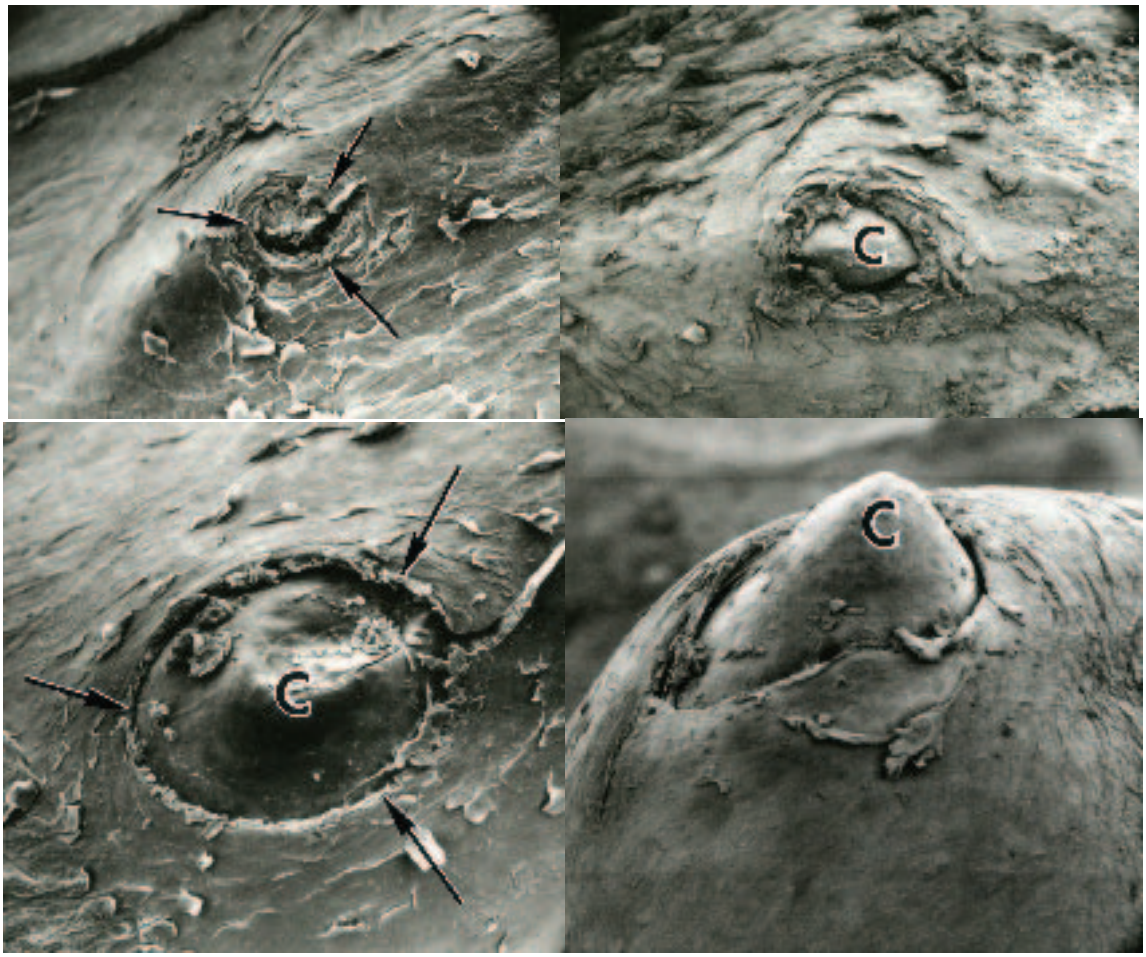

Fig. 1. (*Above left*). A micrograph illustrates the initial formation of a crater (arrows) in the gingival epithelium overlying a canine tooth in the lower jaw of an opossum eleven weeks postnatal. SEM X 100. (*Above right*). The initial emergence of a premolar tooth crown (C) extends from the upper jaw of an eleven-week-old opossum. SEM X 100. (*Below left*). Further emergence of a premolar tooth crown (C) when viewed from above, illustrates that the epithelial crater (arrows) has increased in diameter to accommodate the emerging tooth. An opossum eleven weeks postnatal. SEM X 100. (*Below right*). A scanning micrograph illustrates the emerging crown (C) of a molar tooth from the upper jaw of an opossum eleven weeks postnatal. SEM X 50.

Chapter 19. Esophagus

Synopsis:

The esophagus originates as a minute diverticulum that extends from the floor of the pharynx early in the tenth prenatal day. At the time of birth it is characterized by a wide lumen and lined by epithelium two to three cells deep. This lining epithelium generally is stratified in type although regions of pseudostratified columnar are encountered. A few loosely knit myoblasts organized into two layers constitute the muscularis externa. By the end of the first postnatal week the lining epithelium is arranged into two distinct strata. Cells forming the surface layer are columnar in shape and light staining whereas cells of the basal strata are smaller, dark staining, and irregular in shape. Occasional ciliated and goblet cells occur scattered within the esophageal epithelium. Layers of the muscularis externa also are more clearly defined at this time and an increase in muscle tone accounts for the decrease in luminal diameter observed in the seven-day-old opossum.

The esophageal lining epithelium consists of three basic strata by the end of the third postnatal week. A germinal layer consisting of a single layer of cells, a spinosal layer, and a surface layer of flattened cells that retain their nuclei. Goblet cells and ciliated cells continue to be observed, but usually disappear after the third postnatal week. Ciliated cells, however, do persist in much older opossums but are restricted in distribution to large transverse folds in the distal esophagus. Smooth muscle cells forming the muscularis mucosae appear by the end of the third postnatal week. Coincident with the morphological changes that occur within the esophageal lining epithelium, esophageal glands appear as solid outgrowths that extend from its basal surface at this time. The esophageal glands consist primarily of ducts and mucous cells during the first nine weeks of postnatal life. Serous (light) cells appear at the ends of the secretory units during the eleventh postnatal week. Myoepithelial cells are associated with both serous and mucous cell types of the opossum esophageal glands.

Proximally, the muscularis externa consists entirely of skeletal muscle. Histochemical typing of this musculature indicates that it consists primarily of a type II fiber type. These are fast acting fatigue resistant skeletal muscle fibers. Although type I fibers do occur in the extreme proximal portion of the esophageal wall, these are thought to represent a contribution of fibers from the inferior pharyngeal constrictor muscle. Smooth muscle organized into inner circular and outer longitudinal layers forms the distal half of the esophageal musculature. A mixture of skeletal and smooth muscle cells occurs in between. Motor end plates are most numerous in the proximal end of the esophageal musculature and progressively decrease in number distally. This decrease corresponds to the decrease in skeletal muscle fibers. Likewise, perikarya and ganglia of the myenteric plexus increase in number distally as the amount of smooth muscle in the esophageal wall increases.

Acknowledgments:

Figs. 1, 3 (bottom right), 8 (top), courtesy of and from: Krause, W.J. and J.H. Cutts (1992) Development of the Digestive System in the North American Opossum (*Didelphis virginiana*). Adv. Anat. Embryol. Cell Biol. 125:1-148.

Figs. 2 (bottom), 3 (top), 4, 5 (top), 6 (top left and bottom), 8 (bottom), courtesy of and from: Krause, W.J., J.H. Cutts and C.R. Leeson (1976) The postnatal development of the alimentary canal in the opossum. I. Esophagus. J. Anat. 122:293-314.

Fig. 5 (center), courtesy of and from: Marklin, G.F., W.J. Krause, and J.H. Cutts (1978) Structure of the esophagus in the adult opossum, *Didelphis virginiana*. Anat. Anz. 145:349-361.

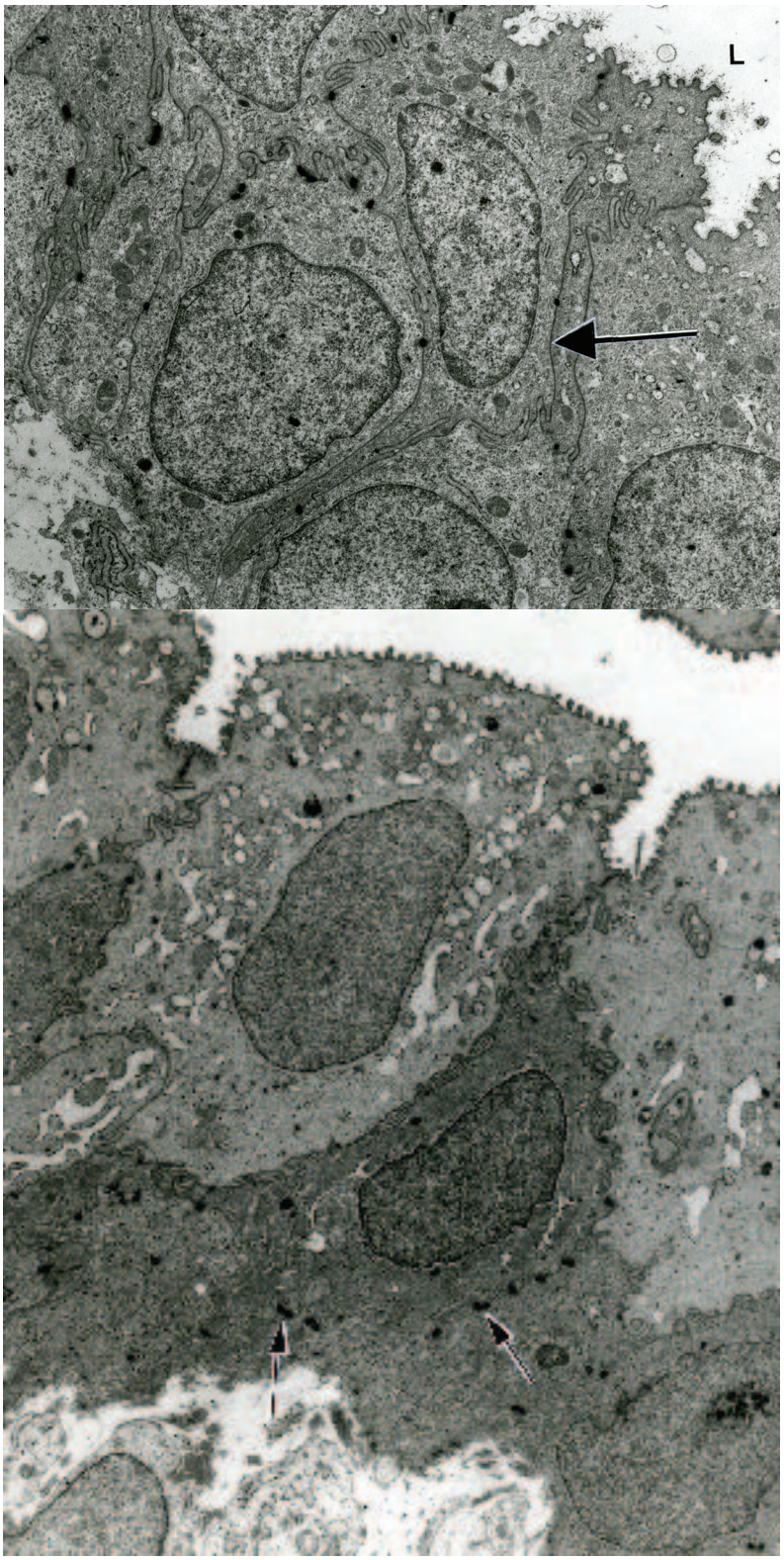

Fig.1. (*Above*). Occasional cells are observed within the esophageal epithelium of the newborn opossum that extend from the basal lamina to the lumen (arrow) presenting a pseudostratified appearance. The esophageal lumen (L) is to the upper right. TEM X 7,000. (*Below*). The esophageal epithelium of an opossum one week postnatal is made up of two distinct layers: a basal layer of small, irregular, dense cells and a surface layer of light staining columnar cells. Numerous desmosomes (arrows) occur between basal cells. TEM X 5,000.

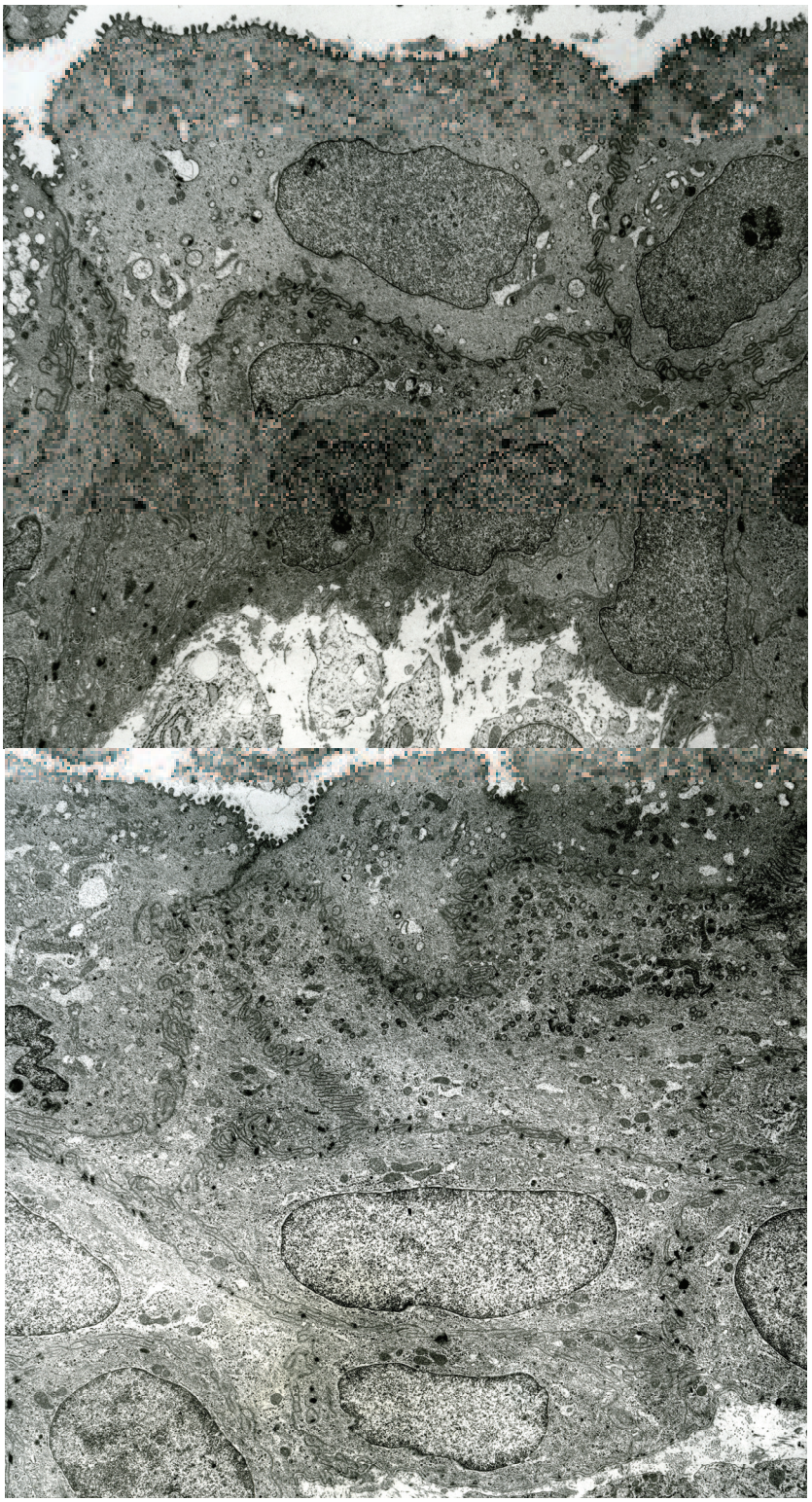

Fig. 2. (*Above*). Surface cells of the esophageal epithelium begin to flatten during the second postnatal week but continue to show stubby microvilli and small cytoplasmic vesicles. TEM X 5,000. (*Below*). By the end of postnatal week two the esophageal epithelium is of greater depth and component cells show an increase in fine cytoplasmic filaments as well as vesicles. TEM X 5,000.

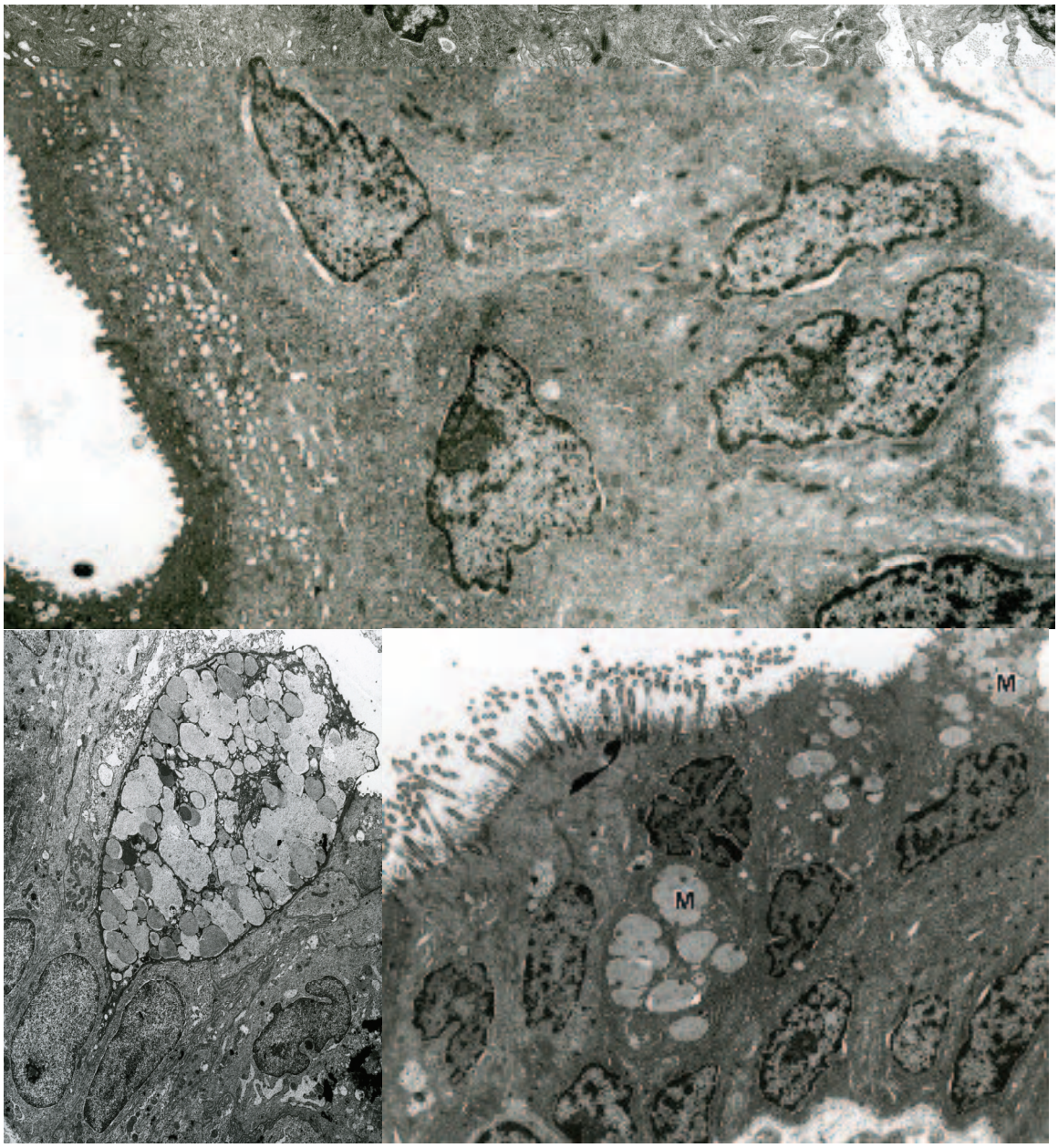

Fig. 3. (*Above*). The majority of surface cells of the esophageal epithelium become flattened, contains numerous vesicles, and show an increase in density by the end of the third postnatal week. TEM X 5,400. (*Below left*). A portion of a goblet cell found within the esophageal lining epithelium of an opossum three weeks postnatal. TEM X 4,000. (*Below right*). A region of esophageal epithelium from a three-week postnatal opossum exhibits both ciliated cells and cells containing mucin (M) granules. TEM X 4,000.

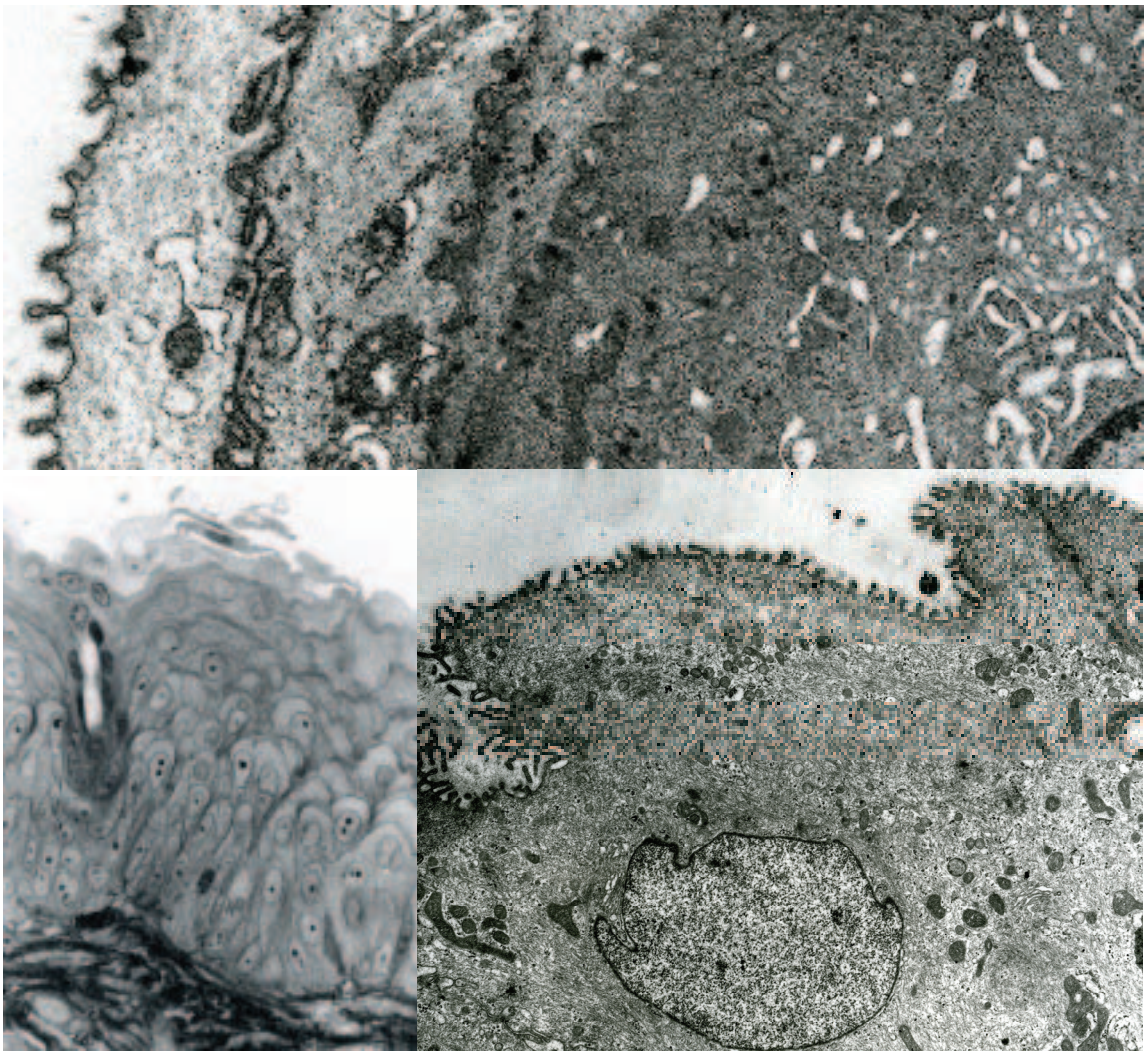

Fig. 4. (*Above*). By the end of the ninth week postnatal cells lining the esophageal lumen continue to exhibit short, stubby microvilli covered by a glycocalyx. The cytoplasm is electron-lucent and contains numerous fine cytoplasmic filaments but few organelles. Cells of the esophageal epithelium located further from the lumen are more electron-dense and contain a larger number of organelles. TEM X 5000. (*Below left*). The esophageal epithelium has increased considerably in depth by the eleventh postnatal week and the surface most cells continue to retain nuclei. The duct of an esophageal gland is shown coursing through the epithelium near the left margin of the photomicrograph. LM X 375. (*Below right*). An individual surface cell from the esophageal epithelium of an eleven-week opossum contains numerous cytoplasmic filaments, scattered vesicles and organelles. Its luminal cell membrane continues to exhibit stubby microvilli covered by a glycocalyx. TEM X 5,000.

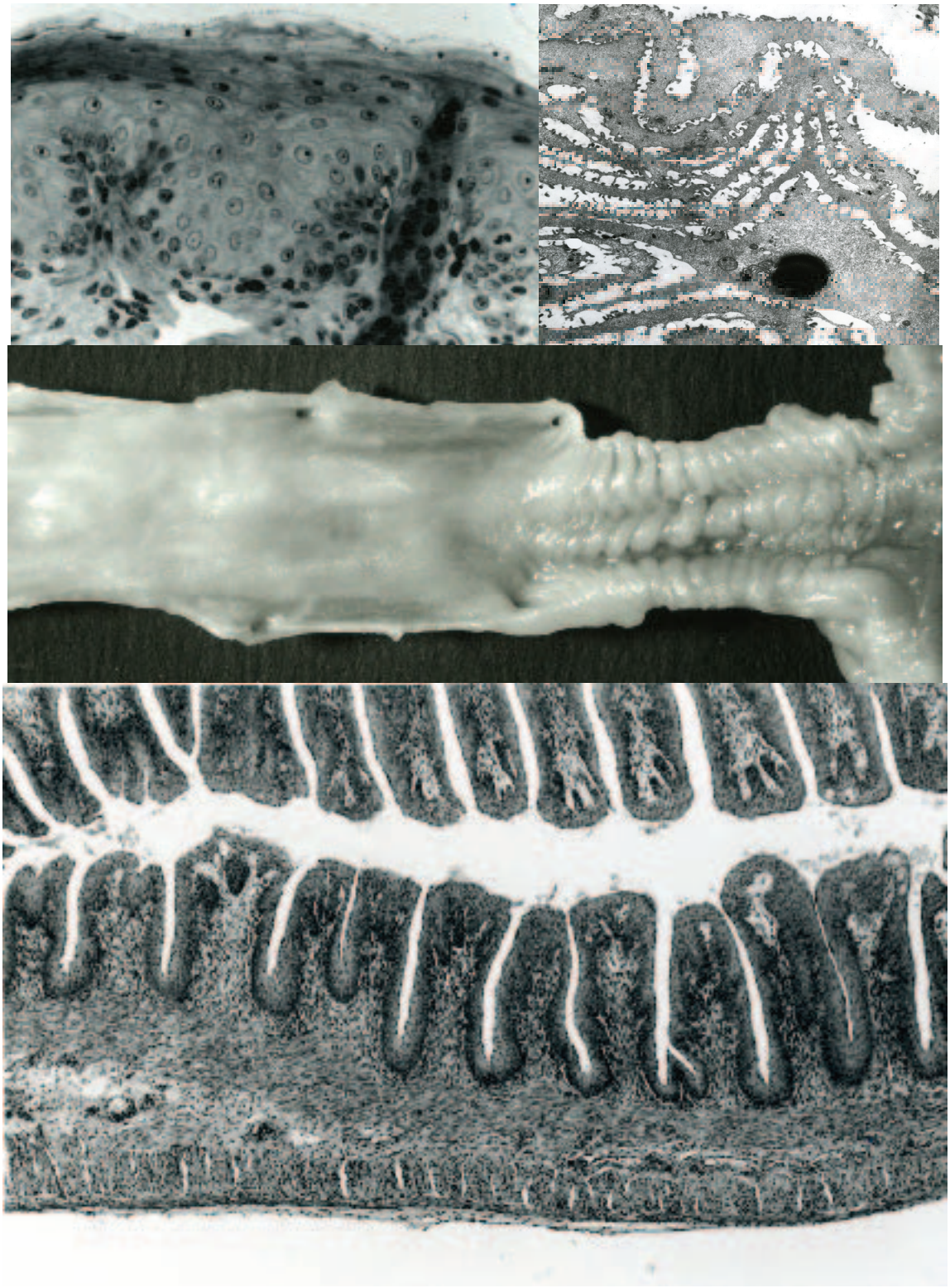

Fig. 5. (*Above left*). A micrograph illustrates the esophageal epithelium of a juvenile opossum. Note the connective tissue papillae projecting into the epithelium and duct of an esophageal gland passing through the epithelium. LM X 200. (*Above right*). Sloughing surface cells from the esophageal epithelium of a juvenile opossum. TEM X 4,000. (*Center*). The distal end of the opossum esophagus exhibits numerous transverse folds. Juvenile. X 5. (*Bottom*). A histological section illustrates the permanent transverse folds characteristic of the distal opossum esophagus. Juvenile. LM X 50.

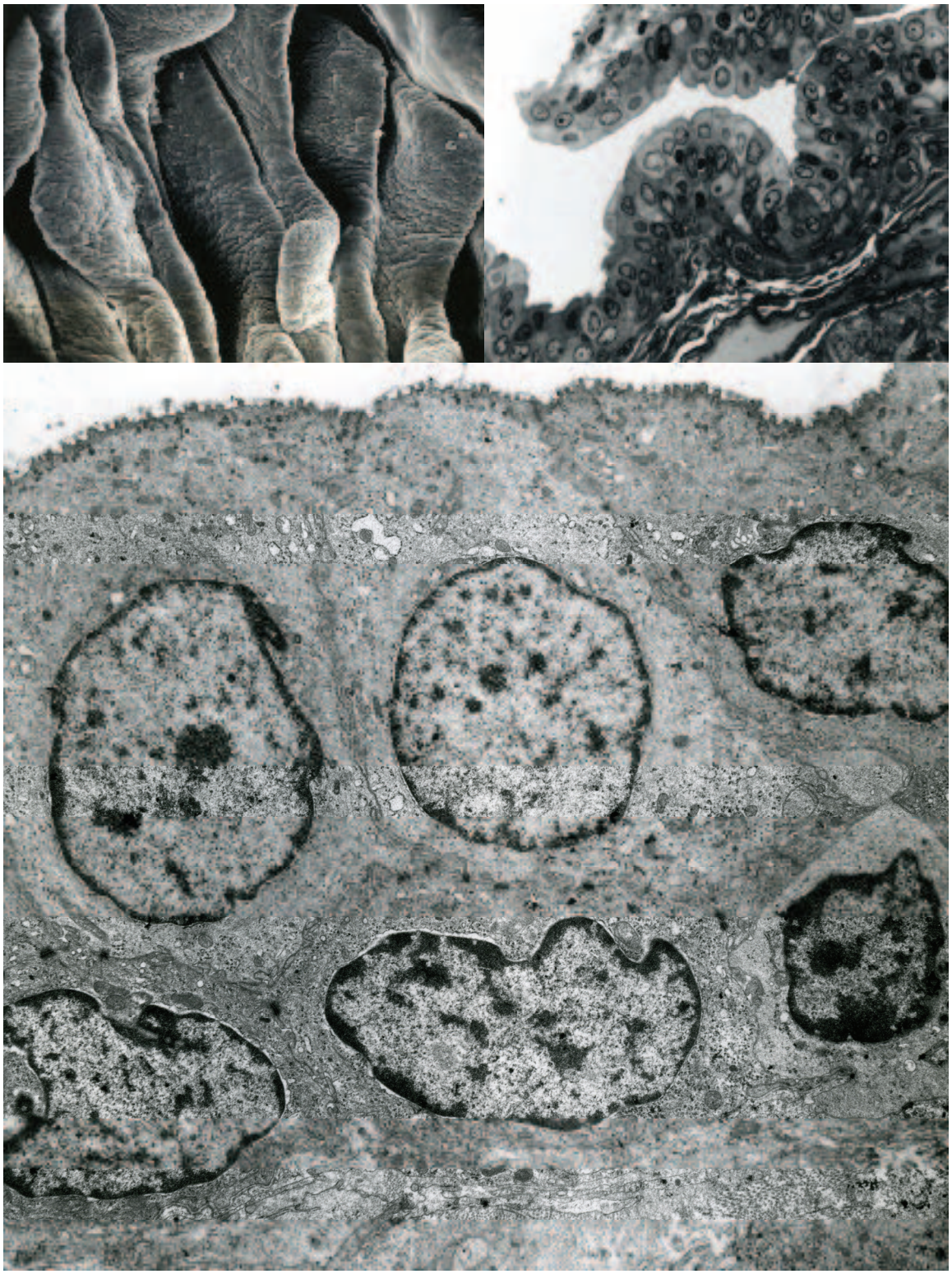

Fig. 6. (*Above left*). The transverse folds of the distal opossum esophagus as seem by scanning electron microscopy. Cell apices appear round rather than elongate as in other regions of the esophagus. Juvenile. SEM X 200. (*Above right*). The esophageal epithelium lining the depths of the transverse folds is two cell layers thick, light staining, and immature in appearance. Ciliated cells may be present. Adult. LM X 400. (*Below*). The esophageal epithelium from the region of the transverse folds consists of two strata. Small electron-dense vesicles occur in the apical cytoplasm of the columnar surface cells. Adult. TEM X 45,000.

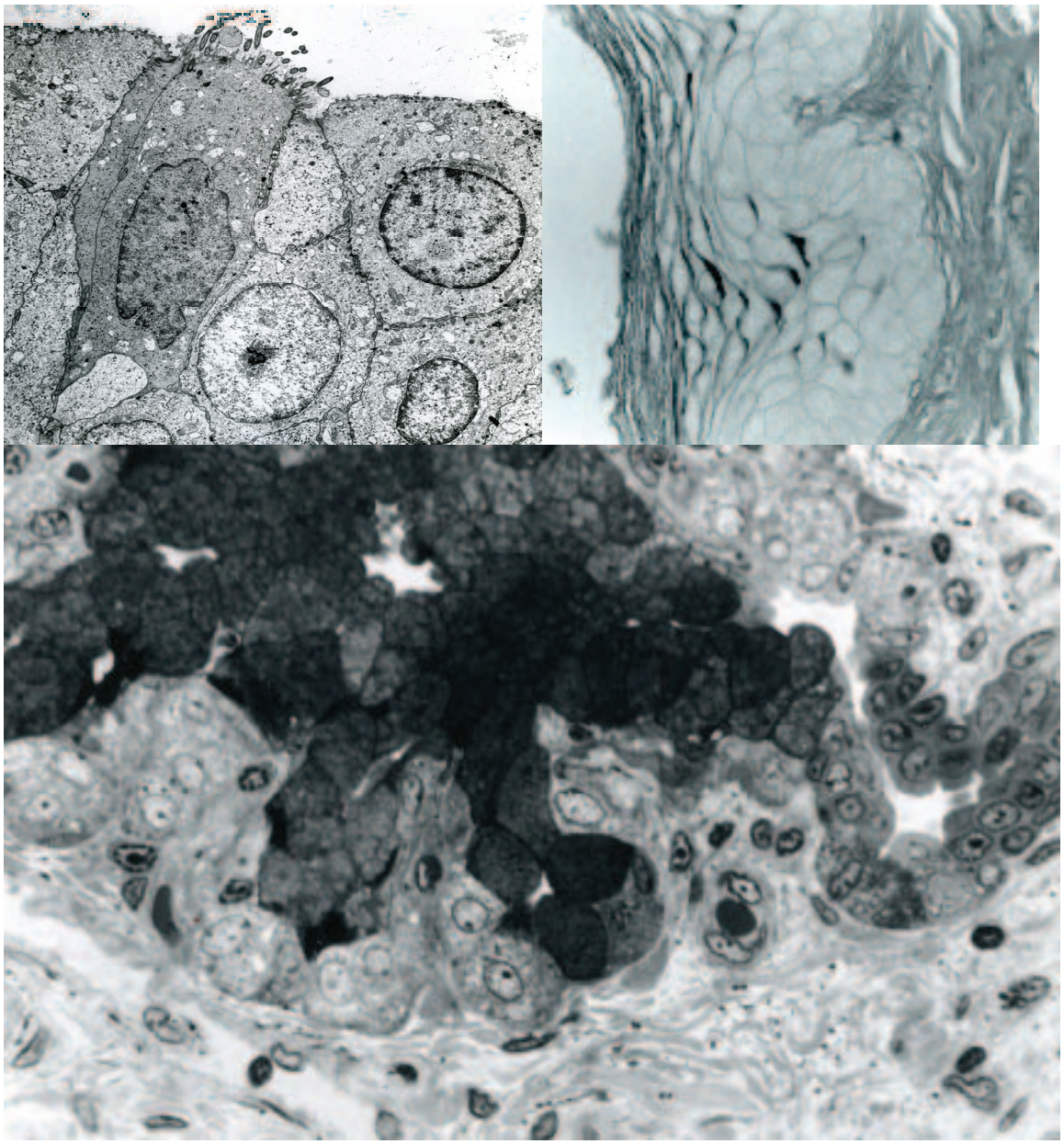

Fig. 7. (*Above left*). A ciliated cell found in the esophageal epithelium lining the region of the transverse folds. Adult opossum. TEM X 4,000. (*Above right*). Areas of intense PAS positive staining (dark) often occur within the cytoplasm of cells forming the central region of the esophageal epithelium. Adult. LM X 400. (*Below).* A region through the esophageal glands of an adult opossum illustrates that the secretory units consist of two distinct cell types. The majority are mucous cells that exhibit dense pyknotic nuclei confined to the basal cytoplasm the remainder of which is filled with mucin granules. Large light staining cells, with centrally placed, round nuclei also are observed that appear limited in distribution to the ends of the secretory units. A duct draining the esophageal gland is shown at the right center of the photomicrograph. LM X 400.

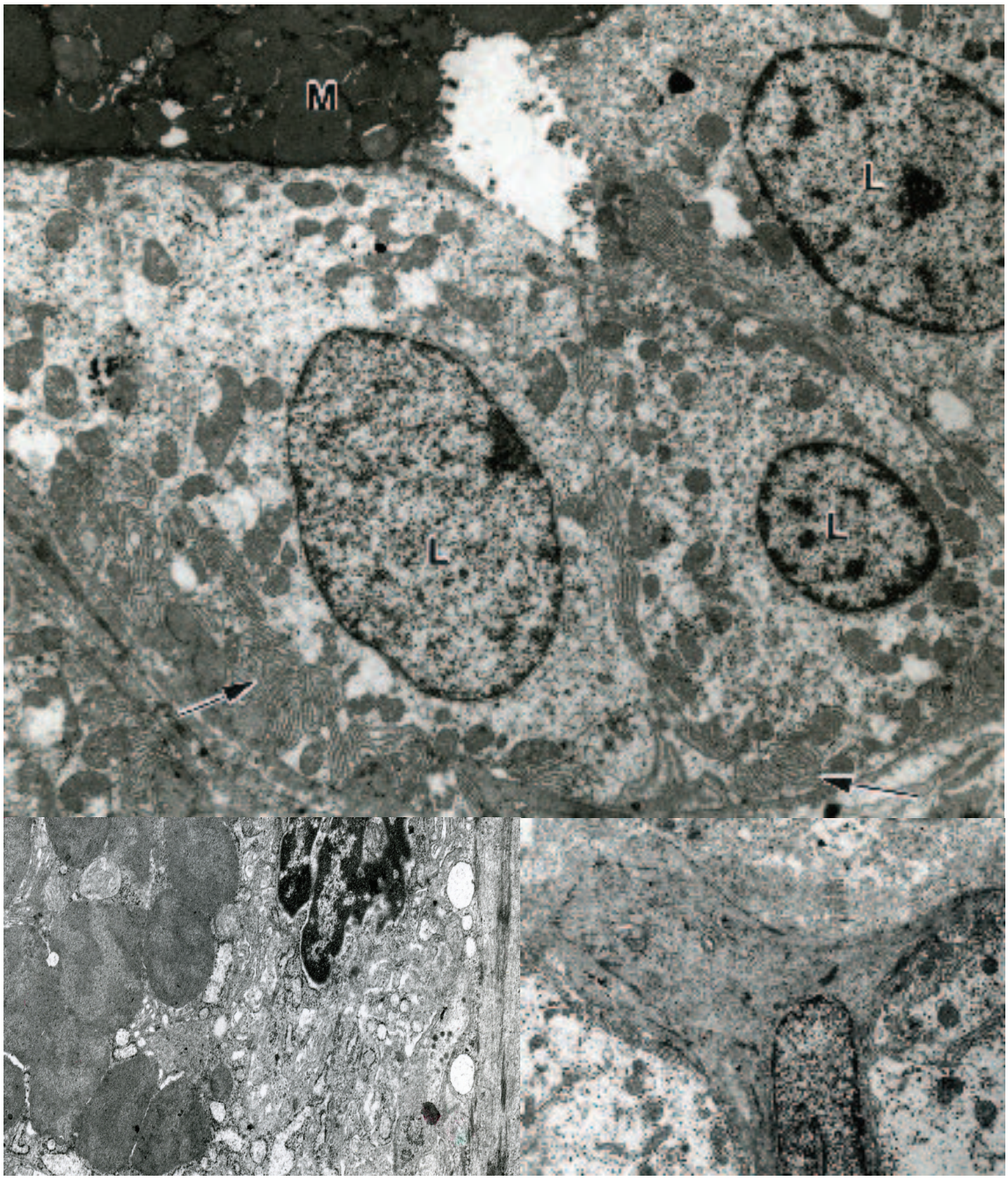

Fig. 8. (*Above*). The large light cells (L) of the opossum esophageal glands exhibit an electron-lucent cytoplasm filled with mitochondria. The light cells are further characterized by extensive infolding of the basolateral cell membranes (arrows) and intercellular secretory canaliculi. A portion of the apical region of an adjacent mucous cell (M) is shown at the upper left of the electron micrograph. Adult opossum. TEM X 8,000. (*Below left*). The basal region of a mucous cell from an opossum esophageal gland illustrates the dense irregular nucleus. The secretory (mucin) granules show an irregular pattern of electron density. A portion of a myoepithelial cell is shown at the extreme right of the illustration. Adult opossum. TEM X 6,000. (*Below right*). A segment of a myoepithelial cell illustrates its nucleus as well as two cytoplasmic processes. The myoepithelial cell embraces three adjacent light cells of an opossum esophageal gland. Adult opossum. TEM X 4,000.

Chapter 20. Stomach

Synopsis:

Stomach formation commences as a distal expansion of the esophagus during the first part of the tenth prenatal day. By the twelfth prenatal day it is lined by a simple columnar epithelium with the remainder of the gastric wall being formed by mesenchymal tissue. Scattered lipid droplets of variable size are found within the cytoplasm of the simple columnar gastric lining epithelium of the newborn. The lipid droplets continue to increase in number and size through the second postnatal week, decrease by the end of the third postnatal week and are an infrequent observation by the end of the fourth postnatal week. Mucin granules may be present in the apical cytoplasm of the gastric lining epithelial cells during the first four weeks of postnatal life, but do not form significant numbers until after this time. These secretory granules consist primarily of neutral glycoproteins. Glands of the stomach (cardiac, oxyntic, pyloric) appear during the postnatal period.

The oxyntic glands are the first to differentiate. Both parietal cells and enteroendocrine cells are present within the gastric lining epithelium of the fundus late in the first postnatal day. The oxyntic glands and their associated foveolae develop simultaneously and begin as clefts within the gastric mucosa in regions that contain parietal cells. Short but definite oxyntic glands are present by the end of the first postnatal week and consist of three cell types: parietal, enteroendocrine, and undifferentiated cells. The latter generally assume a columnar shape and are characterized by numerous free ribosomes. Parietal cells of the newborn opossum exhibit well-developed intracellular canaliculi and a tubulovesicular component of associated cytoplasmic membranes. Parietal cell mitochondria are rich in succinate dehydrogenase at this time. Newborn parietal cells respond to exogenous pentagastrin by producing hydrochloric acid suggesting parietal cell function. The increase in length of the oxyntic glands prior to the seventy fifth postnatal day is due largely to an increase in the number of parietal cells. Chief (pepsinogen-containing) cells do not appear in the oxyntic glands until about the seventy fifth postnatal day and are localized at the bottoms of the oxyntic glands. Opossum chief cells exhibit ultrastructural features typical of those found in other mammals. Pepsinogen- and prochymosin (prorennin)- immunoreactivity is observed however, throughout the early postnatal period in an undifferentiated cell type prior to the appearance of chief cells. Thereafter, primarily the chief cell population produces both gastric proteinases.

The cardiac and pyloric glands develop late in the opossum and begin to differentiate by about the fourth postnatal week but do not become obvious structures until the seventh week postnatal. Argyrophil cells appear scattered within the simple columnar gastric lining epithelium by the eleventh prenatal day and are closely associated with the glands of the stomach as they develop. Five types of enteroendocrine cells have been demonstrated within the argyrophil cell population of the newborn opossum: gastrin-, bovine pancreatic polypeptide (BPP)-, glucagon-, somatostatin-, and serotonin-immunoreactive cells. Gastrin-immunoreactive cells are restricted in distribution to the pyloric glands and show the most prominent increase early in development. Glucagon- and BPP-immunoreactivity are restricted to the oxyntic glands during development and their numbers decrease with age. Somatostatin- and serotonin-immunoreactive cells shift from the cardiac and fundic regions to the pyloric region of the stomach during organogenesis attaining an adult distribution soon after weaning. It is only after the oxyntic glands have been established that the number

of somatostatin-immunoreactive cells equals the number of gastrin cells. The serotonin-, somatostatin- and gastrin-immunoreactive cells are primarily restricted in distribution to a narrow band at the junction between the isthmus of the pyloric glands and the overlying foveolae late in the postnatal period. The muscularis mucosae within the gastric wall is incomplete at birth and consists of only a thin layer of myoblasts. It rapidly increases in thickness to reach a constant width of about 14 μM at the end of the fourth postnatal week. Projections of smooth muscle cells develop that extend from the muscularis mucosae into the lamina propria to form a unique net-like arrangement about individual oxyntic glands. The lamina propria is formed by a delicate connective tissue that contains abundant mast cells, fibroblasts, lymphocytes, macrophages, and eosinophils. The latter are particularly numerous following weaning in response to infestations of gastric round worms and other parasites that plague the opossum. The submucosa is unremarkable during development and consists of typical connective tissue cells, and reticular, collagenous, and elastic fibers embedded in an amorphous ground substance. Neurons constituting the submucosal plexus in the newborn are poorly developed but rapidly increase in number and size through the first four postnatal weeks. Following this period of organogenesis, neurons within the submucosal (Meissner's) plexus form a relatively stable population of cells. The muscularis externa consists only of a thin layer of myoblasts in the newborn opossum and is incompletely separated into outer and inner layers. The outer layer is discontinuous and is formed by a single layer of scattered myoblasts. In contrast, myoblasts of the inner layer form a complete investment around the stomach and is two to three cells in thickness. The muscularis externa is well established and organized into two complete layers by the end of the first postnatal week. As the muscularis externa increases in thickness during the remainder of the postnatal period, the inner layer remains the most prominent. A third innermost oblique layer is present but restricted to the proximal-most portion of the stomach. The primary period of smooth muscle proliferation occurs during the first four weeks with little increase in the total thickness of the muscularis externa. Hypertrophy is the major factor in establishing the total thickness of muscularis externa and begins immediately following the period of proliferation. The muscularis externa then undergoes a second increase in total thickness, which occurs between weaning and adulthood. The myenteric (Auerbach's) plexus is poorly developed initially, but subcomponents increase in size and number through the first four weeks of postnatal life. The neurons of the myenteric plexus constitute a relatively stable population during the remainder of organogenesis of the stomach. Thus, by the time the smooth muscle cell population is established, so are the elements of the myenteric plexus.

Acknowledgments:

Figs. 2 (top), 3, 4 (bottom), 5 (bottom), 6 (top), 7 (top), 8 (top), 9 (top), 10 (bottom), 11, 12, 13 (top), 14, 15 (top), courtesy of and from: Krause, W.J., J.H. Cutts and C.R. Leeson (1976) The postnatal development of the alimentary canal in the opossum. II. Gastric mucosa. J. Anat. 122:499-519.

Figs. 2 (bottom), 6 (bottom), 9 (bottom), 15 (bottom) and 16, courtesy of and from: Krause, W.J. and J.H. Cutts (1992) Development of the Digestive System in the North American Opossum (*Didelphis virginiana*). Adv. Anat. Embryol. Cell Biol. 125:1-148.

Figs. 17 and 18, courtesy of and from: Krause, W.J., J. Yamada, J.H. Cutts and A. Andrén. (1987). An immunohistochemical survey of gastric proteinase (pepsinogen and prochymosin)-containing cells in the stomach of the developing opossum (*Didelphis virginiana*). J. Anat. 154:259-263.

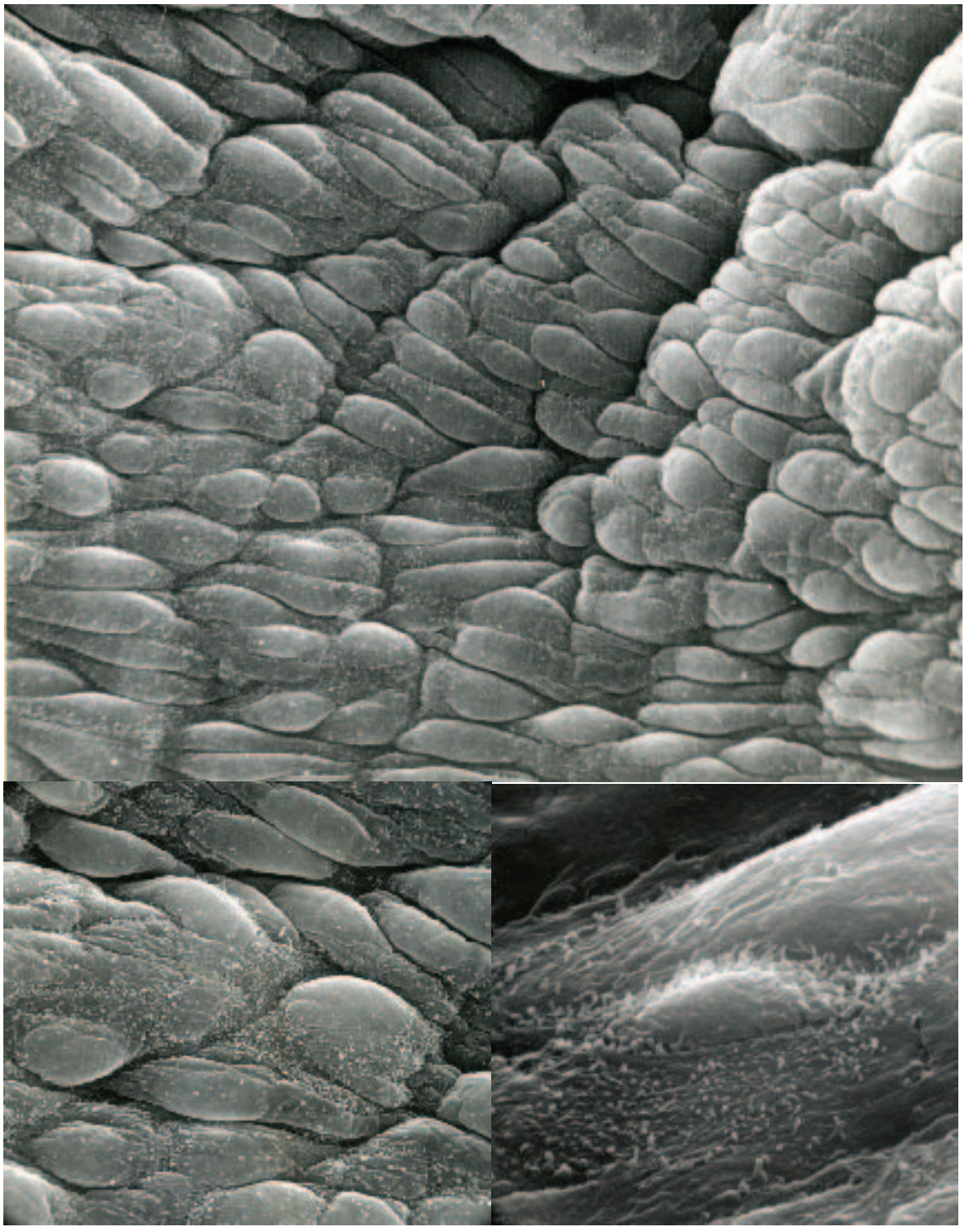

Fig. 1. (*Above*). The gastric mucosal surface of the newborn opossum appears flat and shows few mucosal folds. SEM X 800. (*Below left*). At increased magnification microvilli appear concentrated near cell boundaries. SEM X 2000. (*Below right*). The round profile of a cell within the gastric mucosal surface that is associated with abundant microvilli is thought to be a parietal cell. Newborn opossum. SEM X 5000.

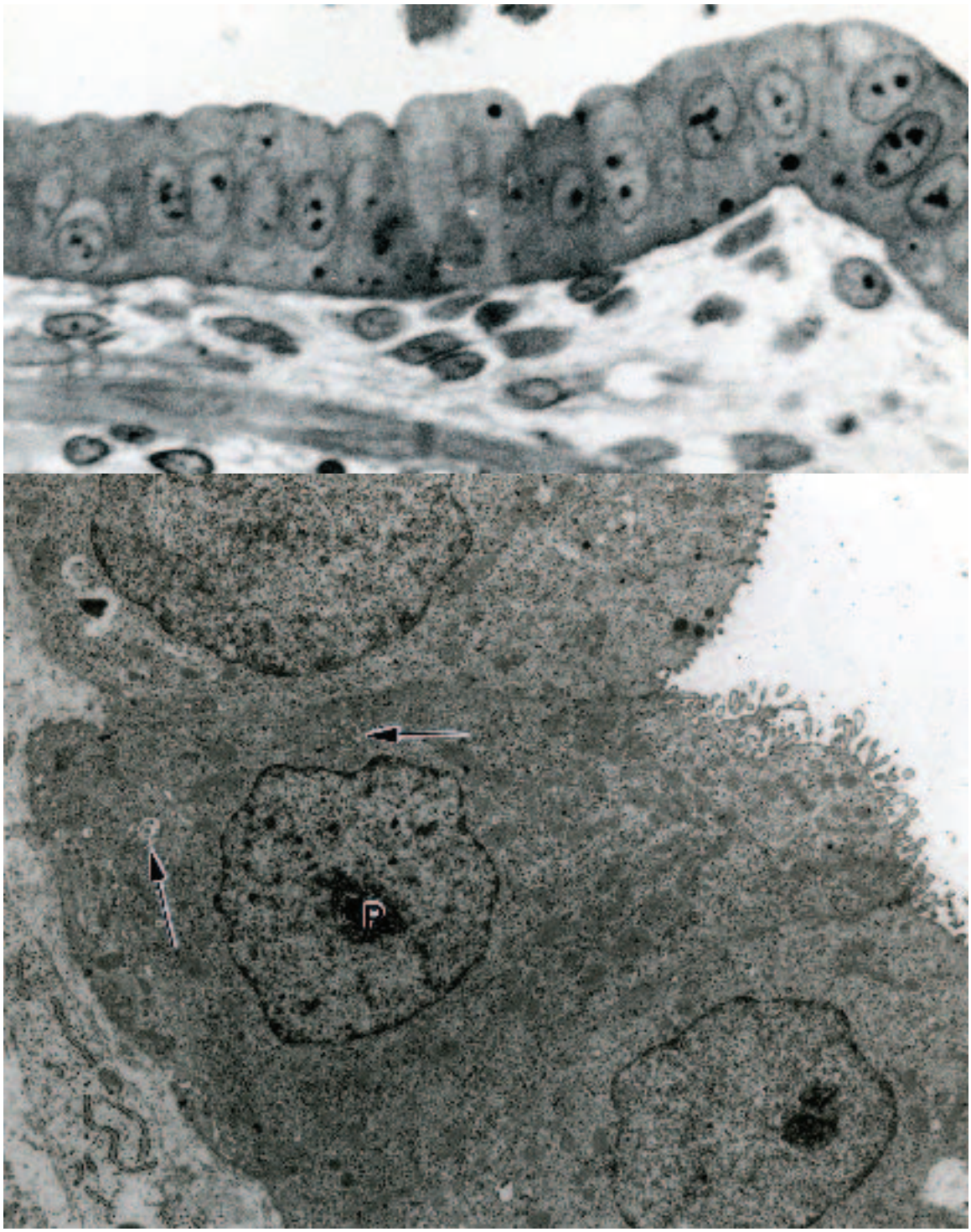

Fig. 2. (*Above*). The epithelium lining the gastric surface of the newborn opossum is simple columnar that contains scattered lipid droplets. Foveolae and glands have yet to develop. Myoblasts of the forming muscularis externa can be observed near the bottom of the photomicrograph. LM X 500. (*Below*). A micrograph illustrates a recently differentiated parietal cell (P) lying within the gastric lining epithelium of a newborn opossum. Note the presence of canaliculi (arrows) and the projection of microvilli into the gastric lumen. TEM X 6000.

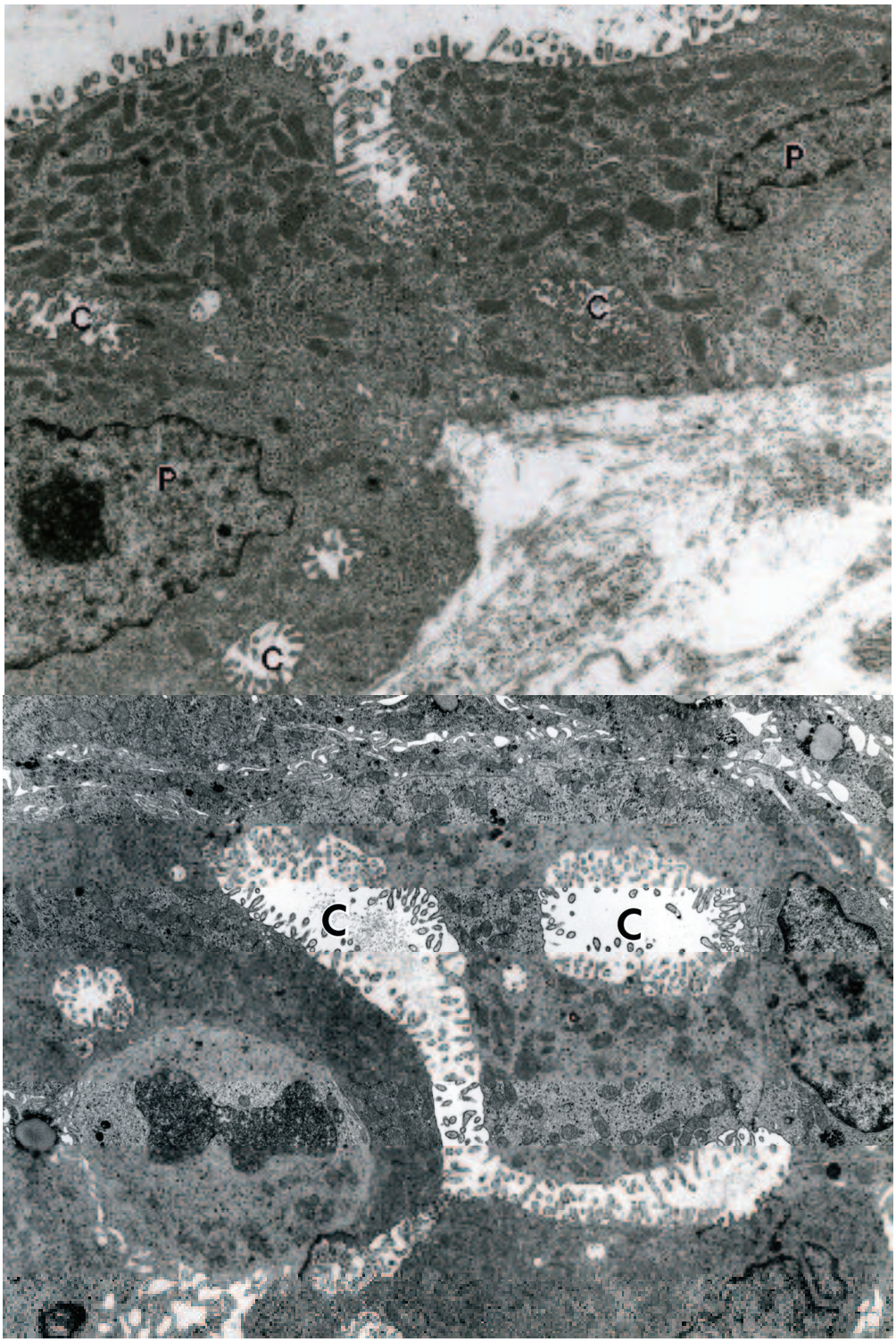

Fig. 3. (*Above*). Regions of the gastric lumen of the newborn opossum are often lined by parietal cells (P) that show numerous mitochondria and well developed canaliculi (C). Note the abundance of microvilli projecting into the gastric lumen. TEM X 5000. (*Below*). An electron micrograph illustrates a cluster of parietal cells from the newborn opossum stomach following stimulation by 6 μg/Kg of pentagastrin. Note the expanded nature of the canaliculi (C) and the mitotic figure at the lower left. TEM X 5000.

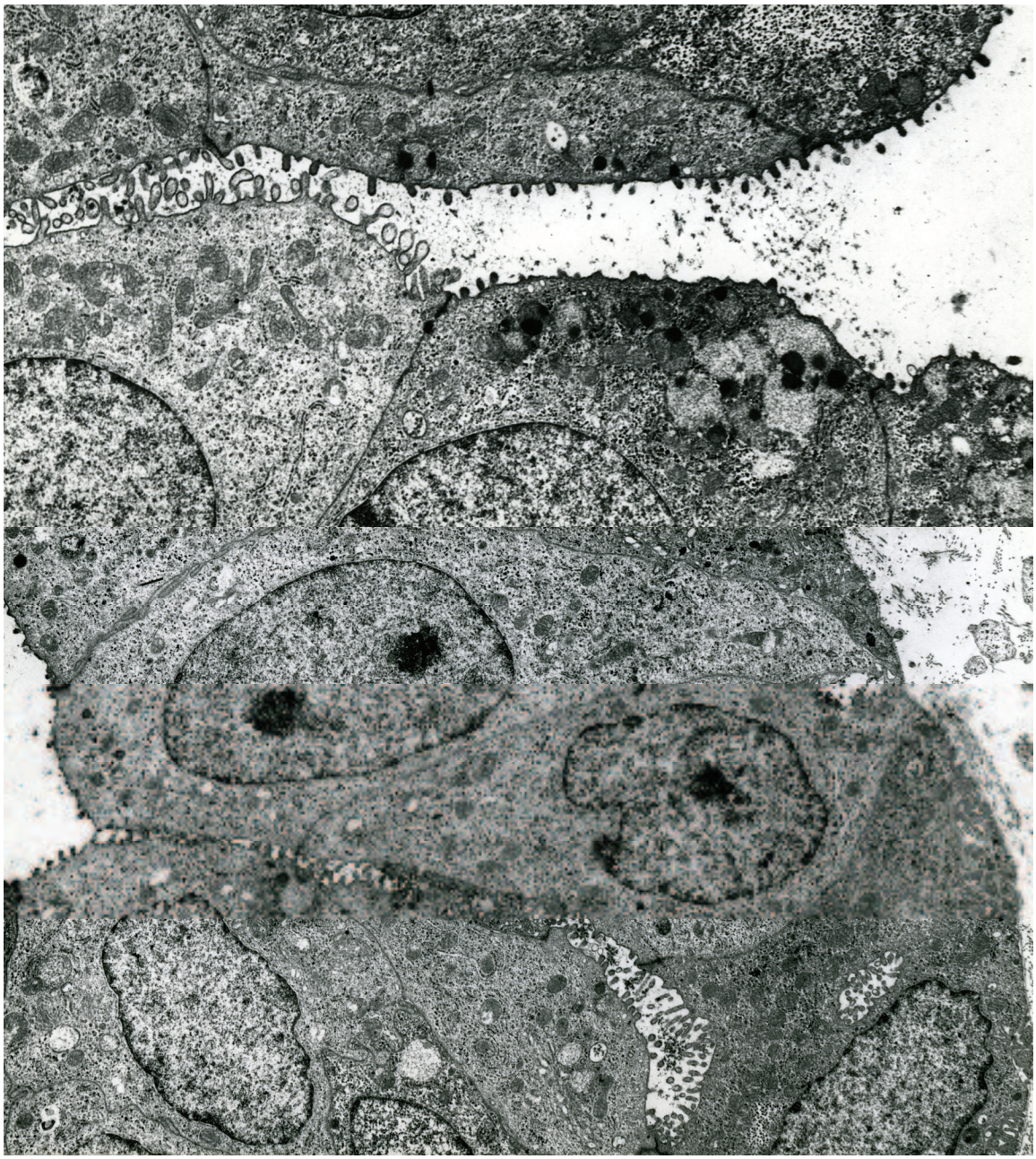

Fig. 4. (*Above*). A region of shallow gastric infolding exhibits a surface lining cell (right) and an adjacent parietal cell (left). The differentiating parietal cell shows numerous broad microvilli projecting into the lumen. The gastric lining epithelial cell contains several secretory granules that exhibit regions of electron density within a flocculent material. Newborn opossum. TEM X 7000. (*Below*). A profile through a gastric cleft of newborn opossum stomach demonstrates columnar shaped surface lining cells and a parietal cell at the base of the invagination. The parietal cell exhibits a greater electron density and contains numerous mitochondria. TEM X 5000.

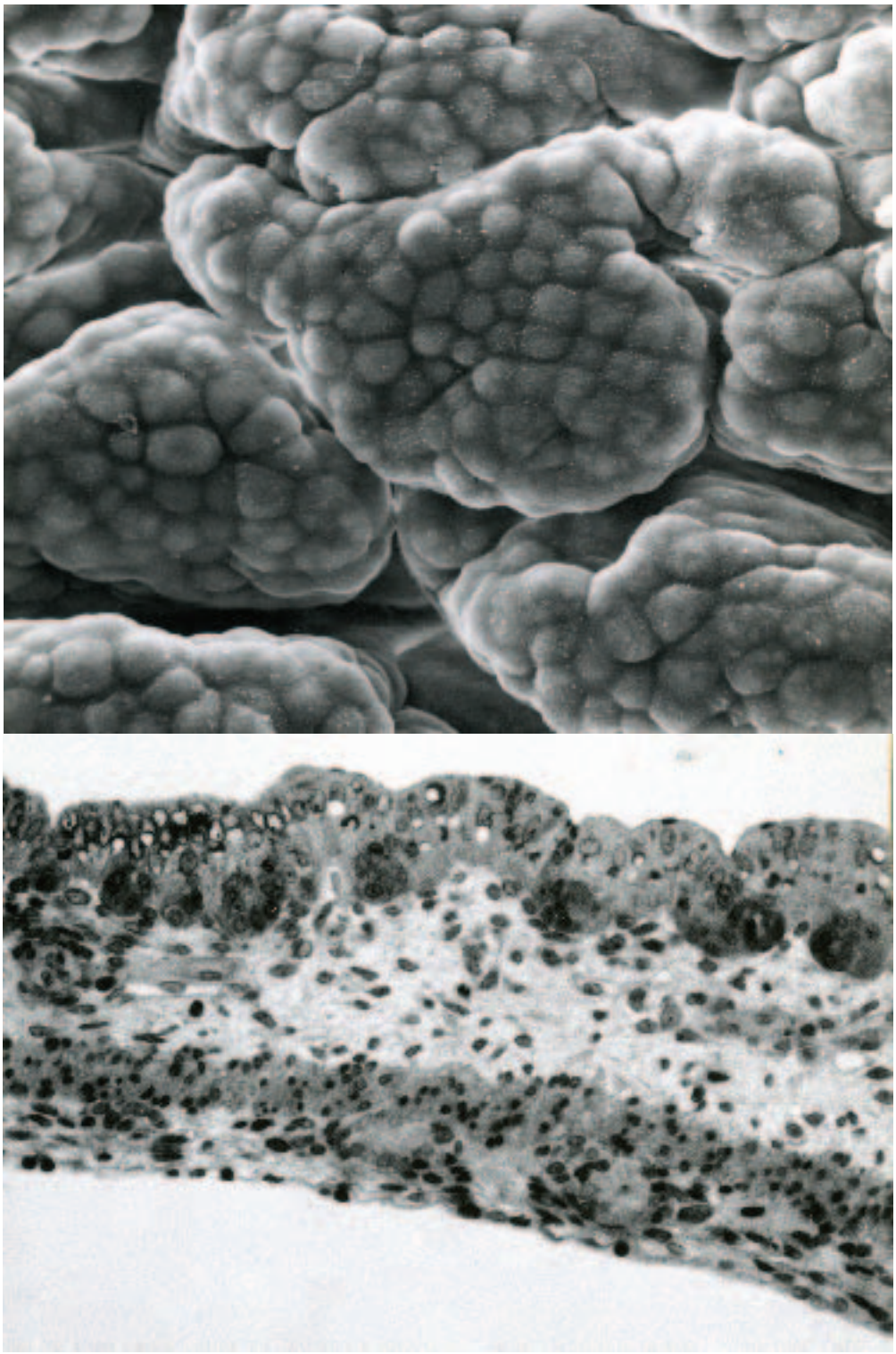

Fig. 5. (*Above*). The gastric mucosal surface of an opossum one week postnatal shows considerable folding. Note that the apices of the lining cells appear rounded in comparison to the elongated form observed in the newborn. SEM X 1000. (*Below*). A region of the stomach wall from an opossum one week postnatal shows the establishment of oxyntic glands and foveolae as well as the muscularis externa. LM X 300.

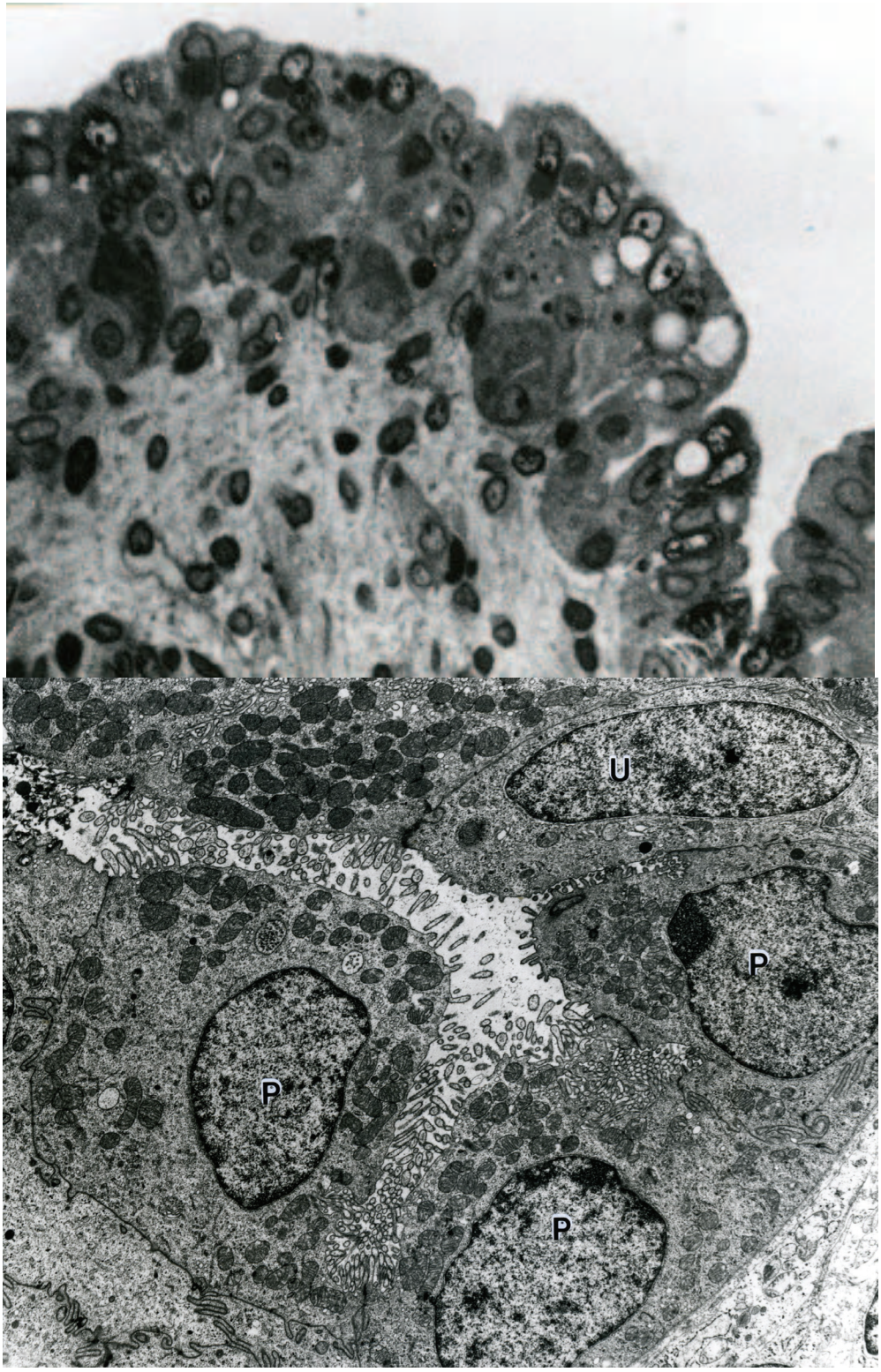

Fig. 6. (*Above*). The gastric mucosa of an opossum one week postnatal as seen at increased magnification illustrates the developing oxyntic glands in greater detail. Note the lipid droplets within the gastric lining epithelium. LM X 400. (*Below*). Three parietal cells (P) and an undifferentiated cell (U) lie at the bottom of an oxyntic gland from a week old opossum. TEM X 5000.

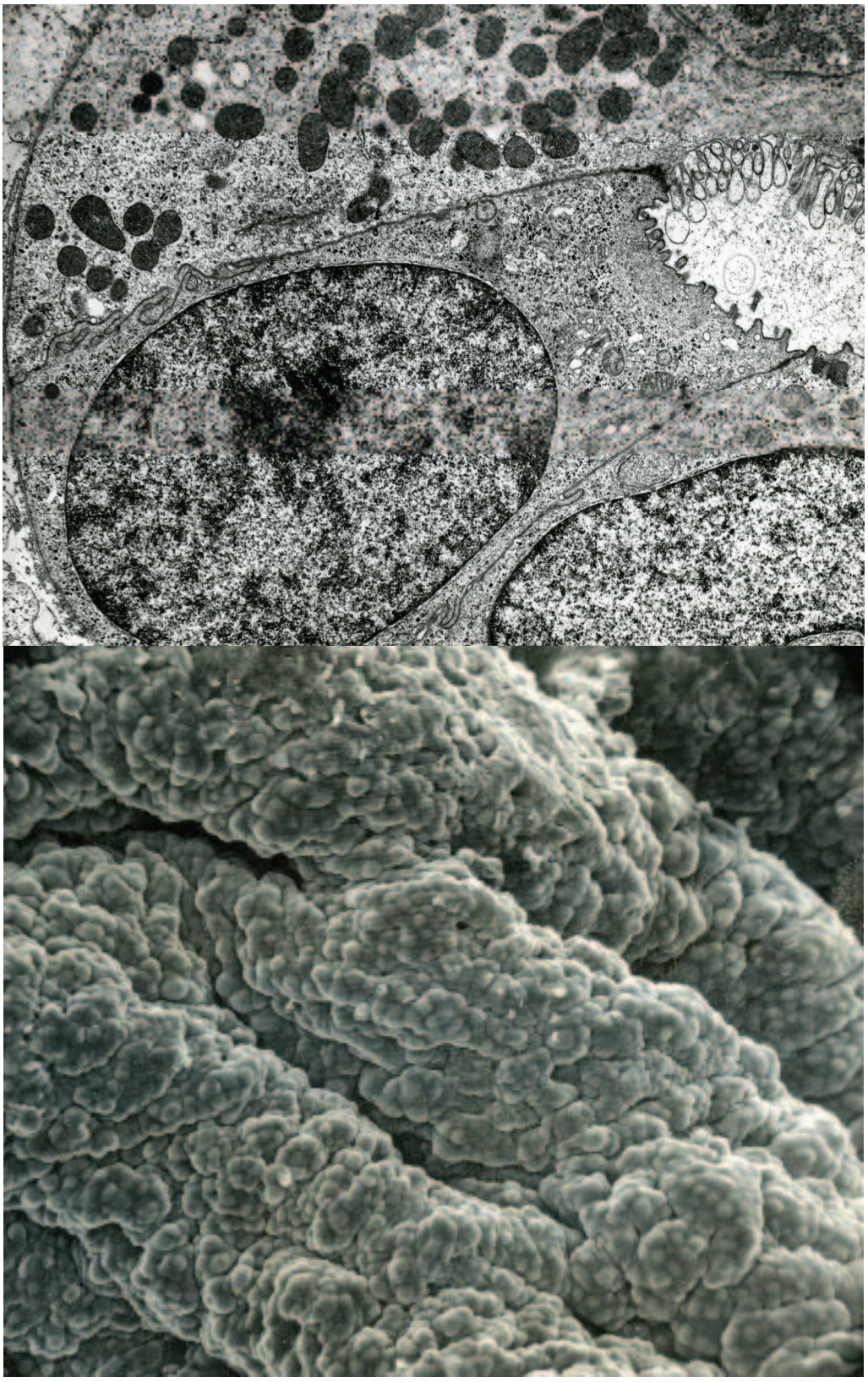

Fig. 7. (*Above*). A columnar shaped undifferentiated cell near the base of an oxyntic gland from an opossum one week postnatal. TEM X 7500. (*Below*). Surface features of the gastric mucosa from an opossum two weeks postnatal illustrate its irregular nature. SEM X 500.

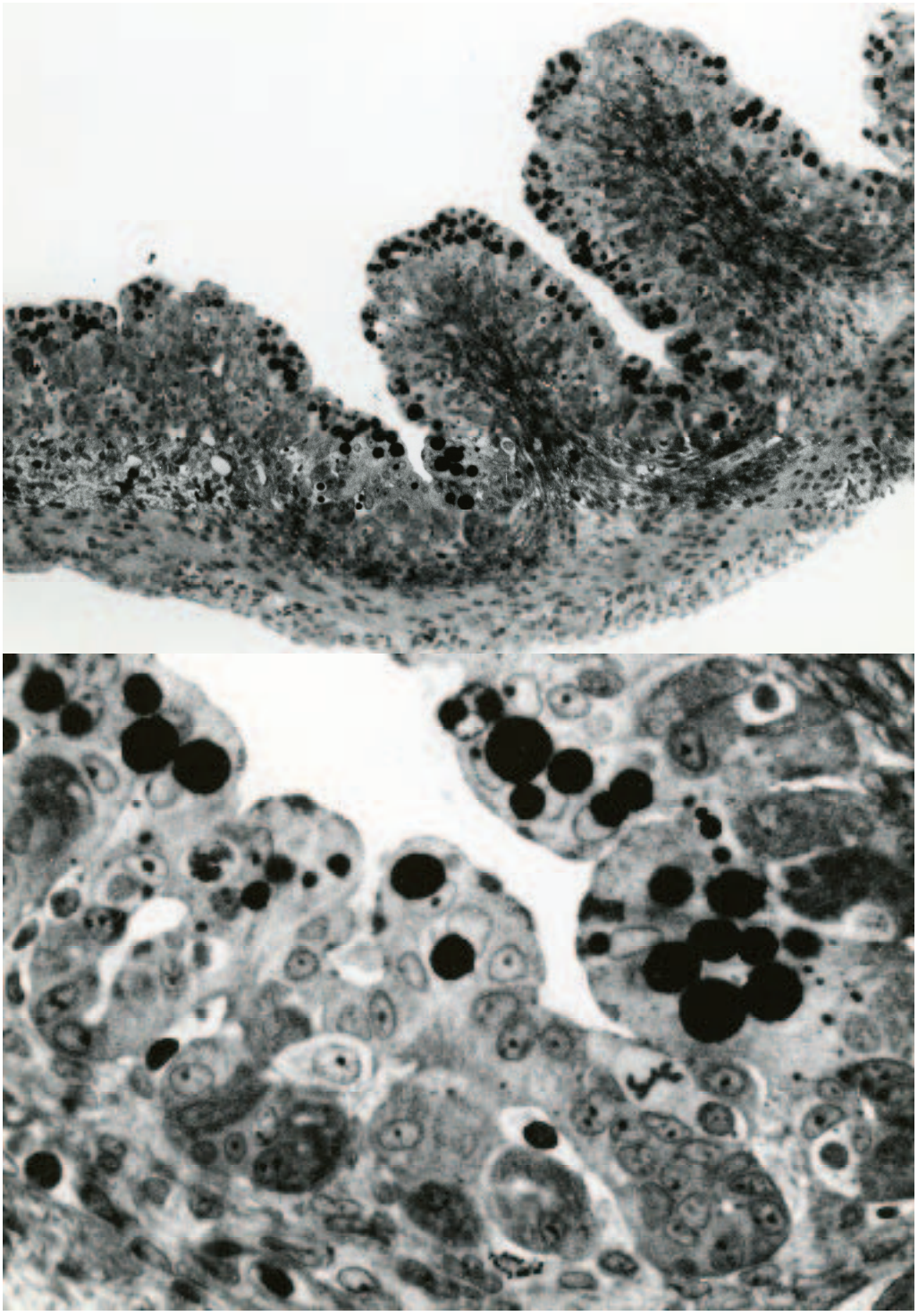

Fig. 8. (*Above*). The gastric mucosa of an opossum two weeks postnatal shows continued development of the oxyntic glands. The gastric lining epithelium shows a marked increase in the number of lipid droplets as compared to younger animals. LM X 150. (*Below*). When the gastric mucosa of the above specimen is examined at increased magnification several light staining cells thought to be enteroendocrine cells also are observed. LM X 400.

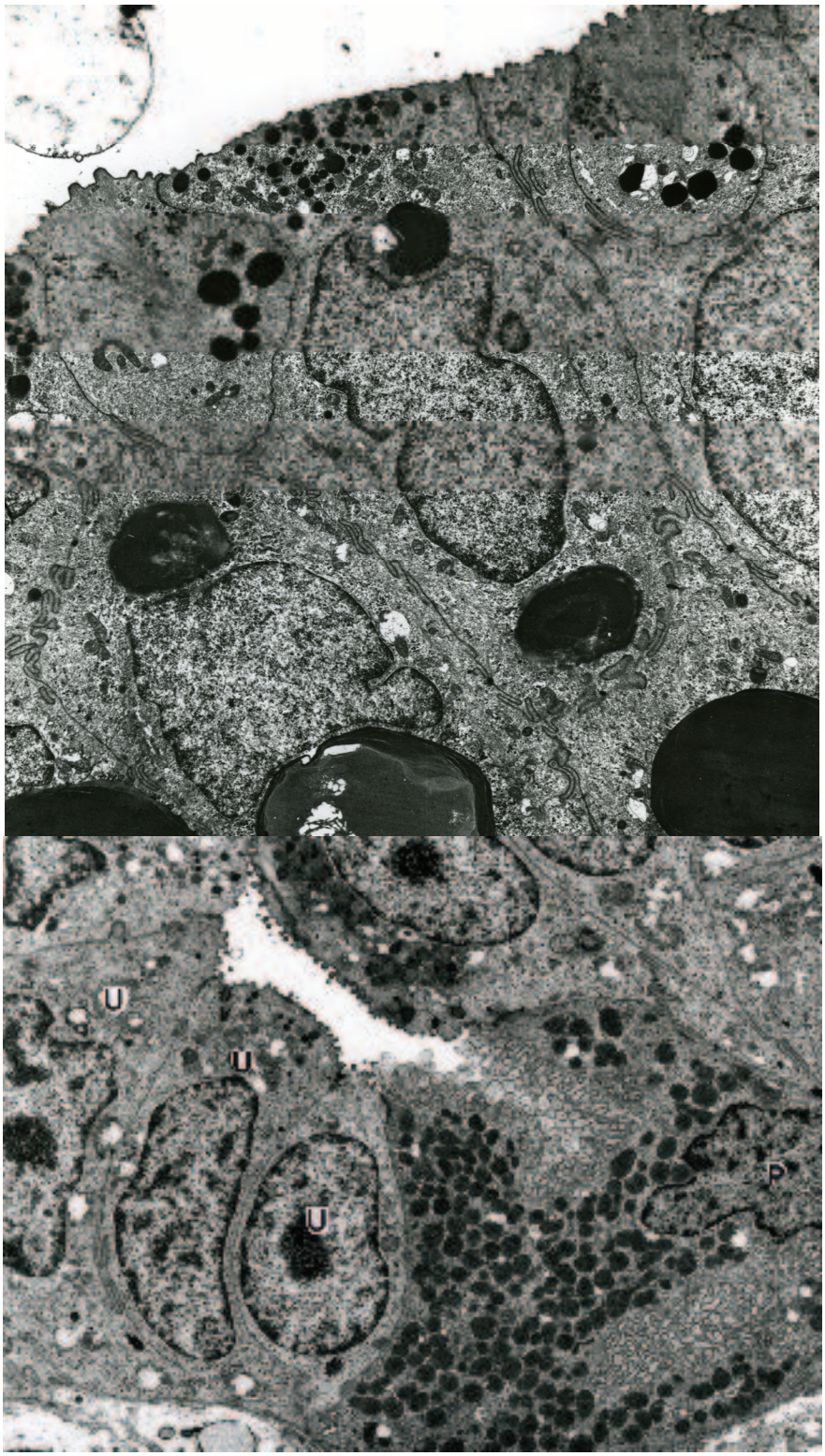

Fig. 9. (*Above*). A region of gastric lining epithelium from a two-week-old opossum illustrates numerous lipid droplets. A membrane does not limit the lipid droplets. The apices of two caveolated cells bordering the gastric lumen at the extreme left and right also are shown. TEM X 7500. (*Below*). A parietal cell (P) and three undifferentiated cells (U) occupy the bottom of an oxyntic gland. Opossum two weeks old. TEM. X 5000.

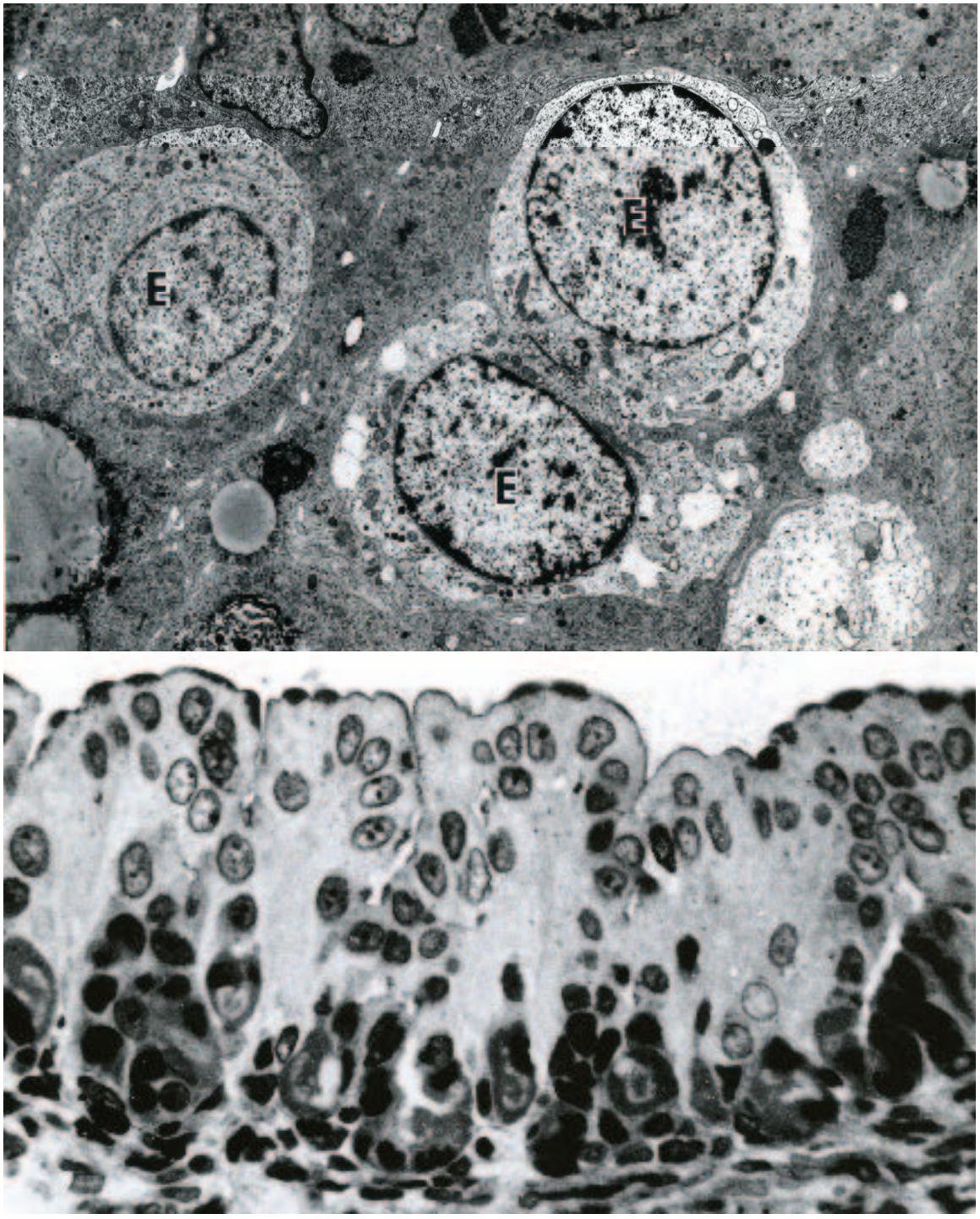

Fig. 10. (*Above*). Three unidentified enteroendocrine cells found within the gastric mucosa of an opossum two week old. TEM X 5000. (*Below*). The foveolae and oxyntic glands show continued expansion with the parietal cells being confined primarily to the bottoms of the glands. Gastric lining epithelial cells show markedly fewer lipid droplets and an increased number of mucin granules. Opossum three weeks postnatal. LM X 500.

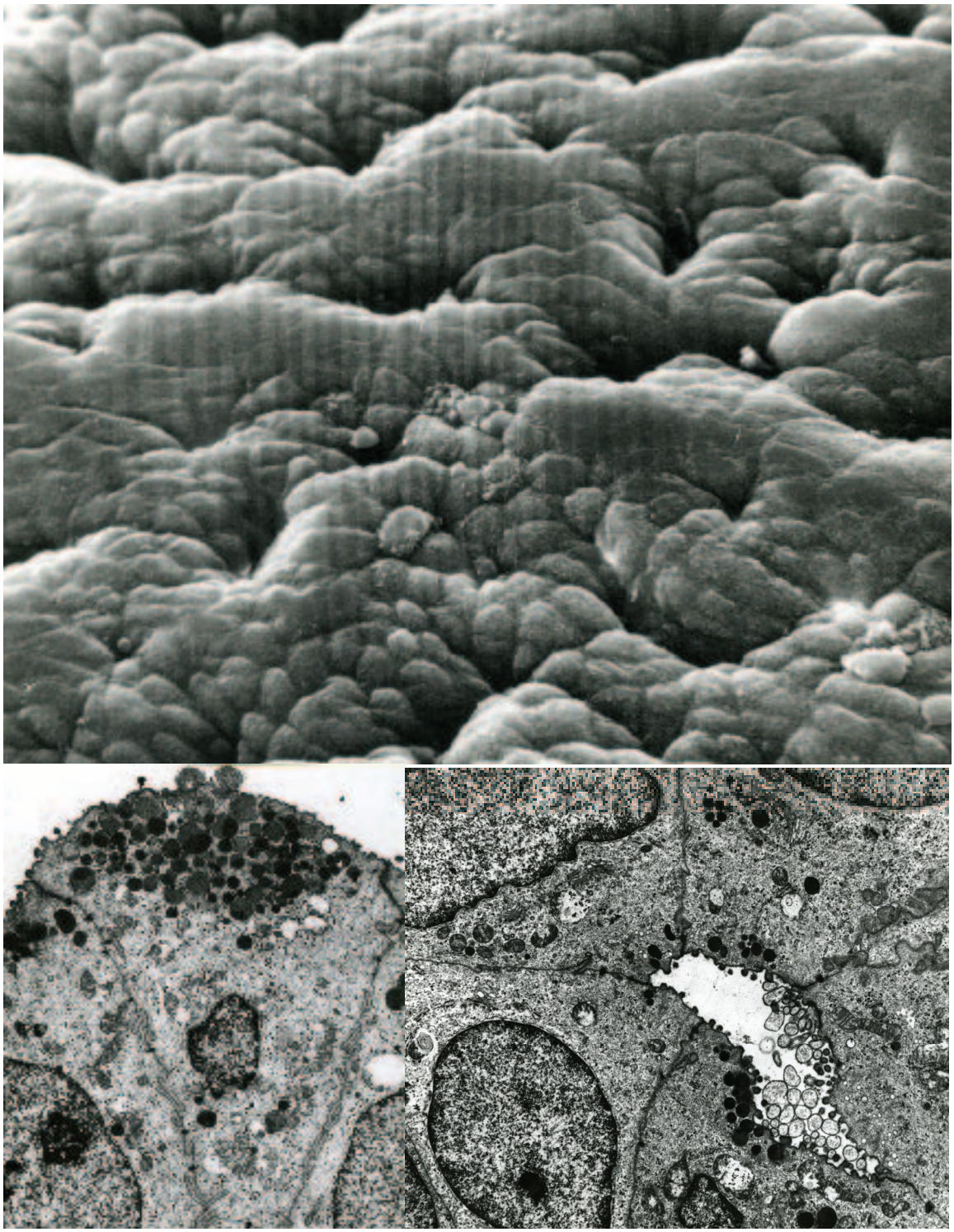

Fig. 11. (*Above*). The gastric surface of a four-week-old opossum exhibits well-established gastric pits and has a more mature appearance. SEM X 800. (*Below left*). A gastric lining epithelial cell from a four week old opossum lacks lipid droplets and is filled with mucin granules some of which are being discharged into the lumen. TEM X 4500. (*Below right*). An electron micrograph illustrates the apices of four differentiating mucous neck cells and a parietal cell (extreme right) from an oxyntic gland of a four-week-old opossum. The former contains scattered electron-dense granules in their apical cytoplasm. TEM X 5000.

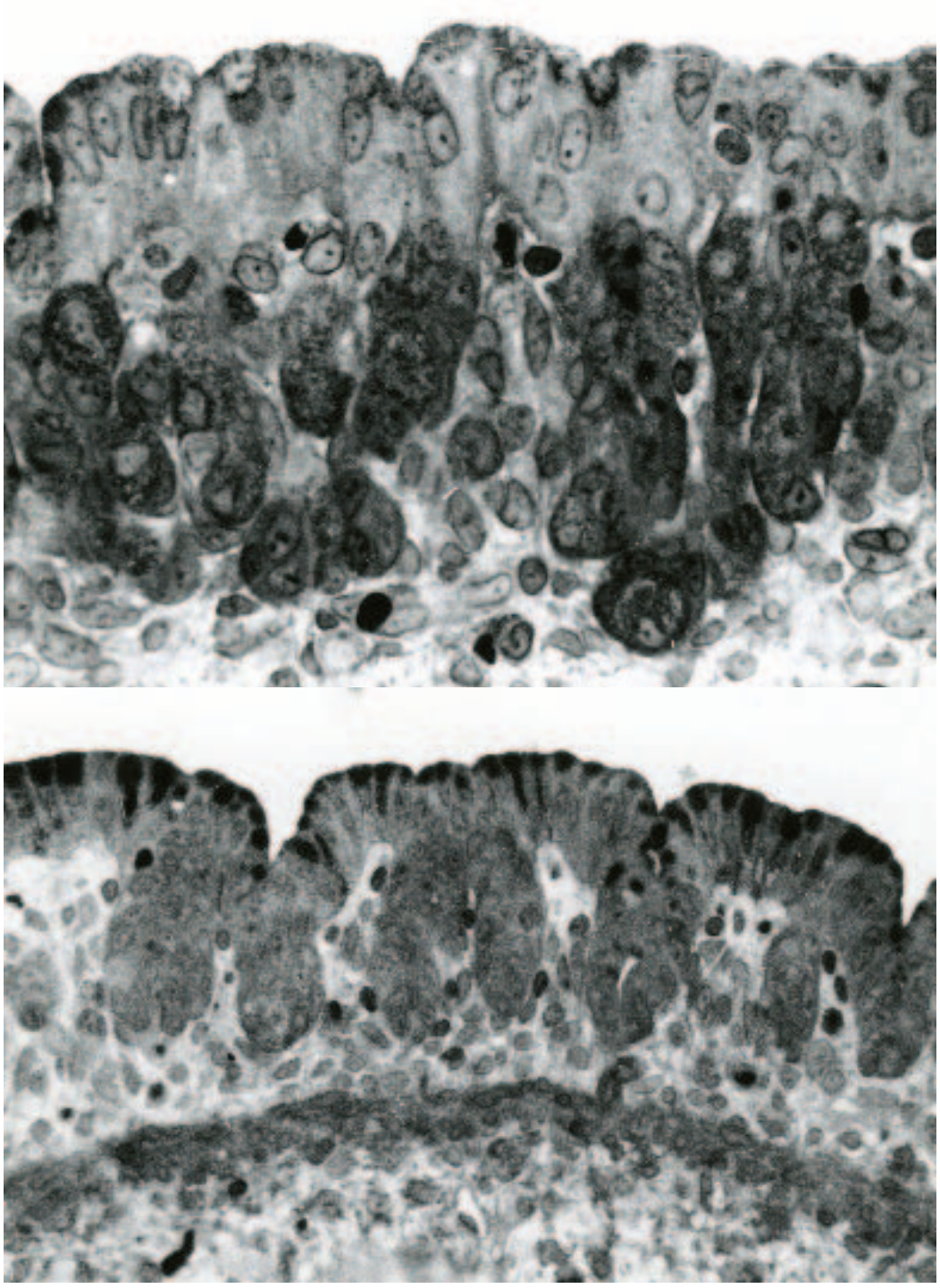

Fig. 12. (*Above*). The oxyntic glands of a seven-week-old opossum show an increase in number of parietal cells and an increase in depth. Gastric lining cells show a continued increase in number of mucin granules. LM X 400. (*Below*). Gastric surface epithelial cells lining the pyloric region of the stomach also show an increase in the number of mucin granules. The pyloric glands are less well developed in comparison to oxyntic glands in an opossum of the same age. Seven weeks postnatal. LM X 300.

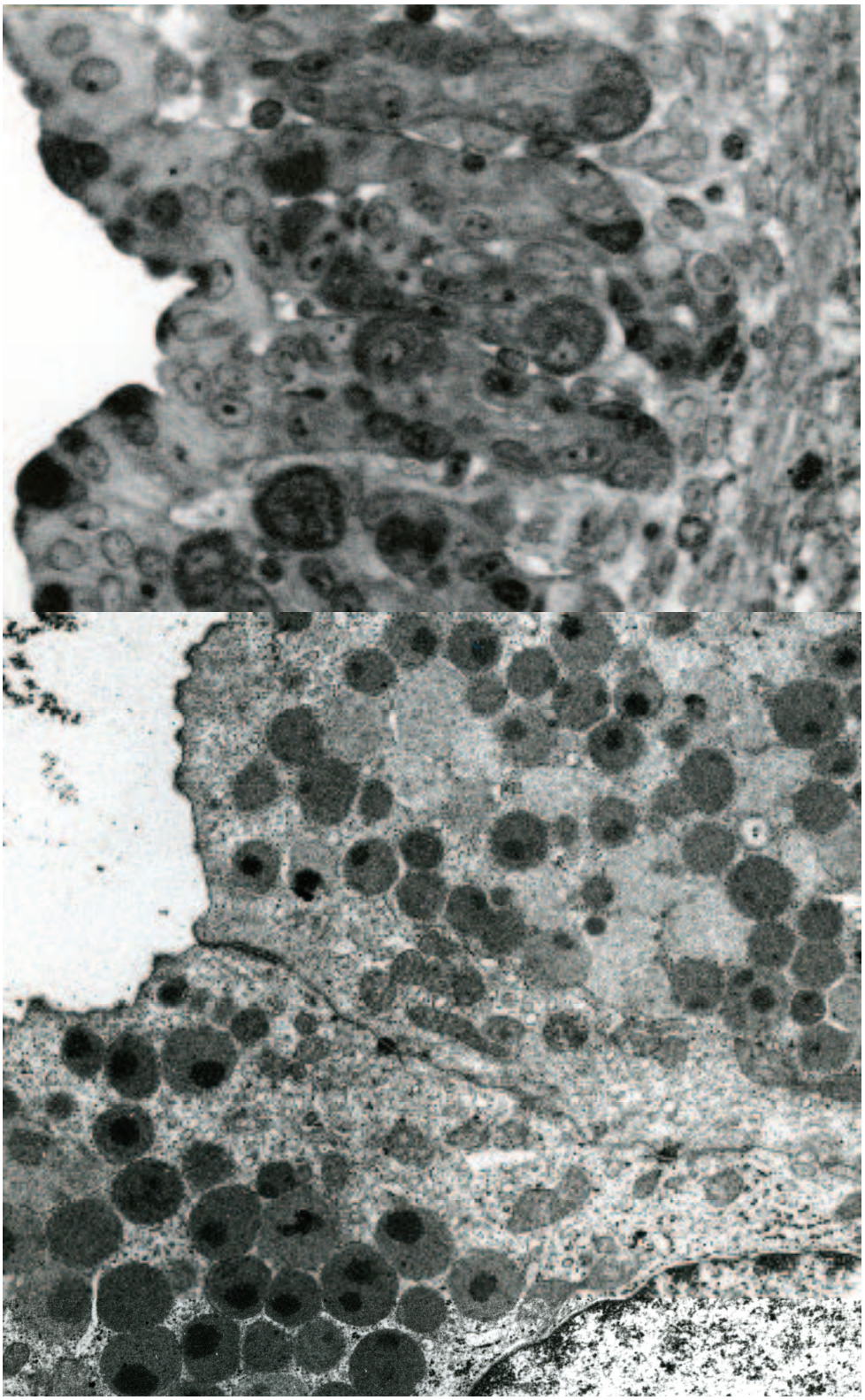

Fig. 13. (*Above*). Gastric glands of the nine-week-old opossum continue to increase in length and consist of parietal, enteroendocrine, and numerous undifferentiated cells. LM X 450. (*Below*). Apices of two gastric lining epithelial cells contain numerous heterogeneous granules that are comprised of a flocculent material limited by a membrane. These secretory granules often show an area of increased electron density. Opossum nine weeks postnatal. TEM X 10,000.

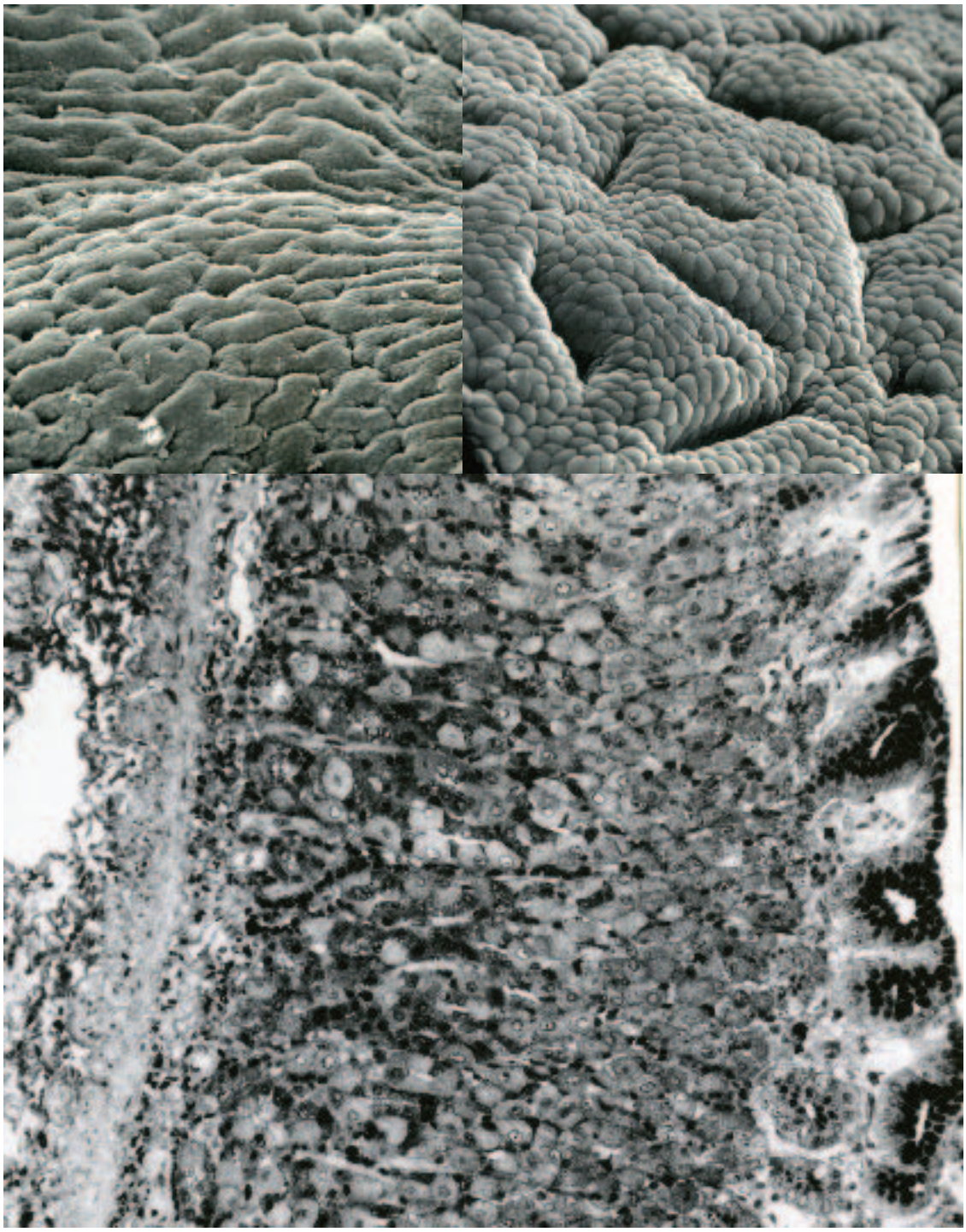

Fig. 14. (*Above left*). The gastric surface of an opossum eleven weeks postnatal shows numerous folds and gastric pits. SEM X 400. (*Above right*). Gastric pits are often slit-like or irregular in appearance in the juvenile opossum. SEM X 750. (*Below*). A profile of the gastric mucosa from a juvenile opossum illustrates the relative depth of the gastric pits (foveolae) and the underlying oxyntic glands. LM X 250.

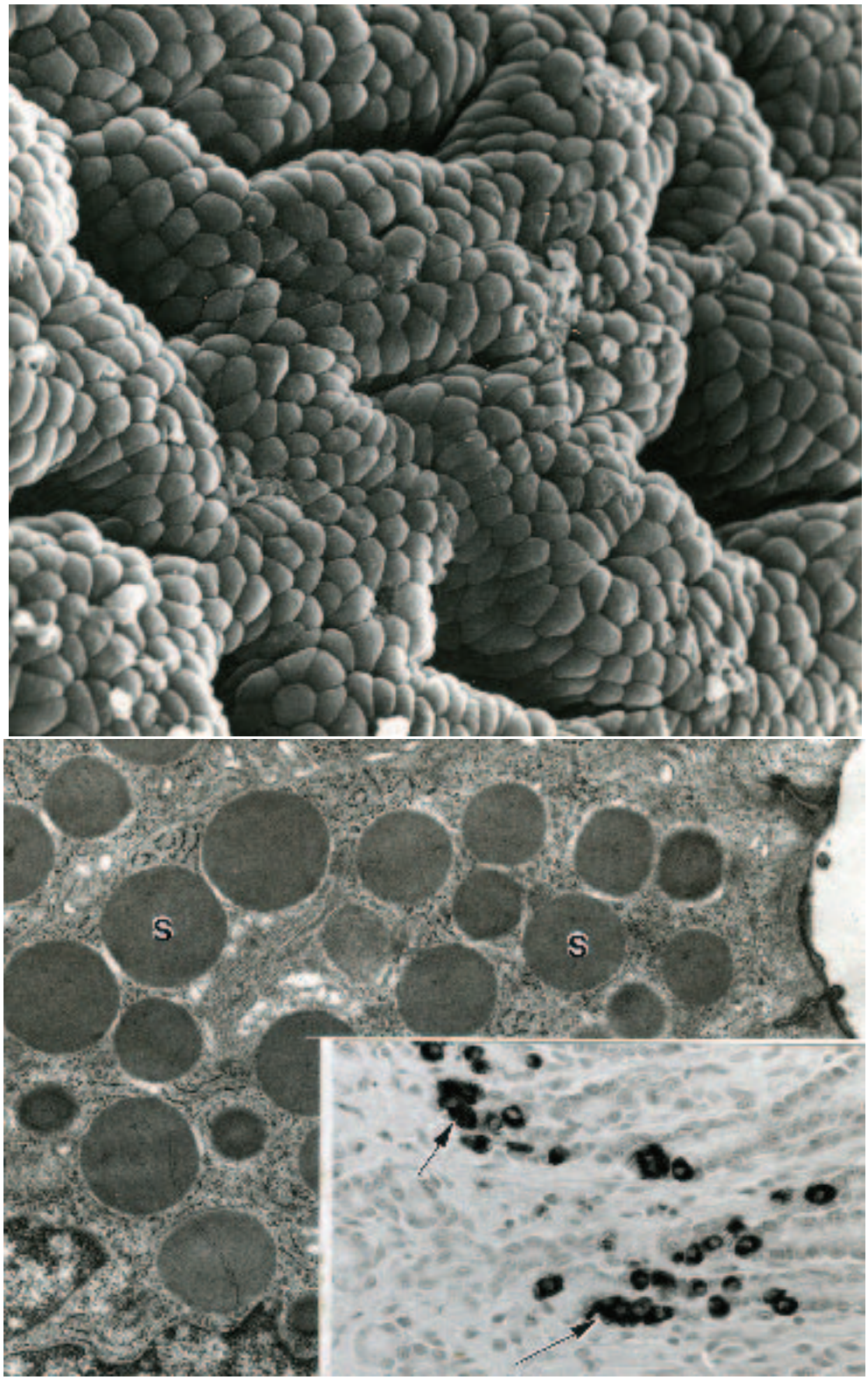

Fig. 15. (*Above*). A scanning micrograph illustrates the mucosal surface and gastric pits of a weaned, juvenile opossum. SEM X 750. (*Below*). The apex of mucous cell from a pyloric gland of a juvenile opossum is filled with electron-dense secretory granules (S). TEM X 10,000. (*Inset*). Gastrin-immunoreactive cells (arrows) concentrated at the junction between the isthmus and neck region of pyloric glands. Weaned juvenile opossum. LM X 250.

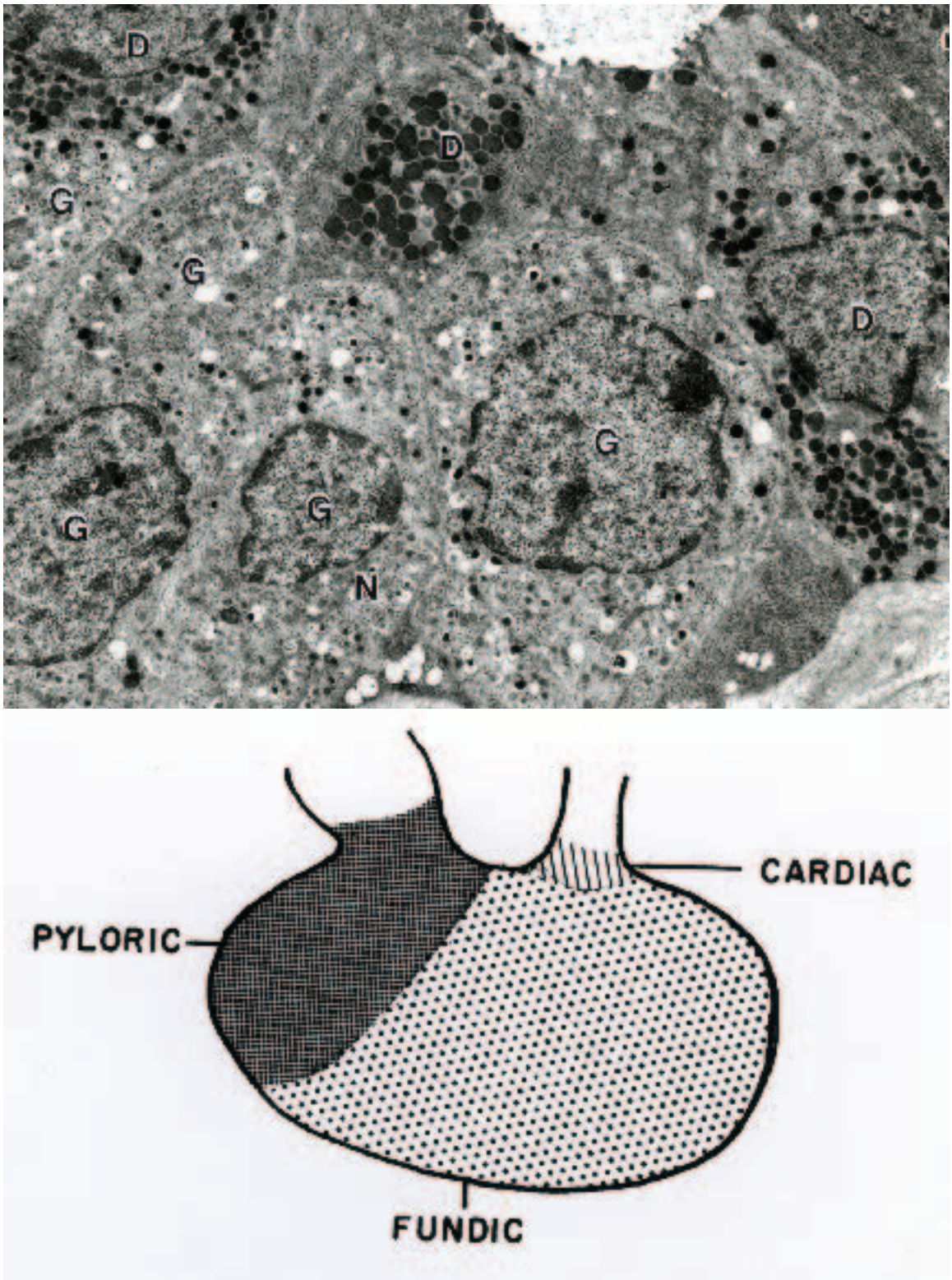

Fig. 16. (*Above*). An electron micrograph through the neck region of a pyloric gland demonstrates five gastrin (G) and three D cells (D) clustered together. TEM X 6000. (*Below*). A line drawing illustrates the distribution of the cardiac, oxyntic (fundic) and pyloric glands within an adult opossum stomach.

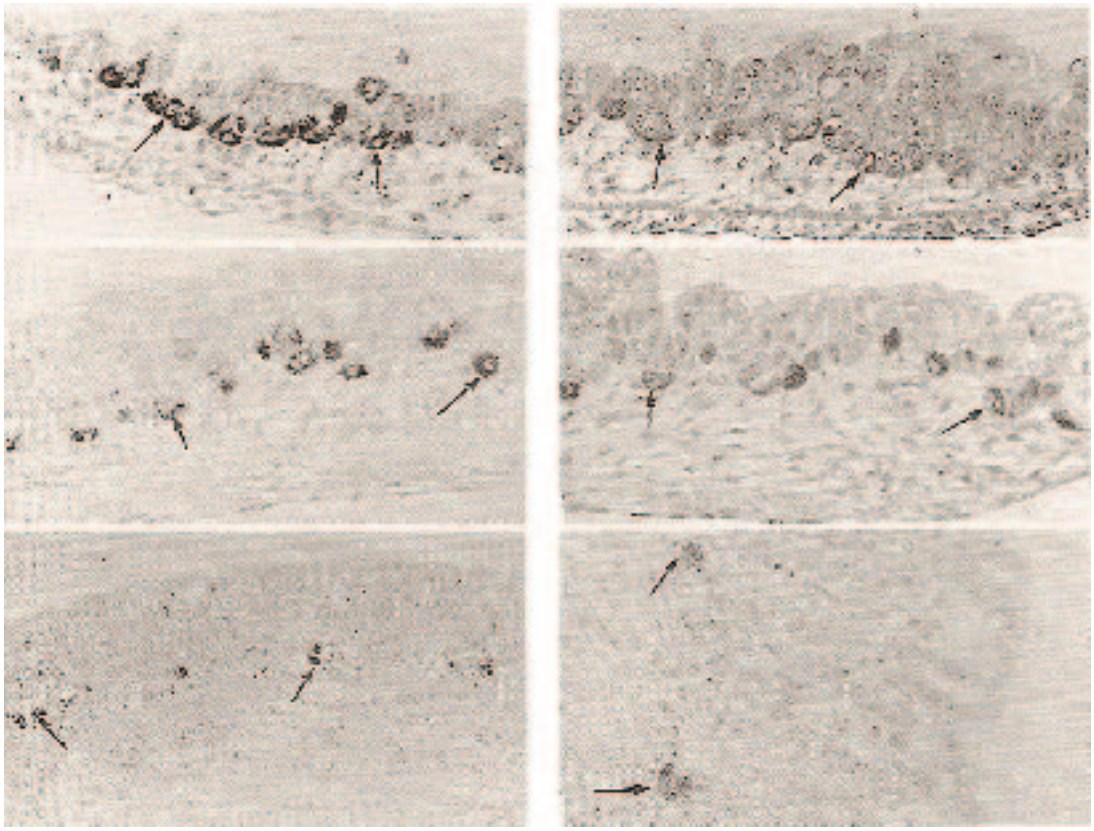

Fig. 17. A series of micrographs illustrate cells within the gastric mucosa of the developing opossum stomach stained immunohistochemically for prochymosin and pepsinogen. (*Above left*). Prochymosin-immunoreactive cells (arrows). Newborn opossum. LM X 250. (*Above right*). Pepsinogen-immunoreactive cells (arrows). Newborn opossum. LM X 250. (*Center left*). Prochymosin-immunoreactive cells (arrows). Opossum one week postnatal. LM X 250. (*Center right*). Pepsinogen-immunoreactive cells (arrows). Opossum one week postnatal. LM X 250. (*Below left*). Prochymosin-immunoreactive cells (arrows). Opossum eleven weeks postnatal. LM X 100. (*Below right*). Pepsinogen-immunoreactive cells (arrows). Opossum eleven weeks postnatal. LM X 250.

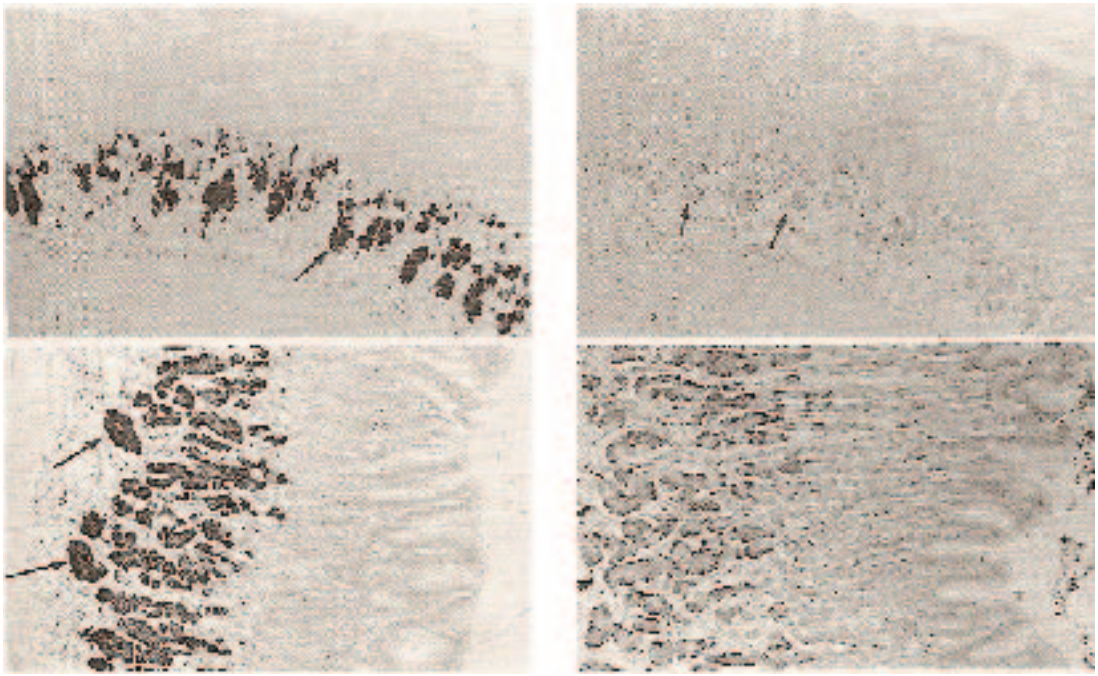

Fig. 18. (*Above left*). Prochymosin-immunoreactive cells (arrows). Opossum thirteen weeks postnatal. LM X 100. (*Above right*). Pepsinogen-immunoreactive cells (arrows). Opossum thirteen weeks postnatal. LM X 100. (*Below left*). Prochymosin-immunoreactive cells (arrows). Weaned opossum. LM X 100. (*Below right*). Pepsinogen-immunoreactive cells (arrows). Weaned opossum. LM X 100.

Chapter 21. Small Intestine

Synopsis:

The narrow intestinal tube of the mid-gut is apparent by prenatal day ten and the hindgut forms the following day. The cecal diverticulum appears early in prenatal day twelve. At birth the luminal diameter of the proximal small intestine is considerable as compared to the distal region, which is quite narrow. Villi are better developed proximally and the intestinal epithelium rests upon a well-developed vascular bed of capillaries. With continued organogenesis villi continue to show differences with regard to height and their state of differentiation. Villi at various stages of development continue to be found until weaning when most have the same height and general conformation. Intestinal glands (crypts of Lieberkühn) are not observed in the mucosa of the intestinal tract until relatively late in the postnatal period (about the seventh postnatal week). They form as simple tubular evaginations from the intestinal epithelium positioned between formed villi. Intestinal glands of the opossum are short in length even in the adult. Enterocytes are the primary cell type constituting the intestinal lining epithelium of both the small and large intestine early in the postnatal period; however scattered enteroendocrine cells of various types also are found. Goblet cells and Paneth cells first appear near the end of the second postnatal week. Mitotic figures are a common observation in the intestinal epithelium but gradually decline until about postnatal week eleven at which time there is a slight peak in mitotic activity, which coincides with the appearance of the intestinal glands. Paneth cells of the opossum are unusual in that they are found within the intestinal epithelium covering the villi as well as within the epithelium forming the intestinal glands. Goblet cells of the small intestine occur in limited numbers early in the postnatal period and do not form a significant population until just prior to weaning. The enterocyte exhibits an extensive endocytic complex, large supranuclear vacuoles, and lipid droplets until about the eleventh week of postnatal life. The endocytic activity appeared most pronounced in enterocytes positioned near the tips of villi. It appears that the enterocytes that line the lumen of the entire small intestine, and to some degree the colon, are modified for macromolecular absorption of materials during the suckling period. Such an adaptation apparently results in the delayed development of intestinal glands and the delayed appearance of other cells types associated with the intestinal lining epithelium of the small intestine. The apical endocytic complex remains a prominent feature of enterocytes lining the small intestine until just prior to weaning. During weaning the apical endocytic complex disappears, first from enterocytes at the base of villi and then progressively towards enterocytes at the tops of villi. Simultaneously, there is a progressive loss of the endocytic complex from enterocytes in a proximal to distal direction within the small intestine lining epithelium. The endocytic complex is important in the uptake of intact macromolecules from the intestinal lumen and is one mechanism by which immunoglobulins from colostrum and milk pass through the intestinal lining epithelium. In this way passive immunity is passed from the mother to the suckling pouch young of this species.

Enteroendocrine cells immunoreactive for secretin, motilin, somatostatin, gastrin, cholecystokinin (CCK), gastric inhibitory peptide (GIP), serotonin (5-HT), bovine pancreatic polypeptide (BPP), and glucagon are found within the intestinal lining epithelium of the newborn opossum. Enteroendocrine cells immunoreactive for neurotensin are unusual in that they appear late in the postnatal period (about eleven weeks postnatal) and when they do appear are concentrated primarily in the distal region of the small intestine. In addition,

they follow a distal to proximal progression in their distribution as they increase in number with age. This is in contrast to the other enteroendocrine cells observed that show a proximal to distal progression in distribution with development. The enteroendocrine cells, although randomly scattered, tend to occur in small clusters component cells of which express the same immunoreactivity. The clustering of specific immunoreactive enteroendocrine cell types at random foci indicates that they differentiate as small clones of cells rather than as individual cells.

As organogenesis of the small intestine continues smooth muscle cells within the lamina propria differentiate from mesenchymal cells but are not well defined until the end of the third postnatal week. The muscularis mucosae is apparent by the end of the fourth week of postnatal life. A unique feature of the opossum small intestine is the appearance of two membranes that limit the lamina propria at weaning. They continue to develop throughout life and may reach a width of 25 μM or more. One forms a series of cup-like structures that envelop the bases of the intestinal glands; the other membrane forms a layer on the luminal side of the muscularis mucosae. As these two membranes form, numerous lymphocytes, plasma cells, eosinophils, and macrophages accumulate between them resulting in a thick, complete sleeve of defensive cells that bounds the intestinal lumen throughout its length. Peyer's patches are few in number in this species.

The muscularis externa is thin and poorly developed in the newborn opossum small intestine. Although both layers can be observed, only the inner layer is complete and consists of a single layer of myoblasts. Mitotic (proliferative) activity occurs primarily during the first four postnatal weeks with little resulting increase in thickness of the muscularis externa. Hypertrophy of the muscularis externa begins at the end of the proliferative period and extends for about the next three weeks into the postnatal period as organogenesis of the small intestine continues. A second period of hypertrophy also occurs and begins at weaning when solid food is being processed by the small intestine.

Acknowledgments:

Fig. 1 (top left), courtesy of and from: Krause, W.J. and J.H. Cutts (1984) Scanning electron microscopic observations on the nine day opossum embryo. Acta Anat. 120: 93-97.

Figs. 1 (bottom), 3, 4 (top left), 5 (top), 6 (top and center), courtesy of and from: Krause, W.J., J.H. Cutts, and C.R. Leeson (1976) The postnatal development of the alimentary canal in the opossum. III. Small Intestine and Colon. J. Anat. 123:21-45.

Fig. 2 (top), courtesy of and from: Krause, W.J. and J.H. Cutts (1992) Development of the Digestive System in the North American Opossum (*Didelphis virginiana*). Adv. Anat. Embryol. Cell Biol. 125:1-148.

Fig. 6 (bottom), courtesy of and from: Krause, W.J., J. Yamada and J.H. Cutts (1985) Quantitative distribution of enteroendocrine cells in the gastrointestinal tract of the adult opossum, *Didelphis virginiana.* J. Anat. 140:591-605.

Fig. 7 (top), courtesy of and from: Krause, W.J., R.H. Freeman and L.R. Forte. (1990) Autoradiographic demonstration of specific binding sites for *E. coli* enterotoxin in various epithelia of the North American opossum. Cell Tissue Res. 260:387-394.

Figs. 7 (bottom) and 8, courtesy of and from: Krause, W.J. and Leeson, C.R. (1969) Limiting membranes of intestinal lamina propria in the opossum. J. Anat. 104:467-480.

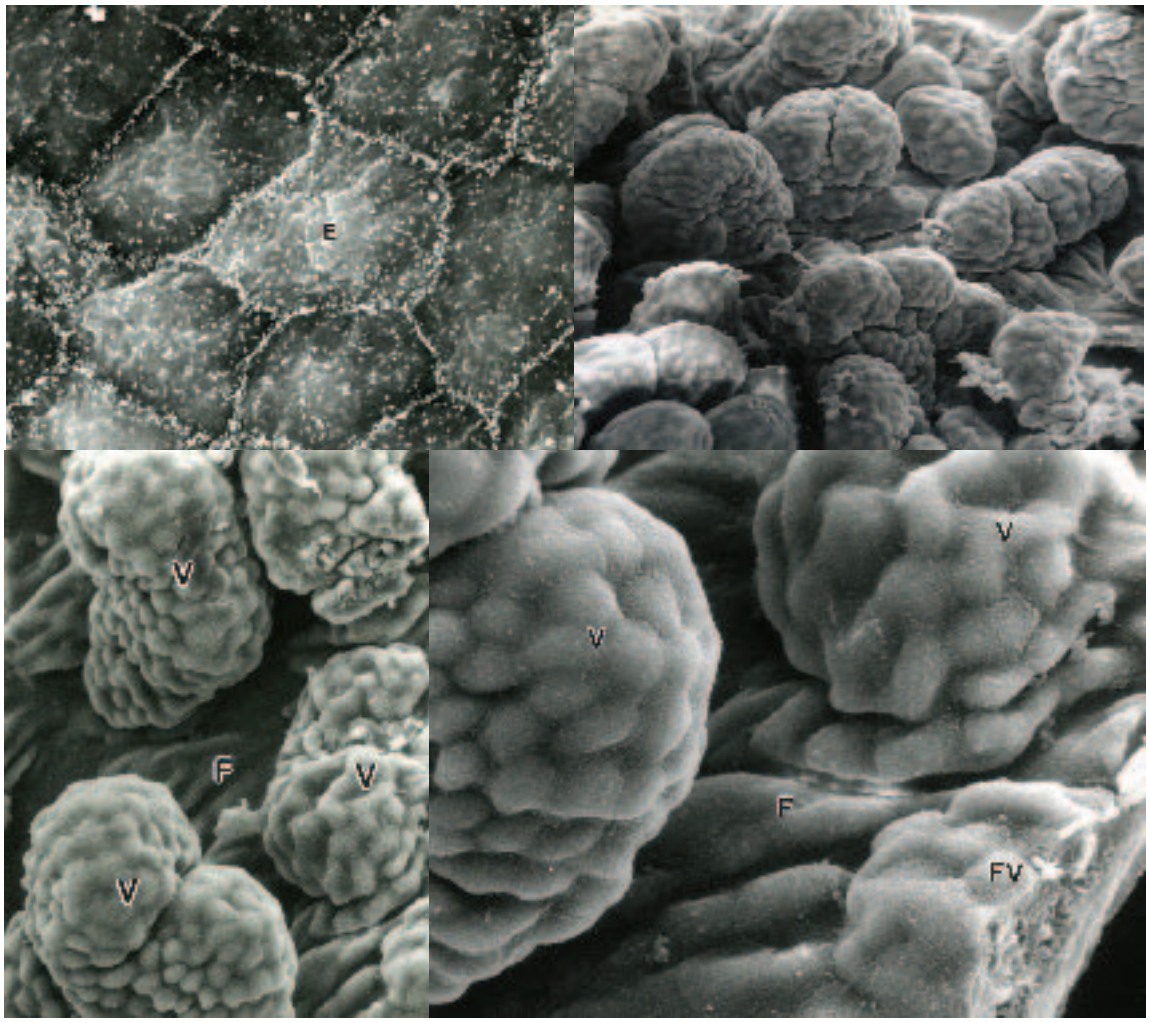

Fig. 1. (*Above left*). The luminal surface of endodermal cells (E) from a nine-day opossum embryo illustrates an epithelium with distinct cell boundaries. SEM X 3,000. (*Above right*). The luminal surface of the duodenum from a newborn opossum illustrates a very irregular contour. SEM X 100. (*Below left*). The duodenum viewed at increased magnification illustrates more clearly scattered intestinal villi (V) as well as the intervening intestinal floor (F). Newborn opossum. SEM X 300. (*Below right*). An evagination into the intestinal lumen forms what is thought to be a forming intestinal villus (FV). Two established intestinal villi (V) and the region of the intestinal floor (F) also are shown. SEM X 800.

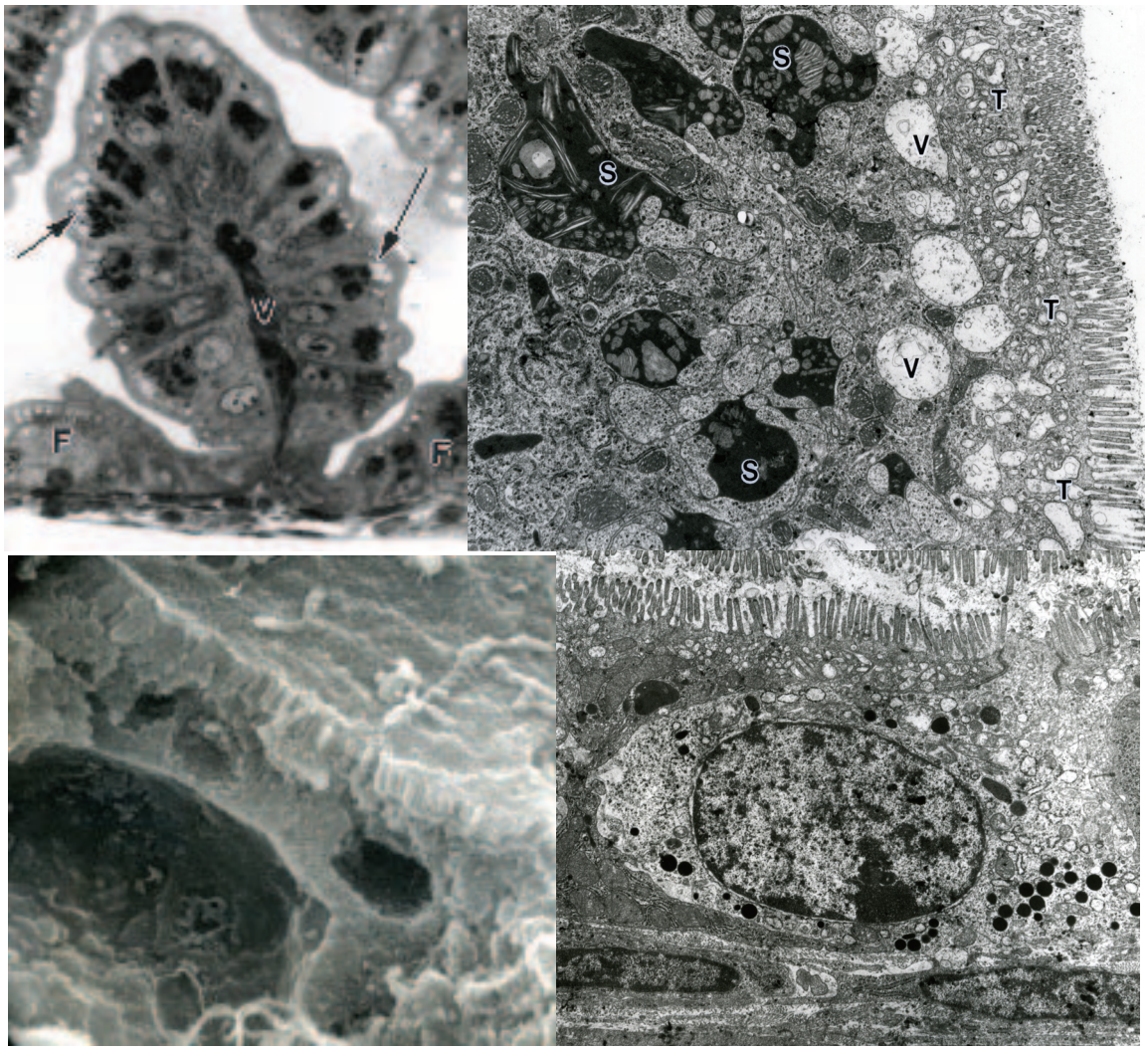

Fig. 2. (*Above left*). A region of the duodenal wall illustrates a primitive villus (V) and adjacent areas of the intestinal floor (F). Enterocytes covering both regions exhibit a well-developed apical endocytic complex (arrows). A scant muscularis externa forms the limiting wall. Newborn opossum. LM X 350. (*Above left*). In addition to microvilli, the apical region of a duodenal enterocyte is characterized by vacuolar (V) and tubulovesicular components (T) of the endocytic complex as well as large supranuclear vacuoles (S) filled with an electron dense material. Newborn opossum. TEM X 6,000. (*Below left*). A freeze fracture preparation illustrates the magnitude of the large supranuclear vacuoles. The microvillus border is shown near the top of the illustration. Newborn opossum. SEM X 5000. (*Below right*). A single, unidentified enteroendocrine cell found within the intestinal lining epithelium of duodenum. Newborn opossum. TEM X 5,000.

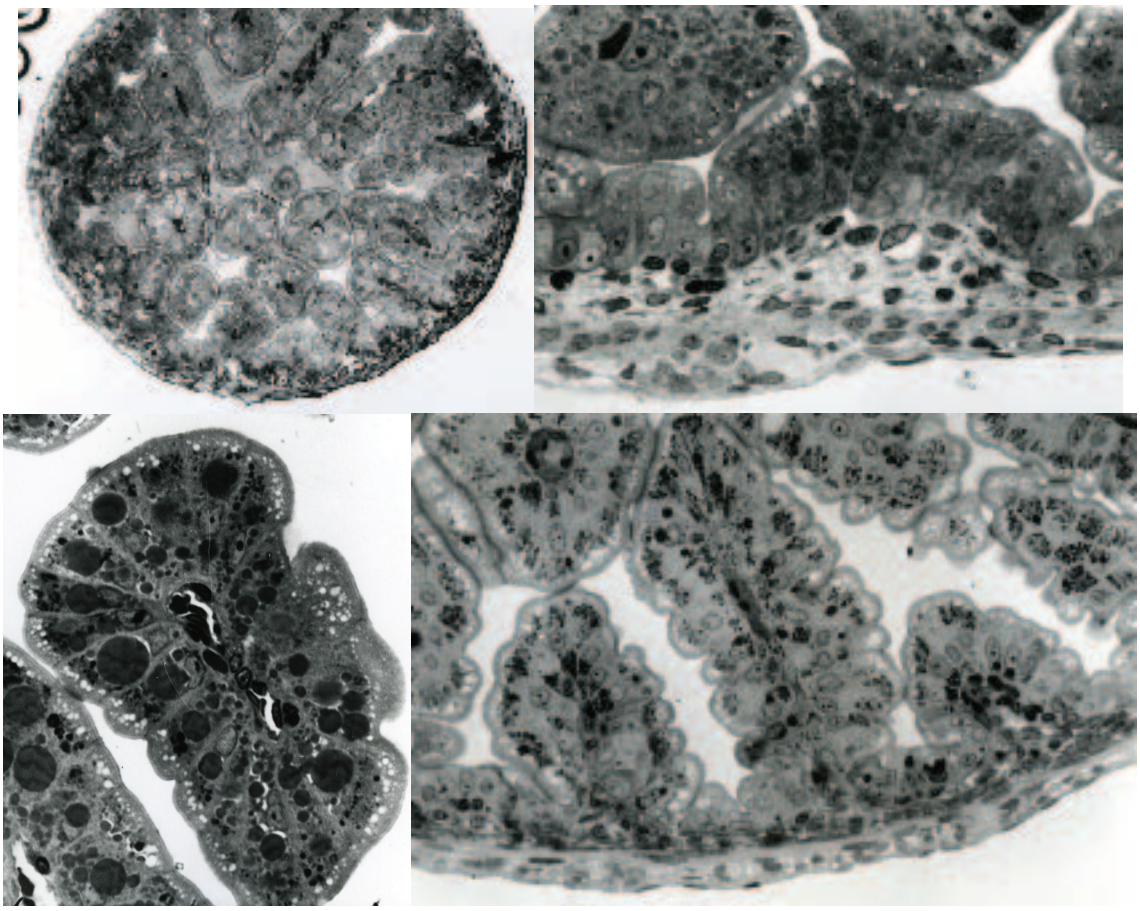

Fig. 3. (*Above left*). A section through the duodenum of a week old opossum demonstrates an increase in the number of villi. LM X 75. (*Above right*). A region through the intestinal wall of a week old opossum as seen at increased magnification shows in greater detail the absorptive activity of intestinal epithelium lining the intestinal floor and the continued development of the muscularis externa. LM X 400. (*Below left*). A segment of a duodenal villus from a week old opossum shows continued absorptive activity by the covering intestinal epithelium. LM X 350. (*Below right*). A region of intestinal wall from an opossum two weeks postnatal illustrates that the villi appear more closely packed together than observed in earlier ages. The villi also vary in height and the muscularis externa continues to expand. LM X 250.

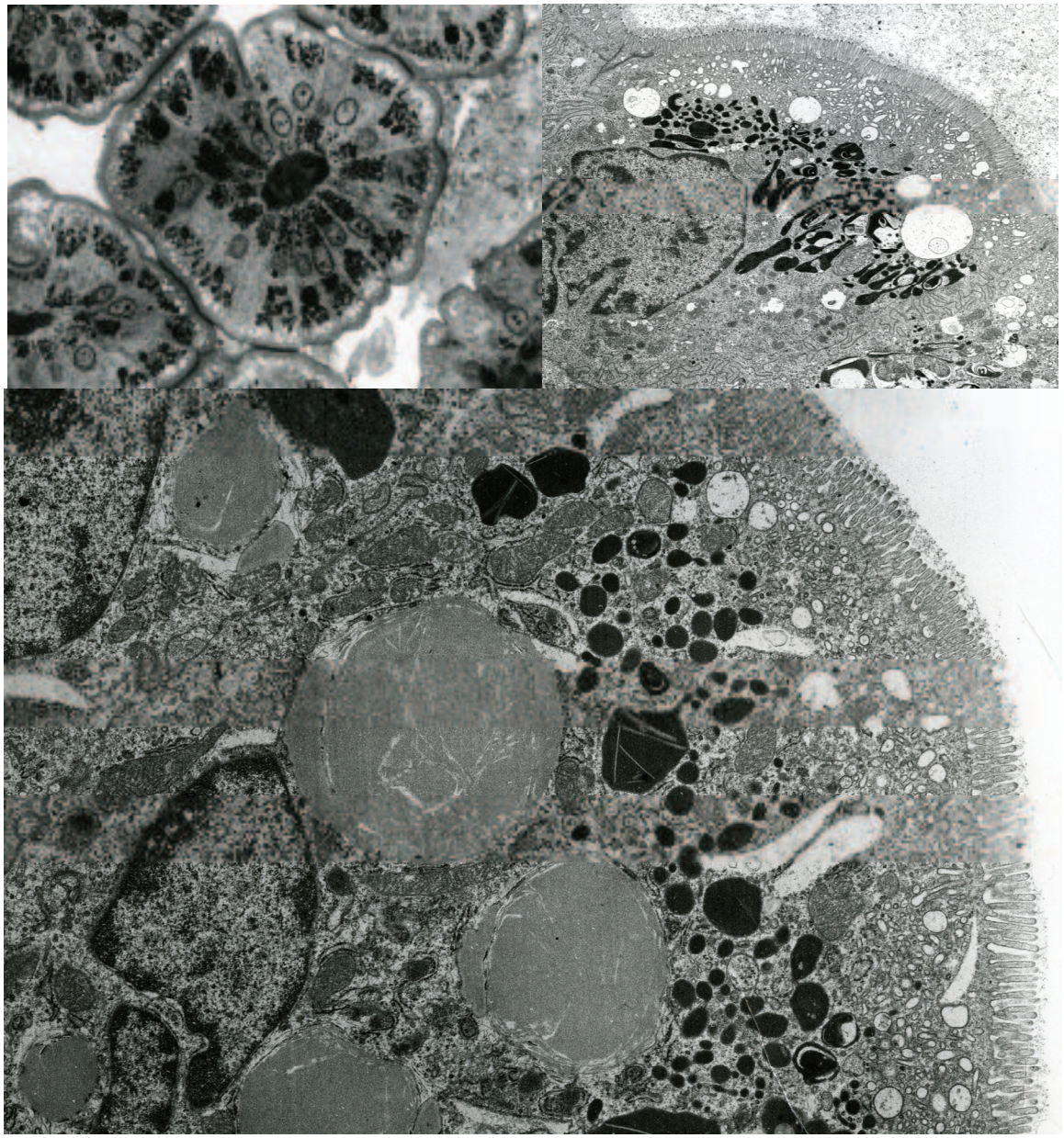

Fig. 4. (*Above left*). Increased magnification of a transverse section through an intestinal villus demonstrates the continued absorptive activity of intestinal epithelial cells in the two-week-old opossum. The apical endocytic complex continues to be a prominent feature of the enterocytes. Note that absorbed materials fill the supra-and sub-nuclear cytoplasm. LM X 400. (*Above right*). An electron micrograph demonstrates the apical endocytic complex of a duodenal enterocyte. TEM X 3,000. (*Below*). The apical and supranuclear regions of an enterocyte from the jejunum of an opossum two weeks postnatal illustrate in greater detail the apical endocytic complex. The supranuclear vacuoles are filled with an electron dense material and large accumulations lipid are observed adjacent to the nucleus. TEM X 6,000.

Fig. 5. (*Above left*). The apical endocytic complex remains a prominent feature of enterocytes covering the top of an intestinal villus from a five-week-old opossum but is not as well developed as that seen in earlier ages. A lone goblet cell occurs near the top of the villus. LM X 375. (*Above right*). Ileal villi of the five-week-old opossum vary in length and may appear club-like or elongate. Note the blebs occurring on the tops of some villi at this stage of development. SEM X 175. (*Below*). By the end of the sixth postnatal week intestinal villi appear more uniform in overall shape but variation in height continues to be a prominent feature. SEM X 200.

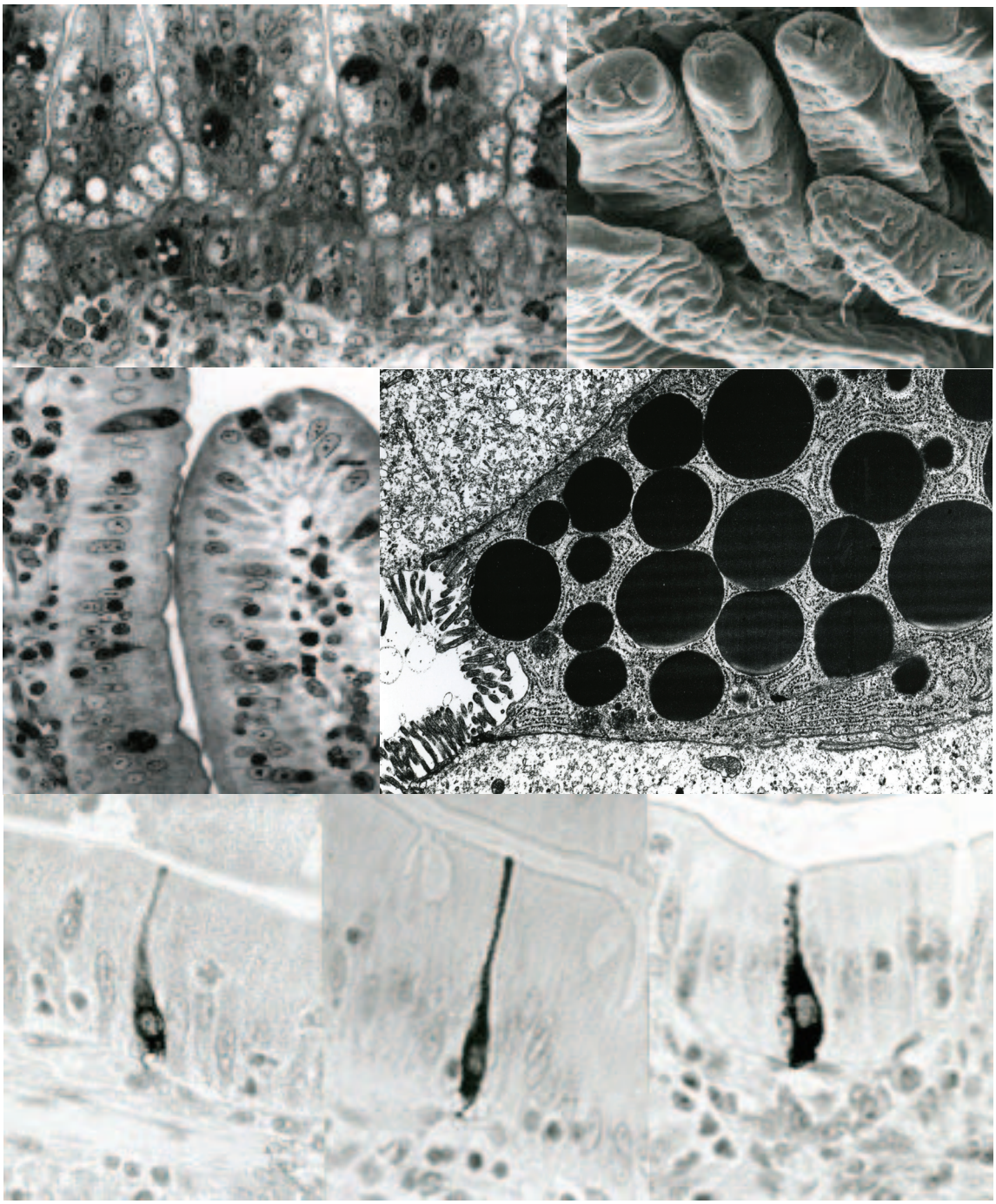

Fig. 6. (*Above left*). Enterocytes lining the distal small intestine of the seven-week-old opossum continue to show vacuolization. Paneth cells (with granules of varying staining density) also are seen. LM X 375. (*Above right*). Duodenal villi of the eleven-week opossum appear large, of uniform height, and finger-like. SEM X 175. (*Center left*). Paneth cells (with granules) of the opossum at thirteen weeks are found scattered within the intestinal epithelium and often occur near the tops of villi. LM X 375. (*Center right*). The apex of a Paneth cell filled with electron dense secretory granules taken from an intestinal villus. Juvenile opossum. TEM X 9,000. Three enteroendocrine cells found within the intestinal lining epithelium of a young adult opossum immunoreactive for gastrin (*Below left*), 5-HT (*Below center*), and secretin (*Below right*). LM X 400.

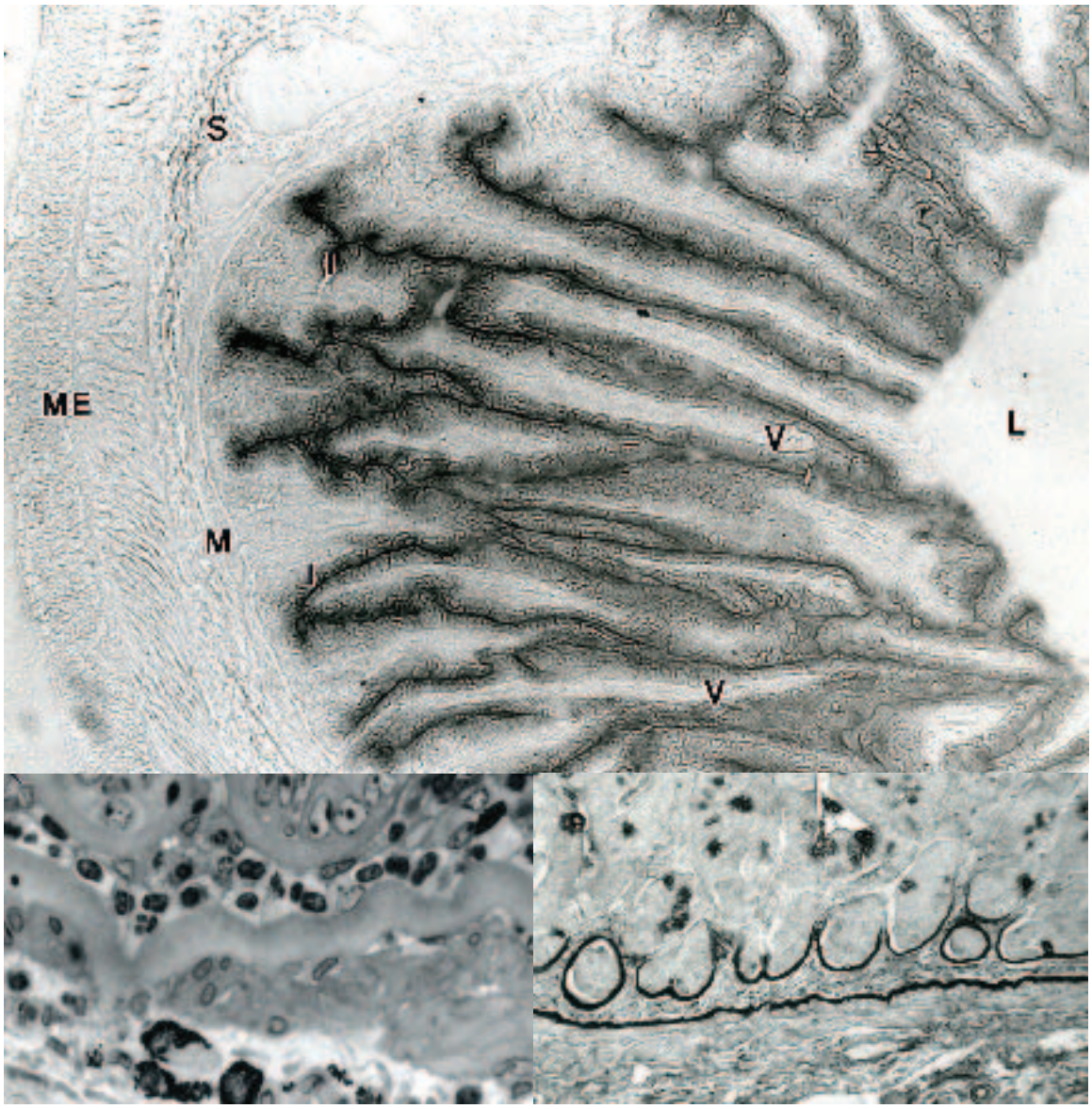

Fig. 7. (*Above*). A section from the proximal small intestine of an adult opossum labeled with ^{125}I-heat stable enterotoxin illustrates receptor localization for heat-stable enterotoxin is confined to the intestinal lining epithelium and not the cores of villi (V), the muscularis mucosae (M), submucosa (S), or the muscularis externa (ME). The intestinal lumen (L) is to the extreme right. Note the increase in receptor localization within the intestinal glands (I) (crypts of Lieberkühn). Autoradiograph X 150. (*Below left*). Two relatively thick homogeneous membranes bound the lamina propria of the adult opossum small intestine. Note the cup-like arrangement of the internal membrane that bounds the crypts of Lieberkühn. The region between the internal and external membranes is filled with connective tissue (defensive) cells. LM X 400. (*Below right*). The two membranes limiting the lamina propria are periodic acid Schiff (PAS) positive when treated with this methodology and resistant to digestion with saliva and diastase suggesting the presence of complex proteoglycan/glycosaminoglycan molecules. LM X 250.

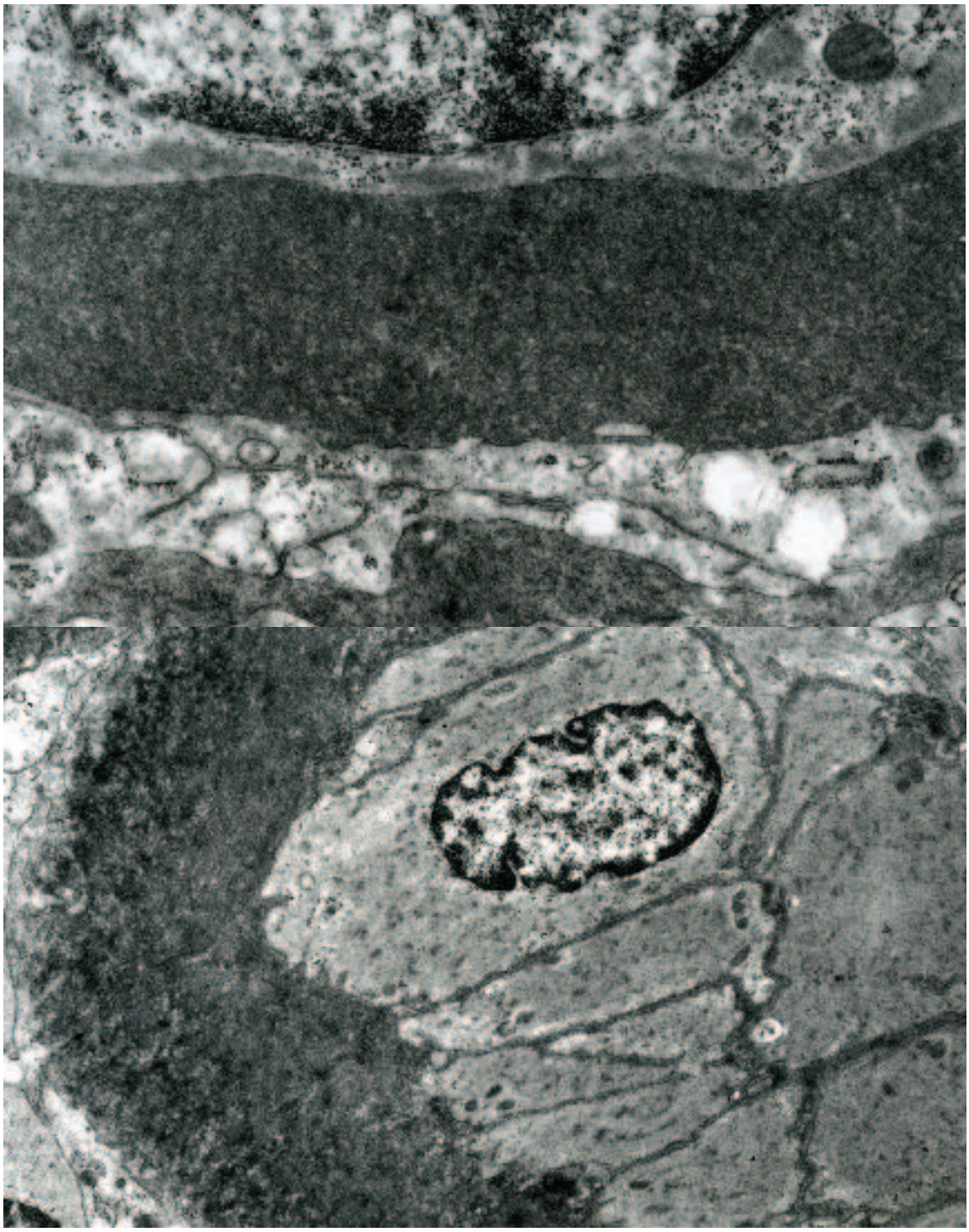

Fig. 8. (*Above*). The structure of the internal membrane limiting the lamina propria appears finely granular or fibrillar in nature and is electron dense. Note the concentrations of a similar electron-dense material between the nucleus and the basal cytoplasm of an adjacent enterocyte (top of micrograph). TEM X 8,000. (*Below*). A micrograph illustrates the ultrastructural appearance of the external membrane, which lies immediately adjacent to muscle cells of the muscularis mucosae. The external membrane appears to have coarse fibrils within it. TEM X 8,000.

Chapter 22. Brunner's Glands

Synopsis:

Brunner's glands are the most unique feature of the submucosa within the small intestine and begin their development just after birth immediately distal to the gastrointestinal junction. These glands differentiate from the intestinal lining epithelium with each invagination resulting in the initial formation of the ductal system of a single gland. With continued development the duct system branches repeatedly, follows a tortuous course, the net result of which is a complex glandular structure. The initial duct system radiates laterally in a stellate fashion and continues to subdivide into numerous intralobular ducts. The first three weeks of organogenesis are concerned primarily with the establishment of the ductal system. Secretory tubules and acini first appear at about the fifth week of postnatal life. Individual duodenal glands develop independently but in close approximation to one another. Such development results in the formation of funnel-shaped depressions in the overlying mucosa. The mucosal depressions may be lined by either gastric and/or intestinal lining epithelium. Thus, the formed Brunner's glands may empty via a single duct either into such depressions or independently into the intestinal lumen between villi. With continued development Brunner's glands form a large, lobed, glandular collar immediately distal to the pyloric sphincter. The complex nature and limited distribution of Brunner's glands in the opossum are features shared by the majority of marsupial species as well as the two monotremes. Brunner's glands of the opossum secrete mucin-type glycoproteins rich in O-linked carbohydrates that contribute to selective barrier functions of the mucosa in this region of the small intestine.

Acknowledgments:

Figs. 1, 2 and 3, courtesy of and from: Krause, W.J. and Leeson, C.R. (1969) Studies of Brunner's glands in the opossum. II. Postnatal development. Am. J. Anat. 126:275-290.

Figs. 4 (top, bottom), 5 (top) and 6, courtesy of and from: Krause, W.J. and Leeson, C.R. (1969) Studies of Brunner's glands in the opossum. I. Adult morphology. Am. J. Anat. 126:255-274.

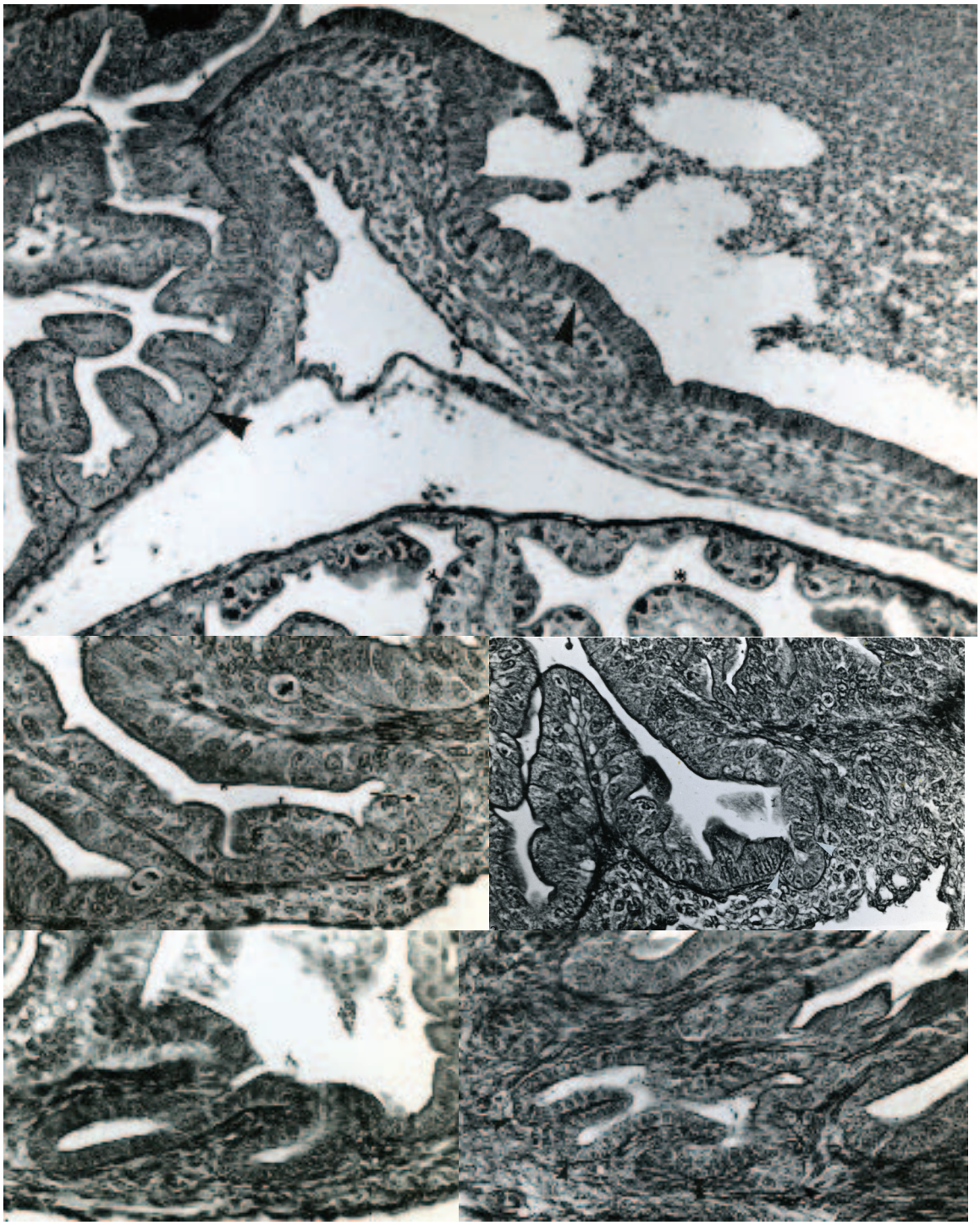

Fig. 1. (*Above*). A histological section through the gastrointestinal junction of a newborn opossum stained with PAS reveals a positive staining basement membrane (arrow heads) underlying both the pyloric (right) and intestinal (left) epithelium. LM X 125. (*Middle left*). A micrograph illustrates the initial point of differentiation of a Brunner's gland (arrow) from the intestinal lining epithelium of the duodenum. Newborn opossum. LM X 250. (*Middle right*). A light micrograph illustrates the initial evagination of a Brunner's gland duct from intestinal epithelium observed in a newborn opossum. LM X 220. (*Bottom left*). By the end of the first postnatal week the developing ductal system of Brunner's glands is well established. LM X 220. (*Bottom right*). The forming intralobular ducts of Brunner's glands exhibit considerable branching (arrow heads) by the end of the second postnatal week. LM X 220.

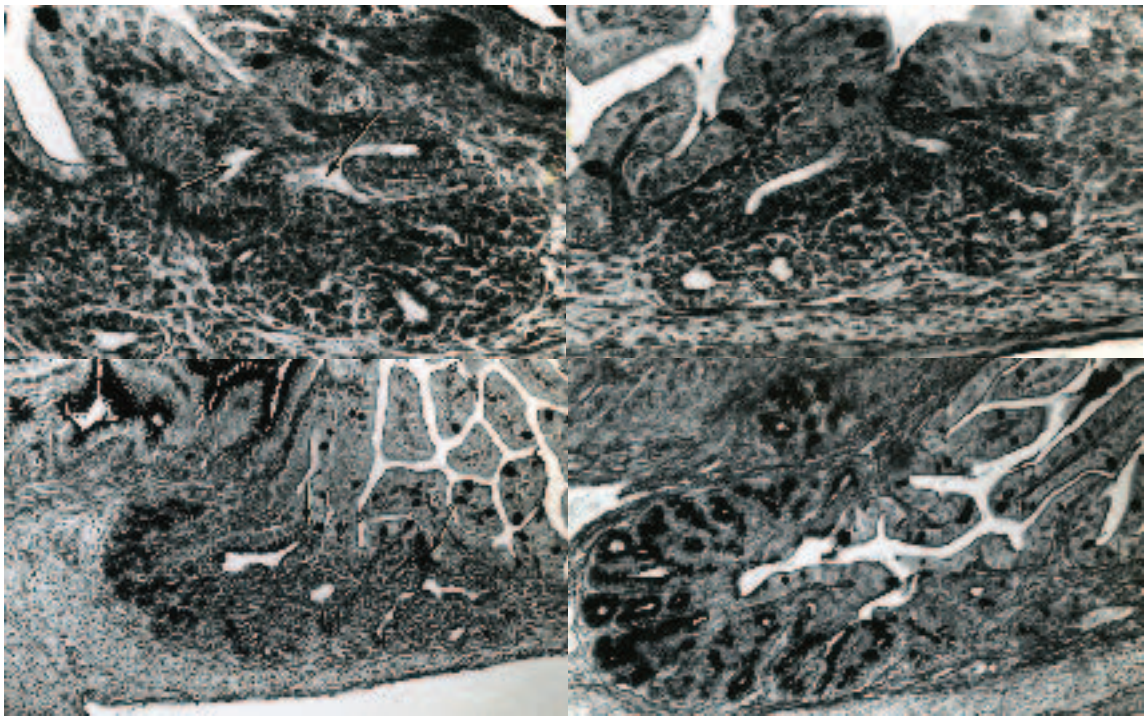

Fig. 2. (*Above left*). The forming intralobular duct system and duodenal sinus (arrows) of a single Brunner's gland from a three-week-old opossum. LM X 220. (*Above right*). Two Brunner's glands the ducts of which drain into a common duodenal sinus. Three-week-old opossum. LM X 220. (*Below left*). By five weeks of age Brunner's glands and their associated duodenal sinuses (arrows) are more clearly established. Note that the proximal gland has well developed secretory units when compared to the Brunner's gland located more distally as revealed by the PAS-positive staining. LM X 90. (*Below right*). A light micrograph illustrates a well-established duodenal sinus with the ducts draining several secretory lobules of surrounding Brunner's glands emptying into it. The glandular units of Brunner's glands create a duodenal sinus by pulling the intestinal or pyloric epithelium after them as they evaginate from the surface. Opossum seven weeks postnatal. LM X 90.

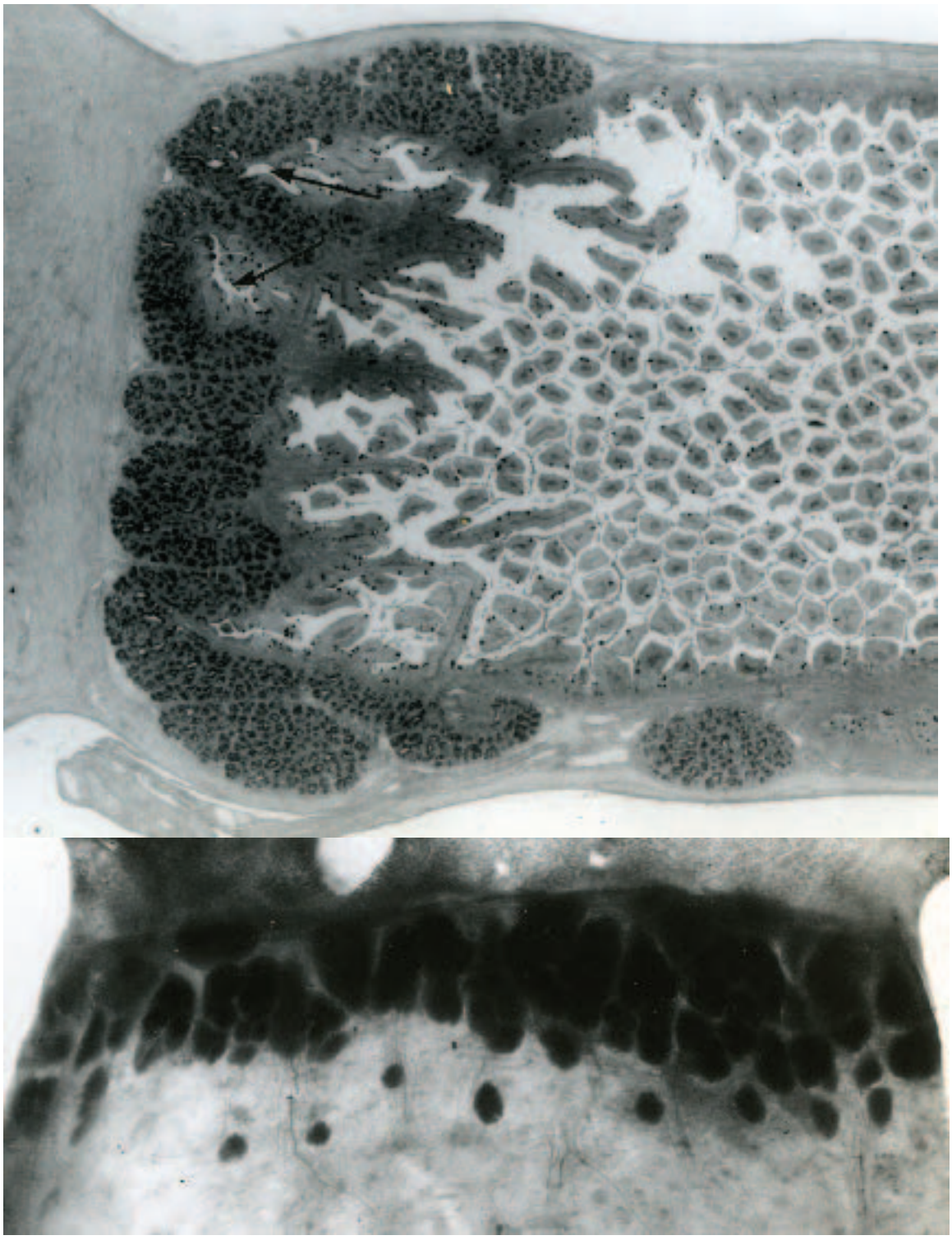

Fig. 3. (*Above*). The distribution and development of Brunner's glands in a twelve-week opossum demonstrated using the PAS staining method. Note the continued expansion of the duodenal sinuses (arrows) in relation to the forming Brunner's glands. LM X 50. (*Below*). The gastrointestinal junction of a fifteen-week old opossum prepared using the Landboe-Christensen method illustrates the overall distribution of Brunner's glands at this time. X 36.

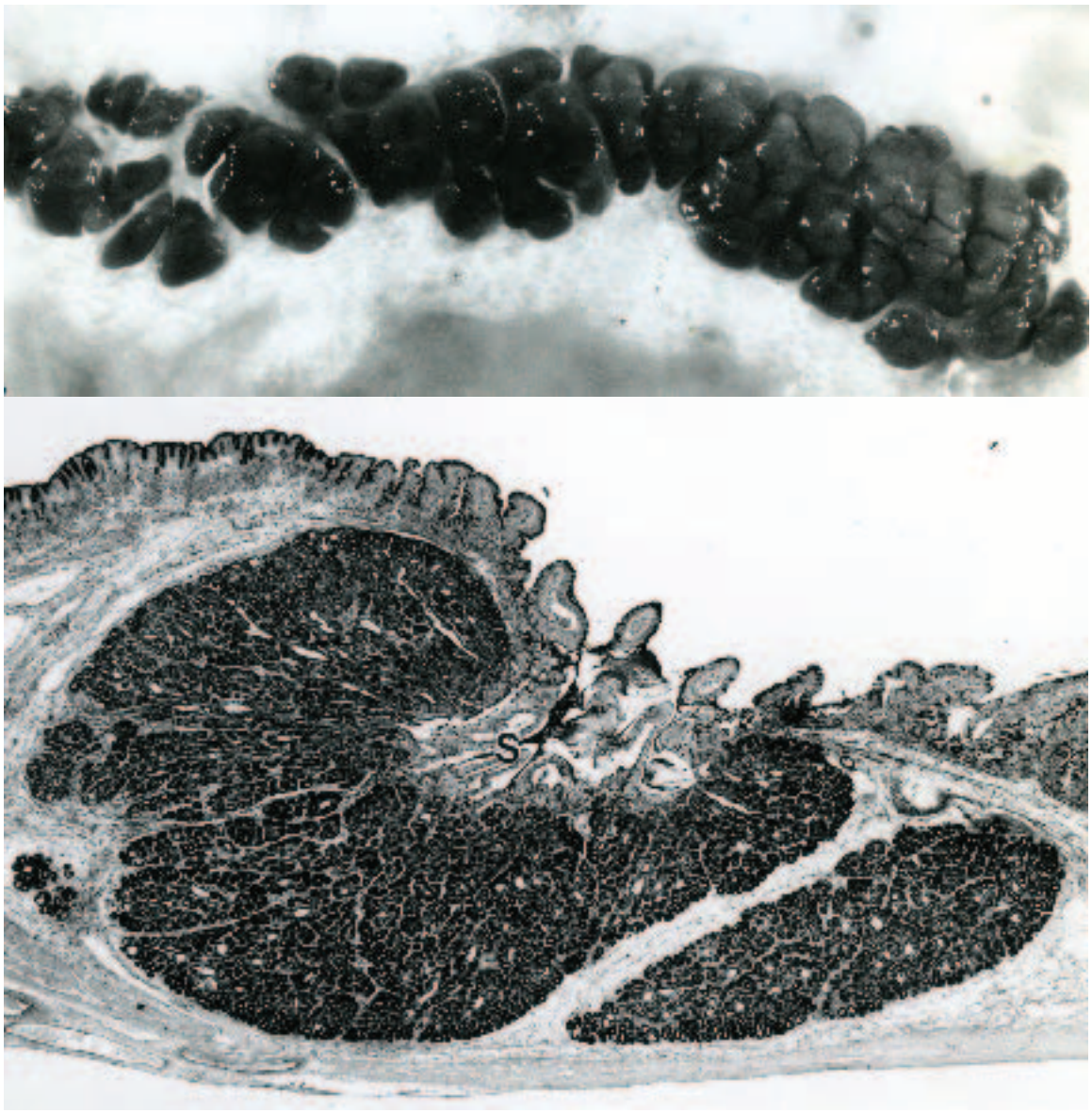

Fig. 4. (*Above*). A photograph illustrates the total distribution and external appearance of Brunner's glands from an adult male opossum as revealed using the Landboe-Christian technique. X 5. (*Below*). A micrograph illustrates a histological section through the central region of a duodenal sinus (S) and the surrounding Brunner's glands that empty into it. Note the numerous intestinal villi projecting into its lumen. The cells comprising the secretory units of Brunner's glands stain intensely with periodic acid Schiff (PAS) method suggesting the presence of complex glycoproteins. LM X 15.

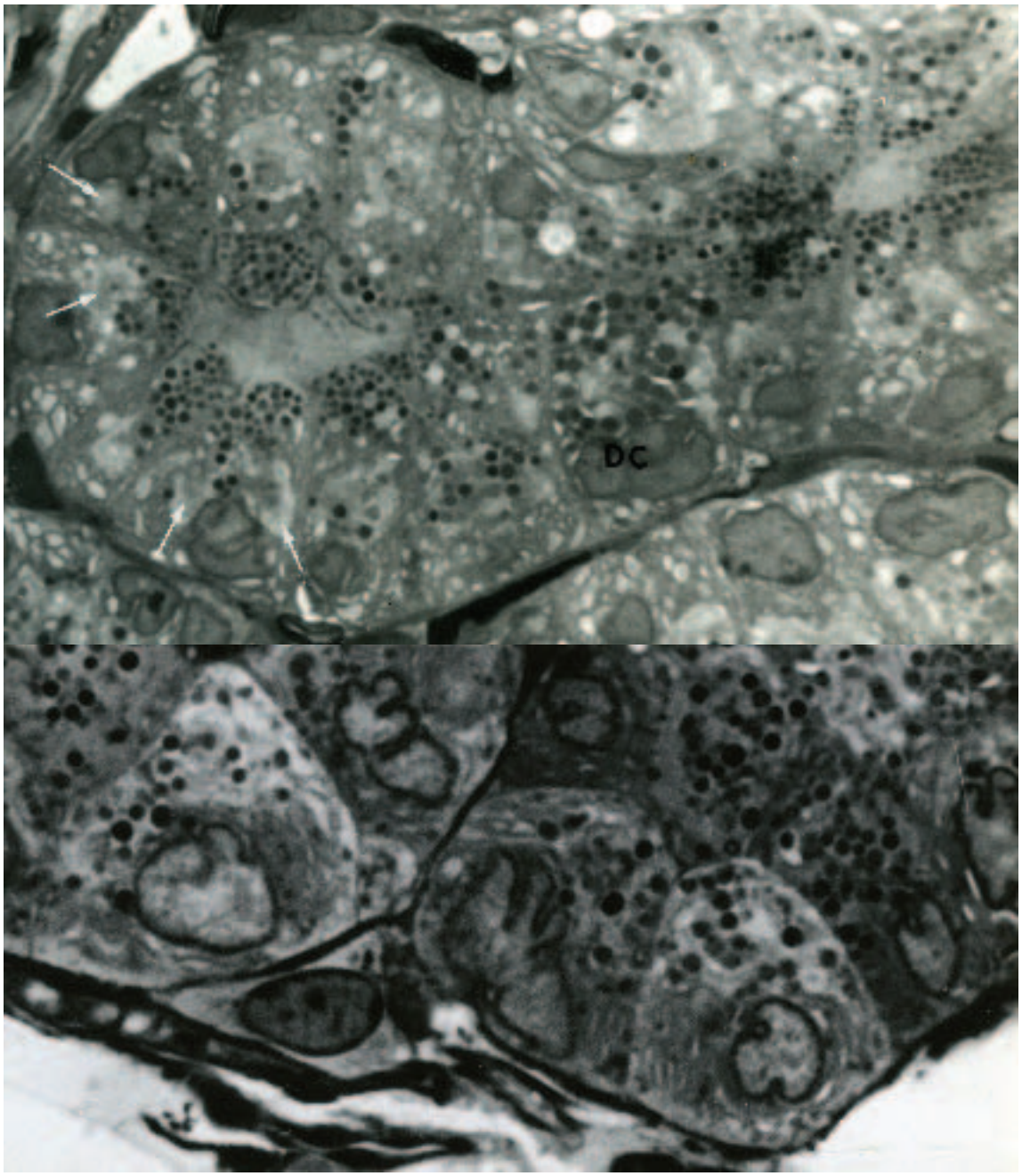

Fig. 5. (*Above*). Large pyramidal-shaped secretory cells form an acinus from an adult female opossum Brunner's gland. Cell apices are filled with secretory granules and large Golgi complexes (arrows) fill the supranuclear cytoplasm. Note the large dark cell (DC) with large secretory granules that fill the apical cytoplasm compressing the nucleus toward the base of the cell. LM X 800. (*Below*). Typical secretory cells of Brunner's glands from an adult male opossum. The cells are pyramidal in shape and show a definite polarity with nuclei occupying a basal position. The nuclei are enveloped by endoplasmic reticulum and secretory granules are found in relation to both a large Golgi complex and the apical plasmalemma. LM X 1500.

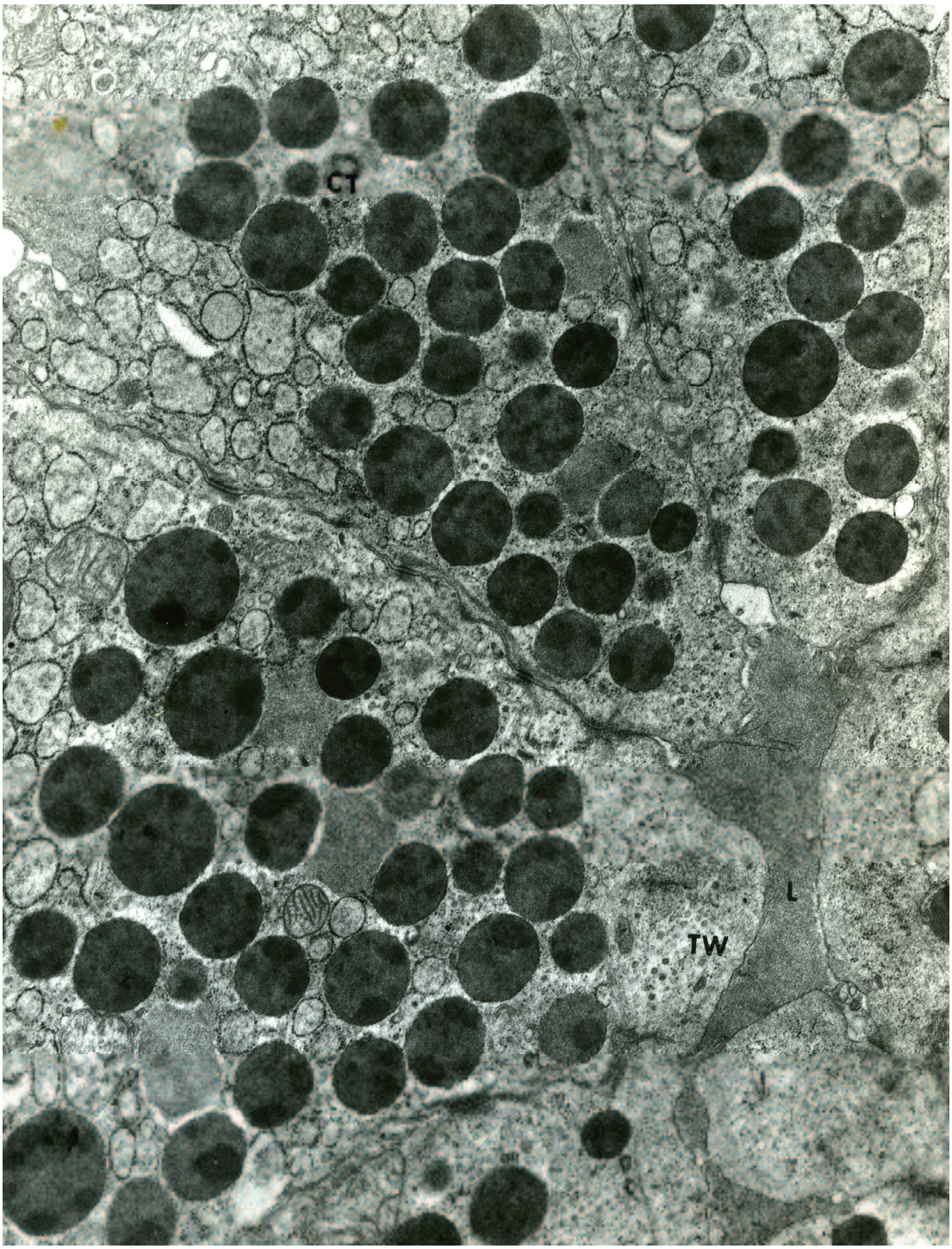

Fig. 6. An electron micrograph illustrates the apices of several cells forming a secretory tubule of Brunner's glands from an adult male opossum. The terminal web (TW) region of individual cells is thick and filled with granular material and vesicles. Desmosomes and tight junctions occur at the interphase between secretory cells. Two morphological forms of secretory granule are evident, one is light, granular and usually without a well-defined membrane; the other being dark, mottled and limited by a membrane. A light, granular material fills the lumen (L) of the secretory tubule. A centriole (CT) also occurs among the secretory granules of one of the cells. TEM X 12,000.

Chapter 23. Colon

Synopsis:

The colon of the newborn opossum has a small lumen lined by pseudostratified columnar epithelium although some proximal regions exhibit a simple columnar epithelium. Enterocytes comprising the colonic epithelium exhibit a well-developed apical endocytic complex and contain numerous large lipid droplets. Goblet cells are present within the intestinal lining epithelium of the newborn colon and make up about 12% of the surface lining cells. Goblet cells increase progressively in number so that by weaning (90-100 days postnatal) they constitute nearly 60% of the cells lining the colon. Villi are not observed in the opossum colon during its development. The intestinal glands (crypts of Lieberkühn), although absent in the newborn, are well established by the end of the first postnatal week and then show a progressive increase in depth during the first weeks of postnatal life. The apical endocytic complex and lipid droplets prominent within enterocytes lining the newborn colon appear only as scattered inclusions by the end of the second week postnatal and completely disappear by the end of third postnatal week.

Enteroendocrine cells immunoreactive for neurotensin, somatostatin or serotonin (5-HT) occur within the intestinal lining epithelium of the newborn colon and increase in number with development. Neurotensin-immunoreactive cells, although found in the newborn proximal colon, do not form a significant population of cells until about the eleventh postnatal week and then are distributed throughout the colonic epithelium. As their numbers increase they show the greatest concentration distally. The muscularis mucosae of the colon is established by the end of the second postnatal week.

In contrast to both the stomach and small intestine, the muscularis externa of the opossum colon is well established at birth with well-defined inner circular and outer longitudinal layers of smooth muscle. Although differing in thickness, the smooth muscle forming the muscularis externa of the colon, like that of the stomach and small intestine, is characterized by an early proliferative period followed by two periods of hypertrophy. As in the stomach and small intestine, the myenteric plexus of the colon is present at birth but poorly developed. The subcomponents of the myenteric plexus (ganglia and nerve fascicles) increase in number and size during the first four weeks of postnatal life and correspond to the period organogenesis when the most active proliferation of smooth muscle cells occurs in the muscularis externa.

Acknowledgments:

Figs. 1 (bottom), 2, 3 and 4, courtesy of and from: Krause, W.J., J.H. Cutts, and C.R. Leeson (1976) The postnatal development of the alimentary canal in the opossum. III. Small Intestine and Colon. J. Anat. 123:21-45.

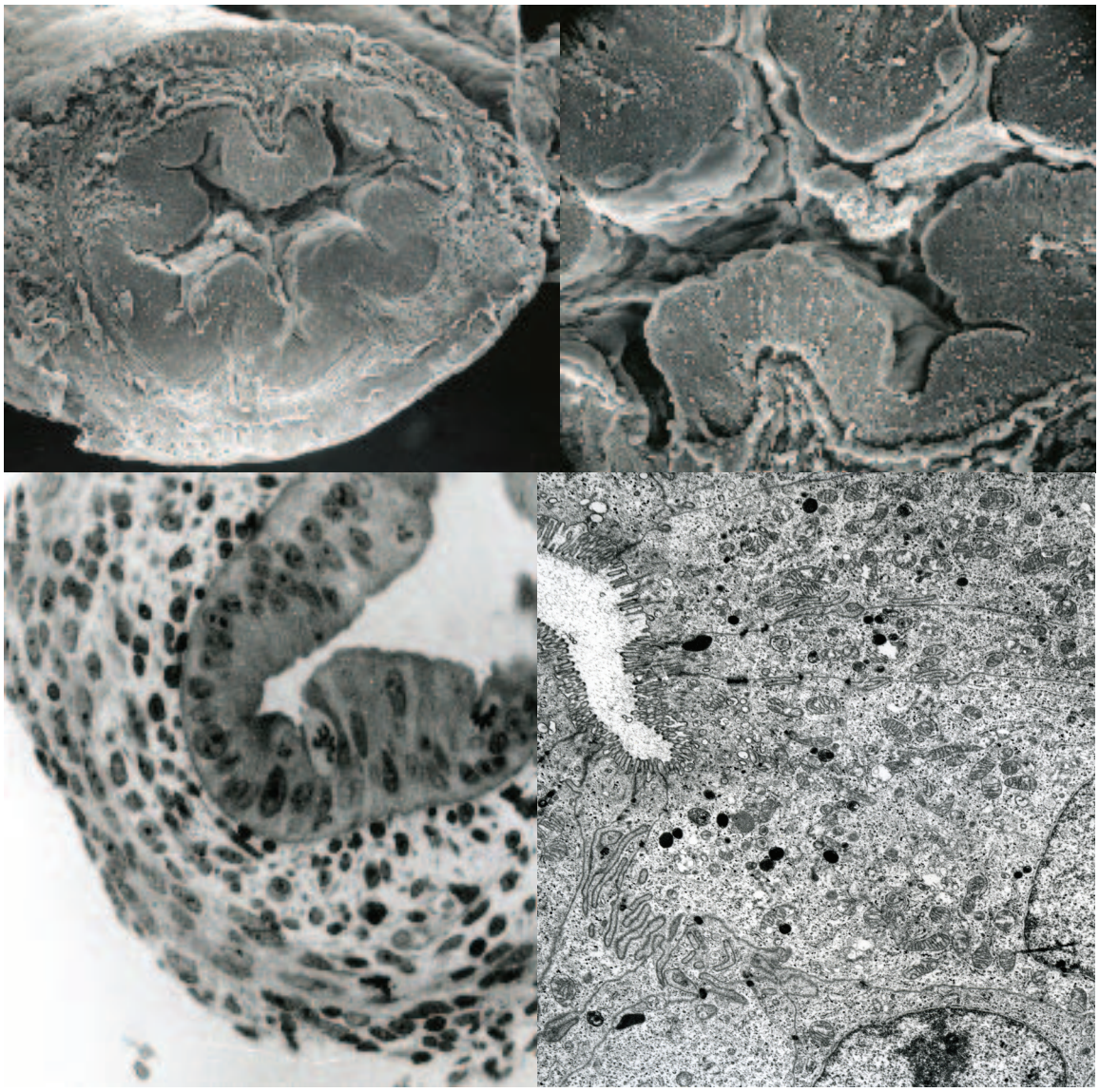

Fig. 1. (*Above left*). A transverse cut through the colon of the newborn opossum as viewed by scanning electron microscopy. The mucosa is organized into longitudinal folds that course parallel to the long axis of the intestinal tract. Villi are absent. SEM X 100. (*Above right*). A micrograph illustrates the mucosa of the colon from a newborn opossum as seen at increased magnification. SEM X 200. (*Below left*). A histological section through the wall of the newborn colon illustrates the immature character of the intestinal lining epithelium and the forming muscularis externa. The latter appears to be of greater depth when compared to the muscularis externa of the small intestine. Note the mitotic figures within the intestinal epithelium. LM X 300. (*Below right*). The apices of intestinal epithelial cells lining the newborn colon exhibit a well-established microvillus border. The apical cytoplasm of these cells contains numerous membrane-bound vesicles; some of which contain material of varying electron density whereas others appear empty. TEM X 8,000.

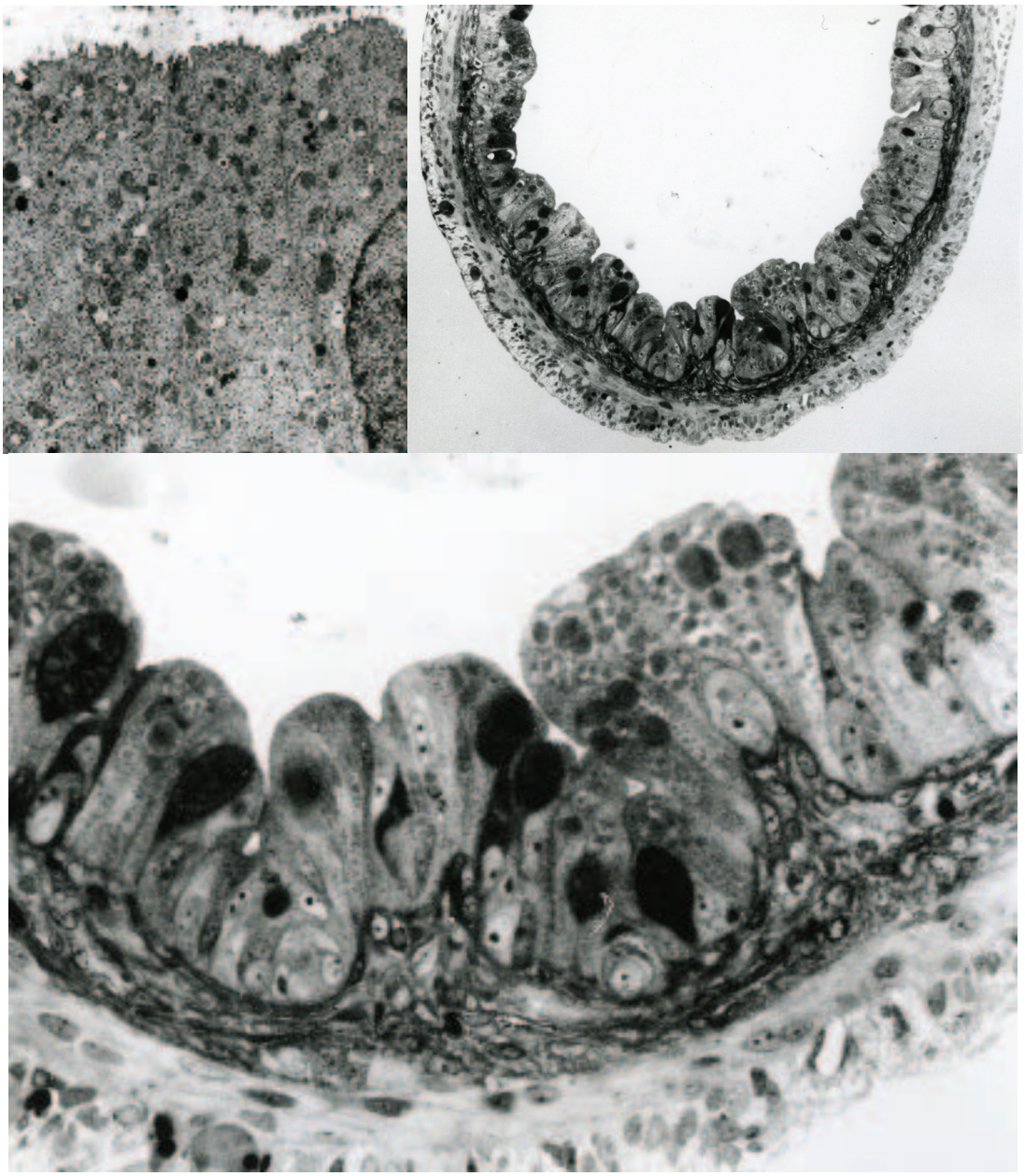

Fig. 2. (*Above left*). The ultrastructure of the colonic epithelium of an opossum three day postnatal appears similar to that of the newborn and contains vesicles some of which appear empty; others contain an electron dense material. TEM X 7,000. (*Above right*). The lumen of the colon increases considerably in diameter by the end of the first postnatal week. Likewise, the muscularis externa shows a considerable increase in thickness and definite outer longitudinal and inner circular layers of smooth muscle have formed. LM X 100. (*Below*). The intestinal lining epithelium of the colon shows initial stages of infolding and appears to be involved in absorption. Some intestinal epithelial cells appear to be filled with lipid droplets. Goblet cells also are present in considerable numbers in the colonic epithelium of the week old opossum. LM X 400.

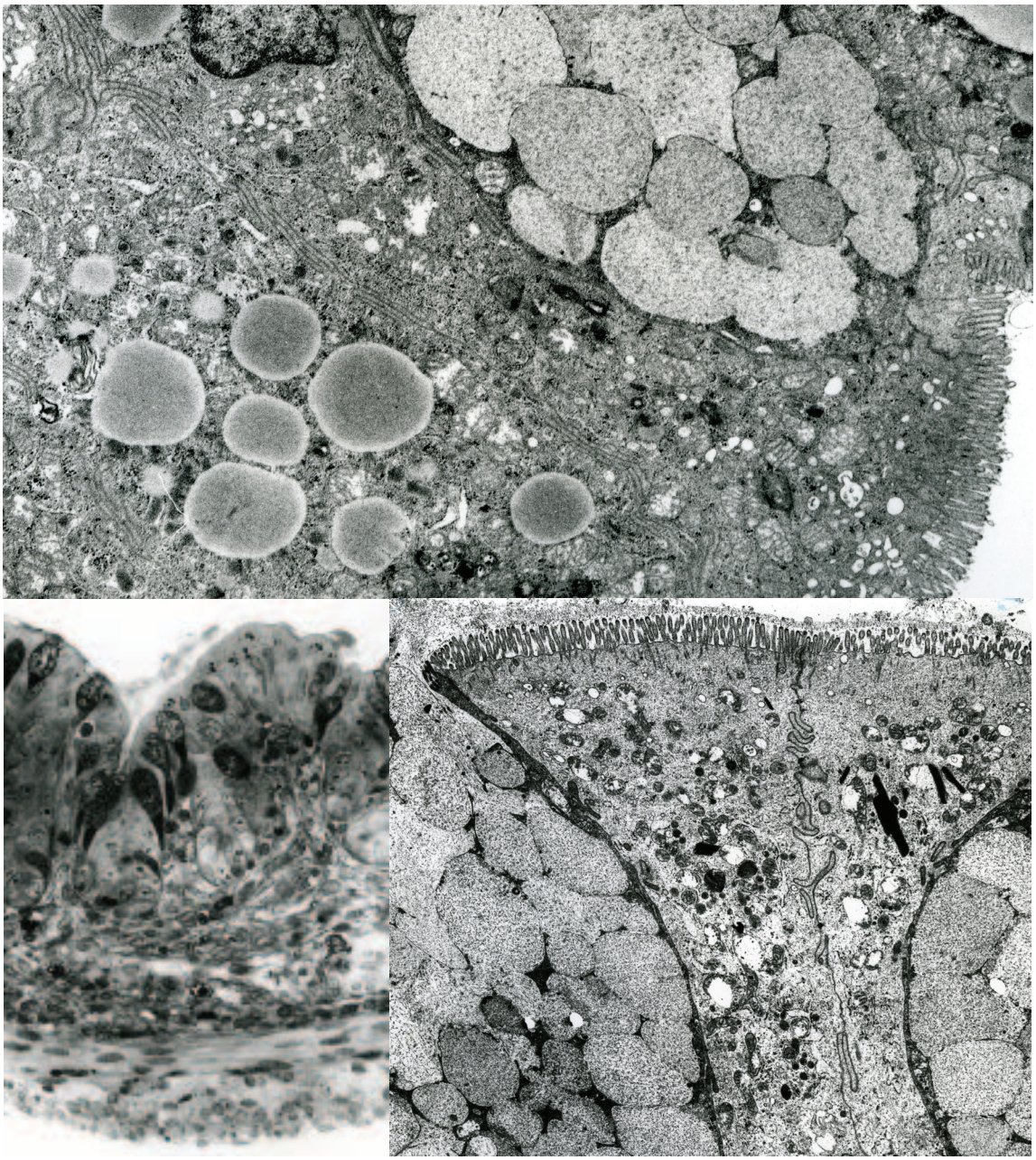

Fig. 3. (*Above*). A region of colonic epithelium one week postnatal illustrates a portion of an enterocyte filled with lipid droplets (bottom of photomicrograph) and a region of an adjacent goblet cell filled with mucin granules (top of photomicrograph). The microvillus border of the enterocyte and the lumen of the colon are shown at the lower right. TEM X 10,000. (*Below left*). By the end of the second postnatal week the crypts of Lieberkühn have differentiated and goblet cells are increased in number. At this time the colonic epithelial cells show only limited amounts of absorbed materials. The muscularis externa continues to increase in depth. LM X 250. (*Below right*). Two intestinal epithelial cells (center) sandwiched between goblet cells of a three week old opossum. Scattered, irregularly shaped, dense crystalline structures are found within the colonic epithelial cells. TEM X 6,000.

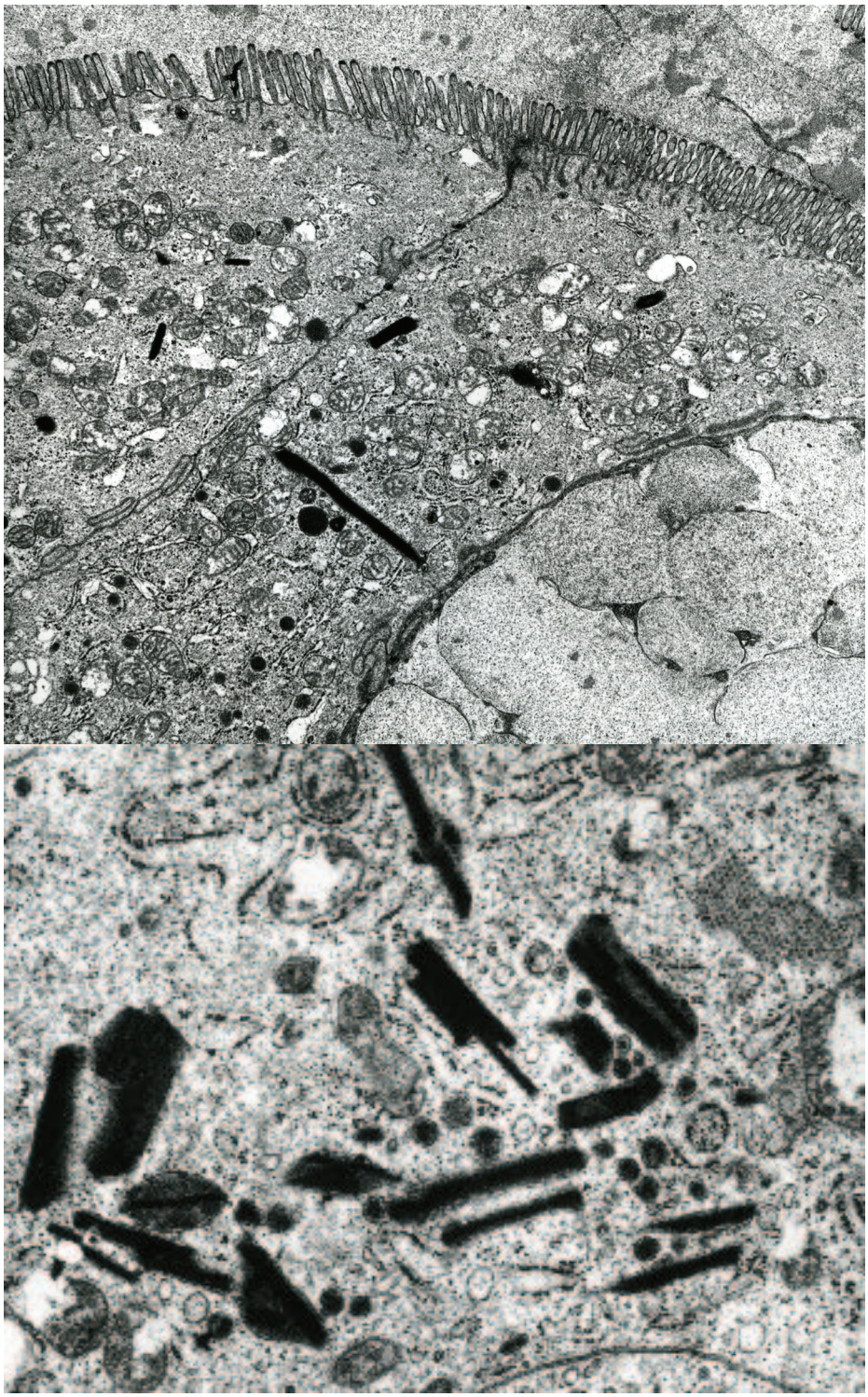

Fig. 4. (*Above*). In addition to the distinct crystalline structures observed in the colonic epithelial cells, scattered small, round electron-dense granules also are observed. A portion of a goblet cell is shown at the lower right. Three-week-old opossum. TEM X 8,000. (*Below*). At increased magnification the crystalline structures appear limited by a membrane and vary in electron density. Note the internal electron-density apparent within some of the crystalline structures. TEM X 15,000.

Chapter 24. Pancreas

Synopsis:

Organogenesis of the opossum pancreas occurs almost entirely during the prolonged postnatal period that typifies this species. However, the general pattern of development for both the exocrine and endocrine components of the pancreas is typical of that observed in other mammals including man. The dorsal anlage of the opossum pancreas originates as an evagination from the foregut late in prenatal day ten. The ventral pancreatic anlage appears during the eleventh prenatal day originating as a branch of the hepatic diverticulum. Just prior to birth (twelve days prenatal) the ventral and dorsal pancreatic anlagen unite. The connection of the dorsal pancreatic anlage with the foregut disappears late in the eleventh prenatal day. As a result, the opossum pancreas is connected to the proximal duodenum by a single duct derived from the ventral anlage. In general, the newborn opossum pancreas has a very immature appearance consisting of primitive exocrine tubules that envelope a central region of endocrine cells. The exocrine tubules terminate in solid clusters of undifferentiated cells among which are proacinar cells and scattered endocrine cells. Cells that form the remainder of the exocrine tubules are smaller than the proacinar cells and range from simple columnar to simple squamous in nature. Numerous mitotic figures are observed within the epithelium forming the exocrine tubules. Regions of stratification are observed also. These regions represent peritubular buds that characterize the differentiating opossum pancreas in its initial phases of organogenesis. Developing acini, centroacinar cells, and small intralobular ducts are present by the end of the first postnatal week. Pancreatic lobules form and progressively enlarge due to continued growth of the differentiating ductal system concomitant with an increase in number of acini. During the first few weeks of postnatal life, the interior of the pancreatic lobule is characterized by small ducts that radiate in a spoke-like fashion from a common, central intralobular duct peripherally toward clusters of differentiating acini. Organogenesis of the pancreas prior to weaning is concerned primarily with the differentiation and formation of ducts, acini, and islets. Development of the pancreas during the post-weaned period appears limited primarily to the expansion of these established pancreatic elements.

Endocrine cells immunoreactive for glucagon, insulin, bovine pancreatic polypeptide (BPP), somatostatin or 5-HT are present either as small groups of cells scattered within the central region of the pancreas or as isolated cells within the exocrine tubules of the newborn opossum pancreas. Boundaries of individual pancreatic islets are difficult to ascertain early in development but become better defined later in the postnatal period. Interlobular (primary) pancreatic islets develop from the central area of the newborn pancreas rich in endocrine cells. A second generation of intralobular pancreatic islets then differentiates from the epithelium forming the exocrine component of the pancreas. Initially, intralobular islets differentiate from the primitive exocrine tubules that constitute the majority of the pancreas during early organogenesis; later in the postnatal period they differentiate from cells lining the intralobular duct system as organogenesis continues. The intralobular pancreatic islet will become the predominate islet, whereas the interlobular islet is a rare observation late in the postnatal period and in the adult. All five types of immunoreactive endocrine cells are associated with both forms of pancreatic islet. Endocrine cells constituting the pancreatic islets of the opossum exhibit a definite organization with regard to distribution within islets. Endocrine cells immunoreactive for insulin occupy the central region of the pancreatic islets.

In contrast, glucagon- and BPP-immunoreactive endocrine cells form an inconsistent peripheral layer, two to three cells deep, around the edge of intralobular islets. Somatostatin-immunoreactive cells also assume a peripheral location, but usually form layer two to three cells deep to the outer margin of the intralobular islet. The small population of 5-HT-immunoreactive cells occurs peripherally as well, scattered among the other endocrine cell types. Dopamine, 5-HT, and BPP can be demonstrated co-localized within the same endocrine cell of some pancreatic islets. Individual (isolated) endocrine cells are observed scattered within the epithelium lining the intralobular duct system and between pancreatic acinar cells throughout the postnatal period and into adulthood.

Acknowledgments:

Figs. 1, 2 (top), 3 (bottom), 4 (top), 5 (bottom), 6, 7 (top), 8 (top and bottom left), 9 (bottom), 10 (bottom), 11 (bottom right), 12, 13, 14, 15, 16 (top left), 17 (bottom), courtesy of and from: King, F.C., (1976) MS Thesis. Postnatal development of the pancreas in the opossum, *Didelphis virginiana*, with special reference to the exocrine epithelium. University of Missouri, Columbia, Missouri, pp 149.

Fig. 16 (top right), courtesy of and from: King, F.C., W.J. Krause and J.H. Cutts (1978) Postnatal development of the pancreas in the opossum. I. Light microscopy. Acta Anat. 101:259-274.

Figs. 4 (bottom), 5 (top), 11 (top), 16 (bottom), 17 (top), 18 and 19 (top), courtesy of and from: Krause, W.J., J.H. Cutts III, J.H. Cutts and J. Yamada. (1989). An immunohistochemical study of the developing endocrine pancreas of the opossum (*Didelphis virginiana*). Acta Anat. 135:84-96.

Fig 2 (bottom), 8 (bottom right), 3 (top), 10 (top), 15 (bottom), 19 (bottom), courtesy of and from: Krause, W.J. and J.H. Cutts (1992) Development of the Digestive System in the North American Opossum (*Didelphis virginiana*). Adv. Anat. Embryol. Cell Biol. 125:1-148.

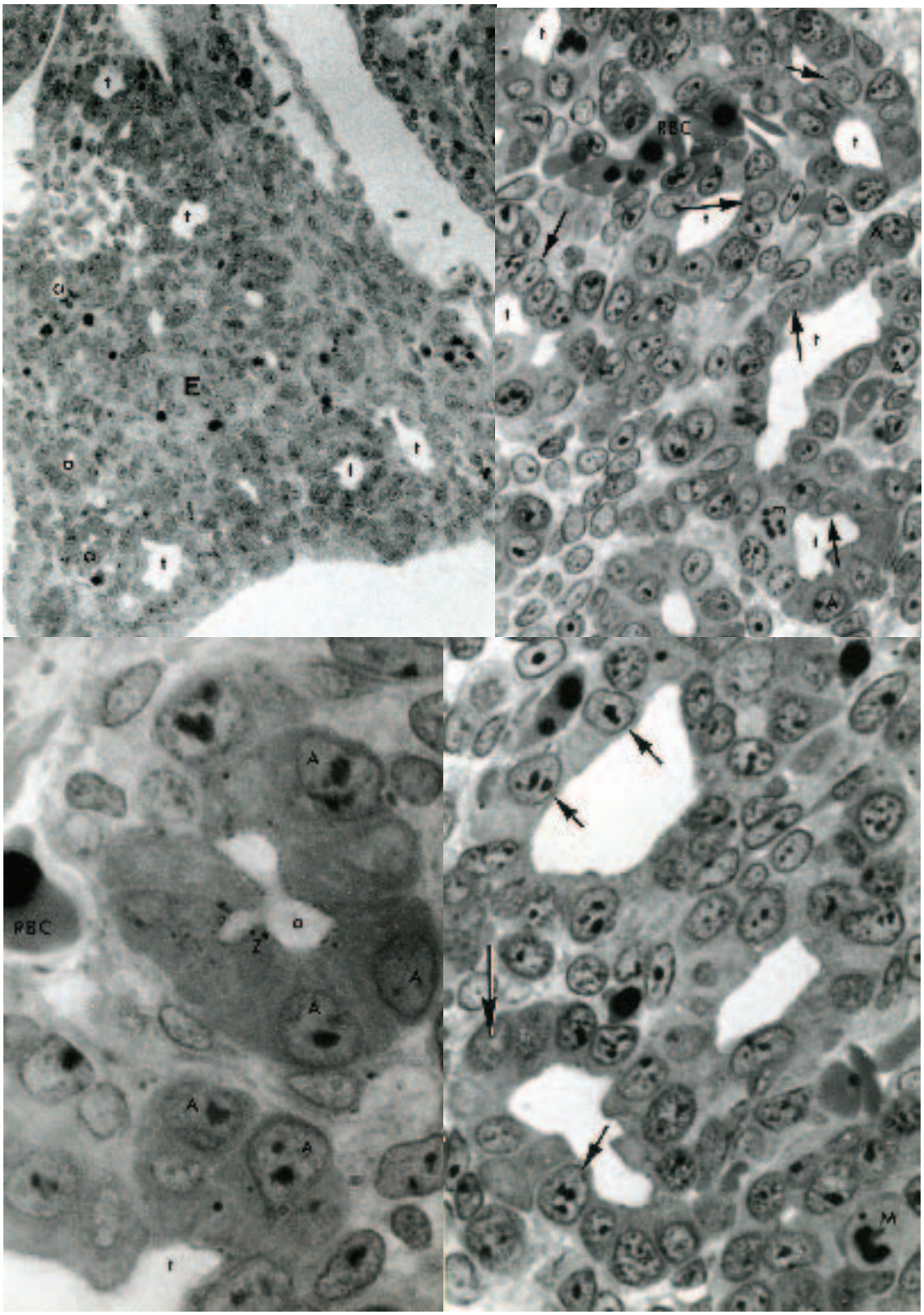

Fig. 1. All are from newborn opossum pancreas. (*Above left*). The pancreas consists of central region of endocrine cells (E) surrounded by differentiating tubules (t) and acini (a). LM X 150. (*Above right*). The periphery of the pancreas exhibits primitive exocrine tubules (t) lined by tubular cells (arrows) and proacinar cells (a). Note the nucleated red blood cells (RBC) and the mitotic figures (m). LM X 400. (*Below left*). Forming acini (a) are comprised of acinar cells (A) that exhibit few zymogen granules (Z). Note the acinar cells (A) within the wall of a primitive exocrine tubule (t). LM X 600. (*Below right*). What appear to be differentiating acinar cells (arrows) within the epithelial lining of primitive exocrine tubules. LM X 400.

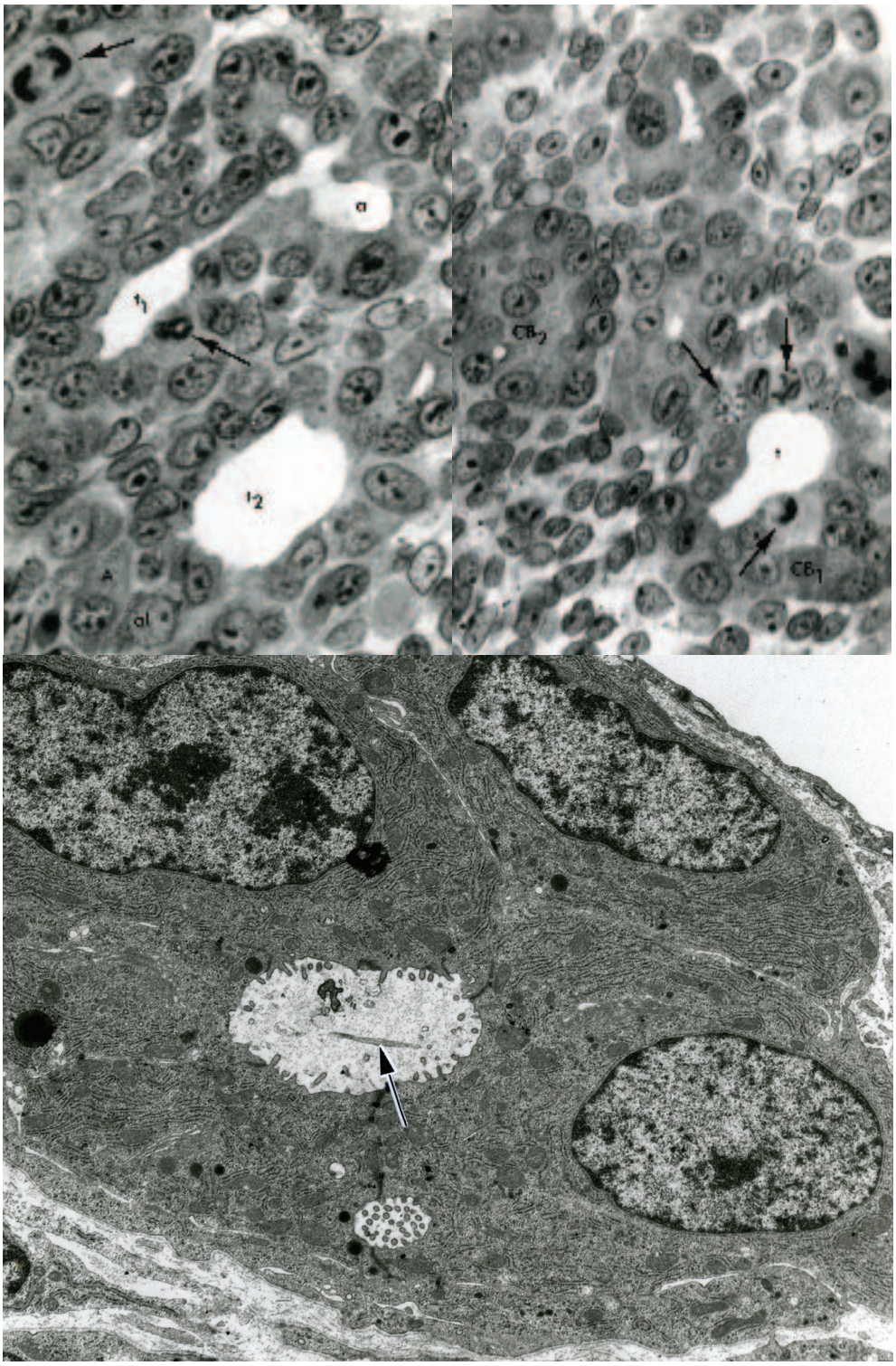

Fig. 2. (*Above left*). A micrograph illustrates a primitive exocrine tubule (t1) from which a differentiating acinus (a) has taken origin. The other tubule shown (t2) exhibits a paratubular bud consisting of differentiating (proacinar) acinar cells (A, al). Several cells are in mitosis (arrows). Newborn pancreas. LM X 400. (*Above right*). A paracellular bud (CB1) extending from a primitive exocrine tubule (t) that shows several mitotic figures (arrows). A second paracellular bud in the field (CB2) consists of differentiating acinar cells. Newborn pancreas. LM X 400. (*Below*). Proacinar cells line an expanding exocrine tubule within the pancreas of a newborn opossum. A cilium (arrow) lies within the lumen of the pancreatic tubule. Note the intercellular canaliculus near the bottom center of the illustration. TEM X 5,000.

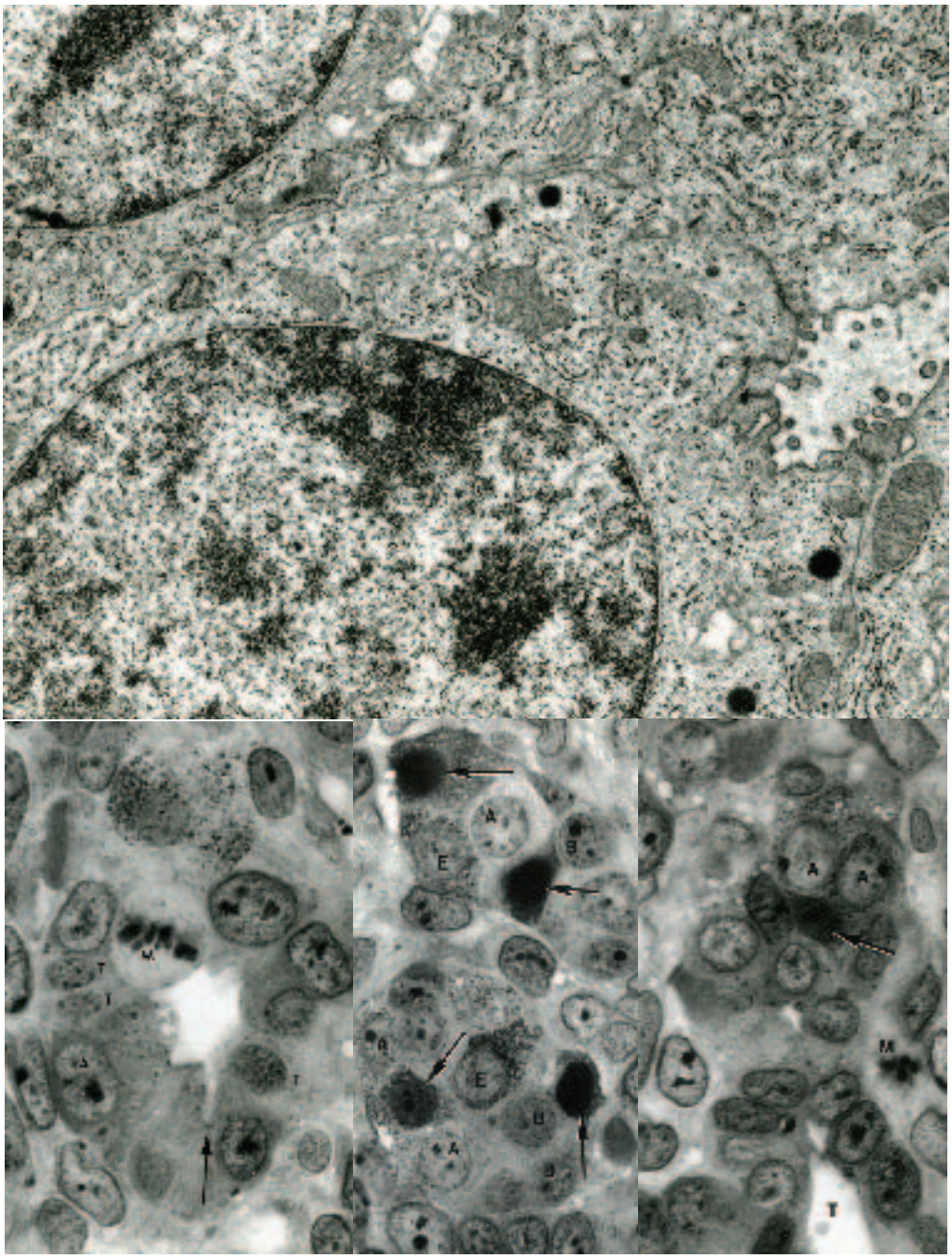

Fig. 3. (*Above*). An electron micrograph illustrates the apical and supranuclear regions of proacinar cells from the pancreas of a newborn opossum. TEM X 10,000. (*Below left*). A region of a primitive exocrine tubule from a newborn opossum pancreas illustrates tubular cells (t), differentiating acinar cells (A) with an associated intercellular canaliculus (arrow), an endocrine cell (E) and a mitotic figure (M). LM X 600. (*Below center*). A paratubular bud from a newborn opossum pancreas consists primarily of endocrine cells (E). Alpha (A), beta (B), delta (arrows) cells are shown. LM X 600. (*Below right*). A region of a paratubular bud of endocrine cells illustrating their origin from a primitive exocrine tubule (T). Two alpha (A) cells and a delta cell (arrow) can be identified. Note also the mitotic figure (M) shown. Newborn opossum. LM X 600.

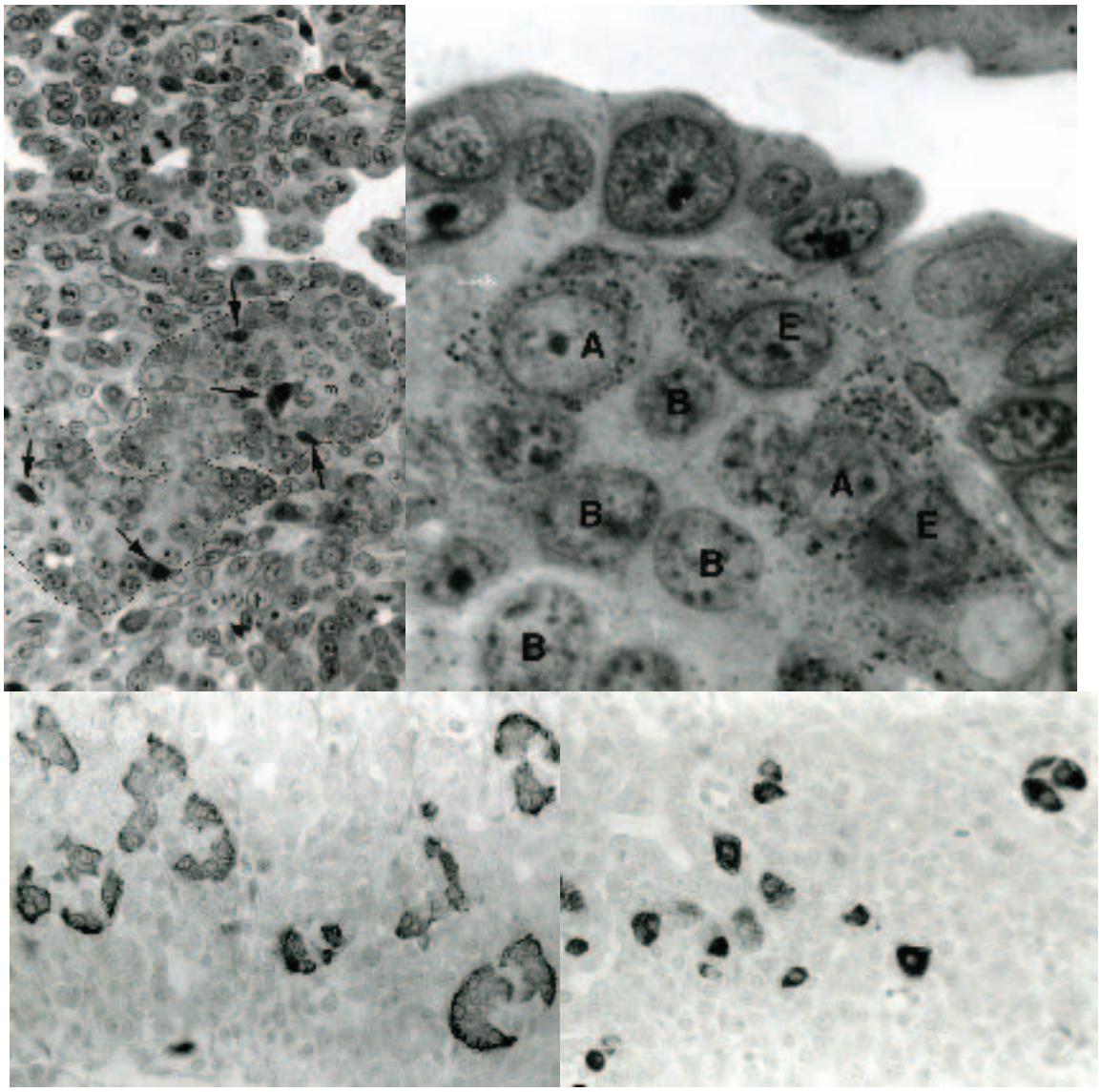

Fig. 4. (*Above left*). A primitive pancreatic islet (outlined) that lies immediately adjacent to a primitive exocrine tubule in the newborn opossum pancreas. What appear to be delta cells (arrows) as well as numerous mitotic figures (m) are observed. LM X 300. (*Above right*). The region of the previous figure where the islet abuts the primitive exocrine tubule when viewed at increased magnification illustrates their intimate association as well as the alpha (A) and beta (B) cells forming this region of the islet. LM X 600. (*Below left*). Glucagon-immunoreactive cells in the newborn pancreas are numerous and concentrated primarily at the periphery of forming pancreatic islets. LM X 275. (*Below right*). Bovine pancreatic polypeptide-immunoreactive cells usually are observed scattered within developing pancreatic islets. Newborn opossum. LM X 300.

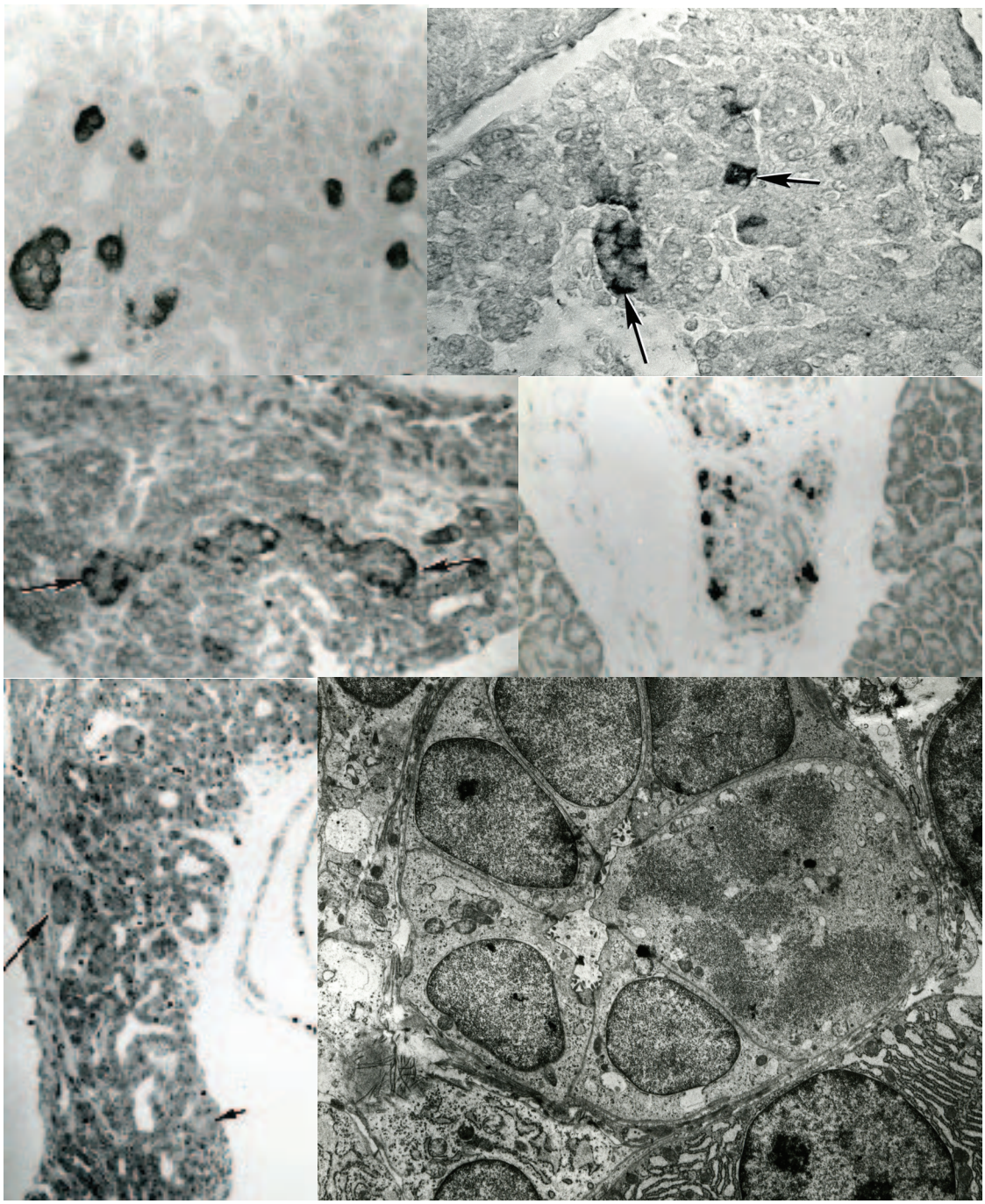

Fig. 5. (*Top left*). Somatostatin-immunoreactive cells in the newborn pancreas form small clusters or may be observed singly in the primitive, expanding pancreatic tubules. LM X 300. (Top *right*). Insulin-immunoreactive cells. Newborn opossum pancreas. LM X 300. (*Center left*). Glucagon-immunoreactive cells associated with an elongate, differentiating secondary pancreatic islet within the exocrine parenchyma. Newborn opossum. LM X 200. (*Center right*). Somatostatin-immunoreactive cells within a primary pancreatic islet located in the interlobular connective tissue. LM X 200. (*Bottom left*). The pancreas of a one-week-old opossum continues to be characterized by numerous primitive exocrine tubules with wide irregularly shaped lumina. Differentiating acini continue to form at the ends of the tubules (arrows) but are few in number. LM X 150. (*Bottom right*). A micrograph illustrates a section through a small intralobular pancreatic duct of a four-day-old opossum. Note the mitotic figure within the epithelium forming its wall. TEM X 5,000.

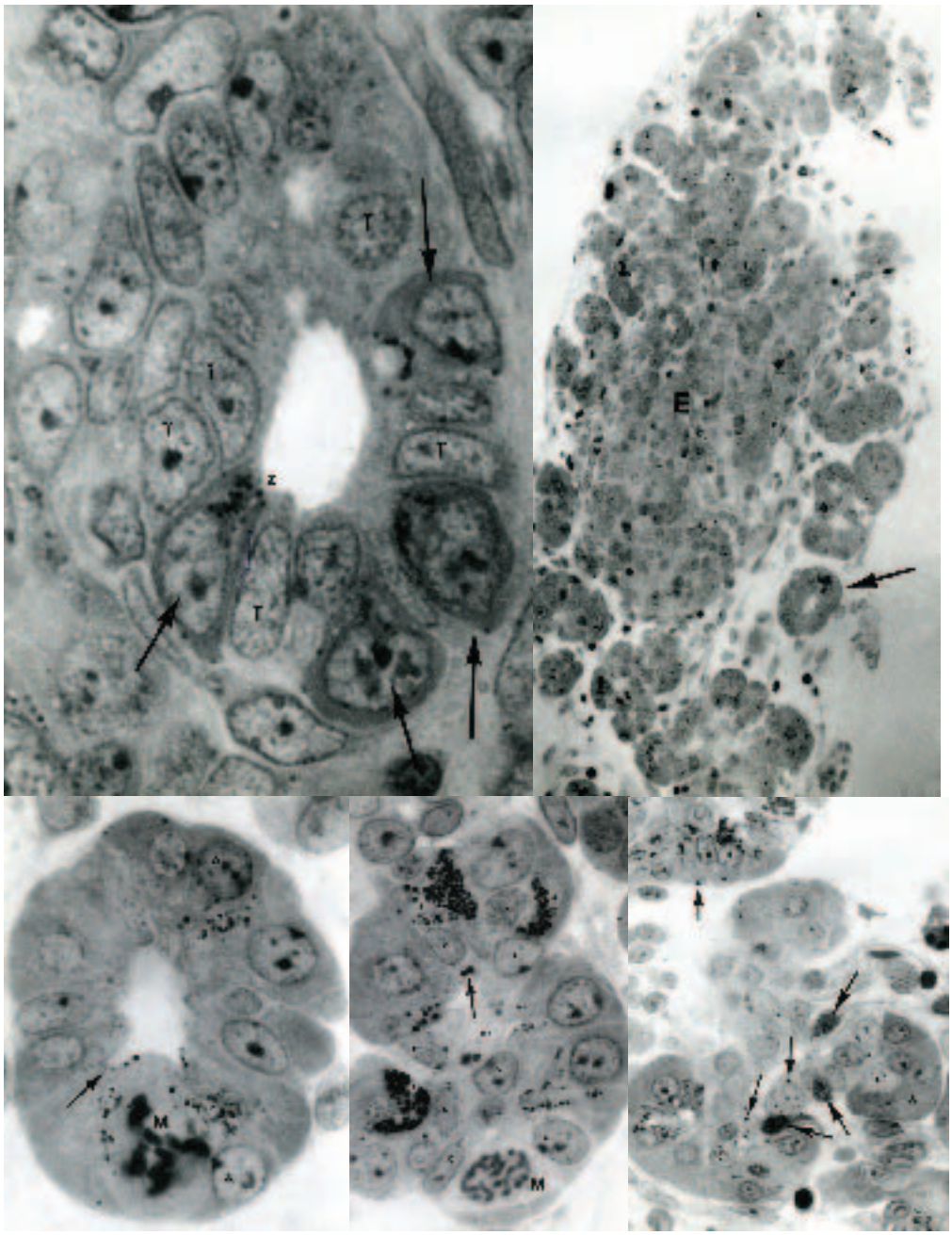

Fig. 6. (*Above left*). A region of a primitive pancreatic exocrine tubule from an opossum one day postnatal that contains differentiating acinar cells (arrows) among the tubular lining cells (T). One of the acinar cells contains numerous zymogen granules (Z). LM X 600. (*Above right*). A region of pancreas from a four-day-old opossum exhibits a central mass of endocrine tissue (E) surrounded by exocrine pancreas (arrow). LM X 150. (*Below left*). A micrograph illustrates a differentiating acinus from a four-day opossum some of the acinar cells (A) of which contain zymogen granules (arrow). One acinar cell is in mitosis (M). LM X 1,000. (*Below center*). Centroacinar cells (C) are apparent in developing acini of the four-day-old opossum pancreas. Zymogen granules fill some acinar cell with occasional lipid droplets occurring in centroacinar cells (arrow). Mitotic figures (M) remain a prominent feature. LM X 1,000. (*Below right*). Lipid droplets are occasionally observed both in the exocrine epithelium (small arrows) and in endocrine cells (large arrows) of the four-day-old opossum pancreas. LM X 500.

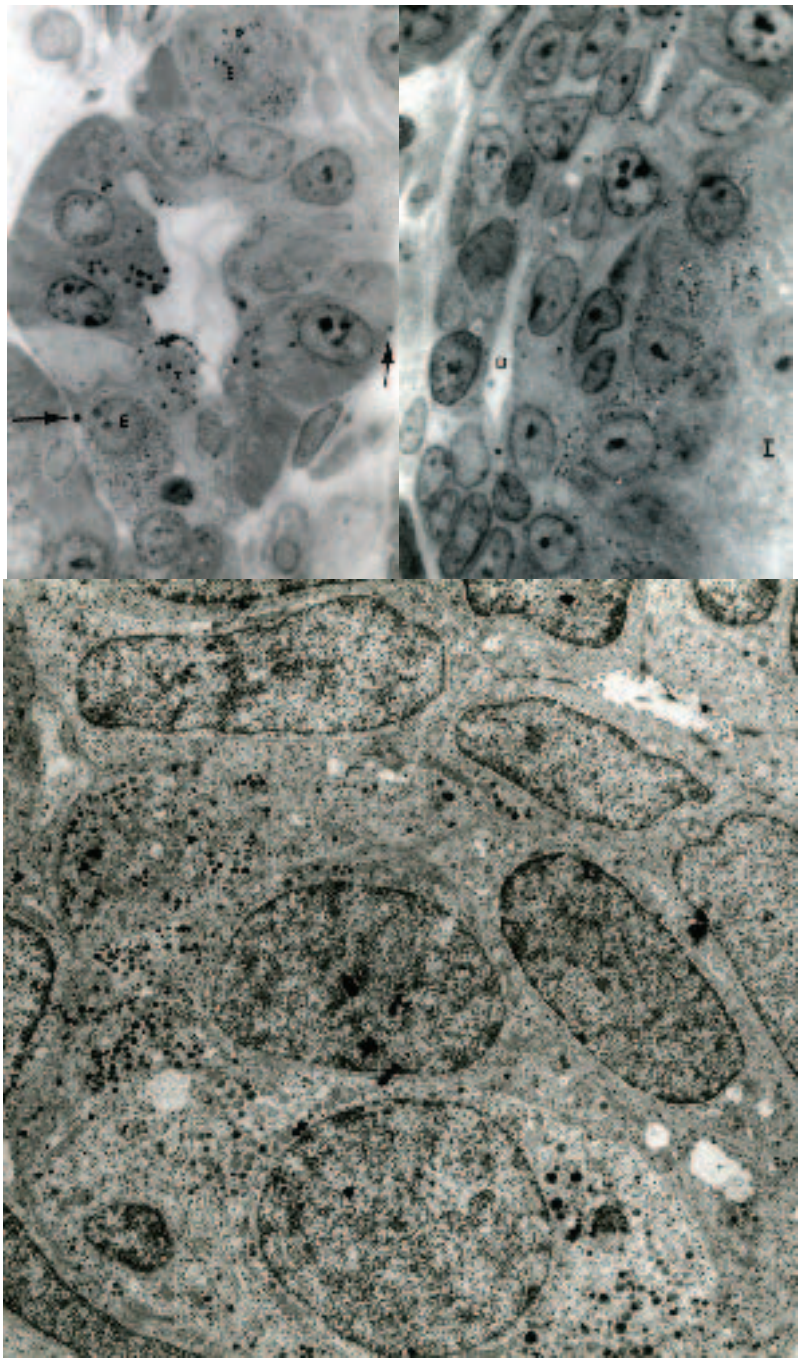

Fig. 7. (*Above left*). A differentiating acinus associated with two endocrine cells (E) whose fine dust-like granules can be distinguished from the larger zymogen granules (Z) within acinar cells. Small lipid droplets (arrows) continue to be observed in the acinar cell cytoplasm. Note the intercellular canaliculus in the upper left portion of the acinus. Four-day-old opossum. LM X 1000. (*Above right*). The edge of a pancreatic islet (I) from a four-day-old opossum that is intimately associated with a small intralobular duct (D). LM X 1,000. (*Below*). A group of five or six endocrine cells form a pancreatic islet. Note the epithelial cells forming a small intralobular duct located in the upper right corner of the electron micrograph. The epithelial cells are united at their apices by tight junctions and define a small lumen. Four-day-old opossum. TEM X 2,000.

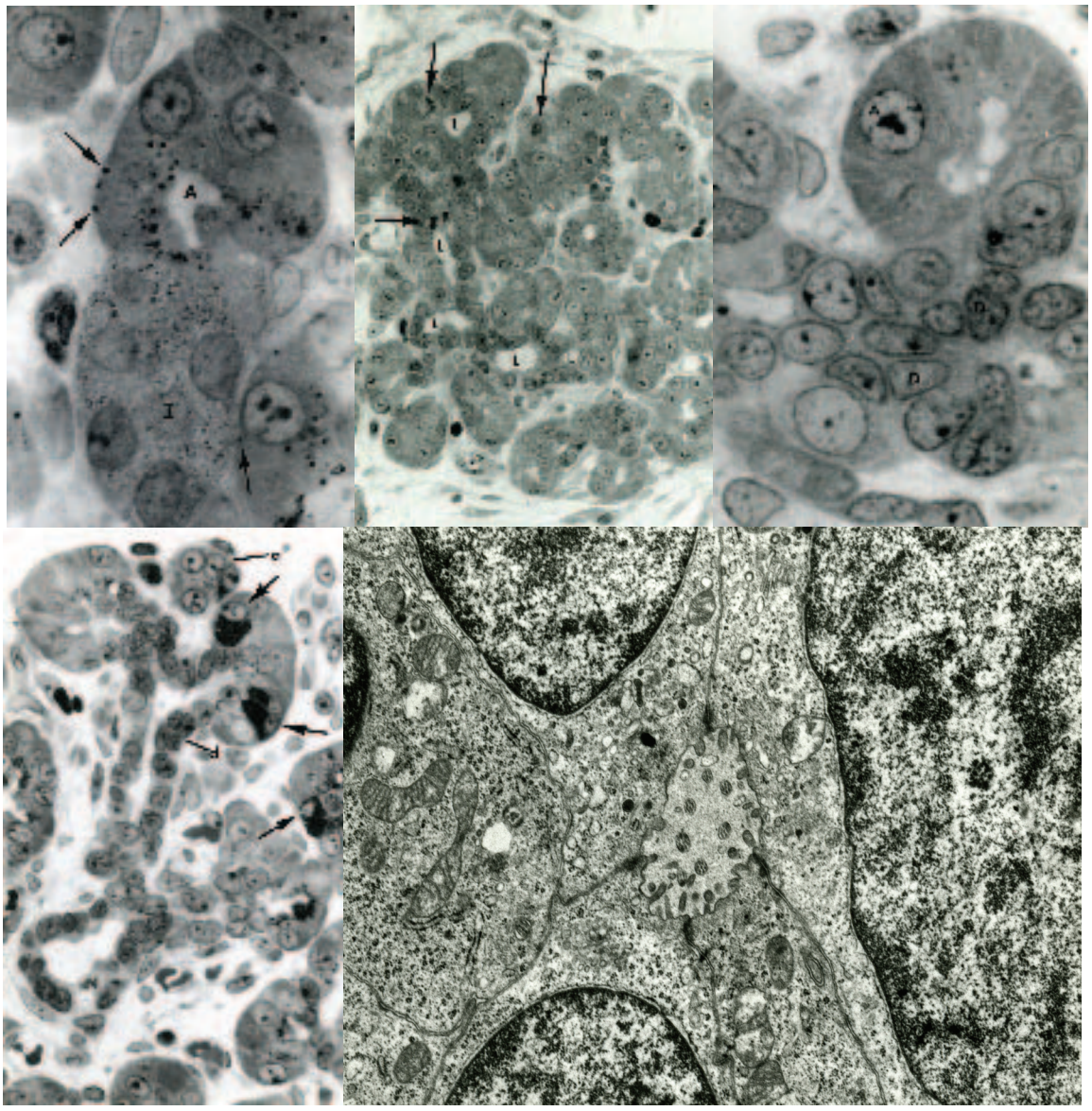

Fig. 8. (*Above left*). A small pancreatic islet (I) intimately associated with the epithelium forming a differentiating acinus (A). Small lipid droplets (arrows) continue to be observed in the basal cytoplasm of acinar cells. Note that the endocrine cells do not directly border the lumen of the acinus. Four-day-old opossum. LM X 1,000. (*Above center*). Lobulation is readily apparent in the pancreas one week into the postnatal period. Note the lumen (L) of the same intralobular duct as it branches and is surrounded by developing acinar units. Note the large number of mitotic figures observed (arrows). LM X 300. (*Above right*). An oblique cut of a small duct as it branches into a forming acinus illustrates that the nuclei of the ductal cells (D) stain more intensely than do the larger spherical nuclei of acinar cells (A). Opossum one week postnatal. LM X 1,000. (*Below left*). A micrograph illustrates a branching intralobular duct (d) that terminates in several forming acinar units (a). Note that a few scattered acinar cells contain an unusually large number of dark staining zymogen granules (arrows). Opossum one week postnatal. LM X 450. (*Below right*). Cilia are often observed within the lumina of differentiating pancreatic acini. Opossum one week postnatal. TEM X 10,000.

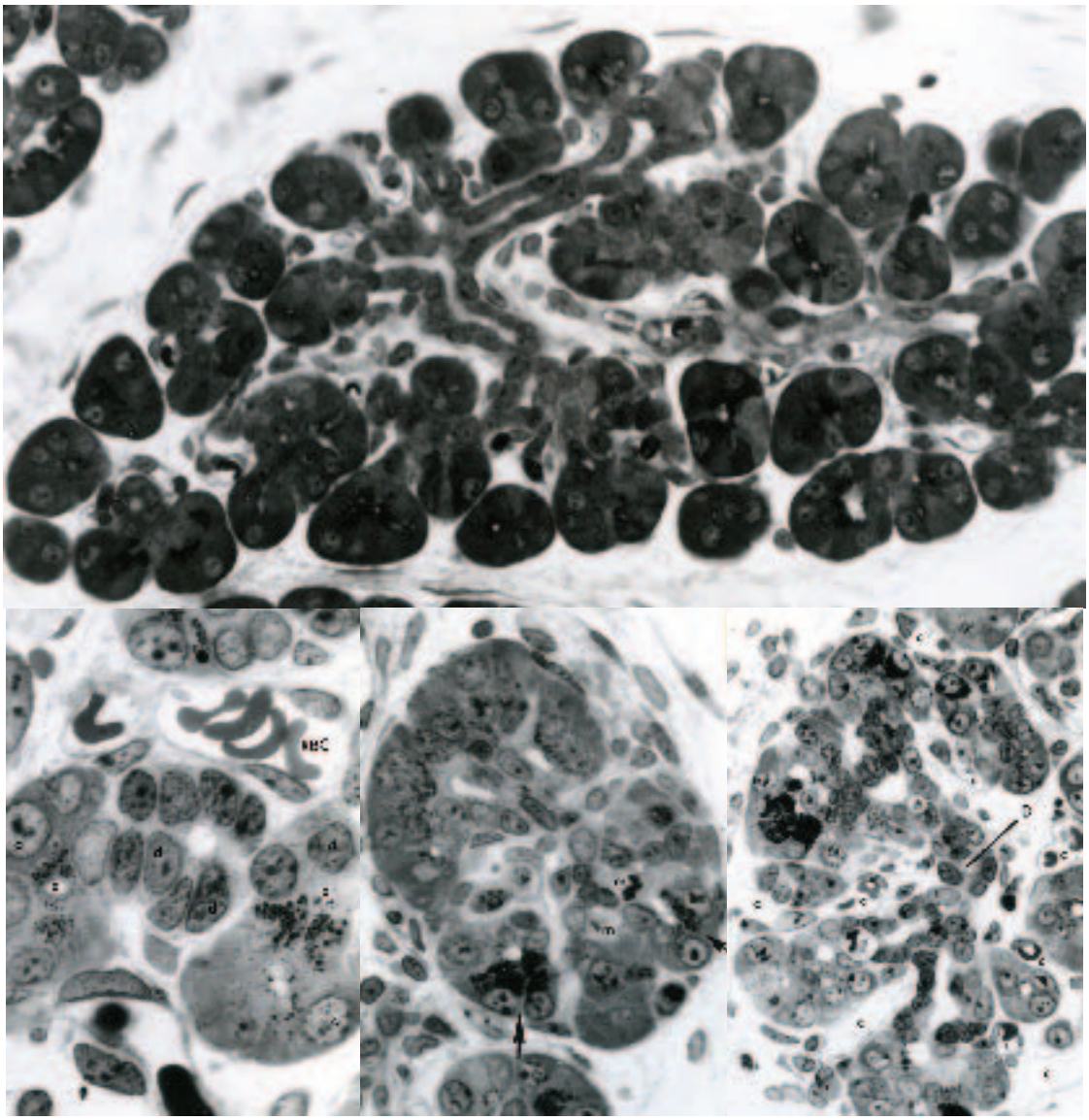

Fig. 9. (*Above*). A region of a developing pancreatic lobule from a week old opossum illustrates the nature of the central branching intralobular ductal system and its relationship to surrounding acinar units in the initial stages of their formation. LM X 400. (*Below left*). A section of a small intralobular duct (d) and two associated forming acinar units (a). Acinar cells nearer the ducts appear to show the greatest number of zymogen granules (Z). Note the presence of red blood cells (RBC) in capillaries on either side of the centrally positioned duct. Opossum one week postnatal. LM X 1,000. (*Below center*). The terminal region of the ductal system branches to end within several surrounding acinar units as centroacinar cells. Note the mitotic activity (m) within the ductal epithelium. A few pancreatic acinar cells are filled with zymogen granules (arrows) whereas the remainder of the acinar cells contains the normal number of zymogen granules form this period of postnatal life. Opossum one week postnatal. LM X 1,000. (*Below right*). Several small intralobular ducts radiate from a common central duct (D) that will eventually differentiate into an interlobular duct with continued development. Note the rich capillary network (c) present adjacent to the expanding ductal system of the developing pancreas. Opossum one week postnatal. LM X 450.

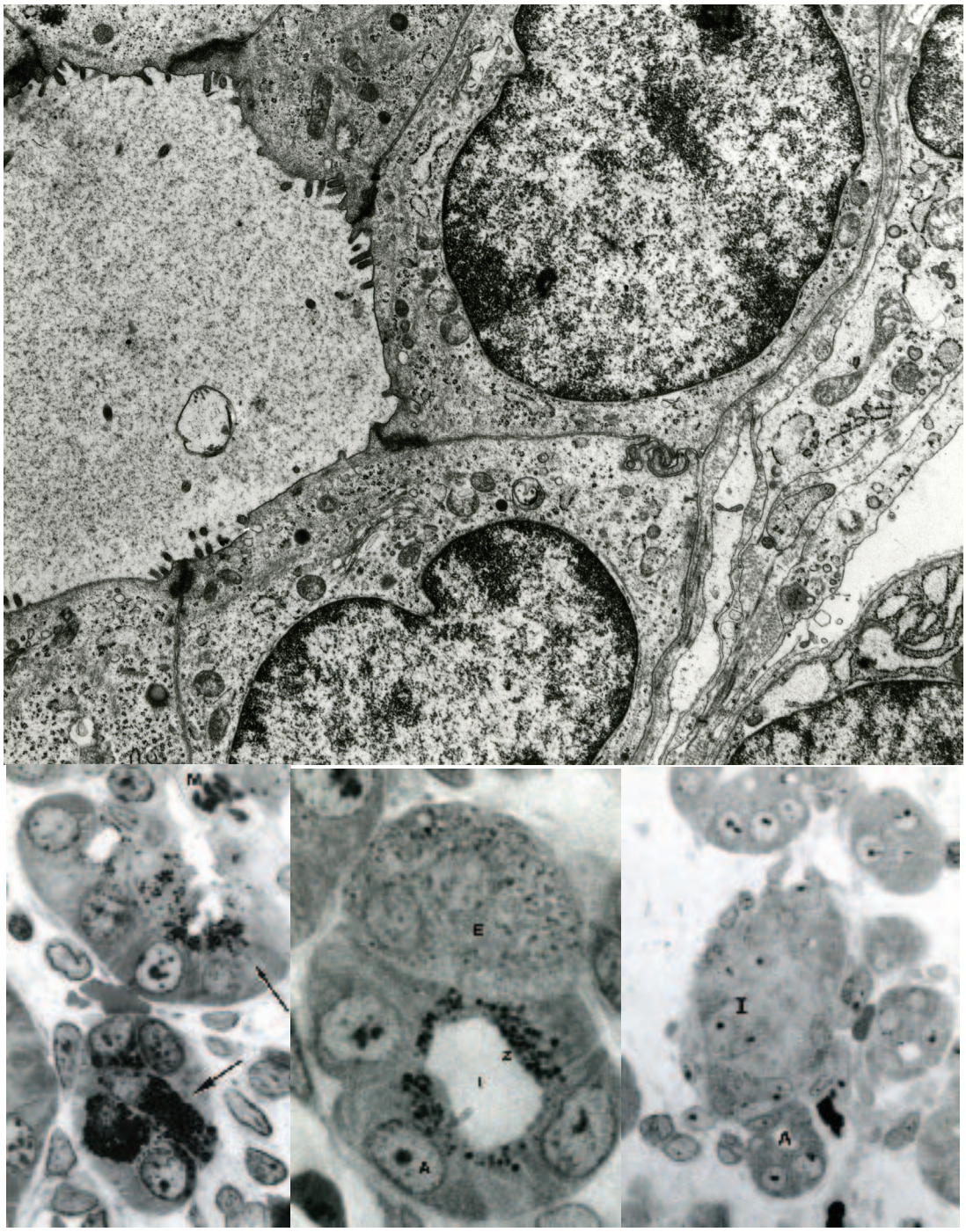

Fig. 10. (*Above*). A micrograph illustrates the structure of epithelial cells lining an interlobular pancreatic duct of a week old opossum. TEM X 6,000. (*Below left*). Most pancreatic acinar cells from the pancreas of a week old opossum contain zymogen granules of a size similar to that observed in adult opossums while others are filled with very large granules (arrows). A mitotic figure (M) is shown in the ductal epithelium. LM X 1,000. (*Below center*). Two endocrine cells (E) intimately associated with cells of an expanding acinar unit (A). The size and distribution of zymogen granules (Z) beneath the plasmalemma that borders the acinar lumen (L) is typical for acinar cells (A) at this period of postnatal life (one week). LM X 1,500. (*Below right*). A micrograph illustrates a larger pancreatic islet (I) from the pancreas of an opossum one week postnatal. Note the adjacent acinar units (A). LM X 450.

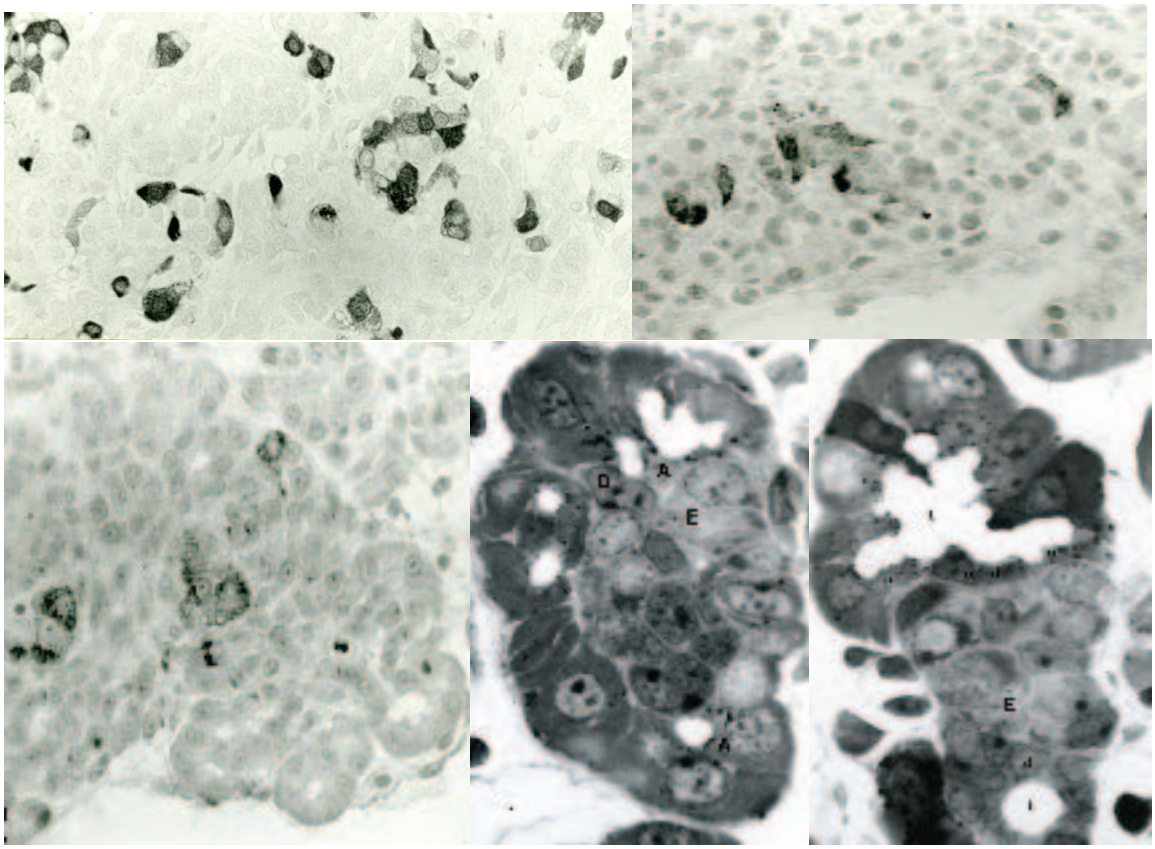

Fig. 11. (*Above left*). Glucagon-immunoreactive cells continue to have a peripheral location in forming pancreatic islets and continue to be the most numerous type of endocrine cell one week into the postnatal period. LM X 300. (*Above right*). Insulin-immunoreactive cells are few in number and scattered within developing pancreatic islets of the opossum one week postnatal. LM X 250. (*Below left*). Cells with 5-HT immunoreactivity are few in number in the week old opossum pancreas and occur as scattered cells within the developing pancreatic islets. LM X 300. (*Below center*). A central mass of endocrine cells (E) and closely associated ductal cells (D) nearly surrounded by acinar cells (A) is a common observation in the opossum pancreas two weeks into the postnatal period. LM X 1,000. (*Below right*). A portion of pancreas from a two-week-old opossum illustrates the lumen (L) and surrounding ductal cells (d) of an intralobular duct and a mass of endocrine cells (E). The latter are positioned between the duct and a differentiating acinar unit near the top of the photomicrograph. Note the irregular outline of the lumen (L) of the developing acinar unit. LM X 1,000.

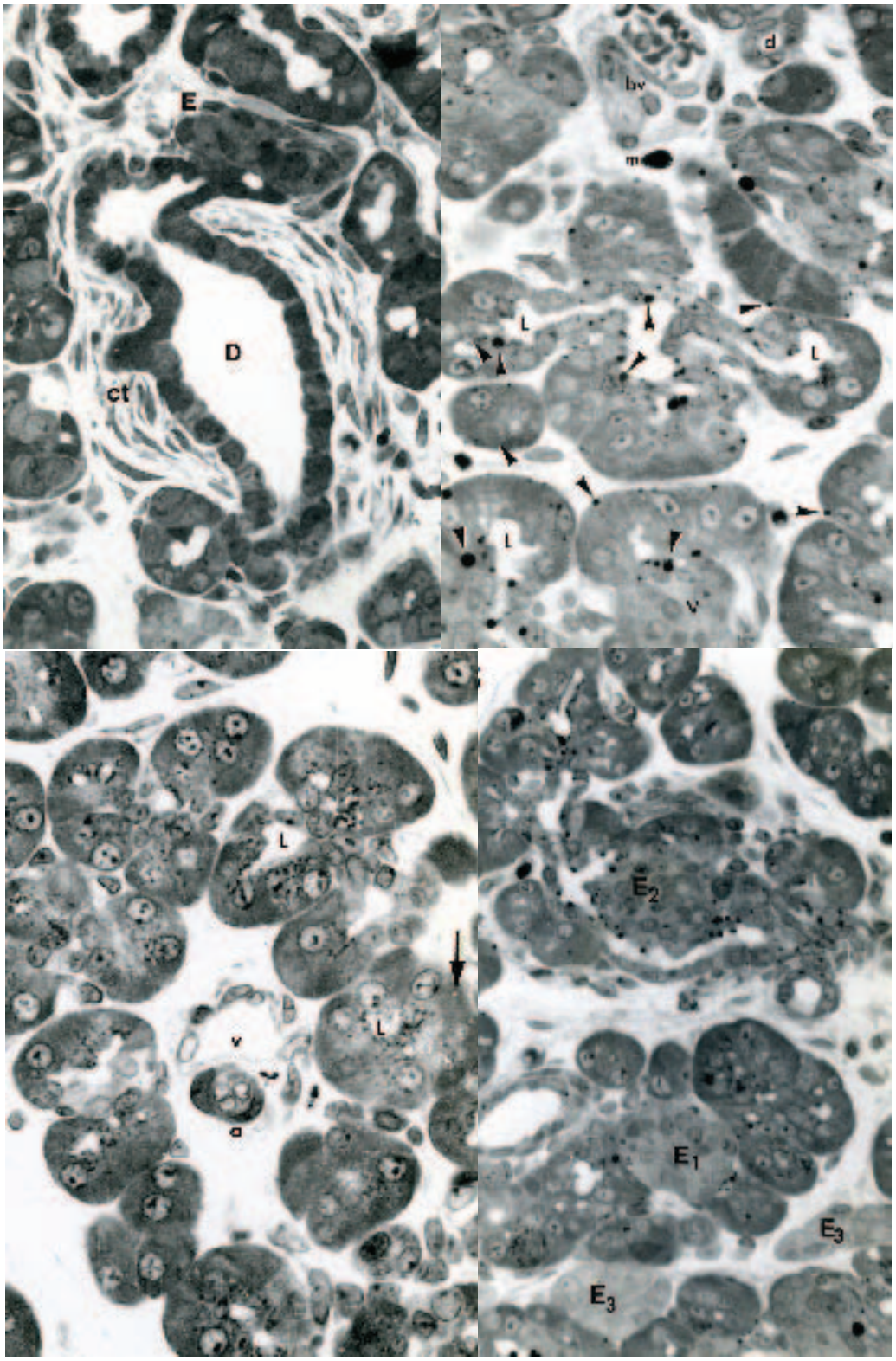

Fig.12. (*Above left*). A well-established interlobular duct (D) lies within the connective tissue (ct) in the center of the field of view. Note the group of endocrine cells (E) intimately associated with one of its intralobular branches (top) and a differentiating acinus with another interlobular branch (bottom). Two weeks postnatal. LM X 450. (*Above right*). A micrograph illustrates centroacinar lumina (L), an intercalated duct (d), and blood vessels (bv) within the pancreas of eighteen-day-old opossum. The arrowheads point to lipid droplets within the exocrine epithelium. LM X 450. (*Below left*). At this stage of development acini are more mature in appearance and centroacinar lumina (L) decrease in size. A venule (v), arteriole (a) and lipid droplet (arrow) also are observed. LM X 450. (*Below right*). Groups of endocrine cells are observed that appear to be associated primarily with either acinar epithelium (E1), ductal epithelium (E2), or isolated within the interlobular connective tissue (E3). Eighteen-day-old opossum. LM X 200.

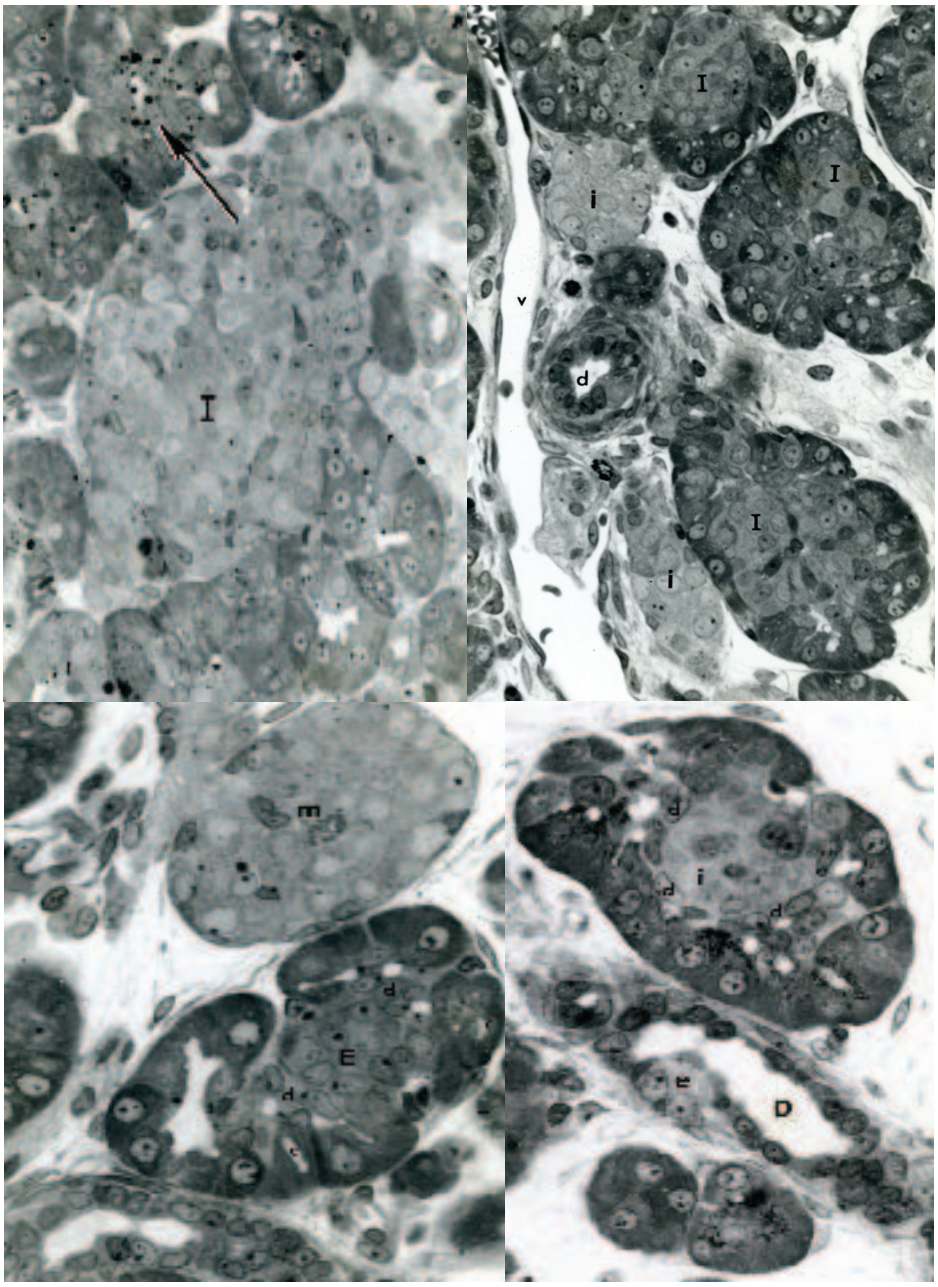

Fig. 13. (*Above left*). A large pancreatic islet (I) that appears intimately associated with the acinar epithelium extends into the interlobular connective tissue. Lipid droplets continue to be observed in the exocrine epithelium (arrow). Eighteen-day-old opossum. LM X 300. (*Above right*). Although a few pancreatic islets continue to be observed within the interlobular connective tissue (i), the majority of islets observed in the four-week-old opossum are enveloped by acinar cells (I). An interlobular duct (d) and a small vein (v) also are shown in this field of view. LM X 300. (*Below left*). An intralobular duct (d) and endocrine cells (E) of a forming pancreatic islet enveloped by differentiating acinar units are shown in this region of pancreas from an opossum four weeks postnatal. Note the continued presence of intercellular canaliculi (c) in the differentiating acinar units. A portion of an interlobular duct (bottom left) and small pancreatic ganglion that contains a mitotic figure (m) also are shown in the field. LM X 450. (*Below right*). In this preparation of pancreas from a five-week-old opossum, the intralobular ductal cells (d) appear to separate a central developing islet (i) from surrounding exocrine epithelium. The latter appears to be developing into acinar units. Note also the two endocrine cells (e) within the wall of the intralobular duct (D). LM X 450.

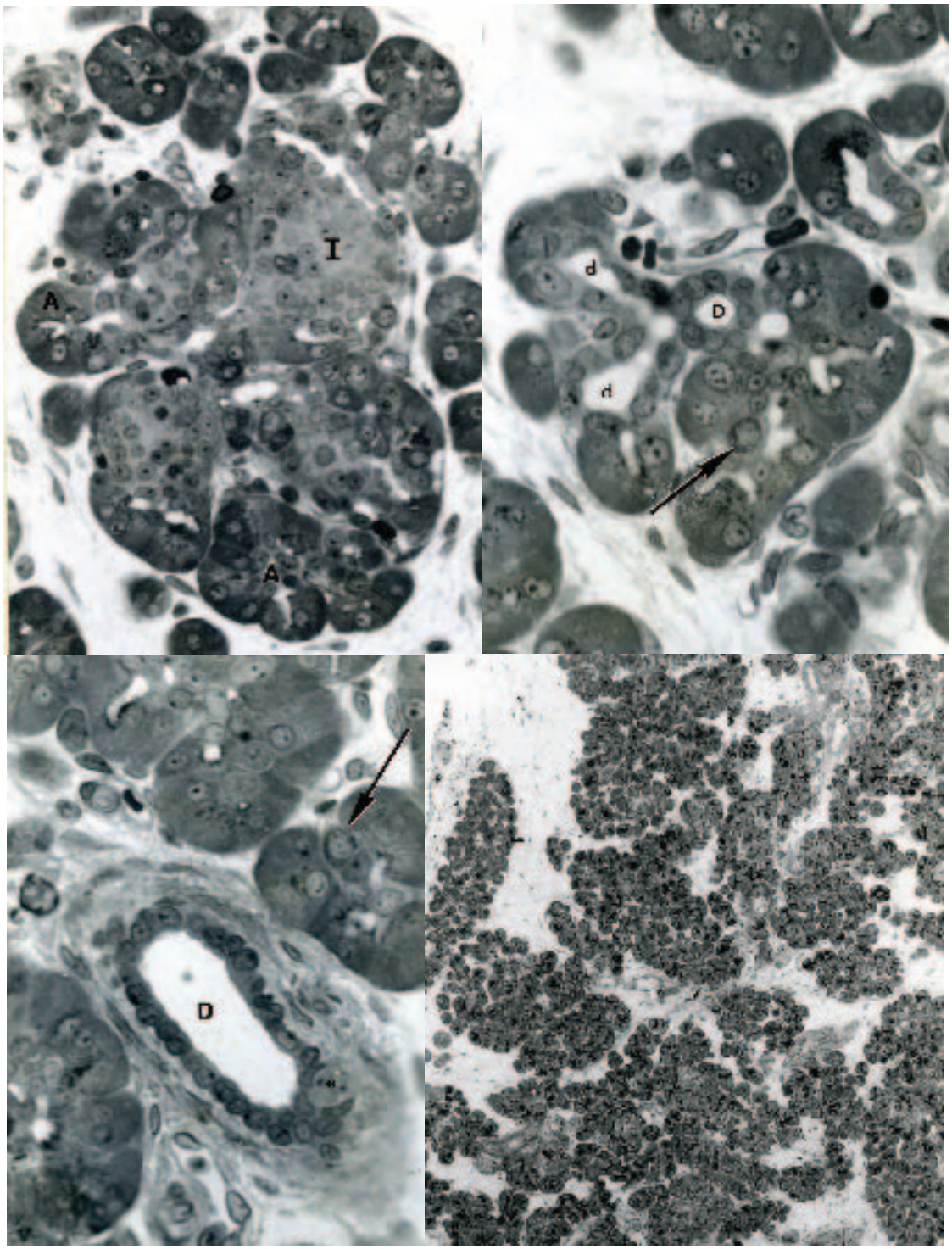

Fig. 14. (*Above left*). As the exocrine epithelium develops into acinar units (A), the pancreatic islets (I) continue to develop and expand into the intralobular connective tissue where the exocrine pancreas ultimately will surround them as development continues. Five-week opossum. LM X 300. (*Above right*). A region of pancreas showing an intralobular duct (D) that branch to provide intercalated ducts (d) two of which unite with acinar units. An isolated endocrine cell (arrow) lies within the epithelium forming an acinar unit. Five-week opossum. LM X 500. (*Below left*). An interlobular pancreatic duct (D) from a five-week-old opossum has a small group of endocrine cells (e) associated with its wall. Note also the isolated endocrine cell (arrow) associated with centroacinar cells within an adjacent acinus. LM X 400. (*Below right*). A micrograph illustrates the architecture of the exocrine pancreas from a ten-week-old opossum. LM X 50.

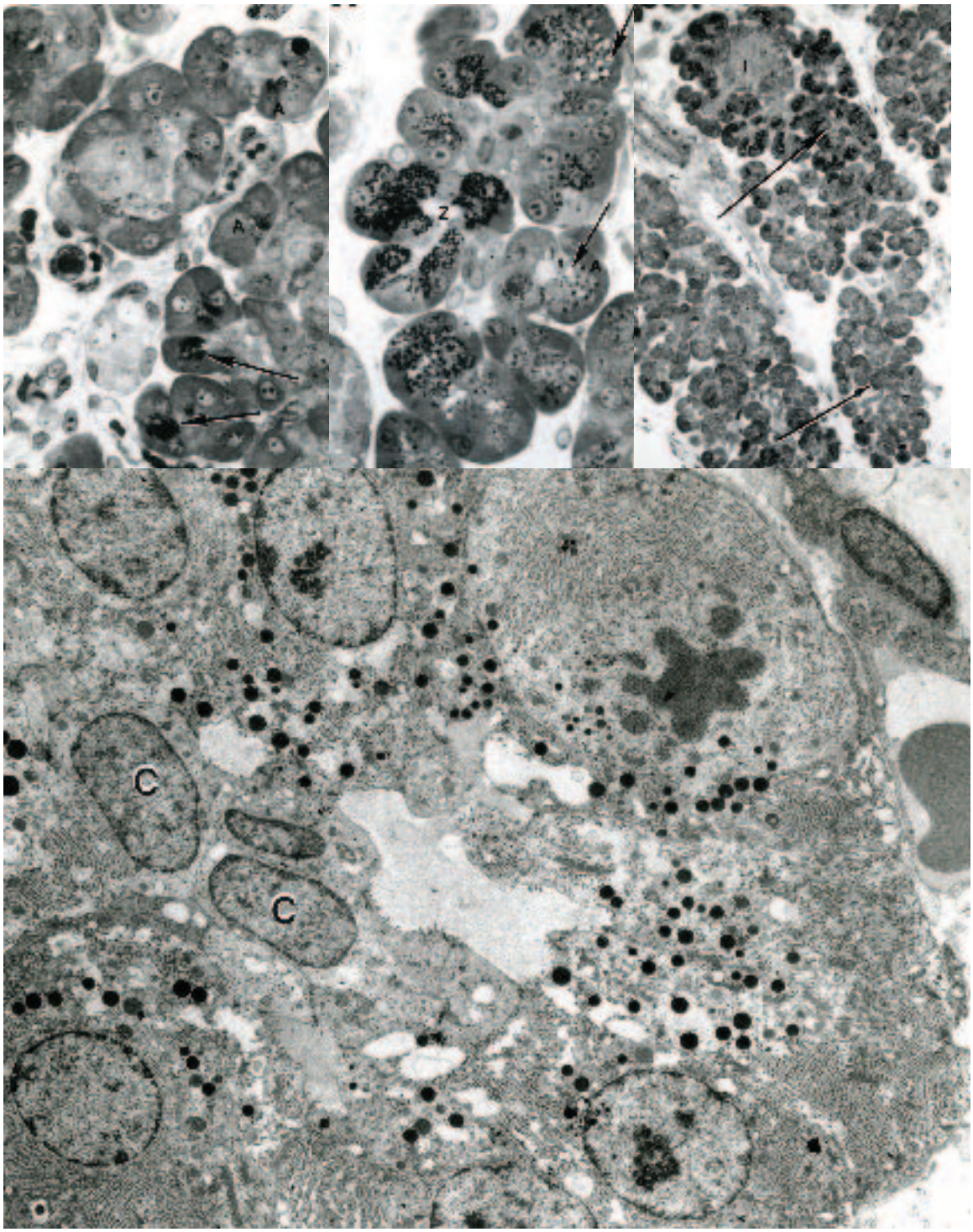

Fig. 15. (*Above left*). Very few acinar cells (arrows) contain a large number of zymogen granules. Six-week-old opossum. LM X 450. (*Above center*). About one-half of the acinar cells exhibit mature zymogen granules (Z) by nine weeks postnatal. The remaining acinar cells (A) exhibit numerous vacuoles (arrows) and what may be immature granules. LM X 500. (*Above right*). The distribution of acinar cells with zymogen granules does not appear to be random. Acinar cells with zymogen granules within the pancreas of the nine-week opossum appear to group together (large arrow) whereas other groups of acini are devoid of zymogen granules (small arrow). Note the large intralobular islet (I). LM X 100. (*Below*). A region of exocrine pancreas from nine-week-old opossum illustrates centroacinar cells (C) and surrounding acinar cells one of which is dividing. Note the increase in amount of rough endoplasmic reticulum and the number of zymogen granules. TEM X 4,000.

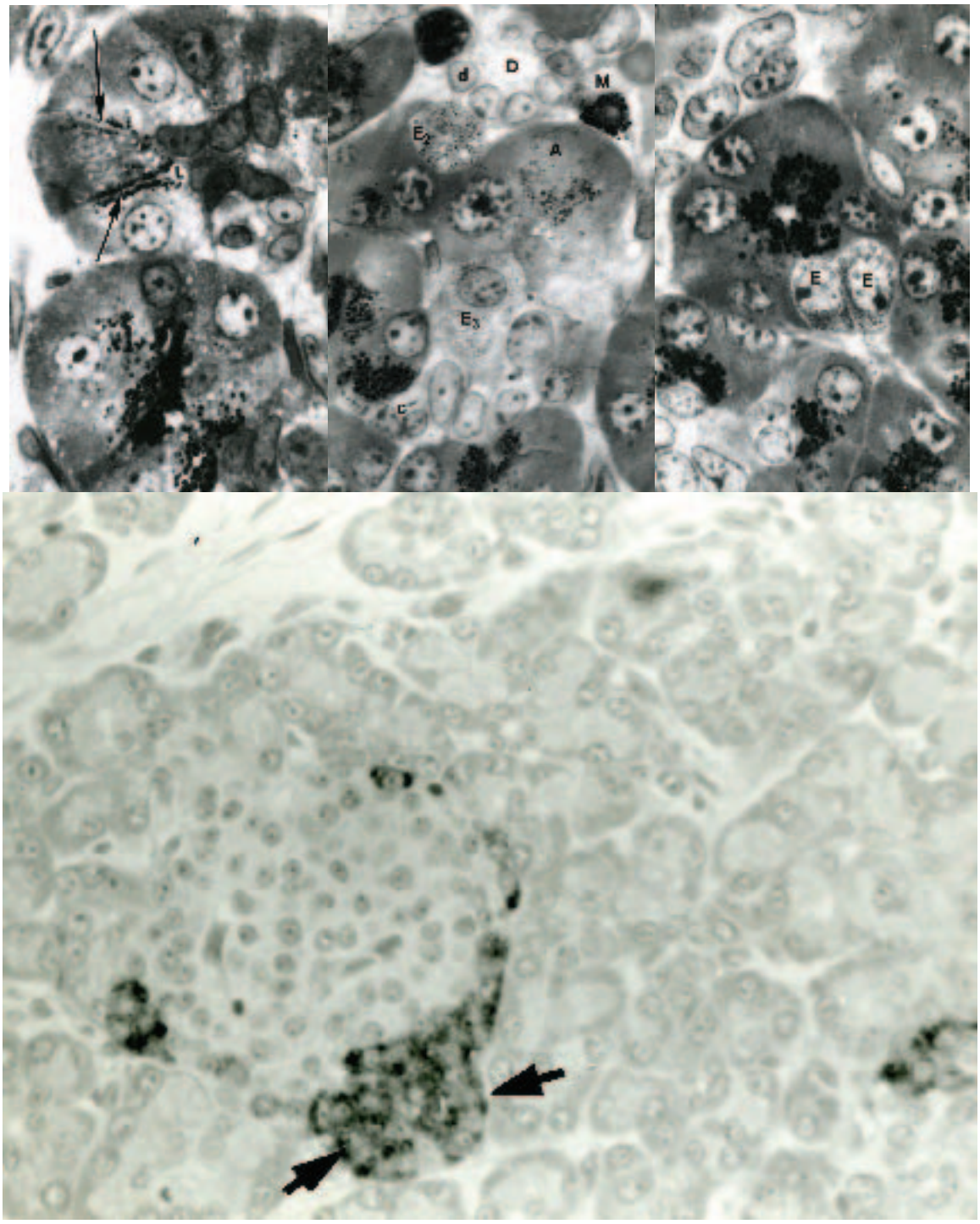

Fig. 16. (*Above left*). A micrograph illustrates adjacent acinar units from the pancreas of a ten-week-old opossum. Note the intercellular canaliculi (arrows) and the alignment of zymogen granules. The lumen (L) of the acinus and the nuclei of several centroacinar cells also can be observed. LM X 1,000. (*Above center*). A region of pancreas from a twelve-week-old opossum illustrates an intercalated duct (D) lined by cuboidal cells (d), centroacinar cells (c) and acinar cells (A). Note the endocrine cells associated with the intercalated duct and acinar cells (E2), and the centroacinar cells (E3). The dark granulated cell adjacent to the intercalated duct is a mast cell (M). LM X 1,200. (*Above right*). Two endocrine cells (E) within an acinar unit of a twelve-week-old opossum. LM X 1,500. (*Below*). Occasional pancreatic islets of opossums eleven weeks into the postnatal period are well established and glucagon-immunoreactive cells occupy a peripheral location. In this figure a cluster of glucagon-immunoreactive cells occurs at one pole of the pancreatic islet (arrows). LM X 400.

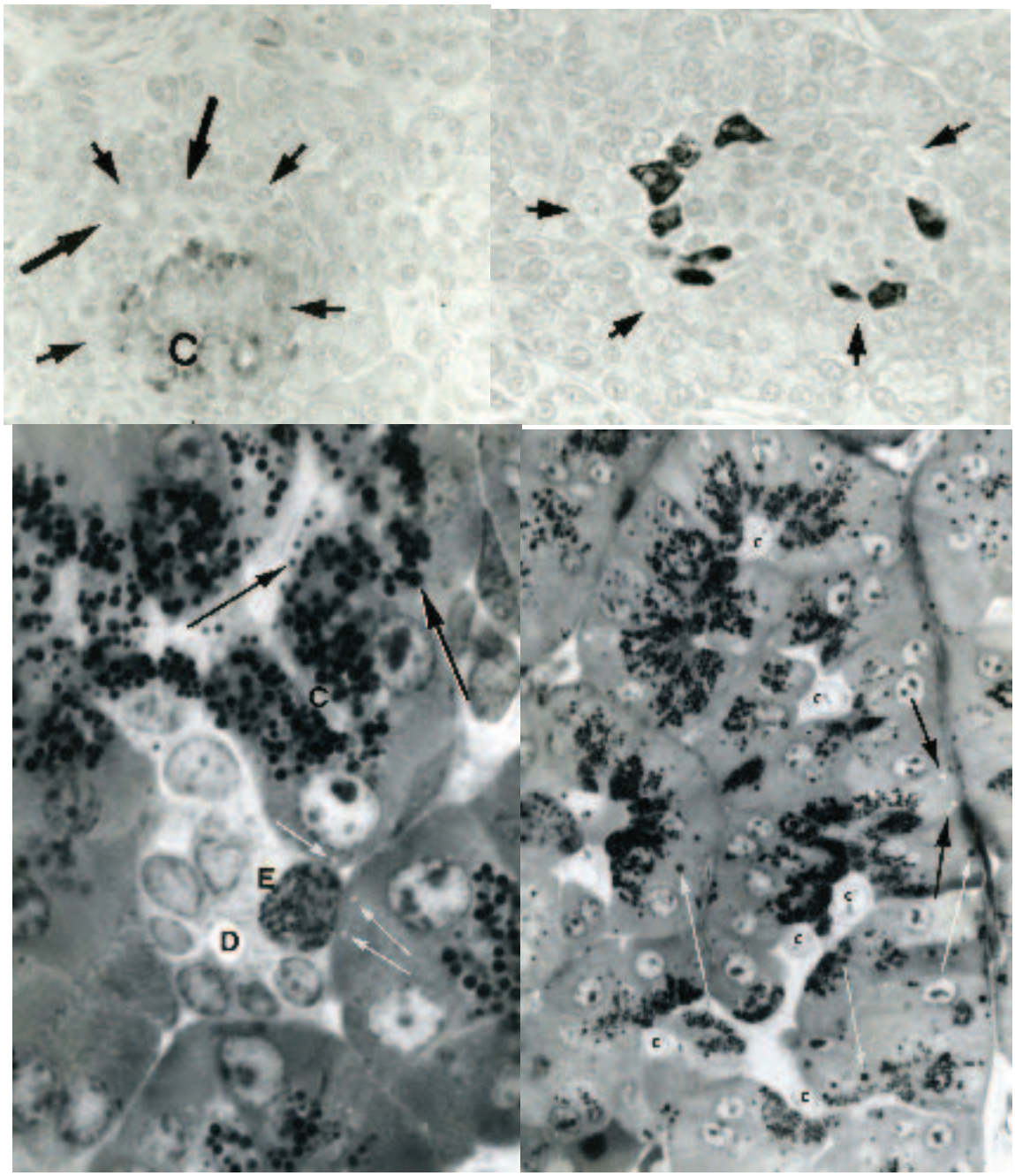

Fig. 17. (*Above left*). By the eleventh week of postnatal life insulin-immunoreactive cells show an adult distribution within pancreatic islets. The small arrows depict the edge of the pancreatic islet. Note that the most intense immunoreactive staining occurs in that region of the endocrine cell cytoplasm adjacent to capillaries (C). The large arrows indicate the position of two ducts associated with this pancreatic islet. LM X 300. (*Above right*). Somatostatin-immunoreactive cells also show an adult distribution in the periphery of pancreatic islets by the end of the eleventh postnatal week. The arrows indicate the edge of the pancreatic islet. LM X 300. (*Below left*). Pancreatic acinar cells of a fourteen-week-old opossum contain zymogen granules that range is size from small (small arrow) to large (large arrow). Small vacuoles (white arrows) continue to be observed in the basal cytoplasm of acinar cells. Note the intercellular canaliculus (C) between acinar cells. A single endocrine cell (E) lies within the wall of an intercalated duct (D). LM X 1,000. (*Below right*). A secretory tubule/acinus from the pancreas of a juvenile opossum consists of numerous acinar cells some of which, in addition to zymogen granules, continue to exhibit lipid droplets (white arrows) and clear vacuoles (dark arrows) in the basal cytoplasm. Several centroacinar cells (c) are present lining the lumen of the secretory unit. LM X 500.

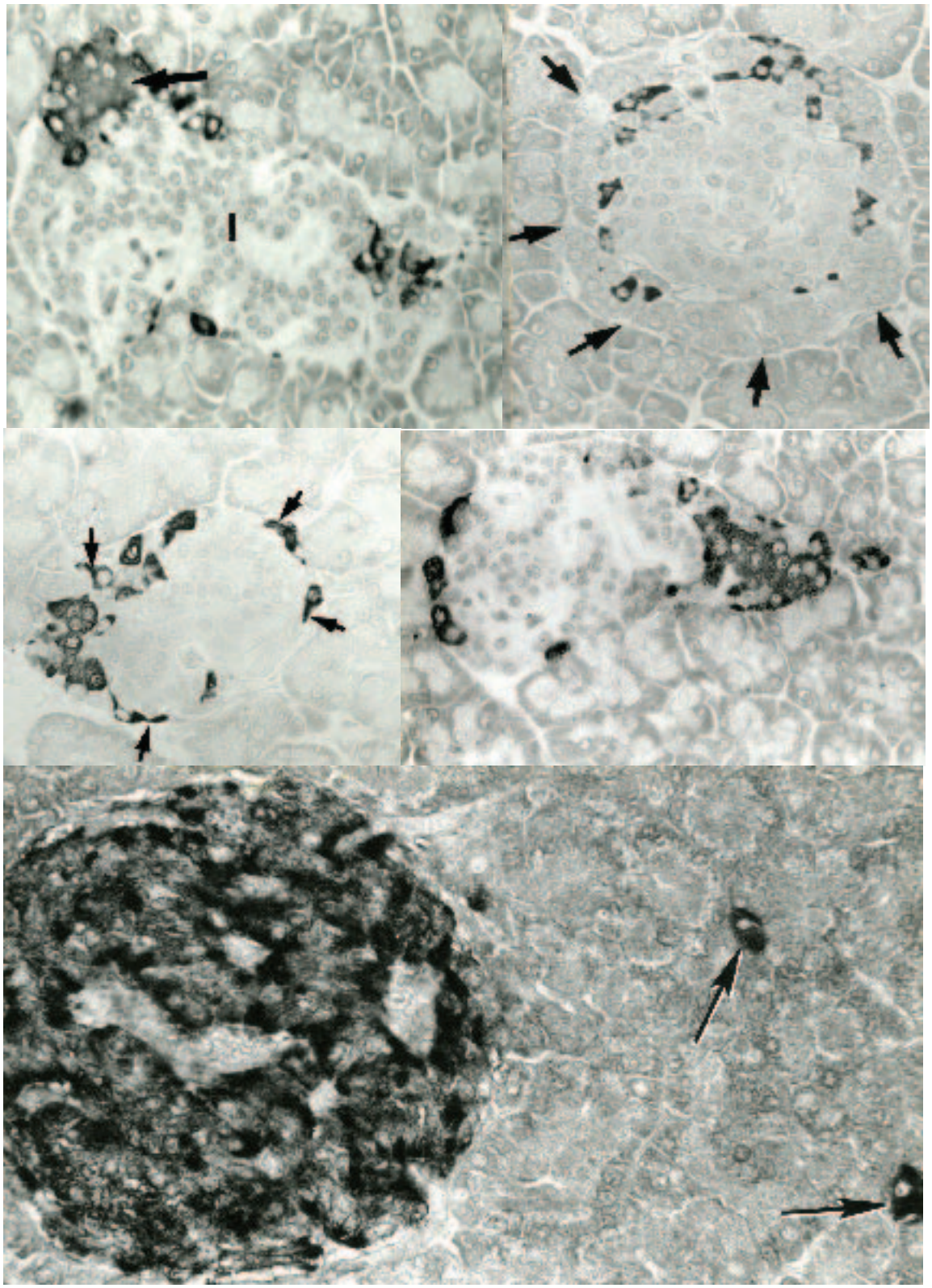

Fig.18. All figures are from juvenile opossums. (*Top left*). BPP-immunoreactive cells usually occupy a peripheral location in pancreatic islets (I) and may form clusters (arrow) is some areas. LM X 300. (*Top right*). Somatostatin-immunoreactive cells often occur in a stratum two to three cells deep from the edge of the islet (arrows). LM X 300. (*Center left*). Some BBP-immunoreactive cells exhibit thin, elongate processes (arrows). LM X 350. (*Center right*). Glucagon-immunoreactive cells. LM X 300. (*Below*). Occasional insulin-immunoreactive cells occur in the exocrine parenchyma (arrows). Note the intense cytoplasmic staining of cells in regions adjacent to capillaries. LM X 400.

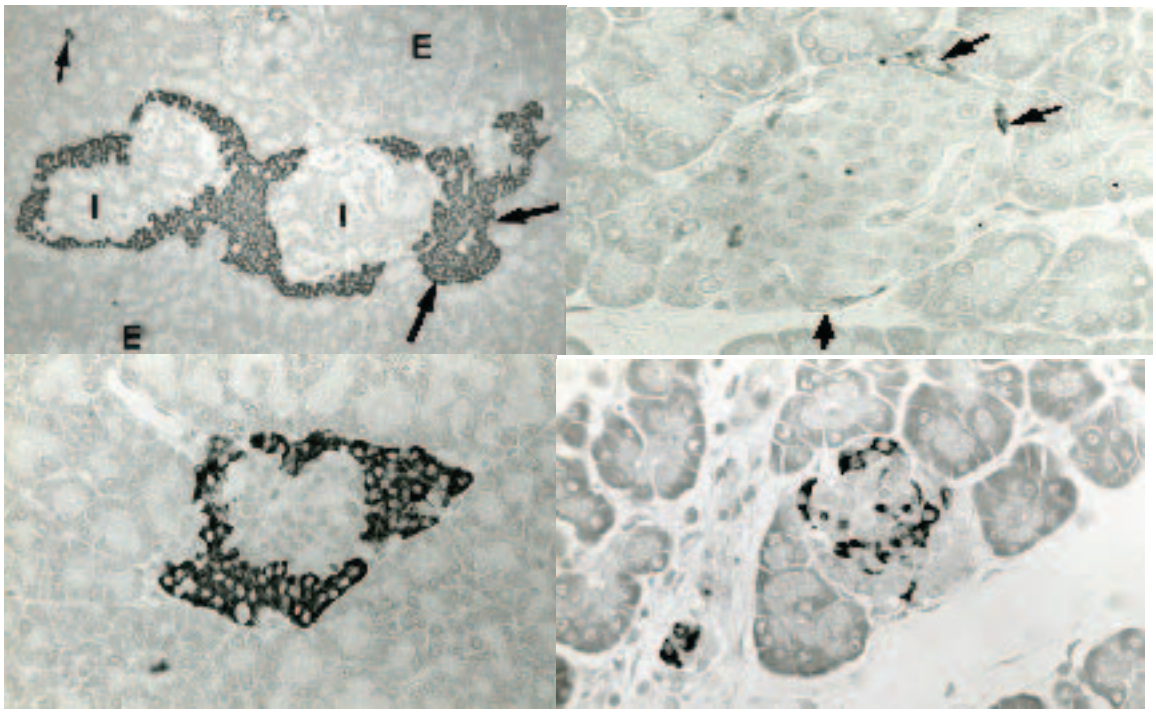

Fig. 19. All figures are from weaned juvenile opossums. (*Above left*). A section through a large, irregular elongate pancreatic islet (I) illustrates numerous glucagon-immunoreactive endocrine cells at its periphery. The large arrows indicate a cluster or knot of immunoreactive cells. Occasional glucagon-immunoreactive cells (small arrow) are observed scattered within the exocrine pancreas (E). (*Above right*). 5-HT- immunoreactive cells (arrows) from a pancreatic islet that also exhibit positive immunohistochemical staining for bovine pancreatic polypeptide. LM X 250. (*Below left*). A micrograph illustrates glucagon–immunoreactive cells within a pancreatic islet. LM X 250. (*Below right*). A micrograph illustrates somatostatin-immunoreactive cells within a pancreatic islet. LM X 250.

Chapter 25. Liver

Synopsis:

A hepatic diverticulum extends from the foregut in the ventral midline during prenatal day ten and by early in the eleventh embryonic day cords of hepatocytes extend from the hepatic duct into the ventral mesentery mesenchyme. The liver enlarges rapidly and is actively hemopoietic, a feature which remains prominent through the first two weeks of postnatal life. Although hepatocytes of the newborn opossum are concentrated around central veins, they are not organized into plates at this time. Instead, hepatocytes occur in clusters separated by islands of hemopoietic cells. Developing sinusoids at this time lack a distinct lining endothelium and hemopoietic cells and hepatocytes are in direct contact with one another. By the end of the first postnatal week hepatocytes show a more uniform arrangement into plates near the central vein and bile canaliculi are observed in these regions. Hepatocytes at the periphery of the forming lobules lack organization into plates. Irregular plates of hepatocytes extend throughout most hepatic lobules by the end of the second postnatal week. Numerous lipid droplets and glycogen deposits characterize the cytoplasm of hepatocytes at this time. The lobular arrangement of the liver continues to be established during the next few weeks and by the end of the sixth postnatal week individual lobules and periportal areas are clearly defined. However, it is not until after weaning that the liver assumes an adult appearance, which is typically mammalian.

Acknowledgments:

Figs. 2 (top), courtesy of and from: Krause, W.J. and J.H. Cutts (1992) Development of the Digestive System in the North American Opossum (*Didelphis virginiana*). Adv. Anat. Embryol. Cell Biol. 125:1-148.

Figs. 3 (bottom), 6, 9, 10, 11, and 12 (top), courtesy of and from: Krause, W.J., J.H. Cutts and C.R. Leeson. (1975) Postnatal development of the liver in marsupial, *Didelphis virginiana.* II. Electron microscopy. J. Anat. 120:191-205.

Fig. 4 (bottom), courtesy of and from: Cutts, J.H., C.R. Leeson and W.J. Krause (1973) Postnatal development of the liver in a marsupial, *Didelphis virginiana.* I. Light microscopy. J. Anat. 115:327-346.

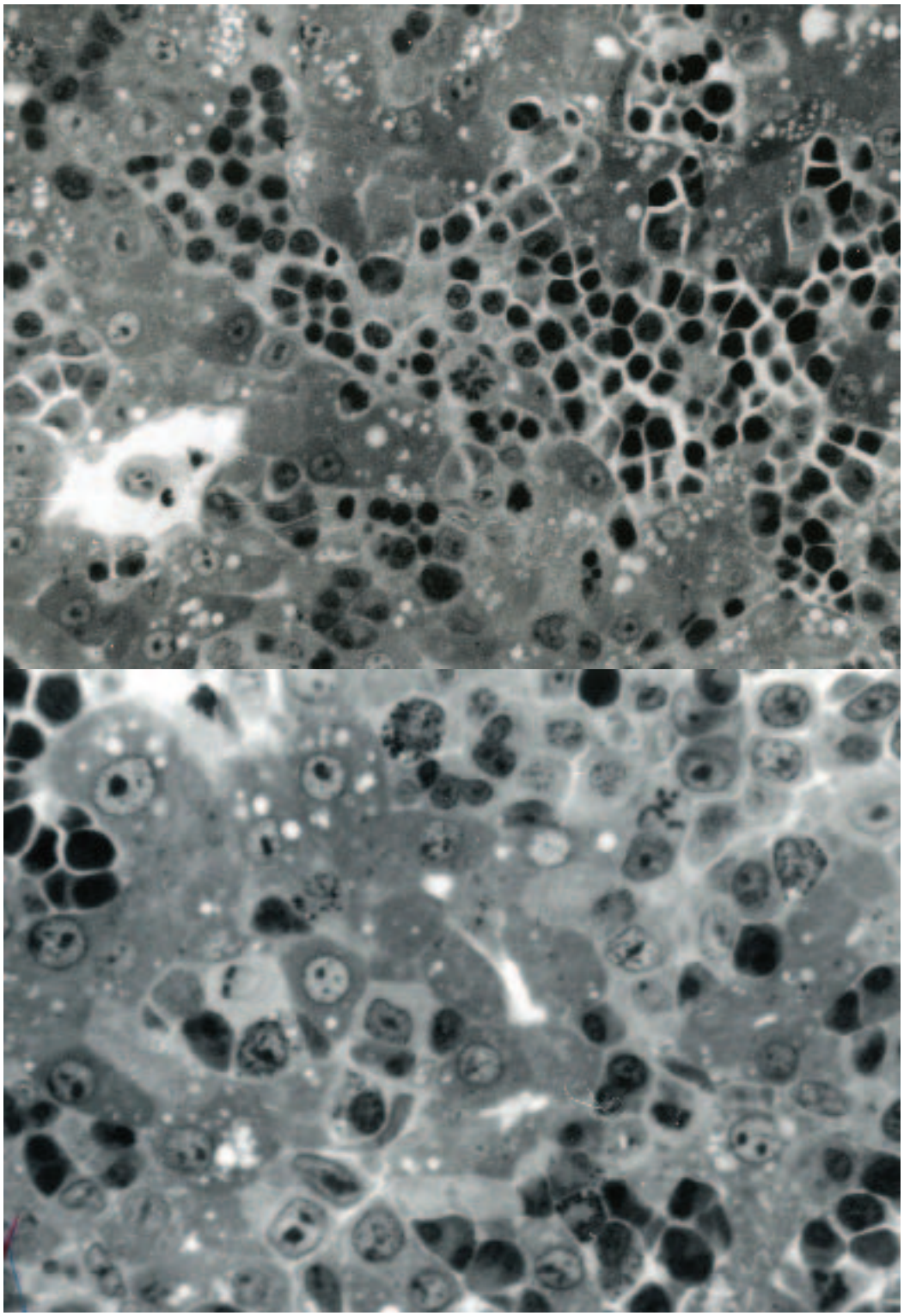

Fig. 1. (*Above*). Hepatocytes contain a finely granular cytoplasm that has a vacuolated appearance due to the presence of discrete lipid droplets. Their pale, vesicular nuclei often show discrete nucleoli. Large islands of hemopoietic cells (center of the field) lie scattered between hepatocytes. Newborn opossum. LM X 400. (*Below*). An intermediate region of a hepatic lobule from the liver of a newborn opossum illustrates the scattered hemopoietic elements that occur between irregular groups of hepatocytes. LM X 600.

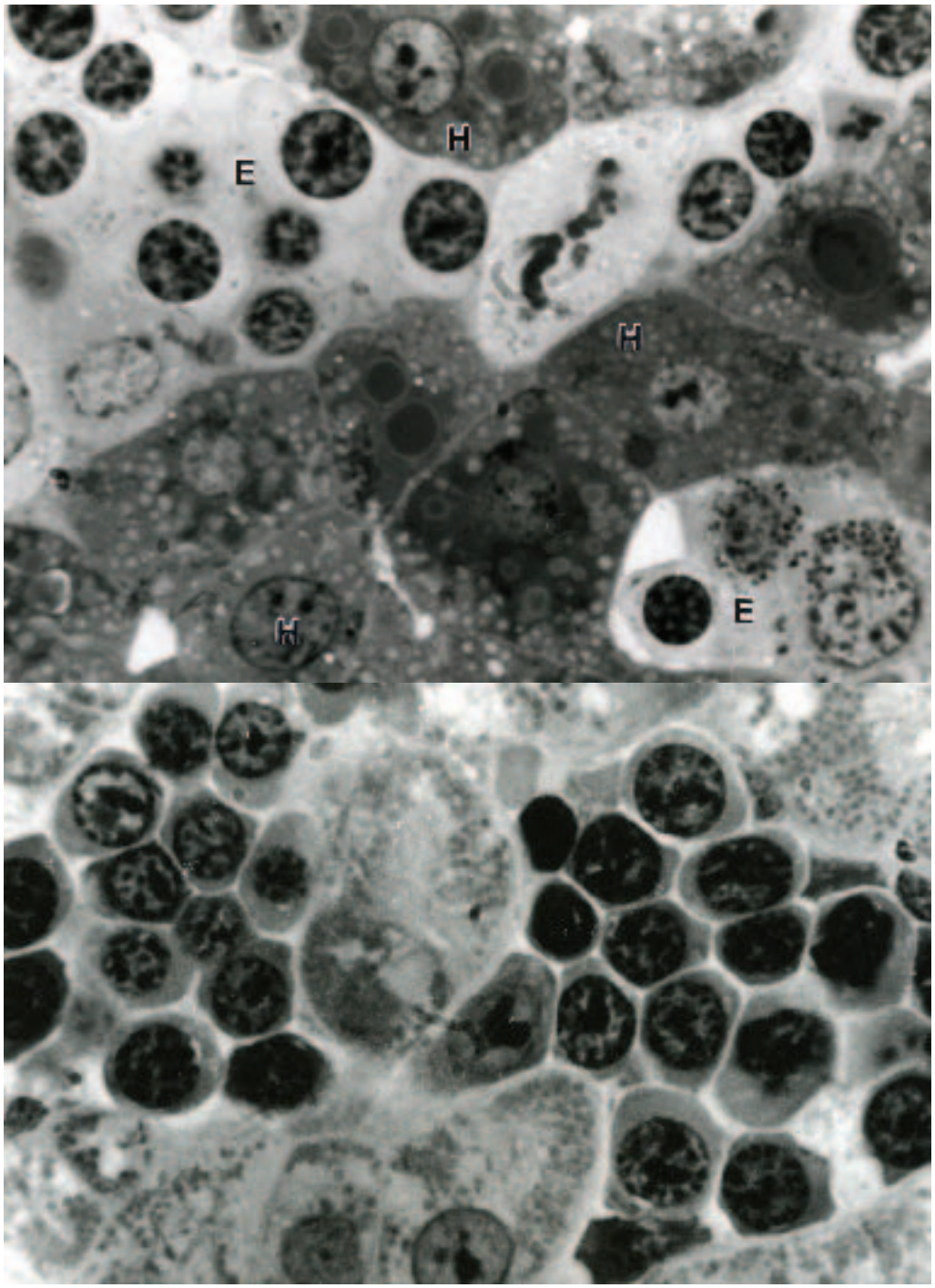

Fig. 2. (*Above*). A region of newborn opossum liver illustrates in greater detail the hepatocytes (H) and hemopoietic elements (E). Two granulocytes can be observed in the lower right portion of the photomicrograph. LM X 1,000. (*Below*). Two islands of hemopoietic cells of the erythroid series separate adjacent hepatocytes. The granules observed in the hepatocyte cytoplasm are in fact mitochondria. Newborn opossum. LM X 1,000.

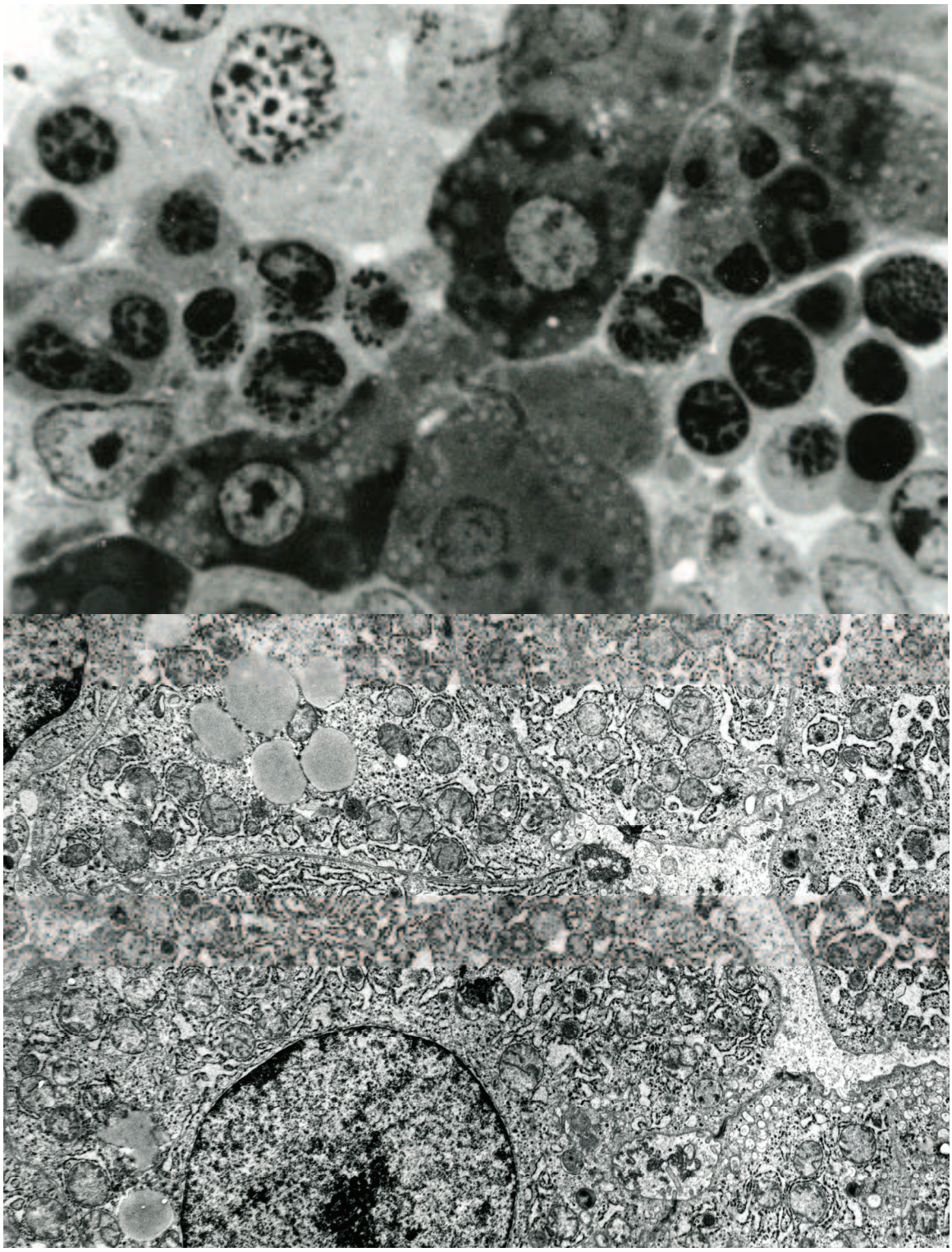

Fig. 3. (*Above*). A cord of hepatocytes crosses the field from lower left to upper right separating hemopoietic elements of both the erythroid and granulocyte series. A light staining megakaryocyte is observed among the hemopoietic cells at the upper left. Note the lipid droplets in the hepatocyte cytoplasm. Newborn opossum. LM X 1,200. (*Below*). The cytoplasm of hepatocytes from the newborn opossum liver contains numerous mitochondria, large amounts of rough endoplasmic reticulum, and scattered lipid droplets. Canaliculi are present between hepatocytes. TEM X 6,000.

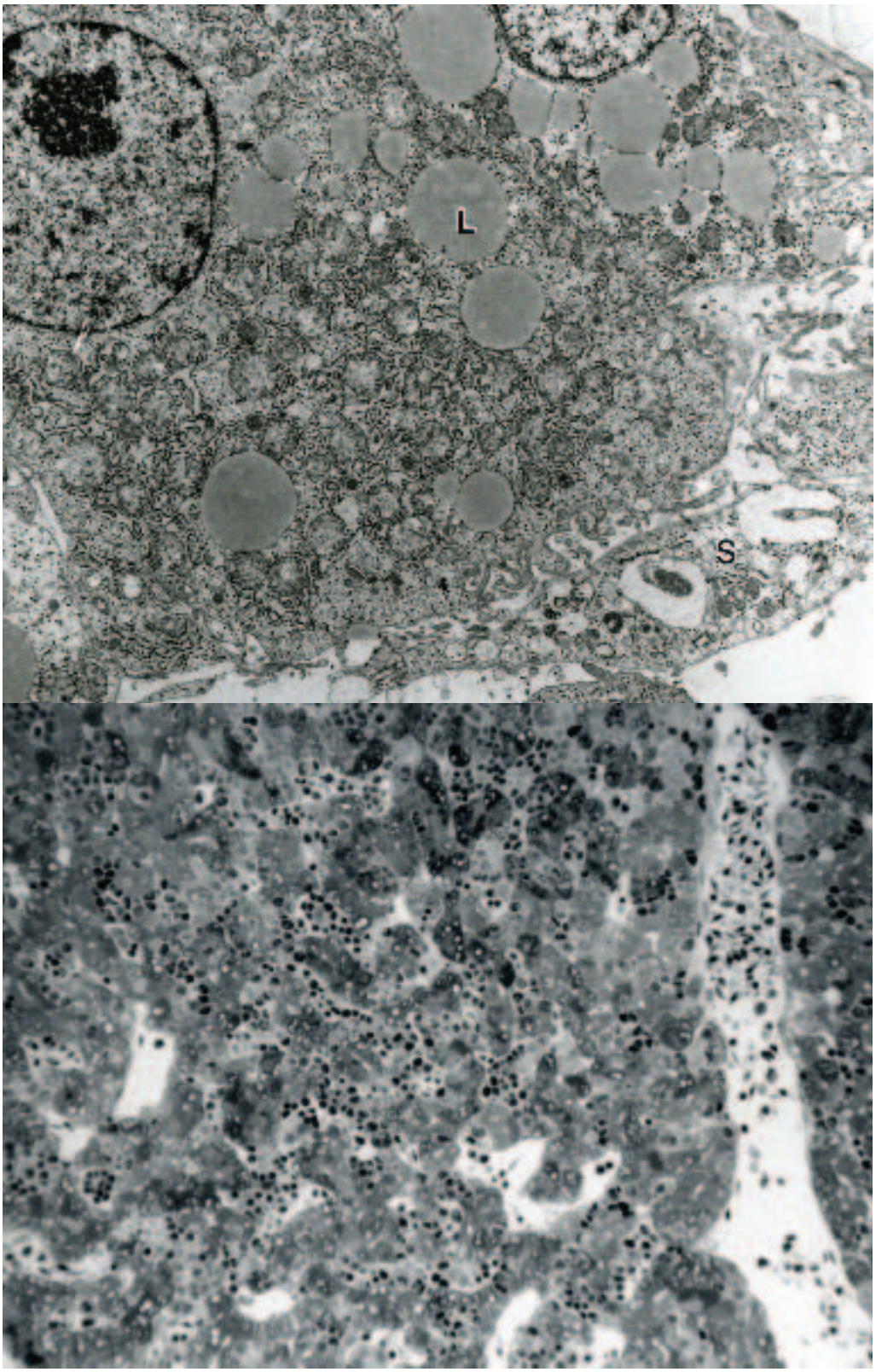

Fig. 4. (*Above*). Microvilli from adjacent hepatocytes extend into a forming space of Disse that separates the hepatocytes from a sinusoidal lining cell (S). Fine collagen fibrils also are observed in this space. Hepatocytes are filled with mitochondria and lipid droplets (L). Newborn opossum. TEM X 6,000. (*Below*). Irregular plates of hepatocytes separated by wide vascular spaces characterize the hepatic lobule of the opossum one week postnatal. Groups of hemopoietic cells occur scattered throughout the lobule. LM X 150.

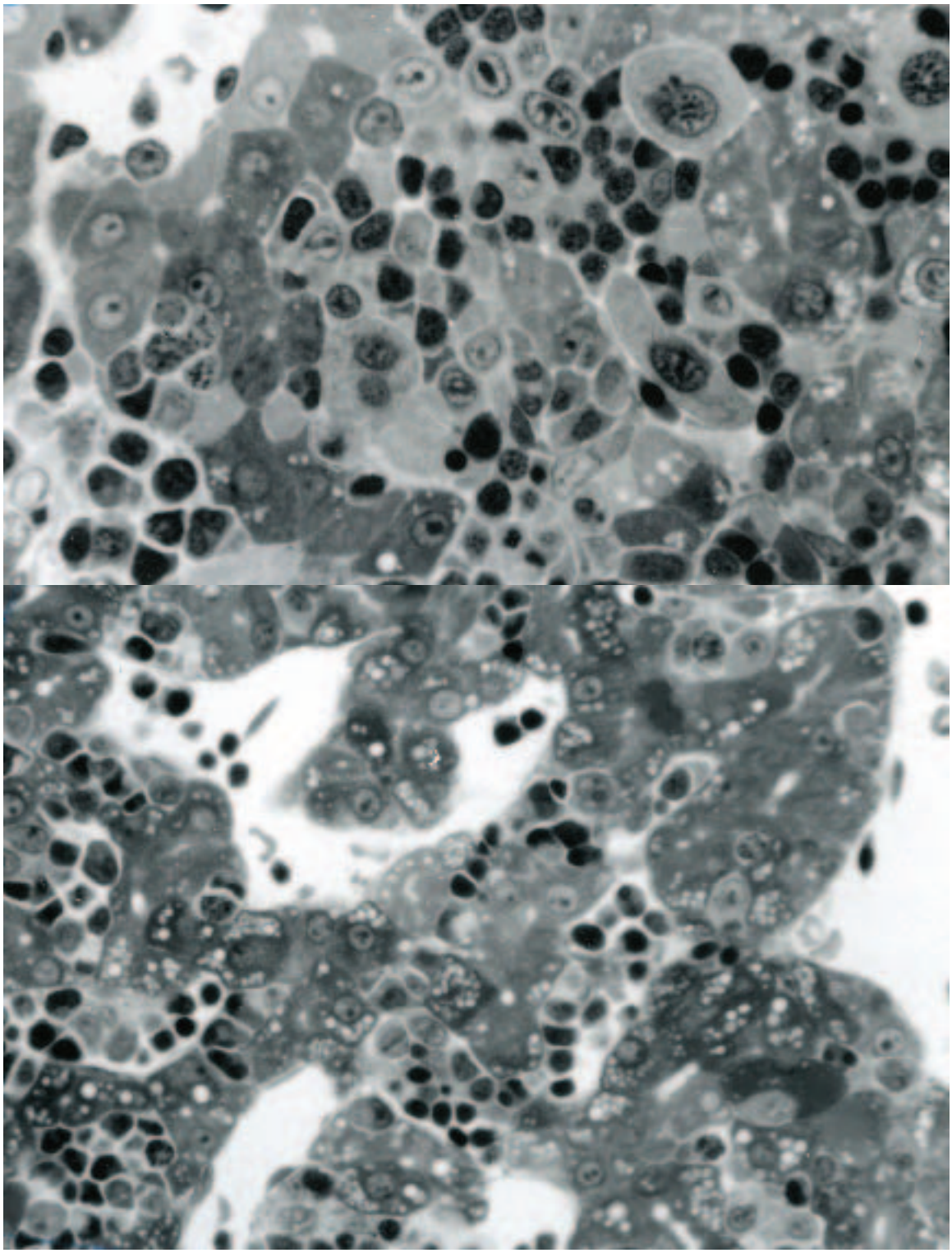

Fig. 5. (*Above*). A micrograph illustrates the central region of a differentiating hepatic lobule from an opossum one week after birth. A portion of a central vein is shown in the upper left corner. Hemopoietic cells of the erythrocyte and granulocyte series as well as megakaryocytes continue to occur between hepatic cells. LM X 400. (*Below*). The peripheral region of a hepatic lobule exhibits wide sinusoidal spaces separating irregular cords of hepatocytes. Flattened endothelial cells line some sinusoidal spaces (bottom). The majority of hepatocytes continue to be laden with lipid droplets. LM X 300.

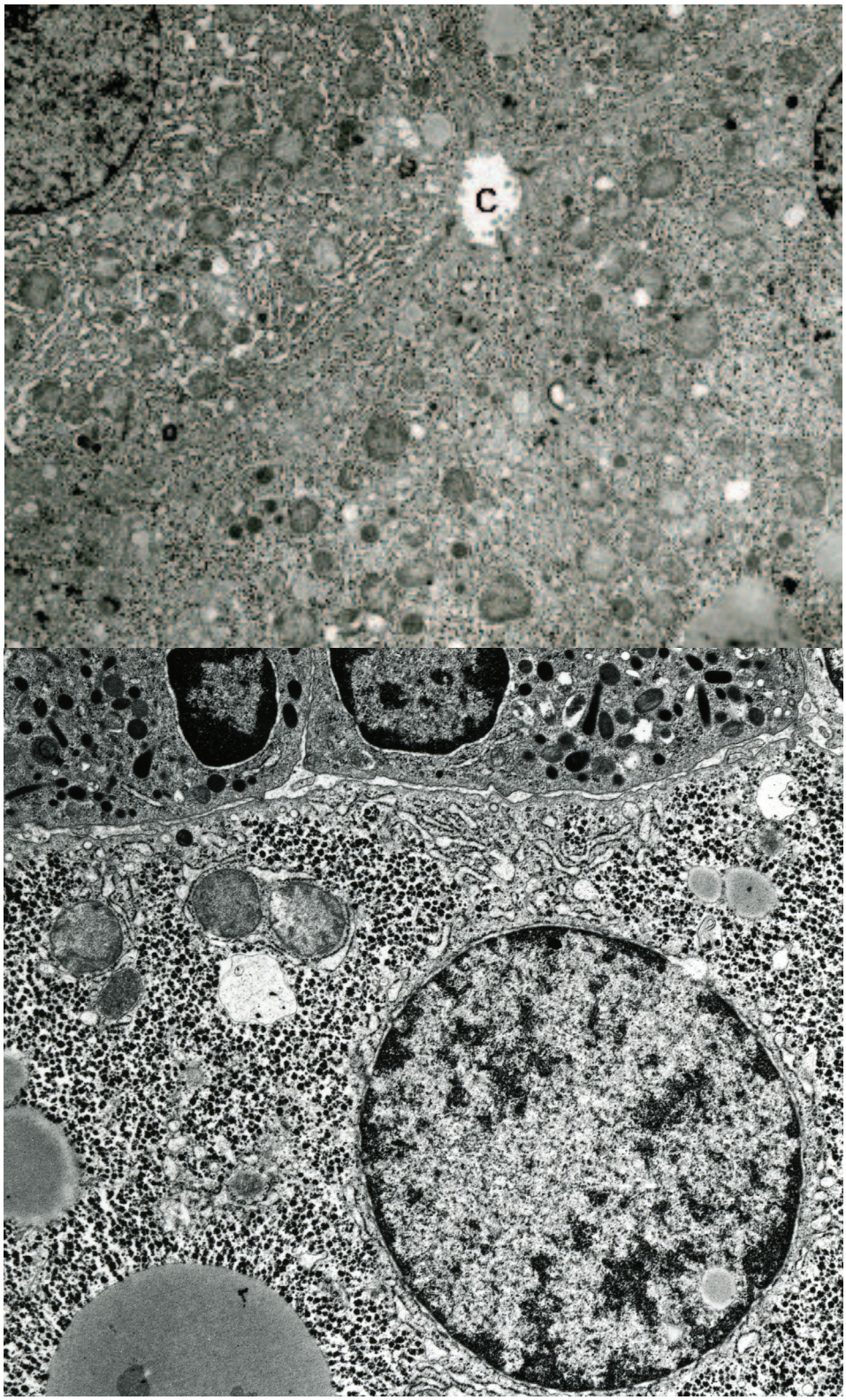

Fig. 6. (*Above*). By the end of the first postnatal week hepatocytes show abundant rough endoplasmic reticulum, scattered dense bodies and accumulations of glycogen. A bile canaliculus (C) is shown near the center. TEM X 6,000. (*Below*). A portion of a hepatocyte from an opossum one week postnatal filled with glycogen and scattered lipid droplets. Note that the neutrophil granulocytes (above) are directly related to the plasmalemma of the hepatocyte. TEM X 6,000.

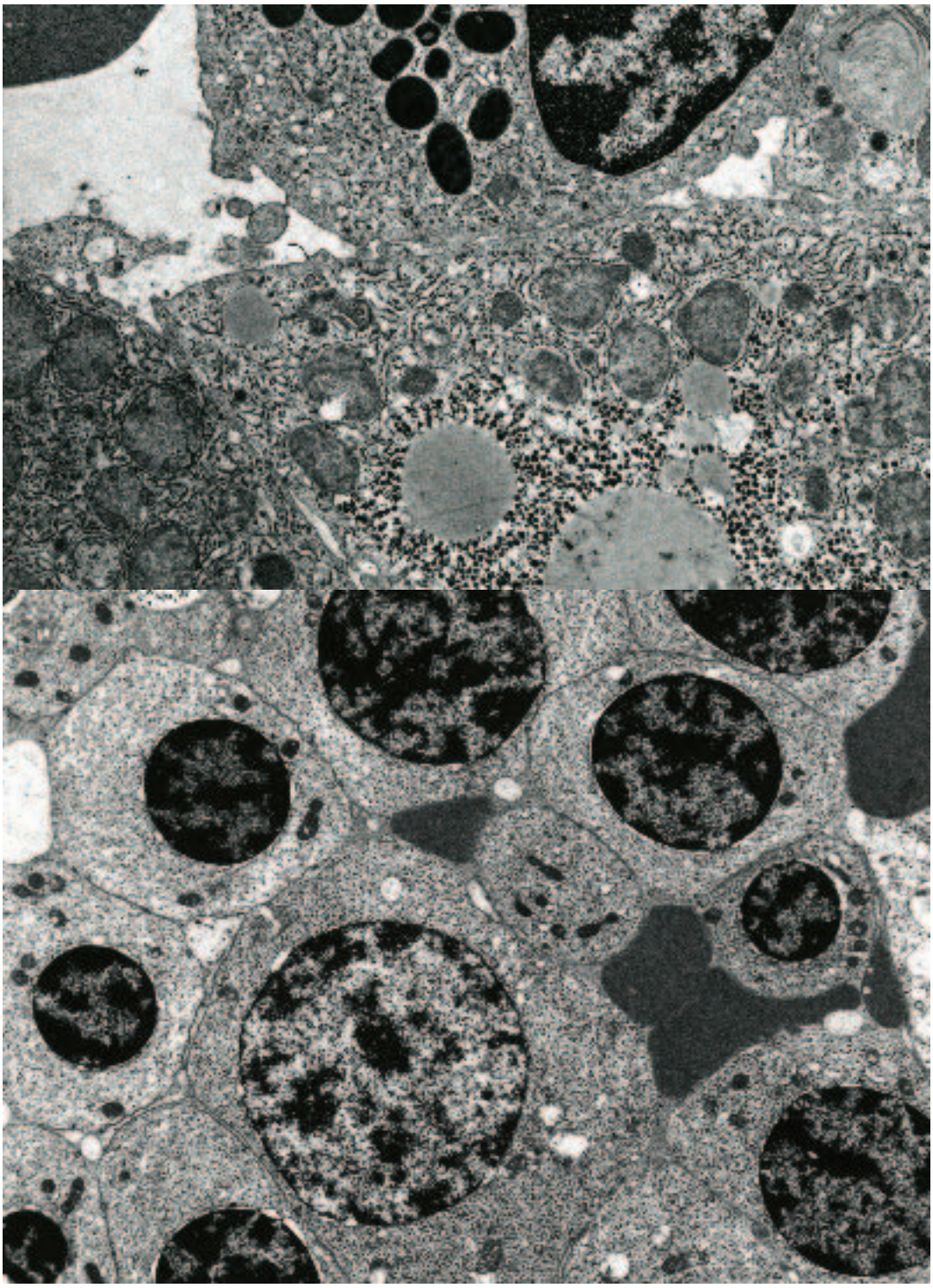

Fig. 7. (*Above*). A region of a hepatic sinusoid where the endothelial lining is incomplete illustrates the close relationship between a hepatocyte and an adjacent eosinophil leukocyte (top). Cytoplasmic processes of a sinusoidal lining cell are seen within the sinusoidal lumen at the extreme left. Opossum one week postnatal. TEM X 8,000. (*Below*). A small island of developing erythrocytes located between hepatocytes of a week old opossum. TEM X 8,000.

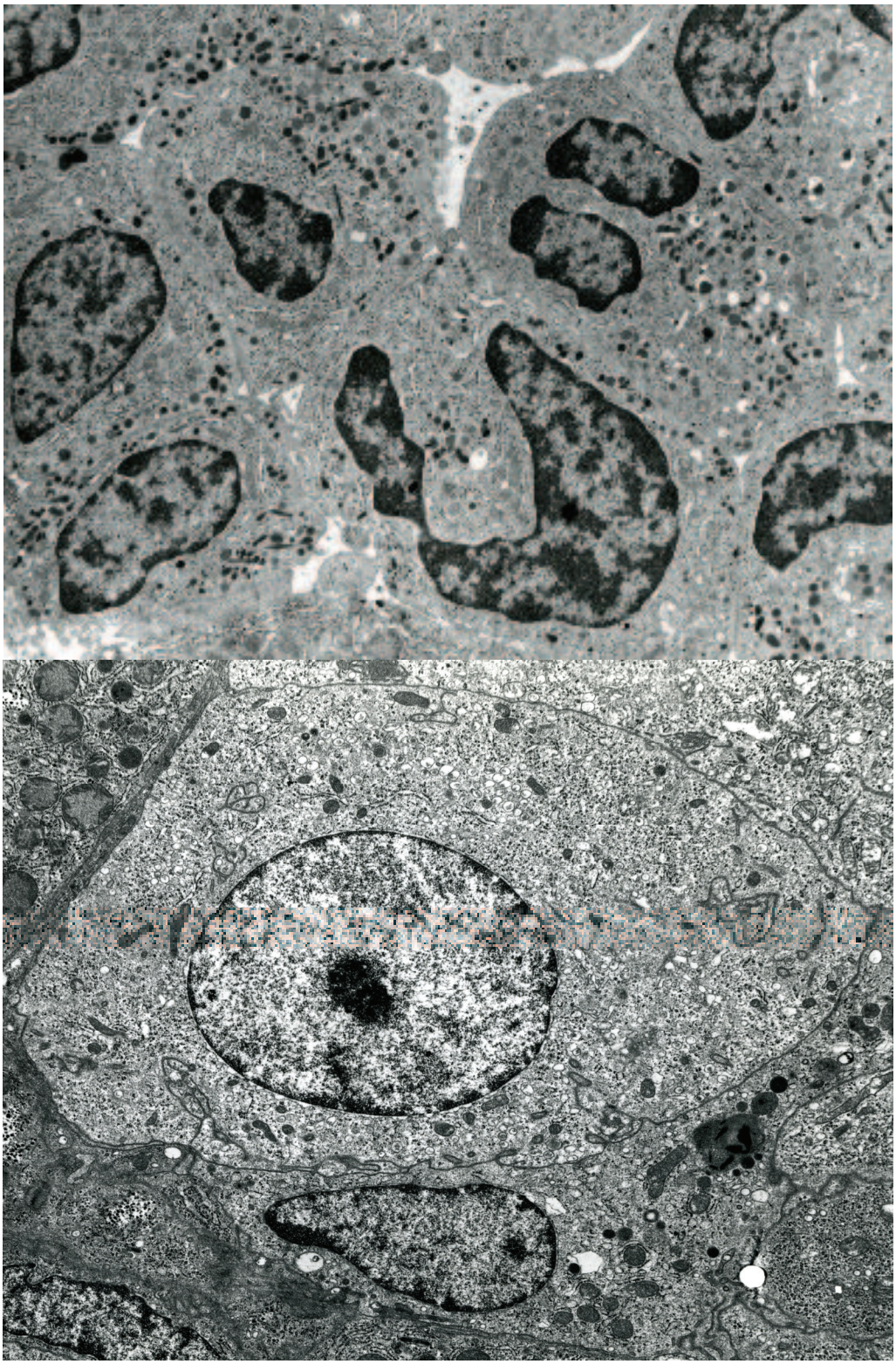

Fig. 8. (*Above*). A small group of differentiating granulocytes (primarily of the neutrophil line) located between hepatocytes of a week old opossum. TEM X 8,000. (*Below*). A megakaryocyte located within a developing hepatic sinusoid of an opossum one week postnatal. TEM X 7,500.

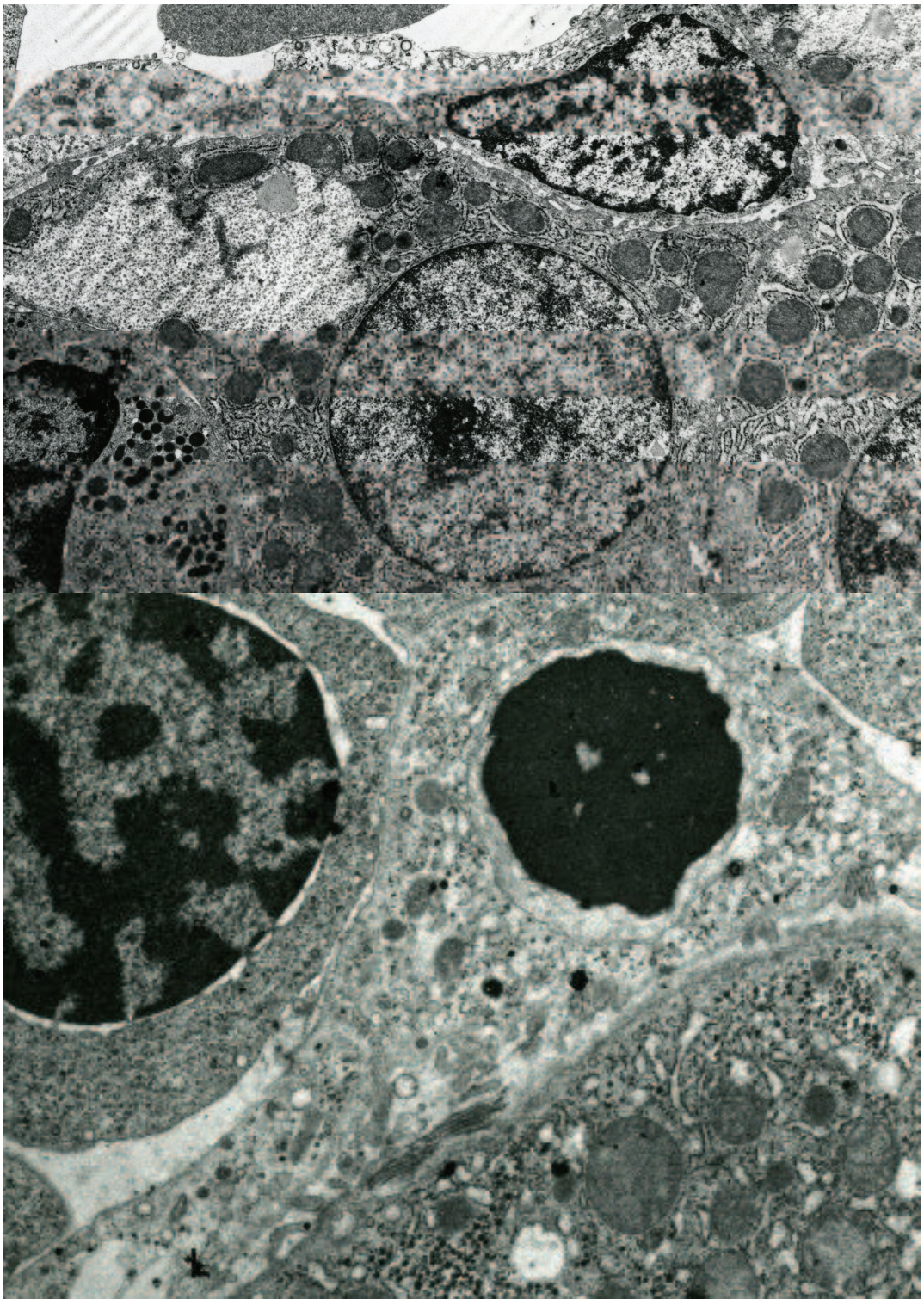

Fig. 9. (*Above*). The hepatic sinusoid (top) is lined by two overlapping sinusoidal cells whereas the region of a sinusoid shown at the lower left is devoid of lining cells and contains a granulocyte. The hepatocyte cytoplasm contains a large accumulation of glycogen and a small bile canaliculus can be observed at the lower right. One-week-old opossum. TEM X 7,500. (*Below*). The cytoplasm of a sinusoidal lining cell (coursing from lower left to upper right) contains a pyknotic nucleus phagocytosed after being extruded from a developing erythrocyte. An erythroblast is shown at the upper left and a portion of a hepatocyte at the lower right. One-week-old opossum. TEM X 8,000.

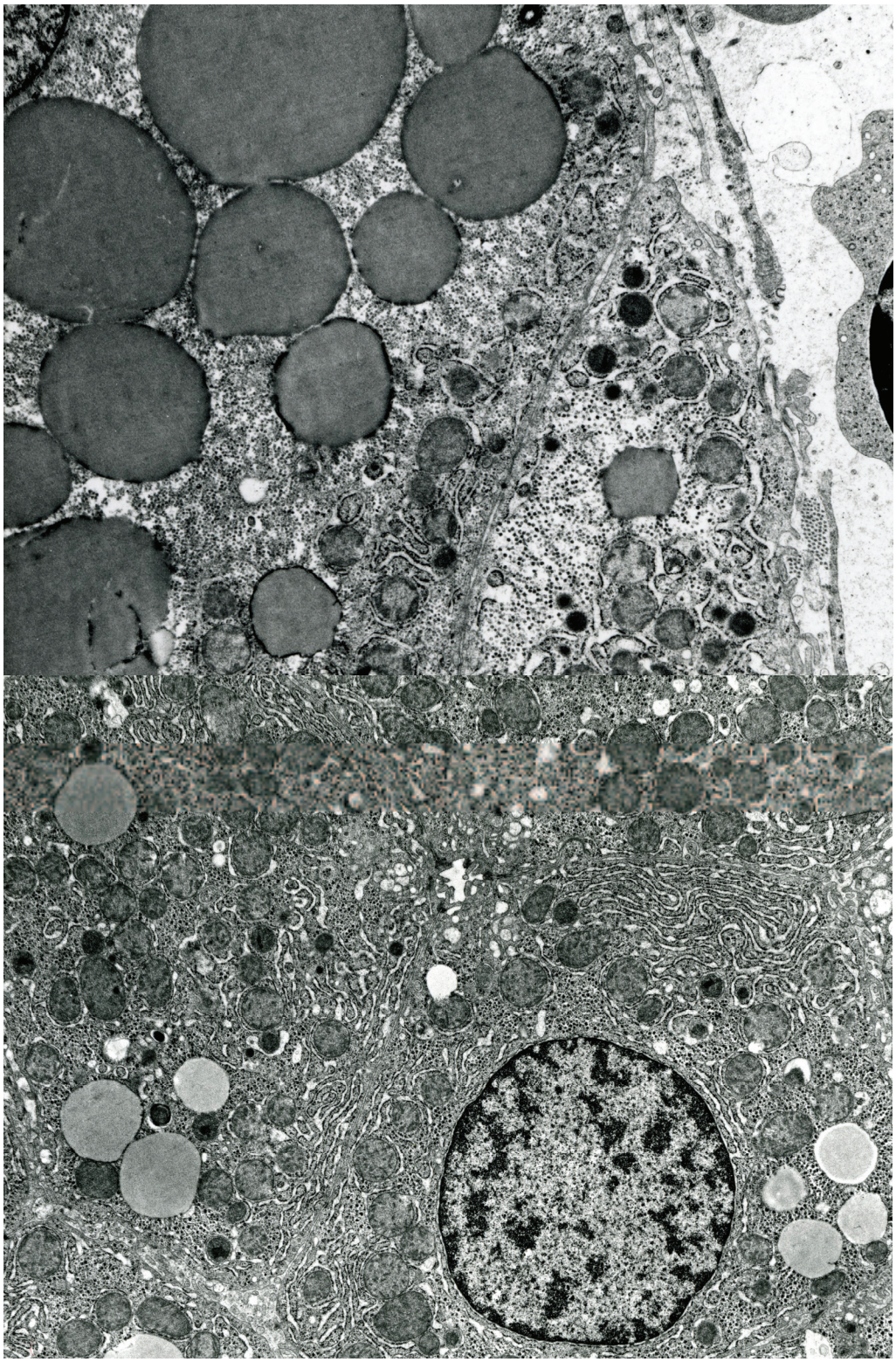

Fig. 10. (*Above*). An increase in the number of lipid droplets, which vary in size, and the amount of glycogen, occurs in hepatocytes of the opossum liver by the end of the second postnatal week. TEM X 6,000. (*Below*). At ten weeks postnatal elements of rough endoplasmic reticulum, scattered glycogen granules, and lipid droplets of medium size characterize the cytoplasm of the majority of hepatocytes. Note the numerous, smooth membrane-bound vesicles of Golgi complexes that lie in relation to a bile canaliculus located near the center of the electron micrograph. TEM X 7,000.

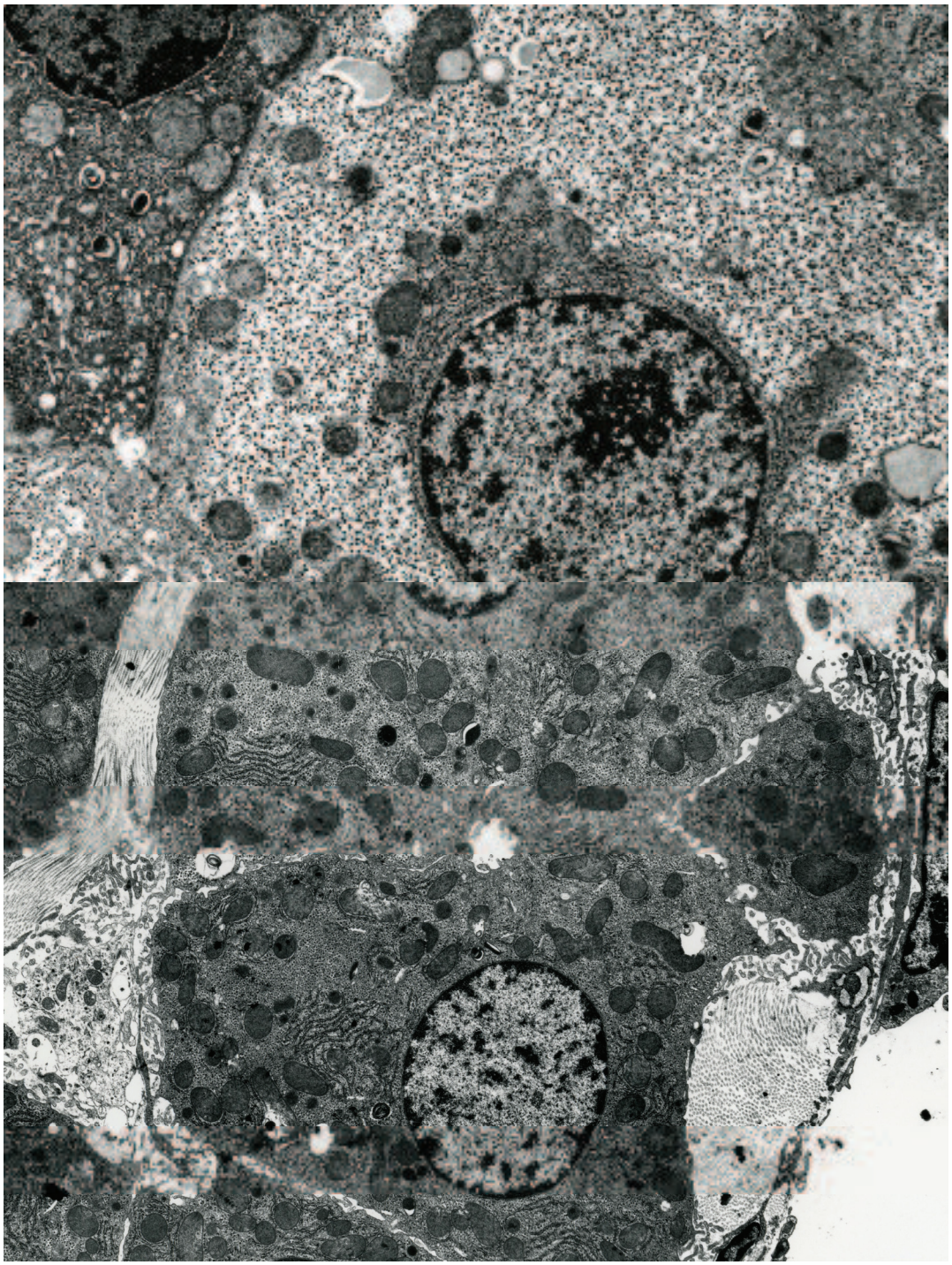

Fig. 11. (*Above*). The liver of the ten-week-old opossum often shows a heterogeneous population of hepatocytes. Some hepatocytes are filled with glycogen, whereas other hepatocytes exhibit considerable electron density (upper left). Note the bile canaliculus (lower left) between hepatocytes. Compare the structure of these hepatocytes with that shown in figure ten. TEM X 9,000. (*Below*). Hepatocytes near a central vein of a liver lobule from a twelve-week-old opossum continue to be characterized by large accumulations of glycogen. Note the bile canaliculus near the center of the field and the large amounts of collagen that lie between hepatocytes and a sinusoidal cell (extreme right). TEM X 6,000.

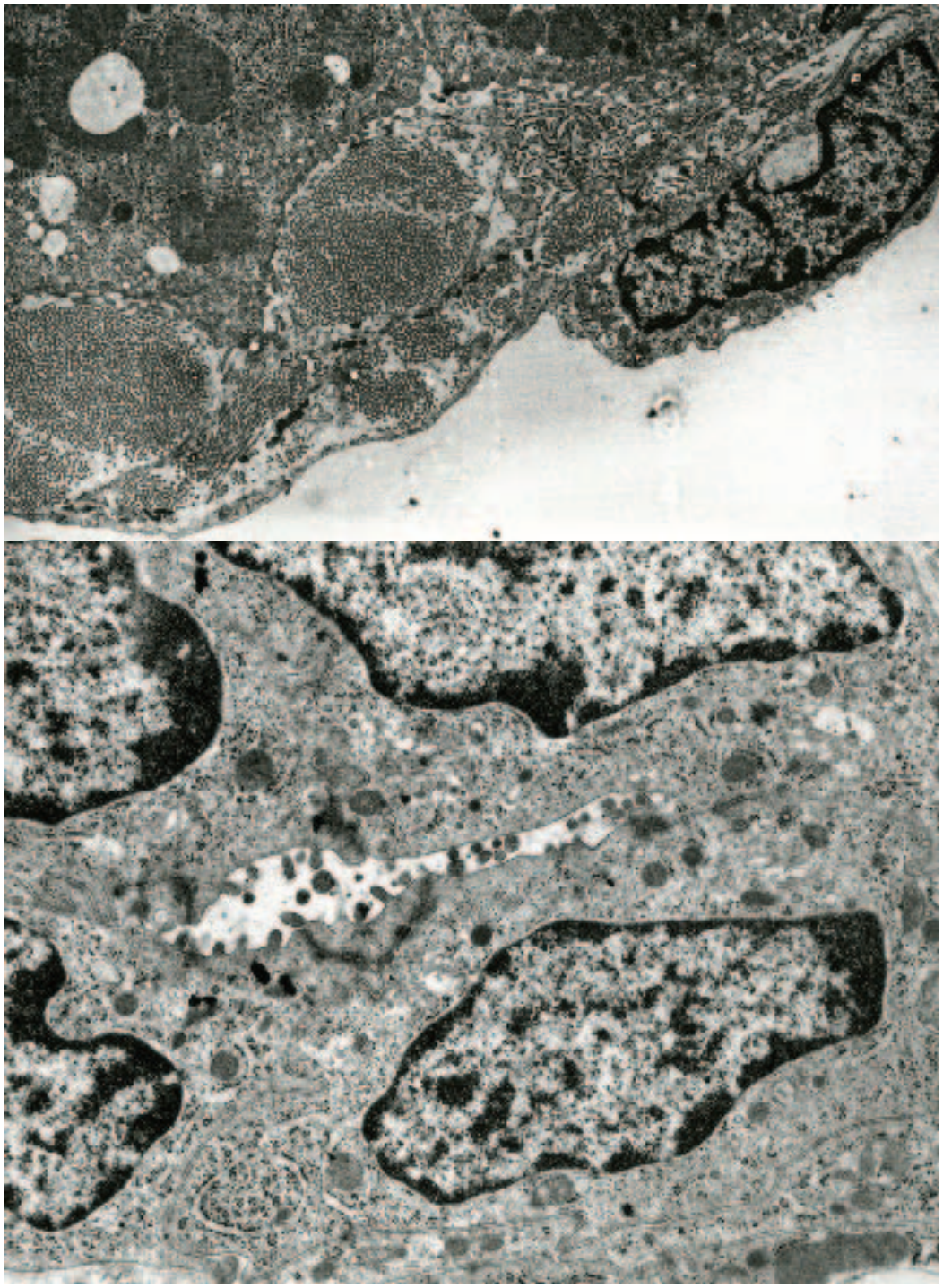

Fig. 12. (*Above*). Large bundles of collagen observed between a hepatocyte (top left) and an endothelial cell lining a central vein of a liver lobule. Juvenile opossum. TEM X 7,500. (*Below*). A segment of a bile ductule (of Herring) formed by cube shaped cells found among hepatocytes of a liver lobule from a juvenile opossum. The bile ductule functions to connect the system of bile canaliculi between hepatocytes to the intralobular bile ducts located in adjacent portal area. TEM X 7,000.

Chapter 26. Spleen

Synopsis:

The spleen of the newborn opossum has a triradiate external appearance and consists primarily of a well-vascularized mesenchymal tissue. The mesenchymal cells show considerable variation in size, shape and in the configuration of their nuclei. Most are characterized by large nuclei with prominent nucleoli and a scant cytoplasm. Scattered between mesenchymal cells are rounded cells of a more uniform size and shape. The spleen capsule consists only of a thin mat of reticular fibers covered by a layer of cuboidal epithelium derived from the peritoneum. Although nucleated erythrocytes are present within forming vascular channels at this stage of organogenesis, there is no evidence of hemopoietic activity in the newborn opossum spleen. Mitotic activity is a common observation among mesenchymal cells during the first four days of postnatal life and there is an increase in number of the uniformly sized, rounded cells. Hemopoietic activity is first observed at about five days postnatal with the appearance of small, scattered foci of developing erythrocytes and a few megakaryocytes. Sinusoid-like spaces lined by attenuated spindle-shaped cells now are observed scattered throughout the spleen. The sinusoid-like vascular spaces continue to be a prominent feature of the spleen through the second postnatal week and are lined by flattened endothelial cells. Extensive overlapping of adjacent lining cells occurs but desmosomal attachments are not observed. Where the vascular spaces occur adjacent to hemopoietic foci, occasional erythrocytes are observed passing through their walls. Arterioles are prominent in areas devoid of hemopoietic activity. The transmural passage of cellular elements through the wall of the sinusoid-like spaces continues to be observed at this stage of development. An additional feature of the spleen at this time and in later stages of development is the appearance of small, darkly stained reticular cells. They are usually closely associated with arterioles. The cytoplasm of these reticular cells is electron-dense and it contains numerous vacuoles and mitochondria of various sizes. The nuclei stain deeply and are oval to fusiform in shape. These reticular cells extend from the arterioles to lie between hemopoietic elements. It is believed that this group of cells may represent a population of dendritic or antigen-presenting cells associated with the spleen. Near the end of the third postnatal week the spleen exhibits ill-defined accumulations of large, medium and a few small lymphocytes adjacent to some arterioles. Elsewhere in the spleen, the differentiating red pulp is filled with developing erythrocytes, granular leukocytes, and megakaryocytes. The initial increase in size of the spleen occurs as a result of growth and expansion at the periphery just beneath the developing capsule. The reticular framework is first laid down as an open-meshwork but soon becomes infiltrated with hemopoietic cells. The hemopoietic cells are in turn replaced by lymphoid tissue. Thus, during the first two postnatal weeks the increase in size of the spleen is due mainly to hemopoietic activity. Subsequent development is concerned primarily with the continued accumulation of lymphatic tissue. By sixty days into the postnatal period, distinct lymphatic nodules are apparent scattered throughout the spleen. As the lymphatic nodules form they are separated from the red pulp by a narrow marginal zone of reticular fibers and cells. The marginal zone becomes a prominent feature in the adult. Germinal centers are not apparent until after weaning. Continued development of the red pulp along the margins of the spleen is thought to account for the late development of the capsule, which is relatively thin even at nine weeks into the postnatal period. The capsule of the spleen in the adult is thick and consists of collagen and reticular

fibers in addition to smooth muscle cells. The latter do not extend into the trabeculae of the spleen.

Acknowledgments:

Fig. 1 (top and center), courtesy of and from: Cutts, J.H. and W.J. Krause (1982) Postnatal development of the spleen in *Didelphis virginiana*. J. Anat. 135:601-613.

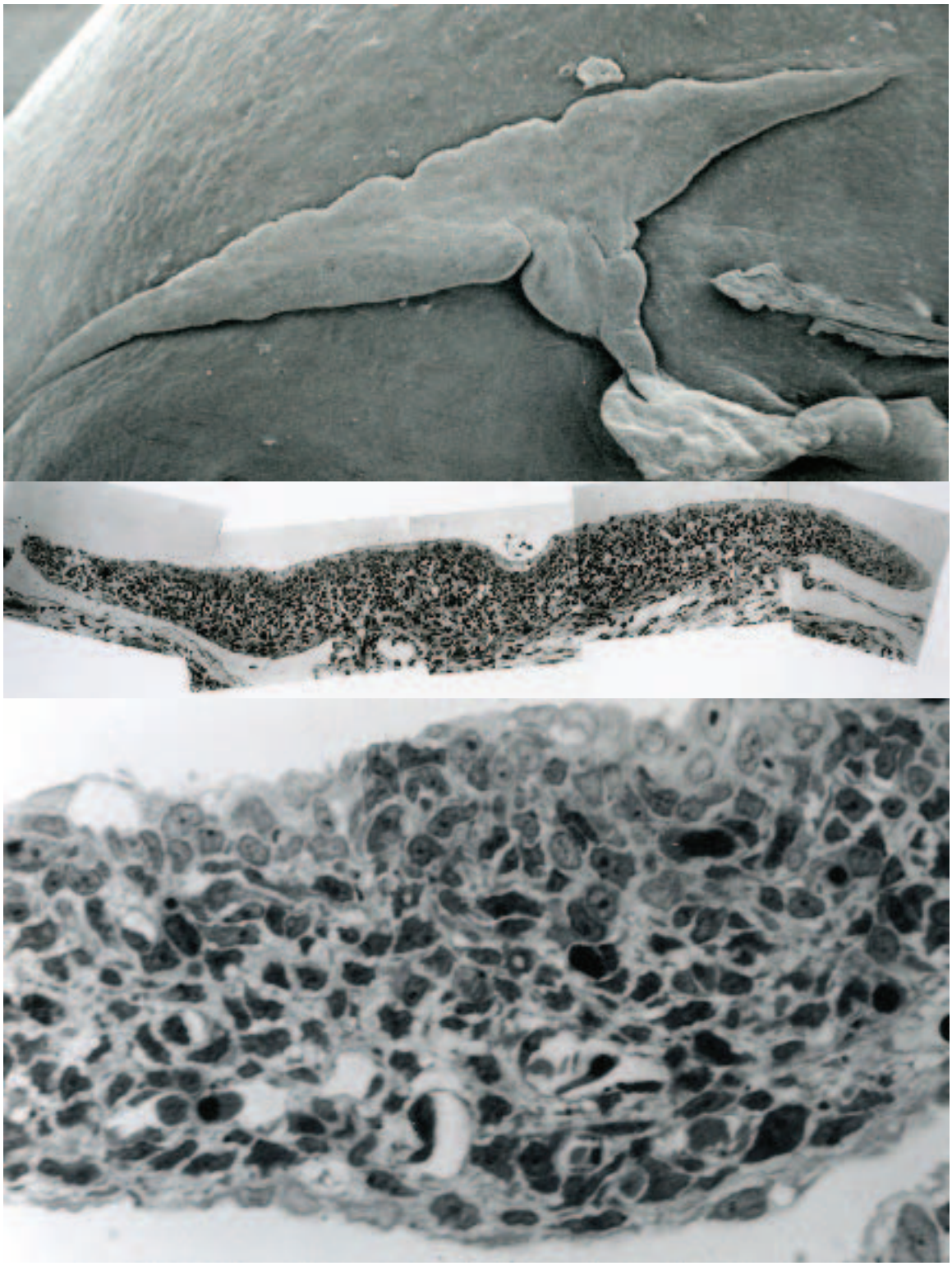

Fig. 1. (*Above*). The triradiate appearance of a newborn opossum spleen. The lateral and inferior margins are concave and end in elongated apices. SEM X 150. (*Center*). A composite of histological sections through the length of the newborn opossum spleen illustrates that it consists primarily of a mass of well-vascularized mesenchymal tissue. LM X 150. (*Below*). Mesenchymal cells are closely packed and exhibit considerable pleomorphism. Nucleated erythrocytes are present in some of the vascular channels. Newborn opossum. LM X 400.

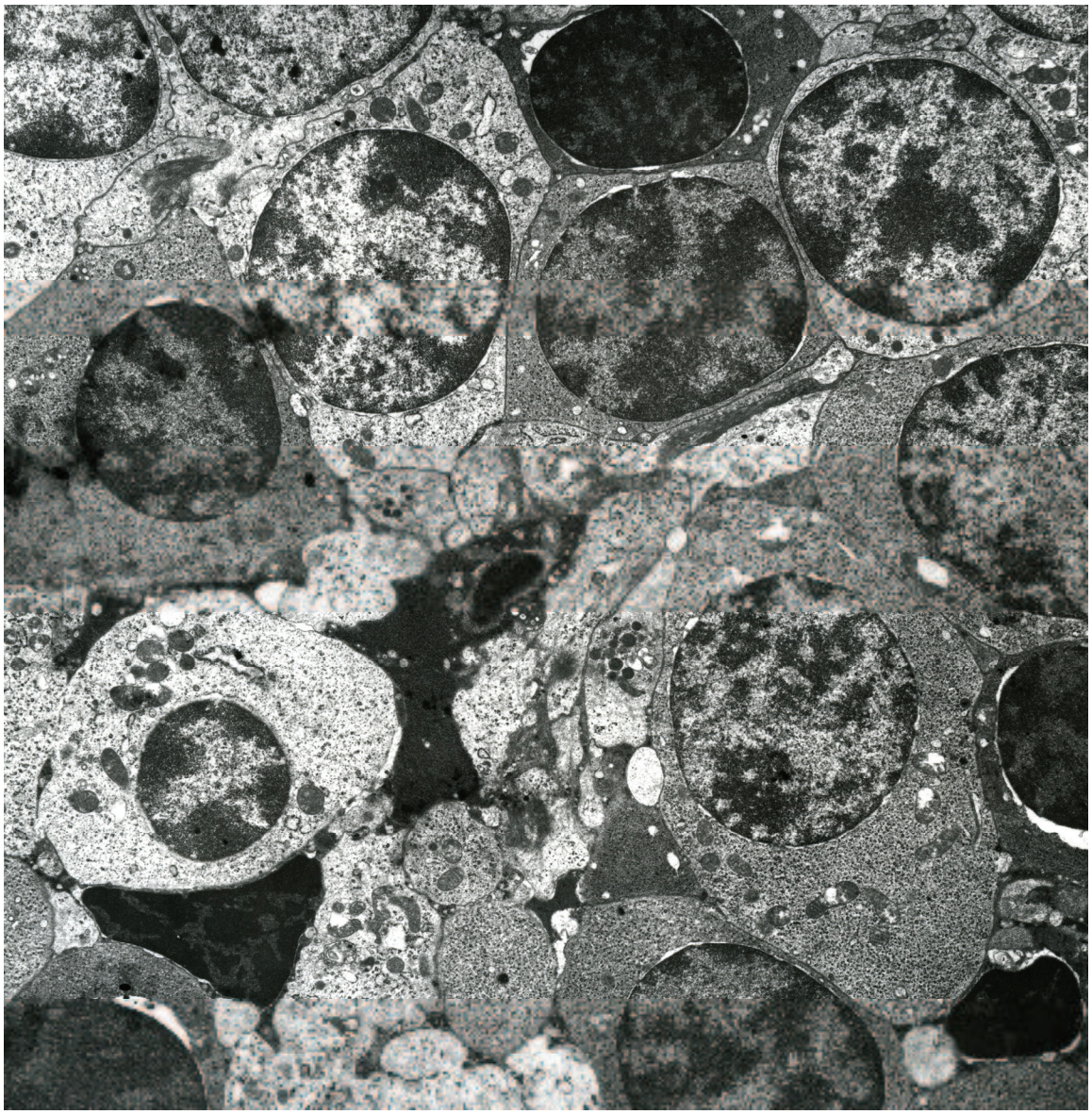

Fig. 2. The spleen of the opossum is an obvious hemopoietic organ by the end of the first postnatal week, with islands of developing blood cells being observed among the mesenchymal cells. These islands tend to be segregated into masses of developing erythrocytes or granular leukocytes. This transmission electron micrograph was taken through the edge of an erythropoietic islet from the spleen of an opossum one week postnatal. Several different stages of erythrocyte maturation can be observed. TEM X 2,000.

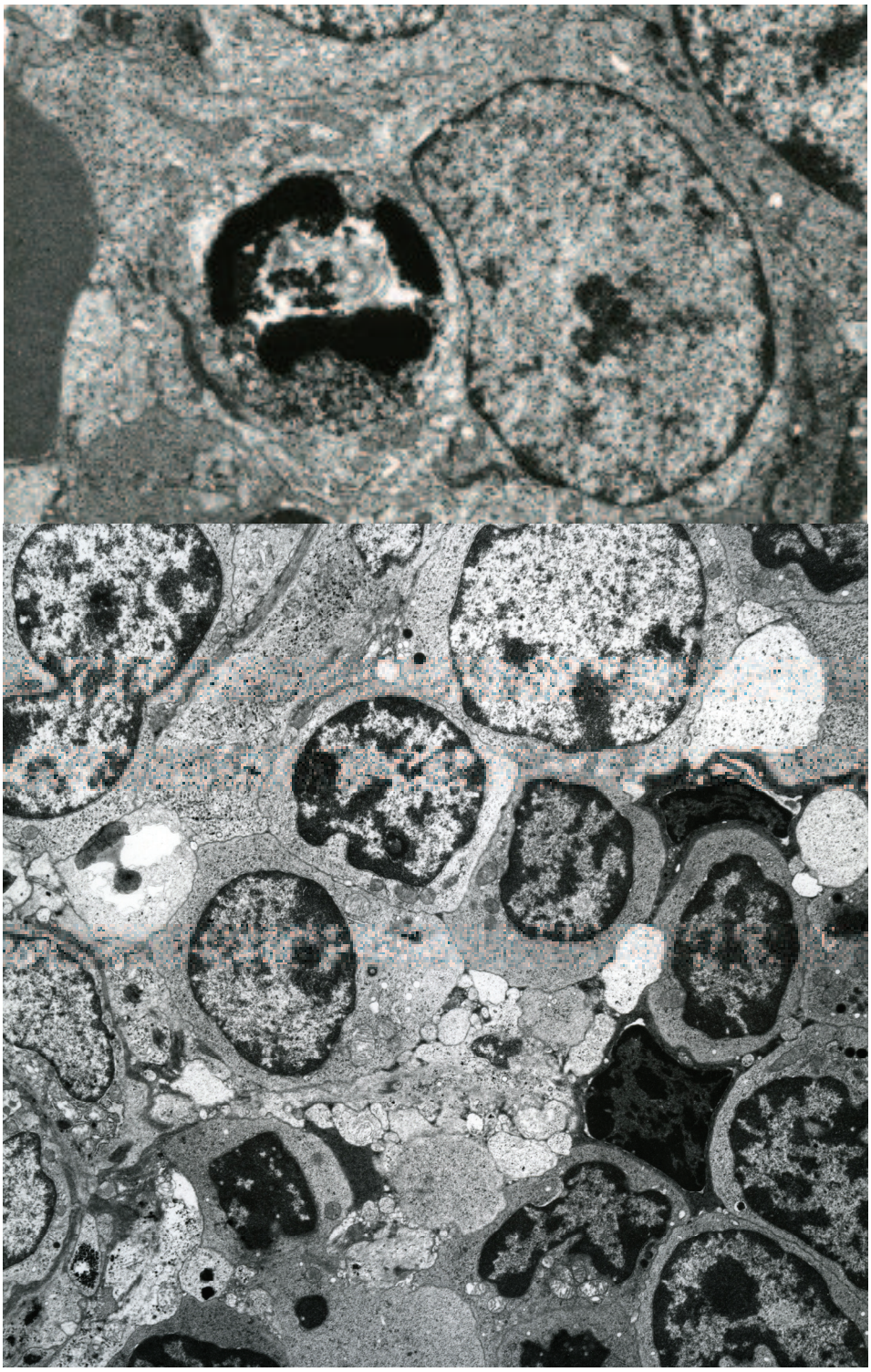

Fig. 3. (*Above*). Phagocytic activity is often observed in and around hemopoietic areas during that time within the postnatal period when hemopoietic activity is prominent. Many of the phagocytic cells contain nuclear debris as shown in the cytoplasm of this macrophage. Opossum two weeks postnatal. TEM X 3,000. (*Below*). Evidence for lymphocyte formation is present in the spleen at the end of the third postnatal week. Note that the lymphocytes shown here form a diffuse cuff around an arteriole the edge of which is shown at the extreme lower left. Note the two darkly stained reticular cells at the right. TEM X 2,000.

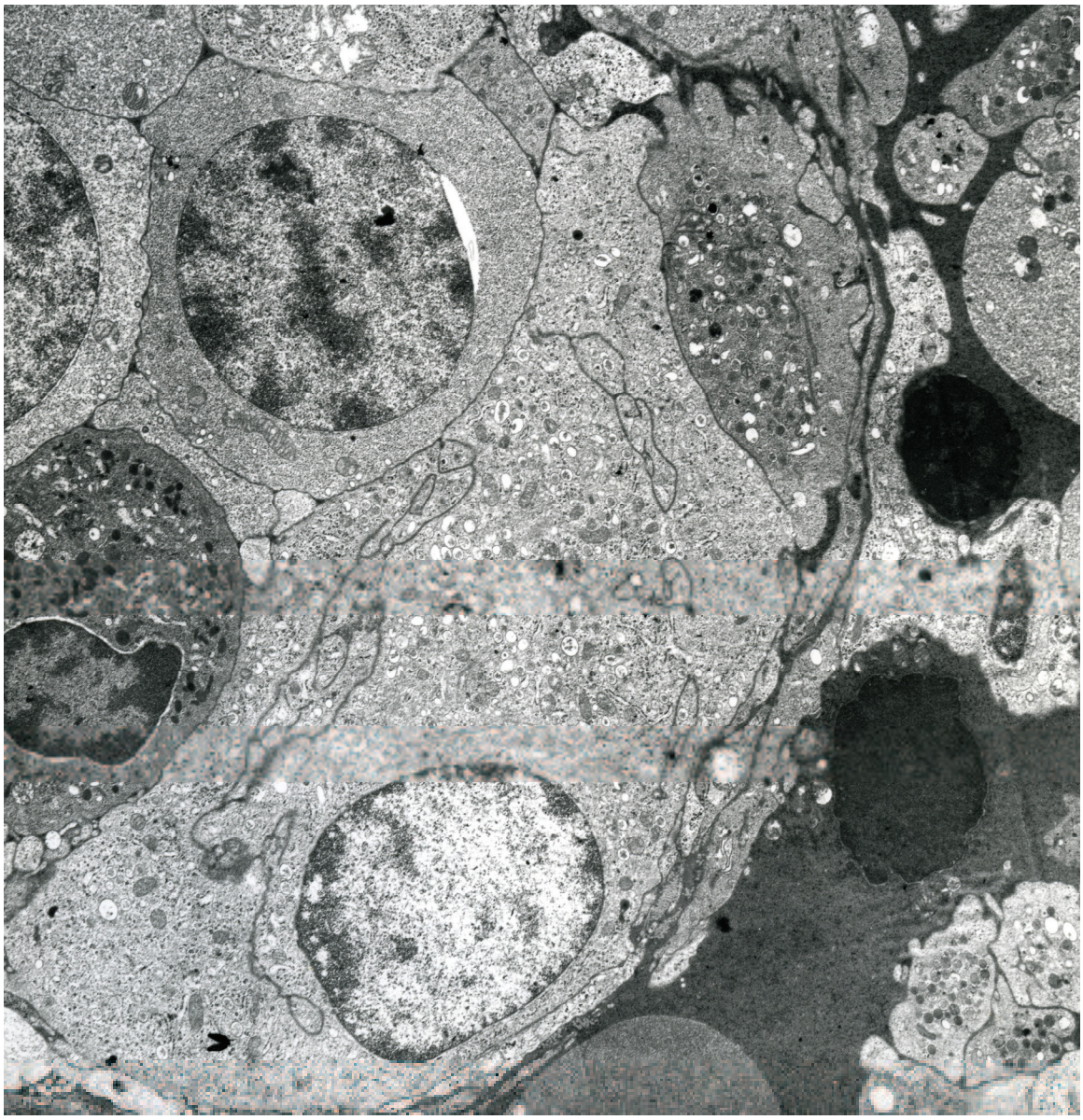

Fig. 4. Megakaryocytes are commonly observed in the developing opossum spleen and exhibit demarcation membranes and platelet fields. A neutrophil and developing erythrocyte are shown to the left of the megakaryocyte located near the center of the field. Two dense staining nucleated erythrocytes are shown to the right of the megakaryocyte. Opossum three weeks postnatal. TEM X 2,000.

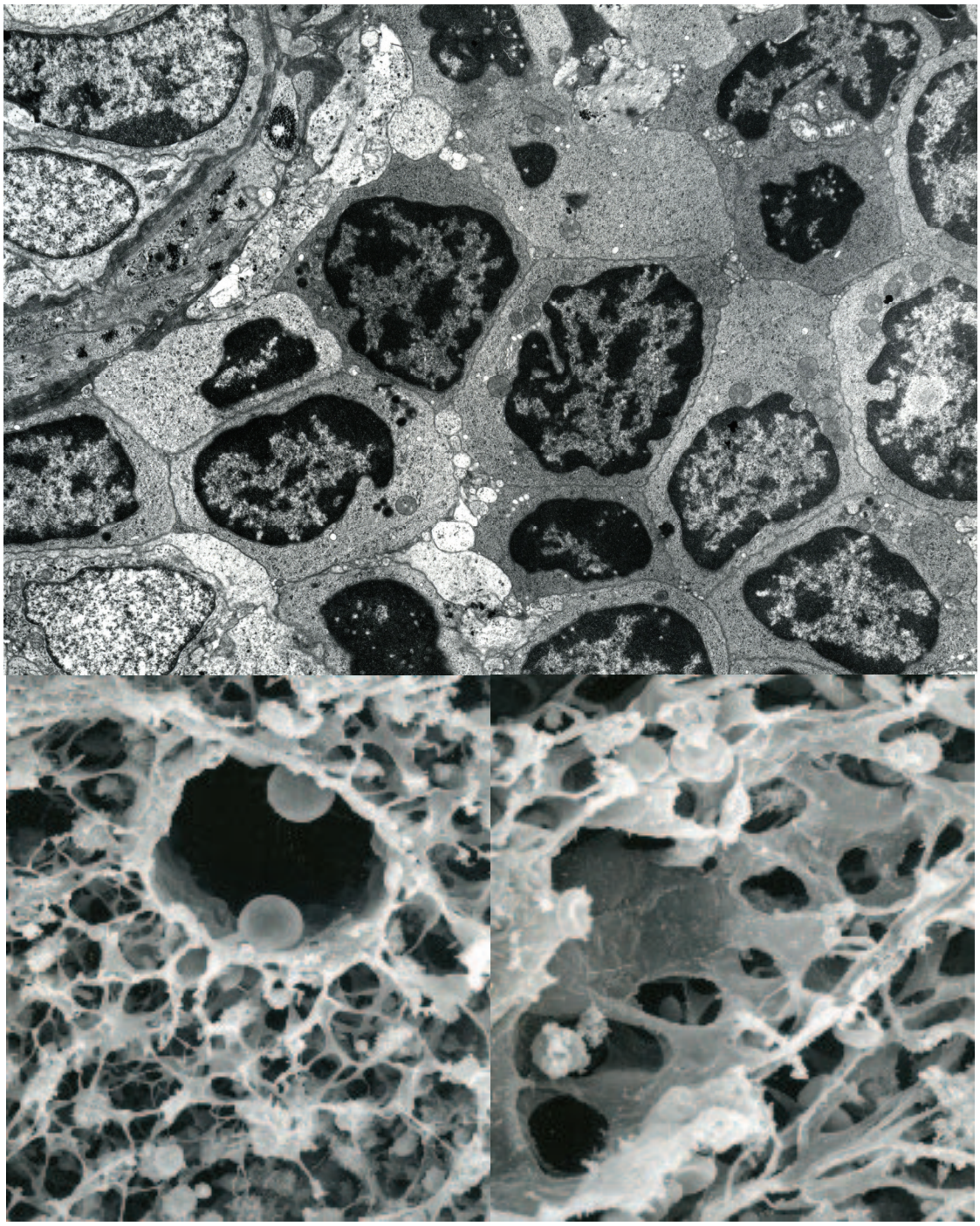

Fig. 5. (*Above*). A transmission electron micrograph through the edge of a splenic follicle from a nine-week postnatal opossum shows a preponderance of small lymphocytes. A portion of a small arteriole is shown in the upper left corner. TEM X 2,200. (*Below left*). A thin walled blood vessel found in the red pulp of a washed spleen taken from a juvenile opossum. Note the surrounding reticular cells. SEM X 660. (*Below right*). A portion of a thin walled, sinusoid-like blood vessel observed in the red pulp of a juvenile opossum spleen by scanning electron microscopy. SEM X 1,600.

Chapter 27. Thymus

Synopsis:

The opossum thymus differentiates from endoderm associated with the third and fourth pharyngeal pouches. During the tenth prenatal day the third pharyngeal out-pocketing differentiates into thymus (III) as well as parathyroid (III). Pouch III elongates and its lumen lost during the shift in position as it follows the heart in its descent into the forming thoracic cavity. The caudal-most region becomes the epithelioid mass that forms thymus III. The remainder of pharyngeal pouch III forms thymic cord fragments that result in occasional accessory thymic bodies located along the path of its migration into the thorax. Thymus IV is derived from endoderm lining the fourth pharyngeal pouch. The resulting four-epithelioid bodies derived from thymus III and thymus IV becomes molded over the upper region of the pericardium as development continues and forms the four-lobed thoracic thymus of the opossum. The newborn opossum thymus is epithelial in character with only scattered large lymphocytes occurring in bordering capillaries between lobules. The stroma consists of closely packed epithelial cells many of which are in mitosis. Scattered desmosomes are found between adjacent epithelial cells. Large lymphocytes account for nearly half of the thymic cells by the end of the second postnatal day. The lymphocytes appear concentrated at the center of each thymic lobule, whereas the peripheral regions continue to consist of large, epithelial stromal cells. Mitotic figures are abundant. The increase in size of the thymus during the remainder of the first postnatal week is due largely to the proliferation of both epithelial cells and lymphocytes. Lymphocytes at the center of each thymic lobule by the middle of the first postnatal week are primarily medium sized lymphocytes with a few small lymphocytes being observed at the end of the first postnatal week. Thymic (Hassall's) corpuscles are present by the end of postnatal week one and the peripheral regions of each lobule continue to be comprised primarily of epithelial cells. Degenerating cells and mitotic figures are observed in large numbers. Scattered electron-dense cells with thin sheet-like cytoplasmic processes that extend between adjacent cell types also are found during the first postnatal week. The origin and function these electron-dense reticular-like (dendritic) cells are unknown at present. During the second postnatal week the number of small lymphocytes increases throughout the thymus and as a result there is less distinction between the center and edge of the thymic lobules. Small lymphocytes extend to the edge of the cortex and form a thin, poorly defined cortex by the end of the second postnatal week. The ratio of cortex to medulla increases during the third postnatal week and now resembles the thymic tissue of a more mature thymus. Thymic corpuscles are abundant and epithelial lined cysts are observed on occasion.

Acknowledgments:

Fig. 1 (bottom), courtesy of and from: Krause, W.J. (1998) A review of histogenesis/organogenesis in the developing North American opossum (*Didelphis virginiana*). Adv. Anat. Embryol. Cell Biol. 143 (I): Springer Verlag, Berlin, pp 143.

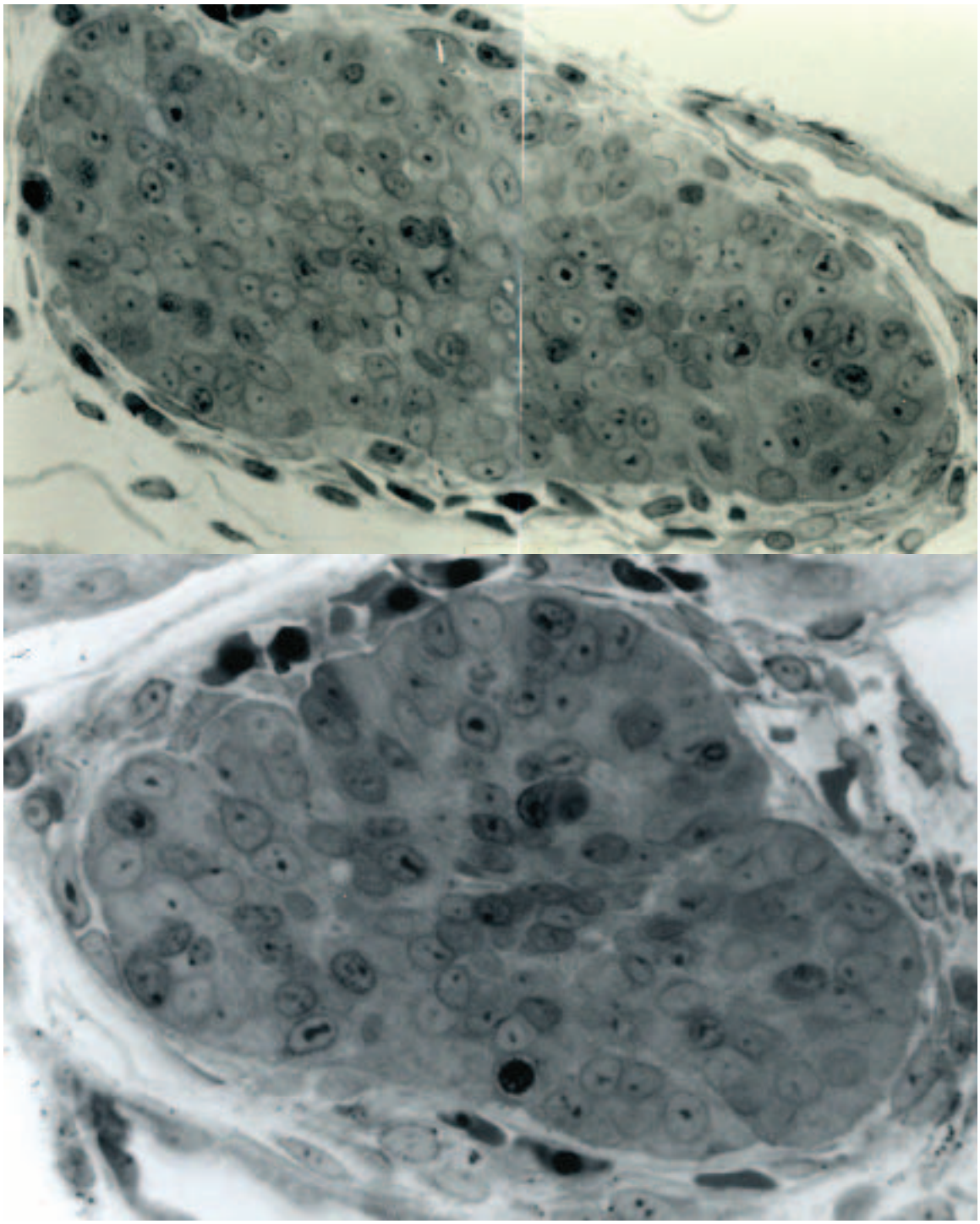

Fig. 1. (*Above*). A composite of two sections through a portion of a lobe from a newborn opossum thymus illustrates the epithelioid character of this lymphoid organ at this stage of organogenesis. LM X 250. (*Below*). When viewed at increased magnification few lymphocytes are observed within the epithelial mass of the newborn opossum thymus. Note the presence of nucleated erythrocytes in capillaries of the surrounding, delicate connective tissue capsule. LM X 350.

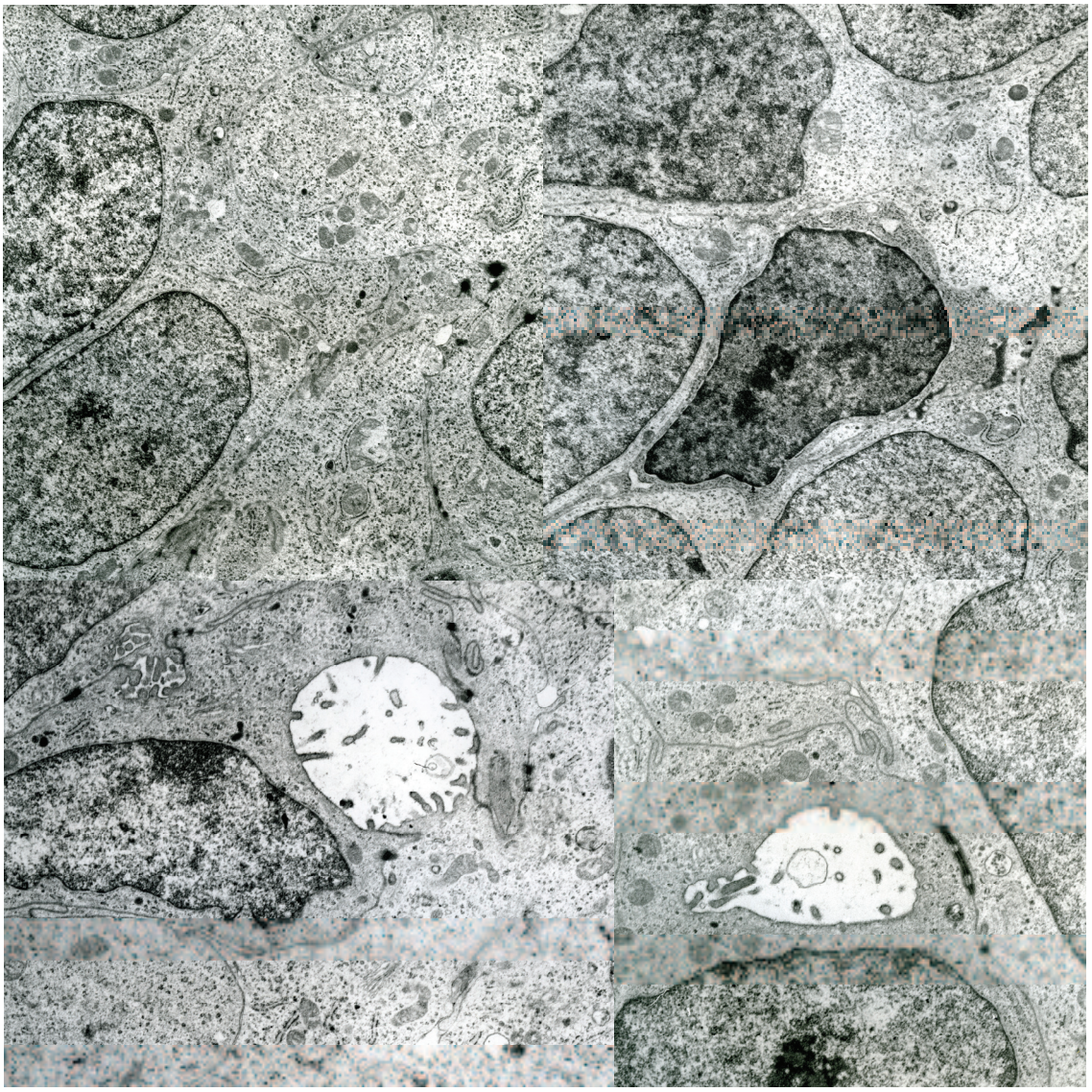

Fig. 2. (*Above left*). The stroma of the newborn opossum thymus consists of closely packed light staining epithelial cells. The cells appear relatively undifferentiated and the cytoplasm contains numerous free ribosomes and scattered mitochondria. Nuclei of most stromal cells are round or oval in shape and characterized by euchromatin. TEM X 2,500. (*Above right*). The dark staining cell (near the center) among the surrounding epithelial cells is thought to be a reticular cell of the thymus. Newborn opossum. TEM X 2,500. (*Below left*). What appear to be intercellular canaliculi that contain numerous microvilli projecting into the lumen (upper left corner) occur between adjacent epithelial cells. Some intercellular canaliculi appear dilated and empty. Note the tight junctions uniting surrounding epithelial cells and the scattered desmosomes between epithelial cells. Newborn opossum. TEM X 5,000. (*Below right*). A region of a thymic epithelial cell exhibits either a profile through an intracellular vacuole or a portion of an intracellular canaliculus. Note the scattered microvilli projecting into the lumen of this structure and the desmosomes shown at the right uniting epithelial cells. Newborn opossum. TEM X 5,000.

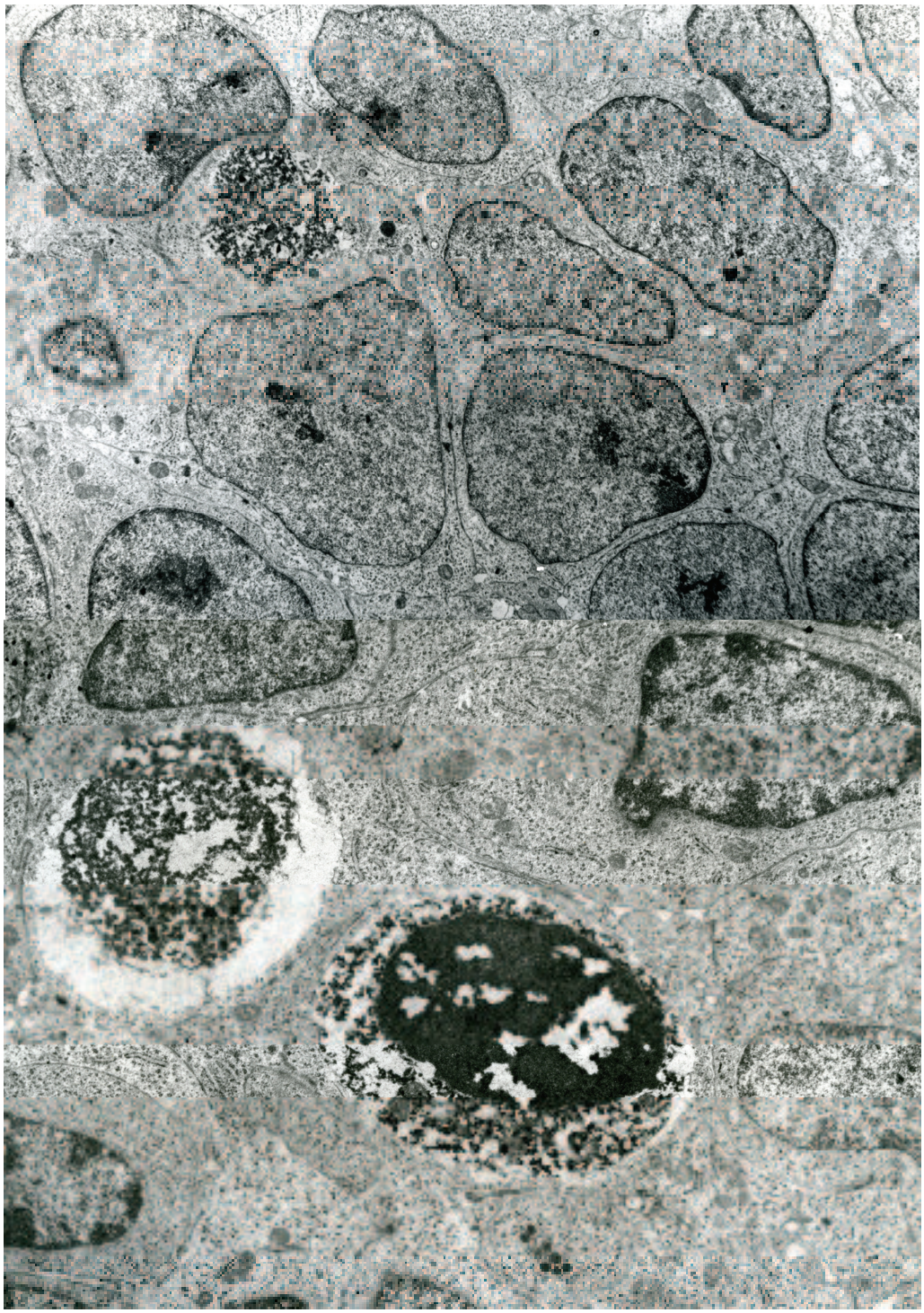

Fig. 3. (*Above*). Scattered, large intracellular vacuoles also are observed in epithelial stromal cells of the thymus, some of which contain electron-dense material (upper left corner). Newborn opossum. TEM X 1,500. (*Below*). Two large intracellular vacuoles observed within epithelial stromal cells of a newborn opossum thymus contain electron-dense material thought to be the remnants of degenerate cells. TEM X 3,500.

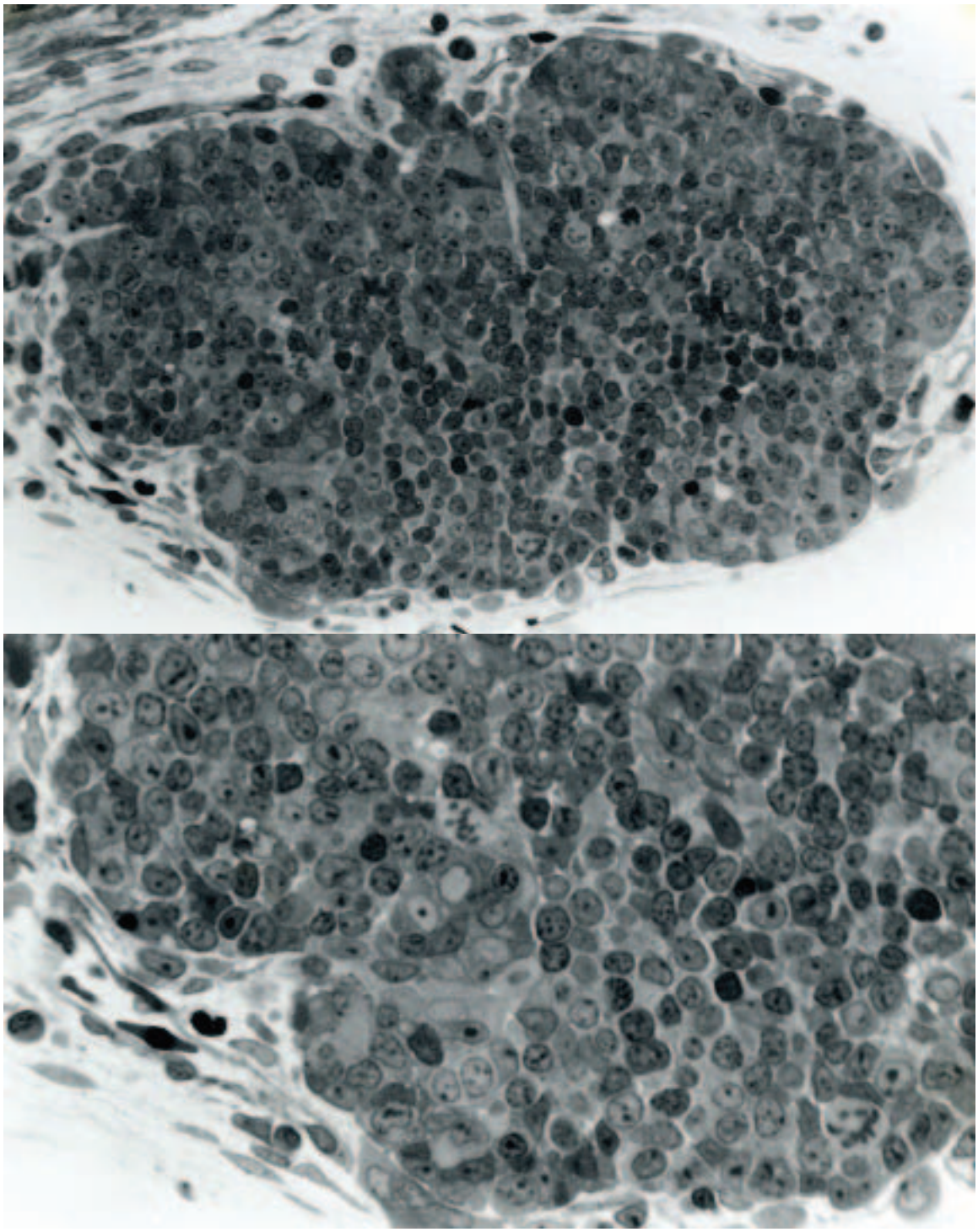

Fig. 4. (*Above*). Numerous lymphocytes are observed within the opossum thymus by the fourth day of postnatal life. Note that the majority of lymphocytes are found within the central region of the lobe. LM X 300. (*Below*). Increased magnification of the peripheral region of a lobe reveals that this area of the thymus has maintained its epithelial character. Numerous mitotic figures also are observed. Opossum four days postnatal. LM X 500.

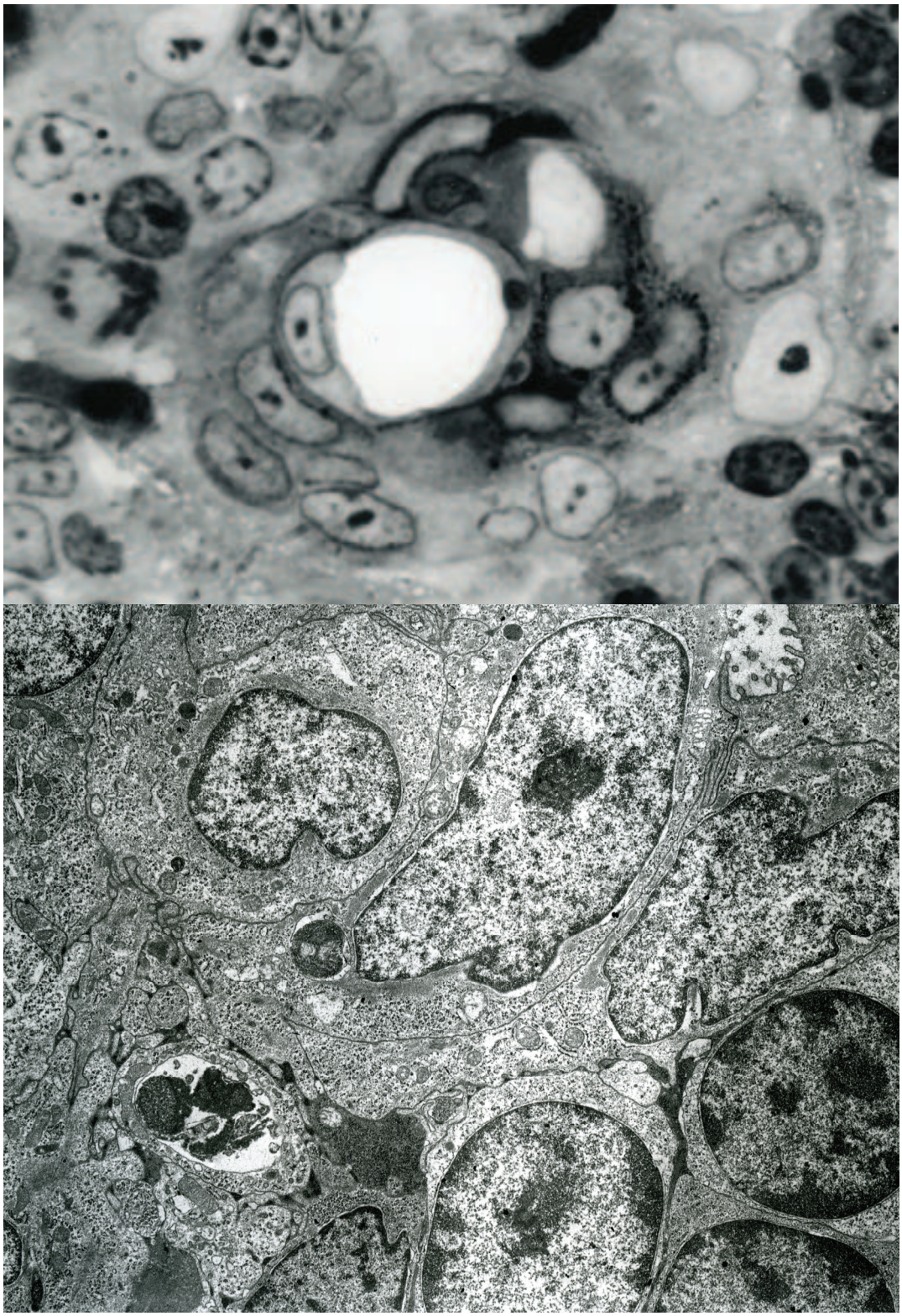

Fig. 5. *(Above*). A developing thymic (Hassall's) corpuscle from the thymus of an opossum one week postnatal consists entirely of epithelial cells. LM X 800. (*Below*). Thymic epithelial cells continue to be associated with intercellular canaliculi-like structures (upper right) though the first postnatal week. Note the lymphocytes at the lower right. Opossum one week postnatal. TEM X 3000.

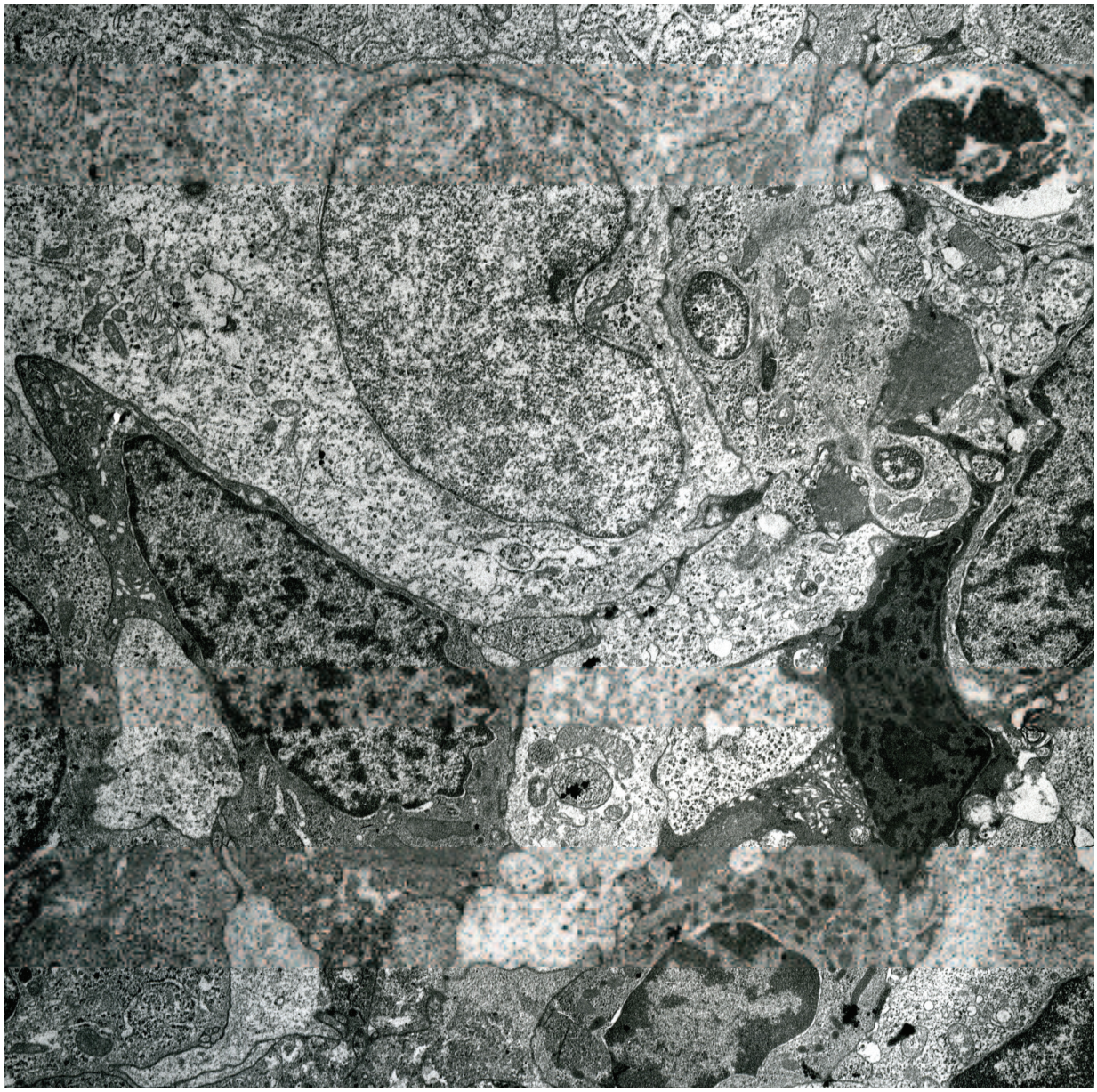

Fig. 6. Scattered electron-dense cells with thin sheet-like cytoplasmic processes that extend between adjacent cells continue to be observed in the thymus through the first postnatal week. Note the cytoplasmic vacuole filled with debris in the upper right corner. TEM X 3,500.

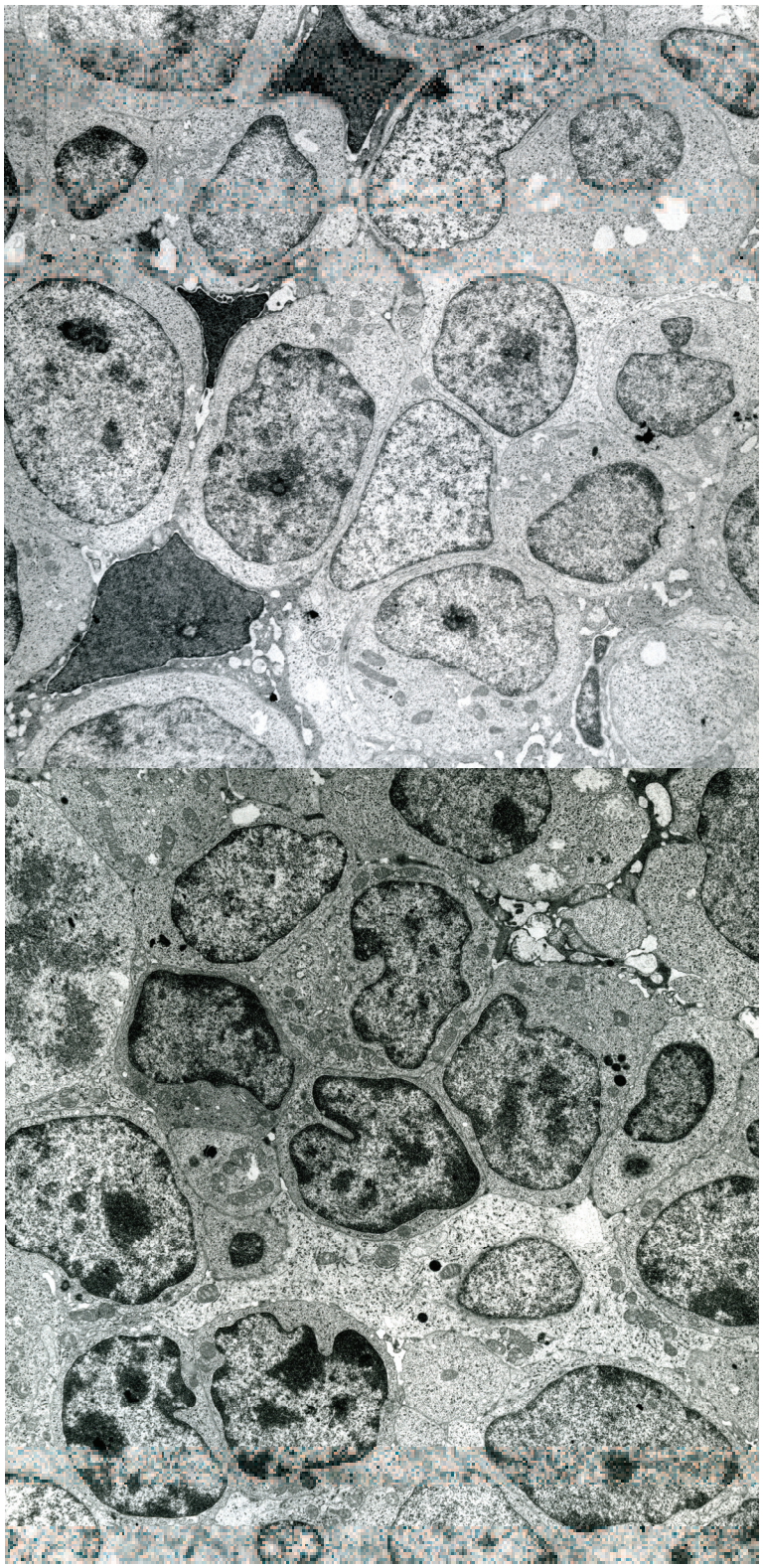

Fig. 7. (*Above*). A peripheral region of opossum thymus one week postnatal illustrates three electron-dense, reticular-like dendritic cells. TEM X 2,500. (*Below*). The central region of an opossum thymus one week postnatal illustrates a field of developing thymic lymphocytes. Note the mitotic figure at the upper left. TEM X 2,500.

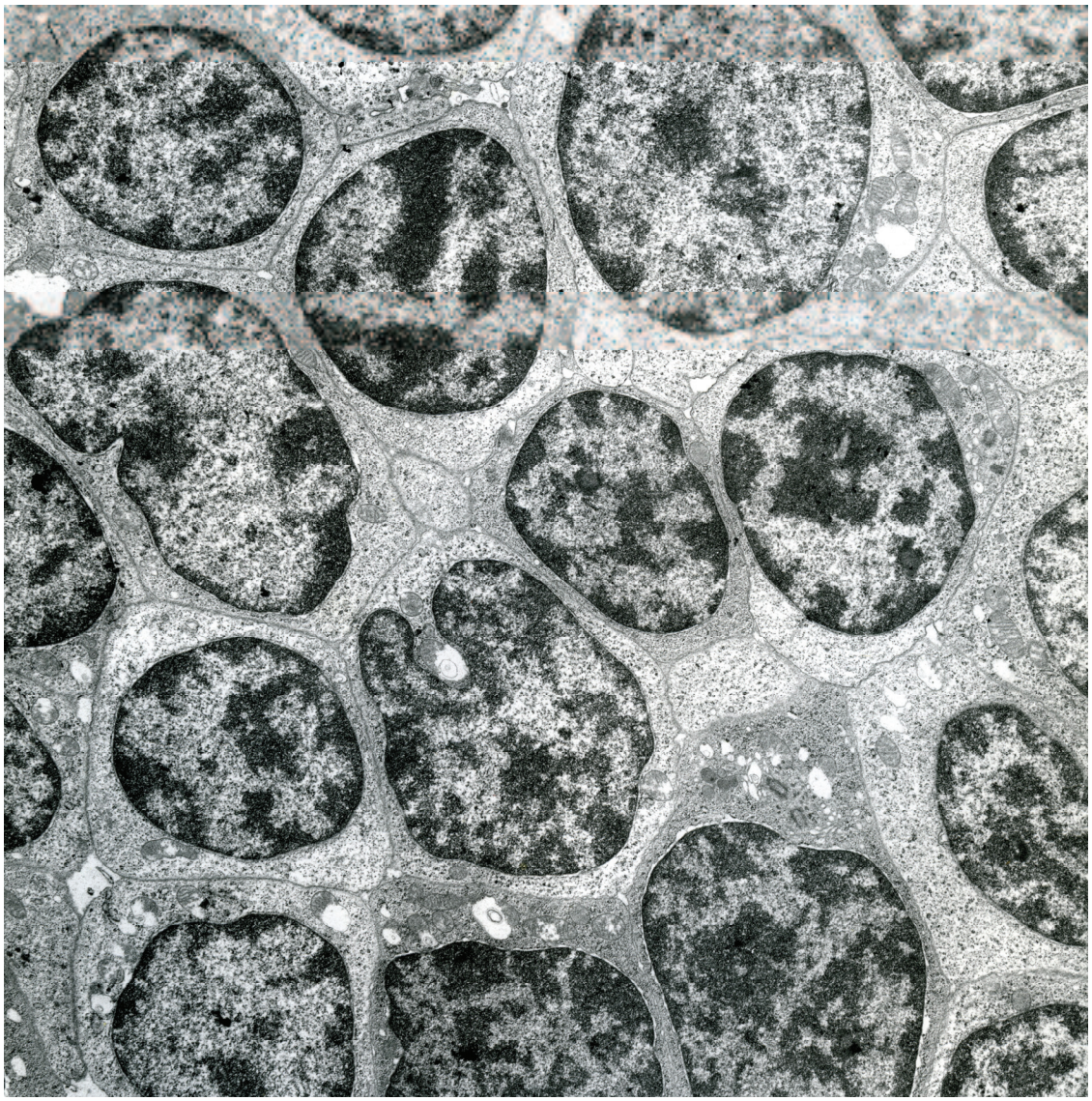

Fig.8. An electron micrograph illustrates a large field of differentiating lymphocytes observed in the central region of an opossum thymus at one week postnatal. TEM X 2,000.

Chapter 28. Blood Cells

Synopsis:

The predominant circulating form of erythrocyte during the first few days of postnatal life is large and nucleated with an elliptic profile of a constant diameter. A few non-nucleated erythrocytes also are seen that are about the same diameter as the nucleated form. Occasional erythrocytes of adult size are present also. The nucleated form of erythrocyte makes up more than 98% of the red cells in the newborn opossum, but these red cells rapidly decrease in number so that non-nucleated erythrocytes predominate by the end of the first postnatal week. The large nucleated erythrocytes disappear following the second postnatal week. As the non-nucleated erythrocytes rapidly increase in number during the first three postnatal weeks their mean diameter decreases by about 25%. During the subsequent eight weeks, erythrocyte diameters remain fairly constant decreasing only by about 10%. It is believed that the large nucleated red cells within the peripheral blood are formed in the blood islands of the yolk sac. The large anucleate erythrocytes present in newborn blood are thought to occur as a result of nuclear loss by some cells in the large nucleated erythrocyte population. The liver is an active hemopoietic organ in the newborn opossum and remains so during the first three weeks of postnatal life. During the first postnatal week the liver is the only source of new erythrocytes as the spleen makes only a minor contribution of erythrocytes at this time. During the time when the total red cell count increases slowly (four to eleven weeks) erythrocyte production is the result of bone marrow hemopoiesis.

Four types of hemoglobin occur in the erythrocytes of the pouch young opossums. Hemoglobins I, II, and IV are found only during the first two weeks of postnatal life. Hemoglobin I occurs only during the first postnatal week. This time corresponds to the time when the large nucleated erythrocytes occur in the circulation. Hemoglobin III is found only after the second postnatal week and is identical to that identified in the adult. The life span of the erythrocyte in the adult opossum is about seventy-seven days.

Circulating leukocytes increase in number from less than $600/mm^3$ at birth to reach a peak forty times this number by the end of the second postnatal week. Leukocytes then decrease in number during the next five weeks. The number of leukocytes then increases with adult numbers being achieved in juvenile animals. Ninety percent of the circulating leukocytes of the newborn opossum are granulocytes and nearly half of these are myelocytes and metamyelocytes. Neutrophils are the most abundant type of granulocyte in both young and adult animals. The increase in total leukocytes during the first two weeks of postnatal life is due primarily to an increase in the number of neutrophils. Eosinophils initially increase in number, then decrease, but remain a considerable proportion of total leukocytes throughout the postnatal period. Basophils also are prominent during the first two postnatal weeks, and then decrease in number and by the seventh week of postnatal life form only a minor proportion of the leukocyte population. Neutrophils and eosinophils show an increase in nuclear lobulation early in the postnatal period. Immature granulocytes have largely disappeared from the peripheral blood by the end of the first postnatal week.

Monocytes are present in the peripheral blood of the newborn, increase slightly in numbers during the first two postnatal weeks, and then are maintained at rather low, but constant numbers throughout development.

Lymphocytes make up less than 4% of all leukocytes in the blood of the newborn opossum. It is only after the third postnatal week that they form a significant number of

circulating leukocytes and become the predominant white blood cell. They continue to increase in number in juvenile and adult opossums. Large lymphocytes are the only lymphoid cells present in newborn peripheral blood and are the predominant form for the first postnatal week. Thereafter they decrease in number and are replaced by medium and then small lymphocytes. Small lymphocytes are absent in the blood of the newborn and do not appear until about the middle of the second week. Thus, the two most striking features of leukocytes in the peripheral blood during development are the early, persistent eosinophilia and the absence of small lymphocytes during the first ten days of postnatal life.

Acknowledgments:

Figs. 2 (bottom left) and 3 (bottom right), courtesy of and from: Cutts, J.H., W.J. Krause, and C.R. Leeson (1980) Changes in erythrocytes of the developing opossum, *Didelphis virginiana*. Blood Cells 6:55-62.

Figs. 2 (top) and 3 (top), courtesy of and from: Krause, W.J. (1998) A review of histogenesis/organogenesis in the developing North American opossum (*Didelphis virginiana*). Adv. Anat. Embryol. Cell Biol. 143 (I): Springer Verlag, Berlin, pp 143.

Figs. 5 (bottom) and 6 (top), courtesy of and from: Paone, D., J.H. Cutts and W.J. Krause (1975) Megakaryocytopoiesis during postnatal development of a marsupial, *Didelphis virginiana*. J. Anat. 120:239-252.

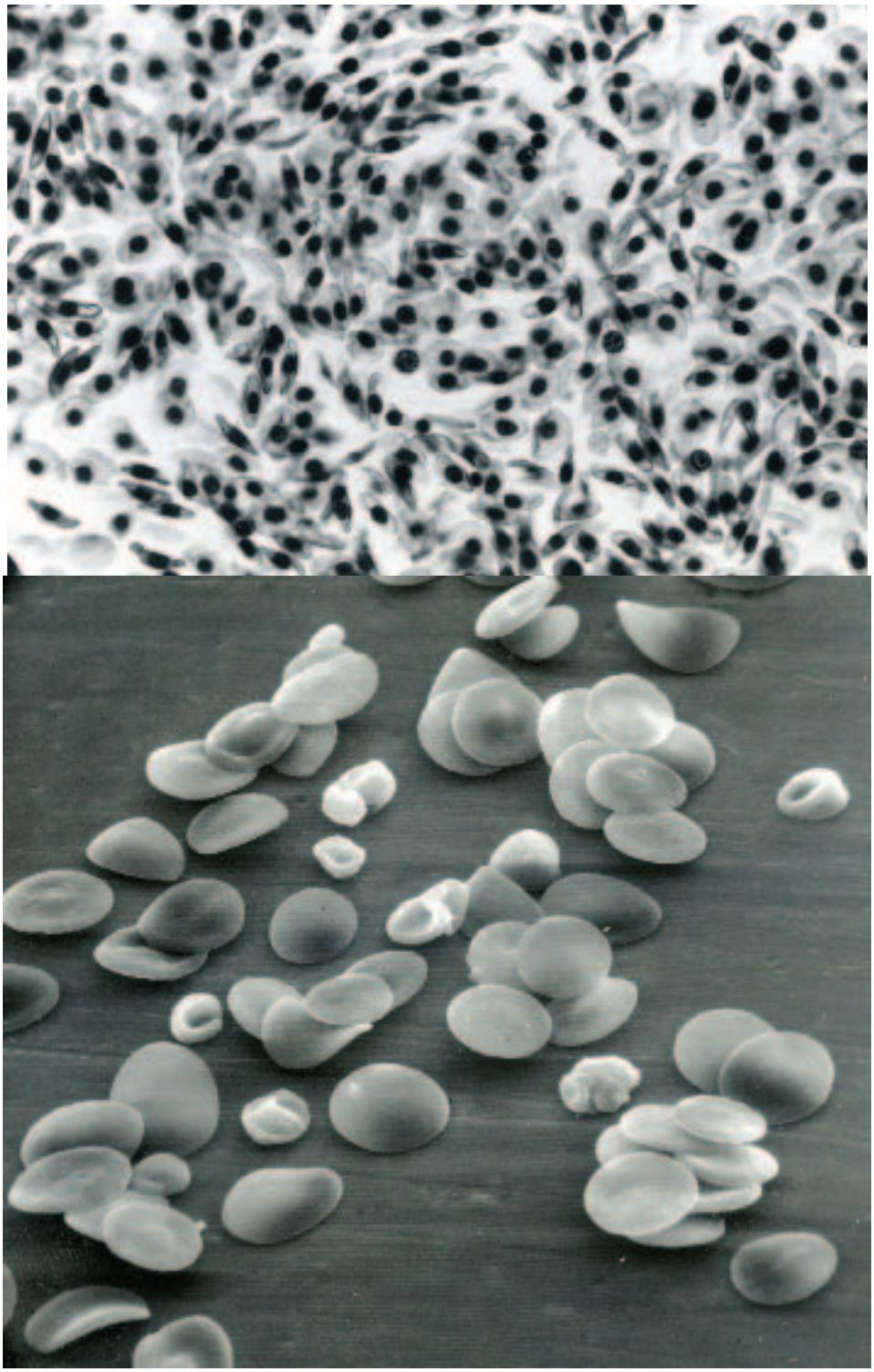

Fig. 1. (*Above*). A histological section through blood in the heart of newborn opossum illustrates that the erythrocytes are nucleated. When viewed in profile erythrocytes appear elliptical in shape whereas when viewed face-on erythrocytes appear disk-like. LM X 300. (*Below*). A scanning electron micrograph of the cells within peripheral blood illustrates the large erythrocytes of a newborn opossum some of which exhibit a central nuclear bulge. Occasional smaller erythrocytes that exhibit a central depression also are observed. SEM X 2,000.

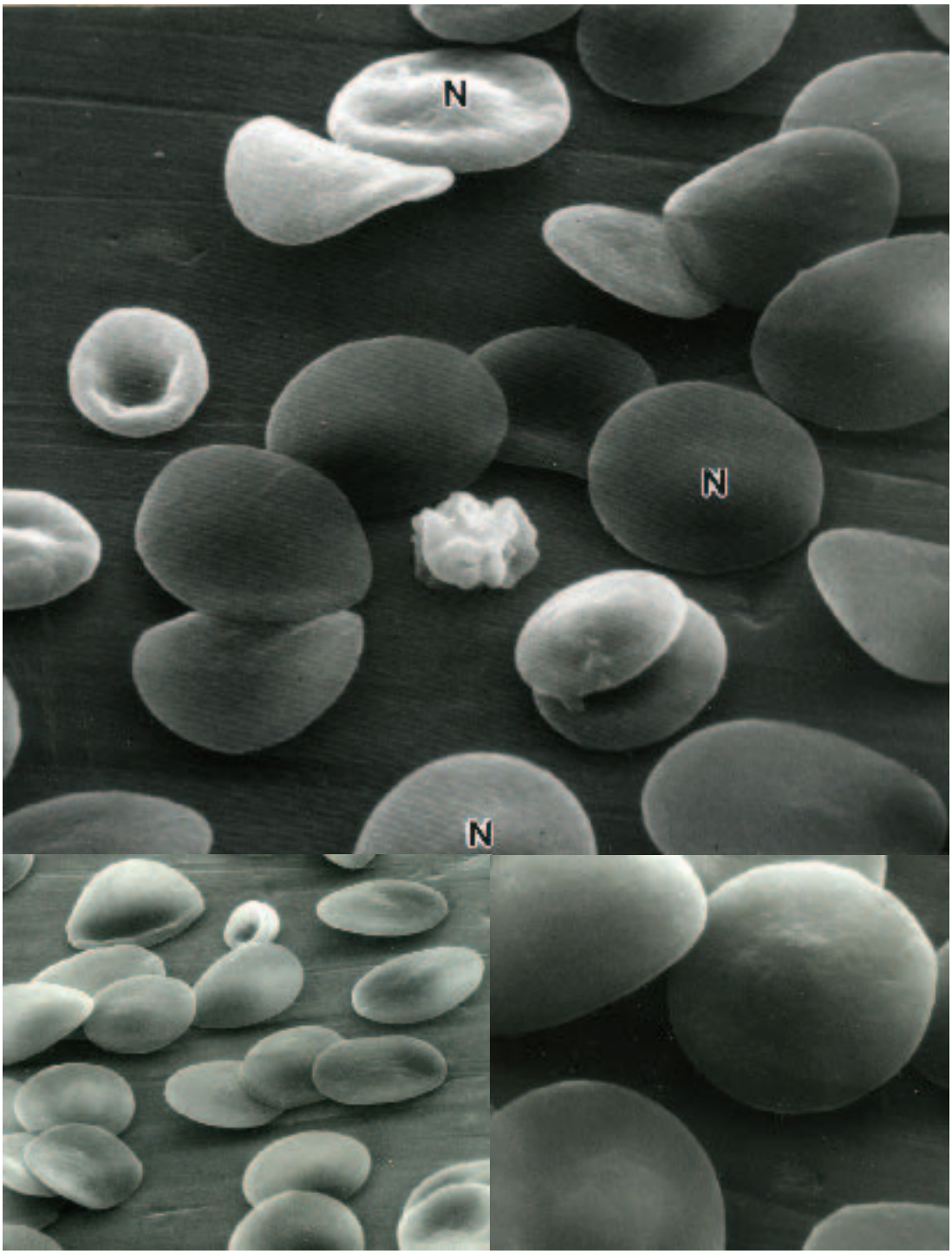

Fig. 2. (*Above*). A scanning electron micrograph of peripheral blood from a newborn opossum illustrates that most erythrocytes appear as large flattened cells with round contours. The majority exhibit a central nuclear bulge (N). Large anucleate forms are seen as well but show no evidence of a central depression. Occasional small erythrocytes are present also. SEM X 4,000. (*Below left*). A micrograph illustrates nucleated and non-nucleated erythrocytes from the peripheral blood of a newborn opossum. A small erythrocyte (a stomatocyte) is shown near top of the micrograph. SEM X 2,000. (*Below right*). Three adjacent nucleated erythrocytes seen at increased magnification. Newborn opossum. SEM X 5,000.

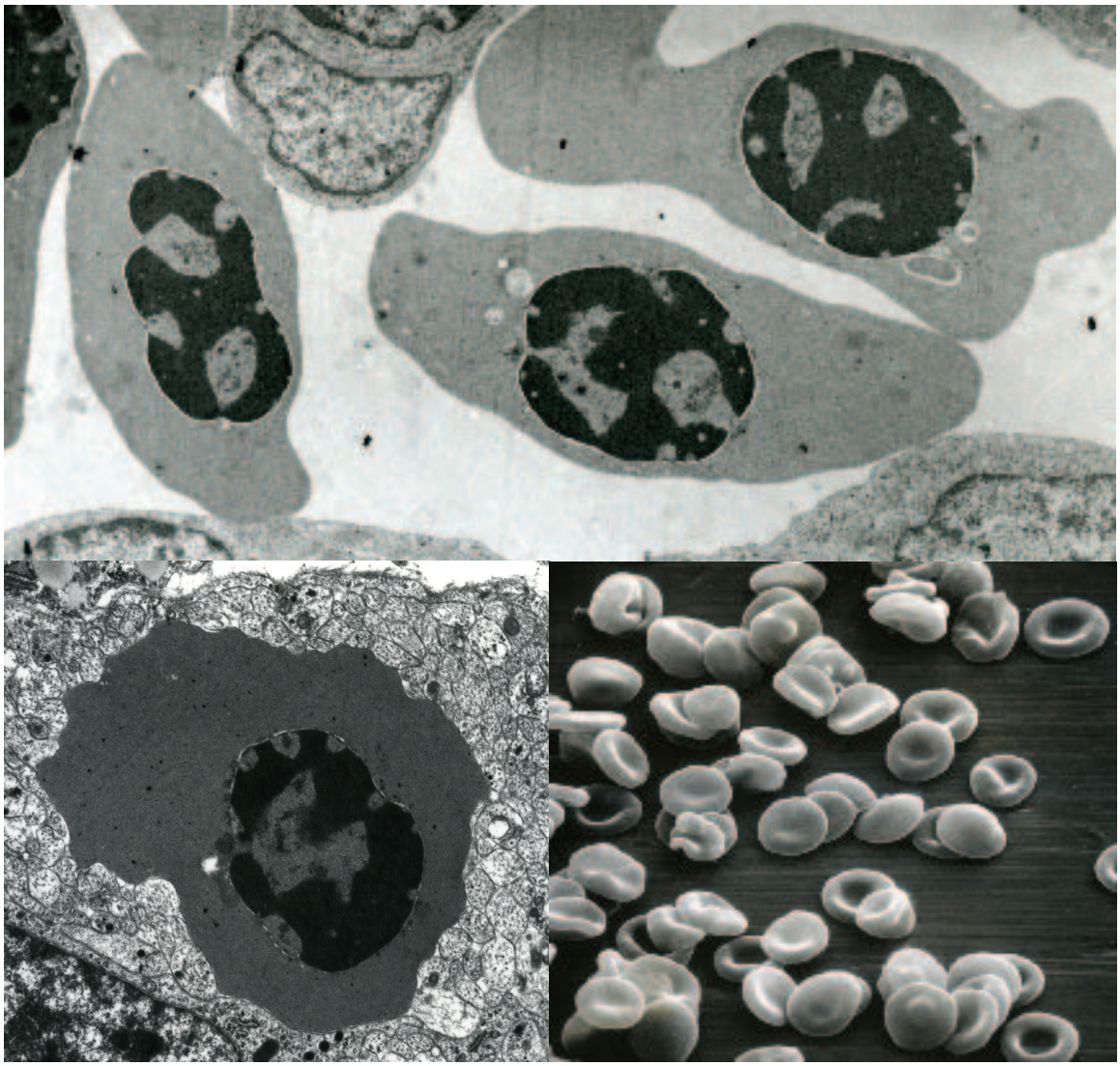

Fig. 3. (*Above*). A transmission electron micrograph through three large nucleated erythrocytes from the peripheral blood of a newborn opossum. TEM X 16,000. (*Below left*). A nucleated erythrocyte within a vessel of newborn opossum thyroid illustrates that few if any organelles occur within the dense, hemoglobin rich cytoplasm. TEM X 16,000. (*Below right*). A sample of peripheral blood from an opossum three weeks postnatal illustrates that the erythrocytes have decreased markedly in size and only a rare nucleated erythrocyte is encountered. SEM X 2,800.

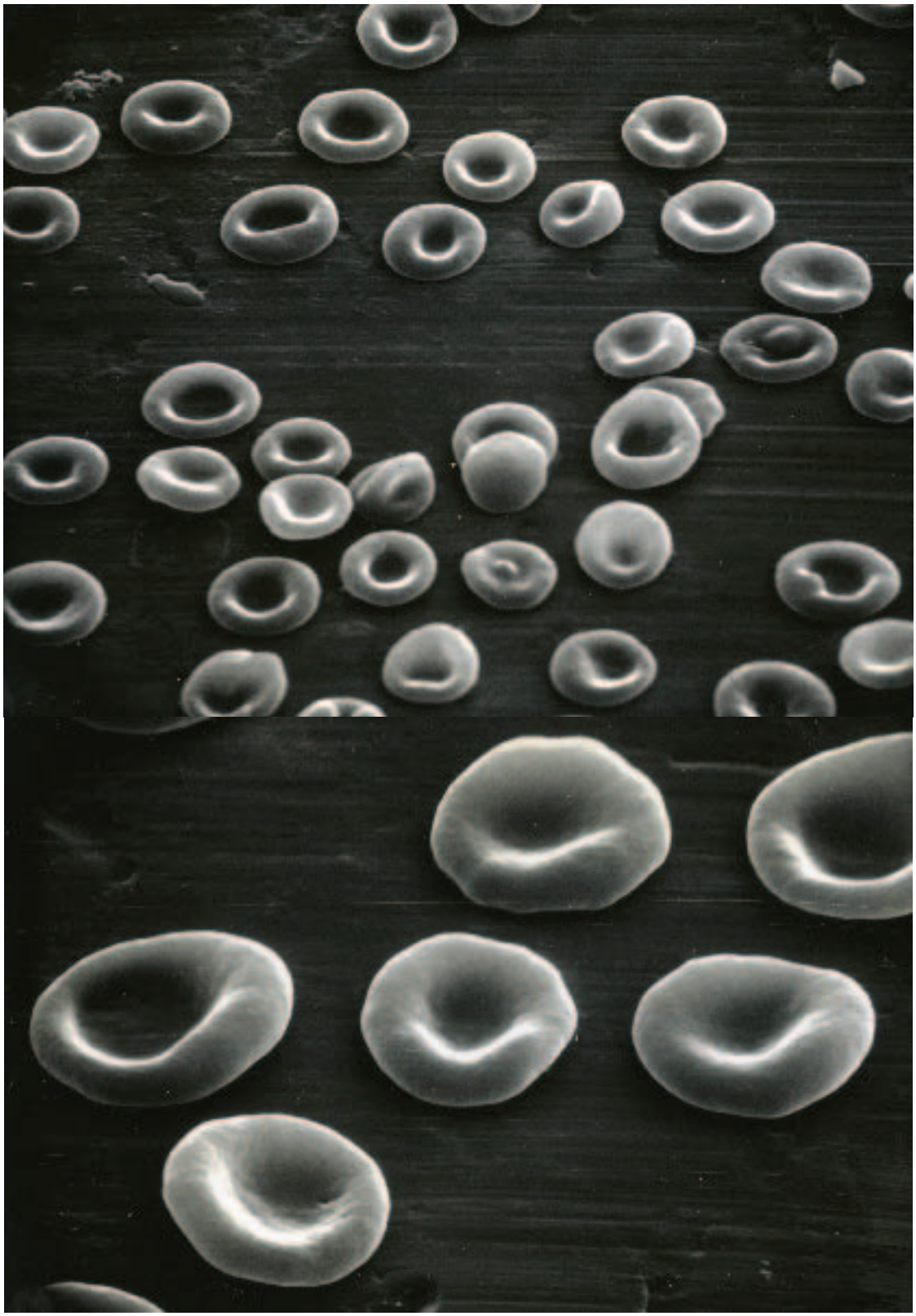

Fig. 4. (*Above*). A micrograph illustrates a field of erythrocytes from the peripheral blood of an opossum four weeks postnatal. SEM X 4,000. (*Below*). Erythrocytes from peripheral blood of an opossum four weeks postnatal viewed at increased magnification. SEM X 10,000.

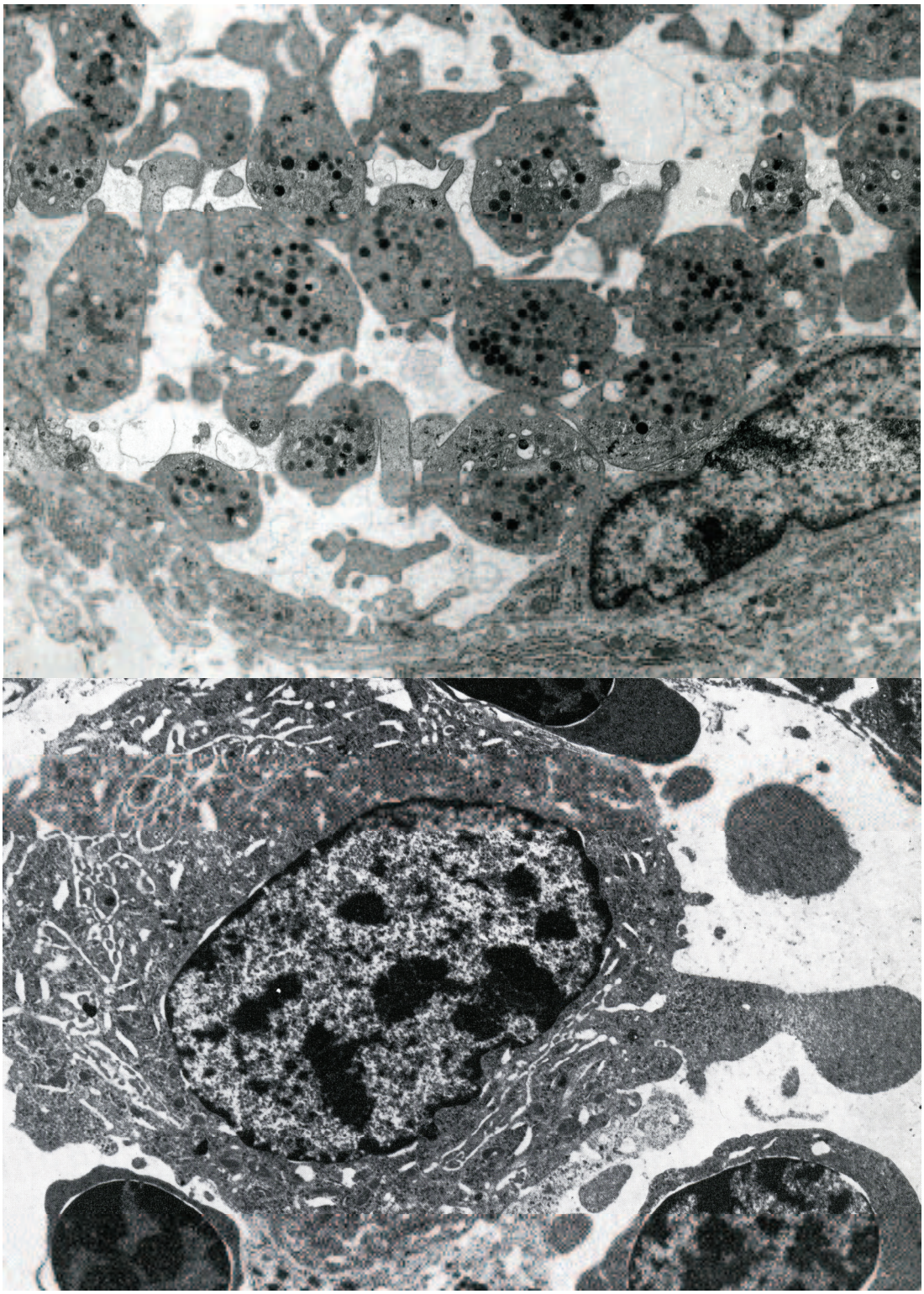

Fig. 5. (*Above*). A field of platelets found within a hepatic blood vessel of a week old opossum. The nucleus of the lining endothelial cell is shown at lower right corner. TEM X 2,500. (*Below*). A hepatic megakaryocyte found within the liver of an opossum one week postnatal. Note the pseudopod extending from this cell and nearby nucleated erythrocytes. TEM X 2,500.

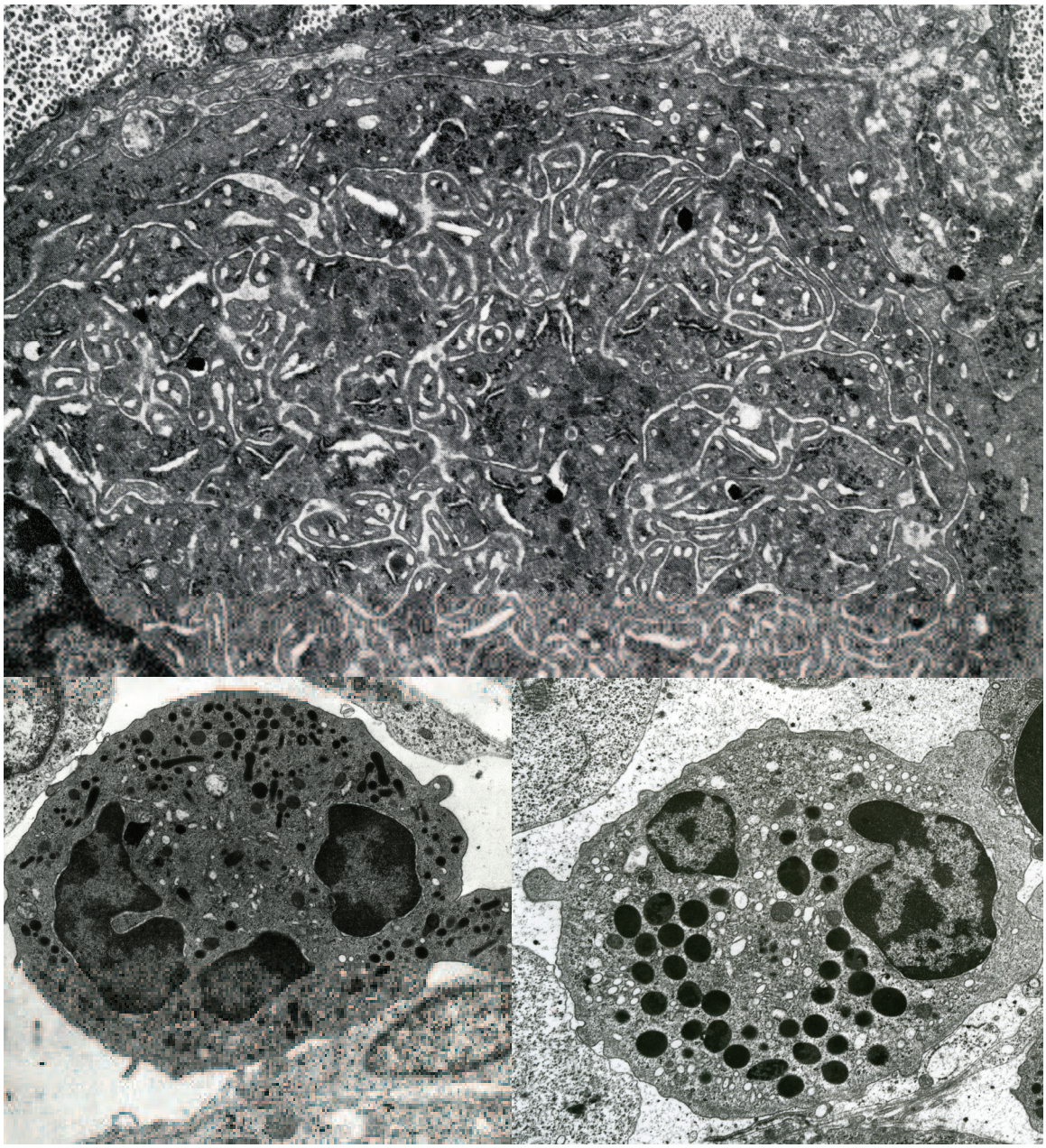

Fig. 6. (*Above*). A region of cytoplasm from a hepatic megakaryocyte illustrates a field of demarcation membranes during platelet formation. TEM X 3,000. (*Below left*). A micrograph illustrates an example of a neutrophil leukocyte taken from the liver of an opossum one week postnatal. The cytoplasm is filled with small, electron dense granules that are irregular in shape. TEM X 2,500. (*Below right*). A micrograph illustrates an example of eosinophil leukocyte taken from the liver of an opossum one week postnatal. Note the large, round cytoplasmic granules some of which show regions of increased electron density. TEM X 2,500.

Chapter 29. Heart

Synopsis:

The provisional heart is first apparent early in prenatal day nine and consists of two separate endothelial lined tubes within the splanchnic mesoderm. They join posteriorly with vitelline vessels from the yolk sac and anteriorly with capillaries coursing through the mandibular mesenchyme. Each hemicardium is a separate tube suspended by a dorsal mesocardium. The paired lateral hemicardia grow forward as development continues and near the head region meet at the midline and fuse into a single median heart. As fusion progresses caudally, the initial region of the endocardium formed is the bulbus cordis. Simultaneously, the vitelline and allantoic veins become confluent to form the sinus venosus. By late in prenatal day nine, the endothelial tubes have fused to form a single, saccular cardiac primordium and the surrounding mesodermal folds merge into a coat of surrounding tissue. With continued organogenesis the endothelial tube will differentiate into the endocardium. The surrounding layer of mesoderm will differentiate into the myocardium and epicardium. Elongation of the single cardiac tube is rapid and because the two ends are anchored to adjacent tissues a cardiac loop is formed. The forming heart twists so that the bulbar region is orientated to the right and the ventricle to the left. The two atria fuse early in prenatal day ten and shortly thereafter the heart begins to beat. Cells covering the external surface of the myocardial coat flatten and together with a differentiating sub-layer of connective tissue form the pericardium. The remainder of the myocardial coat differentiates into an outer compact area of cardiac muscle and an inner region of loosely arranged trabeculae. For much of the postnatal period the myocardium consists of a thin outer compact layer of cardiac muscle and an inner layer of loosely arranged trabeculae. With development the entire myocardial wall becomes more compact except for the trabeculae carnea of the ventricles, which remain as remnants of the spongy network of trabeculae observed earlier in development.

T-tubules are first observed within a few ventricular myocardial cells (two per one hundred cells examined) at the end of the sixth postnatal week. They measure 100-200 nm in diameter and are associated with a basal lamina of moderate electron density. Overall, they appear similar to those observed in other mammals. Myocardial cells are immature in appearance at the beginning of T-tubule formation. The myocardial cells are relatively thin measuring about 5 μM in diameter and contain loosely organized myofibrils. Most myofibrils lie parallel to the long axis of the cardiac myocytes and are separated by columns of mitochondria. Glycogen is scattered throughout the sarcoplasm and the sarcoplasmic reticulum is poorly developed. Invaginations (caveolae) of the sarcolemma also are observed at this time. Intercalated discs occur between myocardial cells at this stage of development and are simple in form. The cardiac myocytes gradually increase in diameter as development continues and by the eleventh postnatal week show characteristics more typical of adult cardiac muscle cells. However, even at this stage of organogenesis only about one tenth of the cardiac myocytes have a well established T-tubule system. The majority of ventricular cardiac muscle cells are fully differentiated by the end of the fifteenth postnatal week. Irregular cylinders of a filamentous material are reported to occur within the sarcoplasm of mature ventricular cardiac muscle cells. They are not bound by membranes and are observed in all orientations with regard to myofibrils.

The differentiation of the cardiac conducting system (sinoatrial node, atrioventricular node, and atrioventricular bundle) occurs gradually in the opossum. Atrioventricular nodal cells, when first apparent, are slightly larger than ordinary cardiac muscle cells. This situation is reversed in the adult due to an increase in size of ordinary atrial and ventricular cardiac myocytes. Although nodal cells remain a constant diameter during development, Purkinje cells increase in size until in the adult they are much larger than ventricular myocardial cells.

Acknowledgments:

Fig.1, courtesy of and taken from: McCrady, E. Jr. (1938) The embryology of the opossum. Am Anat Mem 16: 1-223.

Figs. 2, 3 and 4, courtesy of and taken from: Hirakow, R. and W.J. Krause (1980) Postnatal differentiation of ventricular myocardial cells of the opossum (*Didelphis virginiana* Kerr) and T-tubule formation. Cell Tissue Res 210:95-100.

Figs. 5 and 6 (top), courtesy of and taken from: Leeson, T.S., C.R. Leeson and W.J. Krause (1984) Opossum ventricle: bodies in myocardium. IRSC J Med Sci 12:21-22.

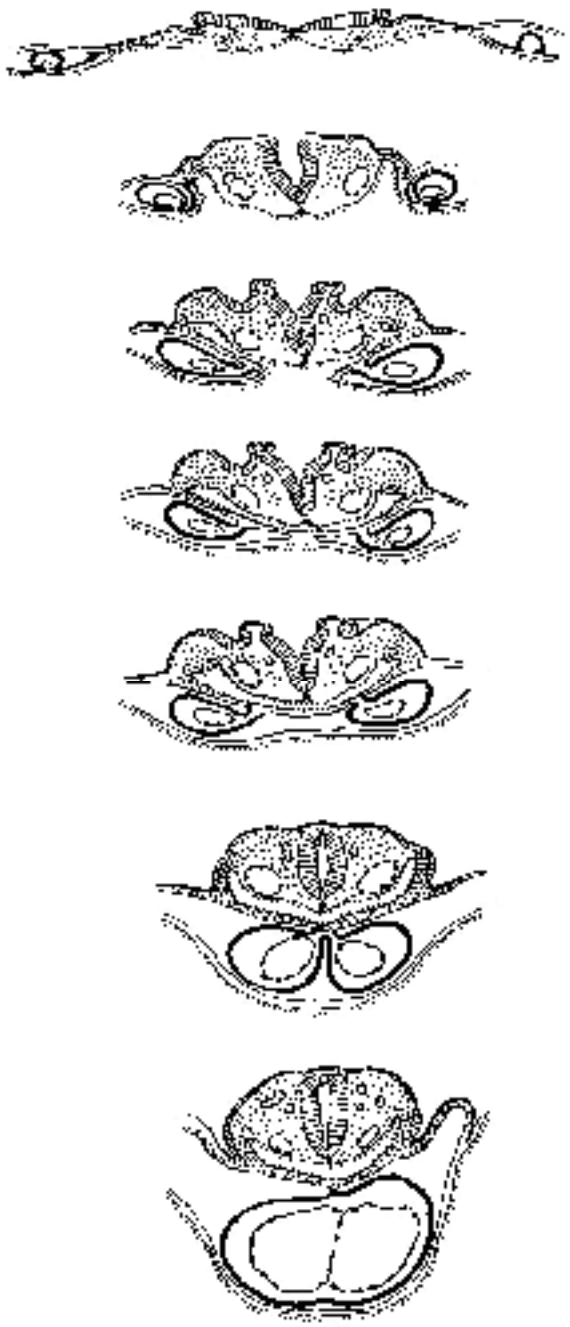

Fig. 1. Line drawings that illustrate the sequence of events that occurs during fusion of the paired hemicardia in the opossum during early embryonic development.

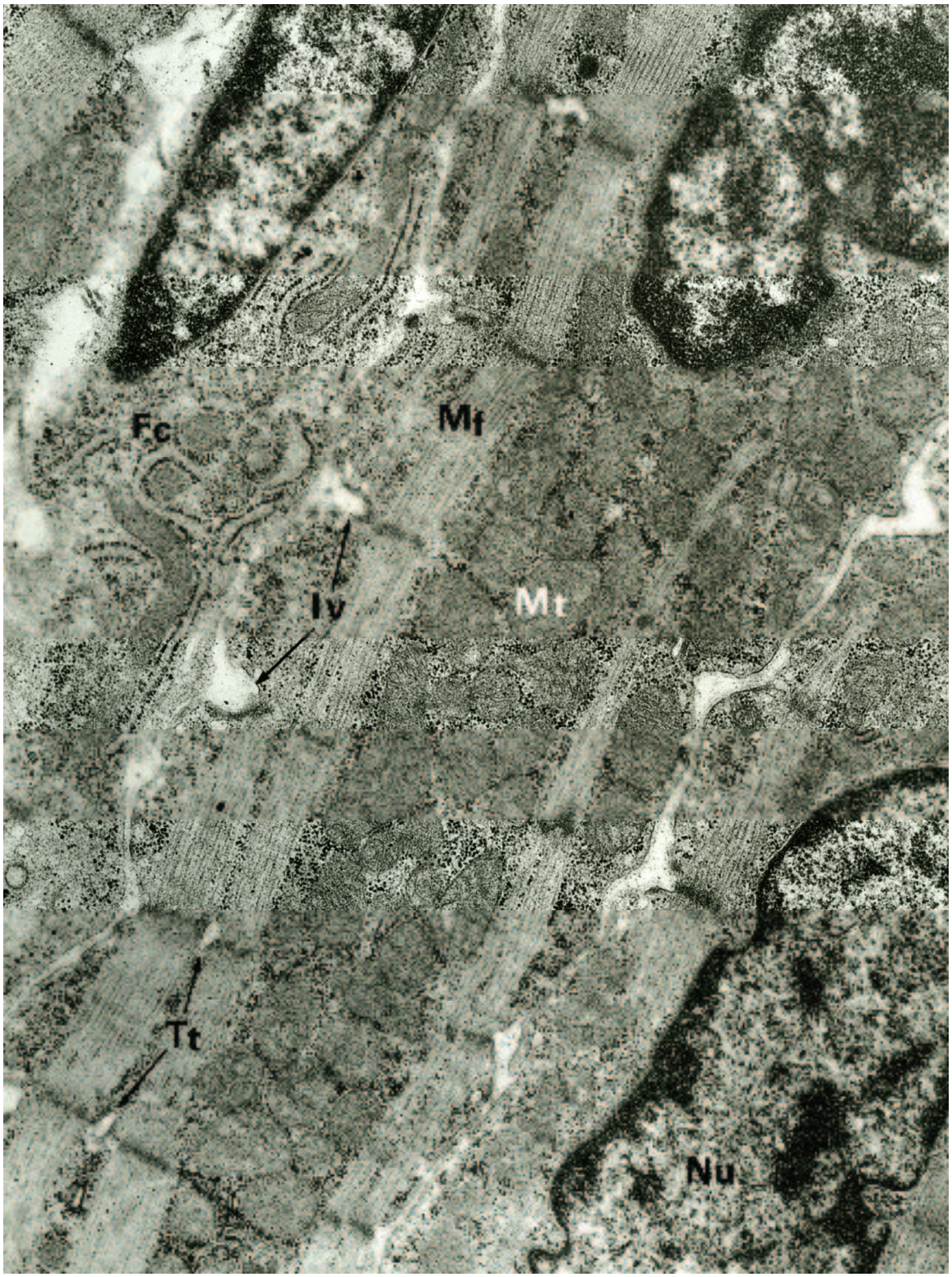

Fig. 2. The ultrastructure of cardiac myocytes from the ventricle of a six-week-old opossum illustrates the presence of sarcolemmal invaginations (Iv), T-tubules (Tt), and numerous mitochondria (Mt) separating forming myofibrils (Mf). The nucleus (Nu) of an adjacent cardiac myocyte is shown at the lower right. A portion of a fibroblast (Fc) is shown at the upper left. TEM X 15,000.

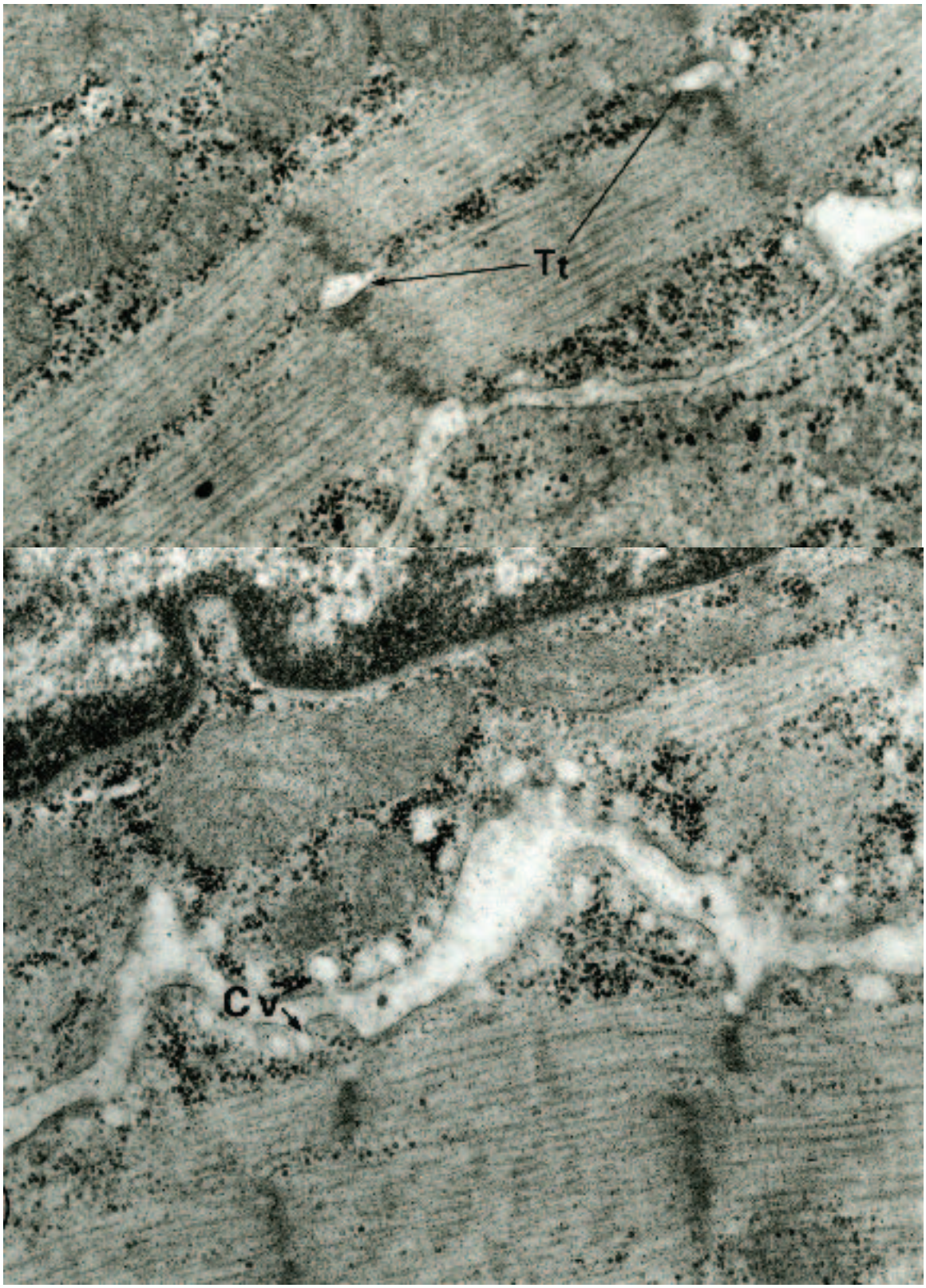

Fig. 3. (*Above*). A region of a ventricular cardiac myocyte from an opossum six weeks postnatal illustrates T-tubules (Tt) at the level of a Z-band of a forming myofibril. Elements of the terminal cisternae lie adjacent to the T-tubules. TEM X 40,000. (*Below*). An electron micrograph illustrates at increased magnification caveolae (Cv) forming from the sarcolemma of a six-week-old opossum cardiac myocyte. Note the forming myofibrils (below) and scattered dense particles of glycogen. TEM X 35,000.

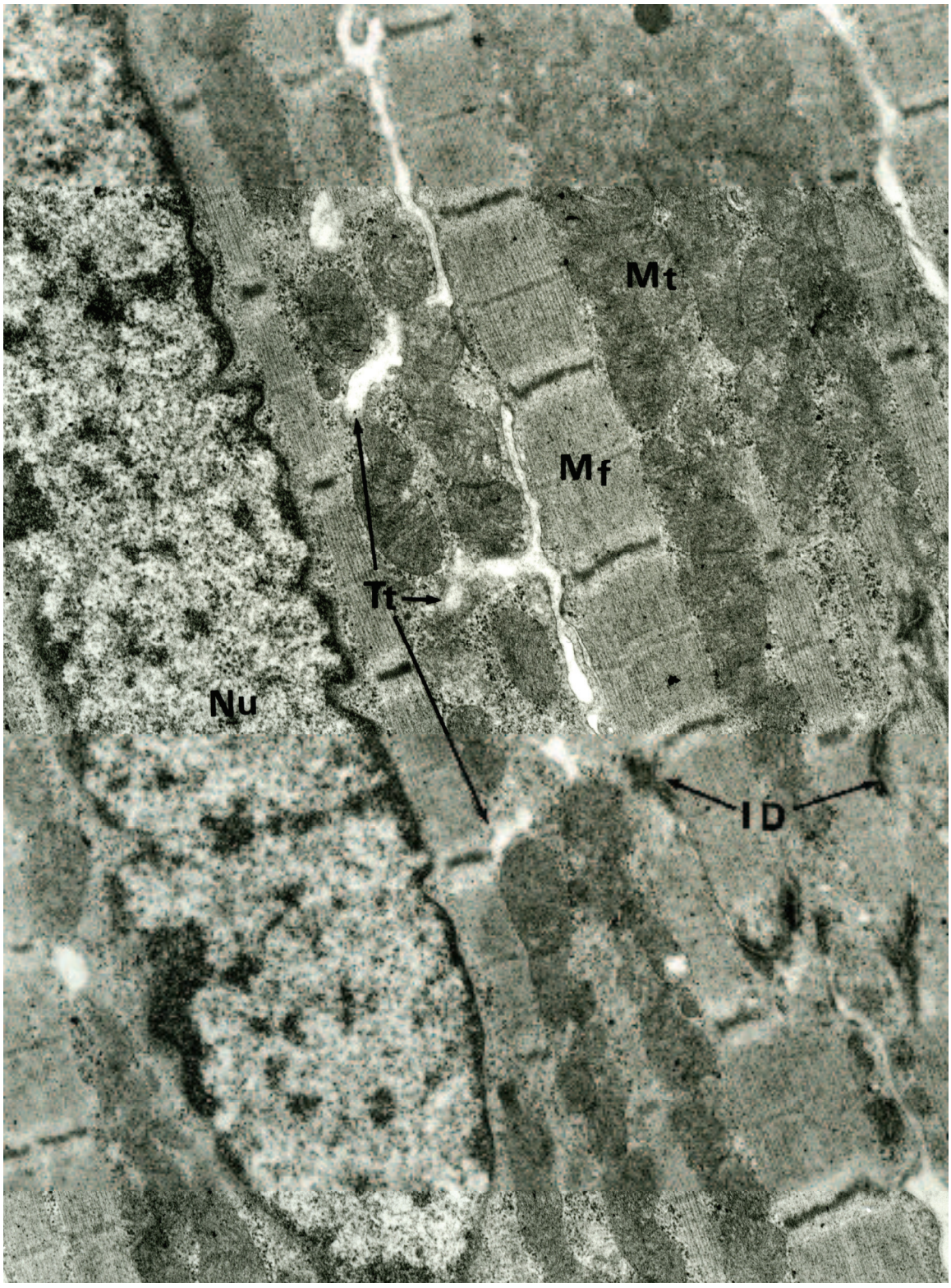

Fig. 4. Ventricular cardiac myocytes from an opossum eleven weeks postnatal illustrate that myofibrils (Mf) are well organized and continue to be separated by numerous mitochondria (Mt). The myocyte to the left exhibits a centrally placed nucleus (Nu) and several profiles of T-tubules (Tt). A well-established intercalated disc (ID) can also be observed. TEM X 15,000.

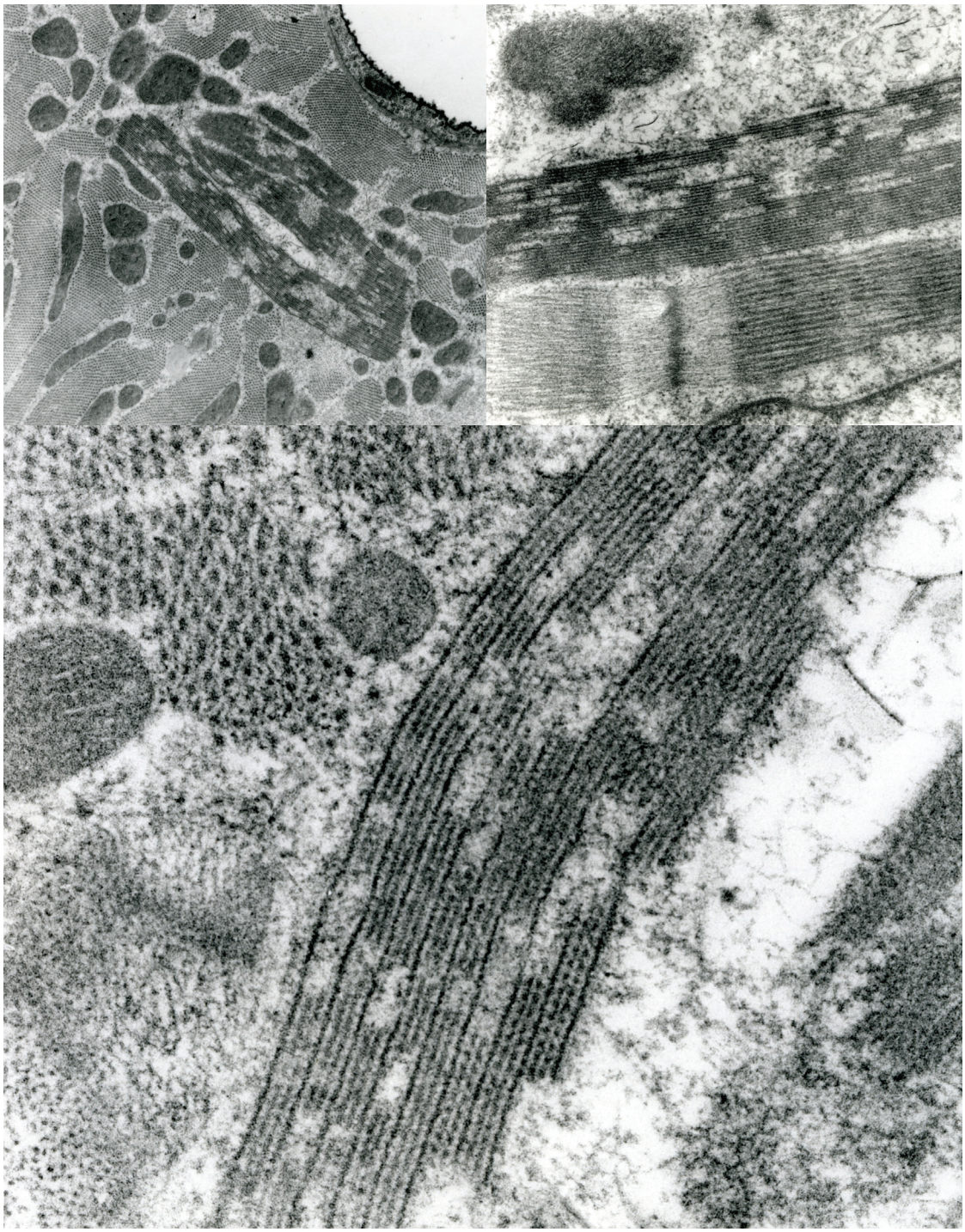

Fig. 5. Transmission electron micrographs illustrate the substructure of several sarcoplasmic bodies from cardiac myocytes within the left ventricle of the adult opossum heart. The sarcoplasmic bodies form irregular cylinders that measure 1 to 2 μM in diameter and range from 1.5 to 8.0 μM in length. Many occur in groups with several cylinders closely apposed. They are found in all orientations with regard to the myofibrils. Although clearly delineated from surrounding structures, the sarcoplasmic bodies lack a limiting membrane. The cylinders appear to be formed by a filamentous material organized in parallel arrays. Some filaments appear complete others have a beaded or interrupted appearance. (*Above left*). TEM X 5,000; (*Above right*). TEM X 15,000; (*Below left*). TEM X 40,000.

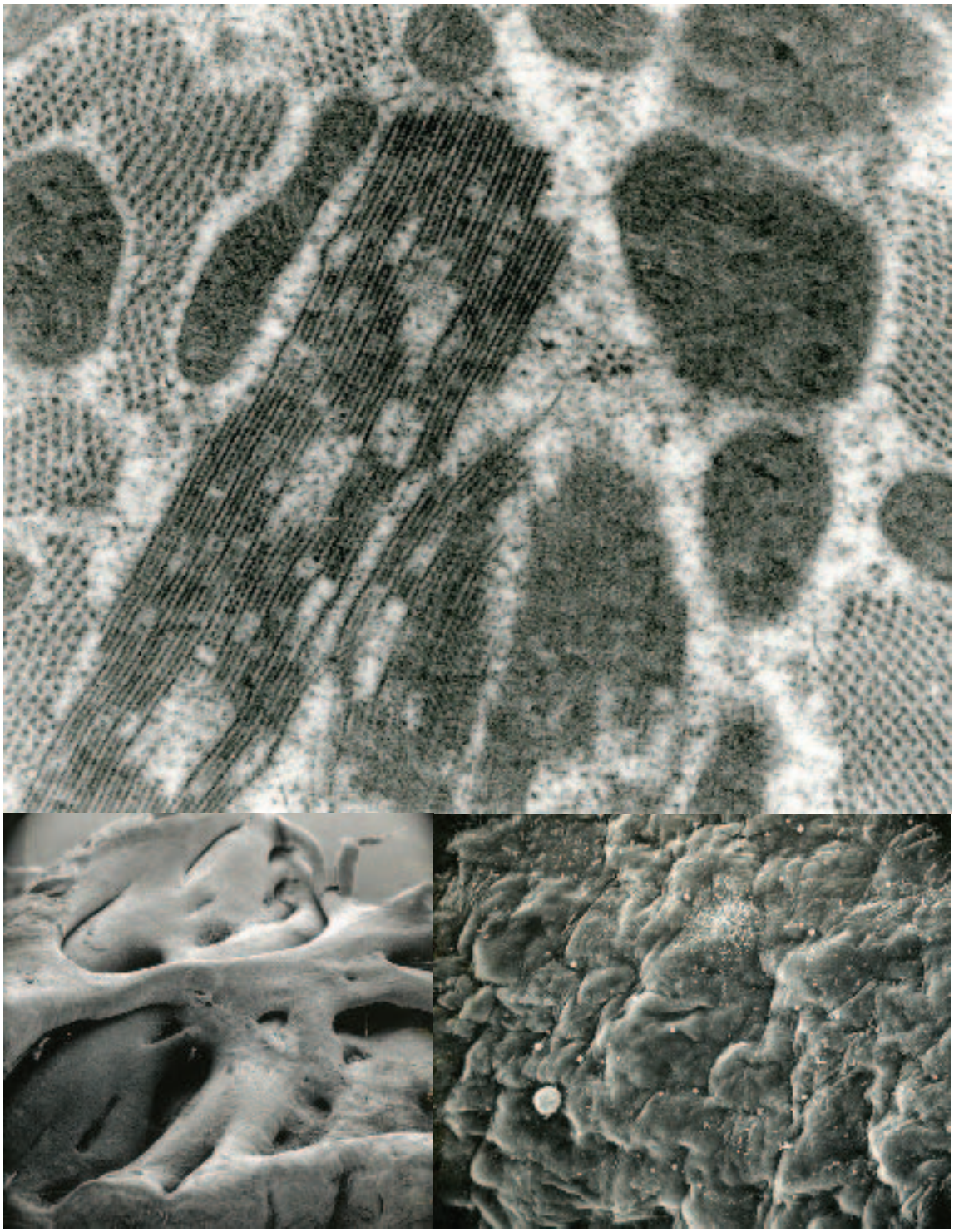

Fig. 6. (*Above*). Sarcoplasmic bodies within an opossum left ventricular myocyte when cut obliquely often present a herringbone appearance. Irregular spaces within the bodies examined are filled by an amorphous granular material. TEM X 35,000. (*Below left*). The interior of a juvenile opossum heart illustrates the trabeculae carnea of a ventricular wall. SEM X 10. (*Below right*). A scanning electron micrograph illustrates the surface features of endothelial cells lining the interior of the left ventricle. Juvenile opossum. SEM X 500.

Chapter 30. Pituitary

Synopsis:

An epithelial lined vesicle derived from Rathke's pouch lies immediately adjacent to the presumptive infundibulum of the opossum diencephalon by the tenth prenatal day. The epithelial wall of the pituitary vesicle is pseudostratified columnar in character and consists of spindle shaped cells. The dorsal wall of the pituitary vesicle remains uniformly thin with continued development and will form the pars intermedia. In contrast, the ventral wall thickens as a result of cellular proliferation and ultimately gives rise to cells that will form the pars distalis of the pituitary. As these events occur, the lumen of the pituitary vesicle is reduced to a flattened, curved cleft at birth but continues to clearly delineate the pars distalis from the pars intermedia. The relationship between the pars distalis, pituitary cleft, pars intermedia and pars nervosa is well established by the end of the second postnatal week and few changes other than size occur during the remainder of pituitary organogenesis. The pars nervosa consists mainly of unmyelinated axons and pituicytes at birth. Electron-dense neurosecretory granules become more abundant within the unmyelinated axons by the end of postnatal week one and are similar in appearance to those described in the adult.

Five cell types (corticotrophs, somatotrophs, lactotrophs, gonadotrophs, and thyrotrophs) are present in the adenohypophysis at birth and corticotrophs, somatotrophs, and lactotrophs can be demonstrated in the pituitary of the eleven-day opossum embryo. By two weeks postnatal the distribution and relative proportions of all five cell types comprising the pars distalis are established. The pars tuberalis is poorly developed in the opossum. Development of both the adenohypophysis and neurohypophysis is substantial during the first two postnatal weeks in the opossum and as a result of differential growth the pars nervosa comes to lie within the center of the pars distalis. These two entities continue to remain separated by the pituitary cleft. The pars intermedia remains a simple epithelial layer about two cells thick. Large, light-staining and small, dark-staining cells as well as scattered granulated cells characterize the epithelium of the pars intermedia by the end of the fifth postnatal week. Cilia may become associated with the large light-staining cells at weaning. The pars intermedia continues to retain its identity as the dorsal wall of the original pituitary vesicle throughout development. Likewise, the ventral wall of the original pituitary vesicle retains its identity as the external wall of the pituitary cleft but is obscured somewhat by the various cell types it shares in common with the pars distalis. Both walls form an epithelial continuum that bounds the space of the pituitary cleft and are limited by a continuous basal lamina.

Acknowledgments:

Figs. 1, 2, 3, 4 (top right and bottom), 5, 6, 7 (top), 8 (bottom), 10 and 12, courtesy of and from: Sherman, D.M. and W.J. Krause. (1990) Morphological, developmental and immunohistochemical observations on the opossum pituitary with emphasis on the pars intermedia. Acta Histochem. 89:37-56.

Figs. 7 (bottom), 8 (top), 9, 11, 13, 14, 15,16 and 17, courtesy of and from: Dunkerley, G.B. and D. M. Sherman, Department of Pathology and Anatomical Sciences, University of Missouri, Columbia, Missouri.

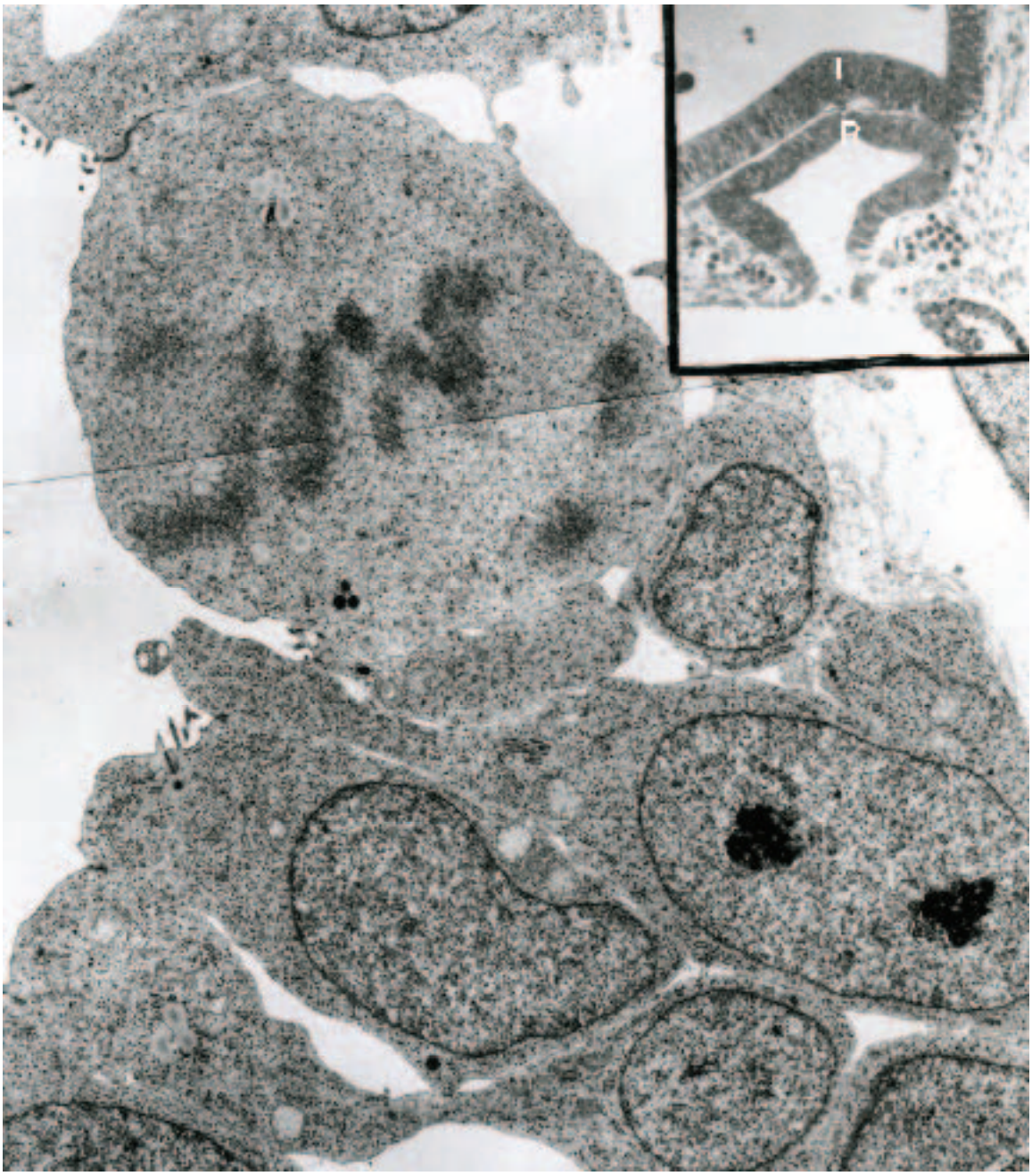

Fig.1. (*Inset*). A section through the region of a developing pituitary illustrates the association between Rathke's pouch (R) and the primordia of the infundibulum (I). The lumen of the oral cavity is shown at the bottom of the photomicrograph. 10.5 day opossum embryo. LM X 250. The epithelial cells of Rathke's pouch are elongated and united at their apices by tight junctions. The epithelial cells lie on a delicate basal lamina and show a definite polarity with the nuclei located in the basal cytoplasm. The cytoplasm is characterized by an abundance of free ribosomes. A mitotic figure is shown within the epithelium of Rathke's pouch at the upper left of the micrograph. 10.5 day opossum embryo. TEM X 7,000.

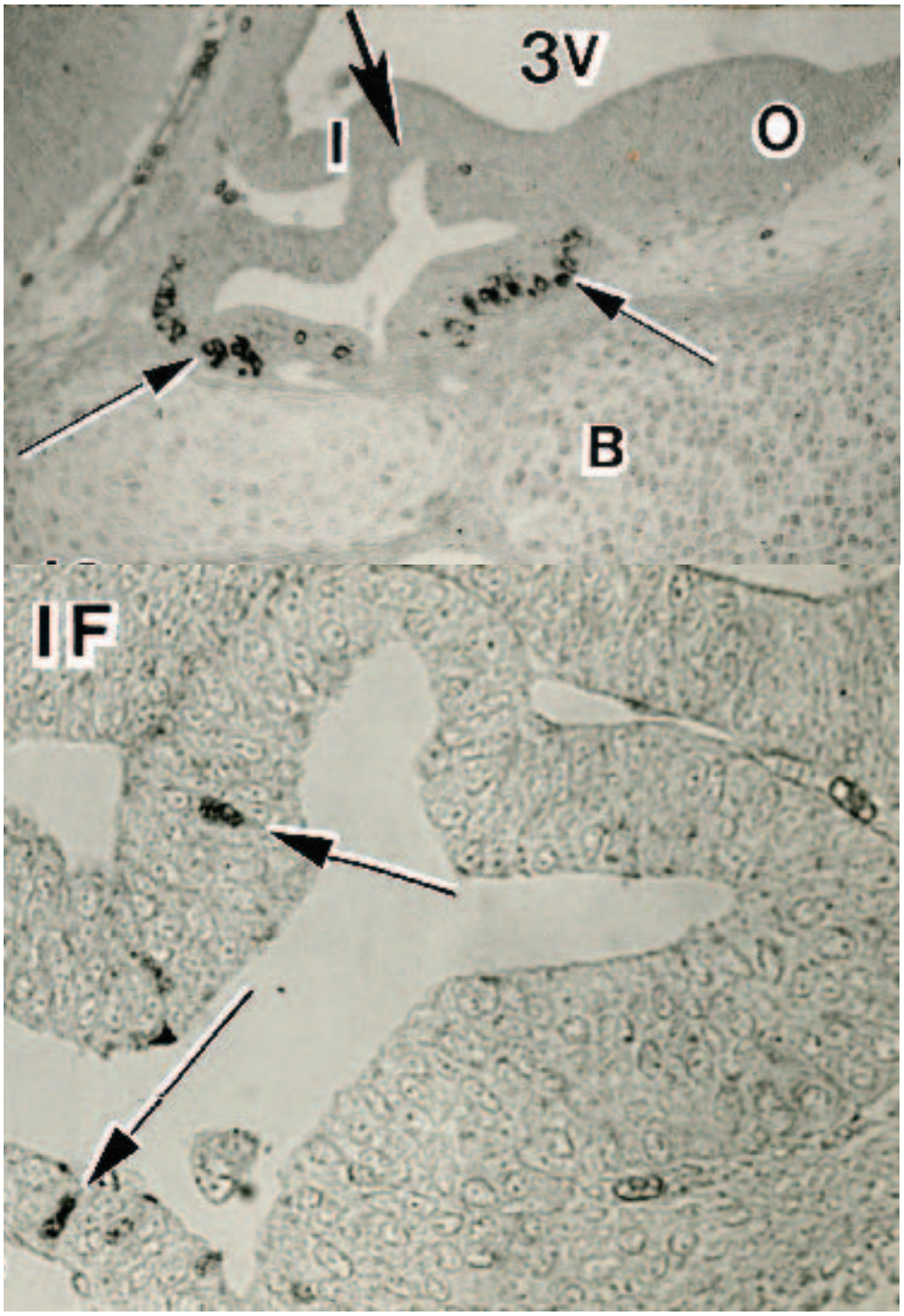

Fig. 2. (*Above*). A section of developing pituitary stained immunohistochemically for ACTH illustrates numerous immunoreactive cells (small arrows). A portion of the third ventricle (3V), infundibulum (I), optic chiasm (O), cartilage of the basisphenoid (B) and the forming pars intermedia (large arrow) also are shown. LM X 200. (*Below*). A region of developing pituitary stained immunohistochemically for somatotropin demonstrates occasional, scattered immunoreactive cells (arrows). A portion of the infundibulum (IF) also is shown. LM X 500. Both illustrations are from an 11.5 day opossum embryo.

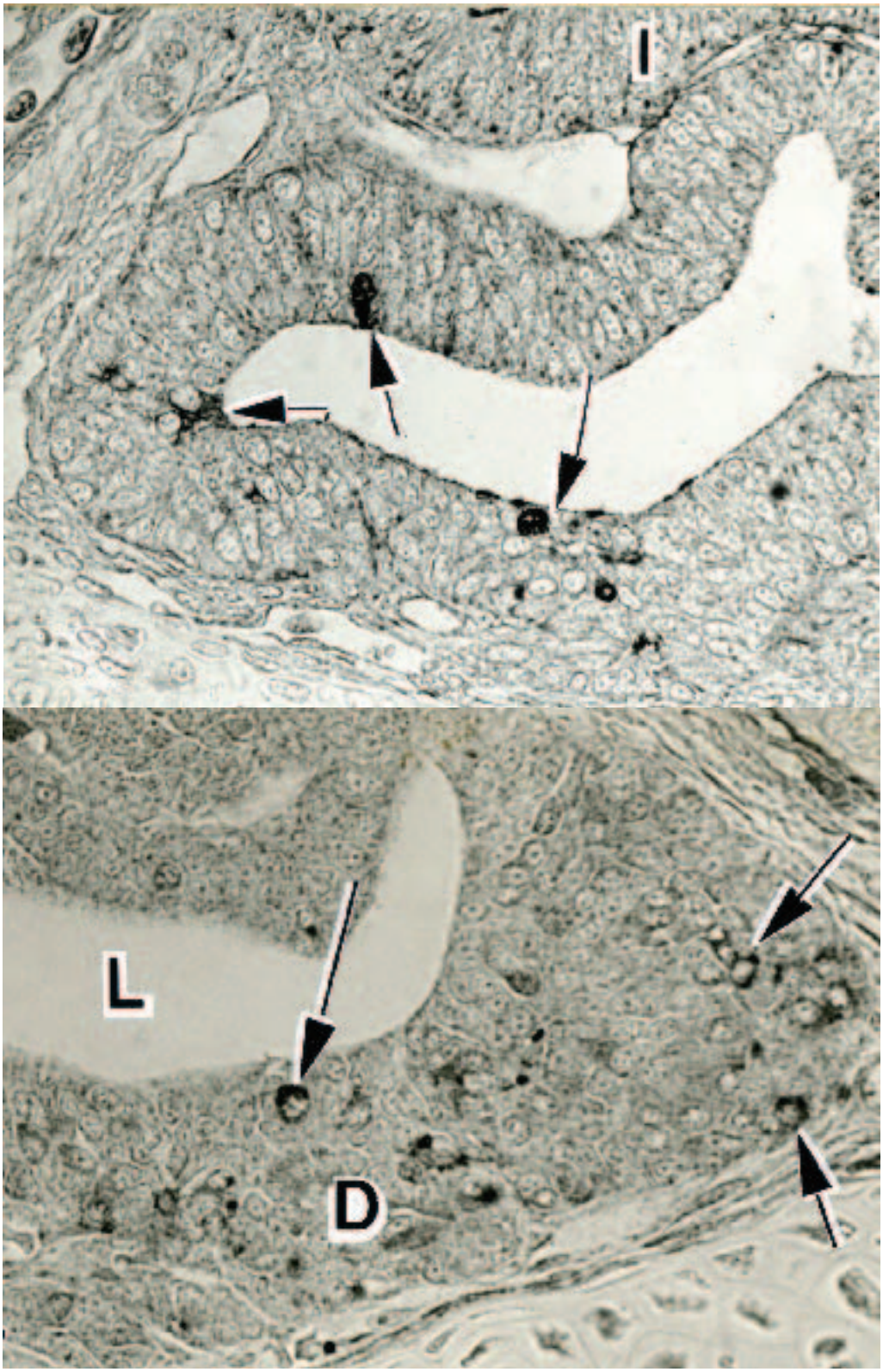

Fig. 3. (*Above*). Developing pituitary stained immunohistochemically for prolactin demonstrates scattered, occasional cells immunoreactive for prolactin (arrows) in the presumptive pars distalis. The infundibulum (I) is to the upper right. 11.5 day opossum embryo. LM X 500. (*Below*). The forming pars distalis (D) stained immunohistochemically for somatotropin demonstrates several immunoreactive cells (arrows). The lumen of the pituitary cleft (L) is shown at left center. Newborn opossum. LM X 500.

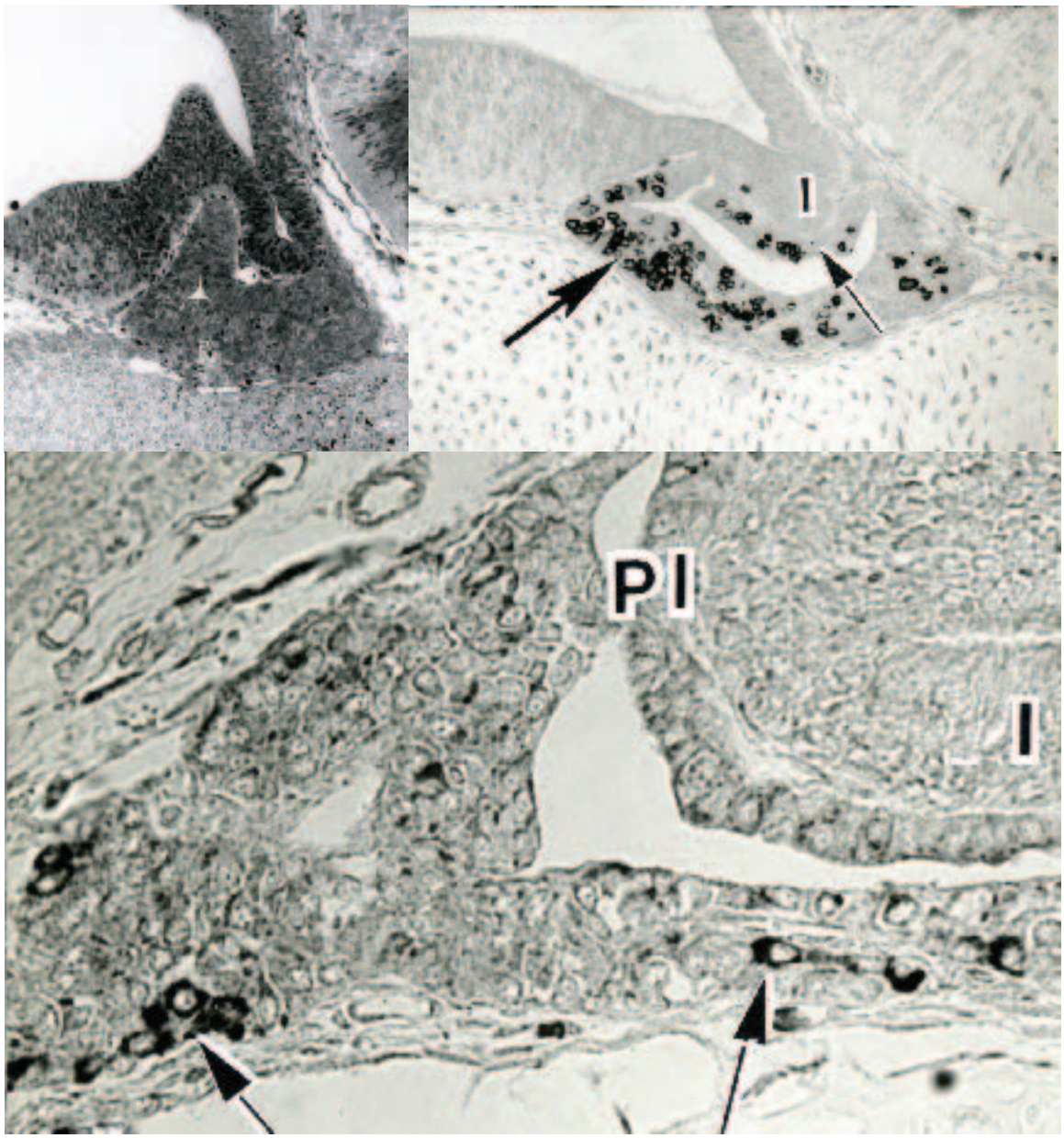

Fig. 4. (*Above left*). The developing pituitary of an opossum examined at one week into the postnatal period. Note the expanding infundibular process into the region of the forming adenohypophysis. The layer of cells immediately adjacent to the infundibular process is the differentiating pars intermedia. LM X 100. (*Above right*). Developing pituitary stained immunohistochemically for ACTH demonstrates numerous immunoreactive cells (large arrow). Note that the definite pars intermedia (small arrow) also contains ACTH-immunoreactive cells and note also its intimate association with the developing infundibular process (I). Opossum one week postnatal. LM X 150. (*Below*). A region of developing pituitary stained immunohistochemically for FSH illustrates only scattered FSH-immunoreactive cells (arrows) in the pars distalis. The nearby infundibulum (I) and pars intermedia (PI) are separated from the pars distalis by the lumen of the pituitary cleft. Opossum one week postnatal. LM X 500.

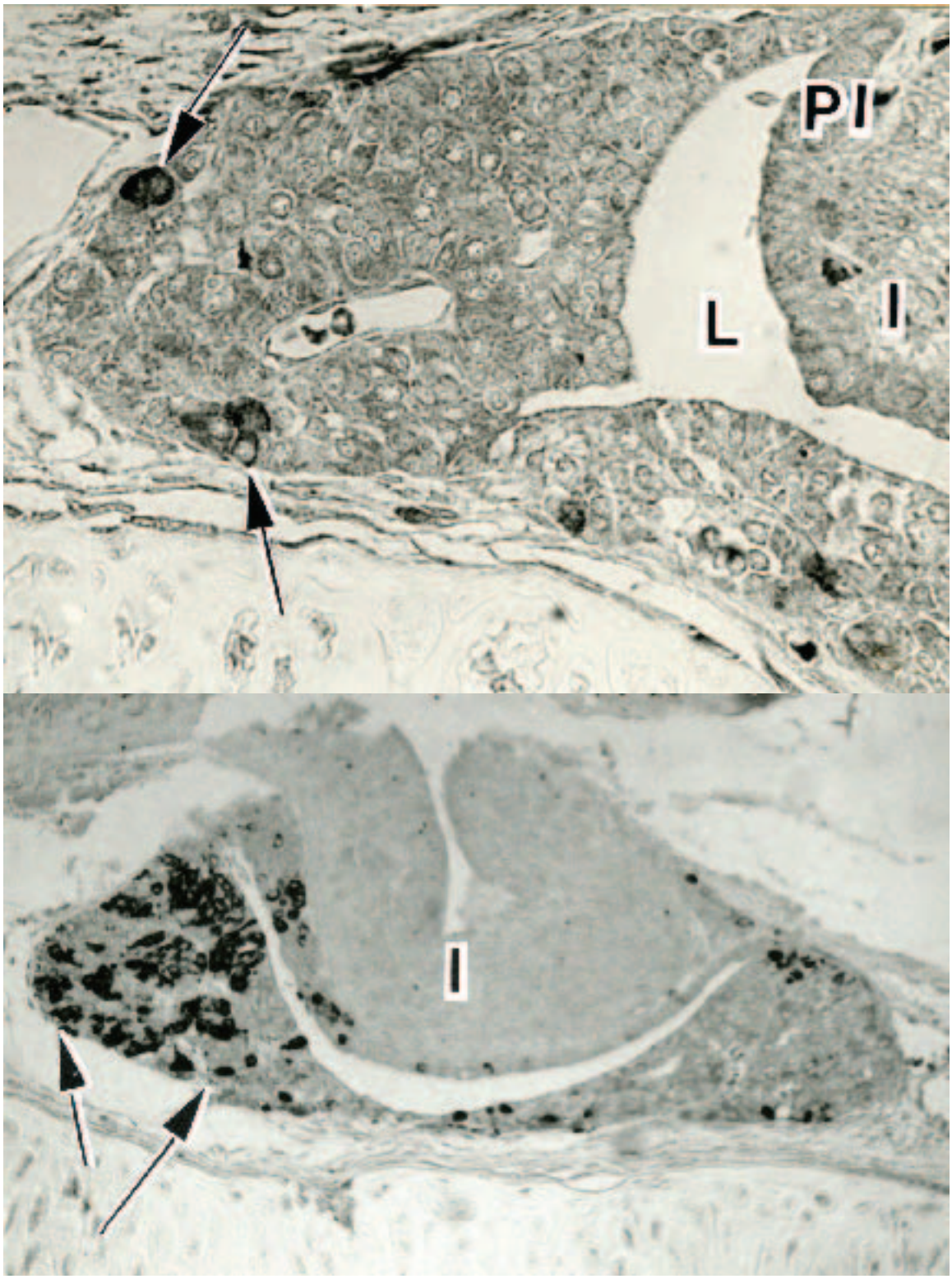

Fig. 5. (*Above*). A region of developing pituitary stained immunohistochemically for luteotropin illustrates scattered LH-immunoreactive cells (arrows) in the pars distalis. The nearby infundibulum (I) and pars intermedia (PI) are separated from the pars distalis by the lumen (L) of the pituitary cleft. Opossum one week postnatal. LM X 500. (*Below*). The pituitary of an opossum two weeks postnatal shows continued growth and expansion. Note that the ACTH-immunoreactive cells shown here continue to be concentrated in the anterior portion of the pars distalis. The infundibular process (I) continues to expand into the center of the developing pituitary. LM X 200.

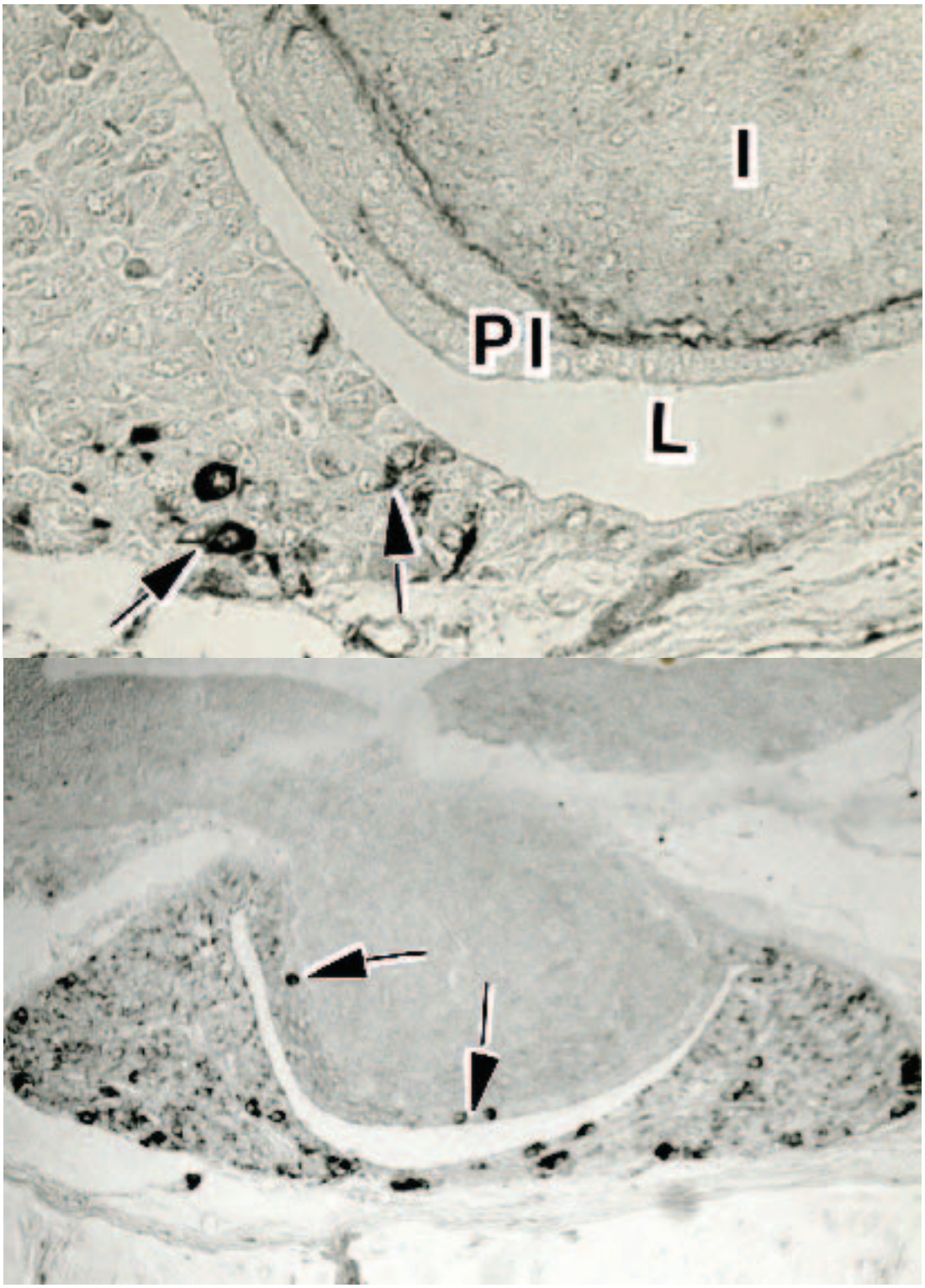

Fig. 6. (*Above*). A region of developing pituitary from an opossum two weeks postnatal stained immunohistochemically for thyrotropin demonstrates only a few, scattered TSH-immunoreactive cells (arrows). Portions of the infundibulum (I), pars intermedia (PI), and lumen of the pituitary cleft (L) also can be observed. LM X 500. (*Below*). An additional section of this specimen stained immunohistochemically to demonstrate luteotropin demonstrates a relatively even distribution of immunoreactive cells throughout the pars distalis. Note the LH-immunoreactive cells (arrows) demonstrated within the pars intermedia. LM X 200.

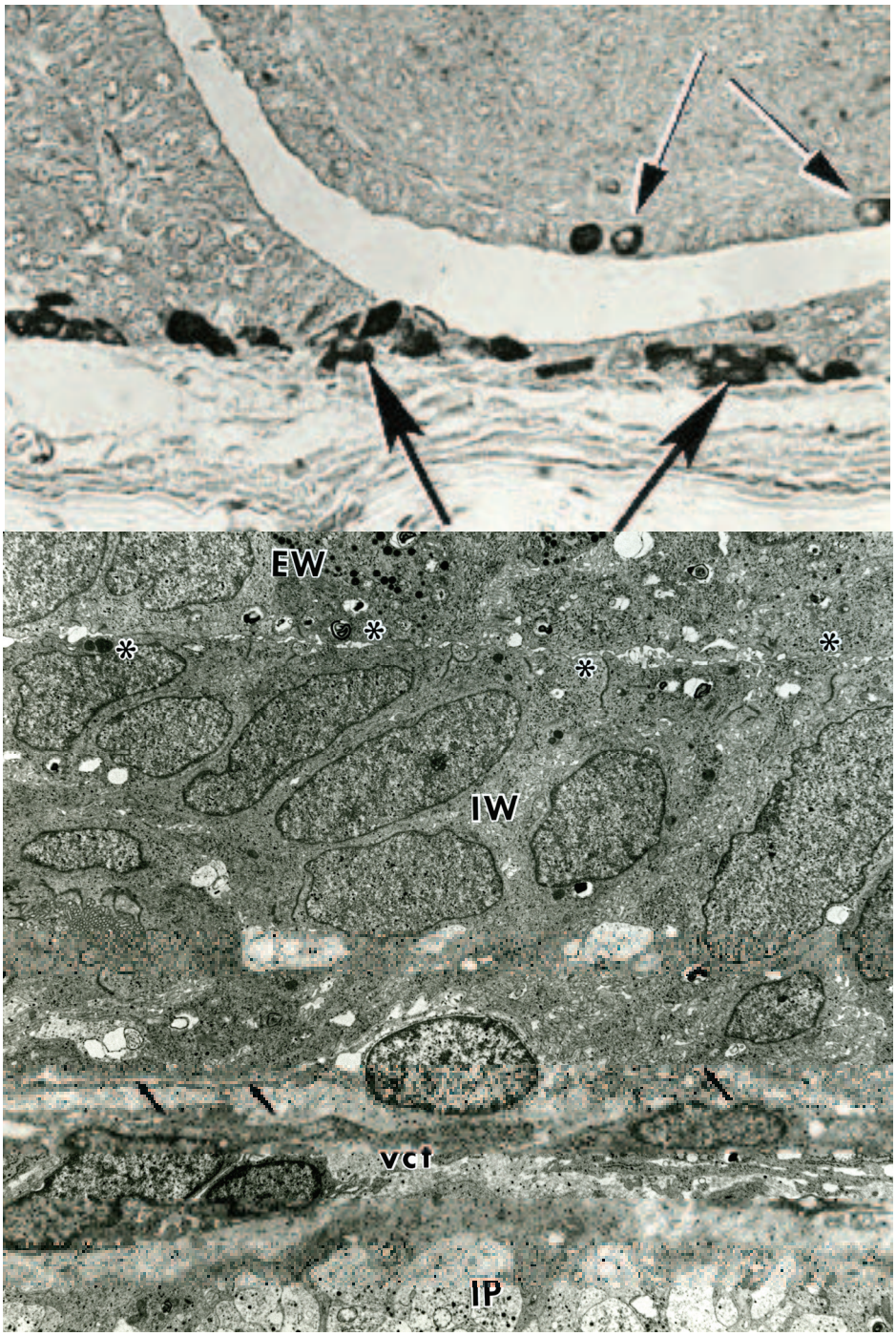

Fig. 7. (*Above*). A region of developing pituitary from an opossum two weeks postnatal stained immunohistochemically for FSH demonstrates several FSH-immunoreactive cells (large arrows) in the narrow region between the larger anterior and posterior portions of the pars distalis. Note that three FSH-immunoreactive cells also are demonstrated within the par intermedia (small arrows). LM X 500. (*Below*). Epithelial cells comprising the internal wall (IW) of the pituitary cleft (pars intermedia) are columnar in shape and appear largely undifferentiated in the two-week postnatal opossum. The cells lie on a distinct basal lamina (arrows) that separates them from the underlying vascular connective tissue (vct), which envelops the infundibular process (IP). Junctional complexes (asterisks) unite the cell apices that border the pituitary cleft of both the external (EW) and internal (IW) walls. TEM X 1,500.

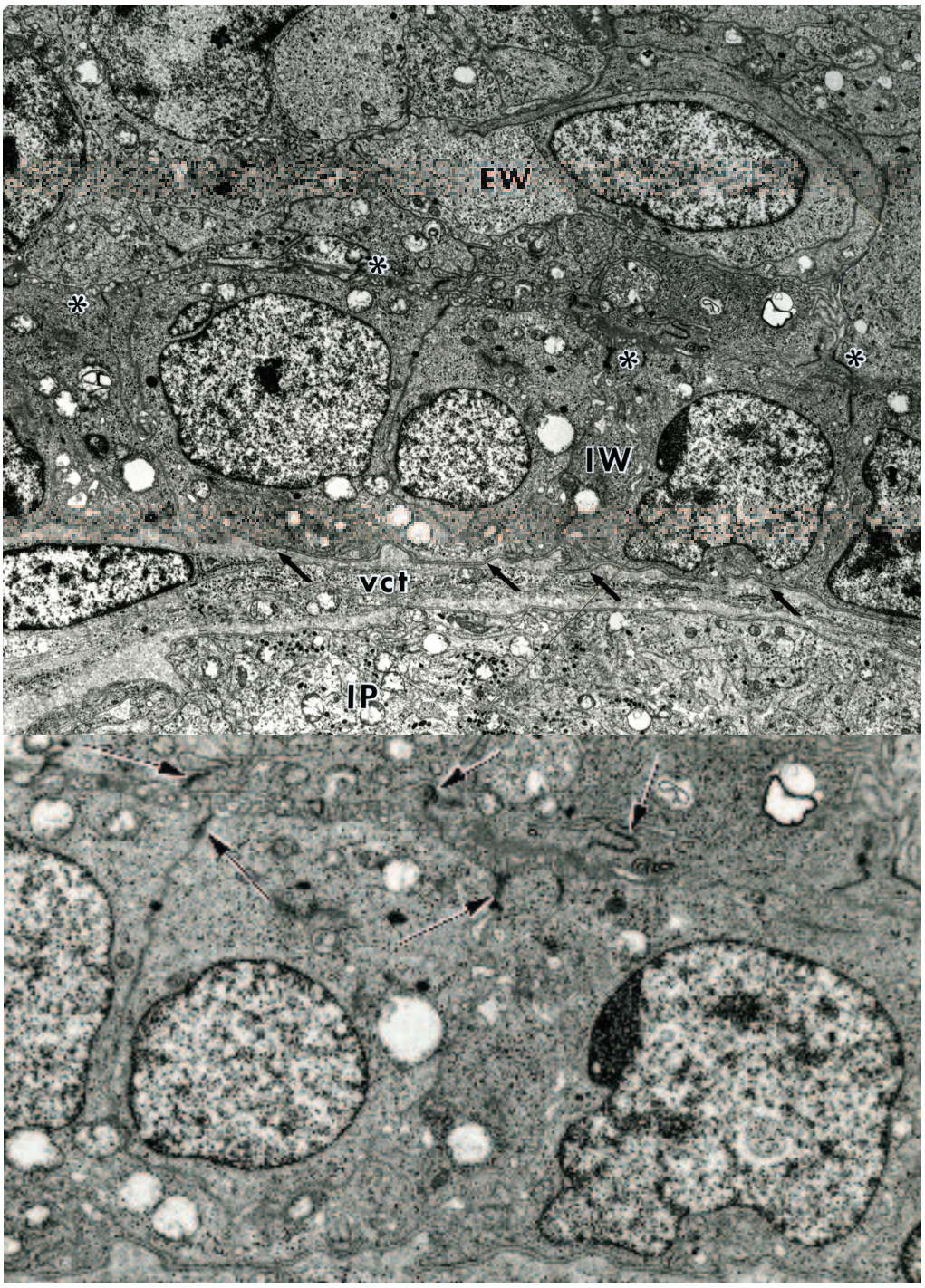

Fig. 8. (*Above*). A region of the pituitary cleft from an opossum five weeks postnatal illustrates both it's the external wall (EW) and internal wall (IW). A well-developed basal lamina (arrows) continues to separate the epithelial cells from the vascularized connective tissue (vct) surrounding the infundibular process (IP). Junctional complexes unite the cell apices that border the pituitary cleft (asterisks). TEM X 1,600. (*Below*). Three columnar cells from the internal wall of the pituitary cleft (pars intermedia) seen at increased magnification illustrate the tight junctions between these epithelial cells as well as those uniting the apices of epithelial cells forming the external wall of the pituitary cleft (arrows). The pituitary cleft is narrow and contains a dense staining, colloid appearing material. Note the prominent basal lamina underlying the epithelial cells forming the internal wall of the pituitary cleft. Opossum five weeks postnatal. TEM X 5,000.

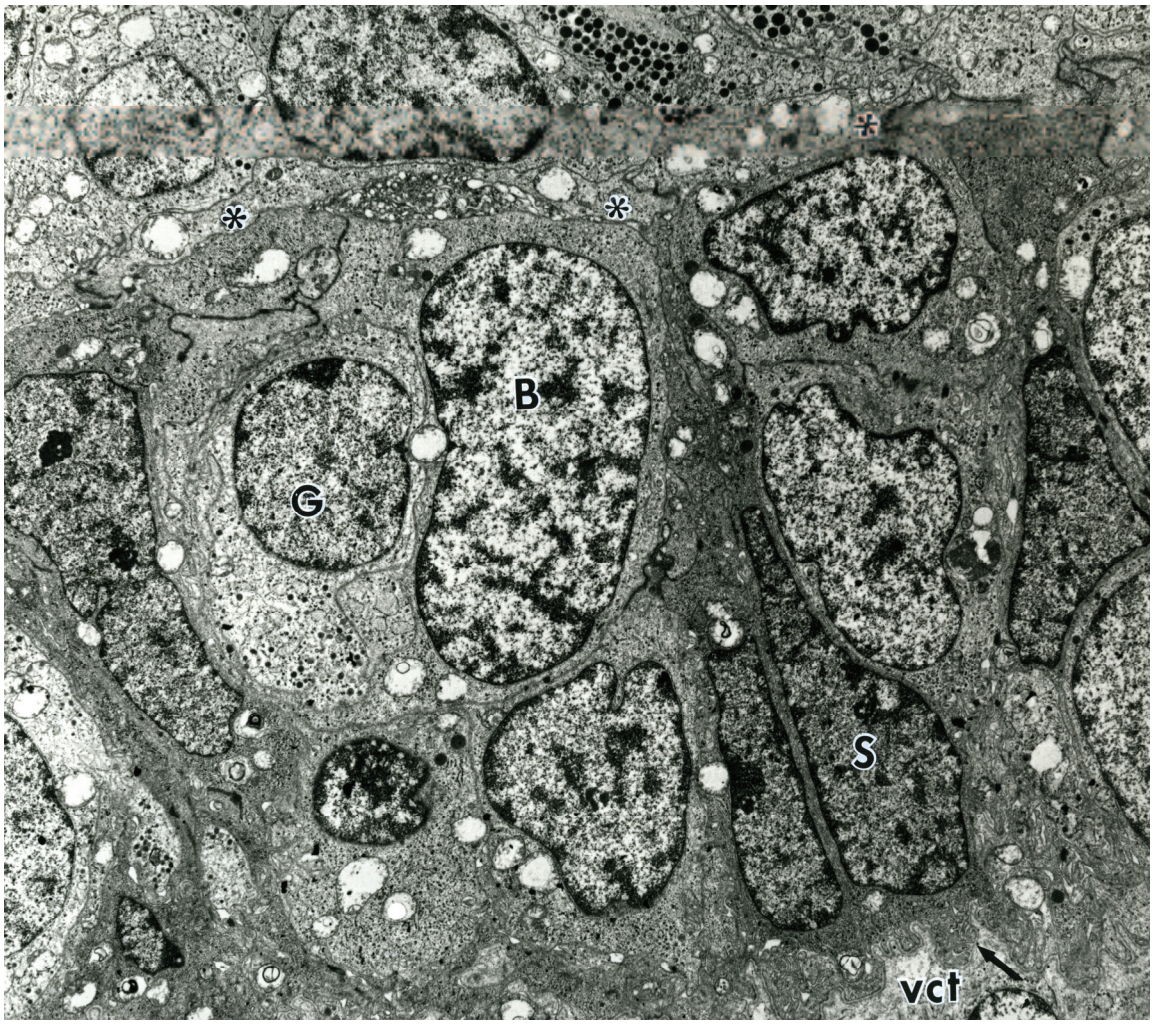

Fig. 9. A segment of the internal wall lining the pituitary cleft (pars intermedia) illustrates the appearance of three different cell types observed in the adult. Differentiating granular cells (G), bulbus cells (B), and spindle cells (S) are observed. Junctional complexes (asterisks) unite the apices of these cells adjacent to the pituitary cleft as well as the apices of cells forming the external wall of the pituitary cleft. A well-defined basal lamina (arrow) continues to separate the epithelium forming the internal wall of the pituitary cleft from the vascularized connective tissue (vct) associated with the infundibular process. TEM X 3000.

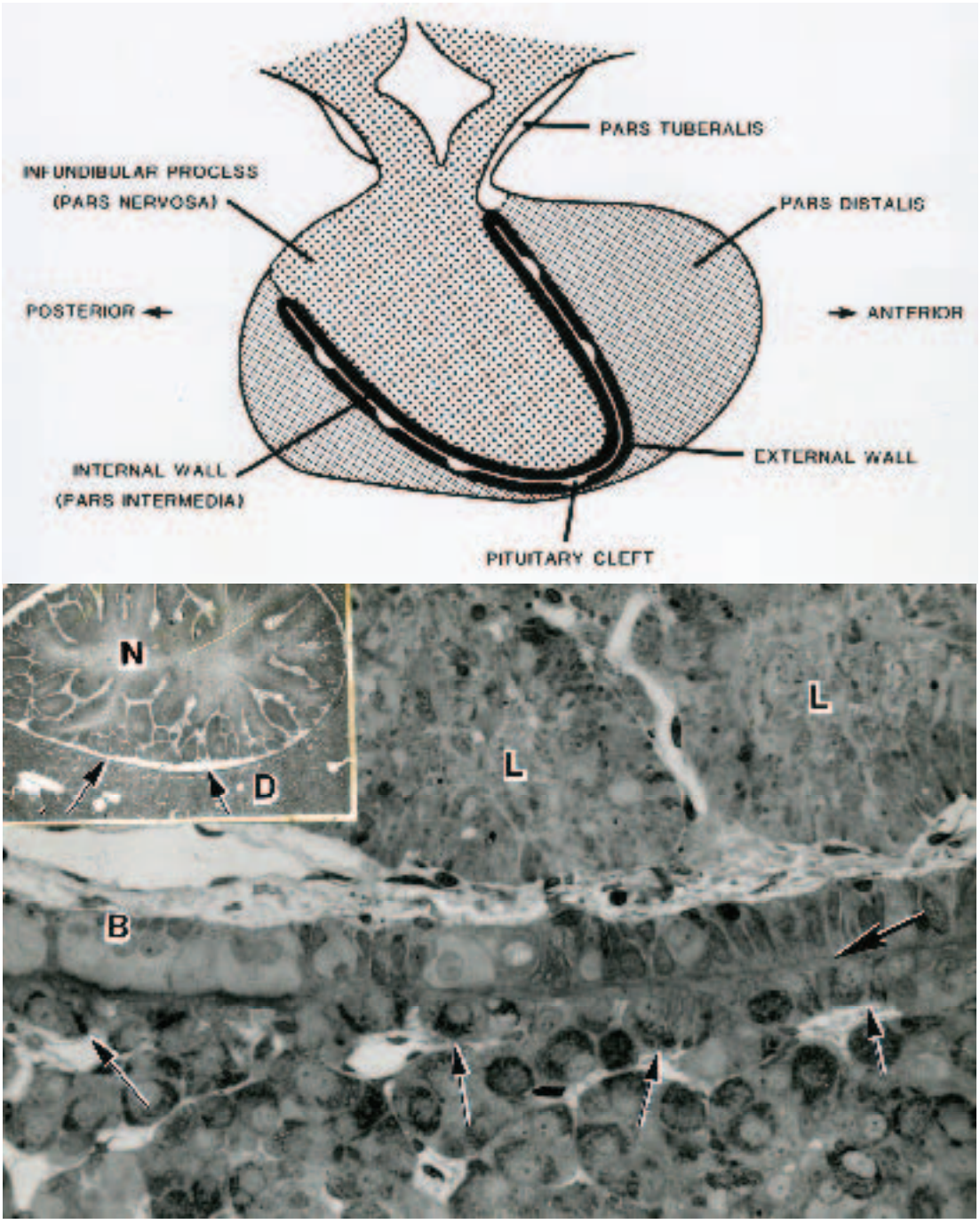

Fig. 10. (*Above*). A line drawing depicting a mid-sagittal section through an adult opossum pituitary illustrates its major subcomponents (pars nervosa, pars distalis, pars tuberalis, pars intermedia) and the position of the pituitary cleft. (*Below*). The lumen of the pituitary cleft (large arrow) is often very narrow with cells forming its internal (pars intermedia) and external walls abutting one another. The internal wall often contains groups of bulbous, light-staining cells (B). The small arrows indicate the extent of the external wall. Two lobes (L) of the pars nervosa are shown at the upper right. LM X 400. (*Inset*). A horizontal section through the pituitary of an adult opossum illustrates the relationship of the pars nervosa (N), pars distalis (D), and the pituitary cleft (arrows). LM X 10.

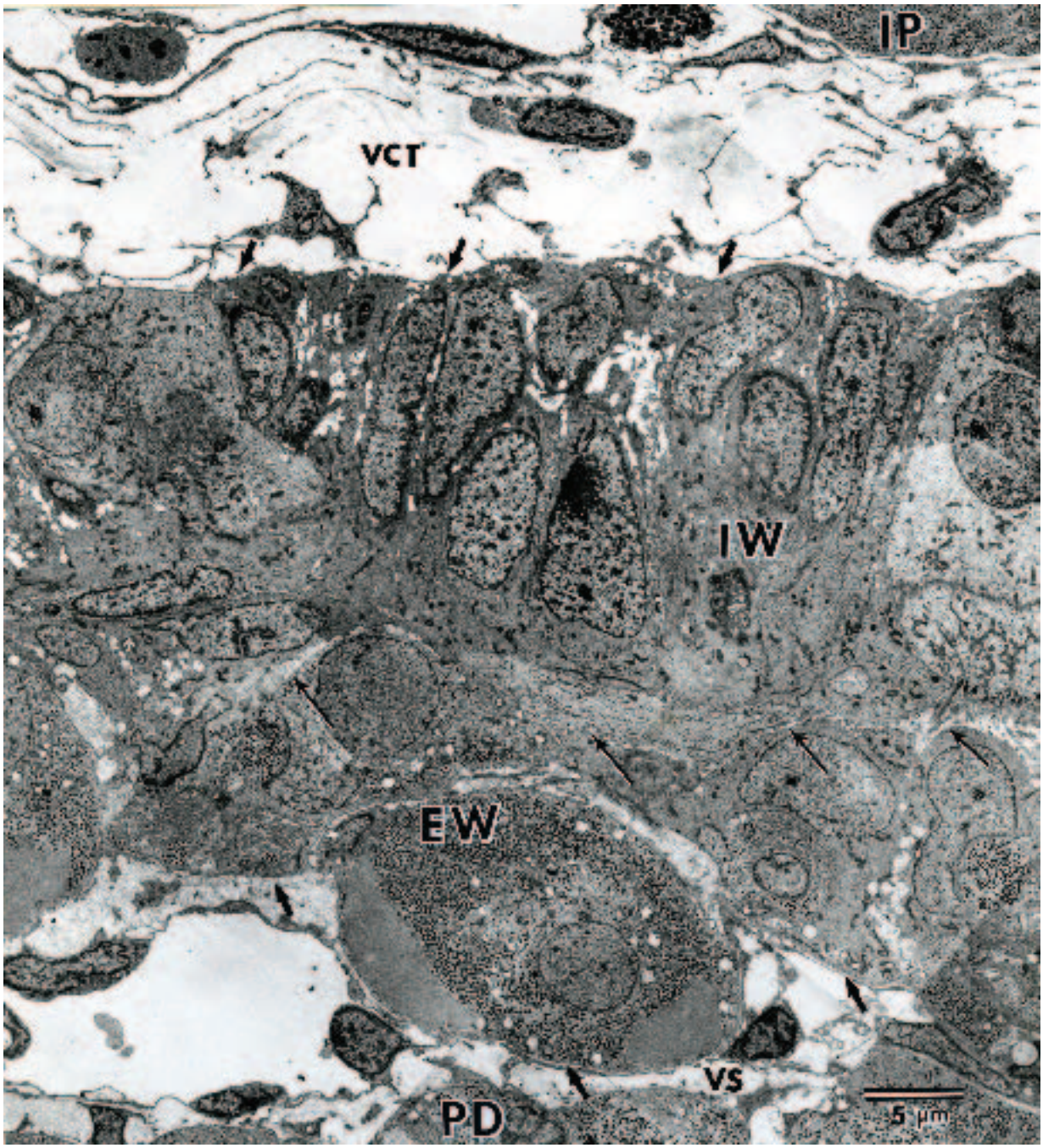

Fig. 11. The pituitary cleft (slender arrows) is collapsed throughout most of its extent, with only a small gap filled with cilia appearing at the far right. The interior wall (IW) of the cleft is separated from the infundibular process (IP) by a thin basement membrane (broad arrows) and a wide vascular connective tissue area (VCT). The internal wall is also known as the pars intermedia. The external wall (EW) of the cleft is separated from the pars distalis (PD) by a thin basement membrane (broad arrows) and a narrow vascular connective tissue space (VS). Adult male opossum. TEM X 3,200.

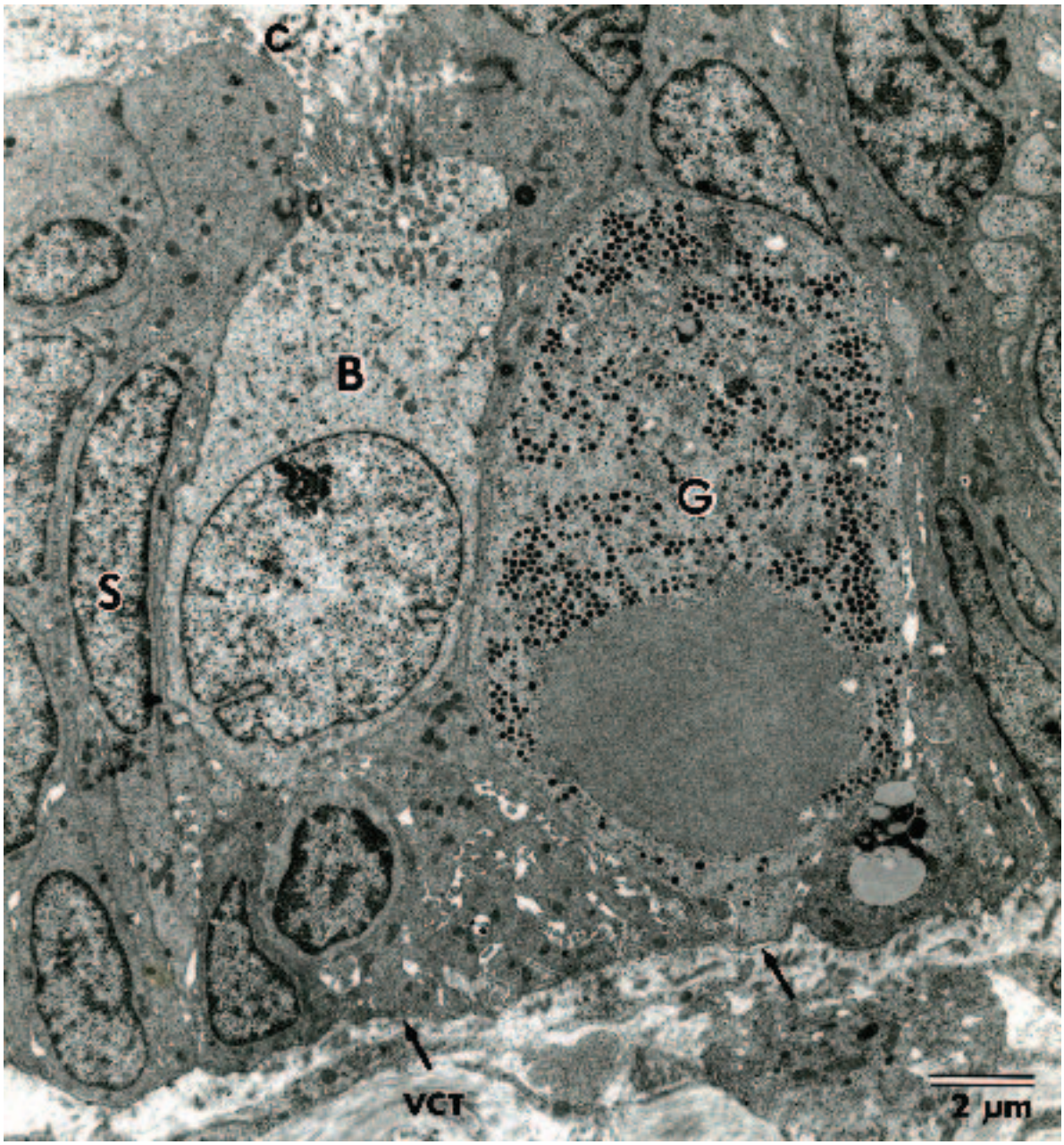

Fig. 12. Three different cell types; granular (G), spindle (S), and bulbar cells (B), can be distinguished in the internal wall (pars intermedia) that limits the pituitary cleft. Note the cilia and microvilli extending from the bulbar cell into the pituitary cleft (C) and the large distended cisterna filled with colloid-like material in the granular cell. A basement membrane (arrows) separates the internal wall from the vascular connective tissue (VCT) covering the pars nervosa. Adult male opossum. TEM X 8,000.

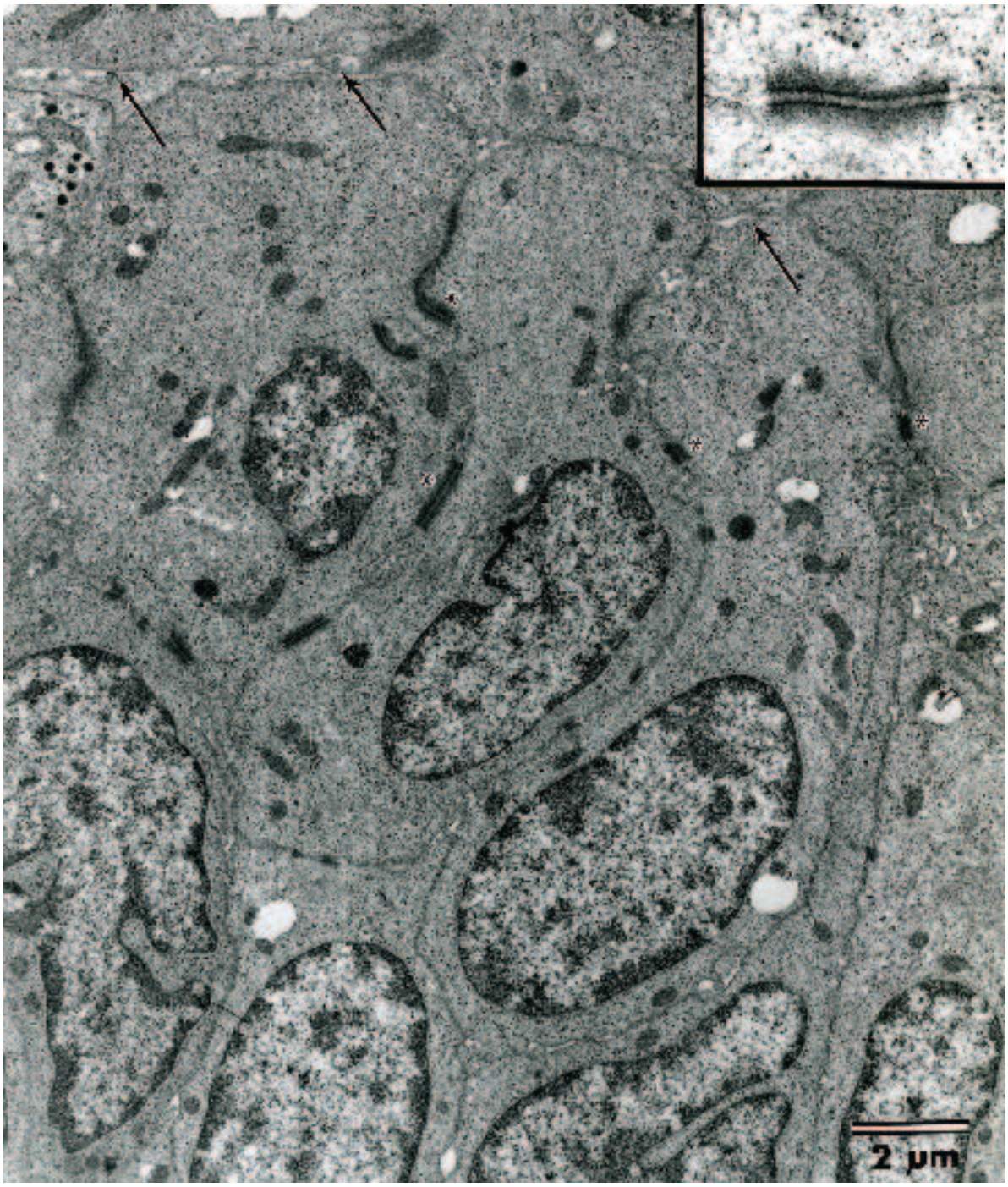

Fig. 13. A portion of the internal wall lining the pituitary cleft (pars intermedia) illustrating a cluster of spindle cells. Zonula occludens (tight junctions) unite the cell apices near the pituitary cleft (arrows) and numerous desmosomes (asterisks) are observed holding the lateral cell membranes in close apposition. Adult male opossum. TEM X 8,400. The inset illustrates a desmosome found between the lateral cell membranes of two spindle cells. TEM X 44,500.

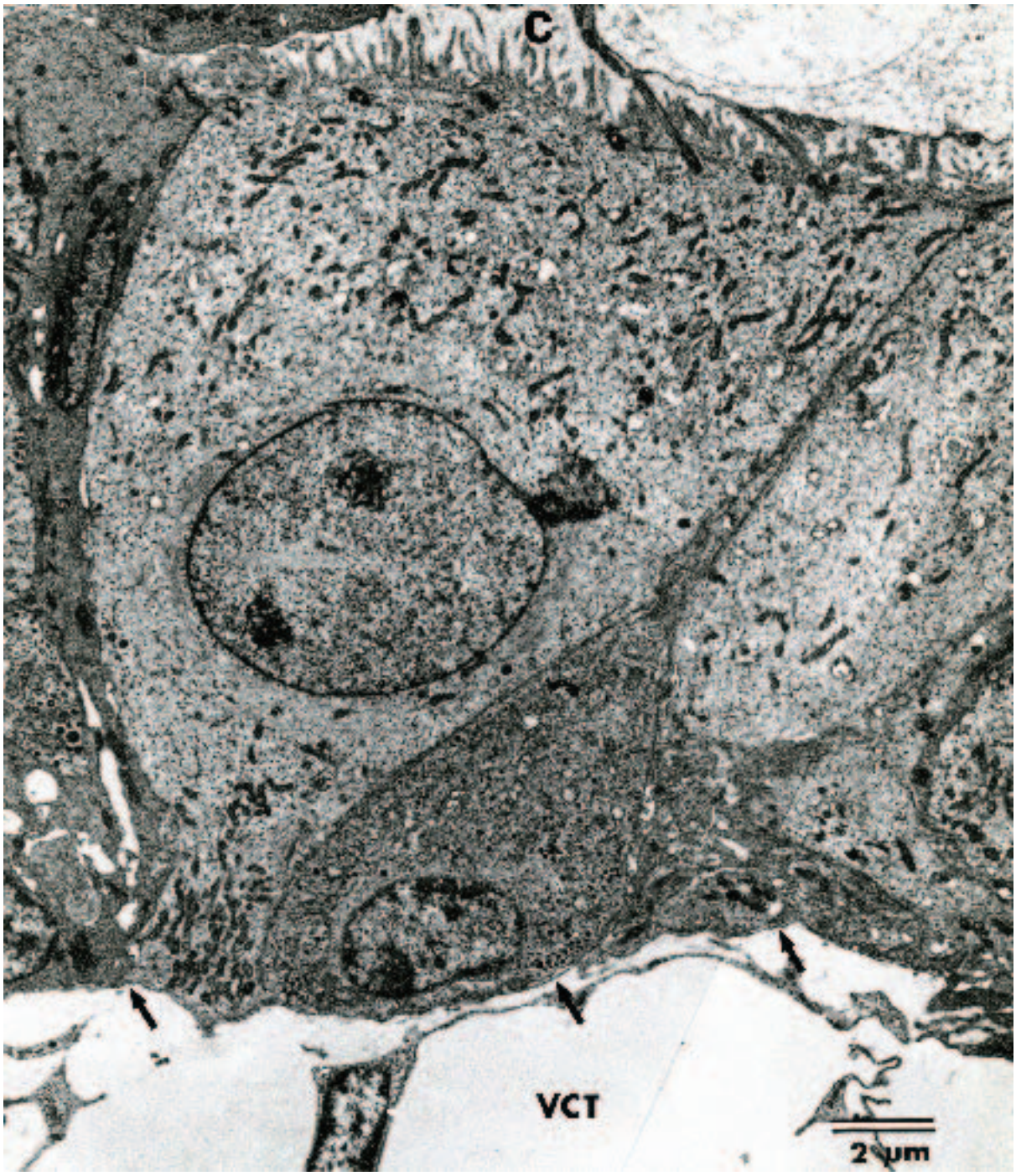

Fig. 14. Bulbar cells within the internal wall (pars intermedia) extend from the limiting basal lamina (broad arrows) to the lumen of the pituitary cleft (C). These cells are characterized by a light staining cytoplasm, exhibit round or oval nuclei, and contain numerous mitochondria that often appear polarized to the apical and basal cytoplasm. The cleft (apical) surface of the bulbar cells exhibits numerous microvilli and cilia. Note that only a thin basal lamina separates the cells forming the internal wall of the pituitary cleft from the adjacent vascular connective tissue (VCT). Adult male opossum. TEM X 7,900.

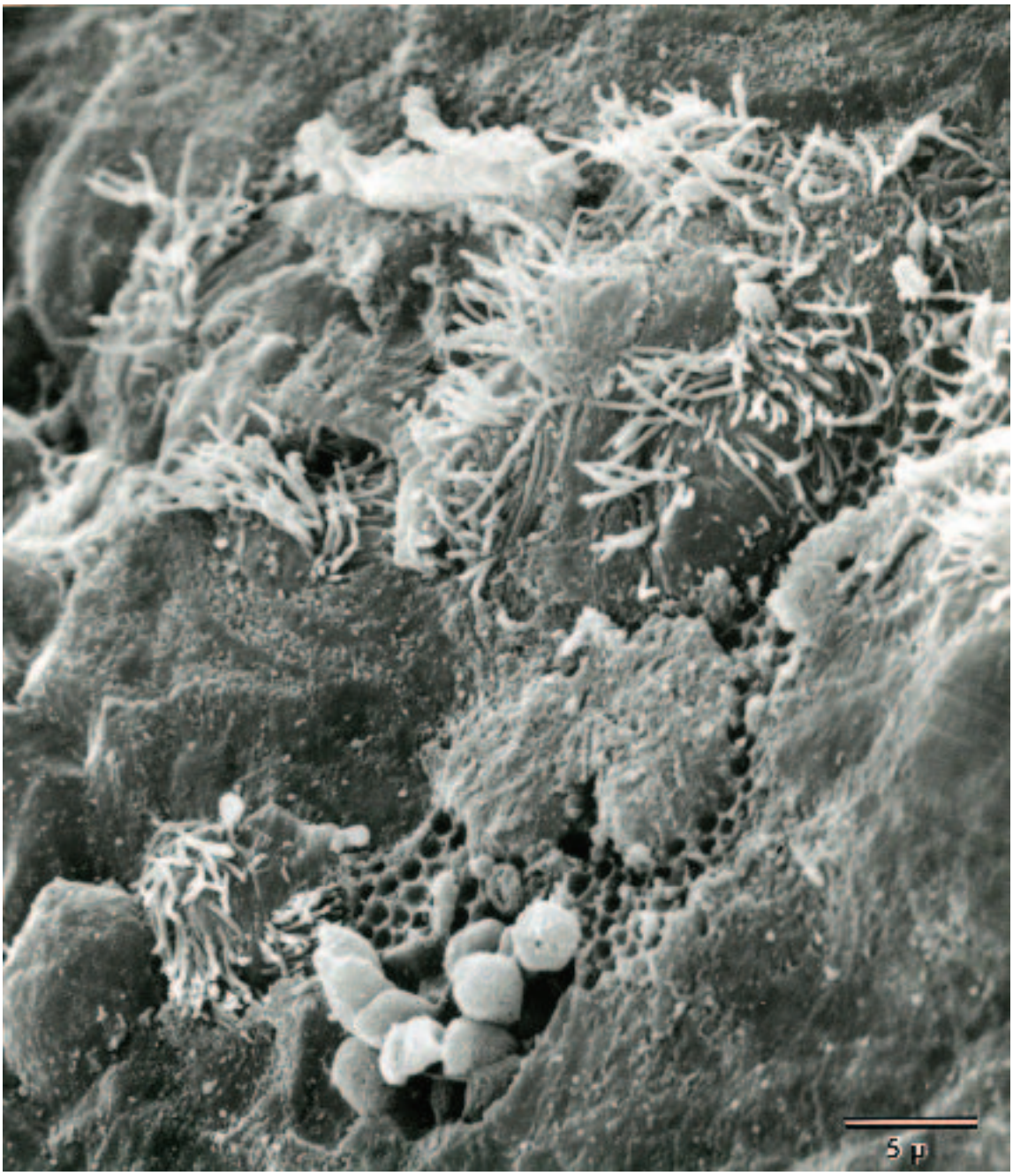

Fig. 15. A scanning electron micrograph of the apices of cells forming the internal wall of the pituitary cleft demonstrates cilia and microvilli projecting into the pituitary cleft. These surface specializations are thought to designate the position of bulbar cells. The honeycomb appearance may represent remnants of fractured secretory granules within the apical cytoplasm of granular cells broken during preparation of the specimen. Juvenile female opossum. SEM X 3,500.

Fig. 16. Two cell types, granular cells (G) and nongranular cells (NG), can be distinguished in the external wall limiting the pituitary cleft. Nongranular cells generally exhibit an oval or elongated nucleus. These cells may extend from the cleft lumen (C) to the limiting basal lamina (arrows), or may be flattened and confined to the cleft surface. The granular cells generally have a round to oval appearing nucleus and their secretory granules may vary in size and density. Adult male opossum. TEM X 9,200. The inset illustrates the basal lamina (arrow) limiting the external wall of the pituitary cleft. TEM X 44,000.

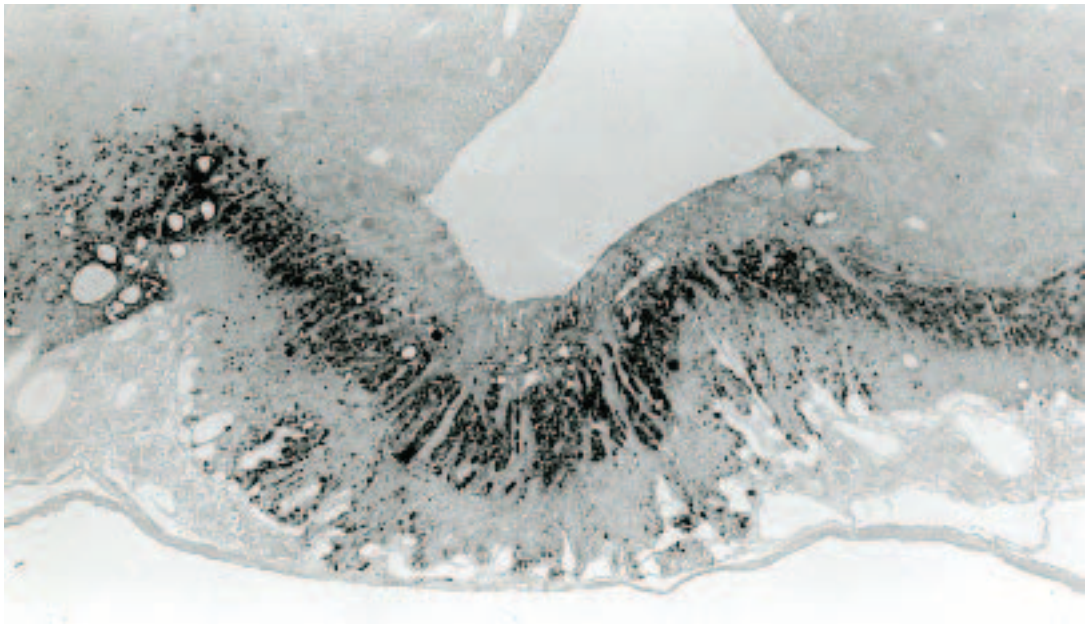

Fig. 17. A region of the median eminence stained immunohistochemically to demonstrate neurophysin. The neurophysin-containing nerve fibers stain black. Note the abundance of dilated capillaries near the base of the specimen. The space shown at the upper center of the photomicrograph is the lumen of the third ventricle. Adult male opossum. LM X 125.

Chapter 31. Thyroid

Synopsis:

Thyroid development in the opossum commences during the tenth prenatal day and is first recognized as an epithelial depression in the medial region of the pharynx between the second and first pharyngeal pouches. This invagination deepens and by prenatal day eleven an epithelial vesicle develops that has separated from the pharyngeal epithelium. The newly formed thyroid vesicle migrates caudally and as it does undergoes lateral expansion to form two lobes late in prenatal day twelve. It is at this time that the thyroid lobes fuse with ultimobranchial tissue (bodies). At birth the two thyroid lobes lie lateral to and on either side of the trachea. During the first postnatal week the thyroid is comprised of small plates or cords of epithelial cells intimately associated with adjacent capillaries. The epithelial cells are cuboidal to columnar in shape, the cell apices of which are united by tight junctions. A minute lumen courses throughout the length of epithelial cords. Cells that contain numerous, small, electron-dense granules also are observed that lie within the basal lamina of the epithelial cords and may represent parafollicular cells at an early stage of differentiation. It is not until about the middle of the second postnatal week that primary follicles are first observed. Evaginations form from the epithelial cords, expand and result in the formation of the primary follicles. Secondary follicles then arise as evaginations from the epithelial walls of the primary follicles. At this time there are morphological indications that the thyroid is engaged is synthetic activity. Epithelial cords are rarely observed in the developing thyroid at the end of the second postnatal week, which is now characterized by numerous, small colloid-filled thyroid follicles. Mitotic figures continue to be observed within the follicular epithelium at this time. As organogenesis continues, the follicles increase in size and number (by budding). Follicular and parafollicular cells exhibit mature features by the end of the fifth postnatal week. The parafollicular cells are found scattered within the follicular epithelium or may form clusters of cells between follicles. Parafollicular cells are more abundant in the upper two-thirds of each elongate thyroid lobe.

Acknowledgments:

Figs. 1, 2, 3, 4, 5 (top) and 6, courtesy of and from: Krause, W.J. and J.H. Cutts (1982) Postnatal development of the thyroid in the opossum, *Didelphis virginiana*. Acta Anat. 116: 322-338.

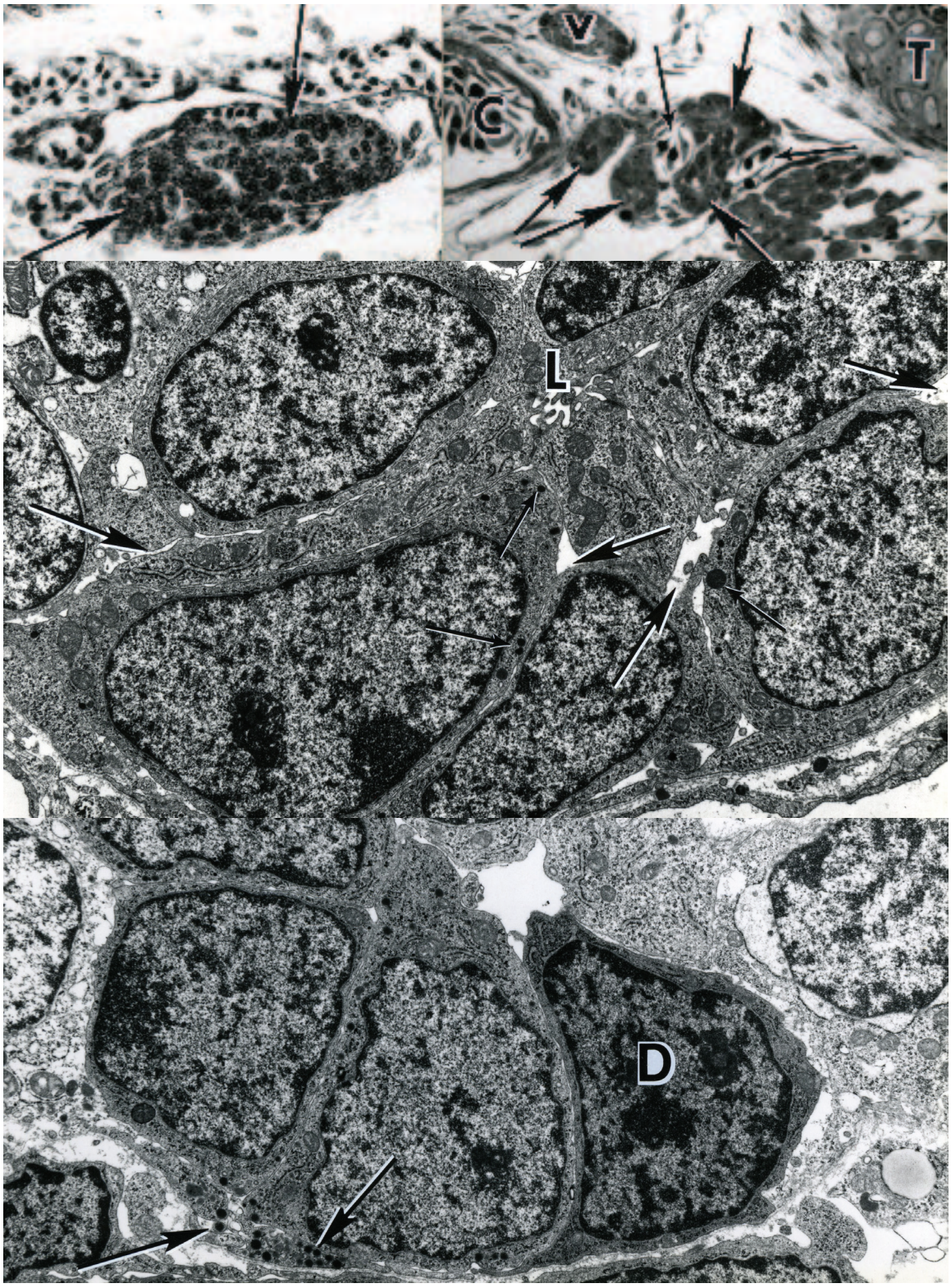

Fig. 1. (*Above left*). The cells of a newborn opossum thyroid (arrows) are organized into cords. LM X 250. (*Above right*). The epithelial cords (large arrows) forming the newborn thyroid are intimately associated with adjacent capillaries (small arrows). Portions of the trachea (T), carotid artery (C), and vagus nerve (V) also are shown. LM X 250. (*Center*). A section through an epithelial thyroid cord reveals a tiny lumen (L) at its center. Tight junctions hold the apices in close apposition whereas wide intercellular gaps occur between cells (large arrows). Small granules (small arrows) of variable size occur in some cells. Newborn. TEM X 4,500. (*Bottom*). Some cells within an epithelial cord appear dark (D) whereas others are lighter staining. Processes of some cells within an epithelial cord exhibit numerous, small granules and are thought to represent differentiating parafollicular cells (arrows). Newborn opossum. TEM X 4,500.

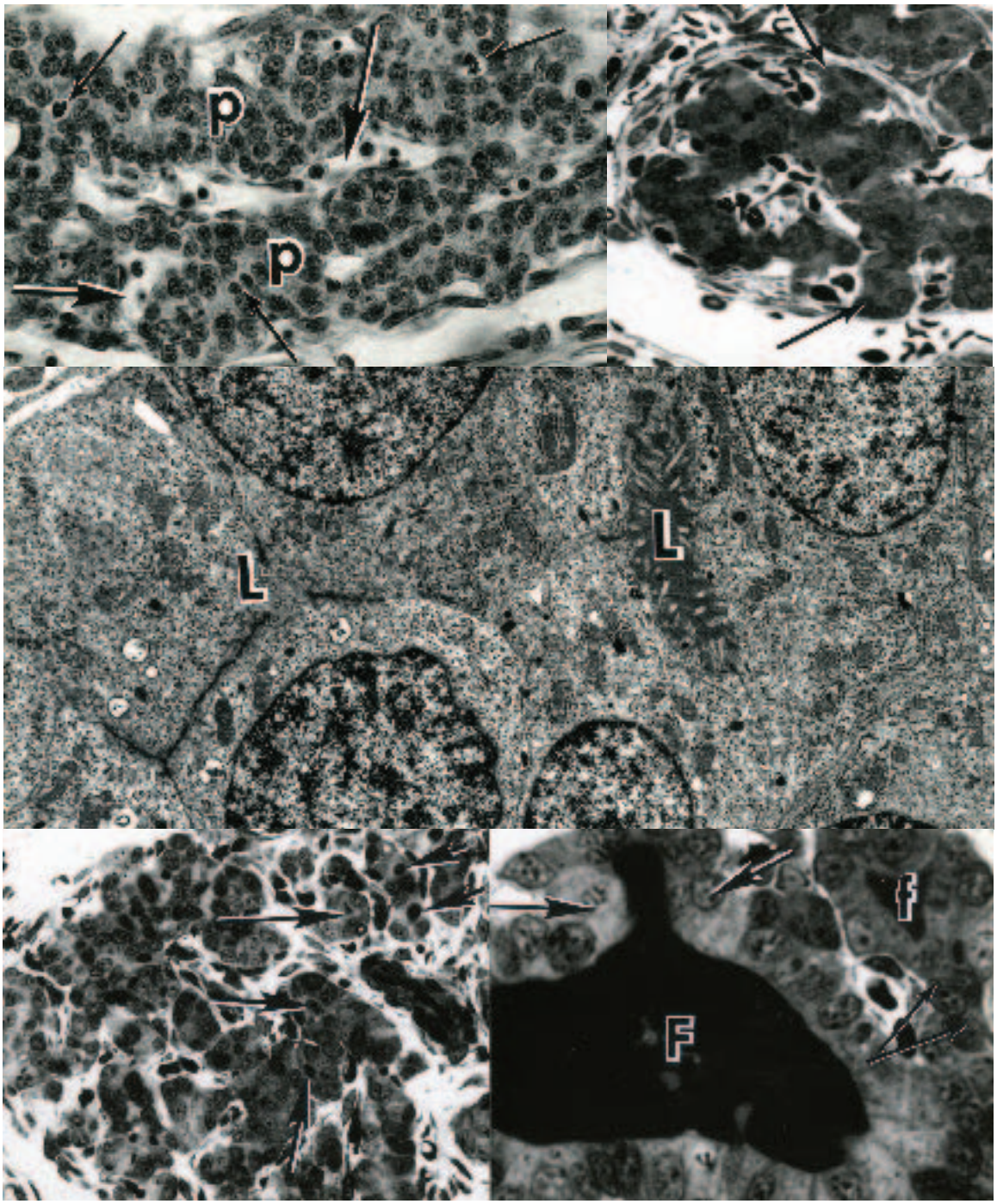

Fig. 2. (*Above left*). The thyroid of an opossum one week postnatal shows continued development and expansion of the epithelial cords (P) and adjacent capillaries (large arrows). Note the abundance of mitotic figures (small arrows). LM X 250. (*Above right*). A transverse section through a developing thyroid lobe illustrates several evaginations or buds (arrows) from the epithelial cords. Opossum one week postnatal. LM X 250. (*Center*). A portion of an epithelial cord illustrates the tortuous course of its central lumen (L), which contains electron-dense material. Opossum one week postnatal. TEM X 4,000. (*Below left*). Lumina (arrows) within the epithelial cords are seen by light microscopy during the second postnatal week and may contain a dense-staining material. LM X 250. (*Below right*). An evagination (large arrows) extending from the wall of a primary thyroid follicle (F). Such evaginations are thought to give rise to secondary thyroid follicles. A small thyroid follicle (f) attached to an epithelial cord (small arrows) is shown at the extreme right. Opossum two weeks postnatal. LM X 400.

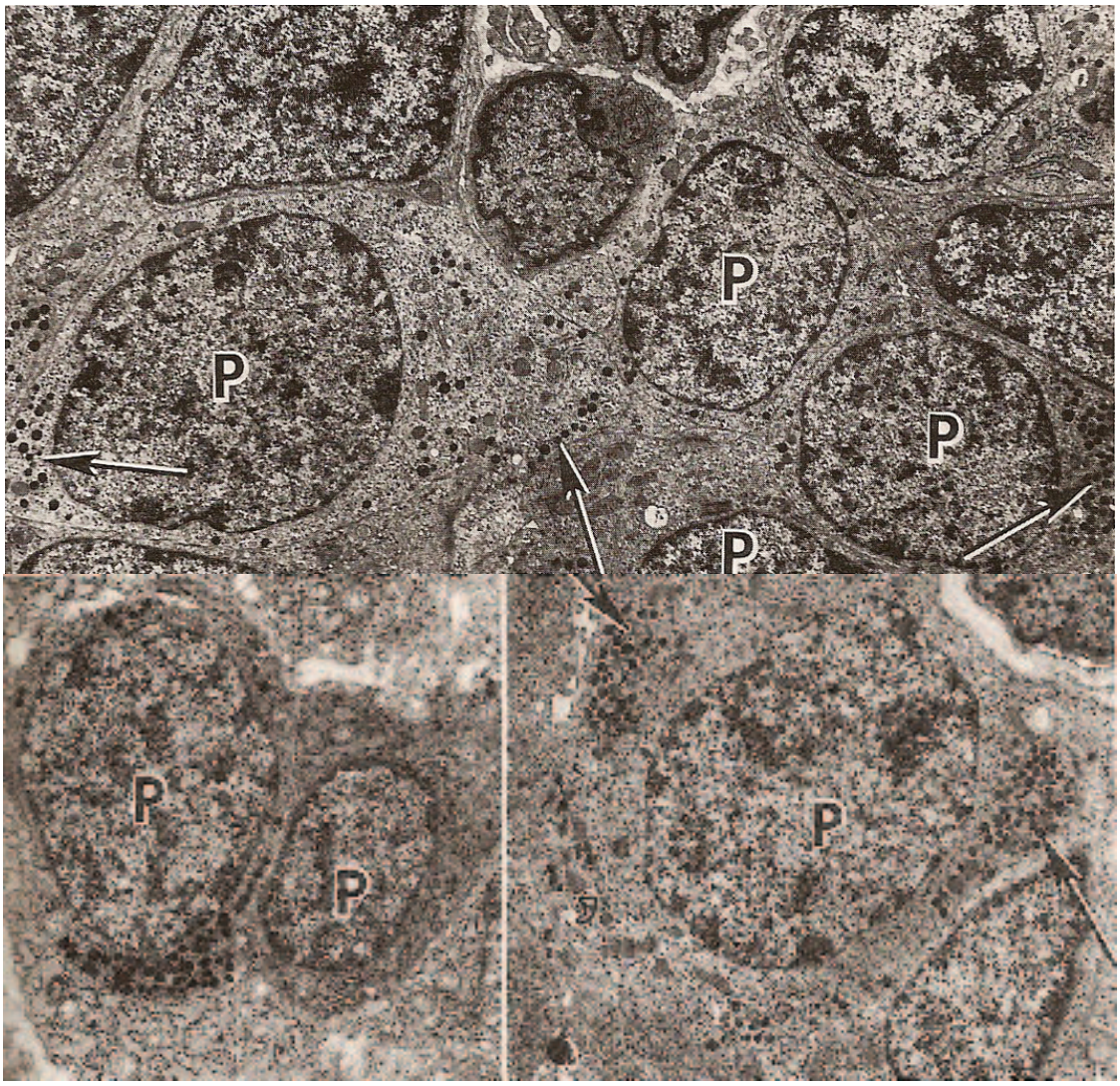

Fig. 3. (*Above*). Groups of parafollicular cells (P) can be identified between epithelial cords of the developing thyroid by the end of the first postnatal week. The parafollicular cells are generally oval in shape with central nuclei and the cytoplasm is characterized by accumulations of small, electron-dense granules (arrows). TEM X 4,000. (*Below left*). Two parafollicular cells (P) identified within an epithelial cord of a developing thyroid lobe. Opossum one week postnatal. TEM X 4,000. (*Below right*). A parafollicular cell (P) from the thyroid of an opossum one week postnatal that contains secretory granules (arrows) that exhibit a greater variation in electron density and more closely resemble those observed in the adult thyroid. TEM X 4,000.

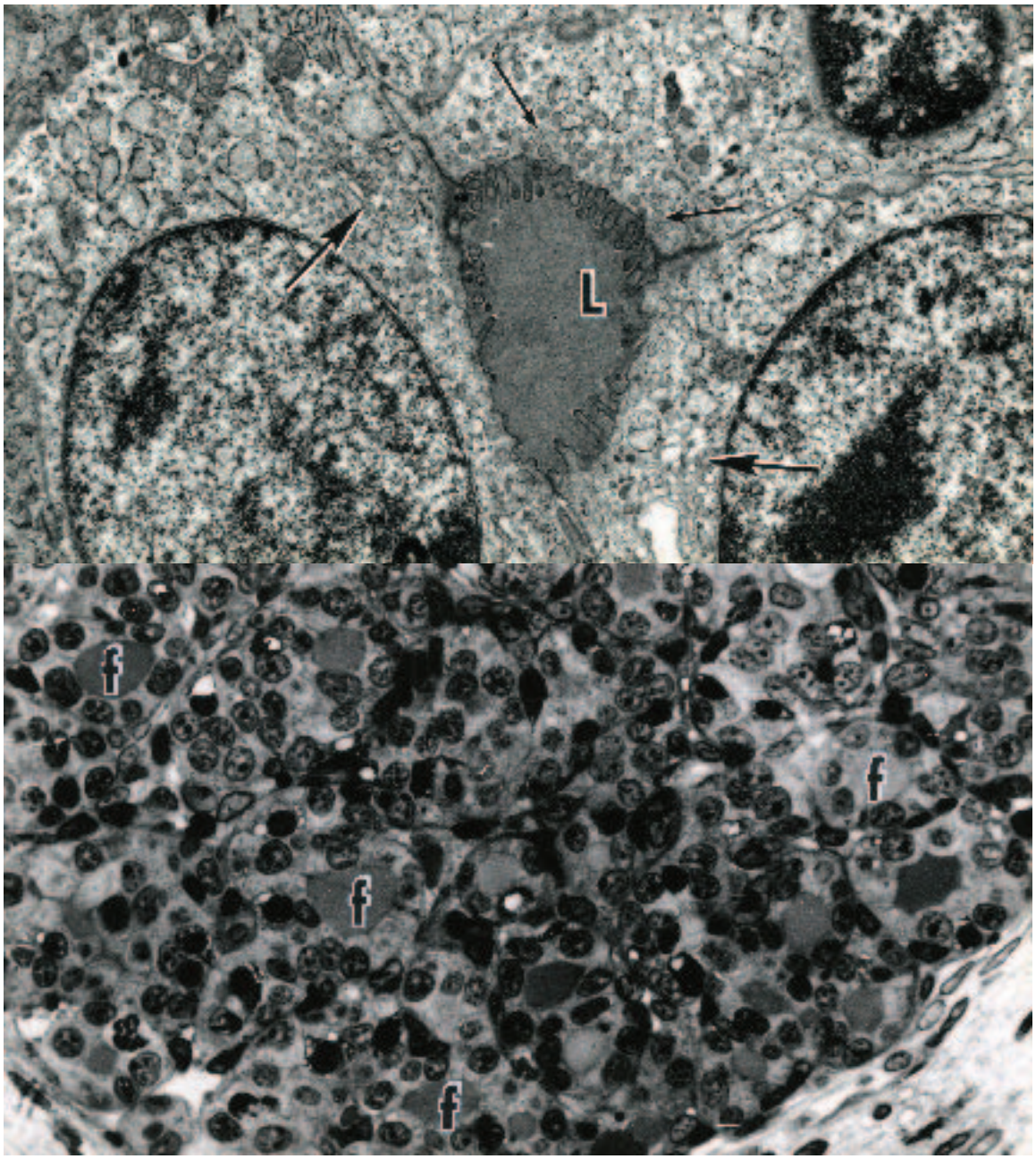

Fig. 4. (*Above*). The cytoplasm of follicular cells from an opossum thyroid two weeks postnatal contains Golgi complexes (large arrows), mitochondria, and scattered profiles of rough endoplasmic reticulum. Numerous, membrane-bound vesicles (small arrows) in the apical cytoplasm that contain material of a similar electron density to that observed in the lumen (L) also are seen. TEM X 10,000. (*Below*). A region of thyroid taken from an opossum at the end of the second postnatal week illustrates its compact nature and the predominance of small thyroid follicles (f). The epithelial cords are now an infrequent observation in the thyroid. LM X 325.

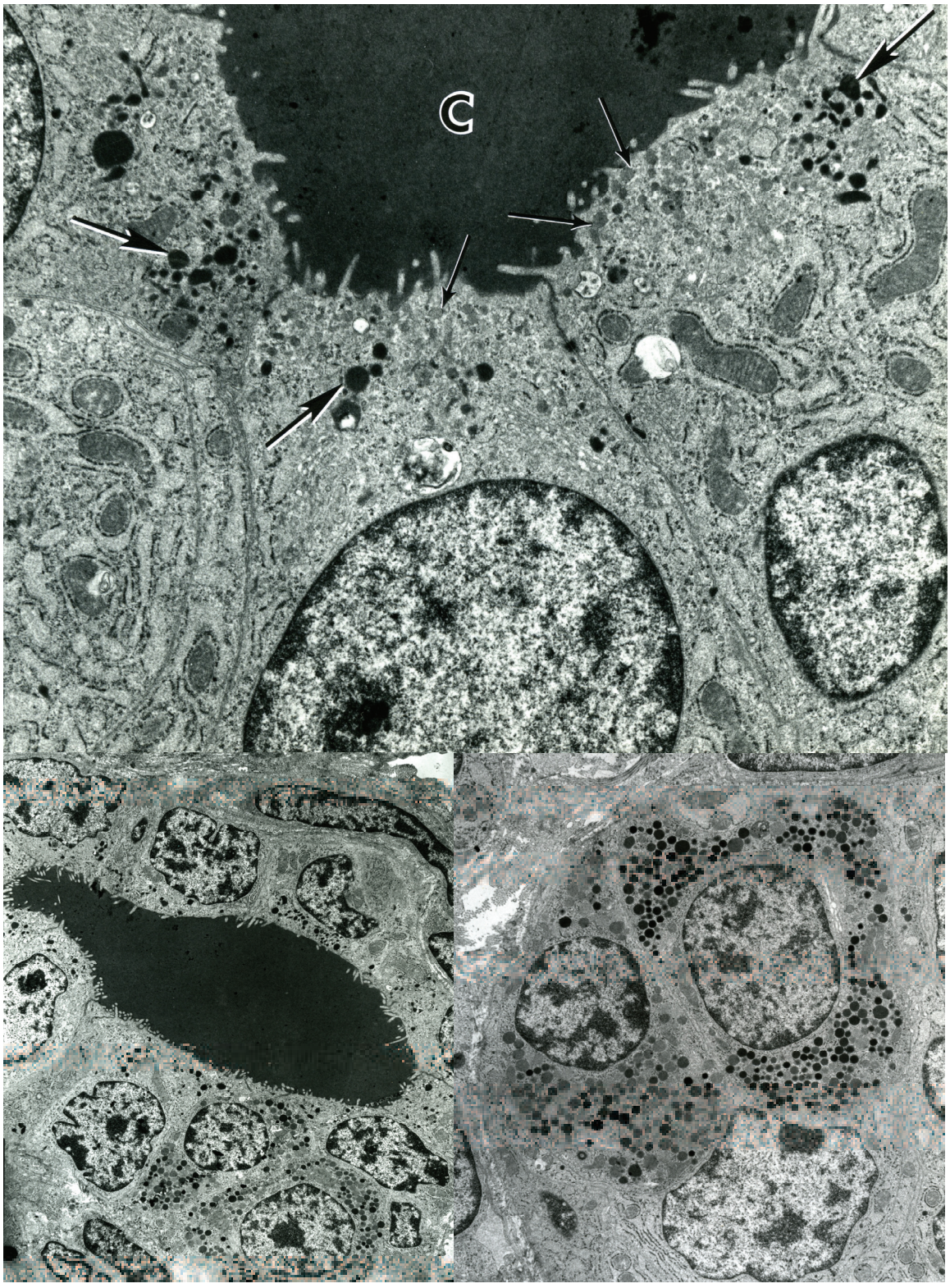

Fig. 5. *(Above)*. Most follicular cells exhibit adult morphological features by the fifth postnatal week including secretion droplets (small arrows) and colloid resorption droplets (large arrows). Note that the staining density of the colloid (C) within the follicular lumen is similar to that observed within colloid resorption droplets. TEM X 8,000. (*Below left*). A portion of a thyroid follicle illustrates two parafollicular cells near the bottom. TEM X 2,000. (*Below right*). Numerous, heterogeneous secretory granules characterize two parafollicular cells within the basal lamina of a thyroid follicle. Opossum six weeks postnatal. TEM X 5,000.

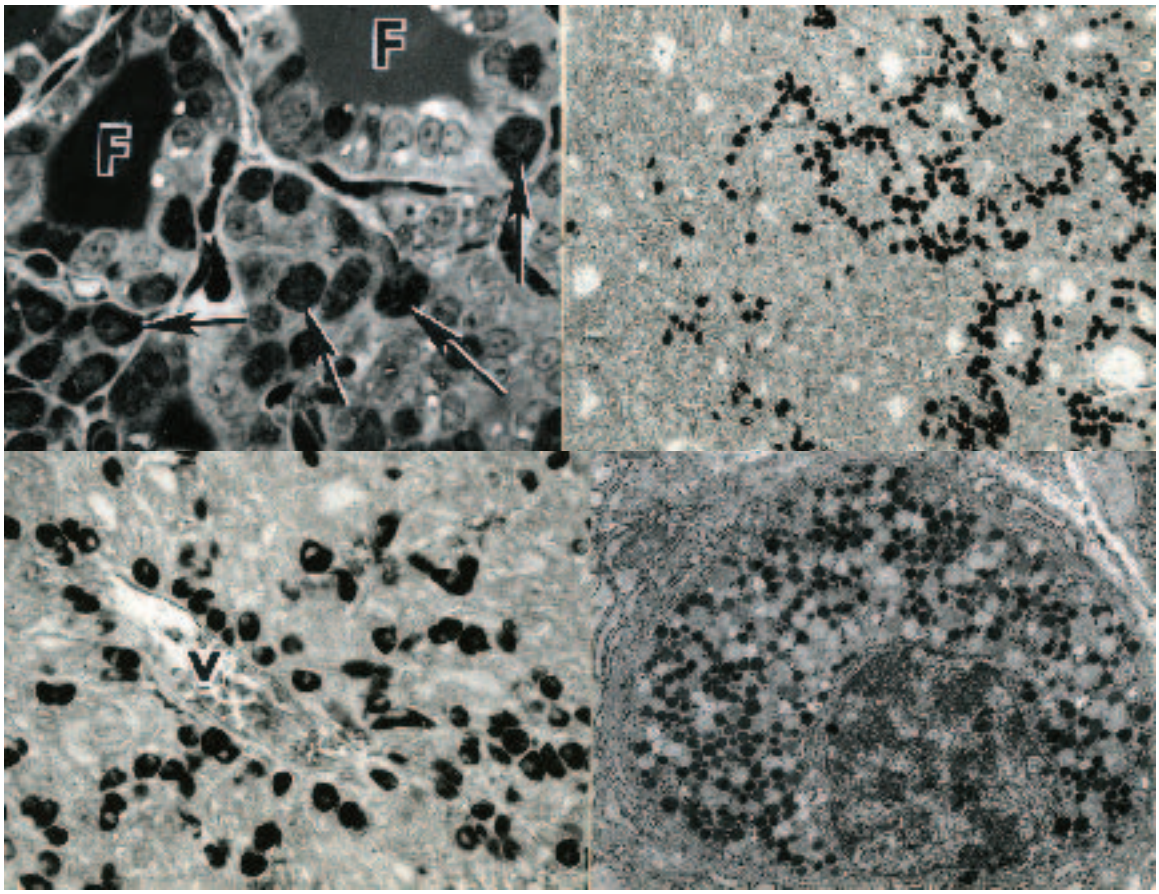

Fig. 6. (*Above left*). A region of adult thyroid illustrates portions of two follicles (F) and an abundance of parafollicular cells (arrows) that occur between follicles as well as within the follicular epithelium. LM X 300. (*Above right*). A central region of adult thyroid stained immunohistochemically to selectively demonstrate calcitonin, illustrates numerous positive parafollicular cells in the direction of the superior pole (right) with relatively few parafollicular cells occurring in the direction of the inferior pole (left). LM X 100. (*Below left*). A region form the superior pole of an adult opossum thyroid stained immunohistochemically for calcitonin reveals a tendency of the parafollicular cells to be aligned immediately adjacent to small veins (V) and capillaries. LM X 250. (*Below right*). A parafollicular cell from the thyroid of an adult male opossum illustrates the heterogeneous nature of the secretory granules that typify this species. TEM X 4,000.

Chapter 32. Parathyroid

Synopsis:

The parathyroid glands of *Didelphis* develop from the epithelium associated with the third and fourth branchial pouches during the early part of prenatal day twelve. Parathyroid III lies near the medial surface of the origin of the internal carotid artery at birth. It consists of a few clumps and irregular cords of epithelial cells. Parathyroid III increases gradually in size during the postnatal period, due primarily to an expansion of the anastomosing cords of epithelial cells. These become associated with numerous capillaries as organogenesis continues. The parenchyma of the parathyroid consists of a homogeneous population of chief or principal cells. Oxyphil cells are not observed in the parathyroid of the opossum. Small, membrane-bound, electron-dense granules characterize chief cells of parathyroid III. Small rod-shaped mitochondria and scattered profiles granular endoplasmic reticulum also are observed in the cytoplasm of the parathyroid chief cells. The location of parathyroid IV is highly variable but is usually found in the thorax. It may be associated with the thoracic thymus, along its course of migration from the branchial pouches, or may be absent altogether. Neither parathyroid III nor IV is anatomically associated with the thyroid of the opossum.

Acknowledgments:

Figs. 1, 2 and 3, courtesy of and from: Krause, W.J. and J.H. Cutts (1983) Morphological observations on the parathyroid of the opossum (*Didelphis virginiana*). Gen. Comp. Endcrinol. 50:261-269.

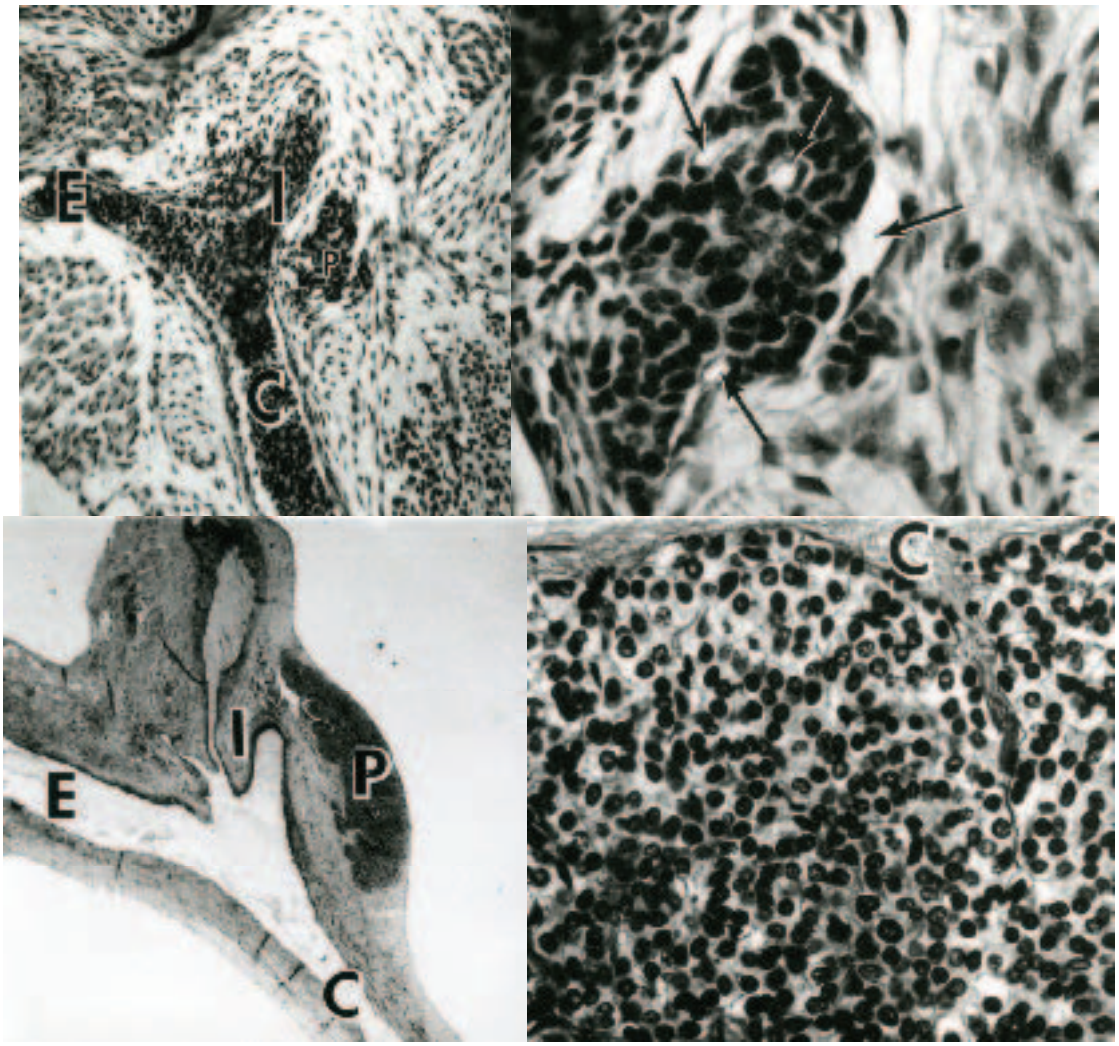

Fig. 1. (*Above left*). A section through the bifurcation of the common carotid artery (C) illustrates the position of parathyroid (P) in the newborn opossum. Portions of the internal carotid (I) and external carotid (E) arteries also are shown. Nucleated erythrocytes typify the blood contained in these vessels. LM X 100. (*Above right*). The parathyroid of a newborn opossum viewed at increased magnification shows the component cells to be arranged in irregular clumps that are associated capillaries (arrows). LM X 250. (*Below left*). A section through the bifurcation of the common carotid artery (C) of an adult female opossum illustrates the continued relationship between the internal carotid artery (I) and the parathyroid (P). The external carotid (E) is shown also. LM X 14. (*Below right*). Epithelial cells constituting the parenchyma of the adult opossum parathyroid gland are round cells with a clear cytoplasm and centrally positioned, intensely staining nuclei. A portion of the limiting capsule (C) is shown at the top of the photomicrograph. Male opossum. LM X 250.

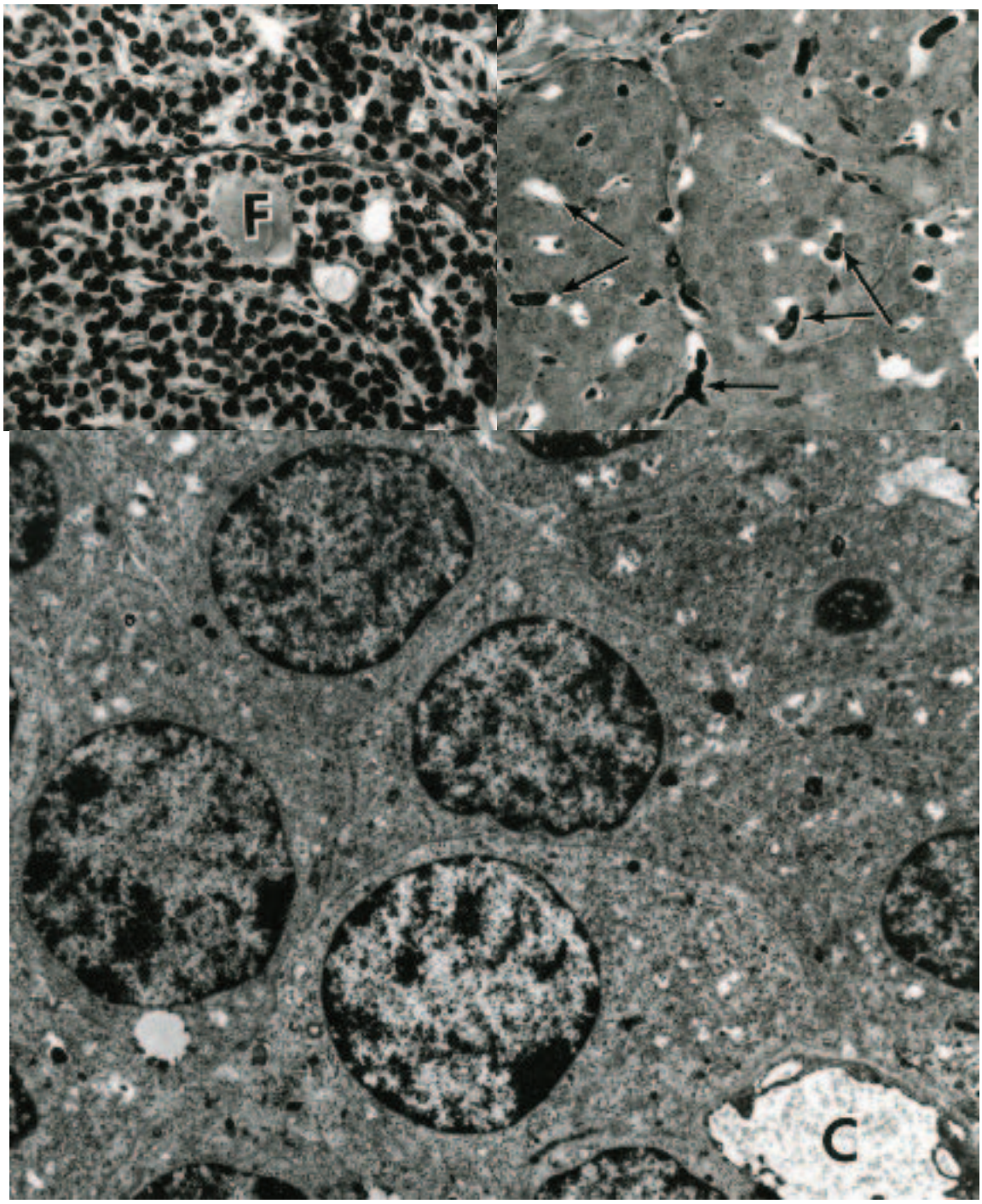

Fig. 2. (*Above left*). A region of opossum parathyroid taken near the center of the gland illustrates that in addition to the clump and cord arrangement of parenchymal cells, cells may be organized into follicle-like structures (F). Some of the follicles may contain a colloid-like material. Adult male opossum. LM X 250. (*Above right*). A region of adult parathyroid fixed by perfusion with glutaraldehyde, embedded in Epon 812, and then stained with Toluidine blue illustrates the component cells to be of uniform size and staining intensity. Adult male opossum. LM X 300. (*Below*). A region of parathyroid containing several chief cells illustrates little obvious difference in the cytoplasmic electron density between cells. A portion of a capillary (C) also is shown. Adult male opossum. TEM X 1,500.

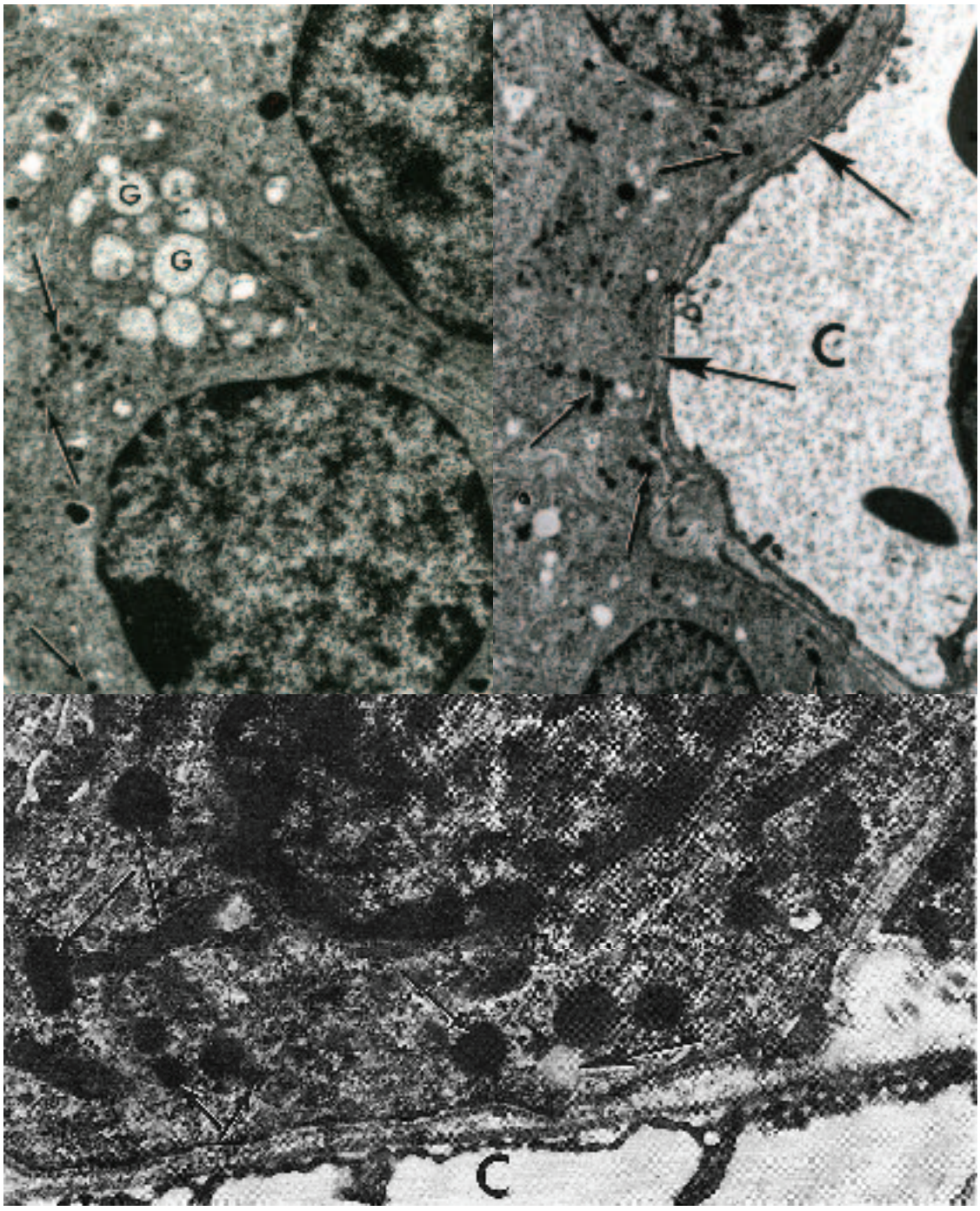

Fig. 3. (*Left*). The cytoplasm of chief cells may contain either small electron-dense granules (arrows) or larger granules (G) that are lighter staining and consist of a flocculent material. Adult male opossum. TEM X 8,000. (*Right*). A region of parathyroid that illustrates chief cells that lie adjacent to a neighboring capillary (C). The chief cells lie on a delicate basal lamina (large arrows). Note that this region of the cytoplasm contains numerous scattered, small electron-dense secretory granules (small arrows). Adult male opossum. TEM X 8,000. (*Bottom*). The cytoplasm of a chief cell adjacent to a capillary (C) contains electron dense granules of variable size (small arrows) and a lipid droplet (large arrow). The endothelial cell lining of the capillary is fenestrated. Note that a limiting basal lamina is associated with the chief cell as well as the endothelial cell. Adult male opossum. TEM X 15,000.

Chapter 33. Adrenal

Synopsis:

The primordium of the adrenal cortex is observed in some opossum embryos late in day eleven and is found in all embryos by the twelfth prenatal day. At this time the adrenal cortex consists of cords of cells that have proliferated from the mesothelial lining of the peritoneal cavity. Capillaries (sinusoids) separate the cords of mesodermal cells. At birth the adrenal gland consists of intermingled stromal, chromaffin and cortical tissue. The intra- and extra-chromaffin tissue consists of primitive sympathetic cells and pheochromoblasts at various stages of maturation. Between the third and fifth postnatal day the adrenal glands begin to become arranged into distinct cortical and medullary regions. The organization of the adrenal cortex into zones begins to occur by the sixth postnatal day and distinct zones are clearly established by the end of the second postnatal week. During this period of organogenesis, cords of chromaffin cells are established in a distinct and separate medulla. The major catecholamine present in the newborn adrenal is norepinephrine (63%) and norepinephrine-containing cells can be identified histochemically and electron microscopically. The percentage of epinephrine-containing cells increases during the first week postnatal to about 58%, which is about the same percentage observed in the adrenal medulla of the adult opossum.

Acknowledgments:

Figs. 1 (top right, bottom), 2, 3 (bottom), 4, 5, 6, and 7, courtesy of and from: Carmichael, Stephen W., Daniel B. Spagnoli, Richard G. Frederickson, William J. Krause, and James L. Culberson (1987) The opossum adrenal medulla: I. Postnatal development and normal anatomy. Am. J. Anat. 179:211-219.

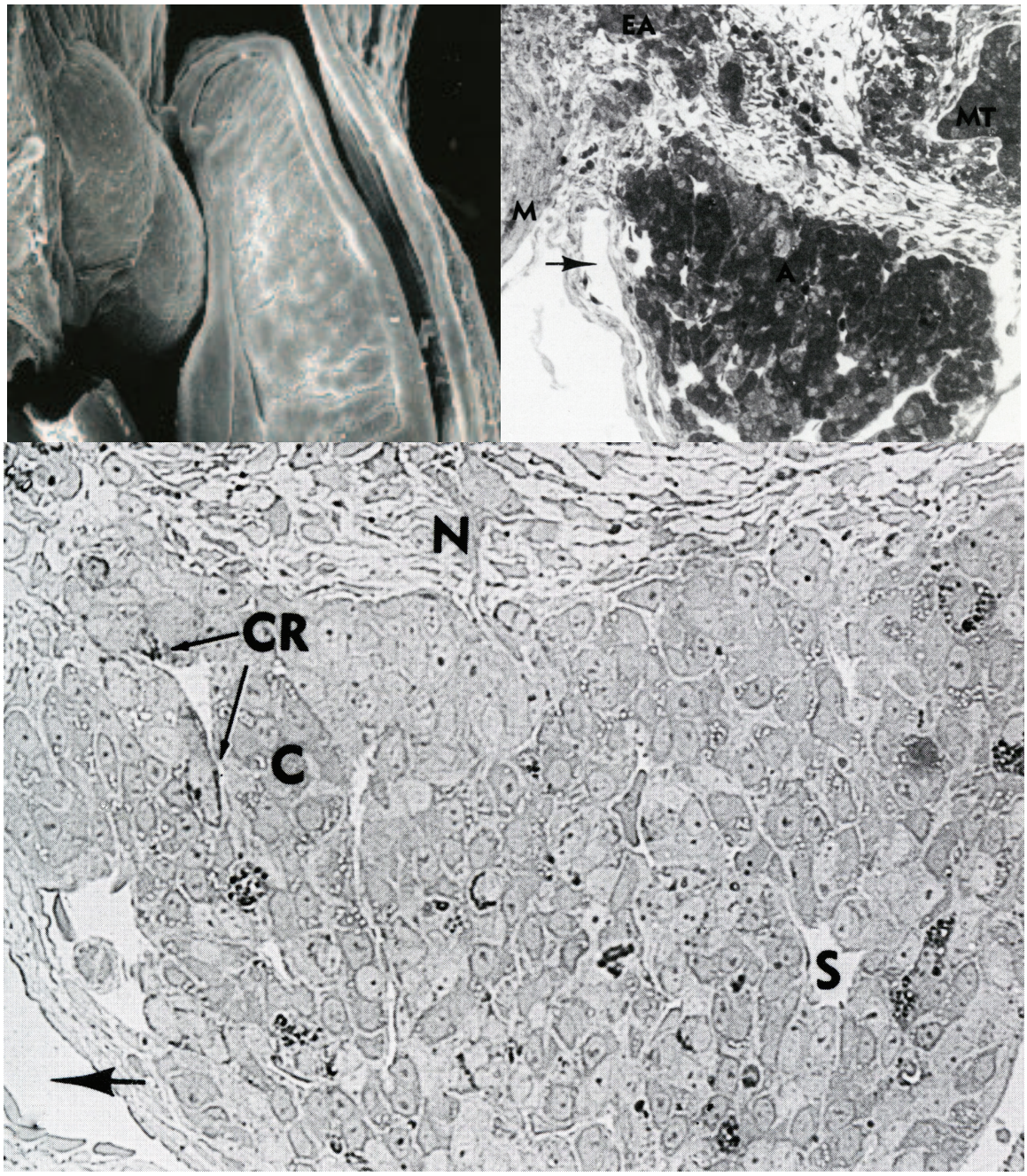

Fig. 1. (*Above left*). The external surface of the adrenal gland from a newborn opossum shown in the upper left corner of this illustration is nearly equivalent in size to the metanephros located immediately beneath it. The genital ridge (bottom center) and mesonephros (right) also are shown. SEM X 25. (*Above right*). A histological section through the adrenal gland (A) and neighboring structures of a newborn opossum. Portions of the inferior vena cava (arrow), metanephric tubules (MT), mesentery (M), and extra-adrenal chromaffin tissue (EA) can be observed. LM X 150. (*Below*). The majority of chromaffin cells are light staining a few of which located adjacent to sinusoids contain dark cytoplasmic argentaffin granules (arrows extending from CR). Unmyelinated nerves (N), a portion of the inferior vena cava (arrow), cortical tissue (C), and sinusoids (S) also are shown in the section. Newborn opossum. Ammoniacal silver preparation. LM X 350.

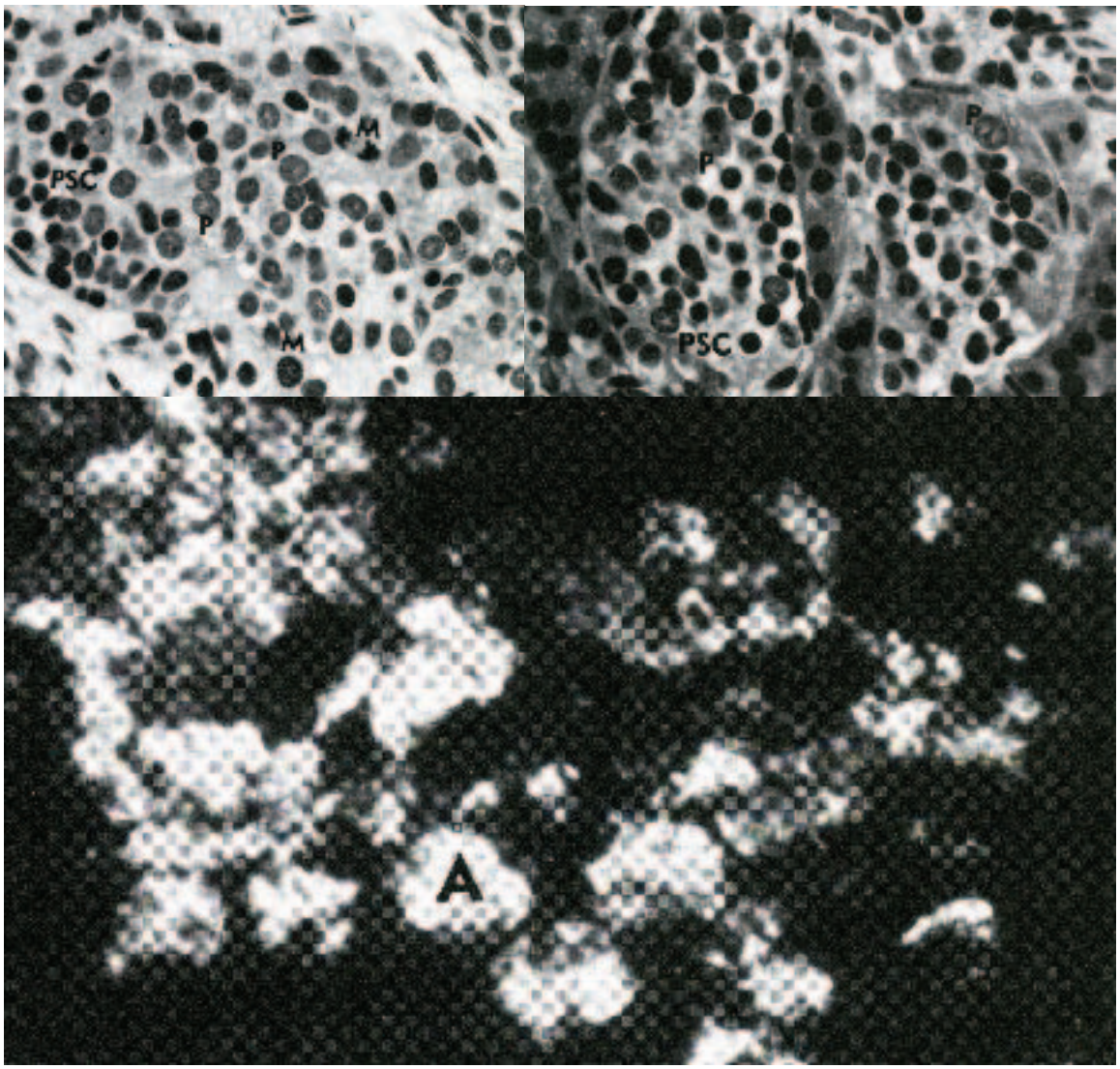

Fig. 2. (*Above left*). Extra-adrenal chromaffin tissue consists of primitive sympathetic cells (PSC) or cells with dark staining nuclei and scant cytoplasm, and pheochromoblasts (P). Numerous mitotic figures (M) also are observed. Newborn opossum LM X 500. (*Above right*). Chromaffin tissue that invades the forming adrenal gland also is characterized by primitive sympathetic cells (PSC) and pheochromoblasts (P). Mitotic figures are a less frequent observation in comparison to the extra-adrenal chromaffin tissue. LM X 500. (*Below*). An intra-adrenal (A) chromaffin region prepared to demonstrate catecholamine histofluorescence illustrates that the chromaffin tissue is fluorescent whereas the adjacent cortical tissue is non-fluorescent. Newborn opossum. Florescence: glyoxylic acid-induced. LM X 250.

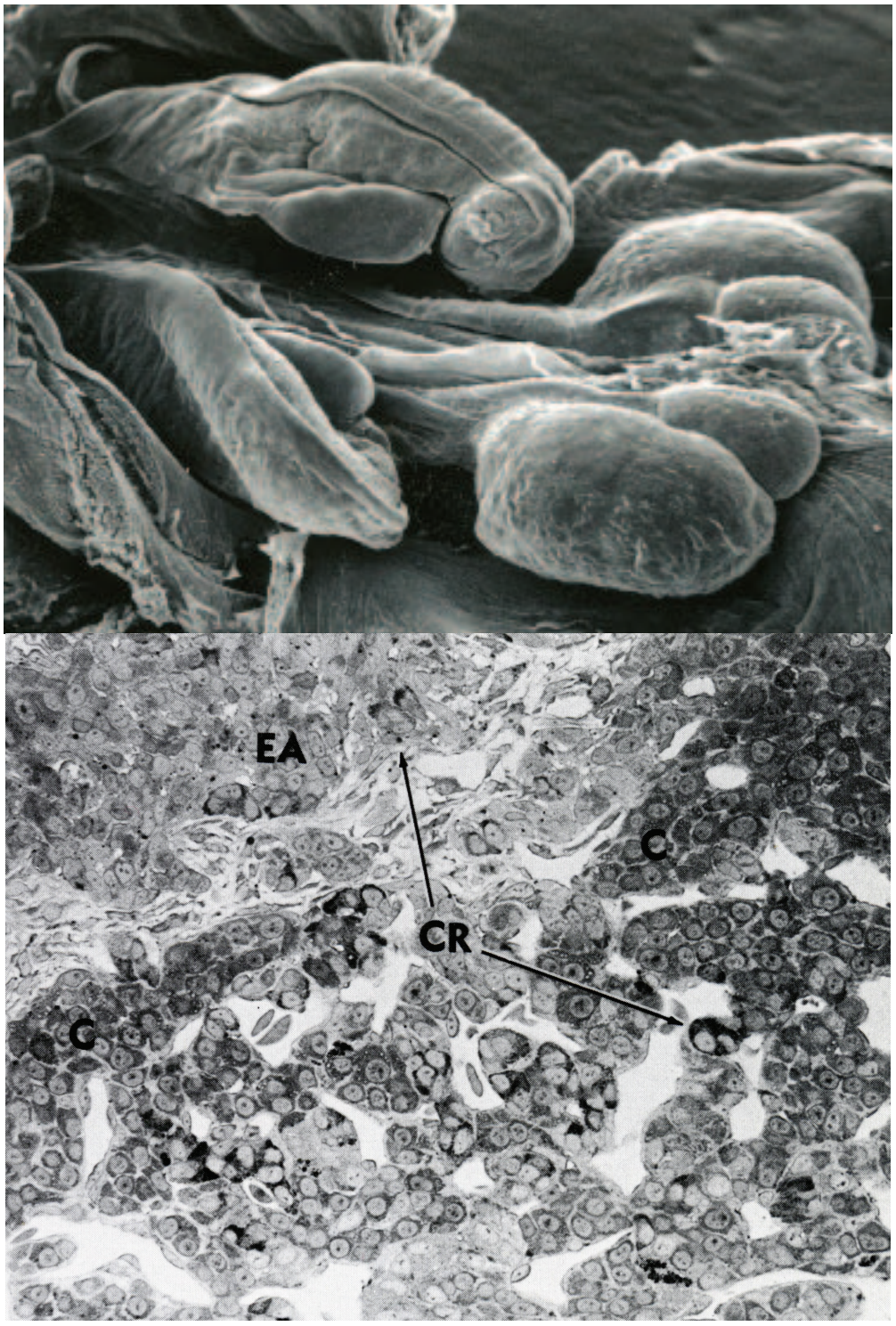

Fig. 3. (*Above*). The posterior abdominal wall of an opossum one week postnatal illustrates that the size of the adrenal glands have increased in comparison to the newborn. The developing metanephros, regressing mesonephros and developing gonad also can be seen. SEM X 40. (*Below*). Chromaffin cells with dark staining argentaffin granules (arrows from CR) are observed in both extra-adrenal (EA) and intra-adrenal locations. Other chromaffin tissue near the CR label is pale staining and only slightly granular. Cells comprising the adrenal cortex (C) are demonstrated at the upper right of the photomicrograph. Opossum one week postnatal. Ammoniacal silver stain. LM X 300.

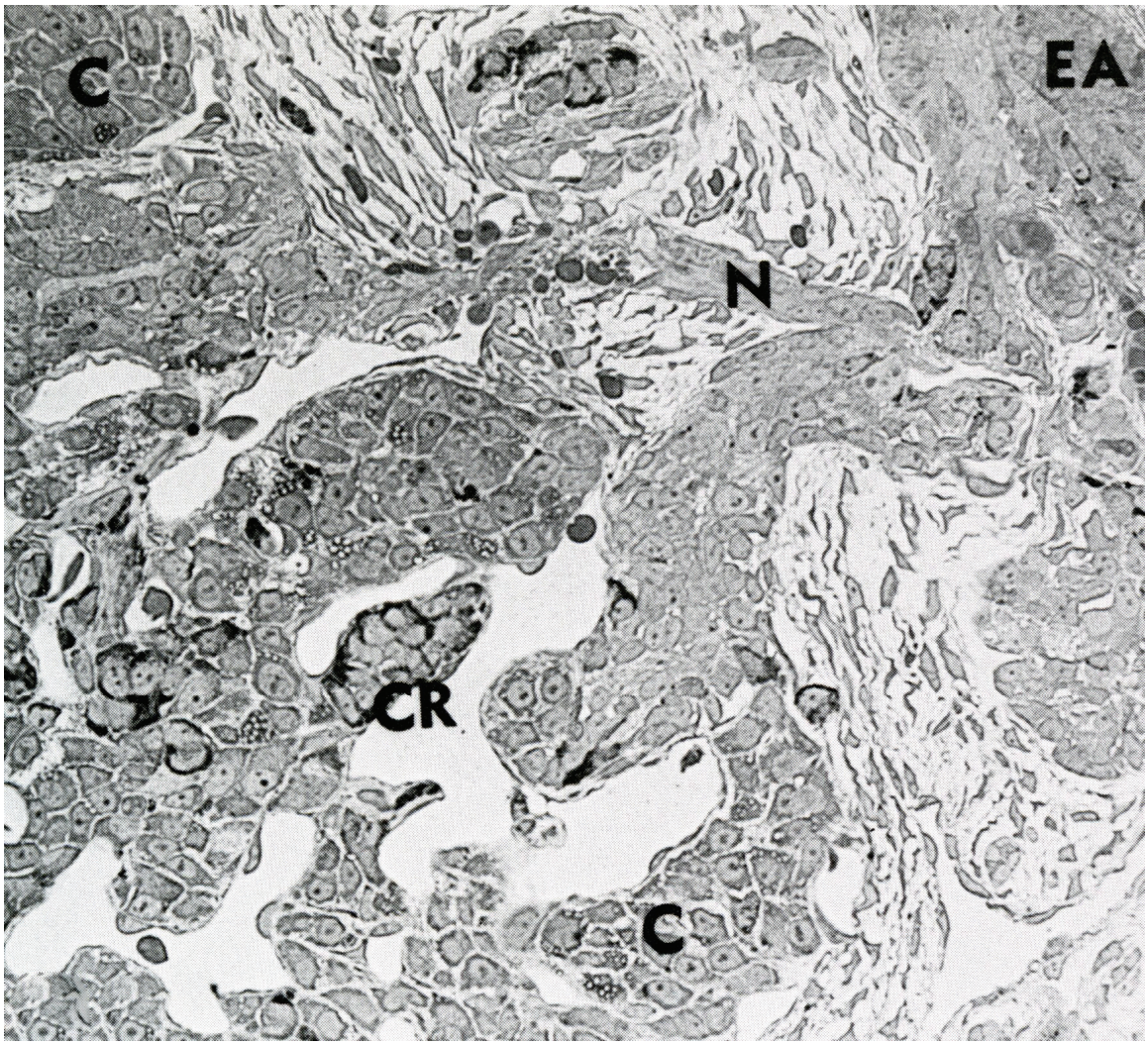

Fig. 4. During the first week of postnatal life the adrenal glands begin to segregate into medullary and cortical regions. In this specimen the cortex (C) of the developing adrenal gland is shown at the upper left and the extra-adrenal chromaffin tissue (EA) is located in the upper right-hand corner of the photomicrograph. A large number of chromaffin cells containing dark appearing argentaffin granules are shown near the label (CR). Note the nerve tissue (N) positioned between the adrenal and the extra-adrenal chromaffin tissue. Ammoniacal silver stain. LM X 300.

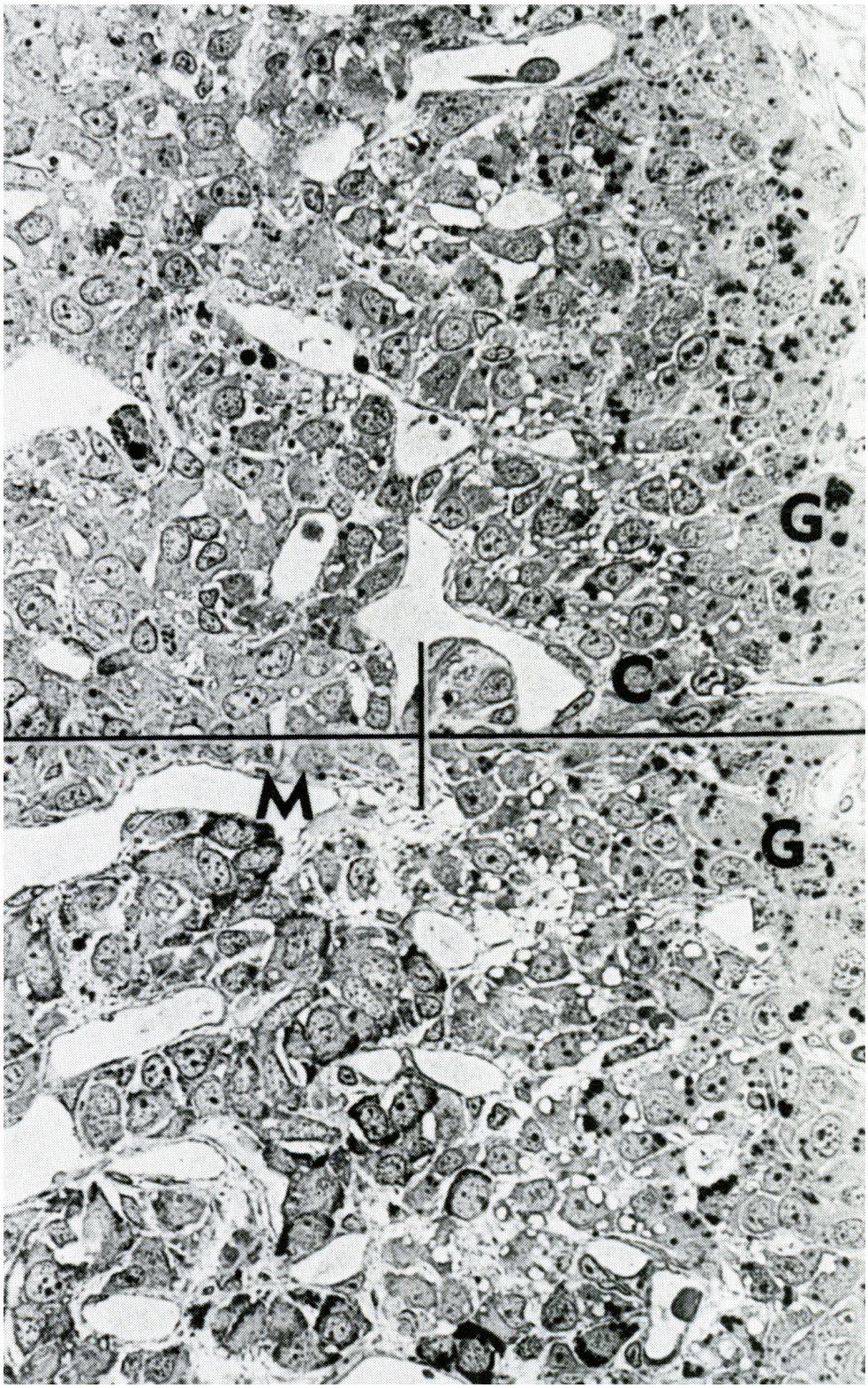

Fig. 5. By the end of the first postnatal week development of the medulla (M) is apparent and cortical cells (C) begin to become organized into distinct cortical zones such as the zona glomerulosa (G). Ammoniacal silver stain. LM X 300.

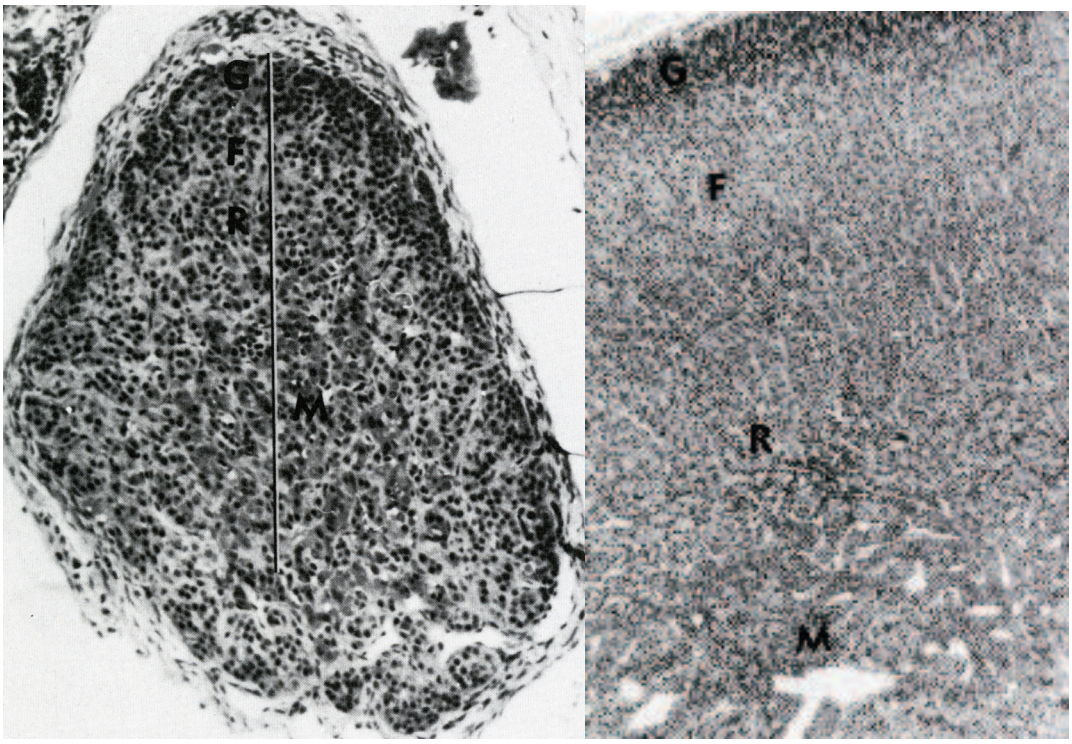

Fig. 6. (*Left*). A section through the adrenal gland of an opossum two weeks postnatal illustrates the initial organization of the cortex into the zones observed in the adult and exhibits a zona glomerulosa (G), a zona fasciculata (F), and a zona reticularis (R). The medulla (M) is located near the bottom center of the photomicrograph. LM X 250. (*Right*). A portion of the adrenal gland from an adult opossum illustrates the basic organization of the cortical region into a zona glomerulosa (G), a zona fasciculata (F), and a zona reticularis (R). The position of the medulla (M) is shown near the bottom of the photomicrograph. Compare this illustration with the illustration shown at the left. LM X 120.

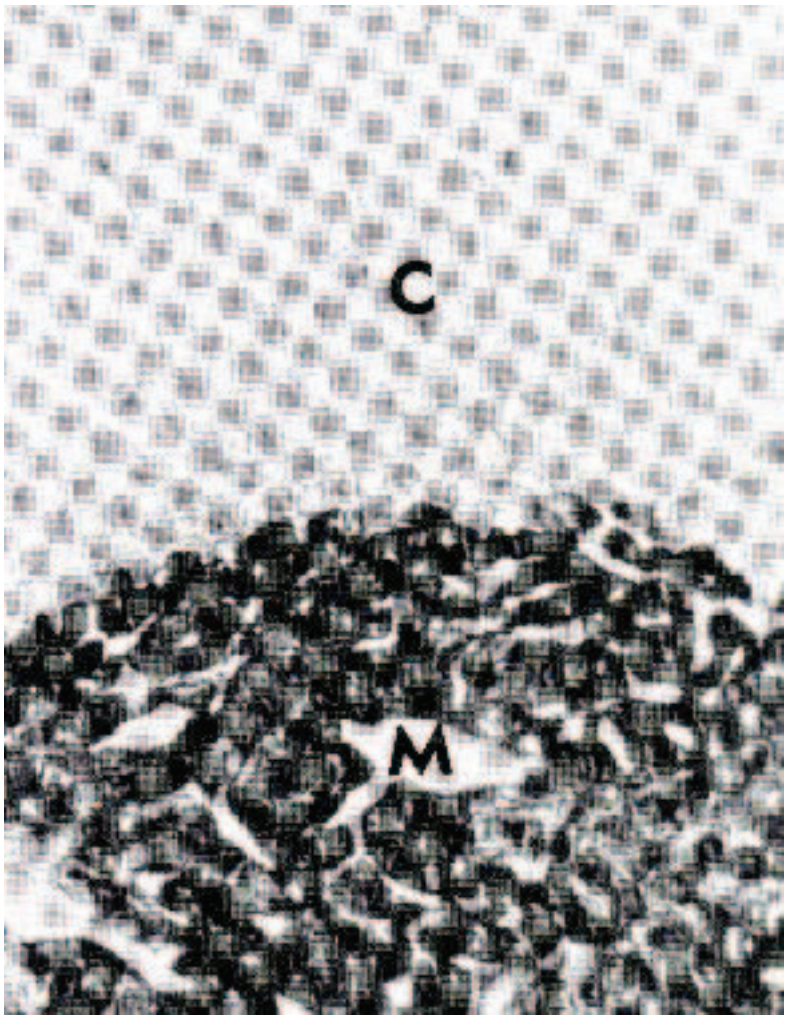

Fig. 7. A portion of an adult opossum adrenal gland fixed in potassium dichromate to illustrate the chromaffin reaction. Cells comprising the medullary region (M) are impregnated by the chromaffin reaction and appear dark whereas the cortical cells (C) are nonreactive. Unstained histological section. LM X 150.

Chapter 34. Brain

Synopsis:

Initial brain formation begins late in prenatal day nine; however, like other major organs, the majority of brain differentiation and development takes place during the postnatal period. Brain organogenesis in the opossum can be subdivided into three morphologically distinct periods. An embryonic period that extends from the ninth prenatal day to the third postnatal day and encompasses the time when the neural tube is transformed into a structure that resembles the overall shape of the brain. The second period of brain development extends from postnatal week one through postnatal week nine. This is a period of brain growth in which regional differentiation occurs and morphologically distinct structures become apparent. A third period of maturation then follows when changes occur within established brain structures.

The neural tube wall during prenatal life consists of a pseudostratified columnar epithelium that forms the ventricular zone. Two lateral expansions occur at the end of the neural tube soon after its closure resulting in the initial formation of the cerebral hemispheres. The telencephalic walls of these evaginations consist of two strata by the eleventh prenatal day: the ventricular zone and a primordial plexiform layer. Both layers remain relatively unchanged during the first portion of postnatal week one. Numerous mitotic figures are observed along the inner surface of the ventricular zone and progenitor cells from within the ventricular zone produce daughter cells that migrate into the primordial plexiform layer during the second half of the first postnatal week. Pro-neurons and pro-glial cells differentiate from this activity and eventually align themselves to form the cortical plate of the neocortex late in the first postnatal week. As a consequence of this cellular migration, the primordial plexiform layer becomes subdivided into outer and inner sub plate zones. Following its formation, the cortical plate expands in both latero-dorsal and antero-posterior directions. With this expansion the cortical plate increases in thickness to six or seven cells by the end of postnatal week two. The cortical plate consists of a layer, ten-twelve cells deep, by the end of postnatal week four. However, the sub plate zone is the most prominent zone within the telencephalon during this period and consists of numerous cells with large oval-shaped nuclei, which tend to be aligned in rows parallel to the cortical plate. Cells with small, round, deep-staining nuclei also are observed in the sub plate zone as well as the cortical plate. As these events occur, the intermediate zone positioned subjacent to the marginal zone expands and is formed by an inner layer of fiber bundles and an outer layer of small oval shaped cells. The nerve fiber layer becomes prominent by the end of postnatal week five. Concurrently the cortical plate becomes increasingly stratified and consists of numerous, more mature appearing cells. The ventricular zone decreases in thickness and mitotic figures are infrequently observed.

The three morphological features characteristic of the neocortex during this period (ventricular zone, sub plate, cortical plate) disappear and the neocortex assumes a striated appearance by the fifth postnatal week. By the end of the ninth postnatal week the cytoarchitecture of the neocortex is well defined and organized into the six layers characteristic of the adult. Regional variation in the six-layered cortex also is apparent at this time. Cell proliferation, elongation of neuroblasts, translocation of perikarya, outgrowth of the axon and formation of dendrites occur in different sequences in various forebrain structures (olfactory bulb, striatum and parietal, cingulate, hippocampal cortex) during

development. Similar events also occur in the auditory centers of the brain stem. The differences in sequence of appearance are related to different architectonic features associated with each region.

The cerebellar cortex also is rudimentary at birth and differentiates during the postnatal period. Axons grow into the cerebellar anlage prior to the formation of distinct cellular layers. Likewise, development of nuclear subdivisions within the olivary complex precedes the lamination of the cortex. The entire process of cortical lamination occurs after birth and continues for about eleven weeks. The external granular layer, the proliferative layer of the cerebellar cortex, reaches its maximum depth between the third and fourth weeks of postnatal life. However, cells from the external granular layer begin to migrate inward from the external surface of the opossum cerebellum late in the first postnatal week. These cells eventually differentiate into basket and stellate neurons, and neurons of the inner granular layer of the definitive cerebellar cortex. The Purkinje cell layer appears near the end of the second postnatal week and the molecular and internal granular layers are established between the third and the eleventh postnatal weeks. Thus, lamination within the neocortex and cerebellar cortex of the opossum brain is a postnatal phenomenon and initially appears and develops at about the same time.

Acknowledgments:

Figs.1 (top), 3 (upper left) and 4 (bottom), courtesy of and from: Krause, W.J. and J.H. Cutts (1984) Scanning electron microscopic observations on the nine-day opossum embryo. Acta Anat. 120:93-97.

Figs. 1 (bottom), 3 (upper top), courtesy of and from: Krause, W.J. (1998) A review of histogenesis/organogenesis in the developing North American opossum (*Didelphis virginiana*). Adv. Anat. Embryol. Cell Biol. 143 (I): Springer Verlag, Berlin, and pp 143.

Figs. 5, 6, 7, 8, 9, 10, 11, 12, 13, 14, 15, 16 and 17, courtesy of and from: Krause, W.J. and N.R. Saunders. (1994). Brain growth and neocortical development in the opossum. Ann. Anat. 176:395-407.

Figs 18, 19, 20 and 21, courtesy of and from: Ulinski, P.S. (1971). External morphology of pouch young opossum brains: a profile of opossum neurogenesis. J. Comp. Neurol. 142:33-58.

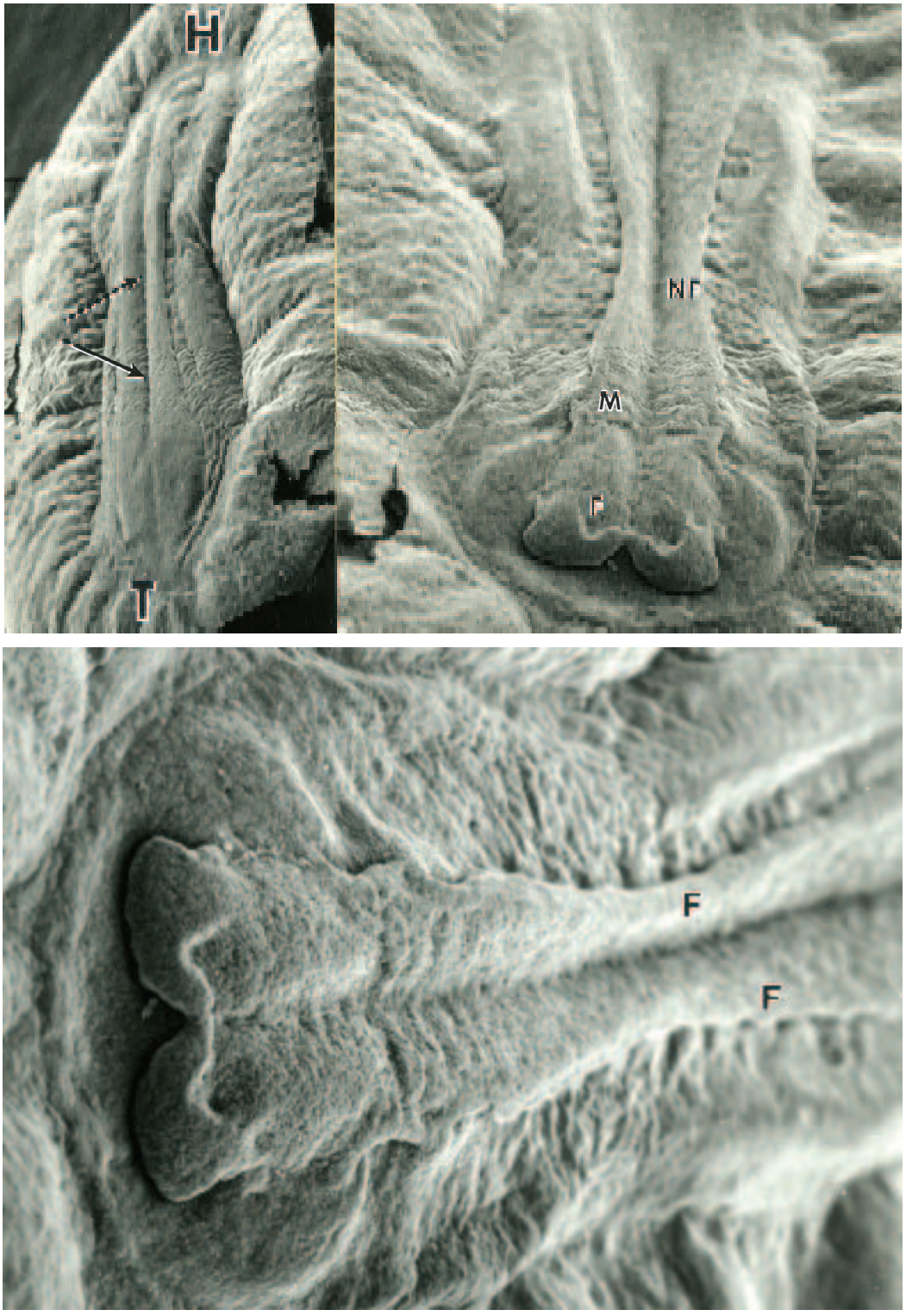

Fig. 1. (*Above left*). A scanning electron micrograph illustrates the head (H) and tail (T) regions of a nine-day opossum embryo. The neural groove (arrows) also can be observed. SEM X 30. (*Above right*). When the nine-day opossum embryo is viewed from a cranial to caudal direction, the forebrain (F), midbrain (M), and neural folds (NF) are readily apparent. SEM X 36. (*Below*). When viewed from a different angle, the initial pattern of brain development is more easily visualized (left). The developing spinal cord, which appears as a deep groove with limiting neural folds (F), courses horizontally along the length of the embryo toward the right. SEM X 80.

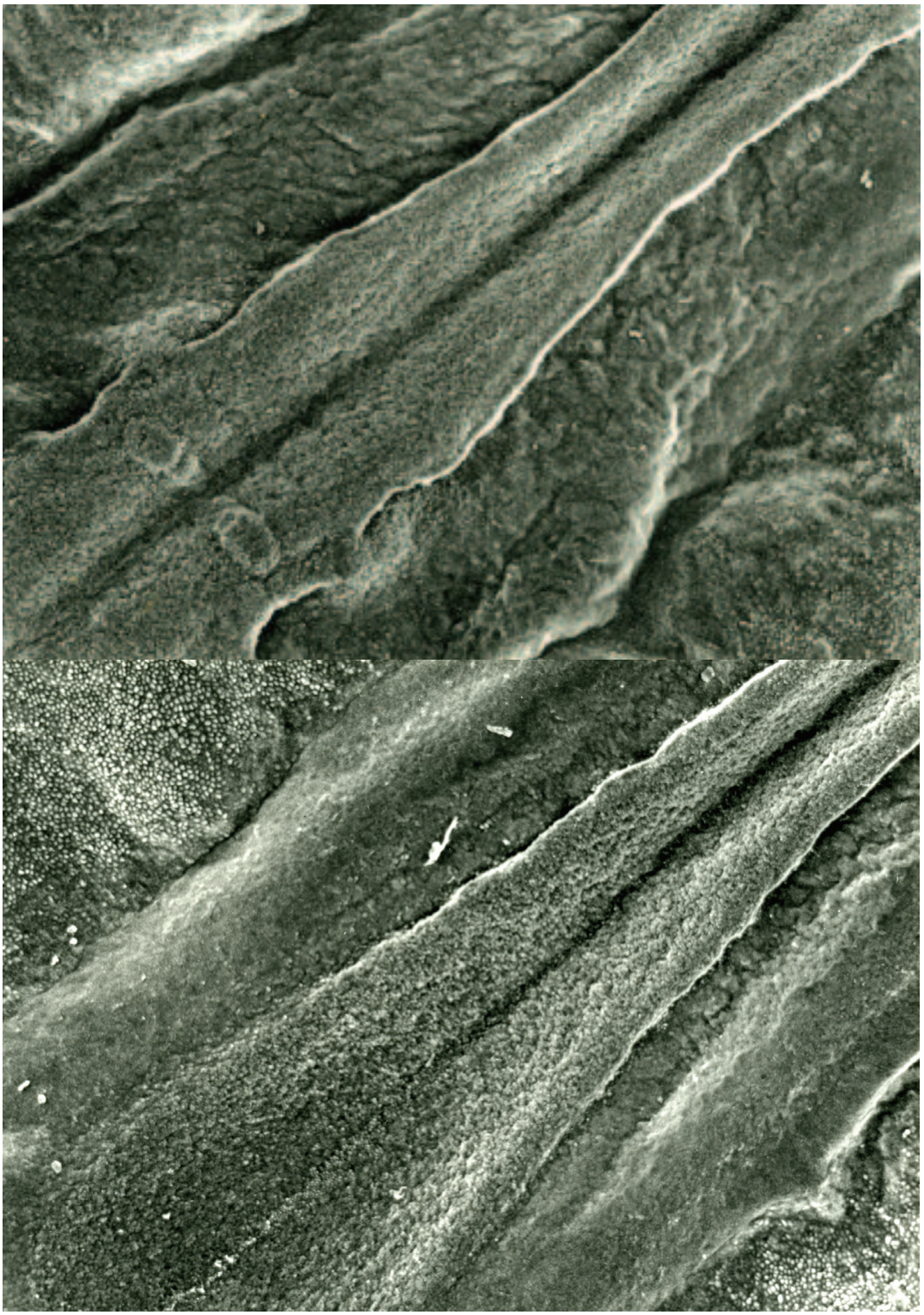

Fig. 2. (*Above*). The developing midbrain region (lower left) and proximal spinal cord of a nine-day opossum embryo seen at increased magnification and viewed from above. SEM X 75. (*Below*). The developing distal spinal cord (upper right) and developing tail region of a nine-day opossum embryo as viewed from above. SEM X 75.

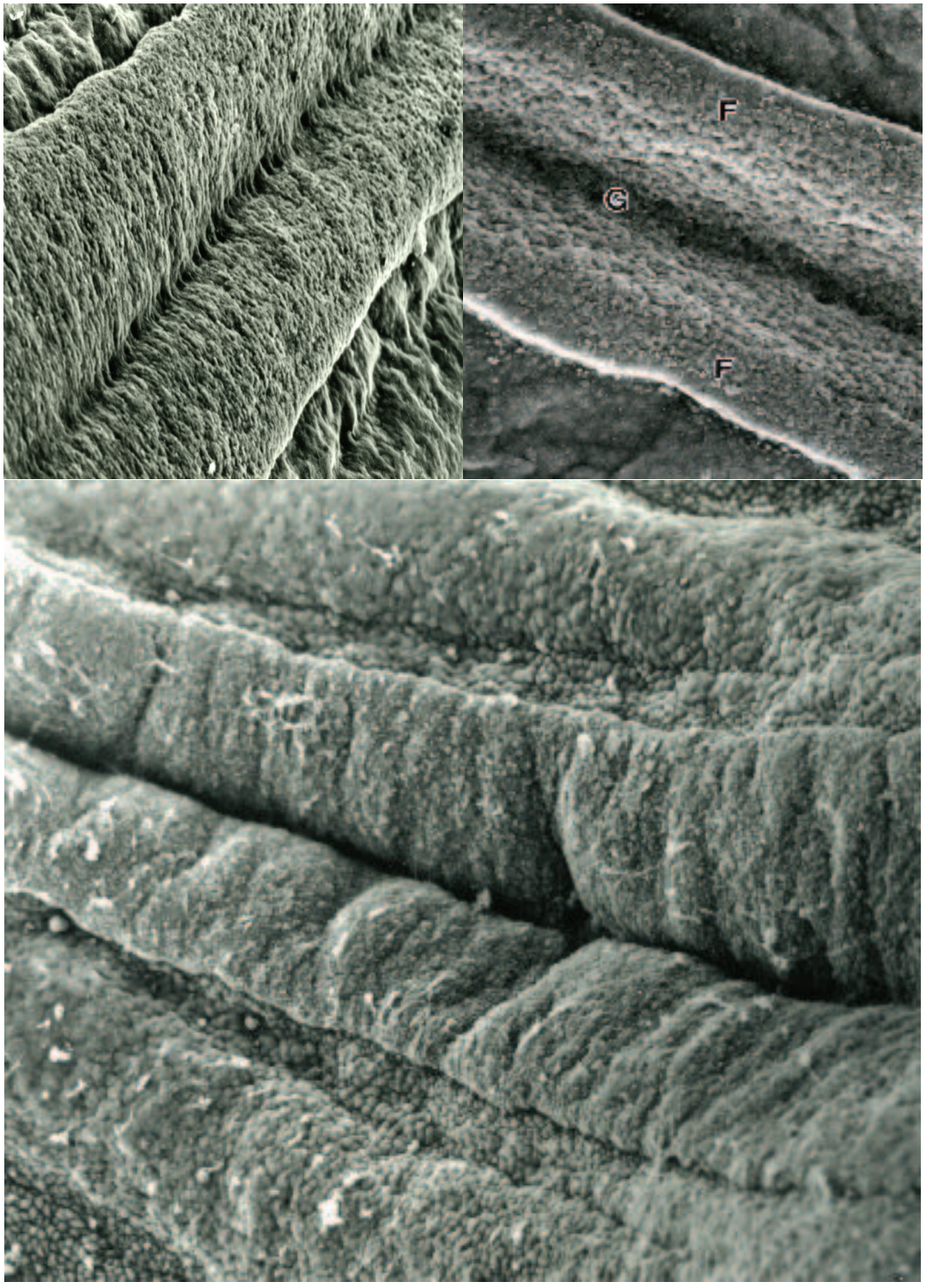

Fig. 3. (*Above left*). Surface features of the neural folds as well as the floor of the developing neural groove viewed from a lateral angle. Nine-day opossum embryo. SEM X 150. (*Above right*). A micrograph illustrates the neural folds (NF) and the neural groove (G)) of a slightly older nine-day opossum embryo viewed from above. SEM X 130. (*Below*). Continued expansion of the neural folds results in the formation of a much deeper and narrower neural groove. Note that the neuroectoderm of the neural folds is continuous with the ectoderm covering the remainder of the embryonic sphere. Nine-day opossum embryo. SEM X 120.

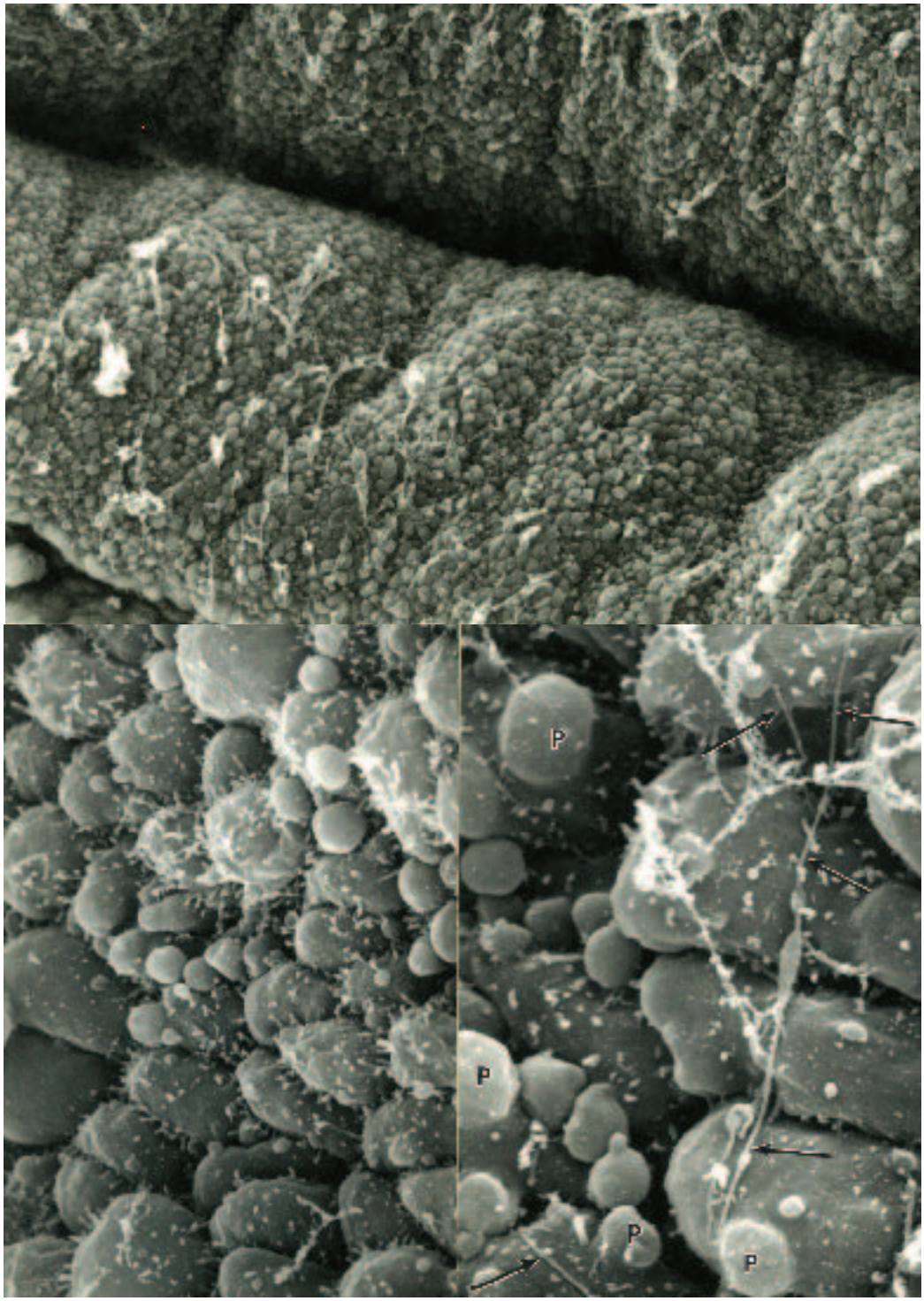

Fig. 4. (*Above*). A region from the neural folds and neural groove of the nine-day opossum embryo shown in figure 2 (bottom) but viewed at increased magnification. SEM X 250. (*Below left*). Increased magnification of the neural ectoderm from the crest region near the neural folds of the opossum embryo viewed above. Note the dome-shaped cell tops and the secondary protrusions as well as scattered microvilli. SEM X 3,000. (*Below right*). Surface features of cells deep within the neural groove of the nine-day opossum embryo illustrates in greater detail the protuberances (P) from cell apices and what appear to be nerve processes (arrows). SEM X 6,000.

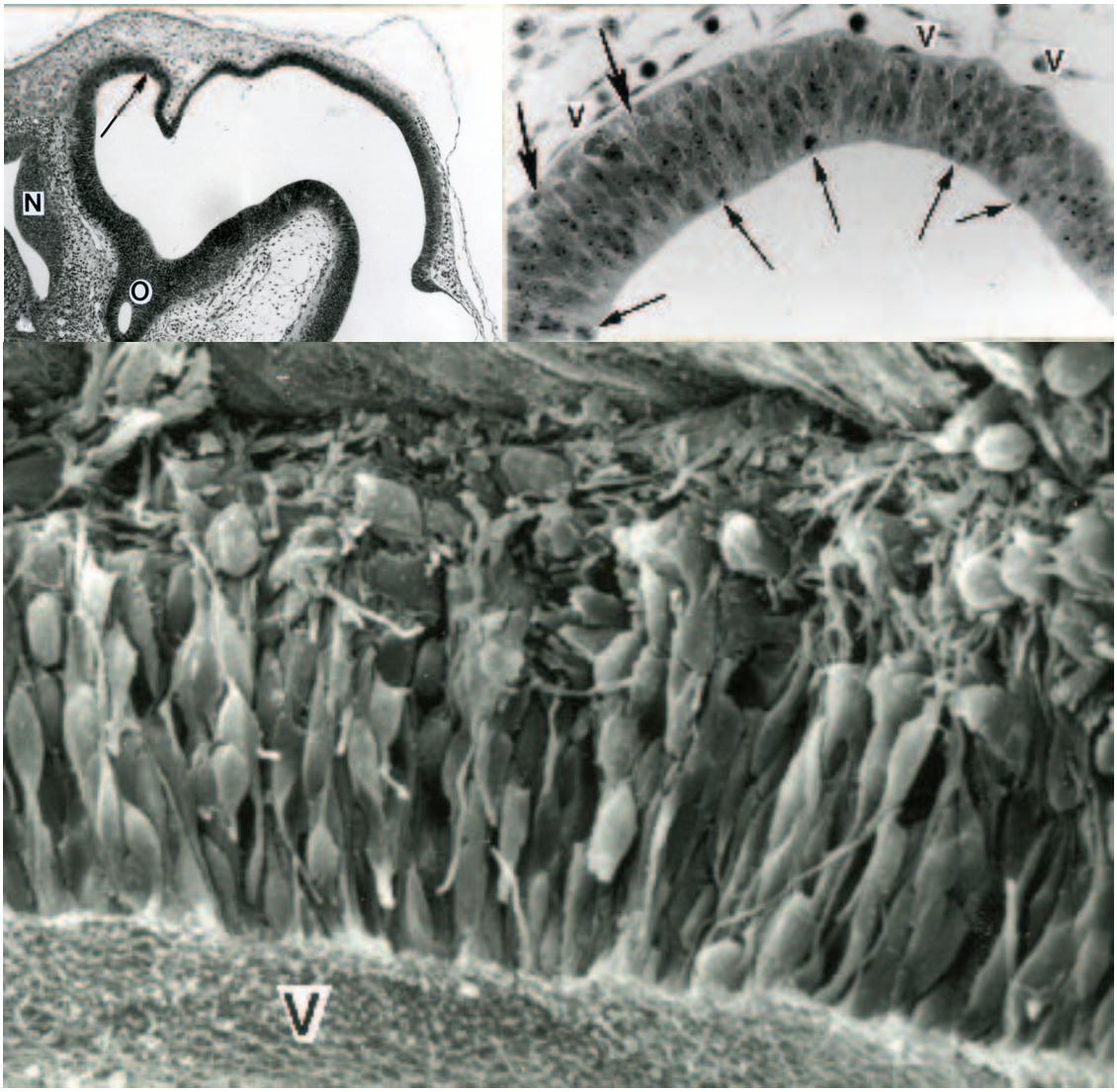

Fig. 5. (*Above left*). A sagittal section through the head of a 10.5 day opossum embryo demonstrates an evagination (arrow) of the developing brain that will result in the formation of a cerebral hemisphere. A region of the developing optic nerve (O) and nasal cavity (N) also can be observed. LM X 50. (*Above right*). A region of the telencephalic wall similar to that illustrated in the left figure but observed at increased magnification. Numerous mitotic figures (small arrows) are found along the ventricular surface. What may be the primordial plexiform layer (large arrows) also is shown. Note the developing vasculature (V) immediately adjacent to the forming brain. 10.5 day opossum embryo. LM X 375. (*Below*). A fractured specimen through the telencephalic wall of a 10.5 day opossum embryo similar to those shown in the above figures. The ventricular surface (V) is shown at the bottom of the micrograph. Note that the fractured surface reveals the three-dimensional appearance of the spindle (oval) shaped cells forming the telencephalic wall. Compare the structure of these cells with those shown in the above right figure. SEM X 1,000.

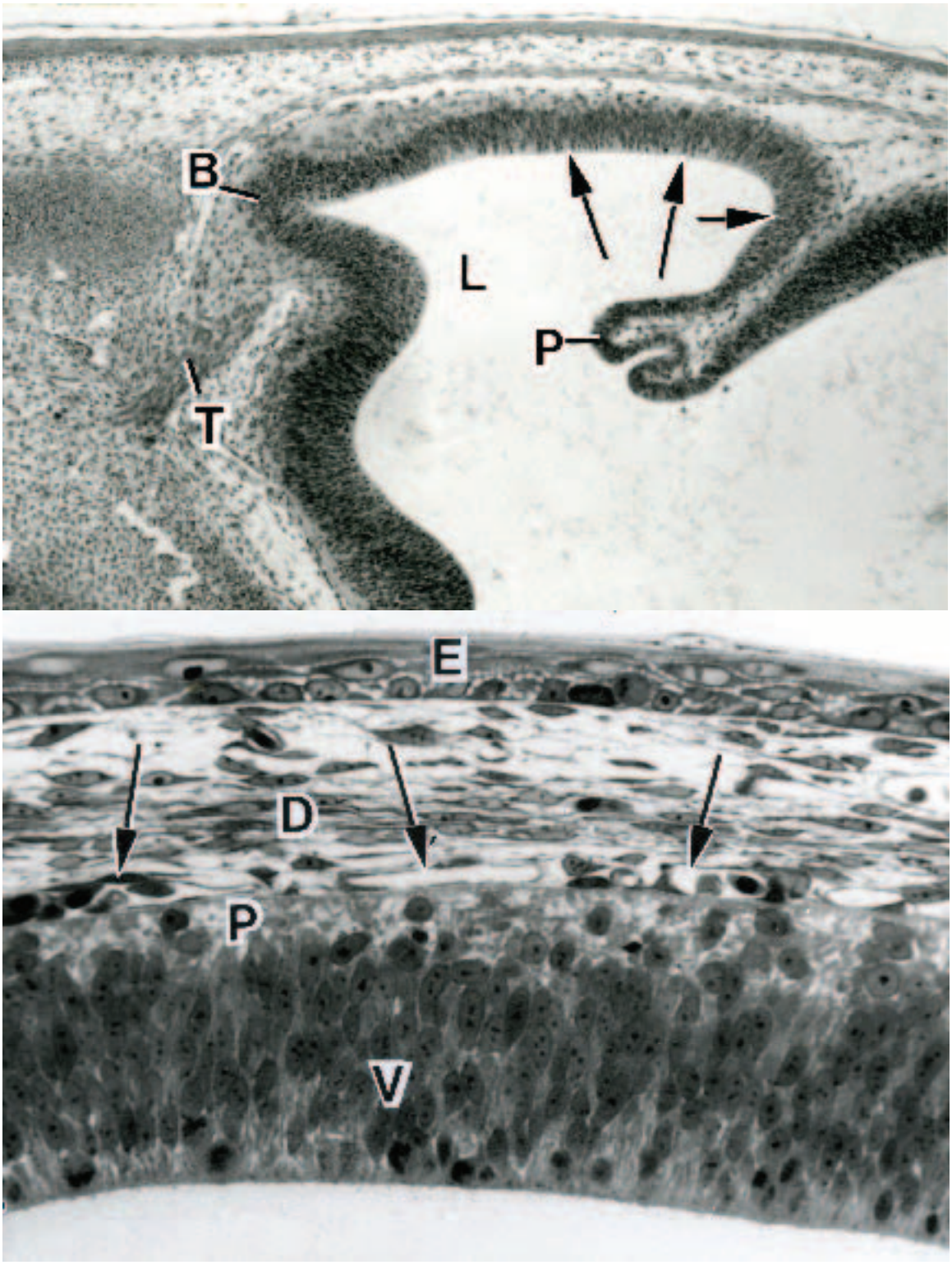

Fig. 6. (*Above*). A portion of the telencephalon (arrows) from an 11.5 day opossum embryo. Regions of developing olfactory bulb (B), choroid plexus (P), lateral ventricle (L) and ganglion terminale (T) also are shown. LM X 125. (*Below*). Increased magnification of the telencephalic wall at this stage of development shows that it consists of two strata: a thin primordial plexiform layer (P) and a thick ventricular zone (V). Numerous mitotic figures occur within the ventricular zone adjacent to the ventricular lumen. Note the abundance of blood vessels (arrows) adjacent to the external surface of the primordial plexiform layer. The epidermis (E) and forming dura (D) also are shown. LM X 850.

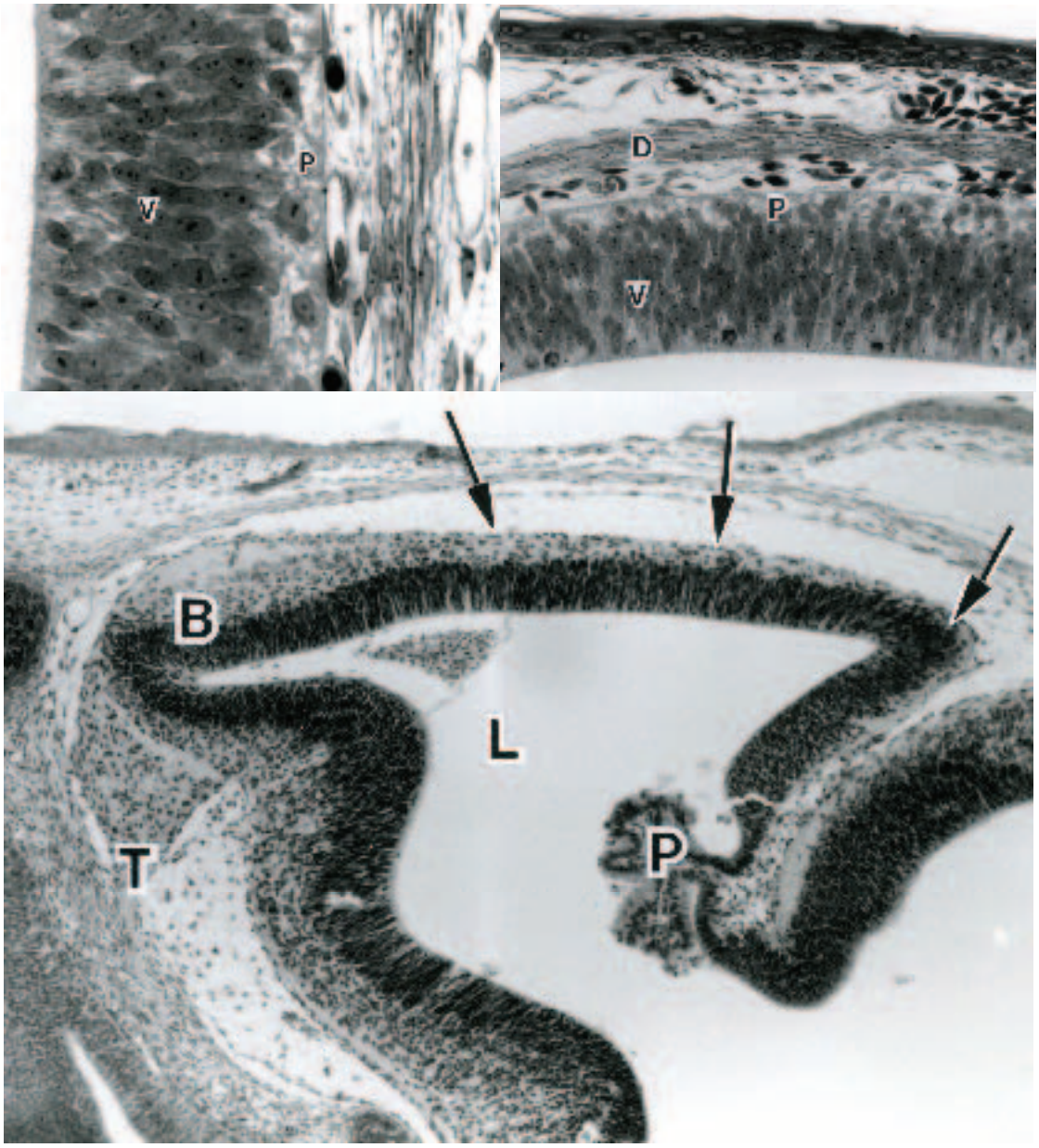

Fig.7. (*Above left*). A region of the telencephalic wall form an 11.5 day opossum embryo illustrates the ventricular zone (V) and primordial plexiform layer (P). LM X 500. (*Above right*). A section through the telencephalon of a newborn opossum demonstrates little if any obvious structural change has occurred within the primordial plexiform layer (P) or ventricular zone (V). Compare with the left figure. The overlying dura (D) has, however, increased in density. Compare with bottom figure six. LM X 450. (*Below*). A sagittal section through the head of an opossum two days postnatal illustrates the expanding lateral ventricle (L), the forming olfactory bulb (B), ganglion terminale (T), and choroid plexus (P). Note the continued expansion of the telencephalon (arrows). Compare this figure with figure six (above) and figure five (above left). LM X 125.

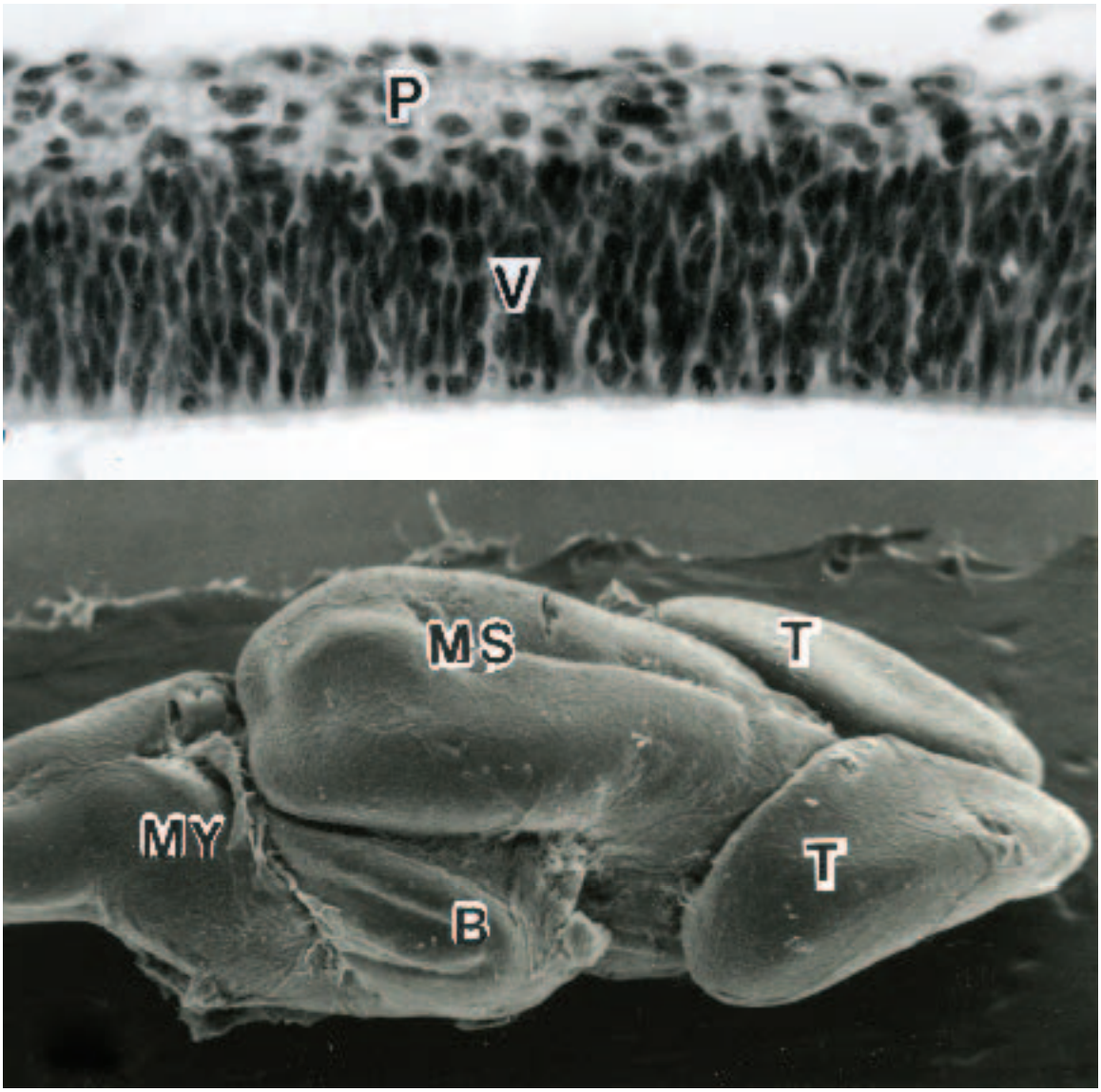

Fig. 8. (*Above*). Increased magnification of the telencephalic wall of a two-day-old opossum demonstrates little if any structural change in the ventricular zone (V). The lumen of the lateral ventricle is located at the bottom of the figure. Note that the primordial plexiform layer (P) now appears to exhibit a slight increase in thickness as compared to earlier ages. LM X 600. The entire brain of an opossum 4.5 days postnatal as viewed by scanning electron microscopy. The expanding cerebral hemispheres (T) of the telencephalon as well as the mesencephalon (MS), myelencephalon (MY) and forming cerebellum (B) can be observed. SEM X 40.

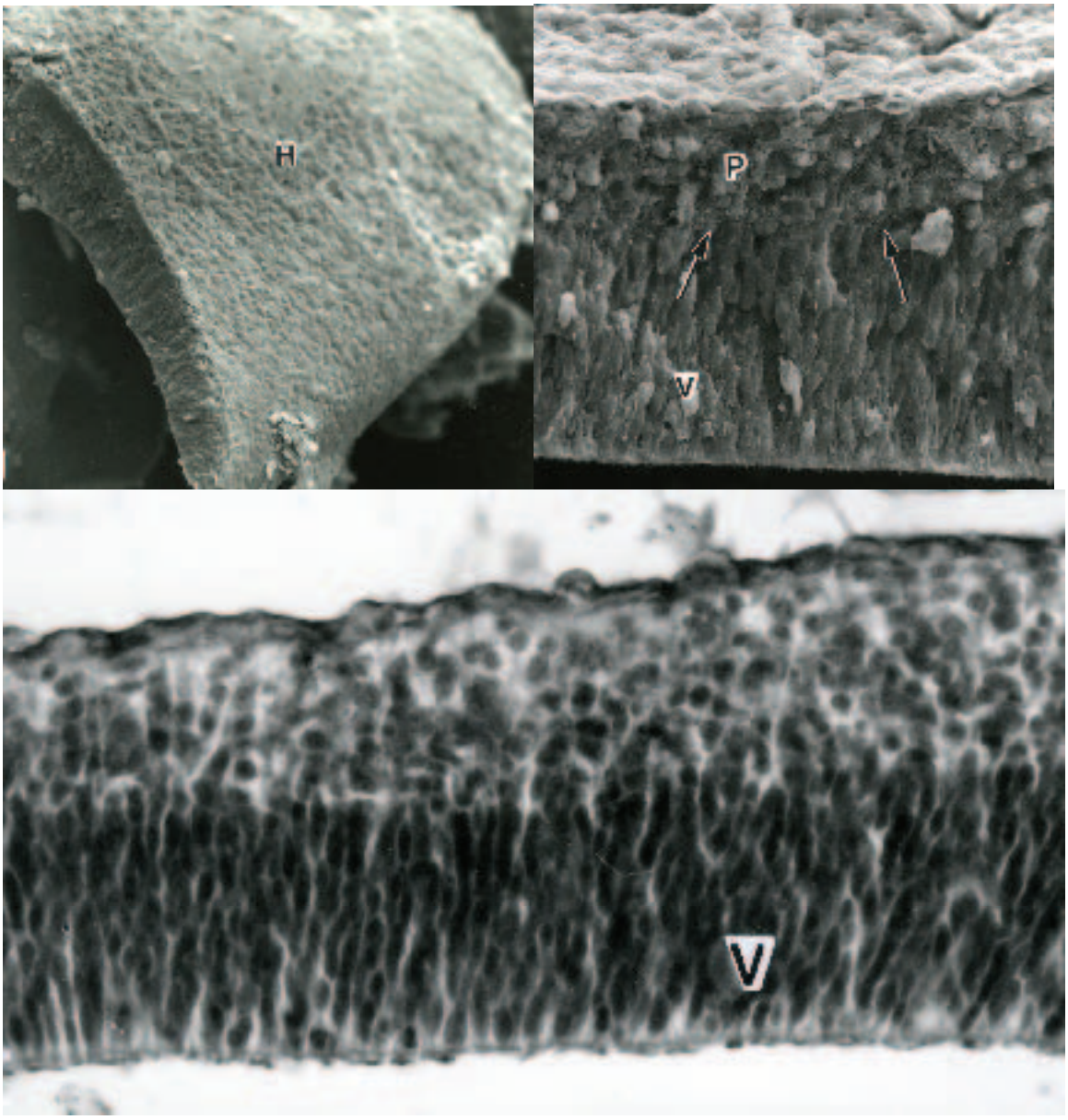

Fig. 9. (*Above left*). A preparation of a cerebral hemisphere (H) fractured transversely midway along its length and viewed from a posterior direction illustrates the depth of the developing telencephalic wall. SEM X 100. (*Above right*). Increased magnification of the fracture plane of the figure to the left illustrates that fracture is not uniform but deviates from a straight line about two-thirds of the way from the ventricular surface at the bottom of the illustration. The deviation of the line of fracture occurs at the boundary (arrows) between the ventricular zone (V) and the primordial plexiform layer (P). Cells within the primordial plexiform layer are for the most part round in shape with intermingling processes. Differences in architecture are believed to cause in the deviation in the plane of fracture between these two layers, which routinely occurs at this boundary in the presumptive neocortex. SEM X 400. (*Below*). A section through a developing cerebral hemisphere of a pouch young opossum 4.5 days postnatal illustrates the increase in thickness of the telencephalic wall. The ventricular zone (V) appears to be of a similar depth to that observed in earlier stages. Compare to top illustration of figure 8. LM X 600.

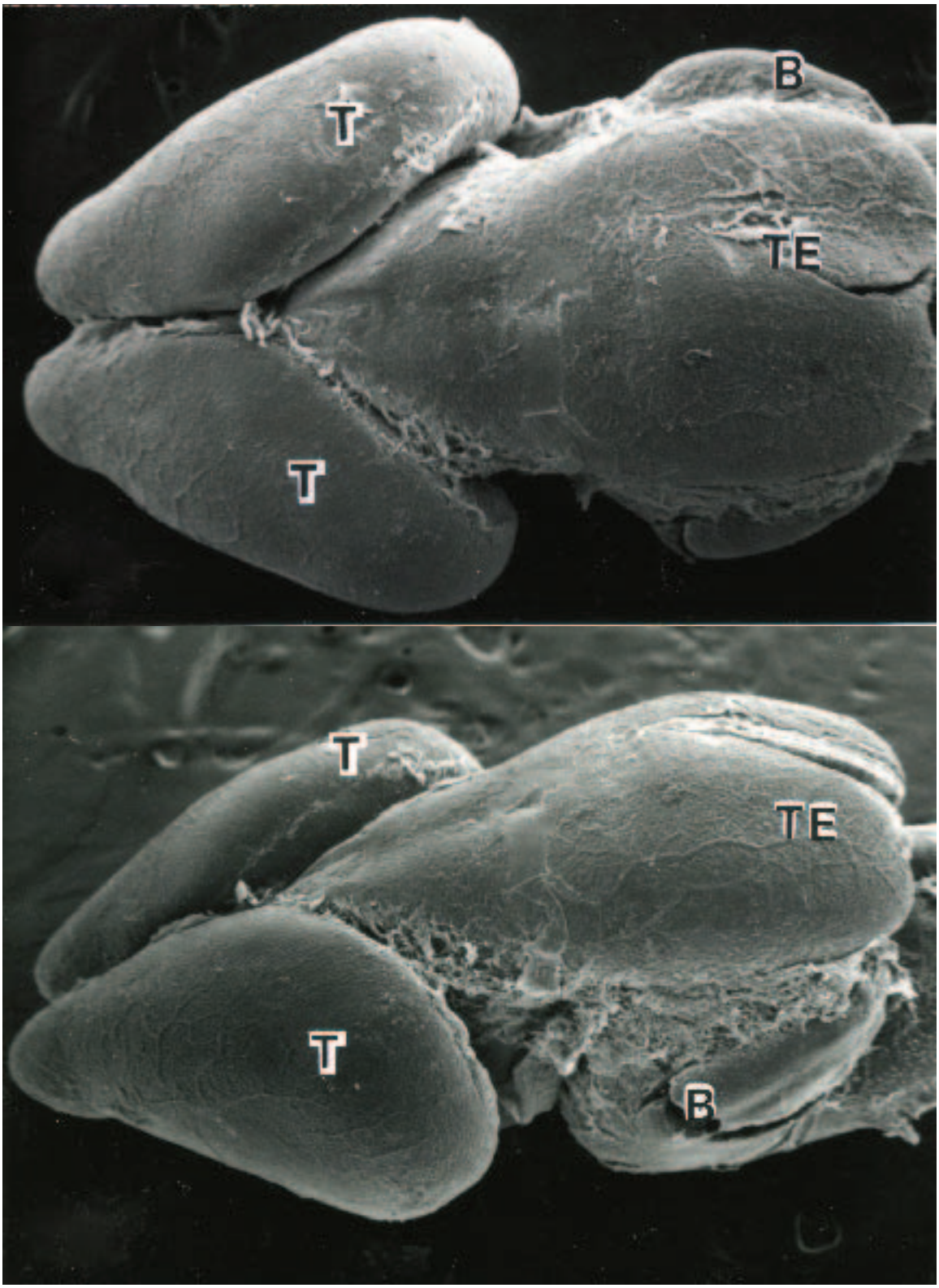

Fig. 10. (*Above*). The telencephalon (T) of an opossum one week postnatal as viewed from a dorsal perspective. Note the expanding cerebral hemispheres, the forming tectum (TE) and cerebellum (B). SEM X 50. (*Below*). The cerebral hemispheres of the telencephalon (T), the region of the forming tectum (TE) and cerebellum (B) of a week old opossum brain as seen from a dorsal lateral perspective. SEM X 50.

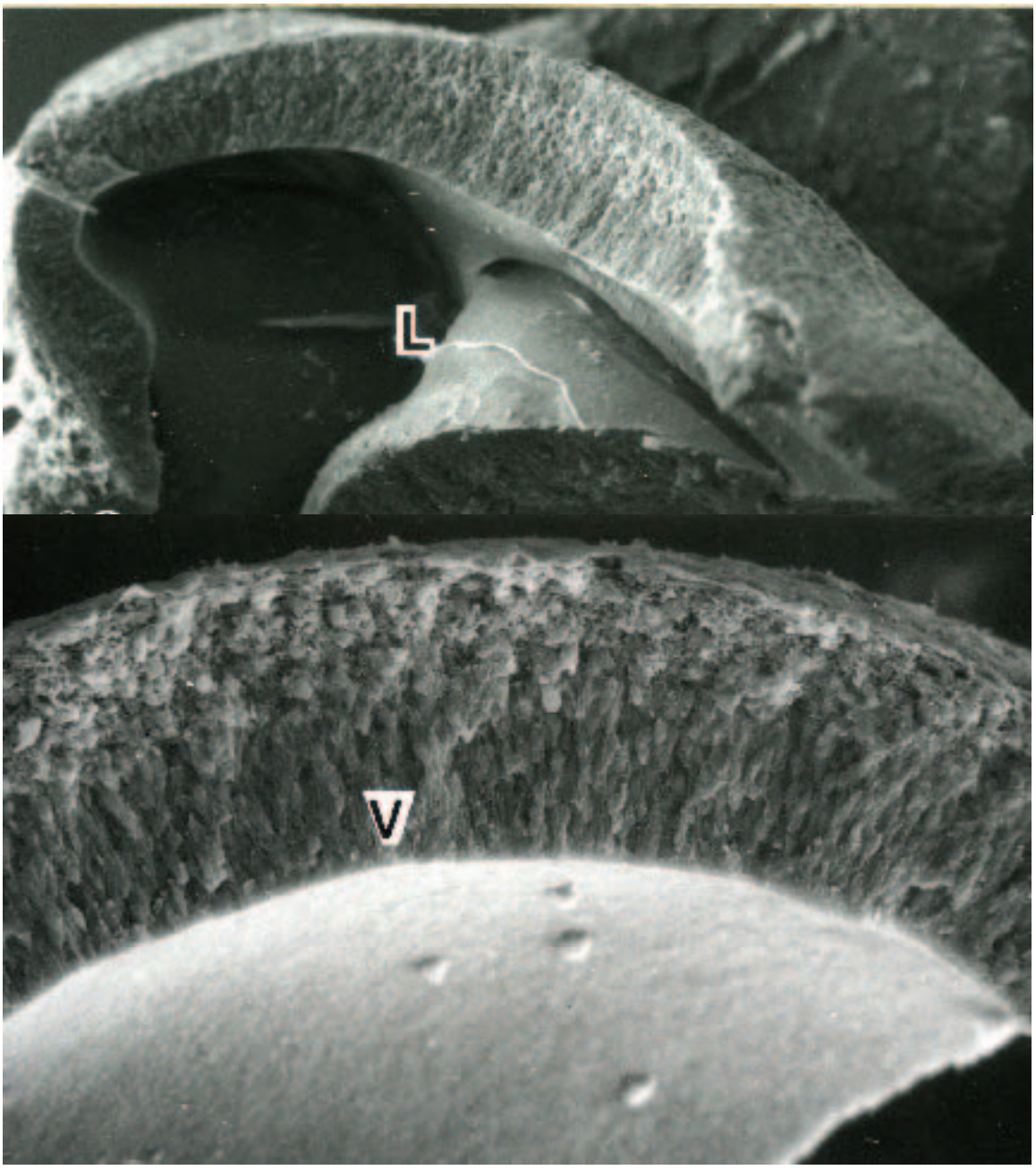

Fig. 11. (*Above*). A fractured cerebral hemisphere viewed from a posterior angle looking into the lumen lateral ventricle (L) illustrates a variation in depth of the provisional neocortex. Opossum one week postnatal. SEM X 100. (*Below*). The ventricular zone (V) continues to be distinguished from adjacent layers of the telencephalon by the plane of fracture in the developing neocortex. Opossum one week postnatal. SEM X 200.

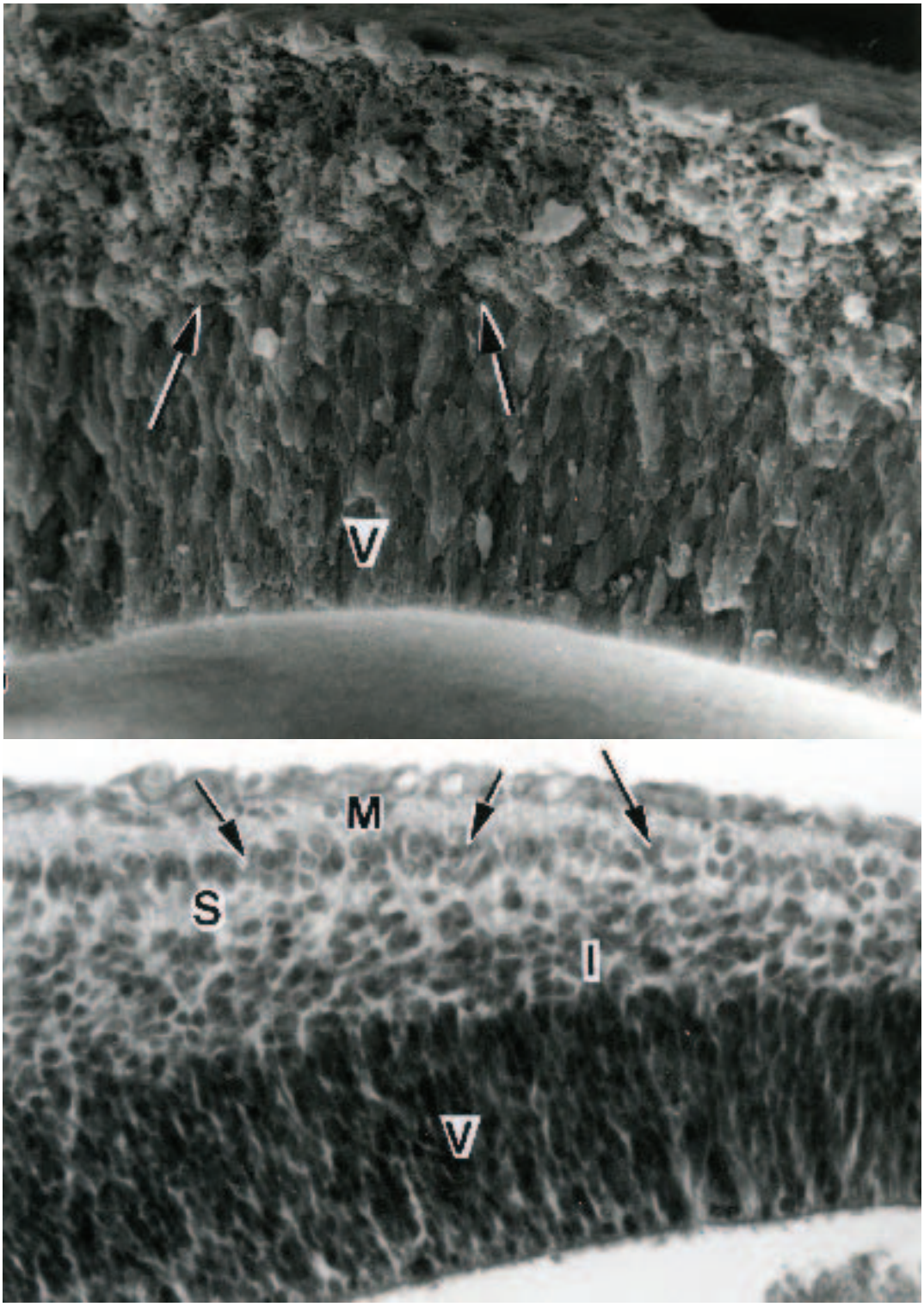

Fig. 12. (*Above*). The ventricular zone (V) continues to be comprised of spindle shaped cells that are arranged parallel to one another. The region external to the fracture line (arrows) consists of rounded cells with intermingling processes. Developing neocortex from an opossum one week postnatal. SEM X 800. (*Below*). The cortical plate (arrows) is present within the opossum telencephalic wall by postnatal day seven and subdivides the differentiating neocortex into four basic strata: a ventricular zone (V), an intermediate zone (I), a sub plate zone (S), and a marginal zone (M). LM X 600.

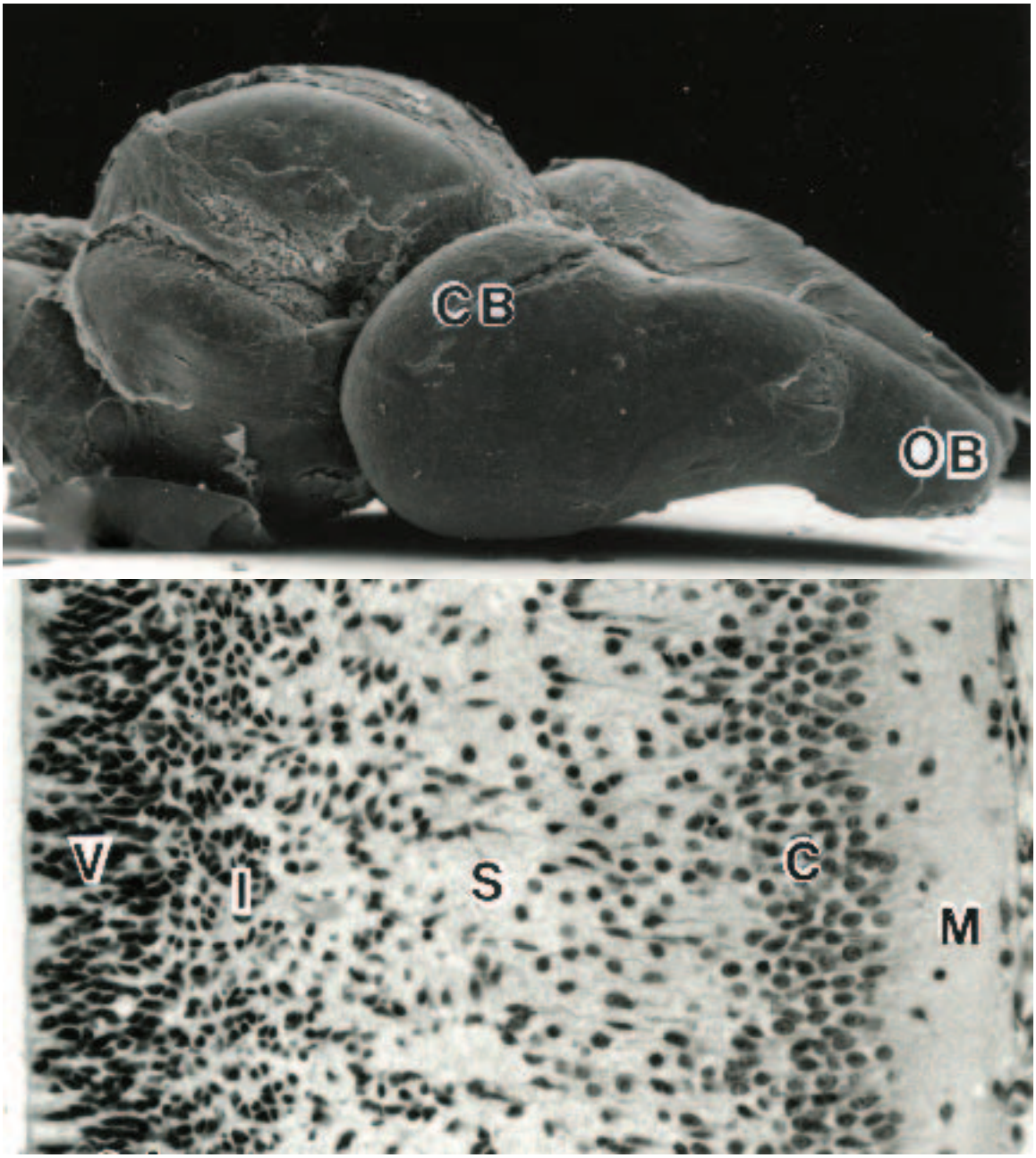

Fig. 13. (*Above*). The developing brain from a pouch young opossum two weeks postnatal. Note the continued expansion of the cerebral hemispheres (CB) and the olfactory bulb (OB). SEM X 40. (*Below*). The cortical plate (C) increases in depth to about six or seven cells and the sub plate zone (S) forms a prominent layer in the neocortex by the end of the second postnatal week. The marginal zone (M) also shows an increase in depth as well as an increase in density of component processes. The intermediate zone (I) expands to consist of several layers of irregularly arranged cells whereas the ventricular zone (V) is now of less depth than earlier stages. However, mitotic figures continue to be observed in this zone immediately adjacent to the lumen of the ventricle. LM X 500.

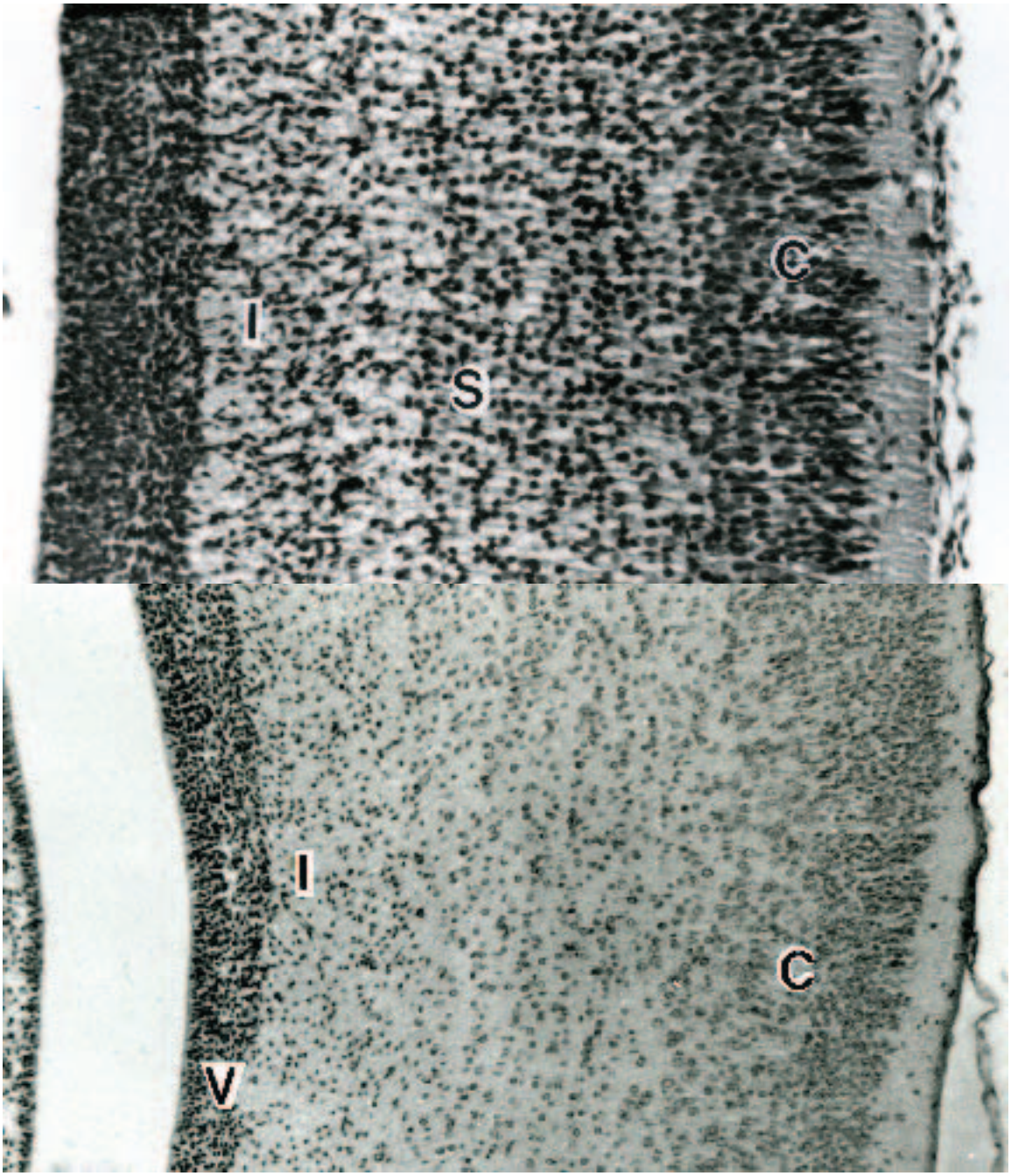

Fig. 14. (*Above*). The cortical plate (C) of the neocortex continues to increase in depth through the fourth postnatal week, as does the sub plate zone (S). Cells of the sub plate zone at this time may appear to be organized into horizontal rows arranged parallel to the cortical plate. The intermediate zone (I) also expands considerably in comparison to earlier stages of development. LM X 400. (*Below*). By the end of the fifth postnatal week, the cortical plate (C) shows considerable stratification and the ventricular zone (V) is reduced in depth. The intermediate zone (I) now consists of two substrata: a sub ventricular layer of nerve fibers and an outer layer of scattered cells. LM X 300.

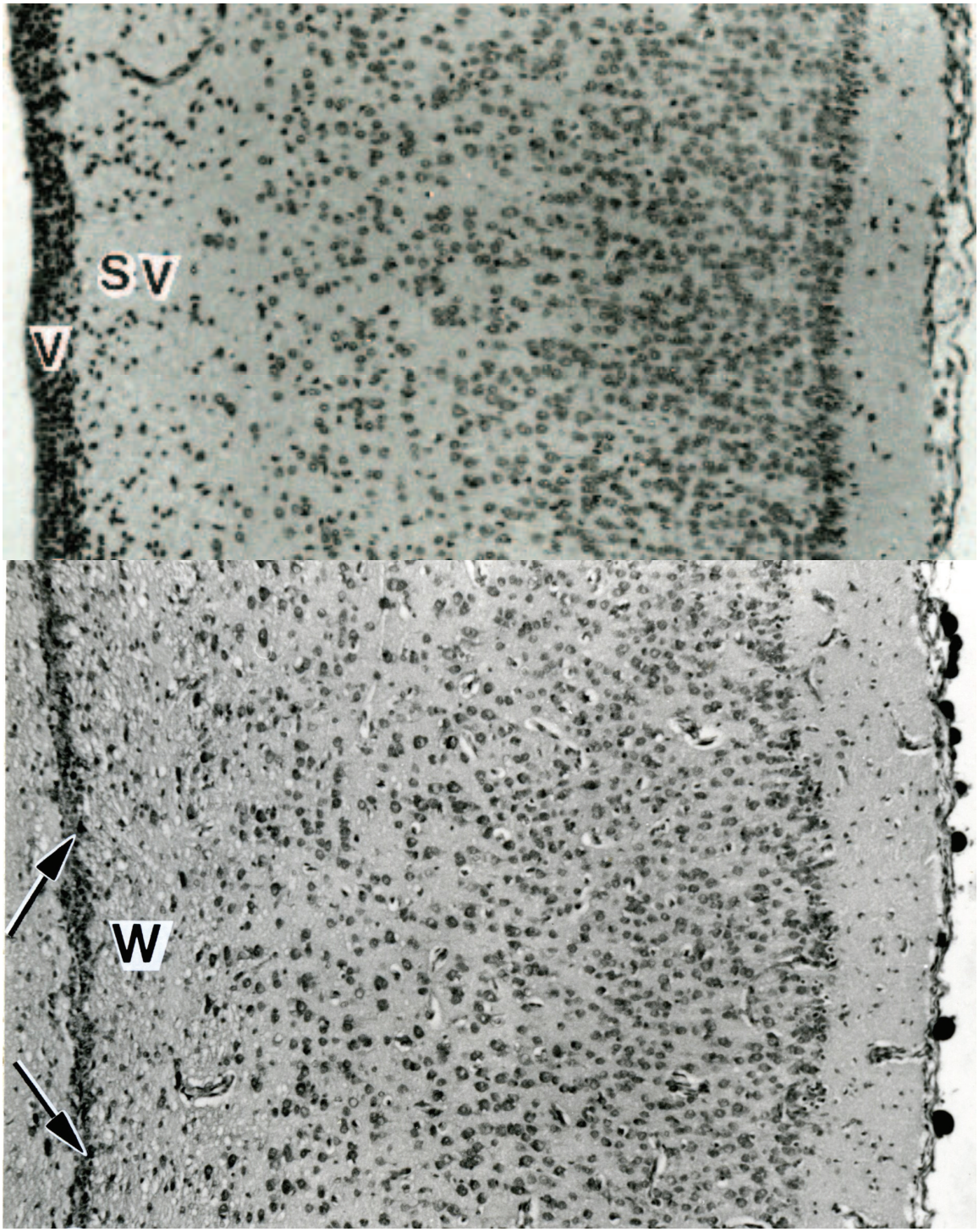

Fig. 15. (*Above*). The ventricular zone (V) continues to thin and the sub ventricular zone (SV) of white matter expands in the neocortex of opossums six weeks postnatal. LM X 350. (*Below*). By the ninth postnatal week, cells within the neocortex show continued stratification and the former ventricular zone (arrows) is reduced to a thin ependymal layer one to two cells thick. Note the expansion of white matter (W) immediately adjacent to the ependymal layer. LM X 275.

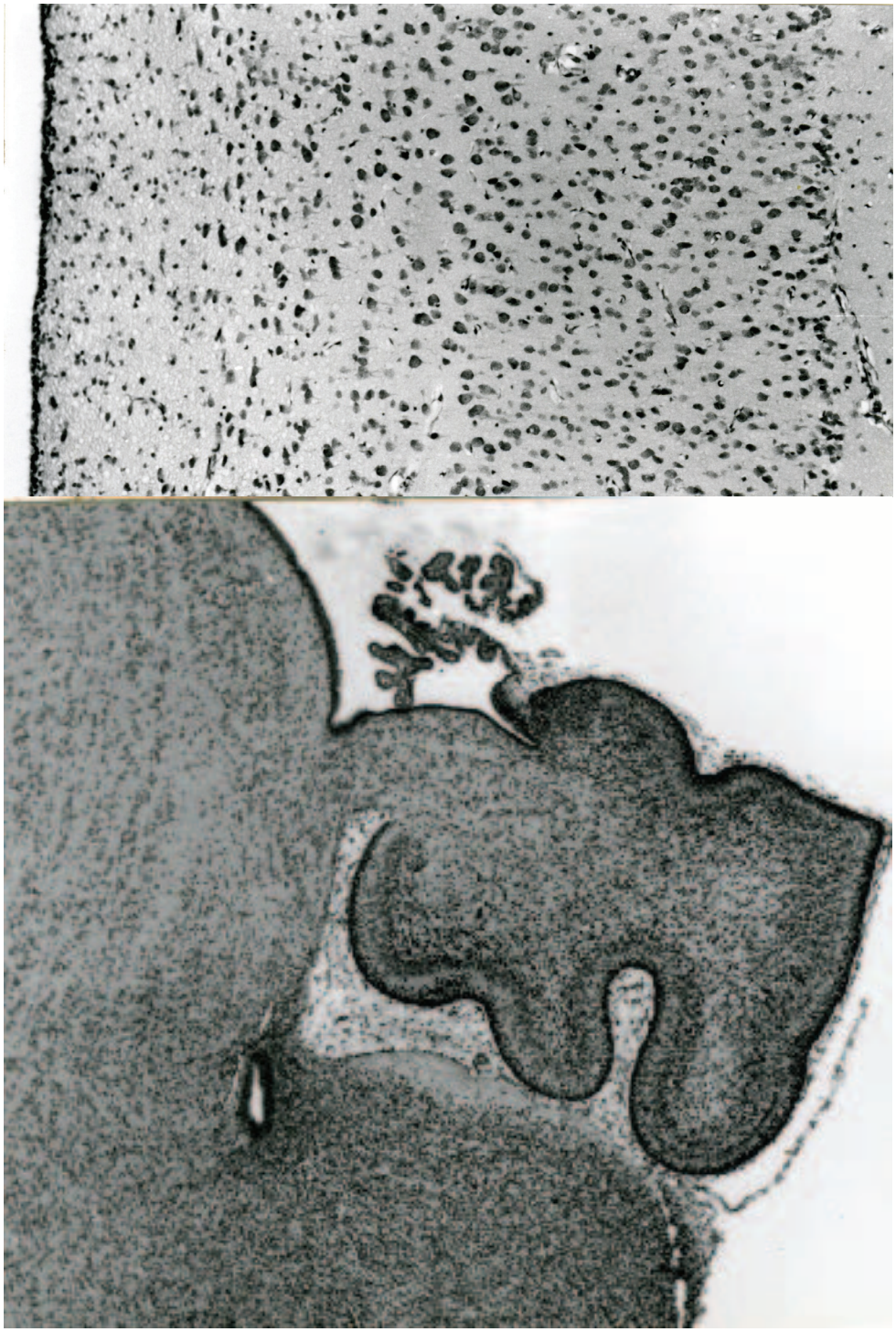

Fig. 16. (*Above*). A section through the neocortex of an opossum twelve weeks postnatal illustrates a stratification pattern similar to that observed in the adult. LM X 250. (*Below*). A section through a region of the developing cerebellar cortex from an opossum four weeks postnatal illustrates its state of organogenesis at this stage of development. LM X 180.

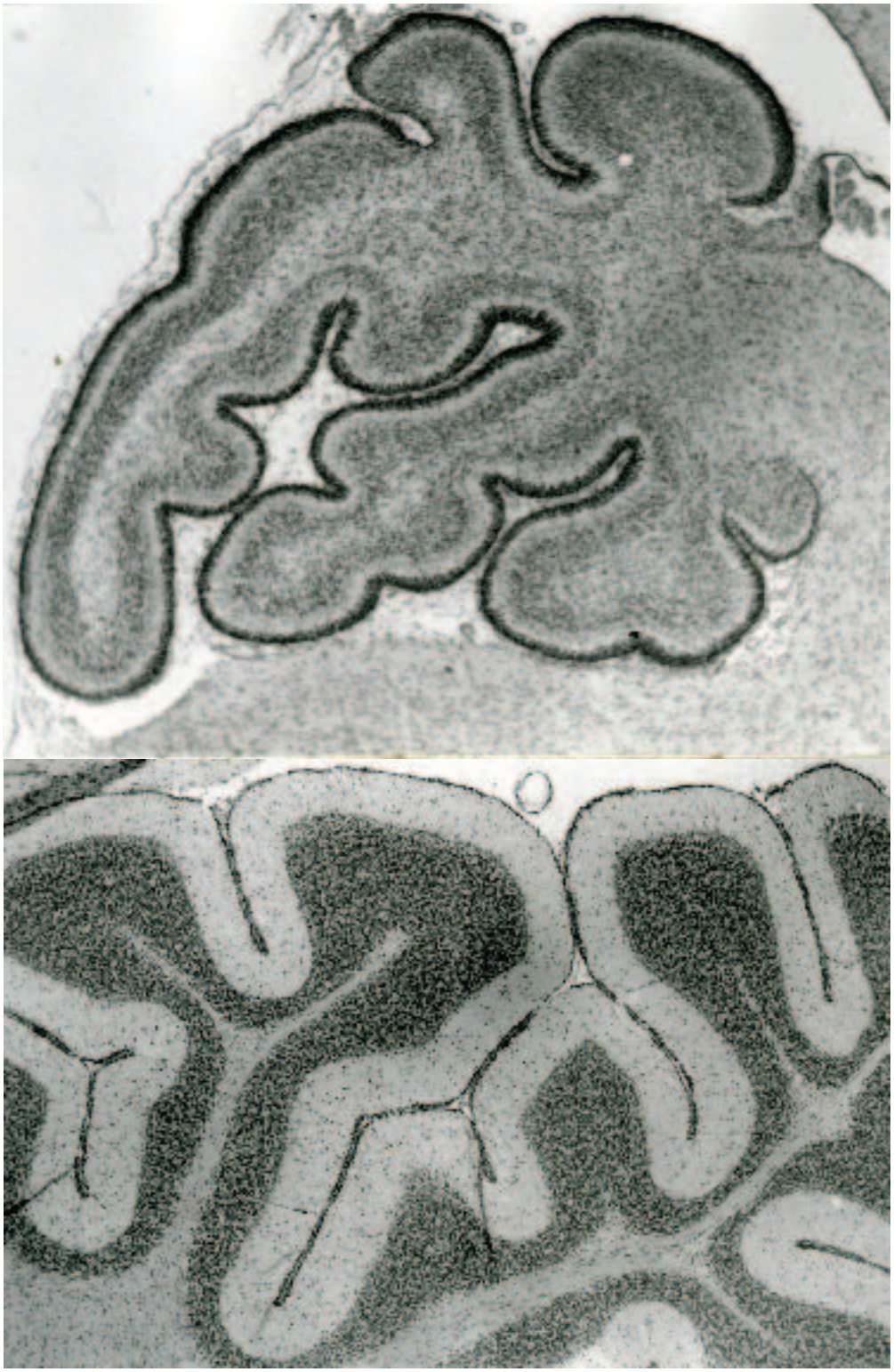

Fig. 17. (*Above*). A section through the cerebellar cortex of an opossum six weeks postnatal illustrates its continued development. Note the density of cells comprising the external granular layer. LM X 180. (*Below*). A section through the cerebellar cortex of an opossum eleven weeks postnatal illustrates a more adult-like appearance. LM X 70.

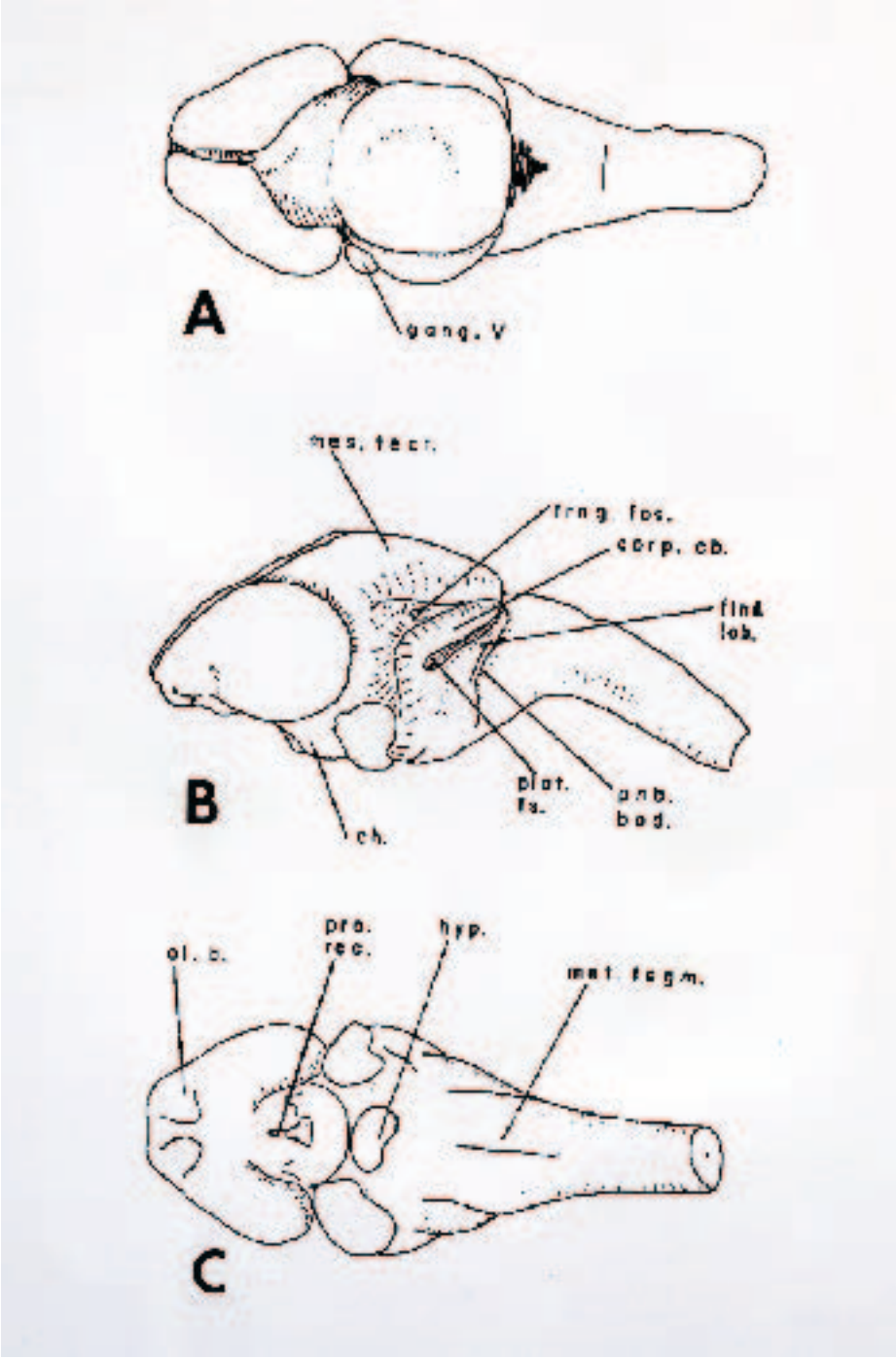

Fig. 18. The dorsal (**A**), lateral (**B**), and ventral (**C**) features of an opossum brain three days postnatal. This stage represents the end of the period of embryonic brain development. Trigeminal ganglion, *Gang. V*, mesencephalic tectum, *mes. tect.*, triangular fossa, *trng. fos.,* corpus cerebelli, *corp. cb.,* flocculonodular lobe, *flnd. lob.,* pontobulbar body, *pnb. bod.,* posterolateral fissure, *plat. fs.,* optic chiasm, *ch.,* olfactory bulb, *ol. b.,* preoptic recess, *pro. rec.,* hypophysis, *hyp.*, and metencephalic tegmentum, *met. tegm.*.

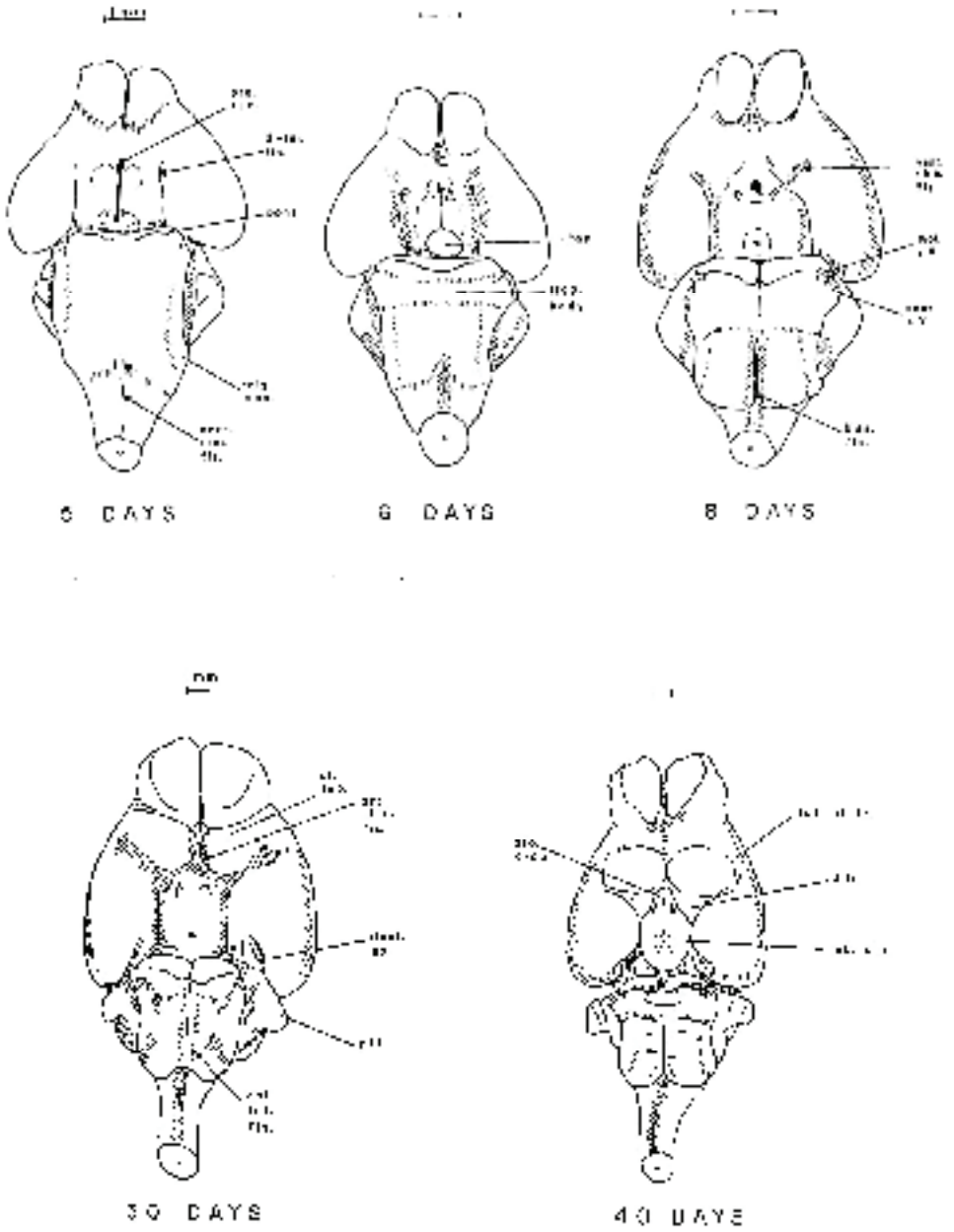

Fig. 19. Line drawings illustrate the ventral brain surface of pouch young opossums from postnatal day five to postnatal day forty. The pons is present by day five and the trapezoid body (*trap. body*) by day six. The basilar fissure (*bas. fis.*) and ventral rhinal fissure (*vent. rhin. fis.*) are visible by day eight. The hypothalamus has acquired adult features (except for the mammillary bodies) by day forty. Hypophysis (*hyp.*), olfactory tubercles (*ol. tub.),* anterolateral fissures (*ant. lat. fis.*), dentate gyrus (*dent. gy.*), preoptic recess (*pro. rec.*), di-telencephalic fissure (*di-tel. fis.*), eminence of the spinal root of trigeminal nerve (*trig. emn.*), ventral median fissure (*vent. med. fis.*), motor root of trigeminal nerve (*mot. r. V*), sensory root of trigeminal nerve (*sens. r. V*), arcuate rhinal fissure (*arc. rhin. fis.*), parafloccular lobe (*pfl.*), tuber cinereum (*tub. cin.*), diagonal band of Broca (*d.b.*), lateral olfactory tract (*lat. ol. tr.*), and preoptic area (*pro. area*).

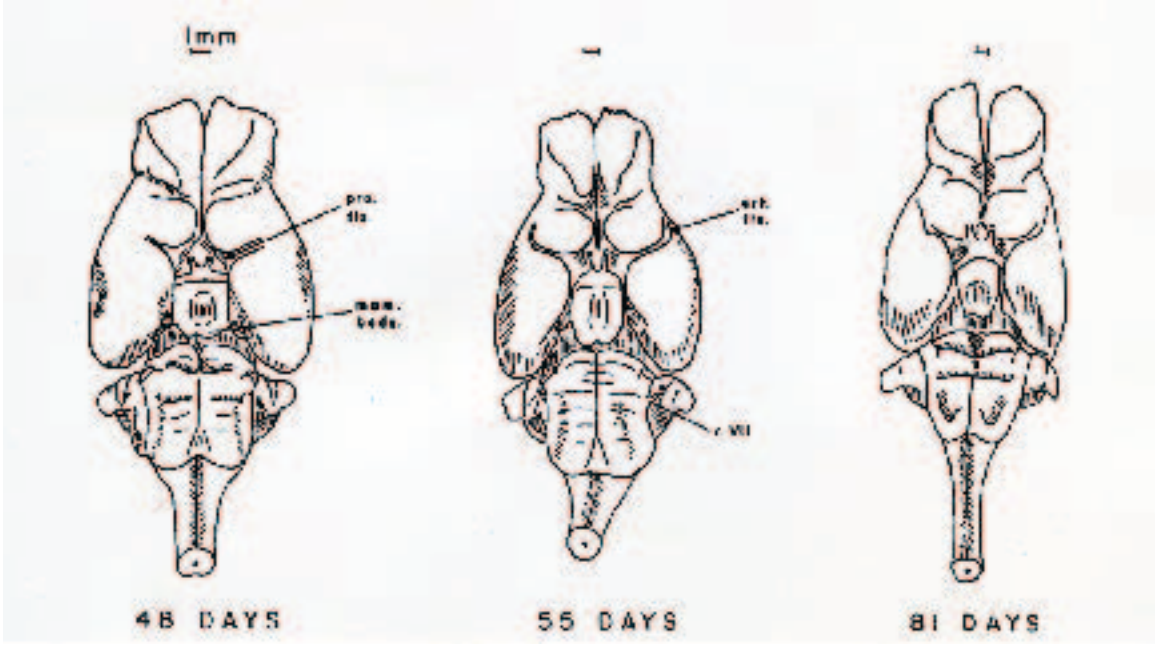

Fig. 20. Mammillary bodies (*mam. bods.*) appear by the end of the seventh postnatal week. The endorhinal fissure (erh. fis.) assumes its adult form by fifty-five days postnatal and the ventral surface of the eighty-one day old opossum brain, except for its size, exhibits the structural features of the adult. Preoptic fissure, *pro. fis.*, fascial nerve, *c VII*.

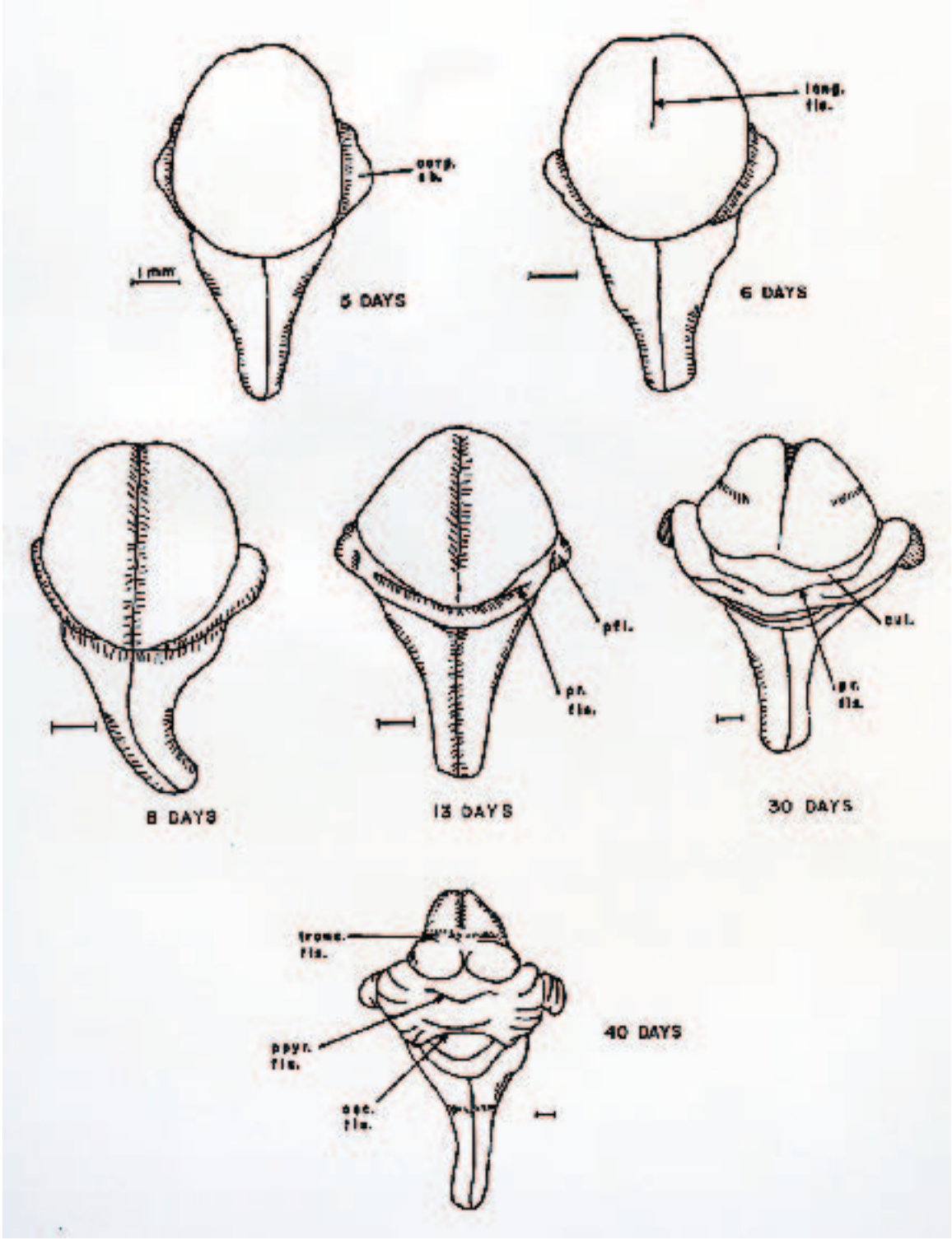

Fig. 21. A line drawing illustrates the development of the dorsal medulla and fissuration of the midbrain tectum of the postnatal opossum brain. The longitudinal fissure (*long. fis.*) is not completely established until day eight and the transverse fissure (*trans. fis.*) not completely formed until postnatal day forty. Corpus cerebelli, *corp. cb.*, parafloccular lobe, *pfl.*, primary fissure, *pr. fis.*, culmen, *cul.*, prepyramidal fissure, *ppyr. fis.*, and secondary fissure, *sec. fis.*.

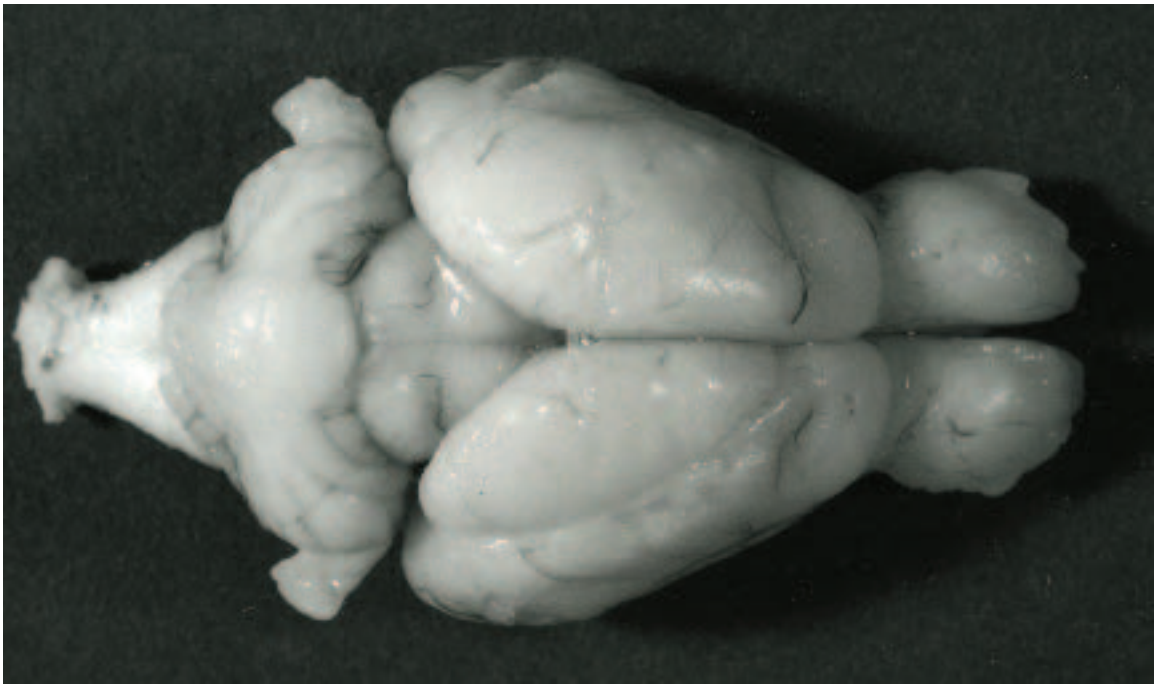

Fig. 22. A photograph illustrates the macroscopic features of the dorsal surface of an adult female opossum brain. The large olfactory bulbs, characteristic of the opossum brain, are shown at the right. Note the relatively smooth cerebral hemispheres, midbrain, and the cerebellum shown at the left. X 5.

Chapter 35. Ear

Synopsis:

The auricle (pinna) of the external ear originates as a proliferation of mesenchymal tissue from around the edges of the first and second pharyngeal arches together with overlying surface ectoderm. The external auditory meatus forms from the first pharyngeal groove. Auricular tubercles are present around the opening of the external auditory meatus late in prenatal day eleven and become more pronounced just prior to birth. At this time periderm covers the forming auricle and the developing external auditory meatus is completely filled with peridermal cells. The auricles appear as swellings of skin along the lateral surfaces of the head by the second week postnatal but it is not until the end of the sixth postnatal week that the auricles are visible as independent flaps of integument. The external auditory meatus becomes partially open at this time; however, it is not until the seventh postnatal week that it is open along its entire length. The auricles continue to enlarge until about thirteen weeks postnatal when they attain adult configuration and size.

In the middle ear anlage of the stapes, malleus, and incus are present by the twelfth prenatal day. The three middle ear ossicles are cartilaginous during the first two postnatal weeks and ossification first occurs in the processus anterior mallei at the beginning of the third week postnatal. The incus exhibits a center of ossification in the corpus by the fifth postnatal week. The majority of the malleus, incus and stapes are bone by the end of the sixth week and only the head of the stapes remains unossified. Thus, ossification of the ossicles occurs in order from malleus, to incus, to stapes in *Didelphis* with the ossification of each ossicle occurring from a single ossification center.

The stapedius anlage is first apparent during the twelfth prenatal day attached to the stylohyal. However, the attachment of the stapedius shifts as a result of degeneration of its ventral muscle cells and the subsequent formation of new dorsal muscle cells attached to the stapes. The tensor tympani muscle also appears at this time and exhibits striations at birth except near the malleus. The stapedius shows few if any striations at this time but does begin to exhibit striations by the second postnatal day.

The tympanic cavity is derived primarily from the first pharyngeal pouch. By the fourth postnatal week the medial aspect of the tympanic cavity has narrowed to a vertical slit where it becomes continuous with the Eustachian tube. Laterally it expands slightly and contacts the membrana propria forming a provisional tympanic membrane. The lining epithelium (endoderm) expands to line the expanding cavity and the inner surface of the tympanic membrane. The external surface of the tympanic membrane is covered by ectoderm from the first pharyngeal groove. During the seventh postnatal week the formed tympanic membrane lies somewhat horizontal, but as the external auditory meatus continues to grow it gradually becomes more erect.

Development of the inner ear begins early during the ninth prenatal day with the appearance of otic placodes. The otic placodes develop as thickenings of ectoderm just lateral to the medullary plate. Neural crest cells lie immediately under the otic placodes and represent the initial formation of the acoustic-fascial ganglion. The otic placode invaginates to form a cup-like structure and finally an otic vesicle late during prenatal day nine. The resulting otocyst separates completely from the overlying ectoderm by early in prenatal day ten. Differential growth rates within various regions of the otocyst will eventually form the various subcomponents of the inner ear during its organogenesis. Development of the opossum inner

ear is typically mammalian; however, about five-sixths of its development takes place after birth while the young are in the pouch. The horizontal ridge that forms within the otic vesicle will result in the formation of the lateral semicircular canal whereas the ventral ridge on the medial aspect of the otic vesicle will result in the formation of the endolymphatic duct. Caudal and cranial borders of the dorsal half of the otic vesicle flatten and will eventually result in the formation of the posterior and anterior semicircular canals, respectively. The ventral half of the otic vesicle will elongate with time and differentiate into the cochlea, utriculus, and sacculus. All semicircular canals appear quite rudimentary and no sensory cells or cristae are observed during the prenatal period. Likewise, sensory cells of the developing cochlea have yet to differentiate. However, a developing macula is present within the utricle the day before birth (twelve days prenatal) and contains approximately twenty sensory cells. The sensory cells are flask-shaped; have a light staining cytoplasm and a large centrally positioned nucleus. Stereocilia extend from the apices of these sensory cells and into an overlying layer of glycosaminoglycans containing otoliths. Nerve fibers within the underlying connective tissue establish an intimate relationship with the overlying sensory epithelial cells. The utricles are thought to function at birth in sensing gravity. Newborn opossums exhibit a negative geotropic behavior at birth and the newborn young move in a direction opposite that of gravity. As a result they climb upwards in the direction of the pouch (the mother sits on her haunches at birth). Other sensory cells associated with either the cristae of the semicircular canals or the organ of Corti within the cochlea are absent at birth. The cristae and maculae do not become prominent structures associated with either a cupula or otolithic membrane, respectively, until after the end of the first postnatal week. At the end of the second postnatal week the utriculus and sacculus open separately into the endolymphatic duct and the cochlear duct has elongated to form the two and one fourth turns characteristic of the adult. Vestibular reflexes can be measured by the sixth week postnatal. By the end of the fourth postnatal week the tectorial membrane extends throughout the length of the cochlea and the scala tympani and scala vestibuli are confluent at the helicotrema. The organ of Corti is present throughout the cochlea by the fifth postnatal week. Histogenesis of cochlear structures initially begins in the second half of the basal coil of the cochlea and then proceeds in both directions. That portion of the organ of Corti first differentiated is the first region responsive to sound, and as differentiation spreads in both directions, the range of hearing spreads to lower and higher tones. Acoustic reflexes are not observed until late during the seventh postnatal week.

Acknowledgments:

Figs. 1 (top) 4 and 5, courtesy of and from: Krause, W.J. (1998) A review of histogenesis/organogenesis in the developing North American opossum (*Didelphis virginiana*). Adv. Anat. Embryol. Cell Biol. 143 (I): Springer Verlag, Berlin, pp 143.

Fig. 6, courtesy of and from: Krause, W.J. (1991). The vestibular apparatus of the opossum (*Didelphis virginiana*) prior to and immediately after birth. Acta Anat. 142:57-59.

Fig. 1. (*Above*). A scanning electron micrograph illustrates the appearance of the pinna and the orifice of the external auditory meatus in an opossum embryo early in the twelfth prenatal day. A well-established eye and the opening to the external nares also are shown. SEM X 40. (*Below*). The external ear of the opossum in the above figure observed at increased magnification and viewed from a different angle details the features of the developing pinna. Note that the developing pinna is covered by periderm. SEM X 100.

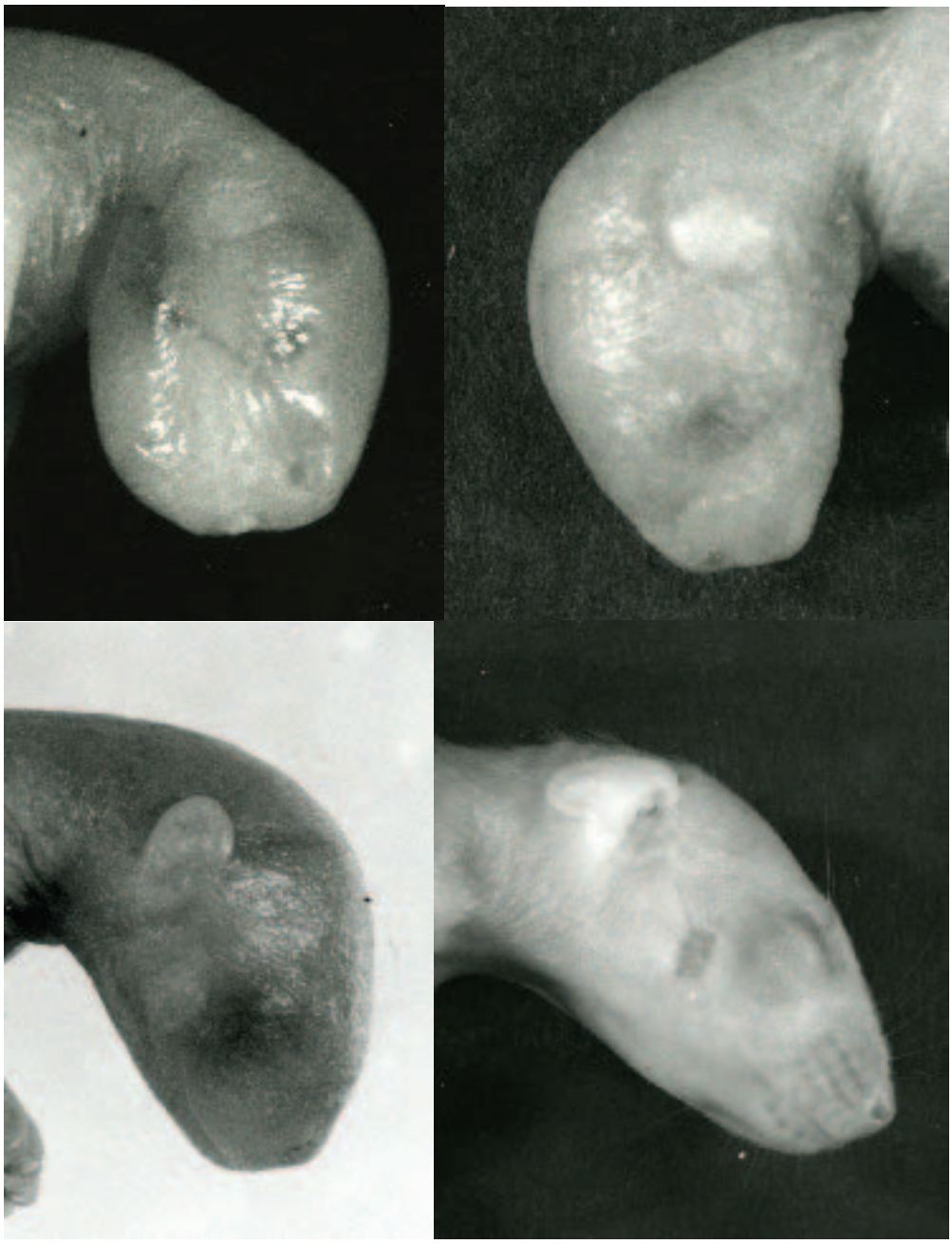

Fig. 2. The postnatal development of the pinna (auricle) of the external ear as observed in a series of postnatal opossums. (*Above left*). The pinna is largely undeveloped and covered by periderm. Pouch young opossum one-week postnatal, snout-rump length 25 mm. (*Above right*). The pinna appears as a swelling along the lateral aspect of the head. Pouch young opossum two weeks postnatal, snout-rump length 35 mm. (*Below left*). The pinna has formed and extends from the integument. Pouch young opossum four weeks postnatal, snout-rump length 45 mm. (*Below right*). Pouch young opossum seven weeks postnatal, snout-rump length 80 mm.

Fig. 3. The postnatal development of the pinna (auricle) of the external ear as observed in a series of older postnatal opossums. (*Above left*). Pouch young opossum nine weeks postnatal, snout rump length 105 mm. (*Above right*). Pouch young opossum ten weeks postnatal, snout-rump length 115 mm. (*Below left*). Pouch young opossum eleven weeks postnatal, snout-rump length 140 mm. (*Below right*). Young adult female opossum. The pinnae of late the juvenile and adult opossums are thin, devoid of hair, and have a leathery consistency. They are deeply pigmented giving them a blue-black appearance. In some animals the black appearing pinnae are tipped with a white band.

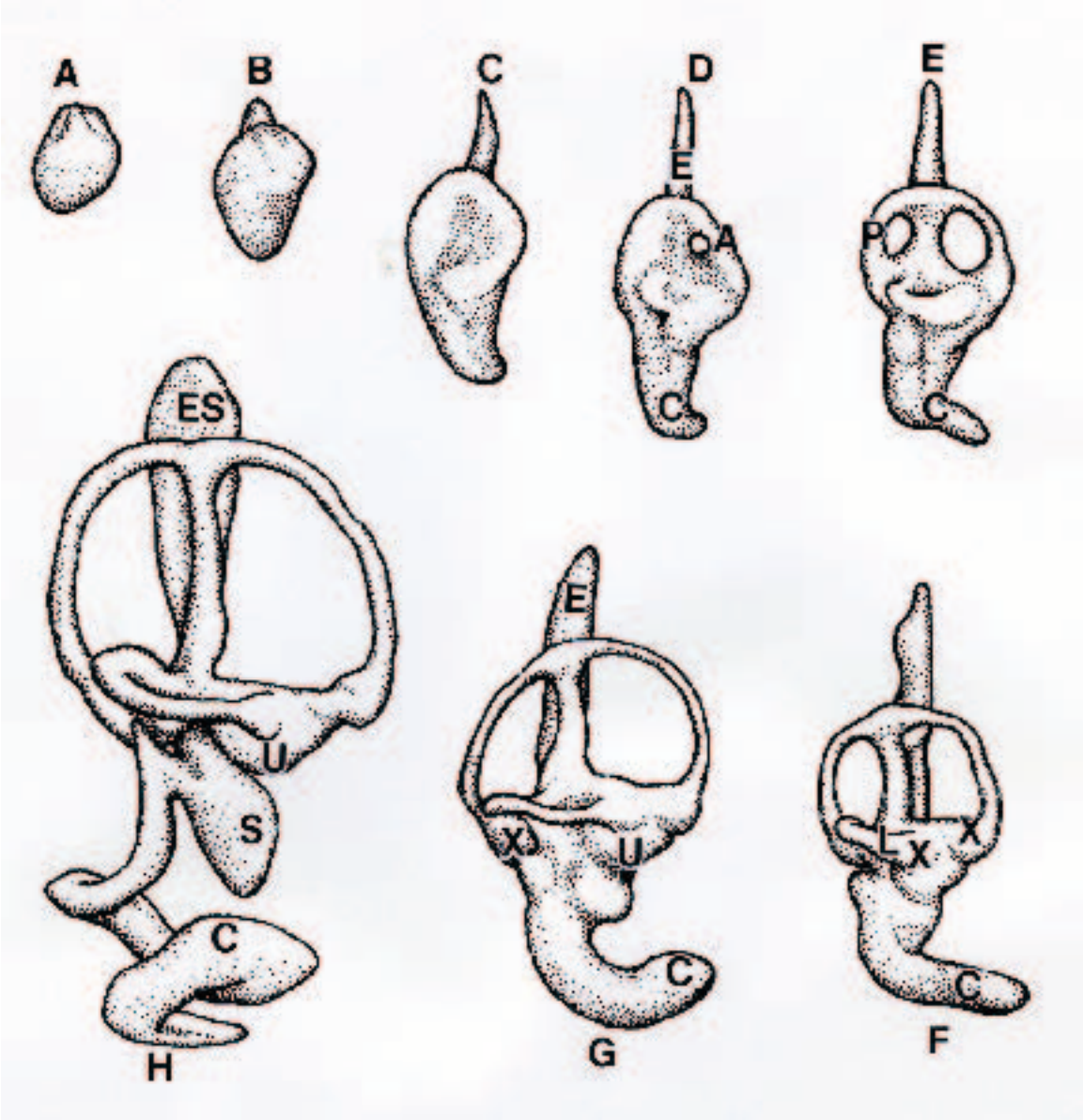

Fig. 4. A line drawing illustrating the developing left otocyst from a series of opossums representing stages from early prenatal day ten to one week postnatal as viewed from a lateral perspective. Six prenatal ages, **A** early prenatal day ten; **B** late prenatal day ten; **C** late eleventh prenatal day; **D** early prenatal day twelve; **E** late prenatal day twelve; **F** just prior to birth, and two postnatal stages **G** just after birth; **H** one week postnatal are depicted. The following structures are labeled: *E*, endolymphatic duct, *C*, cochlea, *A*, anterior semicircular canal, *P*, posterior semicircular canal, *L*, lateral semicircular canal, *X*, ampulla, *U*, utriculus, *S*, sacculus, and *ES*, endolymphatic sac.

Fig. 5. A histological section through the cochlea of an opossum immediately prior to birth illustrates the immature nature of the cochlear duct (C) and adjacent structures at this stage of development. The majority of organogenesis concerned with the inner ear mechanism will take place during the postnatal period. LM X 300.

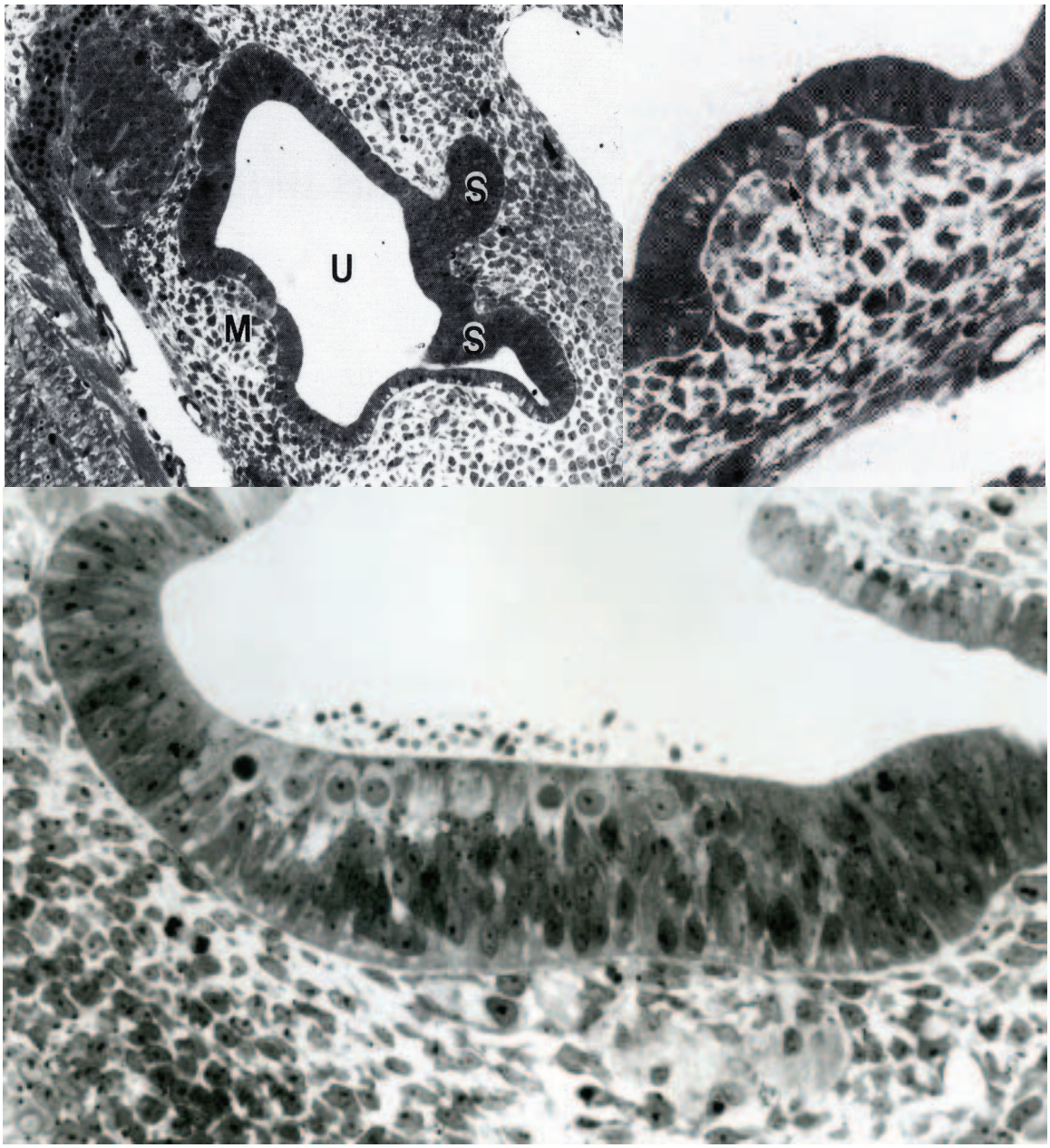

Fig. 6. (*Above left*). The developing utricle (U), macula (M), and two semicircular canals (S) of an 11.5 day-old opossum embryo observed in a histological section. LM X 150. (*Above right*). The developing macula from the illustration shown at the left when examined at increased magnification contains two large, light-staining, flask-shaped cells (arrow). These light-staining cells are believed to be the initial appearance of sensory cells within the epithelial lining of the macula. The surrounding cells are thought to be sustentacular cells. LM X 300. (*Below*). A region of developing macula observed in a histological section of the utricle from a twelve-day-old opossum embryo. Note the presence of several light-staining, flask-shaped sensory cells as well as numerous otoliths overlying this region of sensory epithelium. A small nerve bundle also can be observed underlying the sensory epithelium (lower right) of the macula at this stage of development. LM X 600.

Chapter 36. Eye

Synopsis:

The eyes of the opossum form from neuroectoderm of the embryonic forebrain, surface ectoderm of the head, and mesenchyme that lies between and around these components. With closure of the neural tube, optic grooves on each side of the developing forebrain expand to form the optic vesicles during prenatal day ten. Soon after their formation the distal wall of the optic vesicle collapses into itself forming a double walled optic cup. A small lens vesicle is apparent by the middle of prenatal day ten and by the end of prenatal day ten; the lens vesicle detaches from the surface ectoderm and sinks into the cavity of the optic cup. At this time the presumptive corneal epithelium of the surface ectoderm consists of two – three layers of cells and mesenchyme surrounds the developing optic cup. The inner layer of the optic cup (the future neuroretina) thickens by the end of the eleventh prenatal day and a presumptive vitreous cavity appears between the developing retina and primitive lens at this time. The outer layer of the optic cup (the future pigment epithelium) remains pseudostratified in character; however, melanin pigment granules are present in the apices of these cells. The presumptive choroidal vasculature forms adjacent to the basal surface of the outer layer of the optic cup. A network of loose mesenchymal cells migrates into and occupies a position between the optic cup margin and the surface ectoderm by this period of organogenesis. This mesenchymal network will differentiate into the future corneal stroma and endothelium.

The developing eye and associated surrounding structures show considerable advances in development at birth. In addition to the increase in size of the eye, the eyelids fuse and a large fluid-filled sac separates the eyelids from the eye. The cornea of the newborn opossum consists of two or three layers of epithelial cells resting on a mat of loose mesenchymal cells. The corneal endothelium is not clearly established at this time. The inner layer of the optic cup consists of an outer neuroblastic layer and a thin acellular inner marginal zone. The outer layer of the optic cup, the retinal pigment epithelium, is heavily pigmented. The condensing mesenchyme of the presumptive sclera consists of aggregates of fibrous and non-fibrous elements that extend around the optic cup external to the forming choriocapillaris.

At the end of the first postnatal week the inner neuroepithelial layer (future neural retina) and outer layer (future pigment epithelium) of the retina remain clearly defined. The corneal epithelium consists of a nonkeratinized stratified squamous epithelium, three cells thick, that rests on an irregularly arranged collagenous stroma. The corneal endothelium is present at this time but a distinct Descemet's membrane is absent. The pupillary membrane is poorly defined and the iris and ciliary body have yet to differentiate at this time. The developing sclera consists of a distinct fibrous coat and lies immediately external to a single layer of vessels that forms the choriocapillaris. A rudimentary nictitating membrane and extraocular myoblasts also can be observed by the end of the first postnatal week.

The neural retina continues to consist of inner and outer neuroblastic layers at this time. Considerable mitotic activity occurs in the outer neuroblastic layer particularly in the outer zone adjacent to the optic cavity and at the cup margin. The inner (marginal) zone is no longer acellular but contains cells with large pale staining, irregular nuclei with prominent nucleoli. The inner neuroblastic layer is four to six layers thick centrally, but peripherally only a single neuroblastic cell layer is present. The inner neuroblastic cell layer consists primarily

of ganglion cells and Müllers cells. A partly acellular zone of intertwined cell processes presumed to be the future inner plexiform layer is present but the beginnings of an outer plexiform layer is not observed at this stage of development. The retinal pigment epithelium consists primarily of columnar cells the cytoplasm of which contains numerous mature and immature melanosomes. Cells of the retinal pigment epithelium lie on a thick basal lamina that separates it from fenestrated choroidal vessels. By the end of the second postnatal week nerve fibers extend along the presumptive optic nerve and the corneal stroma is slightly more lamellated. The ciliary body and iris have yet to appear at the end of the second week postnatal.

Rapid organogenesis of the eye occurs between the second and sixth postnatal weeks with most adult structures having differentiated to variable degrees during this period of time. The corneal epithelium is stratified squamous the superficial layer of which is characterized by microplicae. A distinct Bowman's membrane is absent. Now the corneal stroma is characterized by highly organized lamellae of collagen fibers separated by keratocytes and the corneal endothelial cells rest on a prominent Descemet's membrane. By the end of the sixth postnatal week a short iris has differentiated and extends from the optic cup margin anterior towards the lens. A double layer of pigment epithelial cells forms the posterior lining of the iris. The stroma of the iris consists primarily of well-defined collagen fibers and stromal melanocytes filled with melanin granules. Smooth muscle cells of the sphincter pupillae are present, however, a dilator papillae is absent. Well-formed, radially arranged ciliary processes are now present covered by pigmented and non-pigmented ciliary epithelial cells. Both the ciliary body and iris exhibit rapid growth between the second and sixth week postnatal. Likewise, rapid retinal development occurs during this period and a fully laminated retina is observed at the posterior pole of the eye by the end of the sixth week of postnatal life. Development of the peripheral retina continues to lag behind that located along the posterior aspect of the eye.

The posterior retina at this time consists of a nerve fiber layer, a single layer of ganglion cells, a thick inner plexiform layer, an inner nuclear layer six to eight cells deep, and a thin outer plexiform layer which separates inner and outer nuclear layers. By the end of the sixth postnatal week the retinal pigment epithelium is filled with homogeneous cholesterol/lipid droplets in the tapetal region of the retina. In the tapetal region of the opossum retinal pigment epithelium, melanin granules are few in number and restricted to the apical cytoplasm of the pigment epithelial cells. The choroid consists only of a primary layer of vessels at this time of development.

The cornea acquires an adult morphology by the thirteenth postnatal week and the iris is more elongated. The ciliary processes appear thicker and more vascular than earlier developmental stages. A well formed trabecular meshwork positioned internal to a single canal of Schlemm also is present at this time. Although retinal vascularization is present at this time it is restricted to the ganglion cell and inner plexiform layers. The unusual paired retinal capillaries present in the adult opossum retina appear at this stage of postnatal life. The choroid is thicker in comparison to eyes of the sixth postnatal week and the outer choroid consists of vessels that range 30-40 μM in diameter. Elongated rod and cone inner and outer segments, well developed in the central retina, appear less mature in the peripheral retina. Oil droplets in cone inner segments also are present at this time. The eyelids differentiate from folds of integument adjacent to the eyeball and fuse just prior to birth. The time at which the eyelids reopen is variable and not a reliable guide as to age. The eyes may begin to open as early as seven weeks postnatal or may remain closed until the tenth postnatal week.

Acknowledgments:

Fig. 1 (top), courtesy of and from: Krause, W.J. and W. A. Krause (2004) The Opossum: It's Amazing Story. Walsworth Publishing Company, Marceline, Missouri, pp. 71

Figs. 3, 4, 5, 6 and 7, courtesy of and from: McMenamin, P.G. and W.J. Krause (1993). Morphological observations on the unique paired capillaries of the opossum retina. Cell Tissue Res. 271:461-468.

Figs. 8, 9 (top), 10, 11, 12, 13, 14, 15, 16, 17 and 18, courtesy of and from: McMenamin, P.G. and W.J. Krause (1993). Development of the eye in the North American opossum (*Didelphis virginiana*). J. Anat. 183:343-358.

Fig. 1. (*Above*). Eyes of the opossum are prominent, somewhat exophthalmic and black in color. The black appearance of the eyes is due to the fact that eyes are extremely dilated and a large pupil characterizes the front of the eye. The iris is usually not seen except if the opossum is examined with a bright light. (*Below*). A micrograph illustrates the external surface of the cornea from a juvenile opossum similar in age to the opossum shown in the above photograph. Note the rounded curvature of the cornea. SEM X 8.

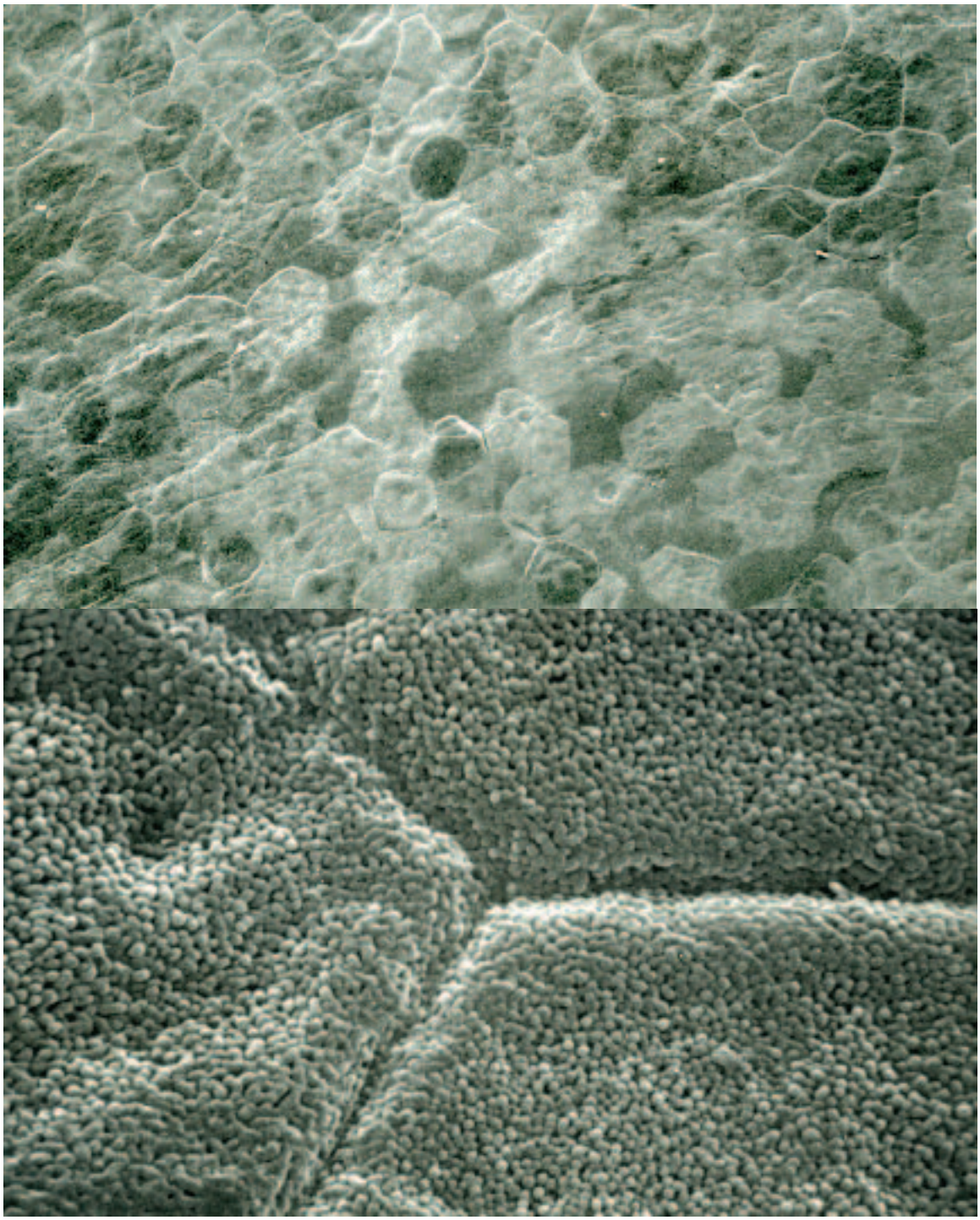

Fig. 2. (*Above*). The corneal surface of a juvenile opossum consists of numerous flattened, irregularly shaped epithelial cells. SEM X 200. (*Below*). The junction between three surface corneal epithelial cells from the cornea of a juvenile opossum examined at increased magnification. Note the extensive development of microplicae with regard to the surface plasmalemma of the corneal epithelial cells. The latter are believed to trap and hold fluid (tears) on the corneal surface to prevent drying. SEM X 8,000.

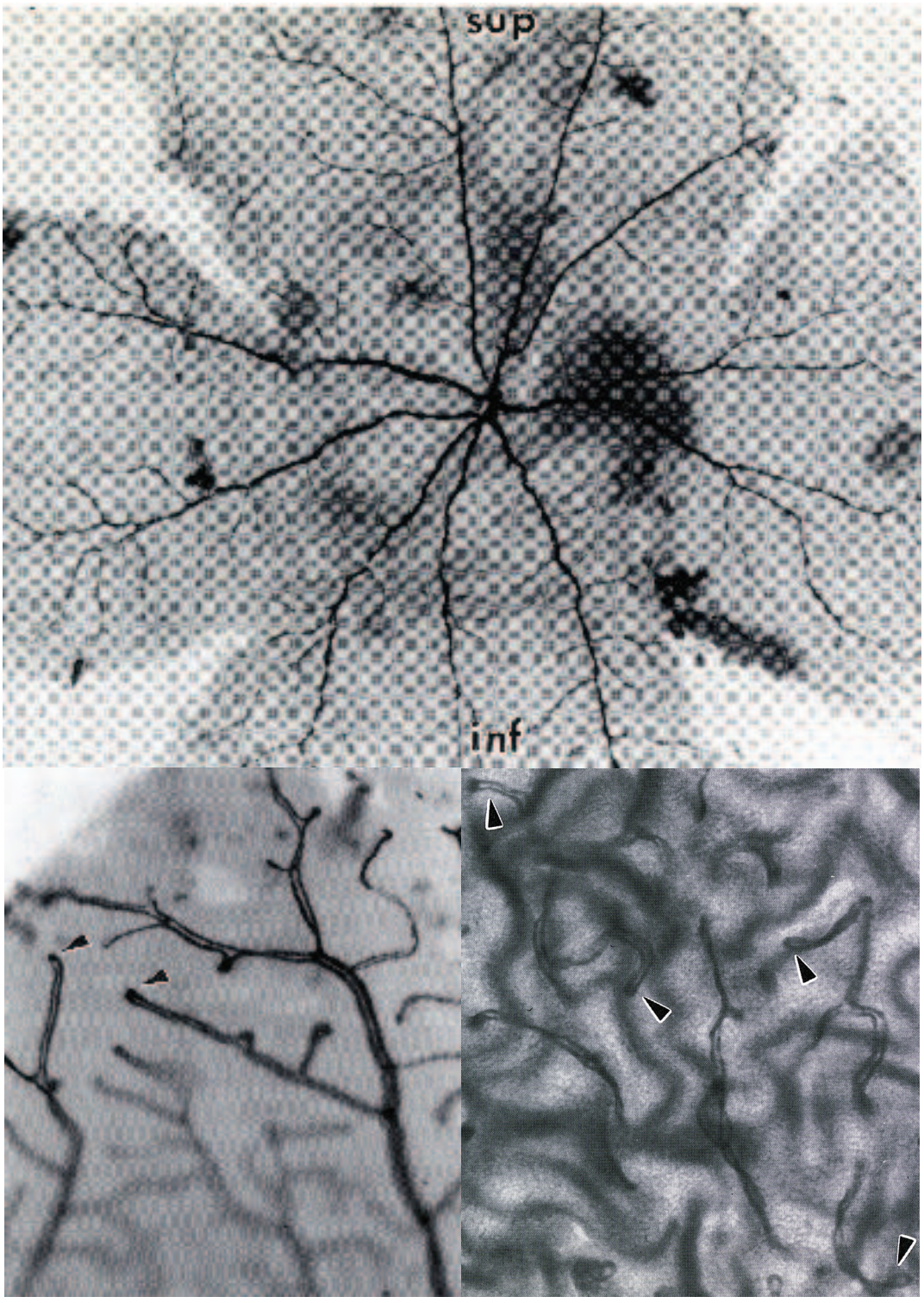

Fig. 3. (*Above*). A whole-mount preparation of adult opossum retina perfused with India ink demonstrates its general vascular pattern. The superior (sup) and inferior (inf) aspects of the retina are indicated. X 30. (*Below left*). Close examination of the India ink injected adult retina demonstrates paired vessels in the nerve fiber layer of peripheral retina that terminate in hairpin loops (arrowheads). X 30. (*Below right*). A whole-mount preparation of adult opossum retina following injection with horseradish peroxidase illustrates the branching pattern of the paired capillaries and the terminal hairpin loops (arrowheads). Focus is through one of the deepest layer of the retina, the outer nuclear layer. X 36.

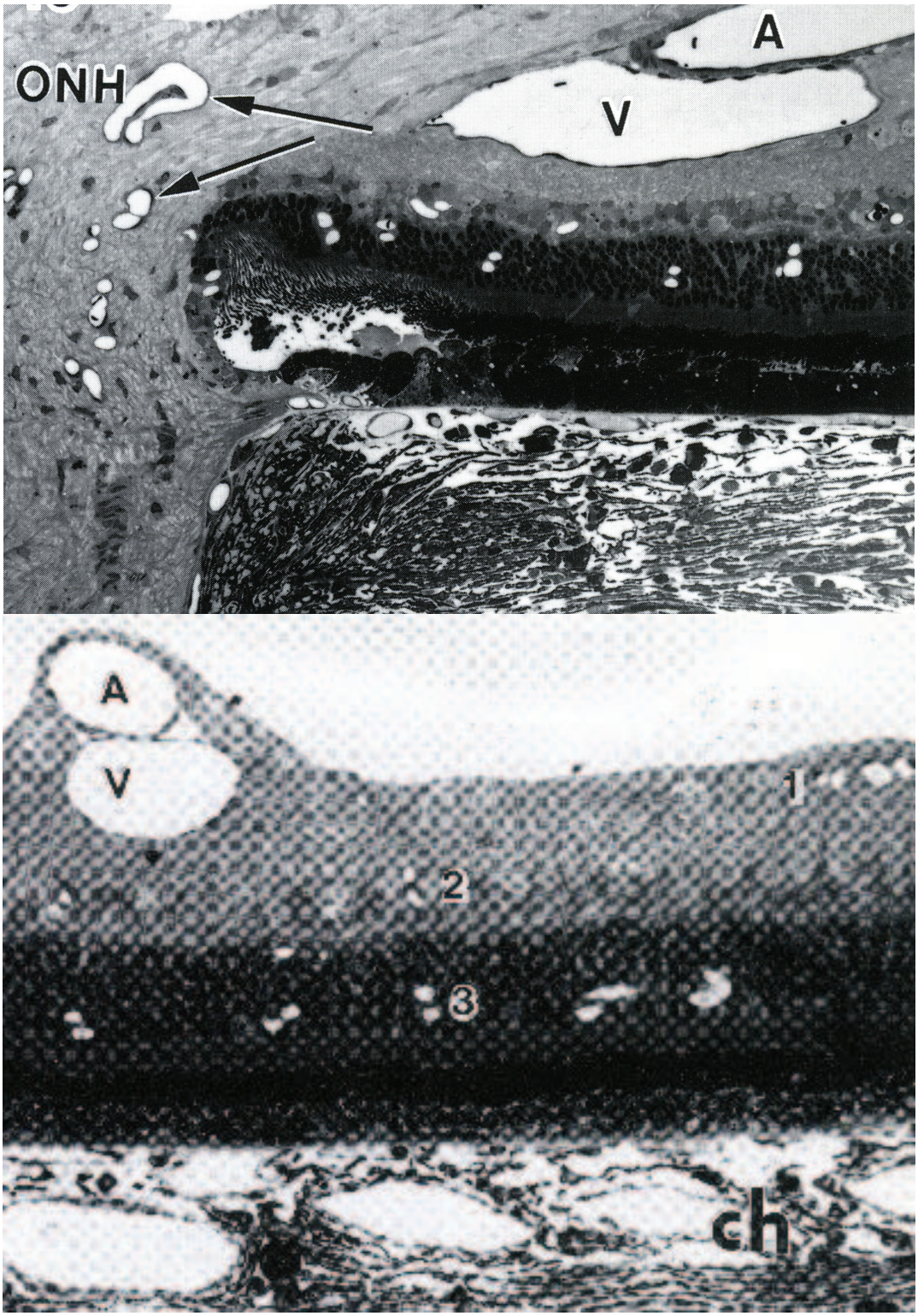

Fig. 4. (*Above*). A section through the region of the optic nerve head (ONH) illustrates the presence of a larger segmental artery (A) and vein (V), which arise from central retinal vessels, as well as paired capillaries (arrows) one of which forms a hairpin loop. LM X 400. (*Below*). Large and small paired vessels observed in the adult opossum retina. The arterial limb (A) lies in a more vitread with respect to the vein (V). This association is maintained as the pairs branch deep within the retina. The paired capillaries are distributed in the three main layers of the retina (1 – ganglion cell layer, 2 – inner nuclear layer, 3 – outer nuclear layer), with the deepest occurring as far as the external limiting membrane. Vessels in the choroid (ch) are large, abundant, and unbranched. The choriocapillaris is well developed. LM X 400.

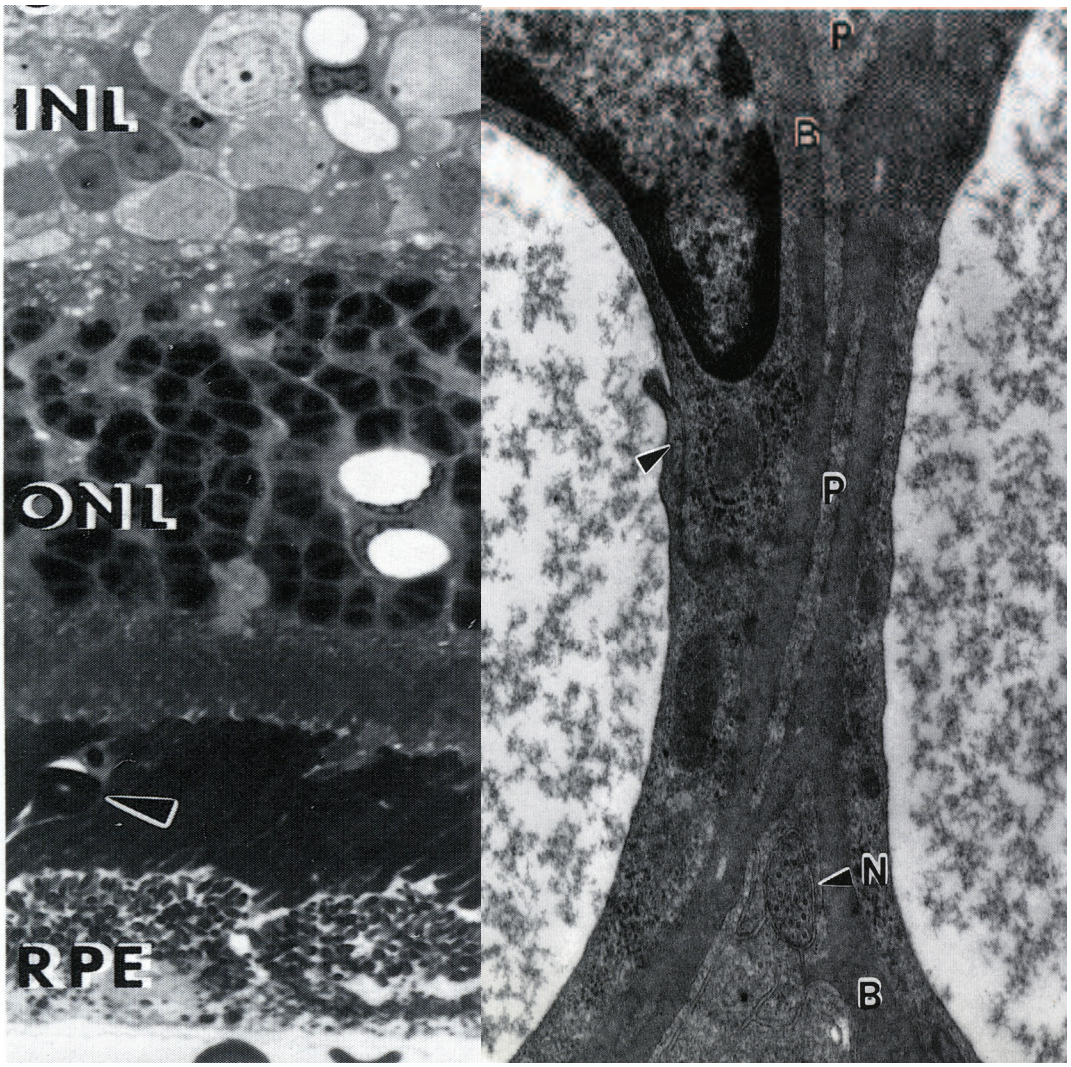

Fig. 5. (*Left*). A region of opossum retina from the previous figure examined at increased magnification shows in greater detail two profiles of the paired capillaries. One pair lies within the outer nuclear layer (ONL), the other pair occurs within the inner nuclear layer (INL). A cone containing a large lipid droplet is shown at the arrowhead. The tapetal retinal pigment epithelium (RPE) and underlying choriocapillaris also are shown. LM X 800. (*Right*). Two closely apposed retinal capillaries each of which is limited by a distinct basal lamina (B) and separated by thin cytoplasmic processes (P) of a pericyte enveloped in the basal lamina. Note the endothelial cell junction (arrowhead) and the small axonal process (N) adjacent to the cytoplasm of a nearby pericyte. TEM X 23,800.

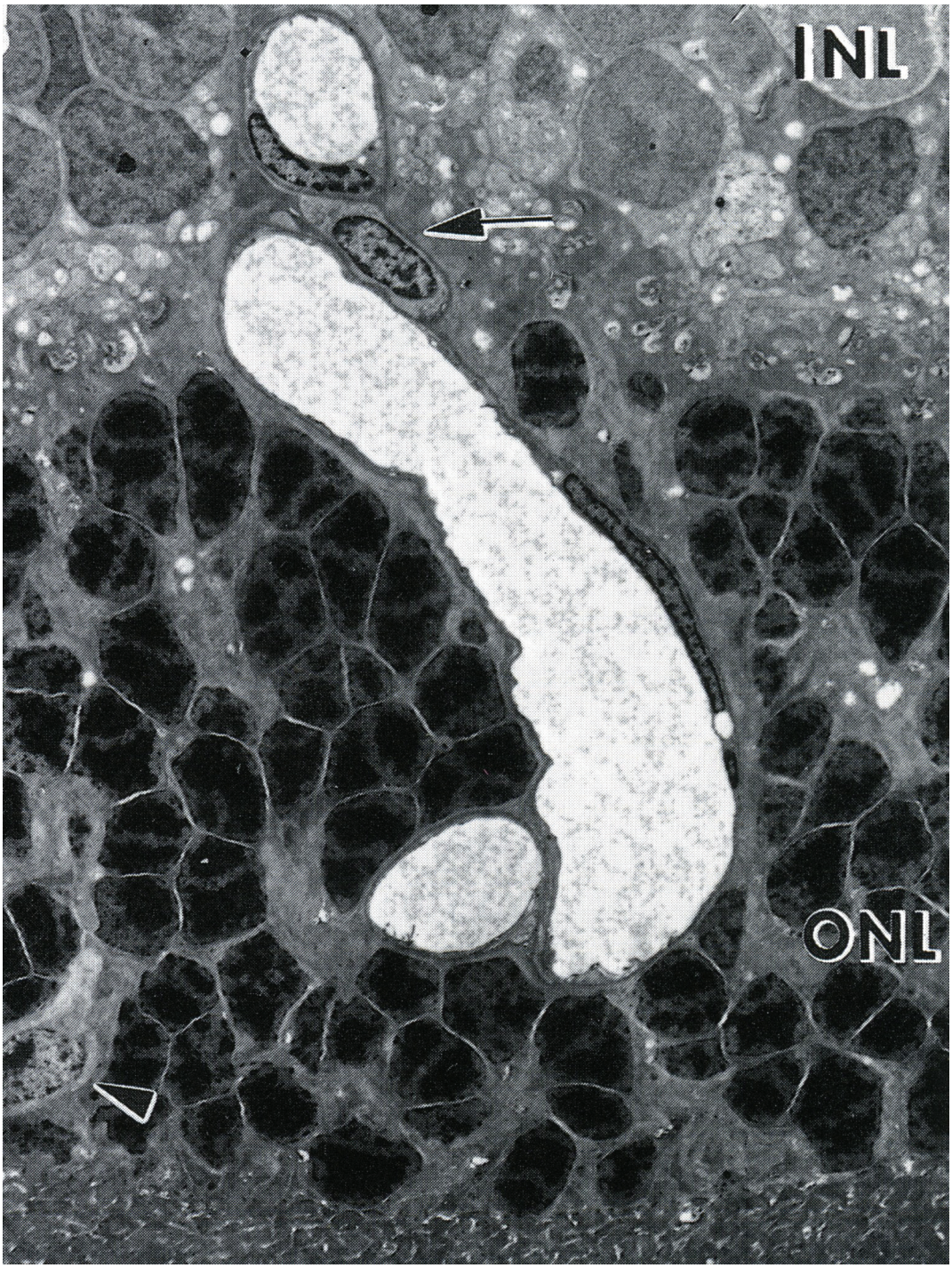

Fig. 6. A segment of a paired capillary extends from the inner nuclear layer (INL) to the outer nuclear layer (ONL) of an adult opossum retina detailed by electron microscopy. Note the absence of pericytes except for shared regions between capillaries (arrow) and the thin attenuated lining endothelium. The nucleus of a cone cell also is shown at the arrowhead. TEM X 3,000.

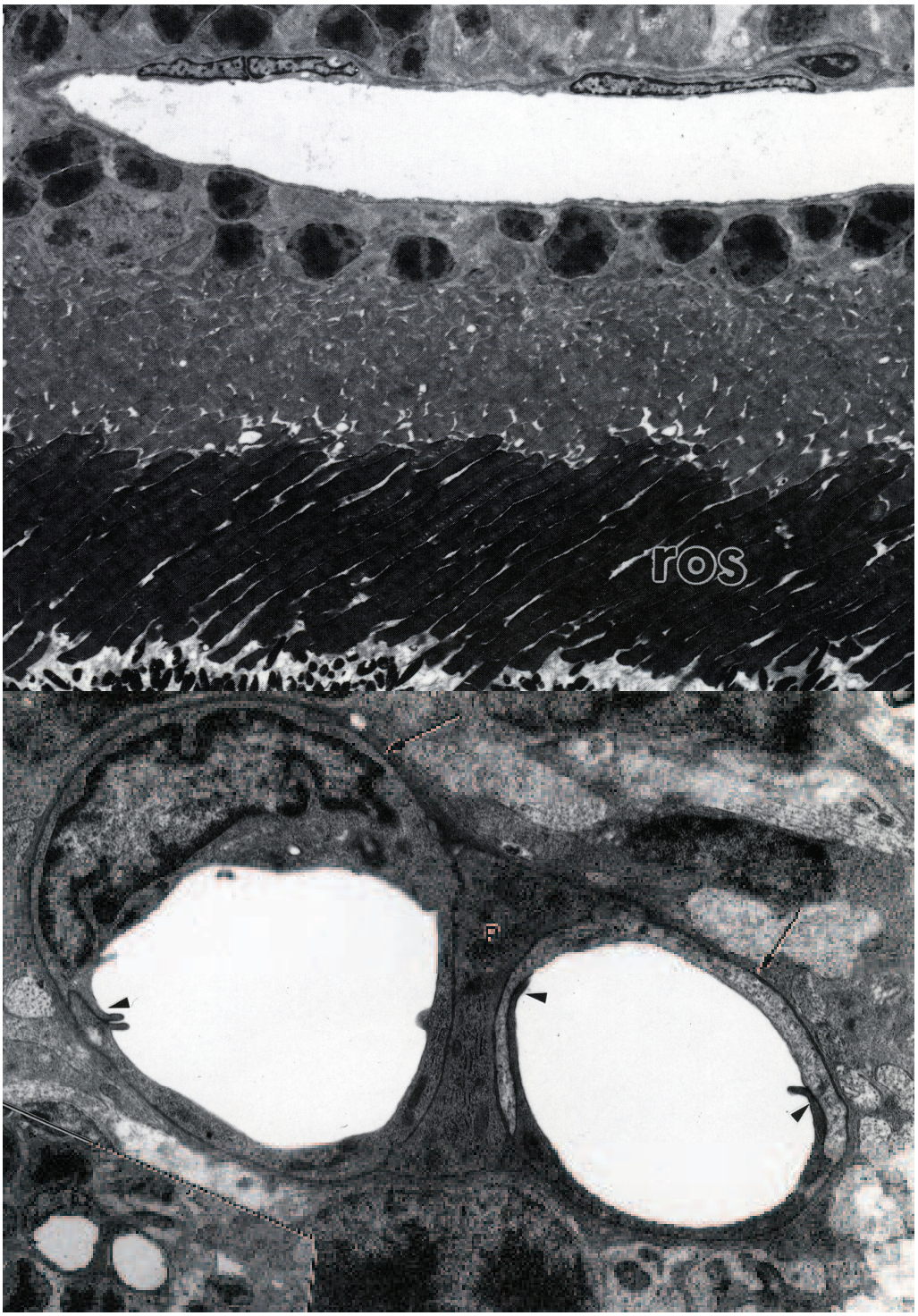

Fig. 7. (*Above*). A region of one paired capillary that runs parallel and close to the external limiting membrane within the non-tapetal portion of the adult opossum retina. The rod outer segments (ros) are shown at the bottom of this electron micrograph. TEM X 2,200. (*Below*). Paired capillaries from the outer nuclear layer of an adult opossum retina. The inset illustrates their appearance at low magnification. The cytoplasm of a pericyte (P) lies interposed between capillaries and is limited by a distinct basal lamina, which fuses with those of the adjacent capillaries. Each capillary is surrounded by a distinct basal lamina (arrows). The capillary to the left (the arteriolar limb) is lined by a single endothelial cell, whereas two endothelial cells of differing electron densities line the capillary to the right. The endothelial cells are united by tight junctions (arrowheads). TEM X 14,000; inset at bottom left X 1,100.

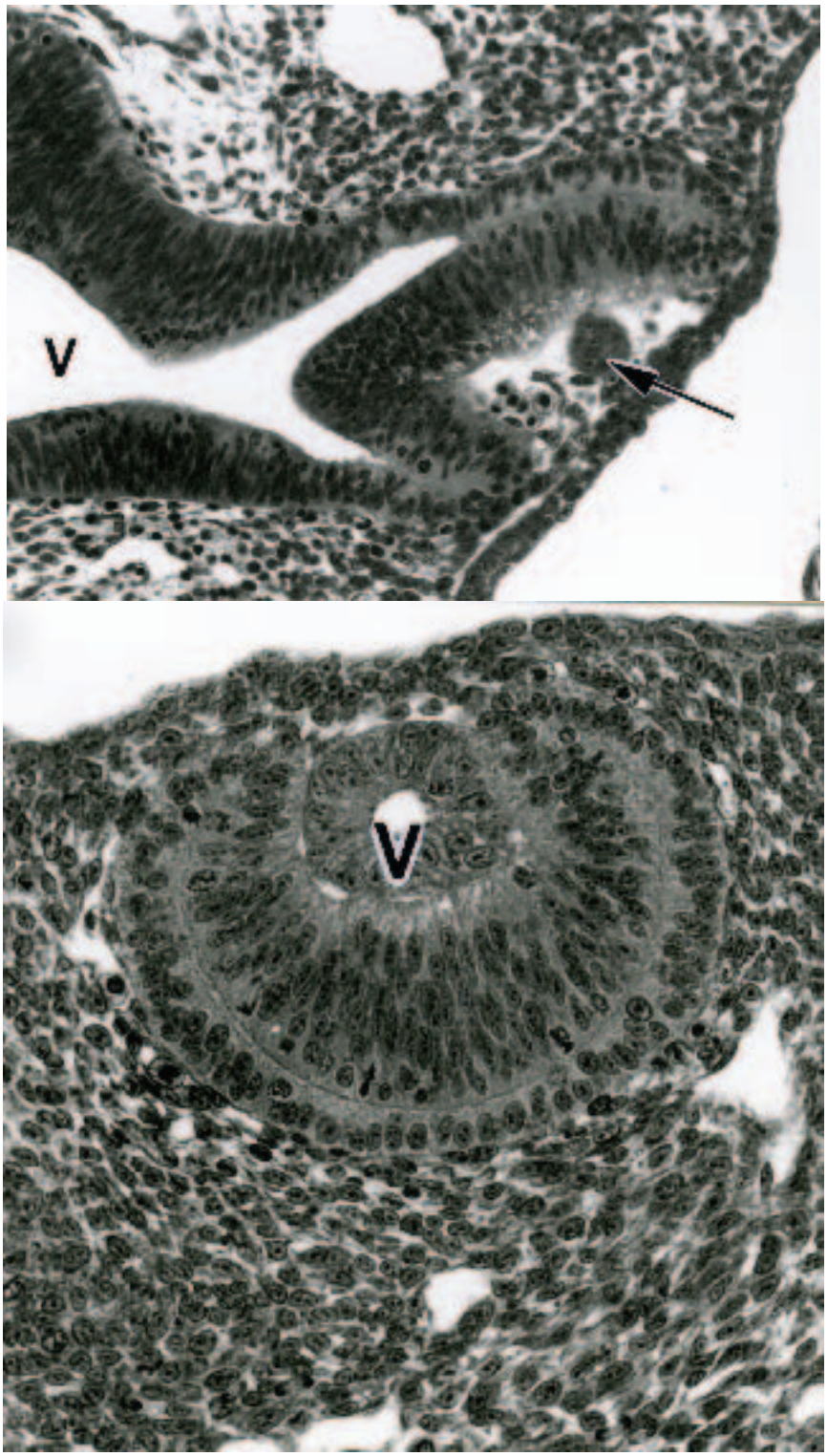

Fig. 8. (*Above*). A region of developing eye from an opossum embryo at 10.5 days gestation illustrates the anatomic continuity of neuroectoderm lining the forebrain ventricle (V) with that of the optic vesicle. A portion of the lens (arrow) positioned immediately under the surface ectoderm also is shown. LM X 300. (*Below*). A histological section through the developing eye of an opossum late in prenatal day ten illustrates that the lens vesicle (V), with its distinct cavity, is now detached from surface ectoderm and tightly encompassed by the surrounding optic cup. Note the number of mitotic figures present within the field. LM X 300.

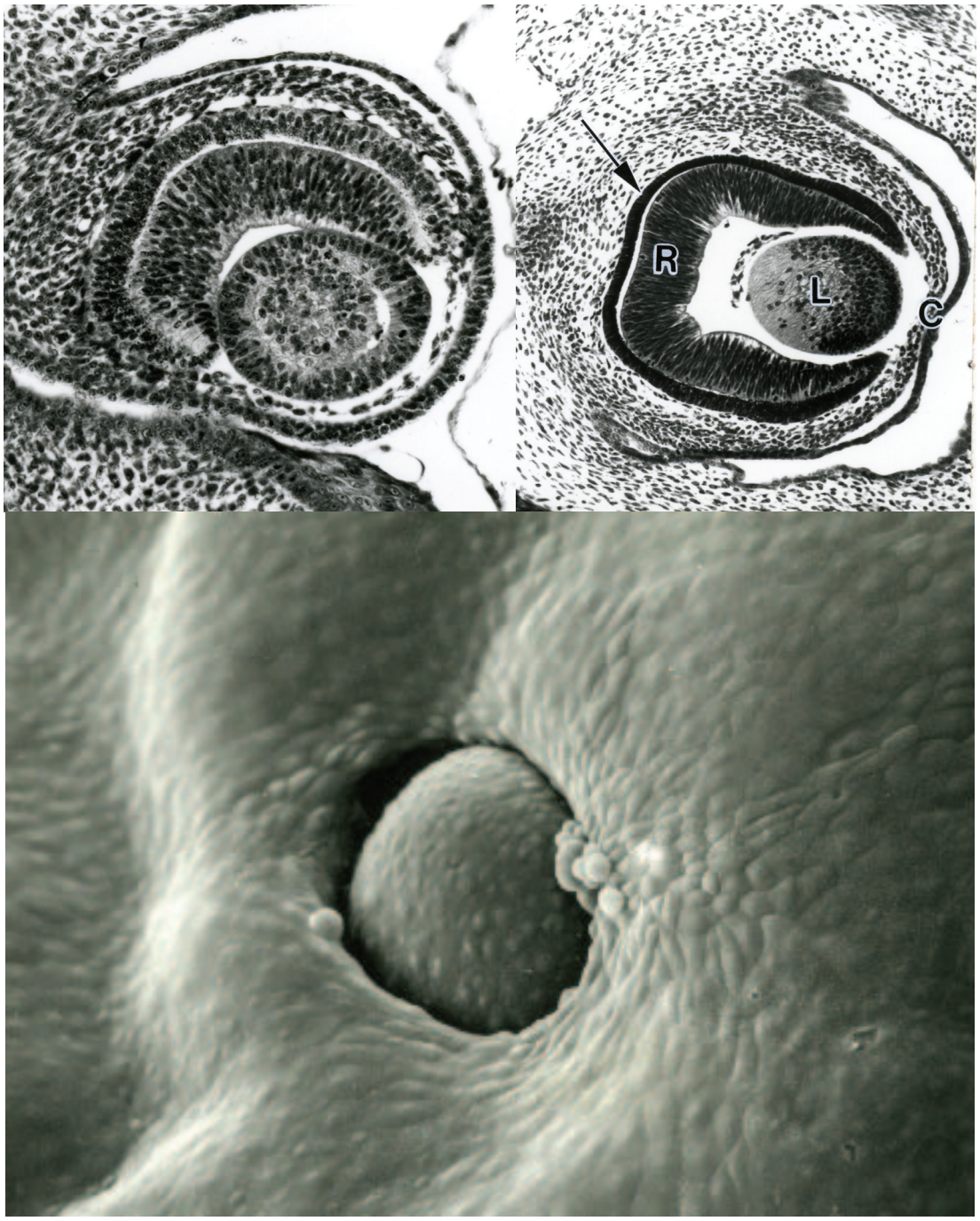

Fig. 9. (*Above left*). The optic cup and surrounding mesenchyme protrude slightly from the head of the eleven-day opossum embryo covered only by a thin layer of surface ectoderm. Note that the mesenchyme has now migrated over the cup margin to lie between the lens and surface ectoderm. LM X 250. (*Above right*). The retinal pigment epithelium (arrow) of the newborn opossum eye contains numerous melanin granules. Note the immature state of development of the neural retina (R), lens (L), and cornea (C). LM X 100. (*Below*). The external features of the developing eye form an eleven-day opossum embryo. The eyelids have yet to form at this stage of development exposing the external layer of cells forming the cornea. SEM X 200.

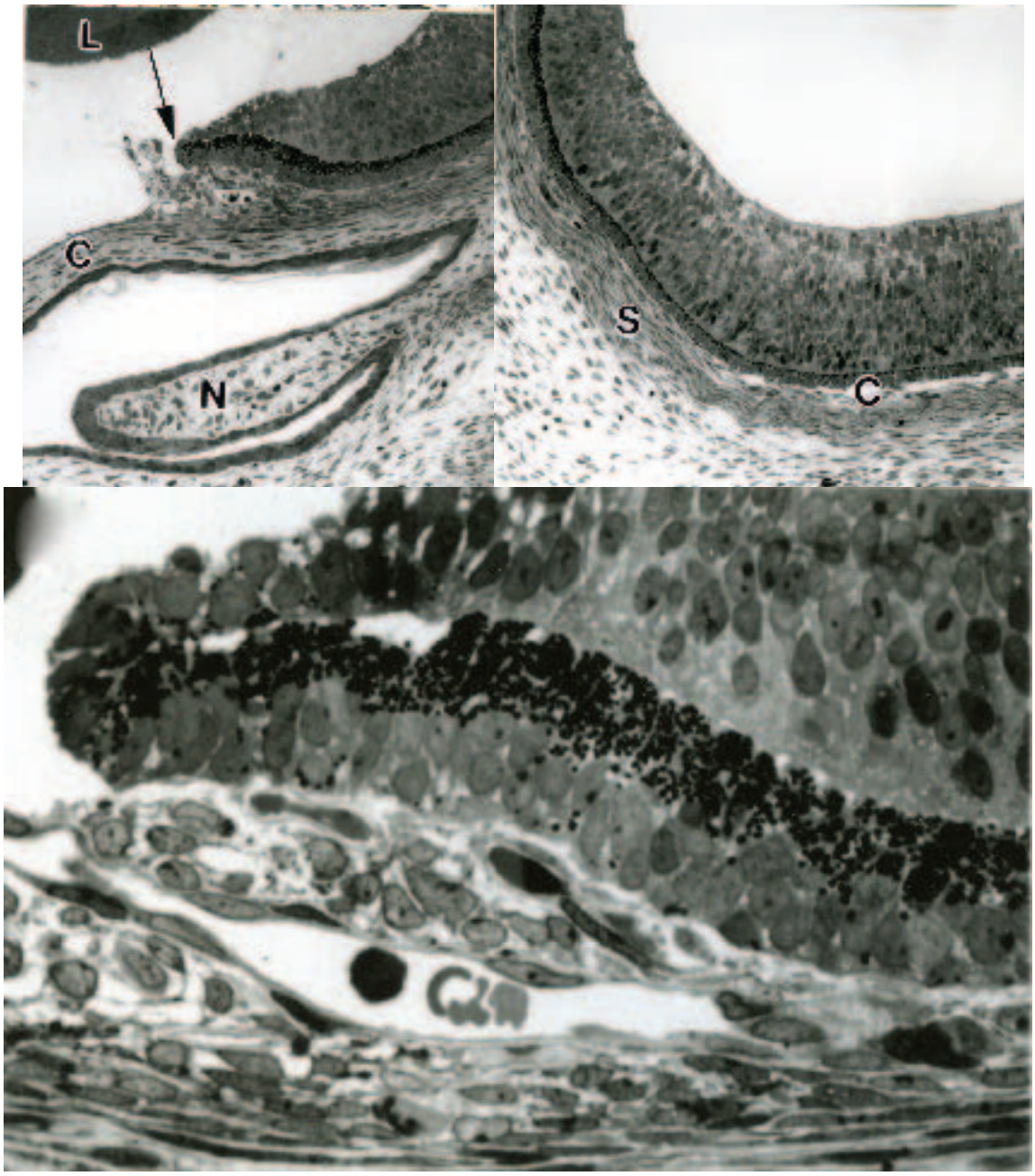

Fig. 10. (*Above left*). A histological section that illustrates the anterior region of the eye from an opossum one week postnatal. The cornea (C) is now well established. The lens (L), anterior cup margin (arrow), and a small nictitating membrane (N) arising from the conjunctival fornix also are shown. LM X 100. (*Above right*). The posterior region of the same eye shown in the figure to the left illustrates that the developing sclera (S), is separated from the retinal pigment epithelium by a single layer of vessels forming the presumptive choroid (C) at this stage of development. LM X 100. (*Below*). The cup margin when viewed at increased magnification illustrates large accumulations of melanin granules within the retinal pigment epithelium. Note that the retina ends close to the cup margin and that the iris and ciliary body have yet to form in the eye of the opossum at one week postnatal. LM X 800.

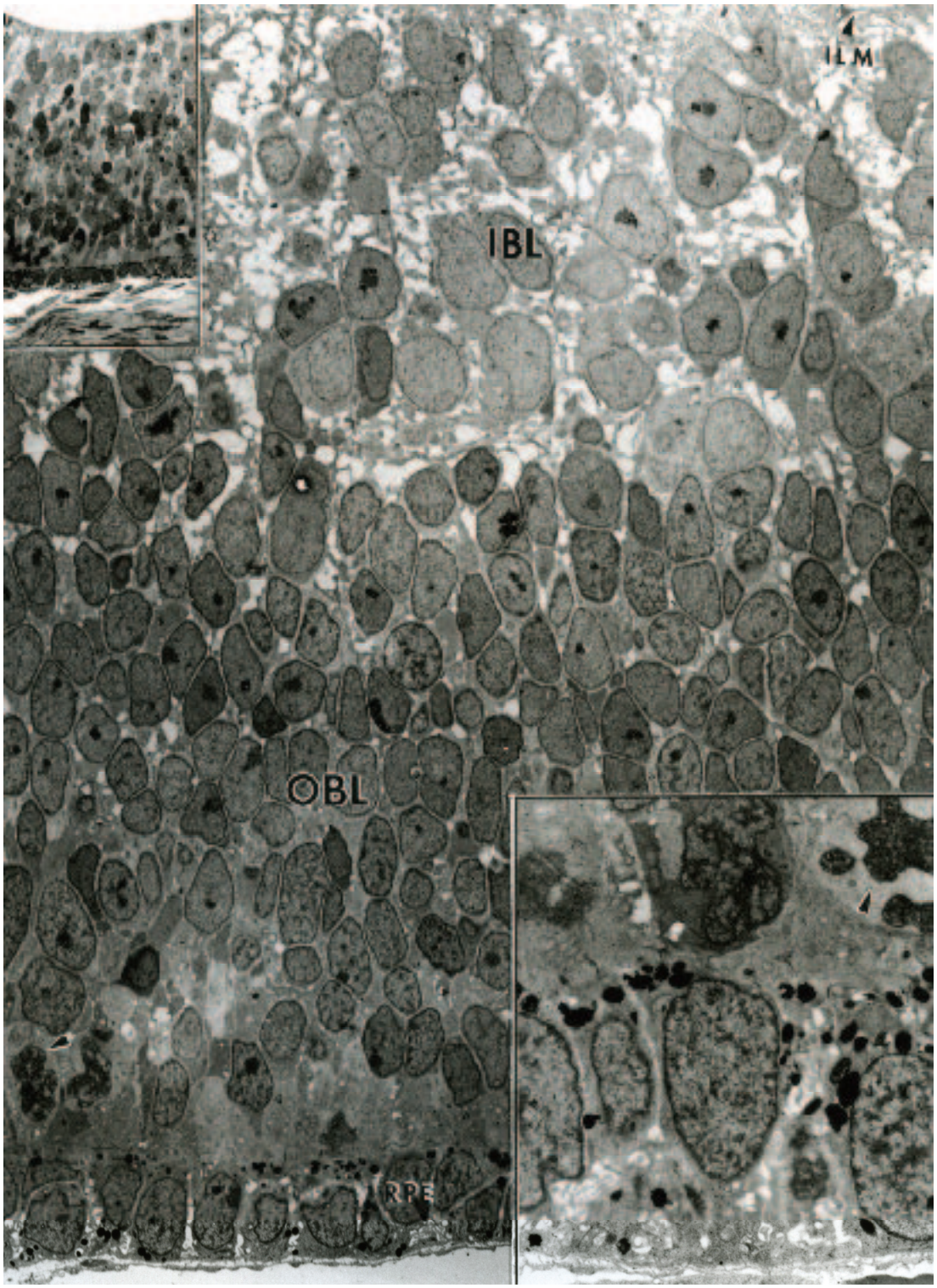

Fig. 11. (*Above left inset*). A micrograph illustrates the depth of the posterior pole of the opossum retina at one week postnatal. LM X 380. (*Primary electron micrograph*). The posterior pole of the retina from the inner limiting membrane (ILM) to the retinal pigment epithelium (RPE) illustrates two distinct populations of cells between: an inner neuroblastic layer (IBL) and an outer neuroblastic layer (OBL) of cells. The arrowhead indicates a mitotic figure. Opossum retina one week postnatal. TEM X 1,710. (*Below right inset*). Note the close juxtaposition of the retinal pigment epithelium and cells of the outer neuroblastic layer one of which is in division (arrowhead). TEM X 3,480.

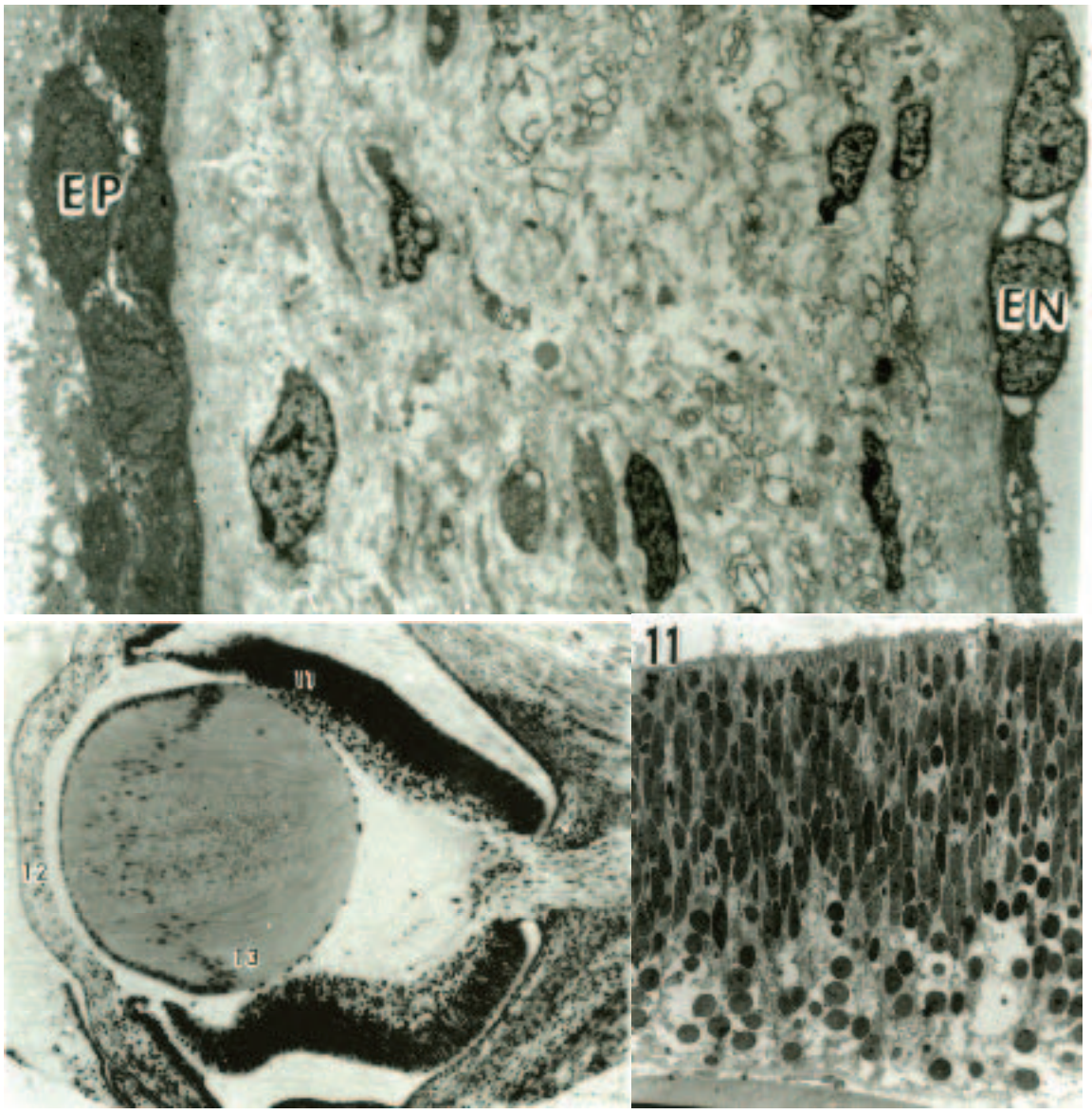

Fig. 12. (*Above*). A section through the cornea of an opossum one week postnatal illustrates the corneal epithelium (EP), the corneal endothelium (EN), and keratocytes within the collagenous corneal stroma. TEM X 2,000. (*Below left*). A section through the long axis of the eye of an opossum two weeks into the postnatal period illustrates the state of organogenesis in various subcomponents. Note in particular regions labeled (11), (12), and (13) which will be presented at increased magnification in the following three electron micrographs. LM X 75. (*Below right, region 11*). The state of retinal organogenesis at two week into the postnatal period is similar to observed in the neural retina of the opossum at one week after birth and consists primarily of inner and outer neuroblastic layers. TEM X 600.

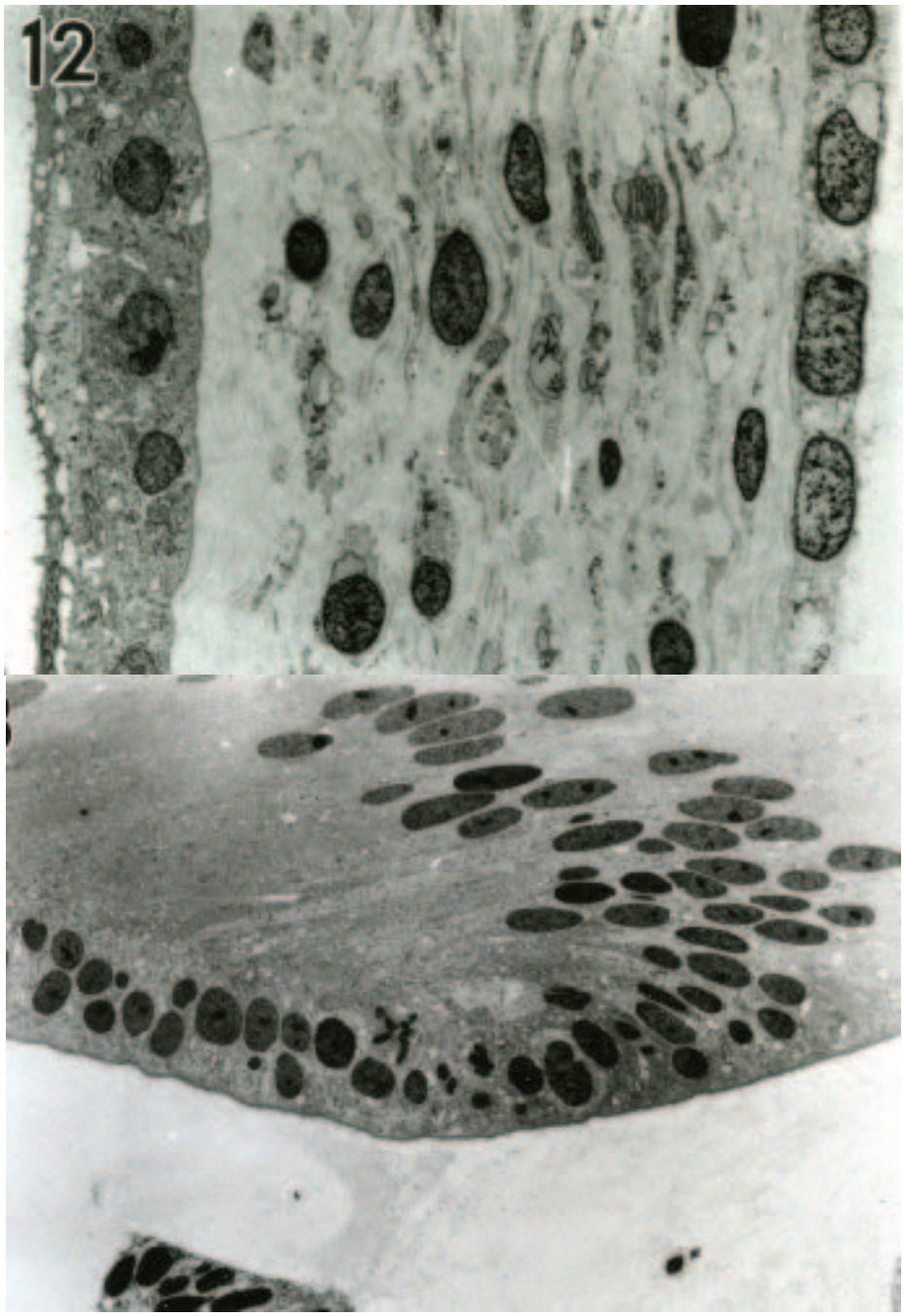

Fig. 13. (*Above, region 12*). The cornea of the two-week postnatal opossum shows continued development and maturation of the corneal epithelium, endothelium and intervening stroma. Note the acellular zone within the corneal stroma immediately beneath the corneal epithelium. TEM X 3,000. (*Below, region 13*). A region of the lens illustrates the anterior lens epithelium (to the left) and the equatorial lens bow. Note the overall size of the lens shown in figure 12 and the well-formed secondary lens fibers. Opossum two weeks postnatal. TEM X 1,500.

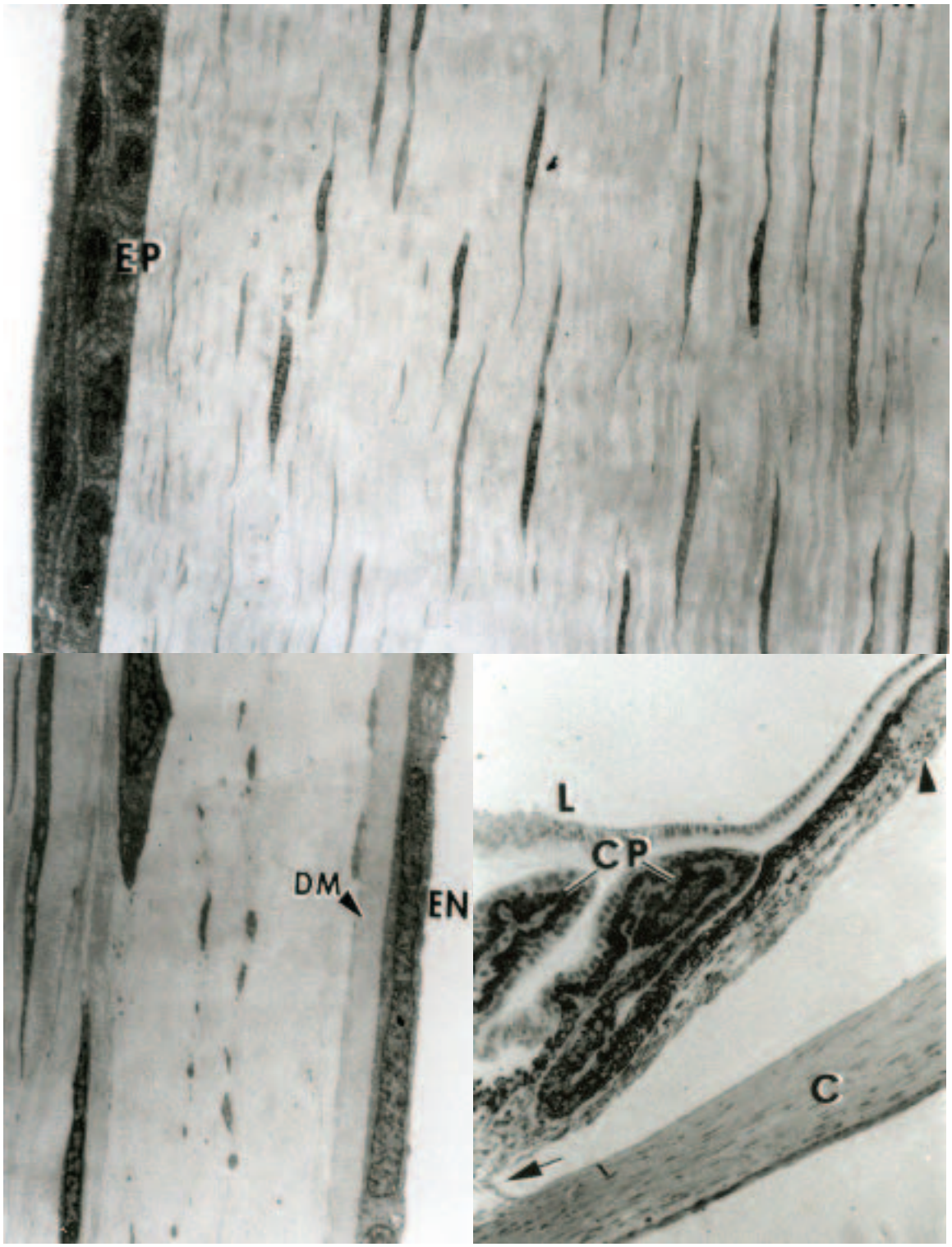

Fig. 14. (*Above*). A region of the cornea from an opossum six weeks postnatal illustrates that the corneal epithelium (EP) is now a three-layered epithelium and that the collagenous lamellae and flattened keratocytes of the corneal stroma show a greater differentiation and organization. Compare this illustration with figures twelve and thirteen. TEM X 2,000. (*Below left*). A region of the cornea interior illustrates the corneal endothelium (EN) resting upon a distinct Descemet's membrane (DM). Opossum six weeks postnatal. TEM 1,500. (*Below right*). The anterior segment of the opossum eye at six weeks postnatal illustrates well-developed ciliary processes (CP), the sphincter pupillae muscle (arrowhead) at the pupil margin, and the iridocorneal angle (arrow). The cornea (C) and lens epithelium (L) also can be observed. TEM X 100.

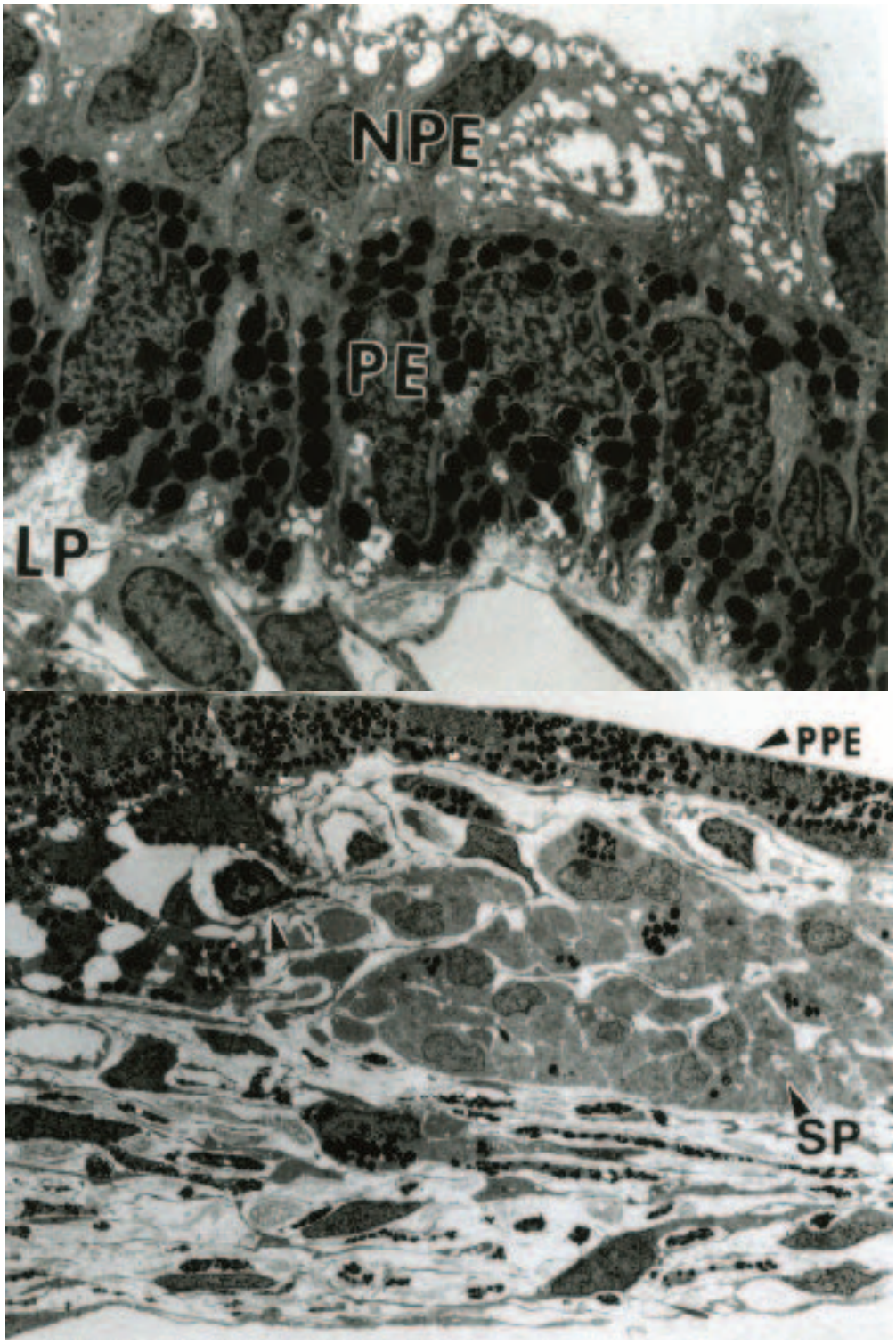

Fig. 15. (*Above*). A segment of a ciliary process illustrates the vascular stroma (LP) covered by pigmented ciliary epithelium (PE) and non-pigmented ciliary epithelium (NPE). Opossum six weeks postnatal. TEM X 1,500. (*Below*). The sphincter pupillae muscle (SP) within the iris and positioned beneath the posterior iris pigment epithelium (PPE) of an opossum six weeks postnatal. Note that the vascular stroma of the iris contains numerous fibroblasts and melanocytes within an irregular collagenous matrix. An occasional mast cell (arrowhead) also is observed. TEM X 1,500.

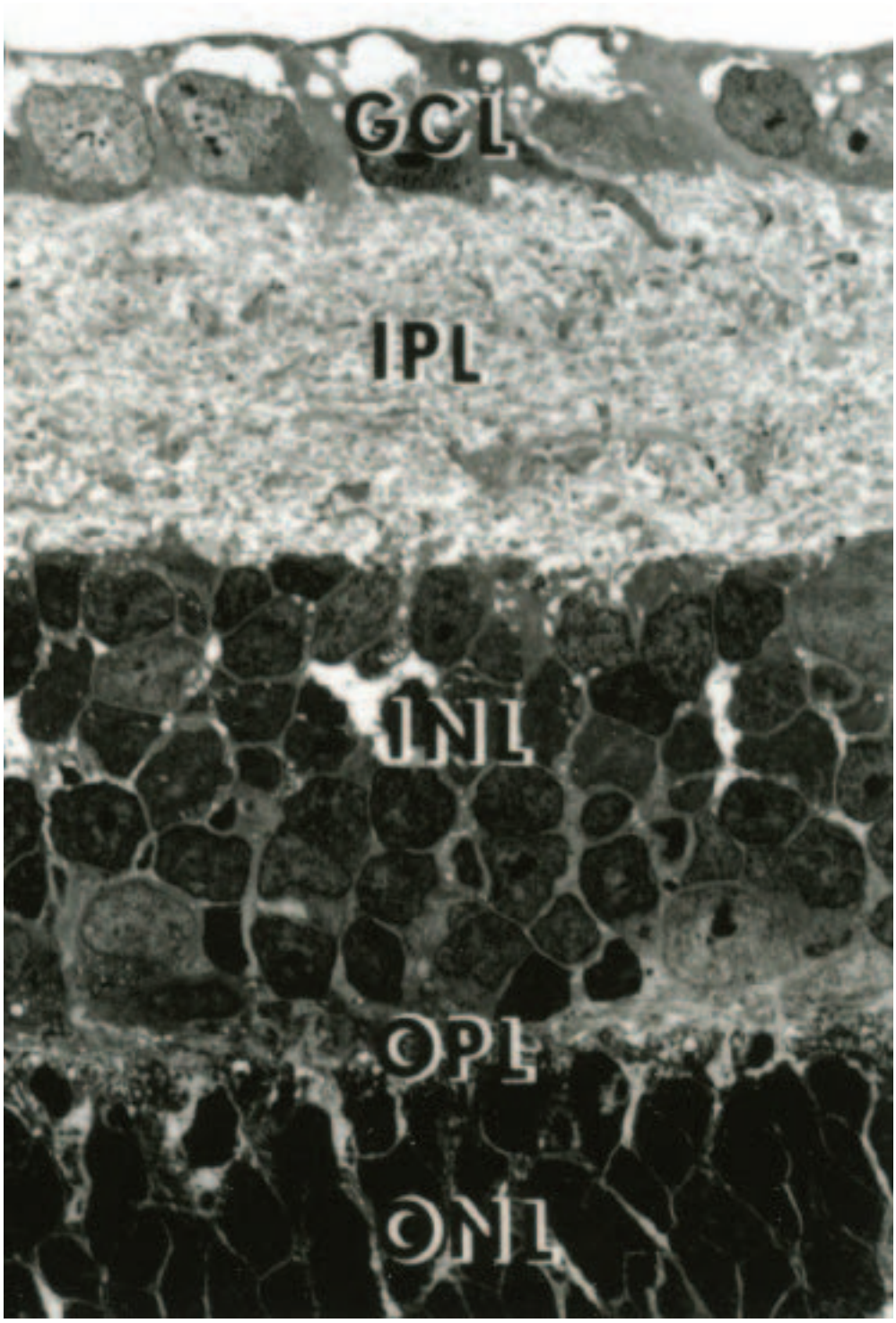

Fig. 16. At six weeks postnatal the inner retina of the opossum eye shows an adult-like arrangement of the ganglion cell layer (GCL), inner plexiform layer (IPL), inner nuclear layer (INL), outer plexiform layer (OPL), and outer nuclear layer (ONL). The retina remains avascular at this stage of development. TEM X 2,100.

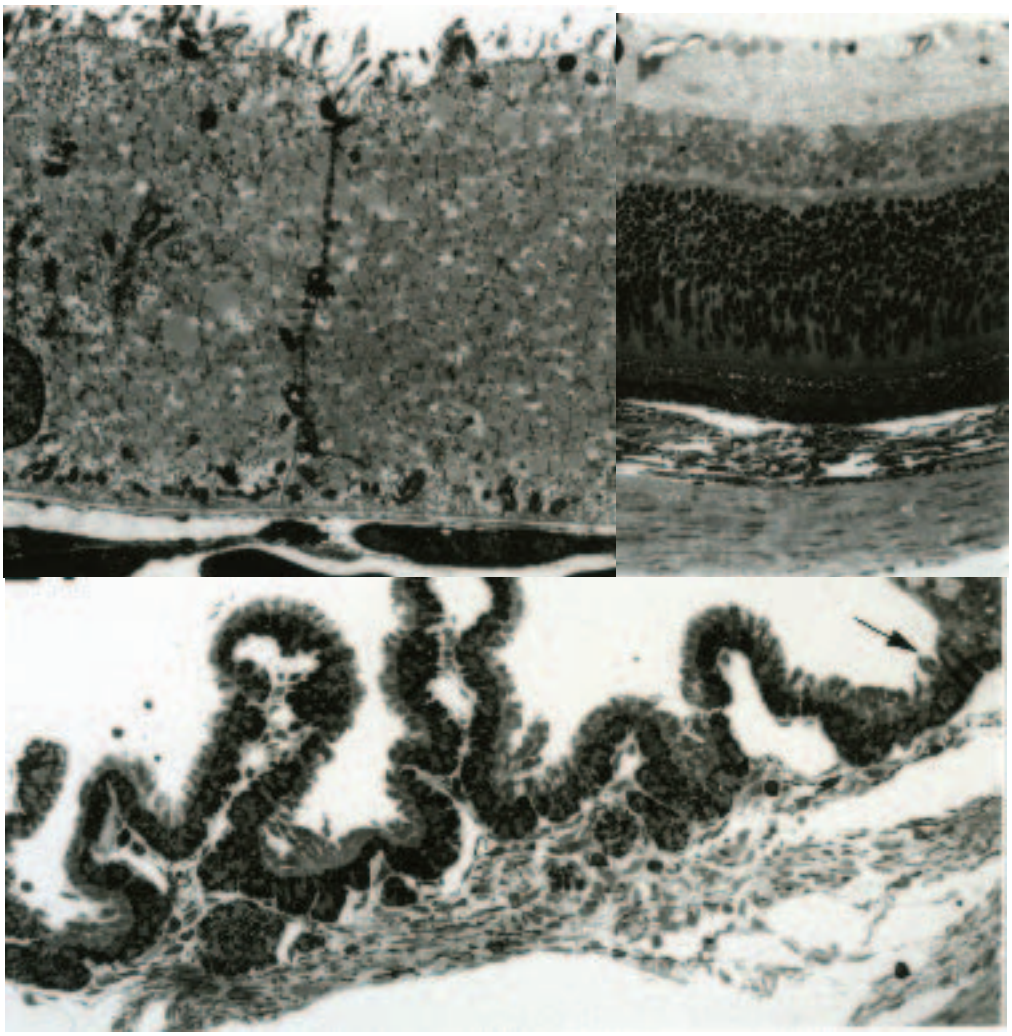

Fig. 17. (*Above left*). A segment of the retinal pigment epithelium that illustrates the tapetal region of the opossum retina six weeks into the postnatal period. Note the abundance of intracytoplasmic lipid droplets and the location of mitochondria positioned along the basal and lateral cell membranes. TEM X 2,500. (*Above right*). The central region of the retina from an opossum thirteen weeks into the postnatal period. The underlying choroid and sclera are positioned at the bottom of the figure. The overall morphology is similar to the adult retina with the exception of a thickened outer nuclear layer. Note that the paired vessels are restricted to the inner retina. LM X 100. (*Below*). The ciliary body of an opossum eye thirteen weeks into the postnatal period. The arrow indicates the pars plana-retinal junction. LM X 400.

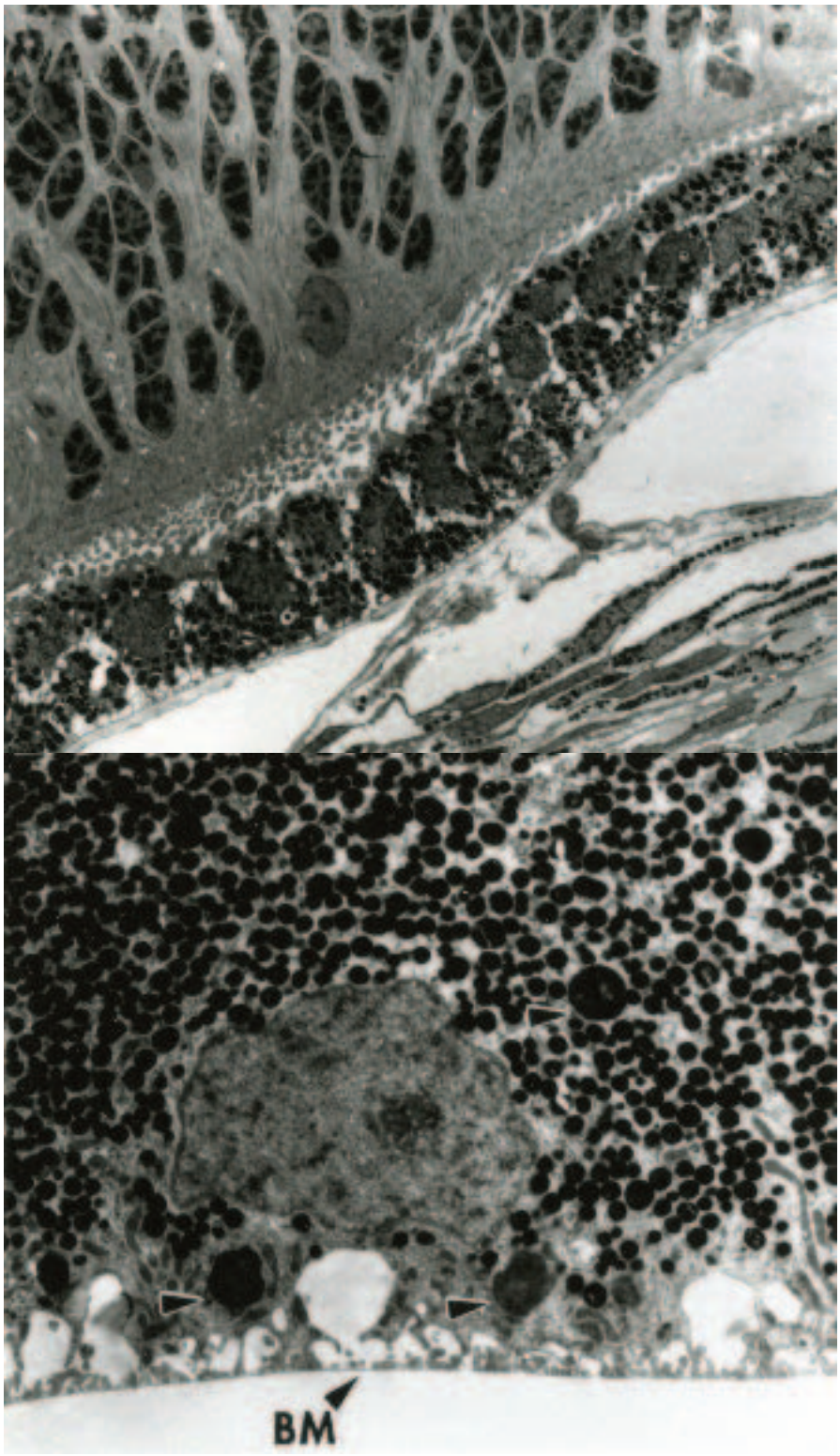

Fig. 18. (*Above*). The peripheral retina of an opossum thirteen weeks postnatal illustrates that the photoreceptors of this region are poorly developed. The retinal pigment epithelium appears stratified is some areas. TEM X 1,000. (*Below*). A micrograph illustrates the central (non tapetal) region of retinal pigment epithelium from a thirteen-week opossum. Large phagolysosomes are show at the arrowheads, evidence for phagocytosis of photoreceptor outer segments. The choriocapillaris is detached from Bruch's membrane (BM) and is not observed in the field of view. TEM X 5,000.

Chapter 37. Harderian Gland

Synopsis:

Only the adult opossum Harderian gland has been examined to date. The Harderian glands of the opossum are large and well developed located behind the eye in the bony orbit. The adult opossum lacks a nictitating membrane. The glands are elongate and enveloped by a delicate connective tissue capsule from which thin septae extend into and subdivide each gland into numerous lobules. The majority of the secretory units are tubuloalveolar in nature with widely dilated lumina filled with secretory product. The secretory units are drained by a well-defined intralobular and interlobular duct system. Both the secretory units and ductal elements are invested by an abundance of myoepithelial cells. Cells lining the secretory units are columnar in shape and are characterized by numerous lipid-containing secretory vesicles suspended in a matrix of considerable electron density. Numerous large irregularly shaped mitochondria also are observed. Likewise, the secretory product within the lumina of the secretory units consists of numerous intact lipid droplets suspended within an amorphous material. Electron-lucent epithelial cells that lack both the lipid-containing vesicles and large mitochondria line the intralobular and interlobular ducts.

In additional to the larger secretory units, a smaller, serous type of secretory unit also occurs near the center of some Harderian gland lobules. The epithelial cells forming the secretory tubules of these units are arranged about a narrow lumen. The serous cells are pyramidal in shape and their cytoplasm is filled with numerous electron-dense secretory granules and scattered profiles of granular endoplasmic reticulum. The basolateral cell membrane of these cells shows extensive infoldings and numerous intercellular canaliculi also are observed. The size of cells forming the serous secretory units is much less than those forming the tubuloalveolar secretory units of the remainder of the Harderian gland.

Acknowledgments:

Figs. 1, 2, 3 and 4, courtesy of and from: Krause, W.J. and P.G. McMenamin (1992). Morphological observations on the Harderian gland of the North American opossum (*Didelphis virginiana*). Anat. Embryol. 186:145-152.

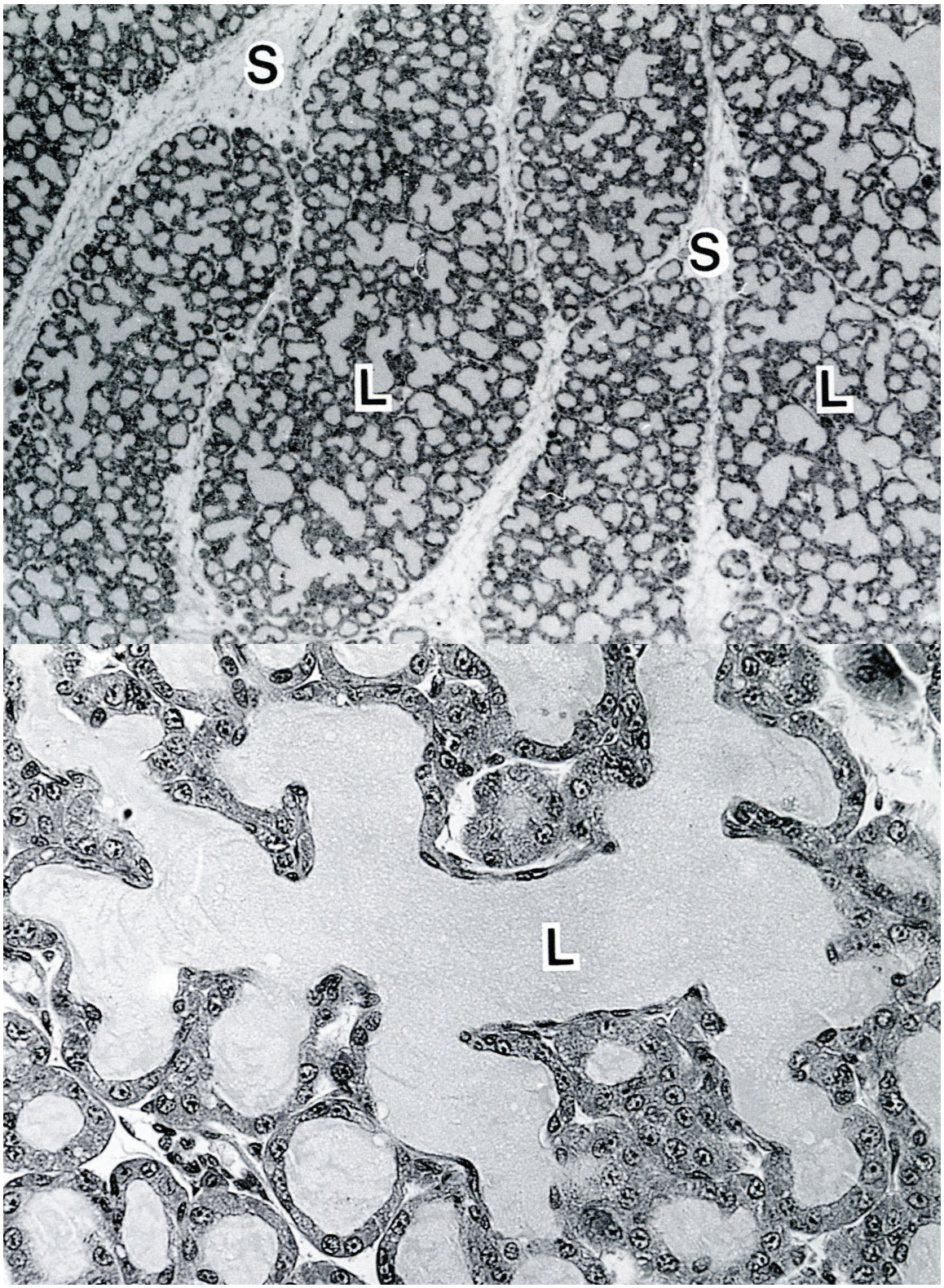

Fig. 1. (*Above*). A transverse section through the center of a Harderian gland illustrates several lobules (L) separated by delicate intervening connective septae (S). Adult female opossum. LM X 160. (*Below*). The lumen (L) of an intralobular duct is shown near the center surrounded by a number of expanded tubuloalveolar secretory end-pieces. LM X 300.

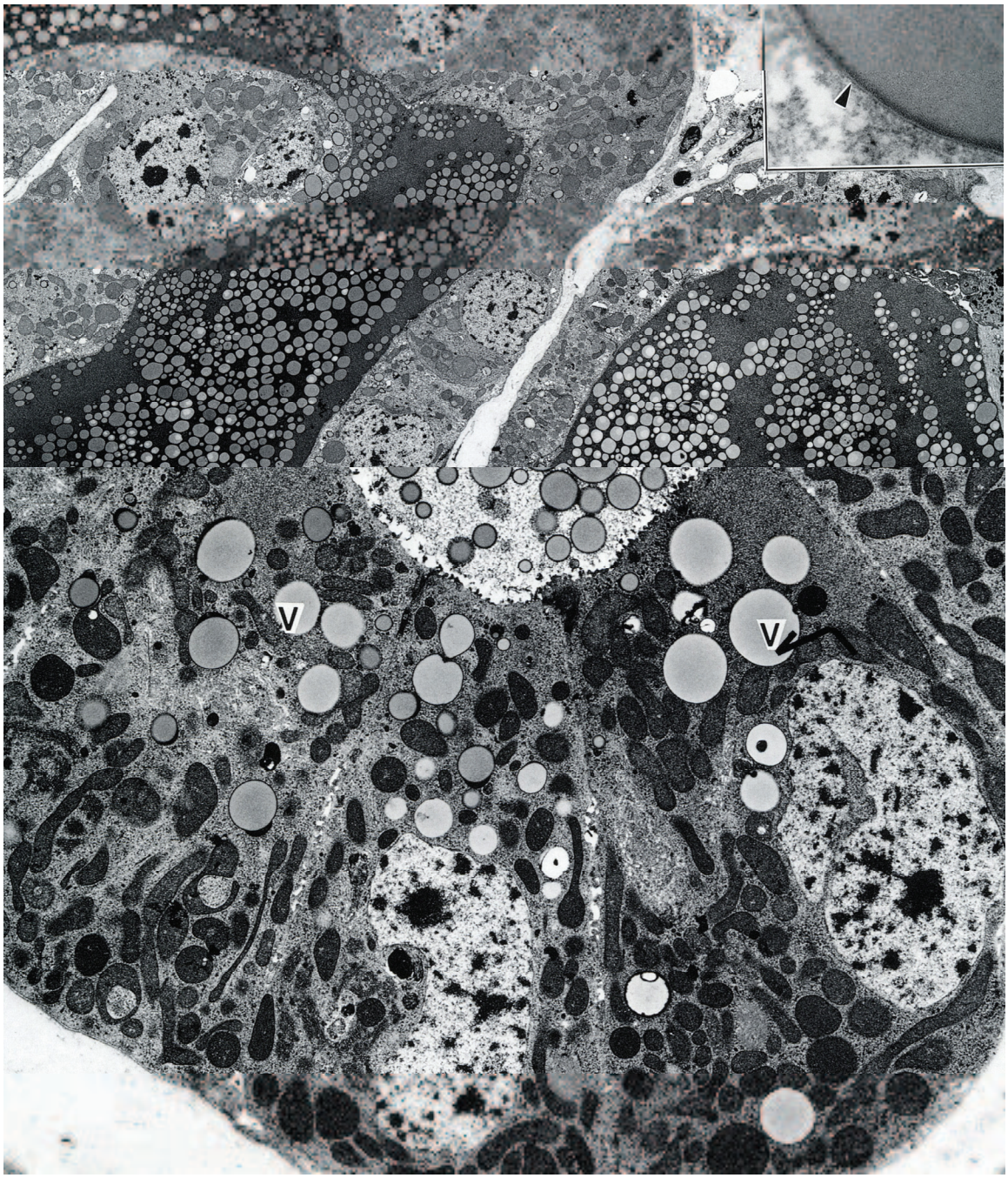

Fig. 2. (*Above*). Epithelial cells lining two adjacent tubuloalveolar secretory end pieces vary considerably in height. Note the number and size of the lipid droplets within the lumen suspended in an electron-dense matrix. The intraluminal lipid droplets appear limited by a membrane (arrowhead; inset at upper right). Adult female opossum. TEM X 1,900. Inset X 84,000. (*Below*). Epithelial cells lining Harderian gland secretory end-pieces contain numerous lipid-containing vesicles (V) of variable size and numerous large mitochondria of varying shapes and sizes. Adult female opossum. TEM X 29,000.

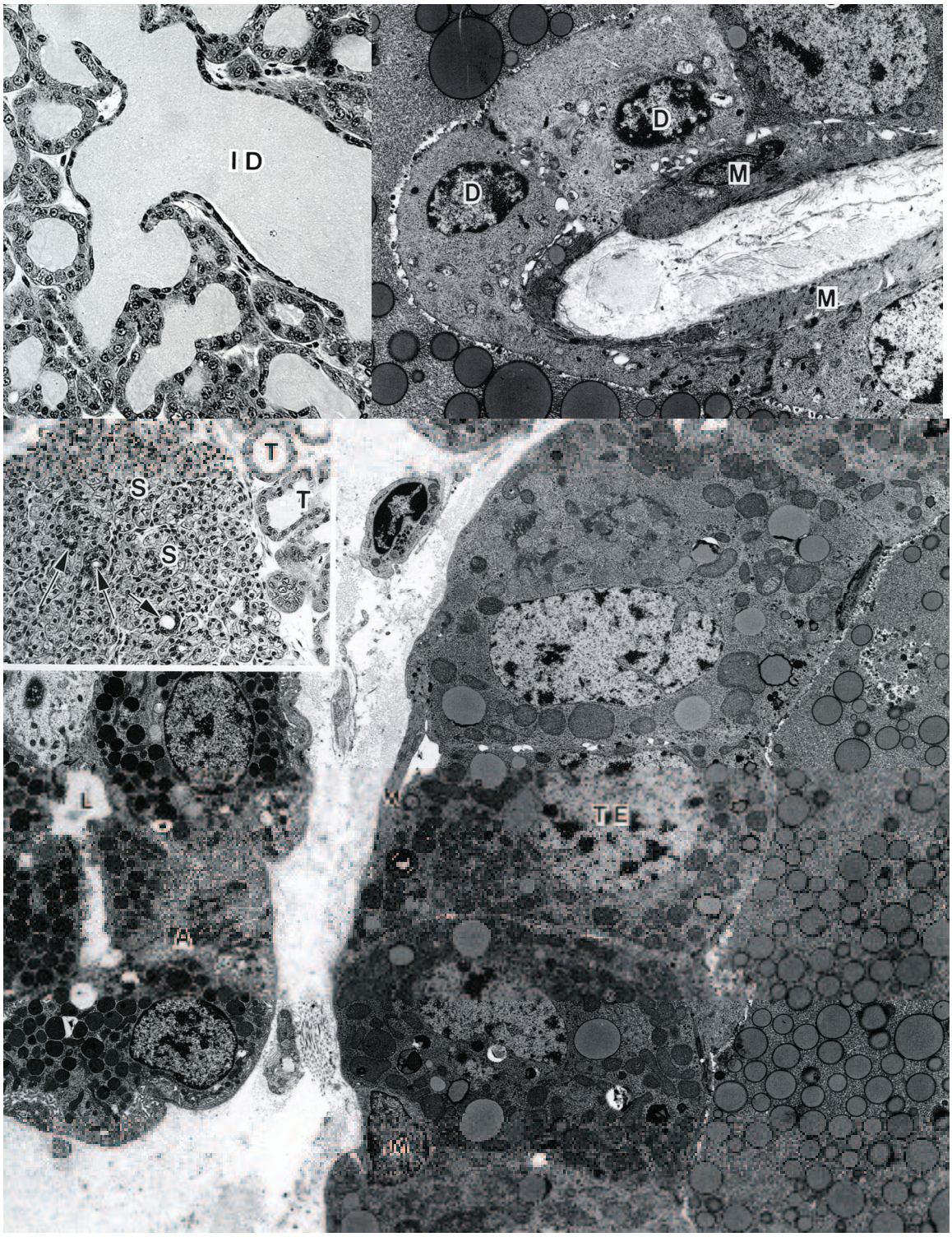

Fig. 3. (*Above left*). An expanded intralobular duct (ID) lined by simple cuboidal epithelium. Note the continuity of the lumina of surrounding secretory end-pieces with that of the intralobular duct. LM X 200. (*Above right*). Ductal epithelial cells (D) are characterized by an electron-lucent cytoplasm and lack lipid droplets. Myoepithelial cells (M) are found between the basal lamina and the ductal epithelium. TEM X 4,000. (*Center left*). A central region of Harderian gland showing expanded tubuloalveolar secretory tubules (T) and smaller, serous tubuloacinar units (S). Intralobular ducts (arrows) are associated with the latter. LM X 170. (*Below*). Compare a portion of a small serous acinus (A) (left) to the expanded tubuloalveolar end-piece (TE) (right). Note that smaller cells surround a small lumen (L) of the serous acinus and that myoepithelial cells (M) are associated with larger cells of the tubuloacinar units. TEM X 3,500.

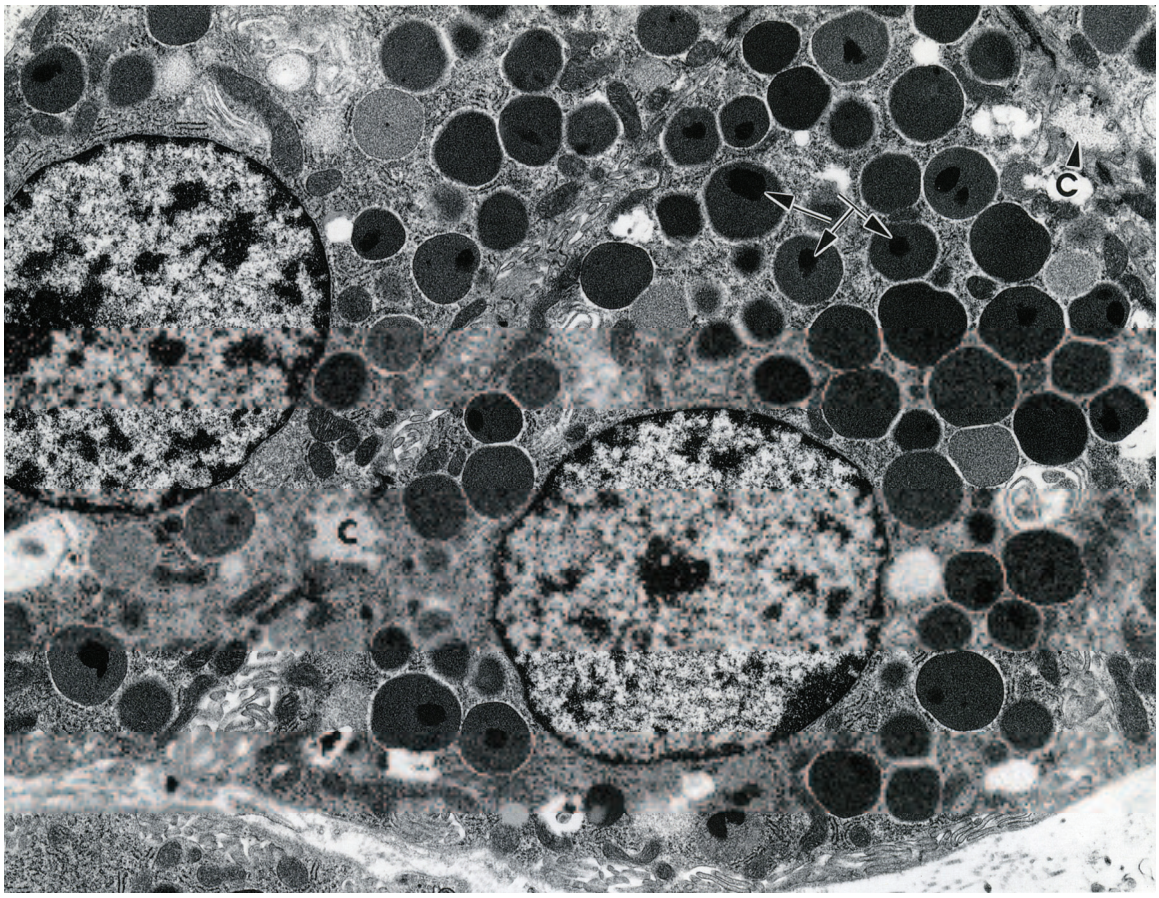

Fig. 4. Two adjacent serous secretory cells from an acinus similar to those depicted in figure 3 (center left and bottom figure). The cytoplasm contains numerous secretory granules some of which vary in electron density. Some secretory granules show a central region of increased electron density (arrows). The basolateral cell membrane exhibits considerable infolding and intercellular canaliculi (C) are a common observation between serous cells. TEM X 9,000.

Chapter 38. Testis

Synopsis:

The testes begin their organogenesis in the urogenital ridge, a thickened region of mesoderm that contains the primordia of both the gonads and kidneys. Proliferation of coelomic epithelial cells late in prenatal day ten on the ventromedial surface of the urogenital ridge signals the initial formation of the gonad. By late in prenatal day twelve definite groups and cords of cells begin to appear in the forming gonad. The epithelial cords of the forming rete are not associated with primordial germ cells and will eventually become incorporated into the hilar region of the developing testis. They will eventually unite the seminiferous tubules with the efferent ductules. The testis is undifferentiated at birth in *Didelphis*. During the first few days of postnatal life the forming testis shortens, rounds up and is closely associated with the regressing mesonephros. At this time primary testis cords are apparent and extend inward toward the center of the forming gonad from the coelomic epithelium. The homogeneous gonad becomes organized into an area of central stroma that eventually becomes associated with rete cords surrounded by a zone of pale-staining cells (medullary epithelial cords) and an outer layer of condensed connective tissue covered by coelomic epithelium. The light cells occupying the middle zone become organized into testis cords. Scattered within the testis cords are occasional large cells thought to be primordial germ cells. The latter are large round, light-staining cells with a prominent nucleus and nucleolus. The testis cords lengthen and extend toward the mesorchium and by the end of the first postnatal week become encapsulated by a primitive tunica albuginea. This is the first morphological indication of testicular differentiation in the opossum. As the rete cords (presumptive rete tubules) become continuous with the testis cords, the latter continue to elongate and differentiate into the seminiferous tubules. Following their union, the solid rete and testis cords then become hollow tubules. As a consequence of the organization of the epithelium around a central lumen, Sertoli cells are arranged peripherally and primordial germ cells occupy a central position within the epithelium lining the seminiferous tubules. The full complement of spermatogenic cells does not appear until puberty. The point of union between the rete and seminiferous tubules lacks germ cells and this region of the seminiferous tubule remains straight forming the tubuli recti. The mesenchymal tissue in which the testis cords develop differentiates into the interstitial tissue (septula testis, connective tissue of the mediastinum, and contributes to the tunica albuginea). Some mesenchymal cells of the stroma between testis cords differentiate into the interstitial cells (of Leydig).

Acknowledgments:

Figs. 1, 2, 3 and 4, courtesy of and taken from: Krause, W.J. (1998) A review of histogenesis/organogenesis in the developing North American opossum (*Didelphis virginiana*). Adv. Anat. Embryol. Cell Biol. 143 (II): Springer Verlag, Berlin, pp 120.

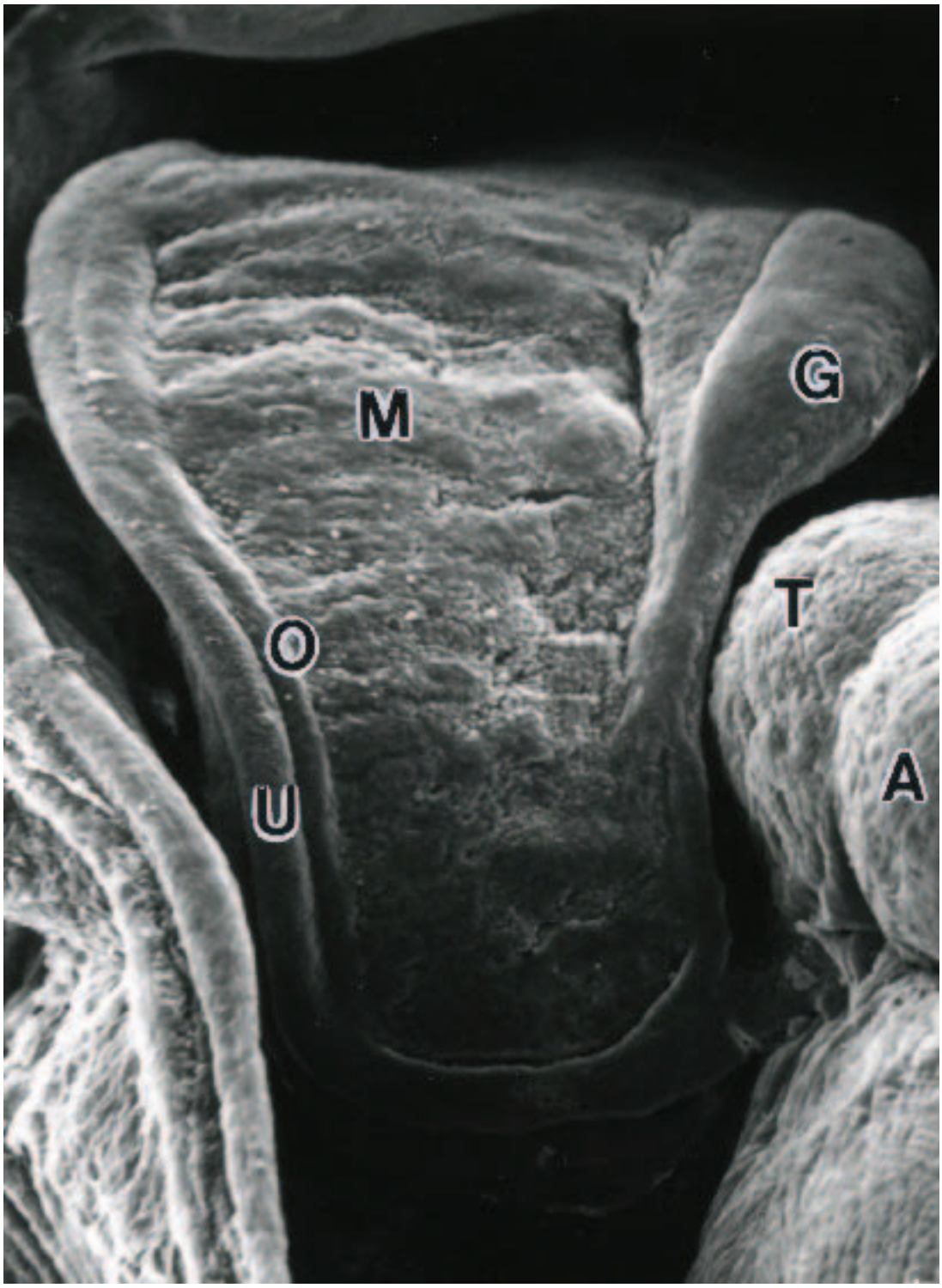

Fig. 1. The proximal urinogenital system of an opossum during the middle of the first postnatal week illustrates a developing gonadal ridge (G), a mesonephros (M) and its associate mesonephric (O) and Müllerian ducts (U) as well as the differentiating metanephros (T) and adrenal cortex (A). SEM X 200.

Fig. 2. The urinogenital region of an opossum after one week of postnatal life shows continued development of the gonad (G), adrenal (A), and metanephros (T). In contrast, the mesonephros (M) appears somewhat reduced in size and shrunken. Note the continued development of the mesonephric duct and the lost of the Müllerian duct in this specimen. SEM X 180.

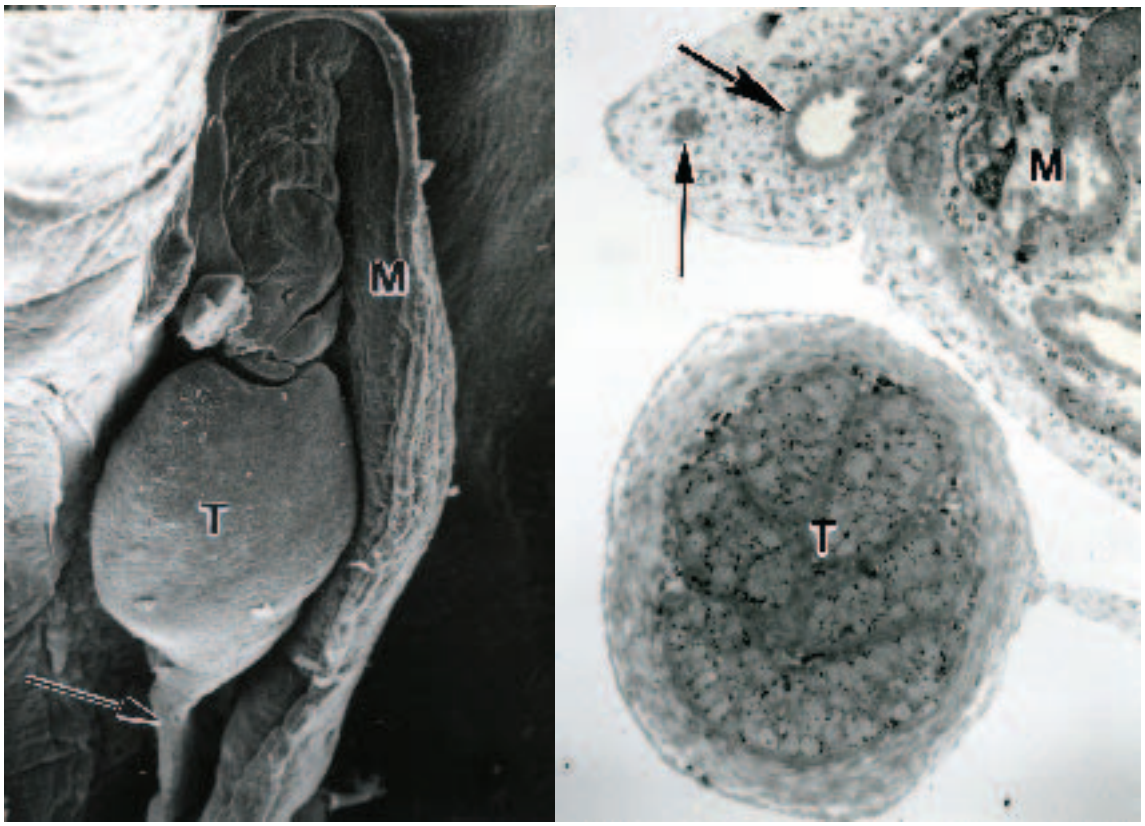

Fig. 3. (*Left*). By the end of the second postnatal week the testis (T) lies immediately medial to the mesonephros (M), which continues to shrink and is reduced in size as compared to younger ages. Note the apparent continued development of the mesonephric duct near the cranial pole of the testis. The caudal pole of the testis is associated with a structure believed to be the gubernaculum (arrow). SEM X 100. (*Right*). A histological section demonstrates the intimate relationship between the regressing mesonephros (M) and the developing testis (T) at the end of the second postnatal week in a male opossum. Note the continued development of the mesonephric duct (large arrow) and the regression of the Müllerian duct (small arrow), which at this stage of development appears only as a remnant. LM X 100.

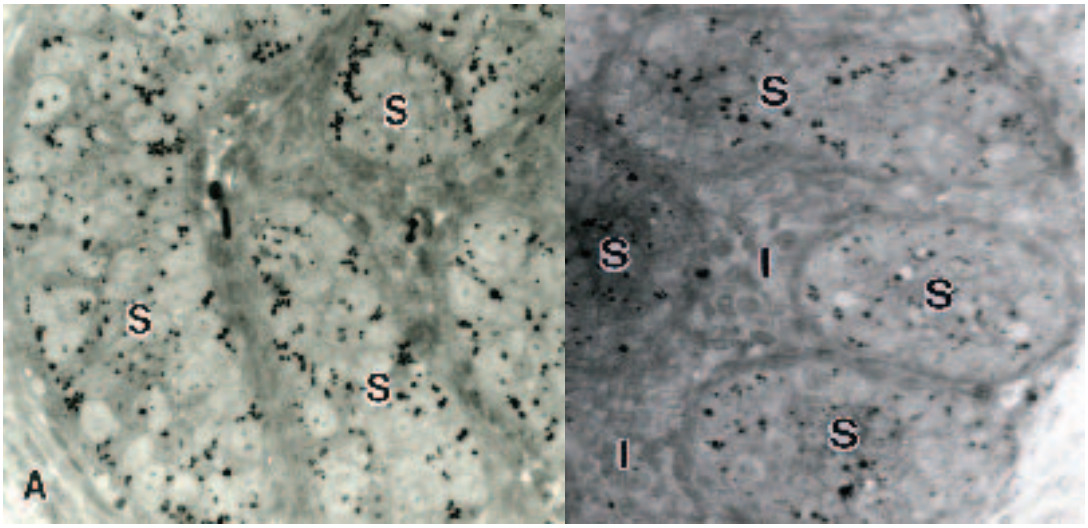

Fig. 4. (*Left*). The seminiferous tubules (S) and limiting tunica albuginea (A) are evident by the end of the second postnatal week. LM X 300. (*Right*). The seminiferous tubules (S) of the opossum are well defined by the end of the third postnatal week and are separated by intervening interstitial connective tissue (I). The tubules consist primarily of Sertoli cells and scattered spermatogonia. The full spectrum of spermatogenic cells will not appear until puberty in late juvenile animals. LM X 300.

Chapter 39. Ovary

Synopsis:

The genital ridge begins its development during the latter part of the tenth prenatal day and appears as a longitudinal thickening of coelomic epithelium along the medial aspect of the mesonephric ridge. The genital ridge develops rapidly during the prenatal period and consists of coelomic epithelium overlying an epithelial cell mass. Large cells associated with the forming genital ridge are thought to be primordial germ cells. Just prior to birth the genital ridge can be subdivided into a posterior mesenteric, middle genital, and an anterior rete region. The opossum gonad (ovary) is indifferent at birth but may exhibit primary gonadal cords. Cells growing from the coelomic (germinal) epithelium covering the presumptive ovary give rise to primary gonadal (sex) cords. Additional gonadal cords also may form from the underlying epithelial cell mass. Growth of mesenchyme separates the primary gonadal cords from the surface (germinal) epithelium and then thickens rapidly to form the tunica albuginea of the ovary. Some primordial germ cells or gonocytes may become incorporated into the gonadal cords whereas others remain under the surface epithelium within the differentiating stroma. Two distinct periods of proliferative activity occur during organogenesis of the ovary. The first is as described previously and results in the formation of the primary gonadal cords. The second period is concerned with the establishment of the ovarian cortex. It begins during the middle of the first postnatal week and continues through the fourteenth postnatal week. As the epithelium continues to proliferate from the gonadal ridge of the newborn, clumps of cells form additional gonadal cords that extend into the underlying mesenchyme. The gonadal cords at the periphery of the provisional ovary establish a primary ovarian cortex. A proliferation of mesenchyme centrally establishes a primary ovarian medulla. The primary gonadal cords are separated into irregular clusters of cells by intervening mesenchyme. The expanding mesenchymal stroma beneath the surface of the ovary separates the remaining gonadal epithelial cords from the surface epithelium and eventually becomes the primary tunica albuginea. As this occurs, rete cords grow into the presumptive ovary from the coelomic epithelium covering the rete portion of the genital ridge. The expanding rete cords are similar to the primary gonadal cords but are not associated with primordial germ cells and follow a more torturous course. A second proliferation of cells from the coelomic epithelium then occurs which gives rise to a new generation of epithelial cords that invade the primary ovarian cortex. These secondary gonadal cords are apparent by the end of the first postnatal week. The primary and secondary gonadal cords are separated by the primary tunica albuginea. At this time a single layer of flattened epithelial cells envelops some primordial germ cells but most are observed with the secondary gonadal cords. The secondary gonadal cords increase in size during the second postnatal week due to continued mitotic activity. They lack any direct connections with the rete cords that extend into the mesovarium of the forming ovary. The appearance of the definitive tunica albuginea occurs during the second postnatal week and permanently separates the secondary gonadal cords from the overlying germinal epithelium. The primary tunica albuginea continues to lie between the primary and secondary gonadal cords. The secondary gonadal cords continue to extend from the periphery of the ovary to its center and exhibit short lumina by the fifth postnatal week. By the seventh postnatal week invading stromal cells subdivide the epithelial cords into clusters of cells that envelop the primordial germ cells (ova). The latter enter prophase of the first meiotic division and are termed

primary oocytes. Primordial germ cells located in or near the medulla of the forming ovary degenerate. A more compact sheath of mesenchyme surrounds the newly formed primordial follicles by tenth postnatal week and the rete continues to expand but remains independent and is free of oocytes. Active follicular formation begins at about this time with granulosa cells being derived from remnants of the gonadal cords and/or stromal cells that took their origin from the germinal epithelium. Granulosa cells of the larger follicles form a layer two to three cells thick by the fourteenth postnatal week. Secondary (antral) follicles are first observed at about the sixteenth week of postnatal life. The ovary doubles its weight between the fourteenth and sixteenth postnatal week and the primary medulla of the ovary is gradually replaced by a fibroelastic stroma seen in the adult. During the first postnatal week the gonads become steroidogenically active and can convert precursor molecules to testosterone and progesterone. By the third postnatal week the differentiating ovaries acquire significant aromatase activity.

Acknowledgments:

Figs. 1 (bottom) and 2, courtesy of and taken from: Krause, W.J. (1998) A review of histogenesis/organogenesis in the developing North American opossum (*Didelphis virginiana*). Adv. Anat. Embryol. Cell Biol. 143 (II): Springer Verlag, Berlin, pp 120.

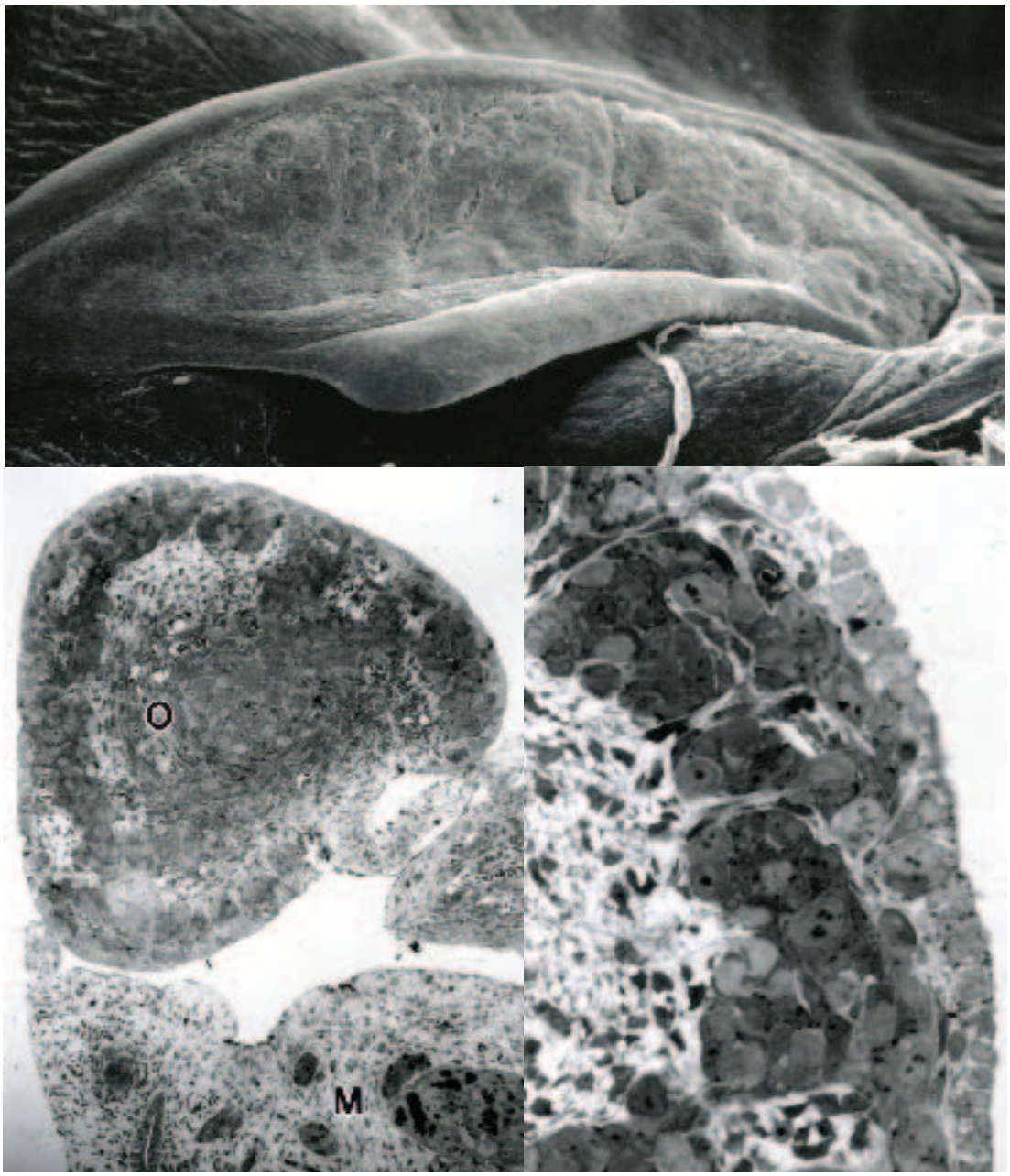

Fig. 1. (*Above*). The mesonephros of newborn opossum viewed by scanning electron microscopy. The elongate genital ridge (shown at the bottom center of the figure) runs parallel to the medial surface of the mesonephros. Note the position of the mesonephric and Müllerian ducts coursing on the lateral surface of the mesonephros near its superior pole (upper right). SEM X 50. (*Below left*). A histological section through the ovary (O) of a two-week postnatal opossum illustrates the state of development of the ovarian cortex during this period of organogenesis. A portion of a degenerating mesonephros (M) is shown at the bottom. Note that at this time the mesonephric duct is degenerative as well whereas the Müllerian duct continues to develop. LM X 50. (*Below right*). When viewed at increased magnification, the germinal epithelium covering the surface of the ovary and the underlying gonadal cords are clearly evident. Note the primitive nature of the mesenchyme filling the presumptive medulla at the left in this ovary of a female opossum at two postnatal weeks. LM X 250.

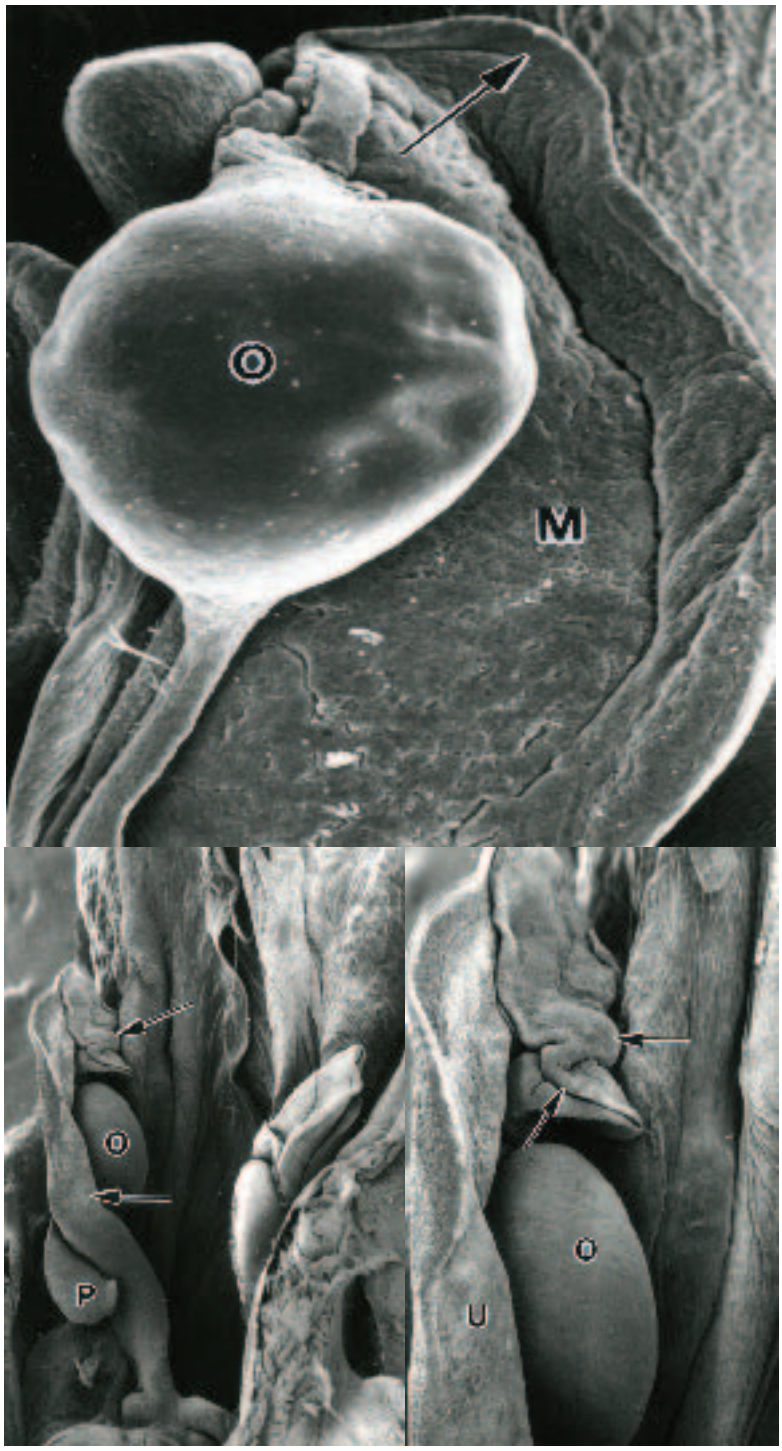

Fig. 2. (*Above left*). The shrunken mesonephros (M) and external surface of the ovary (O) of a female opossum two weeks postnatal. Note the position of the Müllerian duct (arrow) near the top of the photomicrograph. SEM X 50. (*Below left*). Four weeks into the postnatal period, the ovary (O) and the Müllerian duct (arrows) continue to develop as the mesonephros degenerates. Note the appearance of a pigmented body (P) associated with the female gubernacular system. SEM X 20. (*Below right*). At increased magnification the ovary (O) and regions of the Müllerian duct destined to become the oviduct (arrows) and uterus (U) are seen in greater detail. SEM X 50.

Index

Adrenal 397-404
cortex 397, 400-404
medulla 397, 402-404
chromaffin cells 397-400
Allantois 53-60
Alveoli 211, 225
Amnion 30, 40, 43-44
Bartholin's gland 14, 16
Blastocyst 61, 63-70
unilaminar blastocyst 61, 63
bilaminar blastocyst 61, 63
trilaminar blastocyst 61, 63
Blood 352-359
erythrocytes 352, 354-357
leukocytes 352, 359
eosinophils 352, 359
lymphocytes 352, 353
neutrophils 352, 359
platelets 358
Brain 405-428
Bronchi 210-214, 218-225
Bronchial glands 211, 225
Brunner's glands 290-296
Cardiovascular system
heart 360-367
cardiac muscle 360-361, 363-367
fusion of hemicardia 362
myocardial cells 360-361, 363-367
myocardial myofibrils 363-365
T-tubule formation 360, 363-365
sarcoplasmic bodies 366-367
Cervix 14, 16, 22-23
Chorion 30, 40, 43
Cleavage 61, 63
Colon 297-301
Collecting tubules
mesonephros 156, 159, 162, 168-169
metanephros 176, 179-181, 186, 188-189, 191, 193
Corpus luteum 15, 18-20
Cowper's gland 1, 3
Deciduous claws 86-87, 98-99, 123, 125-126
Ductuli efferentes 1, 5
Ductus (vas) deferens 1, 3
Ear 429-436
External ear 429, 485-433
external auditory meatus 429
pinnae 429, 431-433
Inner ear 429
anterior semicircular canal 430, 434
cochlea 430, 434-435
cristae 430
cupula 430
endolymphatic duct 430,434
lateral semicircular canal 430, 434
macula 430, 436
otolithic membrane 430, 436
organ of Corti 430
otic placode 429
otocyst 429
posterior semicircular canal 430, 434
utriculus 430,434, 436
sacculus 430, 434
Middle ear 429
auditory tube 429
ossicles 429
stapedius muscle 429
tensor tympani muscle 429
tympanic cavity 429
tympanic membrane 429
Ectoderm 32, 40, 43, 61, 63, 65-66
Efferent ductule 1, 5
Embryo formation 61-88
Embryos
eight day 64-66
eleven day 83-86
nine day 64, 69-72
ten day 77-82
twelve day 86-88
Endoderm 32, 40, 43, 49-50, 61, 63, 76
endodermal mother cells 61, 63
Enterocytes
colon 297-301
small intestine 279-288
Enteroendocrine cells 258-259, 268, 270, 275-276, 279-280, 283, 287, 297
Epididymis 1,3, 6, 8-9, 11-12
Epiglottitis 210
Epitrichium 88, 136, 138-140
Esophagus 248-257
glands of 248, 256-257
transverse folds 248, 254-256

External nares 84-86, 88, 195-198
Extra-embryonic coelom 40, 43
Eye 437-457
canal of Schlemm 438
choriocapillaris 437
choroid 438, 443, 449
ciliary body 438, 456
ciliary processes 438, 453
cornea 437-438, 440-441, 448-449, 451-453
corneal endothelium 437, 451-453
corneal epithelium 437, 448, 451-453
Descemet's membrane 437, 453
keratocytes 438, 453
iris 438, 454
lens 437, 447-448, 451-452
lens vesicle 437, 447
nictitating membrane 437, 449
optic cup 437, 447-448
optic groove 437
optic nerve head 443
optic stalk 437
optic vesicle 437, 447
paired capillaries 443-446,438
retina 437-438, 442-446, 450-451, 455-457
retinal pigment epithelium 437-438, 447-450, 457
sclera 449
sphincter papillae muscle 453-454
tapetum 438, 456
trabecular meshwork 438
Eyelid 123, 126-135
Female reproductive tract 14-25
Fertilization 14
Fetal membranes 30, 33-34, 40-51, 53-60, 77-78, 84
Gametes 1, 7-8, 10-13, 15, 17
Genital (gonadal) ridge 463-464, 468, 470
Germinal epithelium 469-470
Gonadal cords 468-469
primary 468
secondary 468
Gubernacular apparatus 466, 471
Goblet cells 210-211, 279, 286, 297, 299-301
Harderian gland 458-462
Heart 360-367
Integument 136-155
dermal papillae 136
eccrine swear glands 137, 148
epidermis 136, 138, 141-142, 151, 153-154
Langerhans cells 146
periderm 138-140
stratum basale 136, 138, 141, 143, 146, 152
stratum corneum 141, 144, 147, 151, 153
stratum granulosum 136, 138, 141, 144-145, 147, 151, 153
keratohyalin granules 136, 141, 144, 147, 153
stratum spinosum 136, 138, 141-145, 151, 153
hair 136, 147, 149
hair follicles 136, 145, 150
papillary ridges 136
paracloacal glands 137
sudoriferous glands 137, 155
suprasternal glands 137, 154-155
vibrissae 130, 136, 138
Interstitial (Leydig) cells 463
Intestinal glands 279-280, 288, 297, 300
Lateral vaginal canal 14, 16, 23
Leydig (interstitial) cells 463
Limb formation 89-104
forelimb 77-81, 83-87, 89, 90-92, 94-96, 98-102, 125-135
hind limb 80, 82-87, 89, 93-98, 100-102, 125-135
Lips 100, 125, 127-135
Liver 323-335
bile canaliculi 326, 329, 333, 334
bile ductule 335
hemopoiesis 323-331
megakaryocyte 326, 331, 358-359
hepatic lobules 323, 327-328, 334
hepatocytes 323-335
sinusoids 323, 327-328, 330-332, 334
Lungs 210-226
Male reproductive system 1-13
Mammary glands 118, 121-122, 128
Median vaginal apparatus 14

Mesoderm 30, 32-33, 40, 61, 63-69
extra-embryonic mesoderm 30, 32-33, 40
mesodermal cells 63-68
somatic mesoderm 30, 40
splanchnic mesoderm 30, 40
Mesonephros 156-175
Mesonephric duct 156, 158-159, 163-164, 171, 174-175
Metanephric blastema 176
Metanephros 176-194
Mouth 83-88, 123, 125-135
Migration to pouch ii-iii, 89
Müllerian (paramesonephric) duct 164, 171, 470-471
Muscularis mucosae 259, 272, 280, 288-289
Muscularis externa 248, 259, 262, 265, 268, 280, 284, 288
Musculoskeletal system 105-117
skeletal muscle fibers (cells) 105-106, 116-117
type II fibers 106, 117
during limb development 105-106, 112-116
Myenteric plexus 248, 259, 297
Myoepithelial cells 155, 211, 236, 237, 240, 248, 257
Nasal cavity 195-209
Nephrons
mesonephric 156, 158-164, 166-169, 171-174
metanephric 176-177, 179-194
Nephronogenic zone 176-177, 179-188
Newborn opossum 123, 125
Notochord 105, 107-111
Nervous system (central) 71, 72
brain 71, 405-406, 4011-428
spinal cord 71-72, 407-410
Olfactory epithelium 195-196, 198-204, 207-209
Olfactory placodes 195
Olfactory neurons 195, 198-204, 207-208
Oocytes 14-15, 17
Optic nerve head 443
Oral cavity 83-88, 123, 125-135
Oral shield 85-88
Ovary 14-20, 468-471
cortex 17-18, 468, 470
follicles 14-15, 17
medulla 17, 468-469
primordial follicles 469
rete cords 46
Oviduct 14, 16, 21
Pancreas 302-322
acini 302, 304-306, 309-320
anlage 302
ducts 302, 310-317, 319-320
endocrine cells 302-304, 306-311, 313-322
proacinar cells 302, 304-306
islets 302-304, 3o7-311, 313-322
Panniculus carnosus 118, 122
Parathyroid gland 393-396
principal (chief) cells 393-396
Parturition ii-iii, 14
Pepsinogen 277-278
Periderm 88, 136-140
Penis 3, 129
Phallus 3, 129
Pituitary 368-385
adenohypophysis 368, 372, 378
infundibular process 369-379
median eminence 385
neurohypophysis 368, 378
pars distalis 368, 370-375, 378-379
corticotrophs 368, 370, 372-373
gonadotrophs 368, 372-375
lactotrophs 368, 371
somatotrophs 368, 370, 371
thyrotrophs 368, 374
pars intermedia 368-370, 372-384
pars nervosa 368, 378
pituitary cleft 368, 371-384
pituitary vesicle 368
Placentation 30-52
Pleura 211, 226-227
Postnatal growth (general) 123-135
Pouch 118-122
Primitive streak 64
Proamnion 30, 32-34, 40, 69
Prochymosin (prorennin) 277-278
Pseudovaginal canal 14
Rathke's pouch 368-369
Renal vesicle 176

Rete testis 463
Seminiferous tubules 4, 463, 467
Shell membrane 26-29
Sinus terminalis 30, 40-43
Skeletal development 105-115
Small intestine 279-289
 intestinal glands (crypts) 279, 288
 enterocytes 279, 283-288
 apical endocytic complex 279, 283-286
 enteroendocrine cells 279-280, 283, 287
 goblet cells 279, 286
 Paneth cells 279, 287
 villi 279, 282-288
Spermatozoa 1, 6-8, 10-13
 pairing 1, 10-13
Spleen 336-342
Stomach 258-278
 enteroendocrine cells 258-259, 268, 270, 275-276
 gastric pits (foveolae) 258, 265, 270-275
 glands
  cardiac 258, 276
  oxyntic 258-259, 265-274, 276
   caveolated cells 269
   chief (zymogen) cells 258, 278
   mucous neck cells 271
   parietal cells 258, 261-264, 266, 269-272
   undifferentiated cells 258, 266-267, 269
  pyloric 258, 272, 275-276
Submandibular salivary gland 236-245
 duct system 236-243
 mucous cells 236, 245
 myoepithelial cells 236-237, 240
 proacinar cells 236-238, 240
 secretory tubules (units) 236, 239-240, 243-245
  special serous cells 236, 245
Teeth 246-247
Terminal respiratory chambers 210-211, 213-219, 221-222, 224
Testes 463-467
Thymus 343-351
Thyroid 386-392
 epithelial cords 386-388
 follicle 386, 388, 390-392
  colloid 386, 390-392
  follicular epithelium 386, 388, 390-392
  primary follicle 386, 388
  secondary follicles 386, 388, 390-392
 parafollicular cells 386-387, 389, 391-392
 thyroid vesicle 386
 ultimobranchial body 386
Tongue 228-235
 papillae 228, 231-234
 taste buds 228
Tooth eruption 246-247
Trachea 210-211, 220, 213, 223
Transverse folds (esophagus) 248, 254-256
Trophectoderm 30, 35
Trophoblast 45-47, 51
Type I pneumocytes 210-211, 214, 216-217
Type II pneumocytes 210-211, 214, 216-217
Urogenital sinus 14
Ureteric bud 176
Ureters 1, 16
Urethra 1, 3, 16
 glandular portion 1, 3
  first region (prostate I) 3
  second region (prostate II) 3
  third region (prostate III) 3
Uterine epithelium 22, 25, 30, 37-39, 45-48, 50-52
Uterine glands 22, 25, 30, 36, 39, 45, 52
Uterus 14, 16, 22, 25, 30, 36
Urinary bladder 3, 16, 165, 170
Utricle ii, 123, 430, 434, 436
 maculae ii, 123, 430, 436
Yolk sac placenta 30, 40-43, 45-46, 48-49, 50
 non-vascular yolk sac placenta 30, 40-41, 43, 50
 vascular yolk sac placenta 30, 40-43, 45-48, 51
Zona pellucida 15, 17